Production Forecasting, Performance Analyses and Behavior of Shale Volatile Oil Reservoirs

A Dissertation

Presented to

the Faculty of the Department of Chemical Engineering

University of Houston

In Partial Fulfillment

of the Requirements for the Degree

Doctor of Philosophy (PhD)

in Chemical Engineering

by

Ibukun Makinde

December 2016

Production Forecasting, Performance Analyses and Behavior of Shale Volatile Oil

Reservoirs

Ibukun Makinde

Approved:

Chair of the Committee
Guan Qin, Professor,
Petroleum Engineering

Committee Members:

W. John Lee, Professor,
Petroleum Engineering, Texas A&M

Michael Nikolaou, Professor,
Chemical Engineering

Robert Stewart, Professor,
Earth and Atmospheric Sciences

Arthur B. Weglein, Professor,
Physics

Suresh K. Khator, Associate Dean
Cullen College of Engineering

Michael Harold, Department Chair
Chemical Engineering

Acknowledgements

Firstly, I thank God for bringing this far in my life and career. Next, I thank Dr. W. John Lee for being a supportive mentor/advisor and a great source of inspiration. Working with him has been a valuable experience that has broadened my horizon tremendously. I am grateful for the opportunity and I hope to continue learning from him as my career progresses.

Special appreciation also goes to Dr. Qin, Dr. Stewart, Dr. Nikolaou, and Dr. Weglein for their support and advice as members of my dissertation committee. I will also like to thank the Departments of Chemical Engineering and Petroleum Engineering for their support and provision of a conducive research environment. Further, I will like to appreciate my fellow colleagues, scholars and friends at the University of Houston for their friendship and encouragement.

Last but definitely not the least, I thank my family for their patience, love, support and understanding throughout my studies.

Production Forecasting, Performance Analyses and Behavior of Shale Volatile Oil Reservoirs

An Abstract

of a

Dissertation

Presented to

the Faculty of the Department of Chemical Engineering

University of Houston

In Partial Fulfillment

of the Requirements for the Degree

Doctor of Philosophy (PhD)

in Chemical Engineering

by

Ibukun Makinde

December 2016

Abstract

Due to the continual depletion of non-renewable conventional oil and gas resources and a corresponding rise in the global demand for energy, there are needs for alternative sources of energy. Unconventional resources like shale can provide a possible panacea to this critical energy issue for decades to come. Worldwide, shale resources are vast with several countries having enormous reserves of shale oil and gas. According to Rystad Energy, more than 50% of the United States' oil reserves come in the form of unconventional shale oil, with Texas alone containing approximately 60 million barrels (Matthews, 2016). The combination of horizontal well drilling and hydraulic fracturing has enabled us to produce economic volumes of shale oil and gas in recent years. Therefore, shale oil and gas research is very important to the energy industry as a whole.

The oil and gas industry requires accurate assessment and valuation of unconventional resources. With proper assessment of unconventional reserves, appropriate economic and organizational decisions can be made by companies, investors and other stakeholders. Production forecasting and reserves estimation are vital for correct assessment and valuation of unconventional resources like shale.

A good understanding of the behavior and production mechanisms of shale volatile oil reservoirs enable better reservoir performance analyses and production forecasting. The major focus of this dissertation is to find and explore reliable, easy-to-use ways of forecasting production, estimating reserves as accurately as possible, and in the process increasing our understanding of how shale volatile oil reservoirs behave. This study covers different approaches to production forecasting using reservoir simulation, empirical and statistical methods. Several reservoir simulation models were compared. Improvements

and suggestions for improvement of existing empirical decline curve analysis forecasting methods were thoroughly investigated. Six critical stages in the gas-oil ratio history of shale volatile oil reservoirs were identified and several factors impacting production performance were examined. A new approach to forecasting production and gas-oil ratios from shale volatile oil reservoirs called the Principal Components Methodology was also developed.

The work done in this dissertation will be a valuable contribution to the enhancement of petroleum production and reservoir engineering as well as the growth of the oil and gas industry.

“Except the Lord build the house, they labor in vain that build it…” – Psalm 127:1 (KJV)

To all hardworking scholars

Table of Contents

List of Figures

List of Tables

Chapter 1 – Introduction

1.1. Background and Motivation

The importance of accurate production forecasting and reserves estimation to the oil and gas industry cannot be overemphasized. It is vital for all stakeholders involved. Better economic and management decisions can be made with the availability of good production forecasts and reserves estimates.

Due to the advent of unconventional resources like shale as alternative sources of oil and gas production, it has become necessary for the industry to understand how to reliably forecast production and estimate reserves from these reservoirs. However, the task of appropriately forecasting production and estimating reserves, particularly from liquid rich shale reservoirs is quite difficult. Multiphase flow effects, formation heterogeneity and ultra-low permeability of shales contribute importantly to this challenge. As a result, most conventional methods used for estimating production and reserves are not completely suitable for unconventional reservoirs. The industry needs a good understanding of liquid rich shale reservoir production mechanisms as well as simple, fast and dependable production forecasting techniques.

In this study, I have attempted to tackle some of these problems, with the view of contributing to the ongoing efforts of finding dependable ways to forecast production from liquid rich shale reservoirs. The particular focus of this work is on shale volatile oil reservoirs.

1.2. Unconventional Resources

Unconventional resources are hydrocarbon reservoirs that have very low permeability and porosity. Cander (2012) defined unconventional resources in terms of permeability and viscosity. He defined them as resources in which technology must be used to increase the permeability-viscosity ratio in order to achieve commercial rates of flow. Examples of unconventional resources are tight gas, coal bed methane (CBM), shale gas, shale oil, heavy oil/tar sands and methane hydrates. They differ from conventional resources based on the geological features of the reservoirs, the state of the hydrocarbons and the technology required to extract the hydrocarbons.

Shale reservoirs, such as the Eagle Ford and Bakken, have emerged as extremely viable sources of hydrocarbon reserves. They do not produce economic volumes of oil and gas without some form of stimulation. Figure 1-1 shows basins with assessed shale oil and gas formations worldwide. This figure displays how widespread shale oil and gas resources are globally. There has been a steady increase in productivity of oil and gas from shale plays across the US, due to the emergence of multi-stage hydraulic fracturing and horizontal well drilling technologies. Despite this positive production trend, shale plays have been plagued by relatively low recovery factors in comparison to conventional plays. In the last decade, development of methods for analyzing production data from unconventional resources has gained a lot of attention. It is therefore important for the oil and gas industry to find ways to predict production with “reasonable certainty” from these reservoirs.

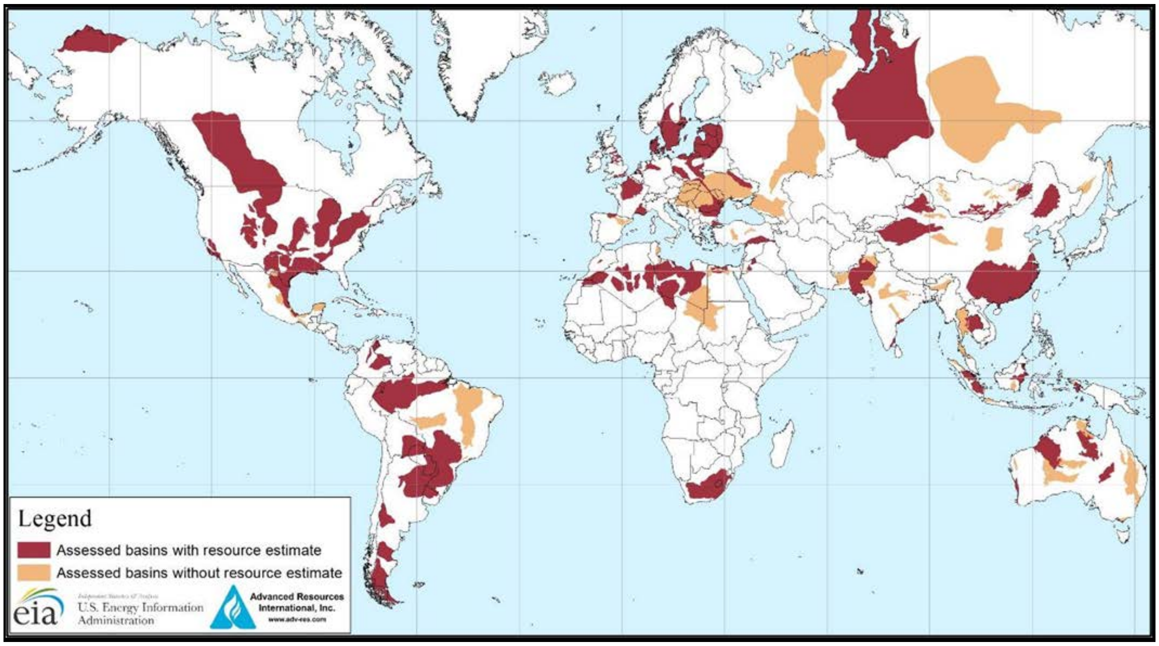

Figure 1-1 Basins with Assessed Shale Oil and Gas Formations (EIA, 2013)

1.3. Volatile Oil

Volatile oils are reservoir fluids with typical oil API gravity of 40°API or higher. They usually contain fewer heavy hydrocarbon components than black oils and are richer in heavy hydrocarbon components than gas condensates. As in black oils, the reservoir temperature is always mostly lower than the critical temperature in the volatile oil pressure-temperature (P-T) phase diagram. In Figure 1-2, we observe that the reservoir temperature is close to the critical temperature; hence volatile oils can also be "near-critical" oils sometimes. The iso-volume lines are closer near the bubble point curve, indicating that a small drop below the bubble point pressure leads to vaporization of a considerable fraction of the oil.

The complicated intermediate properties of volatile oils (between black oils and gas condensates) which become even more complex in the small pores of shale reservoirs, make them an important focal point of research. The need to properly understand the phase behavior of volatile oils in shale reservoirs is important in the bid to accurately forecast production from shale volatile oil reservoirs.

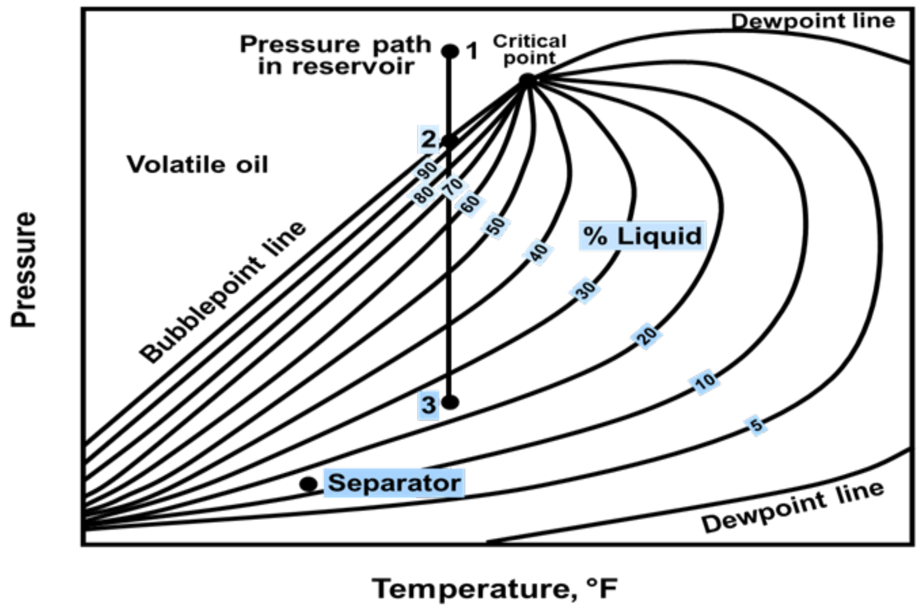

Figure 1-2 Phase Diagram of a Typical Volatile Oil

1.4. Organization of Study

This dissertation is a compilation of six chapters (four research chapters plus the introduction and overall conclusions chapters). Apart from the overall conclusions, there are inferences for each research chapter. Brief descriptions of each chapter (excluding the introduction chapter) are provided in the following paragraphs.

Chapter Two: Can we afford to jeopardize the accuracy of production forecasts by using easier and less time-consuming reservoir simulation methods? How do important parameters affect production performance of shale volatile oil reservoirs when single-phase and two-phase black-oil simulators are used? The results of production forecasts from single-phase and two-phase black-oil simulation models as well as the compositional simulation model are compared here. Also, the influence of fluid sampling errors on production performance is examined.

Chapter Three: How appropriate are traditional decline curve analysis (DCA) methods for forecasting production in shale volatile oil reservoirs? Can we possibly forecast the secondary phase (gas) with some level of confidence using a simple technique? Here, traditional and hybrid (combination) DCA methods were used to analyze production data. Further, a simple method similar to one recently presented in the literature was used to forecast solution gas production.

Chapter Four: How well can we understand the production mechanisms and behavior of shale volatile oil reservoirs? Here, a commercial compositional simulator is used to simulate several scenarios using different fluid samples (volatile oils), in order to evaluate how various factors, affect the production performance and mechanisms of shale volatile oil reservoirs.

Chapter Five: Can we possibly forecast gas-oil ratios (GORs) and estimate solution gas production from shale volatile oil reservoirs? Is it possible to eliminate the complexities associated with existing forecasting techniques and still forecast oil production with "reasonable certainty"? This chapter examines the use of the Principal Components Methodology (PCM) as a possible means of finding solutions to these questions and many more. Here, the oil production forecasts from PCM are also compared to those from traditional and hybrid decline curve analysis (DCA) models.

Chapter Six: The overall conclusions of this study are summarized here.

Chapter 2 – Reservoir Simulation Models – Impact on Production Forecasts and Performance of Shale Volatile Oil Reservoirs

Reservoir simulation is an important tool that can be used to simulate as well as predict production from shale reservoirs. The type of reservoir simulation model used, is significant in this process. Black-oil and compositional simulators can be used for reservoir simulation. Black-oil simulations are easier and less time-consuming than compositional simulations. Nevertheless, how accurate are black-oil simulation results compared to compositional simulation results? Can the results be trusted to some extent? Single-phase and two-phase black-oil simulation results as well as compositional simulation results were analyzed and compared in this chapter. The effects of fluid sampling errors on production forecasts were also studied.

2.1. Reservoir Simulation Models

In black-oil simulation models, oil and gas are represented by two components – one "component" called oil and the other "component", gas. Here, there is an assumption that produced gas, solution gas, injected and free gas in contact with oil all have the same physical properties. In this model, PVT properties of fluid phases are calculated as functions of pressure only. Therefore, the only inputs necessary for black-oil simulators are tables of PVT properties such as oil formation volume factor (FVF), gas FVF, solution gas-oil ratio, viscosity, etc. as a function of pressure.

However, in compositional models, oil and gas phases are represented as multi-component mixtures. Both phases are made up of different amounts of the same components. For example, ethane can be 45% in the gas phase and 7% in the oil phase. Here, the physical properties of the gases are different and the composition of produced gas varies with time. An equation of state is used in this case instead of simple PVT tables. Figure 2-1 shows illustrative descriptions of the oil and gas phases for black-oil and compositional simulation models.

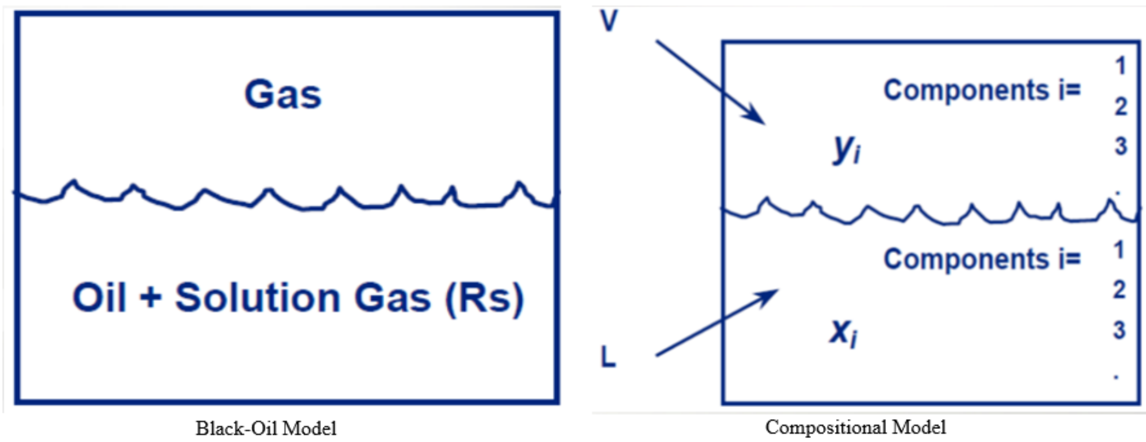

Figure 2-1 Oil and Gas Phases for Black-Oil and Compositional Simulation Models

2.2. Reservoir Model Description

A reservoir basecase model consisting of 8 horizontal wells, with 20 hydraulic fractures spaced 250 ft apart was constructed. The distance between each well is 660 ft, i.e., 330 ft from one well to half adjacent distance of the other. The horizontal well lengths are 5,000 ft. Overall dimensions of the reservoir model are 7,000 ft long, 7,000 ft wide and 250 ft thick. The simulation model is a single porosity system. The fractures are all infinitely conductive. For computational purposes, a fracture width of 2 ft was used. Actual fracture width is about 0.2 inches, but wider fractures make simulation go more smoothly. Fracture permeability is correspondingly reduced to keep the product of width and permeability (of fractures) at an appropriate level. This approach is appropriate because reservoir models with the same fracture conductivity but different fracture widths yield similar results (Alkouh *et al.*, 2012). The initial reservoir pressure is 5,000 psia and the wells produce for 30 years at a minimum bottomhole pressure constraint of 1,000 psia. Figure 2-2 is a pictorial representation of the basecase model after gridding. Tables 2-1 and 2-2 show the reservoir data and the model parameters used. Correlations used to generate PVT properties of oil and gas phases, as a function of pressure are shown in Table 2-3.

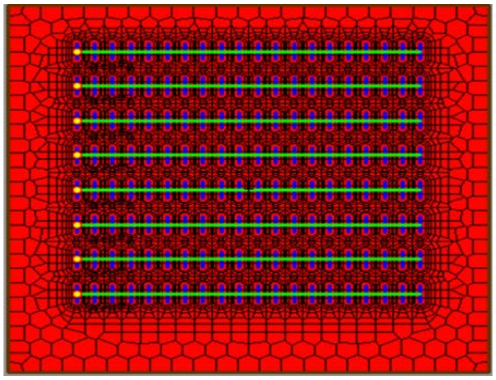

Figure 2-2 Reservoir Basecase Model (after gridding)

Table 2-1 Reservoir Data for the Reservoir Basecase Model

Permeability	0.001 md
Porosity	0.06
Reservoir Temperature	250°F
Initial Reservoir Pressure	5,000 psia
Depth to top of formation	10,000 ft
Reservoir Thickness	250 ft
Corey Relative Permeability Exponent	2.5
Critical gas saturation, S_{gc}	0.05
Residual saturation of oil (gas/oil displacement), S_{org}	0.2

Table 2-2 Parameters for the Reservoir Basecase Model

Number of wells	8
Distance between wells	660 ft
Horizontal well length	5,000 ft
Fracture spacing	250 ft
Fracture half-length	150 ft
Fracture width	2 ft
Oil API gravity	42°API
Initial solution GOR	1,500 scf/STB
Gas specific gravity (Air = 1)	0.75

Table 2-3 Basecase Correlations Used for Black-Oil PVT Tables

Oil		Gas	
Property	Correlation	Property	Correlation
Bubble point pressure, p_b	Standing	Z-factor	Dranchuk
Oil viscosity, μ_o	Beggs - Robinson	Gas viscosity, μ_g	Lee et al.
Solution GOR, R_s	Standing	Gas formation volume factor, B_g	Internal[1]
Oil formation volume factor, B_o	Standing	-	-
Oil compressibility, c_o	Vazquez - Beggs	-	-

2.3. Single-Phase vs. Two-Phase Black-Oil Simulations

30 years of production was simulated using single-phase (oil) and two-phase (oil and gas) black-oil simulators. The simulations were isothermal and simulation results are for the 8 horizontal wells combined. Figures 2-3 to 2-5 show the simulation results comparing single-phase flow with two-phase flow for cumulative oil production, oil recovery factor and average reservoir pressure. There is larger cumulative oil production and oil rate for the two-phase flow than the single-phase flow case. This is likely due to the solution gas drive mechanism in two-phase flow, caused by the presence of the second phase (gas) which is absent in single-phase flow. A higher cumulative oil production correspondingly leads to a higher oil recovery factor for the two-phase flow case. Also, there is lesser pressure drop for two-phase flow compared to the single-phase flow case due to multiphase flow effects.

[1] Internal correlations within the software

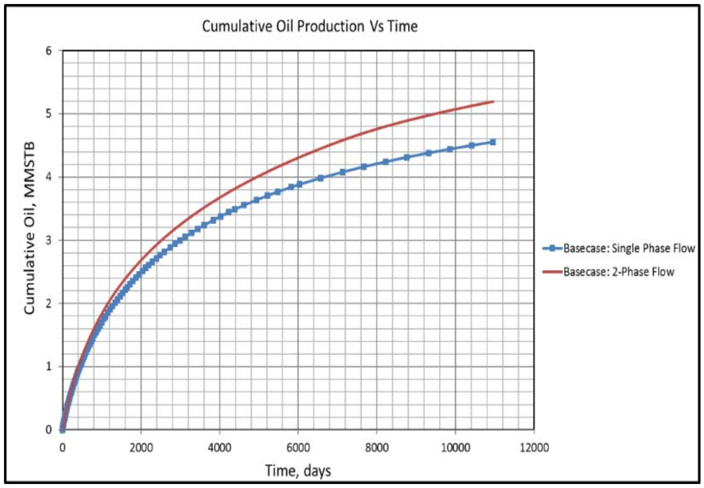

Figure 2-3 Single-Phase Flow vs. Two-Phase Flow – Cumulative Oil Production

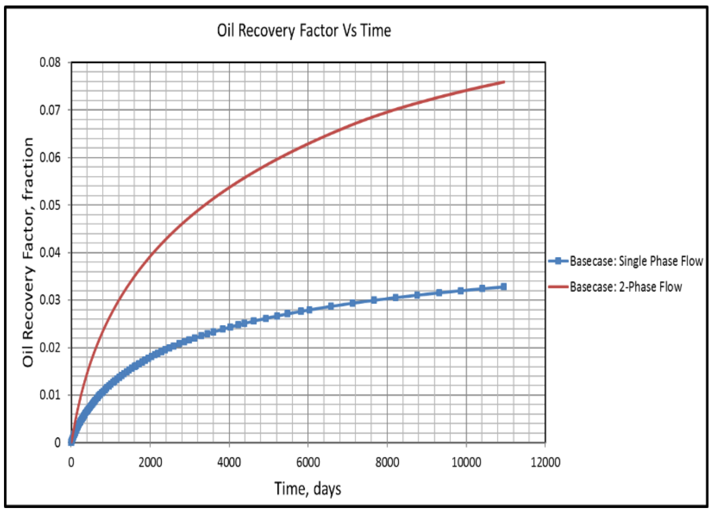

Figure 2-4 Single-Phase Flow vs. Two-Phase Flow – Oil Recovery Factor

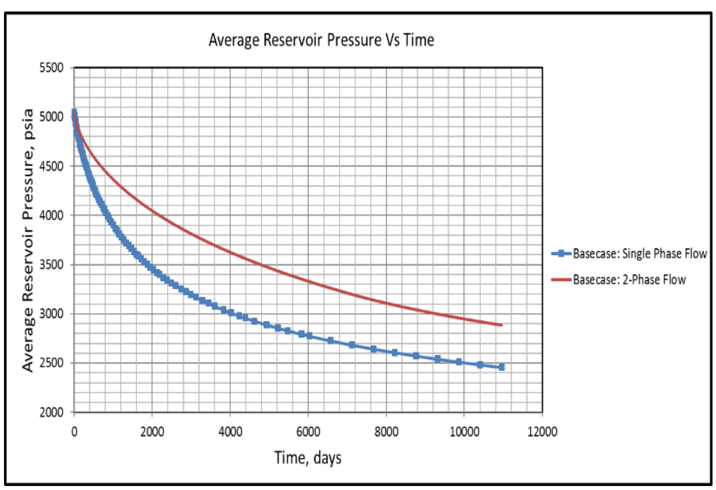

Figure 2-5 Single-Phase Flow vs. Two-Phase Flow – Average Reservoir Pressure

2.3.1. Sensitivity Analyses – Single-Phase Flow vs. Two-Phase Flow Comparisons

How do certain parameters affect the production performance of shale volatile oil reservoirs when single-phase and two-phase black-oil simulators are used to simulate production? Are the results comparable or do they differ? Sensitivity studies were carried out with the aid of isothermal single-phase and two-phase black-oil simulations. The parameters studied include fracture spacing, fracture half-length, oil API gravity and critical gas saturation. These parameters were varied with other variables in the basecase model kept constant.

2.3.1.1. Fracture Spacing – Single-Phase Flow vs. Two-Phase Flow Comparisons

Fracture spacing is an important well completion parameter. The fracture spacing used for the basecase model is 250 ft (20 hydraulic fractures). Two other cases were considered – 100 ft (50 hydraulic fractures) and 500 ft (10 hydraulic fractures). Figures 2-6 to 2-9 show the effect of fracture spacing on cumulative oil production, oil rates, oil recovery factors and average reservoir pressure for single-phase and two-phase flow cases. Simulation results show that closer fracture spacing leads to higher cumulative oil production, higher initial oil rates and higher oil recovery factor for both single-phase and two-phase flow cases. For the oil rate cases, we can observe higher oil rates toward the end of the production period as fracture spacing widens. This is because there is faster drainage of the reservoir with closer fracture spacing, thereby leading to lower oil rates toward the end of the production period in comparison to cases with wider fracture spacing. There is a quicker pressure drop at the beginning of the production period for single-phase flow than for two-phase flow cases. Oil recovery factors, cumulative oil production and oil rates are generally higher for two-phase flow than for single-phase flow cases.

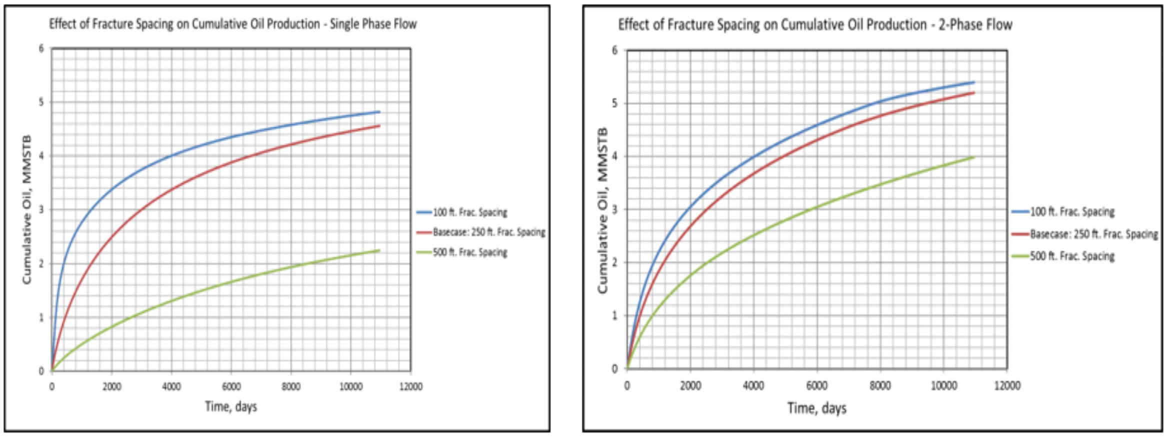

Figure 2-6 Effect of Fracture Spacing on Cumulative Oil Production – Single-Phase and Two-Phase Flow Cases

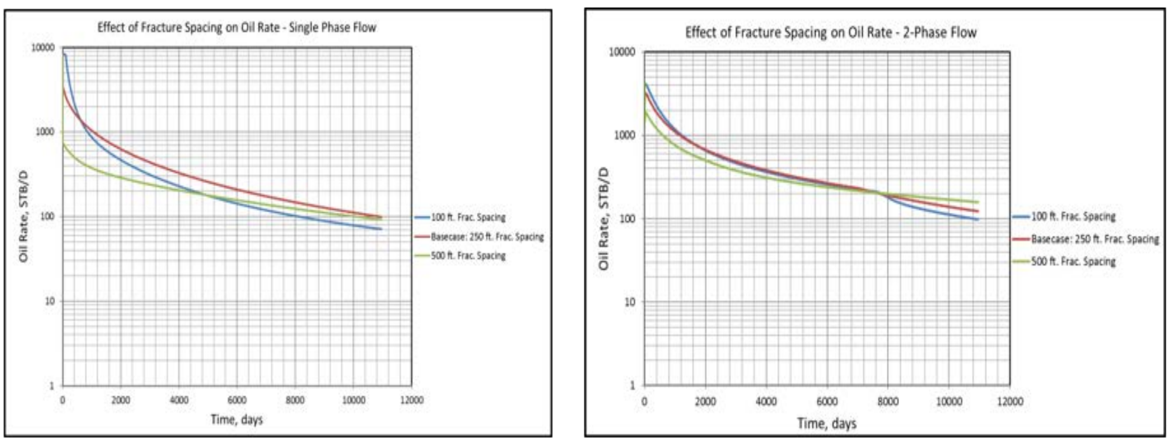

Figure 2-7 Effect of Fracture Spacing on Oil Rates – Single-Phase and Two-Phase Flow Cases

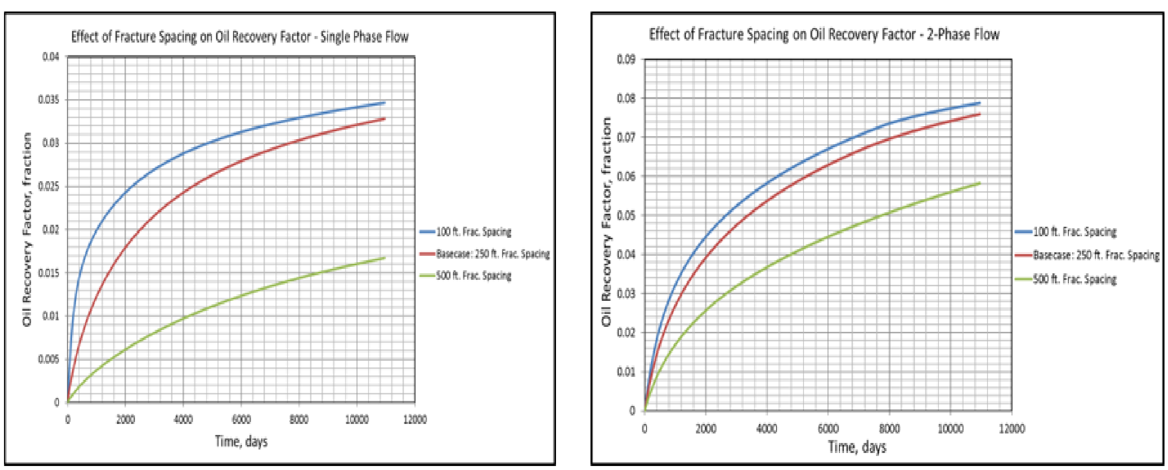

Figure 2-8 Effect of Fracture Spacing on Oil Recovery Factor – Single-Phase and Two-Phase Flow Cases

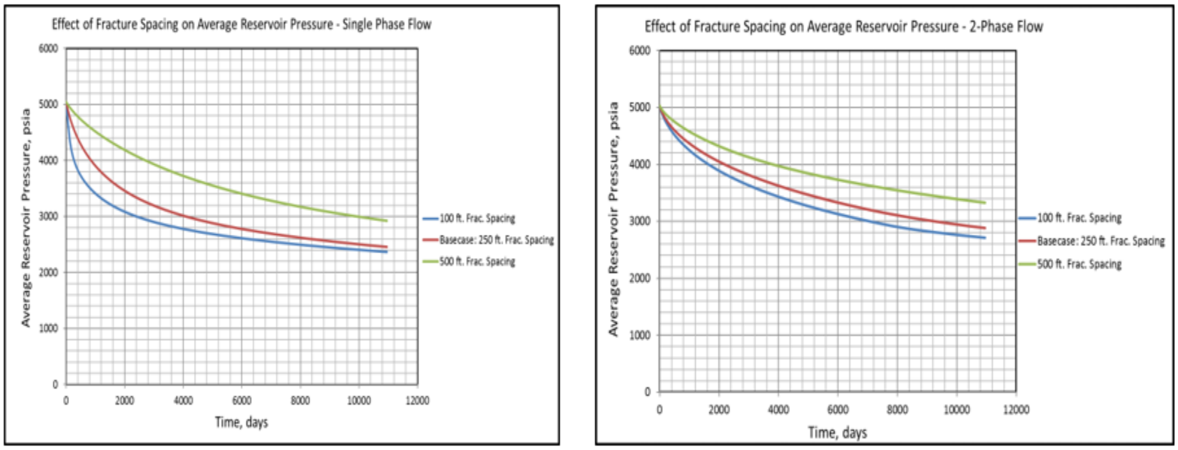

Figure 2-9 Effect of Fracture Spacing on Average Reservoir Pressure – Single-Phase and Two-Phase Flow Cases

2.3.1.2. Fracture Half-Length – Single-Phase Flow vs. Two-Phase Flow Comparisons

Fracture half-length is the distance from the wellbore to the outer tip of a fracture. Three scenarios were considered here – fracture half-lengths of 100 ft, 200 ft and 300 ft. In the basecase model, the fracture half-length is 150 ft. Figures 2-10 to 2-13 show the effect of fracture half-length on cumulative oil production, oil rate, oil recovery factors and average reservoir pressure for single-phase and two-phase flow cases. Results show that the larger the fracture half-length, the higher cumulative oil production, oil rate and oil recovery factor for both single-phase and two-phase flow simulations. There is a more rapid pressure drop (that later flattens out) early in the production period for single-phase flow than for the two-phase flow cases. Oil recovery factors, oil rates and cumulative oil production are mostly higher in two-phase flow than the single-phase flow cases.

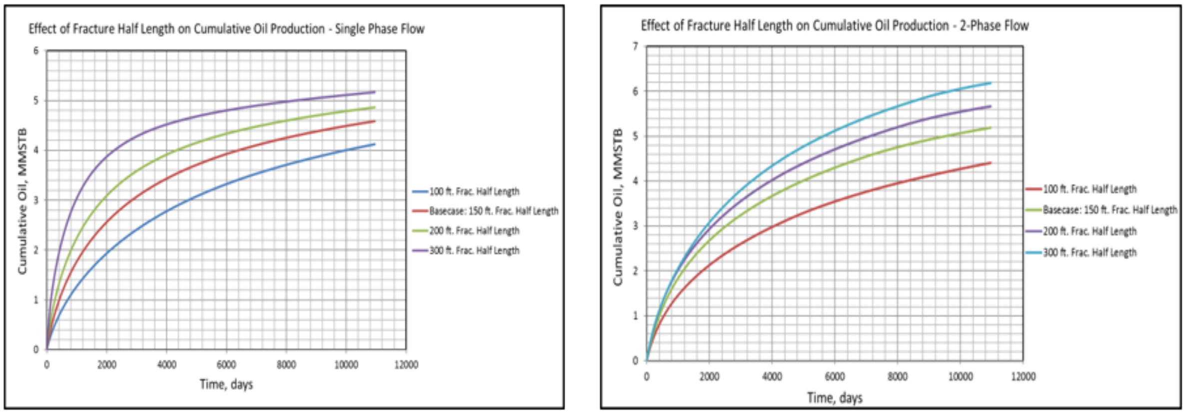

Figure 2-10 Effect of Fracture Half-Length on Cumulative Oil Production – Single-Phase and Two-Phase Flow Cases

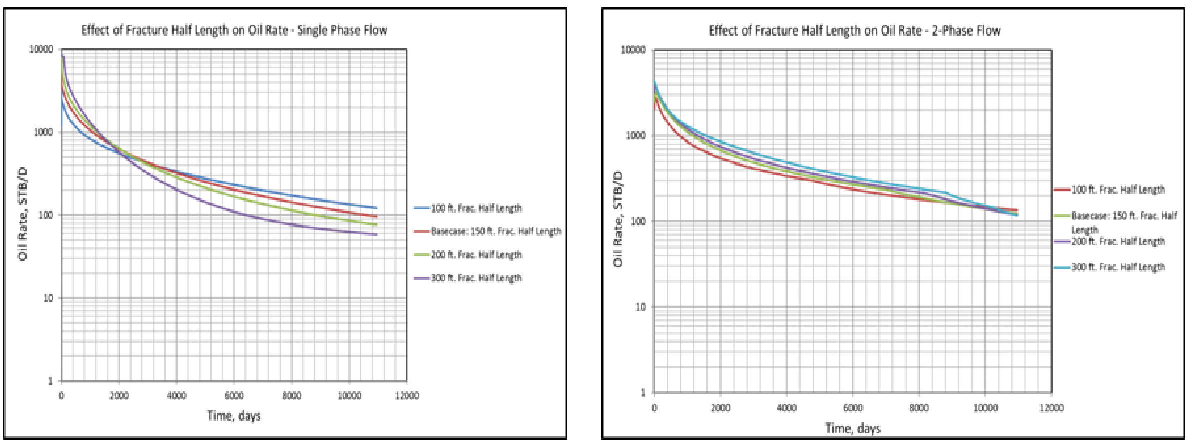

Figure 2-11 Effect of Fracture Half-Length on Oil Rates – Single-Phase and Two-Phase Flow Cases

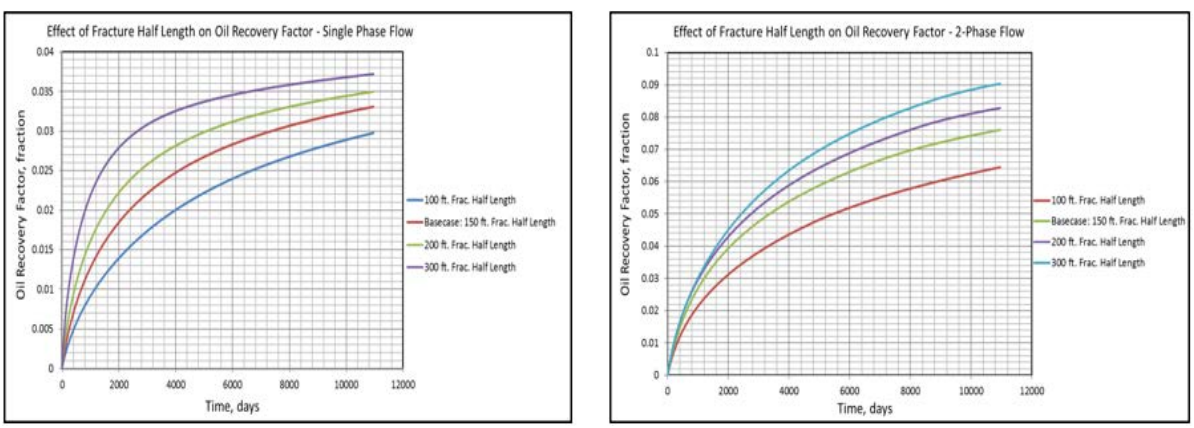

Figure 2-12 Effect of Fracture Half-Length on Oil Recovery Factor – Single-Phase and Two-Phase Flow Cases

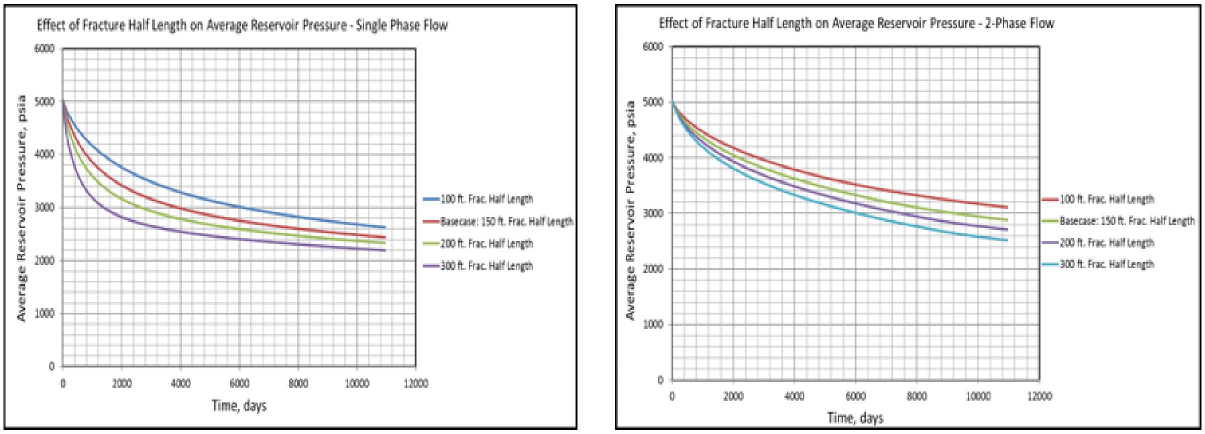

Figure 2-13 Effect of Fracture Half-Length on Average Reservoir Pressure – Single-Phase and Two-Phase Flow Cases

2.3.1.3. Oil API Gravity – Single-Phase Flow vs. Two-Phase Flow Comparisons

Oil API gravity is a very important fluid property. It measures the heaviness or lightness of a petroleum liquid in comparison to water. Oil API gravity is inversely correlated to the specific gravity of oil; therefore, heavier oils have low API gravities and lighter oils, higher API gravities. Oil viscosity increases with lower API gravity and it decreases with higher API gravity. Oil API gravity of 42° was used for the basecase model. The following oil API gravities were considered for the single-phase flow cases - 38°, 40°, 44°, 46° and 50°API. For the two-phase flow simulations - 38°, 40°, 44°, 46°, 50°, 60° and 65° oil API gravities were used. Two additional cases were added for the two-phase flow simulations in order to further demonstrate the impact of this fluid property on the behavior of shale volatile oil reservoirs. Figures 2-14 to 2-17 show the effect of oil API gravity on cumulative oil production, oil rate, oil recovery factor and average reservoir pressure for both single-phase and two-phase flow cases.

For the single-phase flow cases, the higher the oil API gravity, the higher the cumulative oil production and the initial oil production rates. This is because the higher the oil API gravity, the lighter the oil and the lower the viscosity – indicating higher oil mobility. Likewise, the analyses show that the higher the oil API gravity, the higher the oil recovery factor. Also, the lower the oil API gravity, the slower the rate of decline of the average reservoir pressure and vice versa.

Results of the two-phase flow cases provide a good demonstration of shale volatile oil reservoir behavior. As production occurs and reservoir pressure falls below the bubble point, gases start to build up around the wellbore. With time, the increasing gas saturation starts to hinder oil flow to the wellbore – eventually leading to a decline in cumulative oil production. This study illustrates that the higher the oil API gravity, the lower the cumulative oil production. This is shown in Figure 2-14. The higher the oil API gravity of fluids, the more the lighter components they contain. These lighter components of the fluid contribute to gas saturation around the wellbore, thus decreasing cumulative oil production with time. Table 2-4 shows actual production forecast data from two-phase black-oil simulations after 30 years of production. This table clearly shows the numerical value of cumulative oil production decline with increasing oil API gravity. Cumulative gas production on the other hand, increases with increasing oil API gravity. Furthermore, Figure 2-18 shows how average gas saturation increases with increasing oil API gravity. This also corroborates the explanations above on how increasing oil API gravity decreases cumulative oil production. In addition, results from two-phase flow cases show that oil production rates drop with increasing oil API gravity. However, there was an increase in oil recovery factor with increase in oil API gravity, even though above 60°API there was a slight drop in oil recovery factor for the 65°API case. This is shown in Figure 2-16, indicating that with further increase in oil API gravity above 60°API, oil recovery factor will most likely begin to decline. It is also observed from this study that the average reservoir pressure declines at a faster rate with increase in oil API gravity and vice versa. This is illustrated in Figure 2-17.

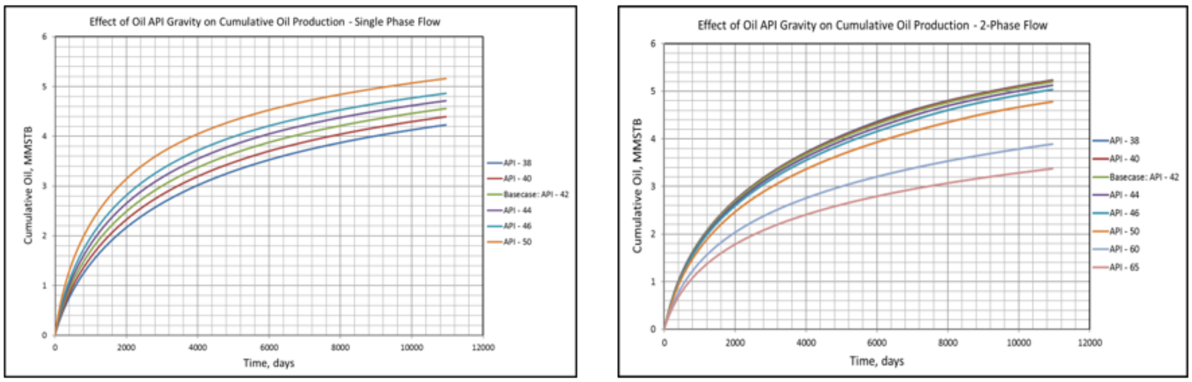

Figure 2-14 Effect of Oil API Gravity on Cumulative Oil Production – Single-Phase and Two-Phase Flow Cases

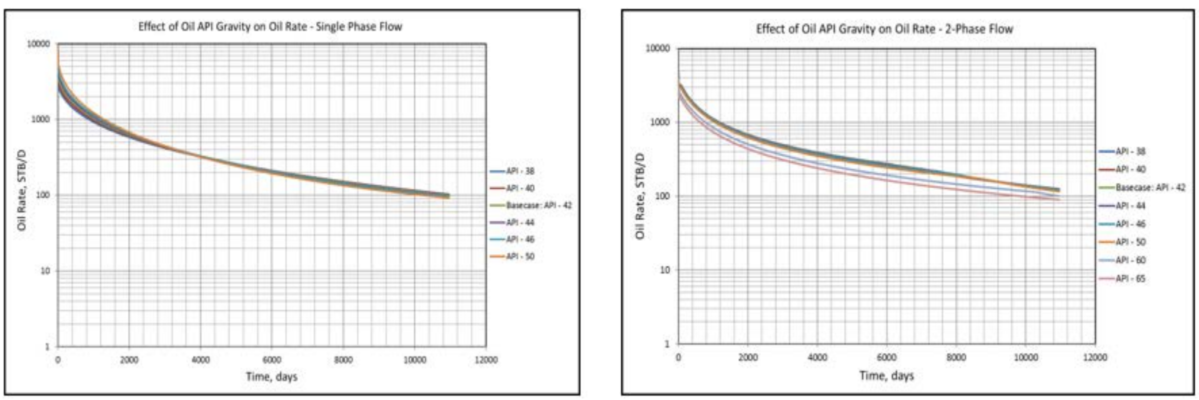

Figure 2-15 Effect of Oil API Gravity on Oil Rates – Single-Phase and Two-Phase Flow Cases

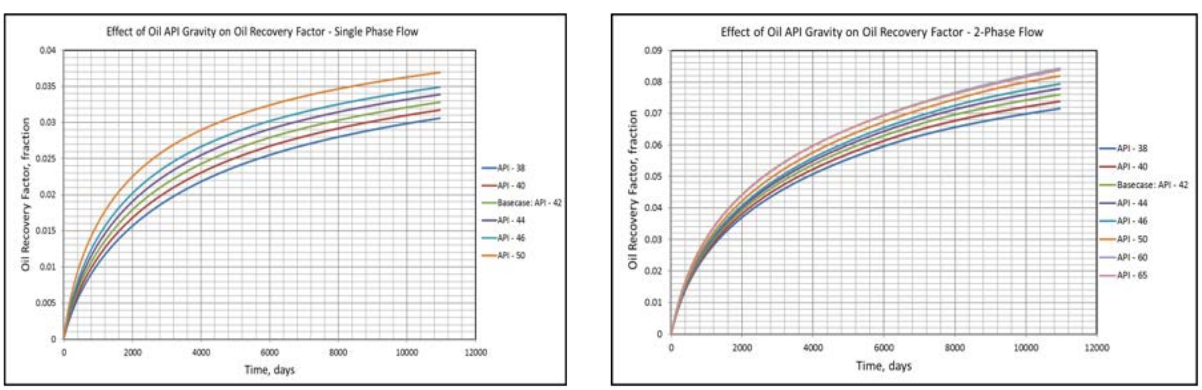

Figure 2-16 Effect of Oil API Gravity on Oil Recovery Factor – Single-Phase and Two-Phase Flow Cases

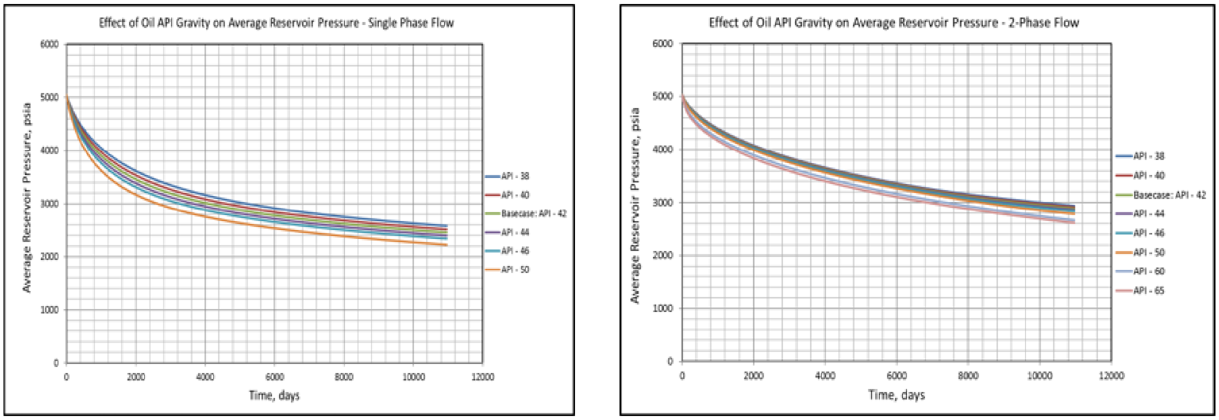

Figure 2-17 Effect of Oil API Gravity on Average Reservoir Pressure – Single-Phase and Two-Phase Flow Cases

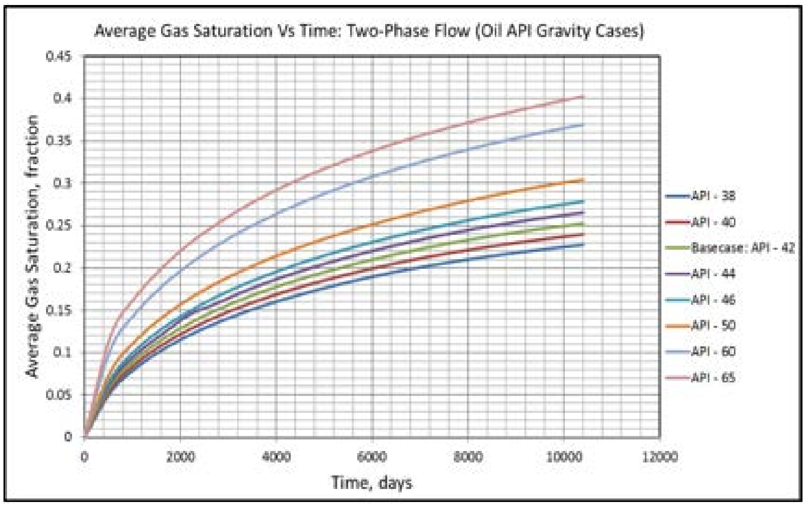

Figure 2-18 Average Gas Saturation – Two-Phase Flow Cases

Table 2-4 Forecast after 30 yrs of Production for Two-Phase Flow (Oil API Gravity Cases)

Oil API Gravity	Cumulative Oil Production, MMSTB	Cumulative Gas Production, bscf
38°API	5.2336	27.4234
40°API	5.2257	28.7767
Base case: 42°API	5.1926	30.1184
44°API	5.1287	31.4301
46°API	5.0368	32.7155
50°API	4.7822	35.1055
60°API	3.8913	39.9792
65°API	3.3757	41.6698

2.3.1.4. Critical Gas Saturation – Two-Phase Black-Oil Simulation Cases

In an oil reservoir, gas evolves out of solution when the reservoir pressure drops below the bubble point. The gas is immobile until it reaches a threshold called the critical gas saturation. At and above the critical gas saturation, the gas phase becomes mobile and begins to flow towards the wellbore. Two-phase black-oil simulations were run with critical gas saturations of 2%, 10%, 15% and 20%. A critical gas saturation of 5% was used for the basecase model. Figures 2-19 to 2-22 show the effect of critical gas saturation on cumulative oil production, oil rate, oil recovery factor as well as average reservoir pressure.

Results indicate that cumulative oil production increases with increase in critical gas saturation. This can be seen in Figure 2-19. The higher the critical gas saturation, the longer the gas stays in the pore spaces, thus pushing out more oil before it becomes mobile and starts to flow. Oil recovery factor also increases with increase in critical gas saturation. For the case with 20% critical gas saturation, the oil recovery factor is almost 12%, while it is approximately 7% for the case with 2% critical gas saturation. Figure 2-21 shows this.

In Figure 2-20, results show that at early times, a constant production rate was observed for the 20% critical gas saturation case, before decline starts to occur. From the graph, it is also observed that oil production rates decline earlier as critical gas saturation decreases. This is because at lower critical gas saturations, evolved gas becomes mobile earlier, leading to earlier decline in oil rate. This phenomenon is vice versa as critical gas saturation gets higher. It also explains why there is a slightly faster decline in average reservoir pressure as critical gas saturation gets lower. This is observed in Figure 2-22.

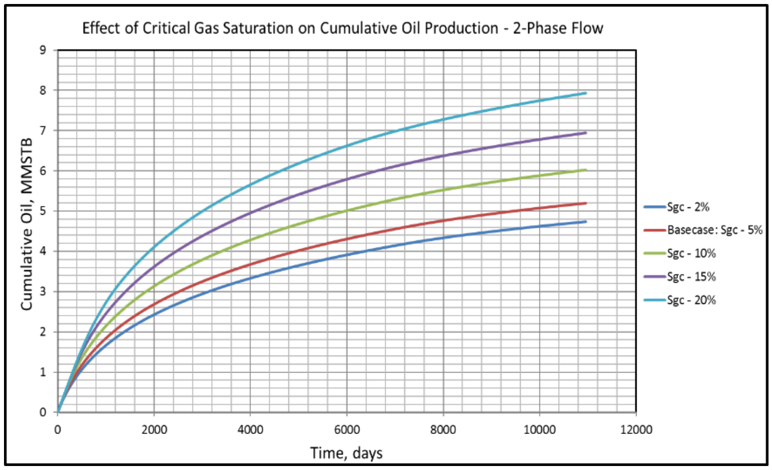

Figure 2-19 Effect of Critical Gas Saturation on Cumulative Oil Production – Two-Phase Flow Cases

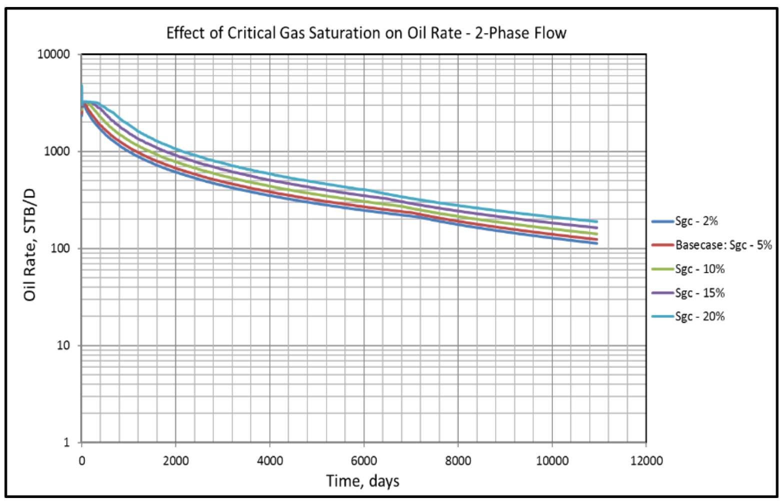

Figure 2-20 Effect of Critical Gas Saturation on Oil Rates – Two-Phase Flow Cases

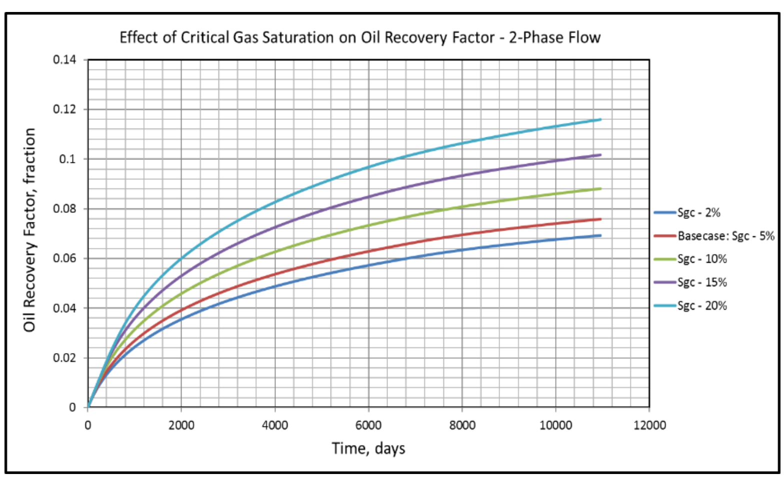

Figure 2-21 Effect of Critical Gas Saturation on Oil Recovery Factor – Two-Phase Flow Cases

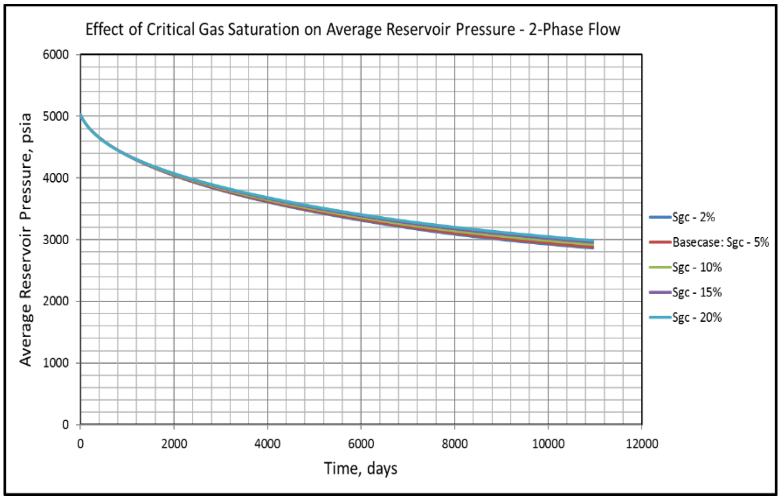

Figure 2-22 Effect of Critical Gas Saturation on Average Reservoir Pressure – Two-Phase Flow Cases

2.3.2. 4-Well vs. 8-Well Cases – Single-Phase Flow vs. Two-Phase Flow Comparisons

Single-phase and two-phase black-oil simulations were run using a reservoir model with four horizontal wells. The distance between the wells is twice that of the original basecase model (8-well case) i.e., 1320 ft (660 ft from one well to half adjacent distance of the other). All other parameters remain the same as the basecase model. An illustration of the two models side by side is shown in Figure 2-23. Simulation results were compared to the 8-well basecase model. Figures 2-24 to 2-27 show the simulation results for single-phase and two-phase flow compared to the basecase model.

For both the single-phase and two-phase flow cases, there is higher cumulative oil production, oil rate and oil recovery factor for the 8-well basecase model compared to the 4-well case. This is an expected result, as there are more wells and more hydraulic fracture stages overall in the 8-well case than in the 4-well case. Also, closer distance between the wells in the 8-well case ensures a larger stimulated reservoir volume (SRV), which ultimately leads to more production. Also, there is a more rapid decline in average reservoir pressure for the 8-well cases compared to the 4-well cases. Generally, cumulative oil production and oil recovery factors were higher for two-phase flow compared to single-phase flow cases.

Figure 2-23 4-Well and 8-Well Reservoir Models

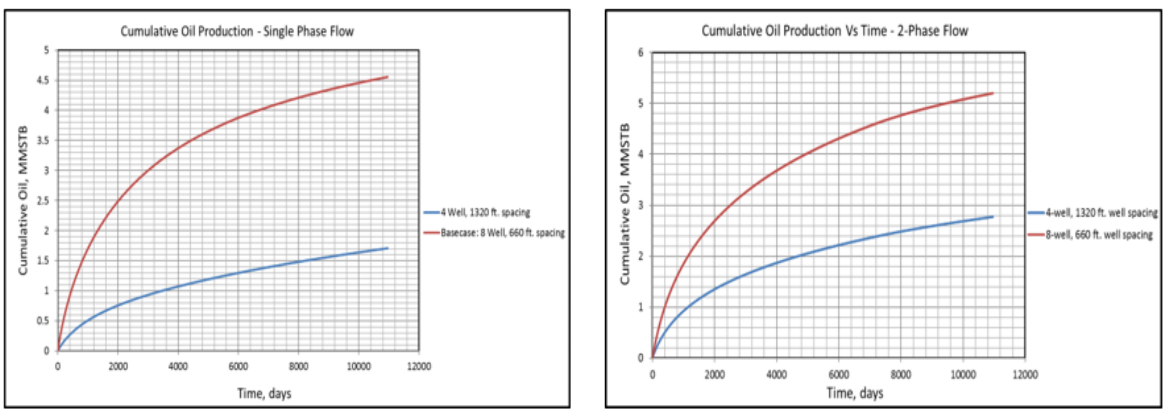

Figure 2-24 Cumulative Oil Production: 4-Wells vs. 8-Wells – Single-Phase and Two-Phase Flow Cases

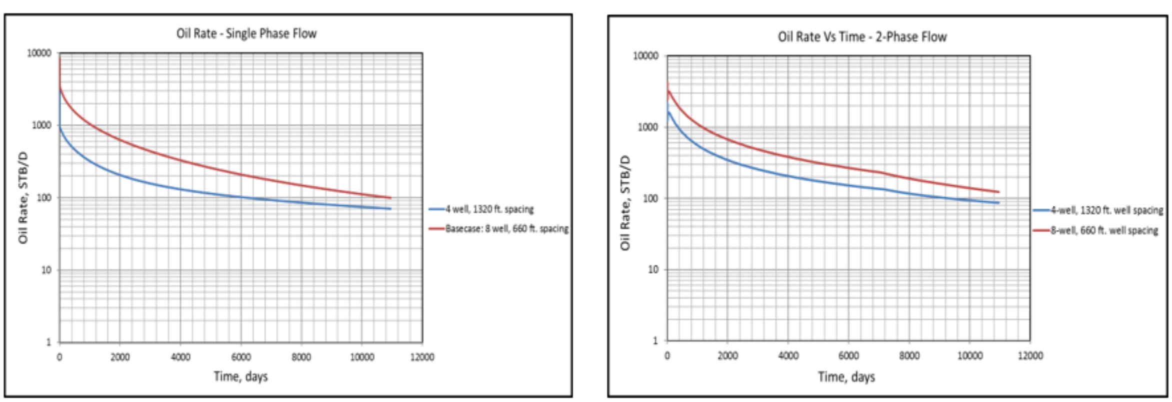

Figure 2-25 Oil Rates: 4-Wells vs. 8-Wells – Single-Phase and Two-Phase Flow Cases

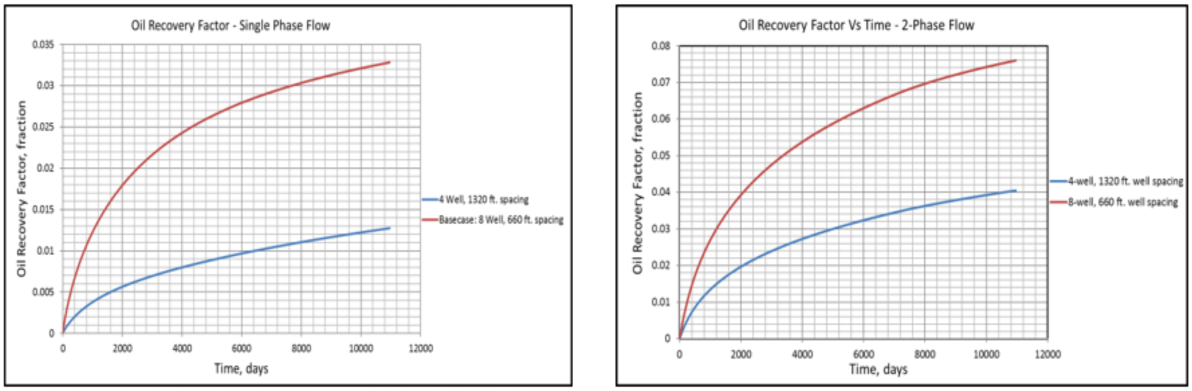

Figure 2-26 Oil Recovery Factor: 4-Wells vs. 8-Wells – Single-Phase and Two-Phase Flow Cases

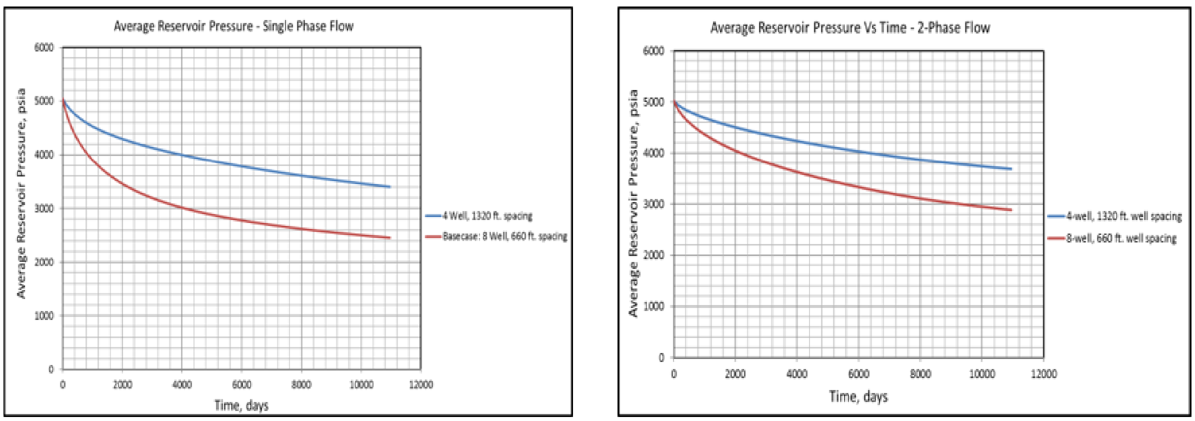

Figure 2-27 Average Reservoir Pressure: 4-Wells vs. 8-Wells – Single-Phase and Two-Phase Flow Cases

2.4. Compositional Simulations

Compositional simulations using different 5 different reservoir fluid samples were run for a period of 30 years. All reservoir parameters remain the same, except that in this case, the Peng Robinson equation of state was used for the PVT instead of correlations. The fluid compositions are shown in Table 2-5. The fluid samples are volatile oils (Fluids 3 and 4 are near-critical fluids). Figures 2-28 and 2-29 show the corresponding P-T diagrams for each of the different fluid compositions. The curves represent the two-phase boundaries; the straight lines going through the curves are the isothermal pressure decrease paths during production and the points on the curves are the critical points. The P-T diagrams were generated using the CMG Winprop software. The positions of the isothermal lines usually help us to determine the reservoir fluid type. In many instances, the isothermal line shows the pressure path in the reservoir. In this case, however, the lines just indicate the positions of the reservoir temperature compared to the critical points. Simulation results were compared to determine the effects of fluid composition on production performance of shale volatile oil reservoirs.

Table 2-5 Fluid Compositions

	Fluid 1	Fluid 2	Fluid 3	Fluid 4	Fluid 5
Components	Composition (%)	Composition (%)	Composition (%)	Composition (%)	Composition (%)
CH_4	58.77	58.07	61.82	53.47	49.43
C_2H_6	7.57	7.43	7.91	11.46	7.28
C_3H_8	4.09	4.16	4.42	8.79	8.02
$I\text{-}C_4H_{10}$	0.91	0.96	1.02	-	2.31
$N\text{-}C_4H_{10}$	2.09	1.63	1.74	4.56	3.61
$I\text{-}C_5H_{12}$	0.77	0.75	0.80	-	1.80
$N\text{-}C_5H_{12}$	1.15	0.80	0.86	2.09	1.79
C_6H_{14}	1.75	1.14	1.21	1.51	2.32
C_{7+}	21.76	22.59	17.59	16.92	22.41
CO_2	0.93	2.32	2.47	0.90	0.16
N_2	0.21	0.15	0.16	0.30	0.87

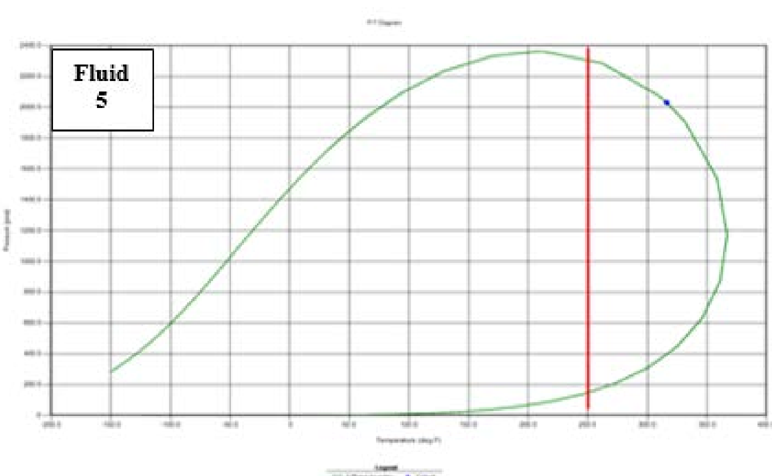

Figure 2-28 P-T Diagram – Fluid 5

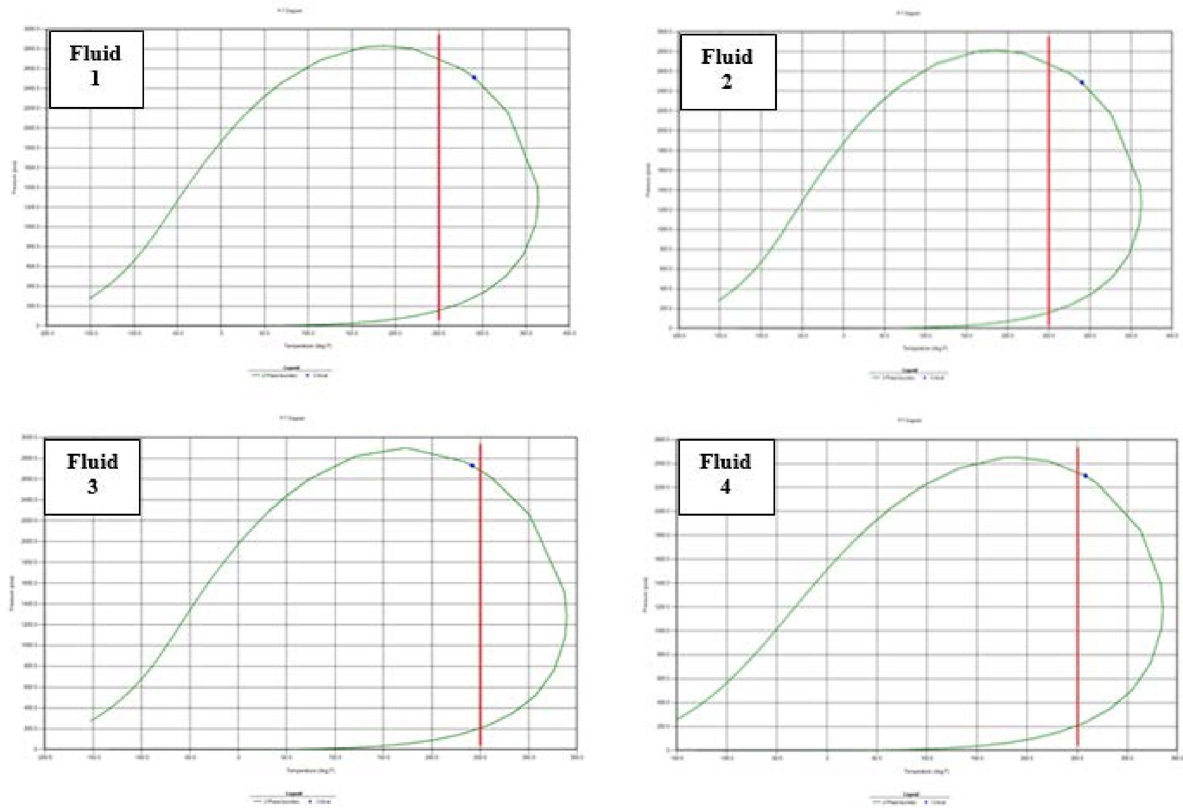

Figure 2-29 P-T Diagrams – Fluids 1-4

McCain (1994) suggested that the heavy components in petroleum mixtures have the greatest effect on fluid characteristics. Results of this study, however, show the importance of not only the heavy components, but also of the light components, especially methane. Figure 2-30 illustrates the effect of fluid composition on cumulative oil production and oil rates. Fluid 5, with the smallest methane composition and relatively high (22.41%) C_{7+} composition has the largest cumulative oil production and oil rate whereas Fluid 3, with the largest methane composition and relatively low C_{7+} composition (though not lowest – Fluid 4 has the least C_{7+} composition), has the smallest cumulative oil production and oil rate. Note that, despite the fact that Fluid 4 has a smaller C_{7+} composition than Fluid 3, cumulative oil production and oil rate for Fluid 4 is higher than for Fluid 3. This indicates that the methane composition plays a major role in reservoir performance. Fluids 1 and 2 are similar in composition (methane compositions are almost the same and the C_{7+} compositions are slightly different) – they therefore have almost the same cumulative oil production and oil rates. Fluid 2, with a slightly smaller methane composition and slightly larger C_{7+} composition, has a slightly higher cumulative oil production and oil rate than Fluid 1. Also, Fluids 5 and 2 have almost the same C_{7+} composition (Fluid 5 – 22.41% and Fluid 2 – 22.59%); however, there is a considerable difference in their methane composition [less – (49.43%) in Fluid 5 than in Fluid 2 – (58.07%)] and results indicate much higher cumulative oil production and oil rate for Fluid 5 than for Fluid 2. The trend generally indicates that the smaller the methane composition, the larger the cumulative oil production and oil rate. This clearly demonstrates the importance of the effect of the methane composition on production performance.

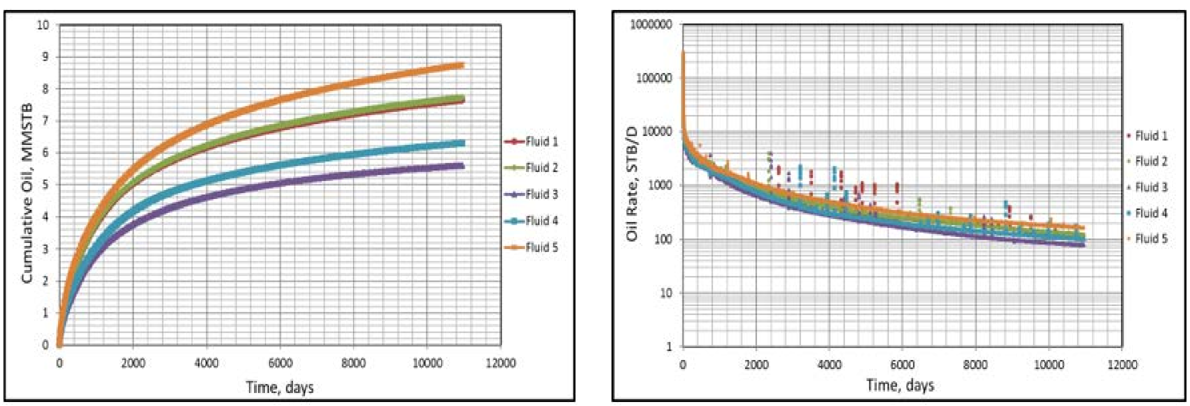

Figure 2-30 Compositional Simulations – Cumulative Oil Production and Oil Rate Comparisons

The heavy components affect cumulative oil production and oil rates because the larger the heavy component composition in the reservoir fluid, the more it contributes to the oil phase production and consequently increases the cumulative oil production and oil rate. However, results of this study indicated that apart from the heavy components, the methane component has a large role to play as well. Note that the spikes in the oil rate curves are probably artifacts due to the numerical solver (in the software) used for the simulation. However, disregarding the spikes, the trends can be clearly observed.

2.5. Two-Phase Black-Oil Simulations – Standing Correlation

Separator tests were done on the fluids and the results of the flash calculations were used as inputs for two-phase black-oil simulations. Two stages of separation were used, with the stock tank as one of the separators. Separator pressure and temperature were 400 psia and 100°F, while the stock tank conditions were 14.7 psia and 60°F respectively. The results of the flash calculations are shown in Table 2-6. This was done to provide a reasonable basis for comparison of the compositional simulation and the black-oil simulation results.

Table 2-6 Flash Calculation Results

	Fluid 1	Fluid 2	Fluid 3	Fluid 4	Fluid 5
Gas-Oil Ratio, SCF/STB	3,024	3,043	4,081	3,967	2,561
API @STC	63.50	63.04	63.52	64.94	65.22
Average Gravity of Total Surface Gas (Air = 1)	0.743	0.753	0.756	0.841	0.851
Oil FVF, RB/STB	3.558	3.551	-	4.806	3.529
Condensate-Gas Ratio, STB/MMSCF	-	-	245.0	-	-
Dry Gas FVF, (ft^3/SCF)	-	-	6.5E-3	-	-
Wet Gas FVF, (ft^3/SCF)	-	-	5.1E-3	-	-
Well Stream Gas Gravity (Air = 1)	-	-	1.246	-	-

First, a case where Standing's correlation was used for bubble point pressure estimates was considered. The simulation results were different from those obtained in the compositional simulations and show no notably observable trends. Figure 2-31 shows the results for cumulative oil production and oil rates. Fluid 1, in this case, has the largest cumulative oil production and oil rate, while Fluid 5 has the smallest. Incorrect bubble point pressures estimated with the correlations might have led to discrepancies in the results.

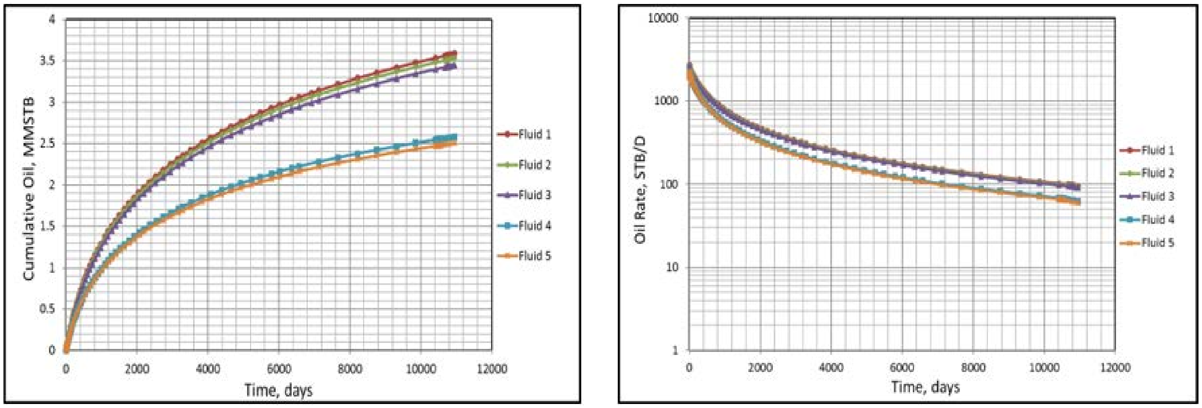

Figure 2-31 Two-Phase Black-Oil Simulations: Standing – Cumulative Oil Production and Oil Rate Comparisons

2.6. Two-Phase Black-Oil Simulations – Vazquez-Beggs Correlation

Black-oil simulations were repeated using the Vazquez-Beggs correlation to estimate bubble point pressure. The Vazquez-Beggs correlation is generally applicable and the data used in the development of the correlation covers a wide range of temperatures, pressures and oil properties. Simulation results show similar trends (Fluid 1 – largest cumulative oil production and oil rate and Fluid 5 – smallest cumulative oil production and oil rate) as in cases where Standing's correlation was used to calculate the bubble-point pressure. However, the values of the cumulative oil production and oil rates were relatively larger in this case. The results for cumulative oil production and oil rates are shown in Figure 2-32.

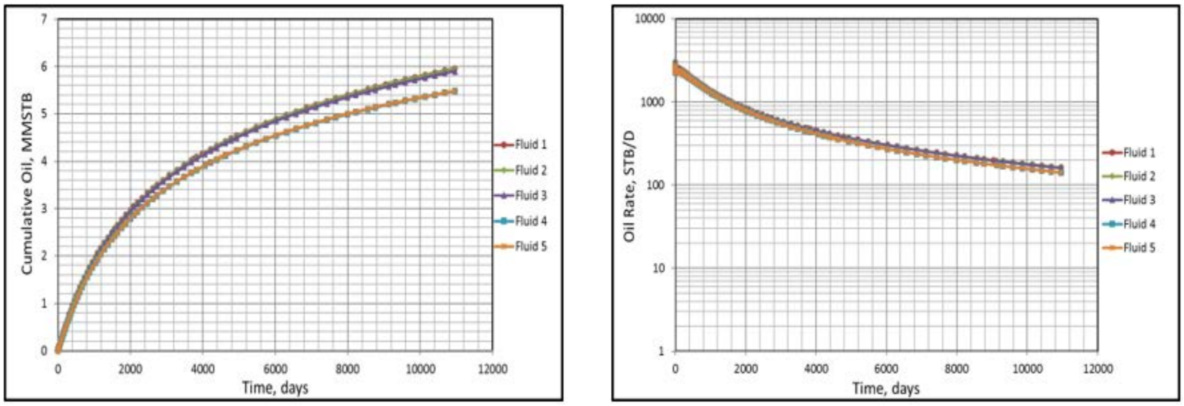

Figure 2-32 Two-Phase Black-Oil Simulations: Vazquez-Beggs – Cumulative Oil Production and Oil Rate Comparisons

The inconsistencies in the results for the black-oil simulations are most likely due to inaccurate bubble point estimates using empirical correlations. In Table 2-7, the approximate bubble point estimates calculated with the Standing and Vazquez-Beggs correlations are shown. Note that the initial reservoir pressure is 5,000 psia. Therefore, the bubble point pressure estimates calculated are higher and lower than the initial reservoir pressure depending on the fluid type considered. Predicted values of bubble point pressure (using correlations) could be in error by 25 percent or more depending on the circumstance (McCain *et al*., 1998). This definitely affects the accuracy of production forecasts.

Table 2-7 Approximate Bubble Point Estimates

	Standing	Vazquez – Beggs
Fluid 1	4,870 psia	4,650 psia
Fluid 2	4,870 psia	4,650 psia
Fluid 3	6,150 psia	5,850 psia
Fluid 4	5,270 psia	5,020 psia
Fluid 5	3,570 psia	3,450 psia

2.7. Compositional Simulations vs. Two-Phase Black-Oil Simulations

Simulation results from the compositional and black-oil simulations were compared for each of the fluid samples under consideration. Results generally show greater cumulative oil production and greater oil rates from compositional simulation than from black-oil simulations. Black-oil simulations using Vazquez-Beggs correlation for calculation of most of the oil PVT properties produced results that are closer to the compositional simulation results than black-oil simulations in which Standing's correlations were used. Therefore, we conclude that proper use of correlations or the development of better correlations for black-oil simulations can lead to results that are close to or almost the same as compositional simulation results. Results of cumulative oil production and oil rate comparisons for each of the fluid samples (apart from Fluid 3) are shown in Figures 2-33 to 2-36.

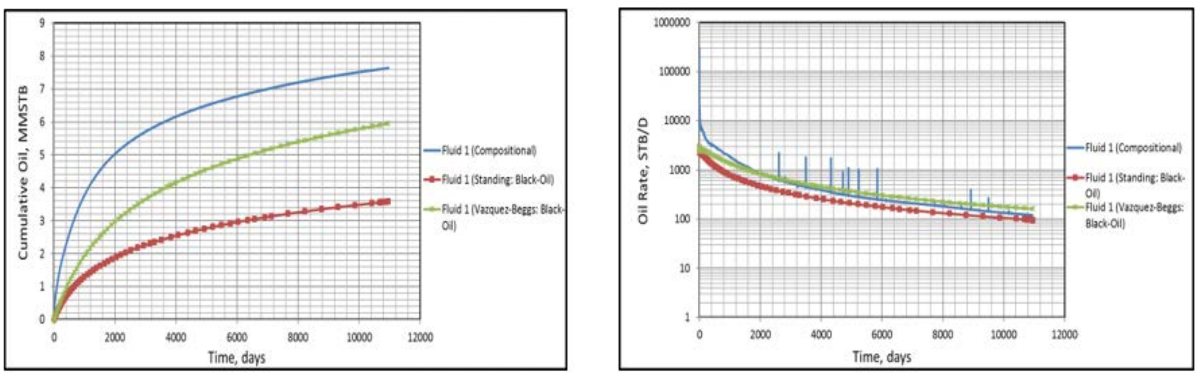

Figure 2-33 Compositional vs. Two-Phase Black-Oil Simulations – Fluid 1 Cumulative Oil Production and Oil Rate Comparisons

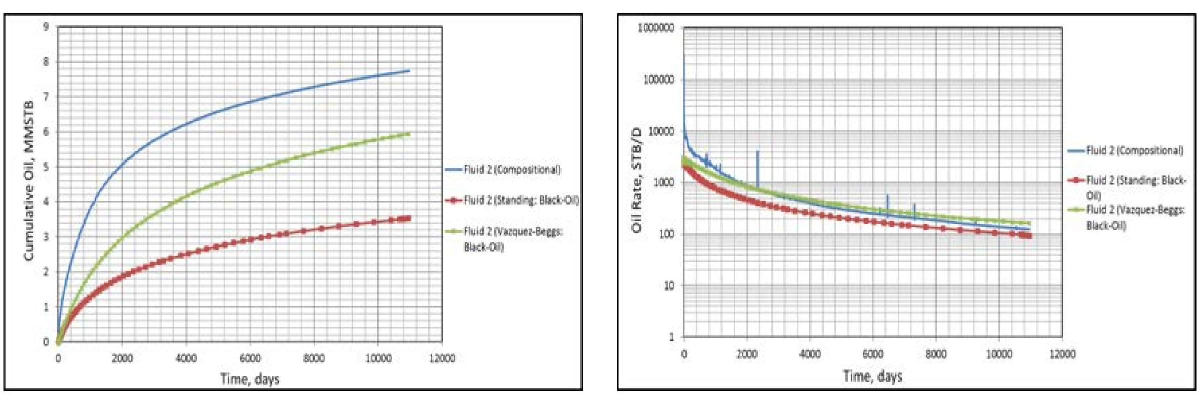

Figure 2-34 Compositional vs. Two-Phase Black-Oil Simulations – Fluid 2 Cumulative Oil Production and Oil Rate Comparisons

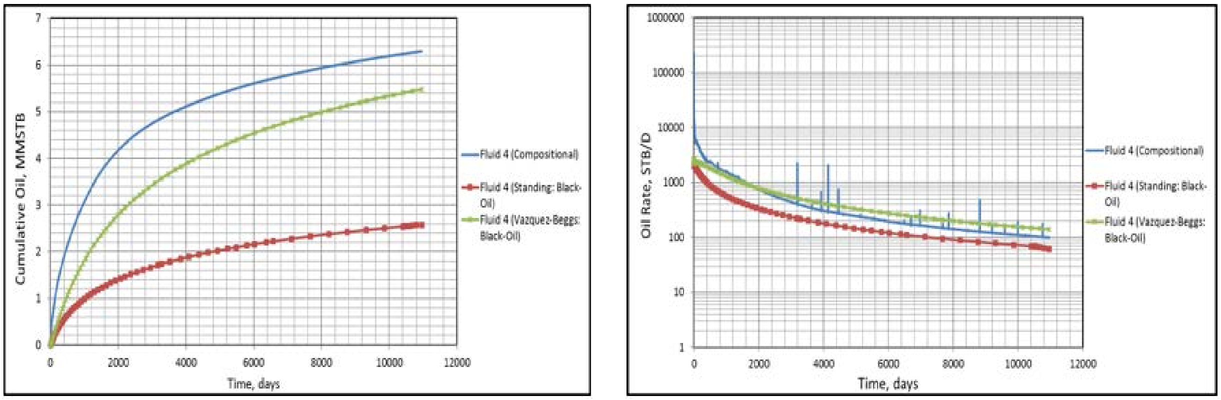

Figure 2-35 Compositional vs. Two-Phase Black-Oil Simulations – Fluid 4 Cumulative Oil Production and Oil Rate Comparisons

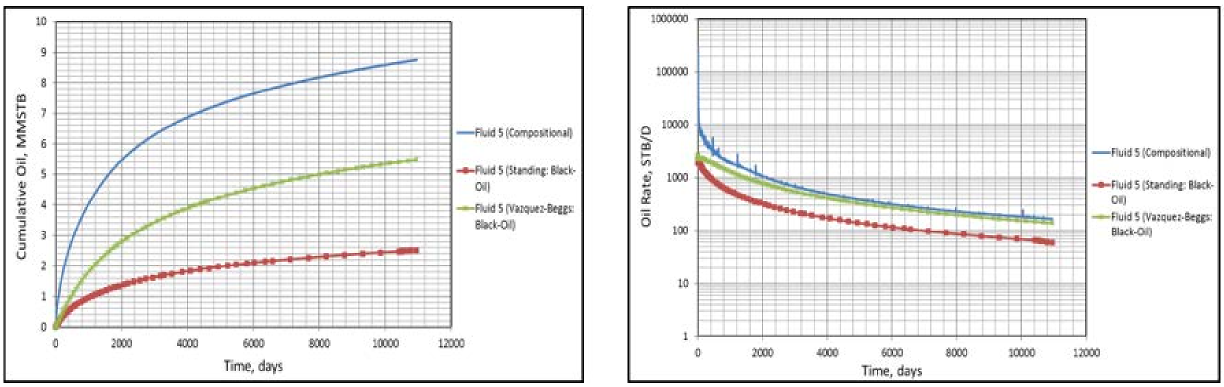

Figure 2-36 Compositional vs. Two-Phase Black-Oil Simulations – Fluid 5 Cumulative Oil Production and Oil Rate Comparisons

2.7.1. Near-Critical Fluid: Fluid 3 Case

Fluid 3 is a near-critical fluid; therefore, an additional simulation was run by modeling it as a gas condensate using modified black-oil (MBO) simulation. MBO simulation of gas condensates takes into consideration the condensate-gas ratio, R_v, which is the amount of vaporized oil in gas.

When Fluid 3 was modeled as a gas condensate (using MBO), the result was similar to the original black-oil simulation case (when modeled as a bubble point fluid using Standing's correlation). When modeled as a bubble point fluid using the Vazquez-Beggs correlation, the cumulative oil production is a little closer to the compositional simulation case except toward the end of the production period. This highlights the difficulties inherent in modeling near-critical fluids, especially when using black-oil simulators with dependence on empirical correlations. Figure 2-37 illustrates the results for the cumulative oil production and oil rates.

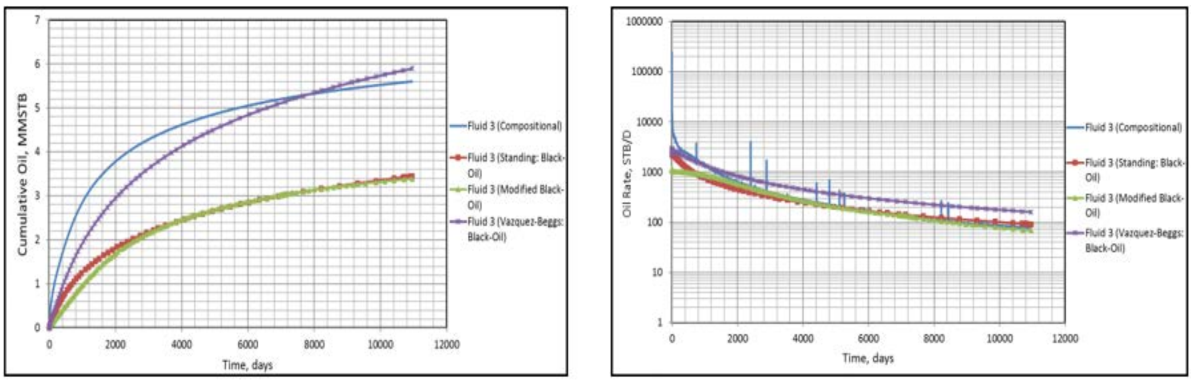

Figure 2-37 Compositional vs. Two-Phase Black-Oil Simulations – Fluid 3 Cumulative Oil Production and Oil Rate Comparisons

2.8. Recombination of Fluids

To quantify the effects of recombination/sampling errors on production forecasting, we recombined the separator liquid and vapor compositions of the Fluids (1 – 5) at the separator (i.e., with the aid of gas-oil ratio at the separator with pressure of 400 psia and temperature of 100°F) as a base case. Field evidence suggests that sampled GORs can be off by as much as 20%; therefore, recombination ratios (GOR at the separator) were varied by +/-20%. Compositional simulations were then done for each of the cases. The recombined fluid compositions are shown in Tables 2-8 and 2-9.

Table 2-8 Recombined Fluid Compositions

	Fluid 1A (GOR = 2268 scf/bbl)	Fluid 1B (GOR = 1815 scf/bbl)	Fluid 1C (GOR = 2722 scf/bbl)	Fluid 2A (GOR = 2302 scf/bbl)	Fluid 2B (GOR = 1841 scf/bbl)	Fluid 2C (GOR = 2762 scf/bbl)	Fluid 3A (GOR = 3102 scf/bbl)	Fluid 3B (GOR = 2482 scf/bbl)	Fluid 3C (GOR = 3722 scf/bbl)
CH_4	56.72	53.05	59.54	55.79	52.21	58.53	59.25	56.06	61.64
C_2H_6	9.284	9.033	9.478	9.109	8.863	9.298	9.683	9.454	9.854
C_3H_8	4.755	4.892	4.650	4.847	4.986	4.741	5.246	5.388	5.140
$I\text{-}C_4H_{10}$	0.976	1.047	0.922	1.037	1.112	0.980	1.113	1.193	1.053
$N\text{-}C_4H_{10}$	2.195	2.388	2.048	1.711	1.862	1.596	1.848	2.012	1.726
$I\text{-}C_5H_{12}$	0.767	0.860	0.699	0.751	0.841	0.683	0.801	0.902	0.726
$N\text{-}C_5H_{12}$	1.142	1.284	1.033	0.799	0.898	0.723	0.858	0.972	0.774
C_6H_{14}	1.711	1.950	1.528	1.112	1.268	0.992	1.179	1.358	1.045
C_{7+}	21.22	24.33	18.83	22.04	25.30	19.55	17.07	19.84	15.00
N_2	0.149	0.138	0.157	0.110	0.102	0.116	0.119	0.112	0.124
CO_2	1.080	1.027	1.121	2.699	2.568	2.800	2.834	2.716	2.923

Table 2-9 Recombined Fluid Compositions (Contd.)

	Fluid 4A (GOR = 2527.01 scf/bbl)	Fluid 4B (GOR = 2021.608 scf/bbl)	Fluid 4C (GOR = 3032.412 scf/bbl)	Fluid 5A (GOR = 1581.90 scf/bbl)	Fluid 5B (GOR = 1265.52 scf/bbl)	Fluid 5C (GOR = 1898.28 scf/bbl)
CH_4	50.81	47.66	53.22	48.14	44.39	51.13
C_2H_6	13.57	13.22	13.84	8.565	8.310	8.768
C_3H_8	9.987	10.27	9.769	8.859	9.123	8.650
$I\text{-}C_4H_{10}$	-	-	-	2.404	2.568	2.273
$N\text{-}C_4H_{10}$	4.710	5.120	4.397	3.689	3.986	3.452
$I\text{-}C_5H_{12}$	-	-	-	1.784	1.968	1.637
$N\text{-}C_5H_{12}$	2.043	2.298	1.848	1.762	1.952	1.610
C_6H_{14}	1.448	1.653	1.292	2.259	2.527	2.045
C_{7+}	16.20	18.61	14.35	21.75	24.45	19.60
N_2	0.218	0.203	0.230	0.611	0.556	0.654
CO_2	1.012	0.964	1.048	0.182	0.172	0.189

Figures 2-38 to 2-40 and Tables 2-10 to 2-14 are graphical representations of the analyses as well as the errors and percentage errors in cumulative oil production (after 30 years) for each of the cases compared to the basecases. Additional columns containing cumulative gas production (after 30 years) and corresponding errors and percentage errors were also included in each of the tables. From the results, we observe that the percentage error in cumulative oil production forecasts due to sampling errors can be as high as 21%. The smallest error was around 11%. For cumulative gas production, the percentage error was as large as about 16% and the smallest error was about 4%. These analyses have helped to quantify the effects that sampling or recombination errors can have on oil recovery estimates as well as gas production forecasts. It is also generally observed that recombined fluids from separator GOR with -20% error (compared to the separator GOR of the basecases) have higher cumulative oil production in comparison to the basecases and vice versa (lower) for the recombined fluids from separator GOR errors of +20% (compared to the GOR of the base cases). The inverse is the case for cumulative gas production. This pattern conforms well to the compositional simulation fluid analyses done earlier.

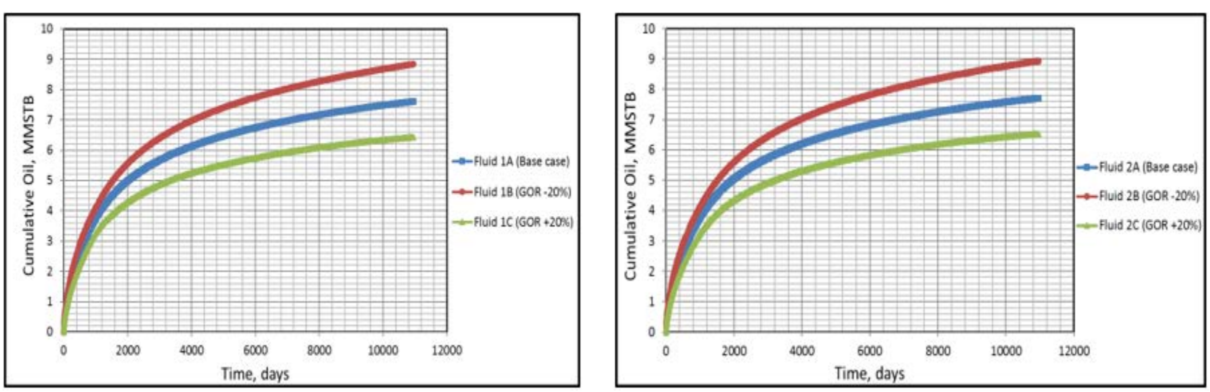

Figure 2-38 Recombined Fluids 1 and 2 – Cumulative Oil Production Comparisons

Table 2-10 Cumulative Oil, Gas and Errors – Recombined Fluids 1

	Recombination ratio, scf/bbl	Cumulative Oil (after 30 yrs), MMSTB	Error (absolute value), MMSTB	Percentage Error, %	Cumulative Gas (after 30 yrs), bscf	Error (absolute value), bscf	Percentage Error, %
Fluid 1A (Base case)	2268	7.605	0	0	58.01	0	0
Fluid 1B	1815	8.836	1.231	+13.93	49.92	8.091	-16.21
Fluid 1C	2722	6.428	1.177	-18.31	63.91	5.897	+9.23

Table 2-11 Cumulative Oil, Gas and Errors – Recombined Fluids 2

	Recombination ratio, scf/bbl	Cumulative Oil (after 30 yrs), MMSTB	Error (absolute value), MMSTB	Percentage Error, %	Cumulative Gas (after 30 yrs), bscf	Error (absolute value), bscf	Percentage Error, %
Fluid 2A (Base case)	2302	7.703	0	0	58.00	0	0
Fluid 2B	1841	8.930	1.227	+13.74	49.88	8.113	-16.26
Fluid 2C	2762	6.531	1.172	-17.95	63.87	5.868	+9.19

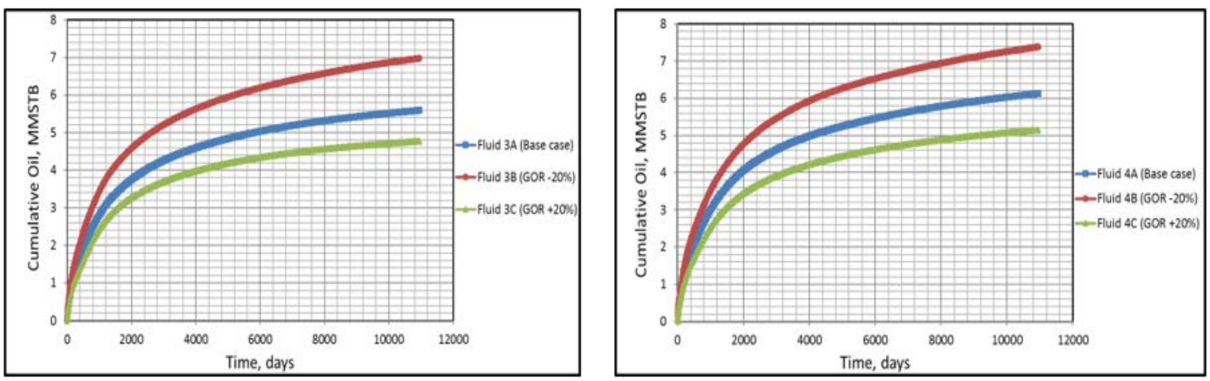

Figure 2-39 Recombined Fluids 3 and 4 – Cumulative Oil Production Comparisons

Table 2-12 Cumulative Oil, Gas and Errors – Recombined Fluids 3

	Recombination ratio, scf/bbl	Cumulative Oil (after 30 yrs), MMSTB	Error (absolute value), MMSTB	Percentage Error, %	Cumulative Gas (after 30 yrs), bscf	Error (absolute value), bscf	Percentage Error, %
Fluid 3A (Base case)	3102	5.594	0	0	67.89	0	0
Fluid 3B	2482	6.978	1.384	+19.83	60.96	6.932	-11.37
Fluid 3C	3722	4.774	0.820	-17.18	73.53	5.644	+7.68

Table 2-13 Cumulative Oil, Gas and Errors – Recombined Fluids 4

	Recombination ratio, scf/bbl	Cumulative Oil (after 30 yrs), MMSTB	Error (absolute value), MMSTB	Percentage Error, %	Cumulative Gas (after 30 yrs), bscf	Error (absolute value), bscf	Percentage Error, %
Fluid 4A (Base case)	2527	6.129	0	0	64.09	0	0
Fluid 4B	2022	7.385	1.256	+17.01	56.84	7.258	-12.78
Fluid 4C	3032	5.148	0.981	-19.06	69.71	5.618	+8.06

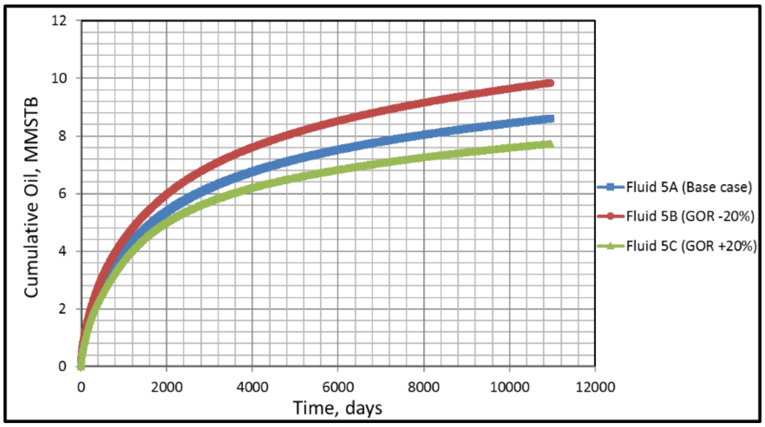

Figure 2-40 Recombined Fluids 5 – Cumulative Oil Production Comparisons

Table 2-14 Cumulative Oil, Gas and Errors – Recombined Fluids 5

	Recombination ratio, scf/bbl	Cumulative Oil (after 30 yrs), MMSTB	Error (absolute value), MMSTB	Percentage Error, %	Cumulative Gas (after 30 yrs), bscf	Error (absolute value), bscf	Percentage Error, %
Fluid 5A (Base case)	1582	8.601	0	0	48.02	0	0
Fluid 5B	1267	9.842	1.241	+12.61	41.35	6.664	-16.12
Fluid 5C	1898	7.727	0.874	-11.31	54.60	6.581	+12.05

2.9. Inferences

1. Sensitivity studies done with the aid of single-phase and two-phase black-oil simulators, showed that fracture spacing, fracture half-length, oil API gravity and

critical gas saturation are important parameters that affect oil production and oil rates in shale volatile oil reservoirs;

2. From the analyses of the oil API gravity cases, it is obvious that imperfect fluid samples (errors in calculation of fluid properties) can have significant impact on oil recovery estimates;
3. The gas phase in two-phase flow has a considerable effect on oil production in shale volatile oil reservoirs;
4. Results from black-oil simulations are markedly different from compositional simulations. Compositional simulations are more accurate than two-phase black-oil simulations, while two-phase black-oil simulations are more accurate than single-phase black-oil simulations;
5. Volatile oil production cannot be properly modeled using black-oil simulations (especially when PVT properties are estimated with empirical correlations);
6. Inaccurate bubble point pressures and PVT properties estimated using correlations can have huge impacts oil production forecasts, whereas identification and use of more appropriate correlations for PVT property estimates can lead to production estimates that can be almost the same as those obtained from compositional simulations;
7. Reservoir engineering calculations for volatile oils should treat the reservoir fluid as a multi-component mixture, i.e., compositional simulation is necessary for thorough analysis of volatile oil production, especially in shale volatile oil reservoirs;

8. Light components, particularly methane composition in reservoir fluids, can have a substantial effect on shale volatile oil reservoir production performance;
9. Proper identification and classification of fluid samples prior to modeling and simulation is important (especially for black-oil simulations);
10. Near-critical fluids are very difficult to model;
11. Sampling or recombination errors can have significant impact on oil and gas recovery estimates as well as on major decisions affecting reservoir management and economics.

Chapter 3 – Forecasting Production of Shale Volatile Oil Reservoirs Using Empirical Models.

Because of its relative simplicity, an empirical method of forecasting production such as the Decline Curve Analysis (DCA), is an appealing alternative compared to reservoir simulation and analytical techniques. However, traditional DCA models like Arps, Stretched Exponential Production Decline (SEPD), Duong and YM-SEPD have not been completely adequate for reliably forecasting production from unconventional reservoirs. Multiphase flow effects resulting in lengthy transition periods between transient linear flow and boundary dominated flow (BDF) in liquid rich shale reservoirs have further complicated this quest. Therefore, further research efforts led to the use of combination (hybrid) models. For example, the use of a model like YM-SEPD for transient flow combined with Arps' hyperbolic model for the BDF regime is a hybrid decline model. In this chapter, DCA (traditional and hybrid) methods were compared and some cogent factors affecting empirical methods of forecasting were highlighted. Also, solution gas production was forecasted with a simple procedure similar to one published recently in the literature.

3.1. Decline Curve Analysis (DCA) Models

Some of the available DCA models for production forecasting in shale reservoirs applied in this study are briefly described here.

3.1.1. Arps' Decline Model

Arps (1945) presented a decline model that has been the basic foundation for DCA. The Arps hyperbolic decline model is valid assuming boundary dominated flow (BDF), i.e. flow affected by the reservoir boundaries. Many unconventional reservoirs reach BDF regimes only after many years, thereby making the use of Arps' hyperbolic decline models generally inappropriate for reserves evaluation in these instances.

For the hyperbolic decline model, the decline rate, D varies and the b value (decline exponent) is more than 0 and less than 1 ($0<b<1$). Production rate in this case is expressed with the following equation

$$q = \frac{q_i}{(1 + bD_i t)^{\frac{1}{b}}} , \tag{1}$$

where q_i is the initial production rate and D_i is the initial decline rate.

The exponential and harmonic decline models are special cases. For exponential decline, the rate of decline, D is constant and the b value is 0. Here, the production rate is expressed as

$$q = q_i exp(-D_i t) . \tag{2}$$

In the case of harmonic decline, the rate of decline, D also varies but is directly proportional to the production rate, and the b value is 1. Production rate in this instance is

$$q = \frac{q_i}{(1 + bD_i t)} . \tag{3}$$

In unconventional reservoirs, the use of b values (decline exponents) greater than 1 may be encountered. Decline exponents greater than 1 causes forecasted cumulative production to increase toward infinity, (i.e., they are unbounded), which is not possible in reality. However, since unconventional reservoirs like shale have very low permeabilities and exhibit lengthy transient flow, b values greater than 1 provide "best-fits" to production data in certain situations.

3.1.2. Duong's Model

Duong (2011) proposed a model assuming long-term linear (or bilinear) flow. The assumption of linear or near-linear flow for the entire well life in this model leads to overestimation of reserves in shale plays. The Duong equations are:

$$q = q_1 t(a,m) \text{ and} \tag{4}$$

$$t(a,m) = t^{-m} e^{\frac{a}{1-m}(t^{1-m}-1)}, \tag{5}$$

where a and m are the intercept and slope of the log-log plot of inverse material balance time (MBT), q/N_p versus time, t,

$$\frac{q}{N_p} = a t^{-m}. \tag{6}$$

From equation (6), the slope is negative but m is always positive. For shale reservoirs, m values are mostly greater than 1. In equation (4), q_1 is the flow rate at time, t equal to 1.

3.1.3. YM-SEPD Model

Yu and Miocevic (2013) introduced a modified form of the SEPD model proposed by Valko and Lee (2010). A specialized log-log plot of ln(qo/q) versus time (Yu plot) is used to define the parameters n and τ for the SEPD model. For this model to be applicable, one must ensure that points on the Yu plot used to generate n and τ, are on a straight (or nearly straight) line. In most instances, points on the Yu plot become straight (or nearly straight) only after about two or more years of historical production data. Therefore, with little historical production data of a year or less, this model can be quite inappropriate. In such cases, Yu suggests that we can obtain more accurate forecasts if we use the Duong model forecasts to the suggested minimum of 3 years of history. This model considerably improves forecasts in shale reservoirs. However, short production histories, an uncertain time-zero rate and the nature of production data can hinder the effective application of this model. The parameter n is the slope on the Yu plot while τ is calculated from the intercept of the plot as

$$\tau = exp[\frac{-ln(intercept)}{n}]\,. \tag{7}$$

3.2. Reservoir Model Description

A horizontal well, with 20 hydraulic fractures spaced 250 ft apart was modeled. The horizontal well length is 5000 ft. The simulation model is a single porosity system. The fractures are all infinitely conductive with half lengths of 150 ft. Fracture width of 2 ft was used to make simulation easier. Fracture permeability was correspondingly reduced to keep the product of width and permeability (of fractures) at a proper level. A commercial compositional simulator was used to simulate production with four different reservoir fluids. The well produced for 30 years at a minimum bottomhole pressure constraint of 1000 psia. Logarithmically-spaced local grid refinement (LS-LGR) was used to model pressure drop and fluid flow as accurately as possible. Figure 3-1 shows an illustrative representation of the reservoir model. Tables 3-1 and 3-2 show the reservoir data and the reservoir fluid compositions used.

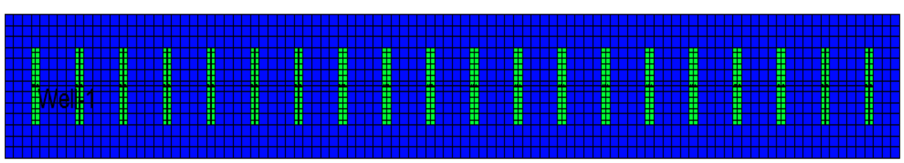

Figure 3-1 Multi-Fractured Horizontal Well (MFHW) Model

Table 3-1 Reservoir Data for the MFHW Model

Permeability	0.001 md
Porosity	0.06
Reservoir Temperature	250°F
Initial Reservoir Pressure	5,000 psia
Depth to top of formation	10,000 ft
Reservoir Thickness	250 ft
Corey Relative Permeability Exponent	2.5
Critical gas saturation, S_{gc}	0.05
Residual saturation of oil (gas/oil displacement), S_{org}	0.2

Table 3-2 Fluid Compositions

	Fluid 1	Fluid 2	Fluid 3	Fluid 4
Components	Composition (%)	Composition (%)	Composition (%)	Composition (%)
CH_4	58.07	61.82	53.47	49.43
C_2H_6	7.43	7.91	11.46	7.28
C_3H_8	4.16	4.42	8.79	8.02
$I\text{-}C_4H_{10}$	0.96	1.02	-	2.31
$N\text{-}C_4H_{10}$	1.63	1.74	4.56	3.61
$I\text{-}C_5H_{12}$	0.75	0.80	-	1.80
$N\text{-}C_5H_{12}$	0.80	0.86	2.09	1.79
C_6H_{14}	1.14	1.21	1.51	2.32
C_{7+}	22.59	17.59	16.92	22.41
CO_2	2.32	2.47	0.90	0.16
N_2	0.15	0.16	0.30	0.87

3.3. Diagnostic Plots

Before applying DCA techniques for production forecasting, diagnostic plots are essential for proper flow regime identification. This is important as use of decline models without appropriate flow regime identification may lead to highly inaccurate forecasts.

Log-log rate-time and log-log rate-MBT (Material Balance Time) plots are the most commonly used diagnostic plots for flow regime identification. Transient linear flow can be identified with a slope of -1/2, bilinear flow – slope of -1/4 on both diagnostic plots and boundary dominated flow (BDF) with a slope of -1 on the log-log rate-MBT plot. On the rate-time plot, data in BDF will eventually have a slope more negative than -1, as on the familiar Fetkovich type curve. However, the time at which the slope reaches a value of -1 appears to coincide with the actual start of BDF. This will be demonstrated in the next subsection.

3.3.1. Flow Regime Identification – Fluids 1 to 4

Each decline model is valid only for the flow regime for which it was derived (Khanal *et al*., 2015). This further highlights the importance of flow regime identification before application of DCA methods for forecasting production. Hence, prior to applying DCA techniques to the simulated production data, log-log rate-time and log-log rate-MBT diagnostic plots for each of the fluid samples under consideration were plotted.

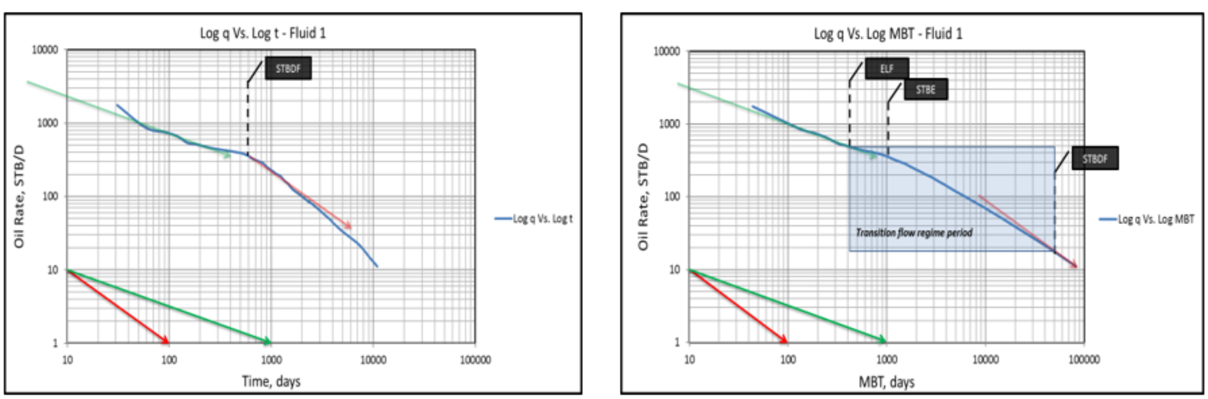

Figure 3-2 Log q vs. Log t and Log q vs. Log MBT – Fluid 1

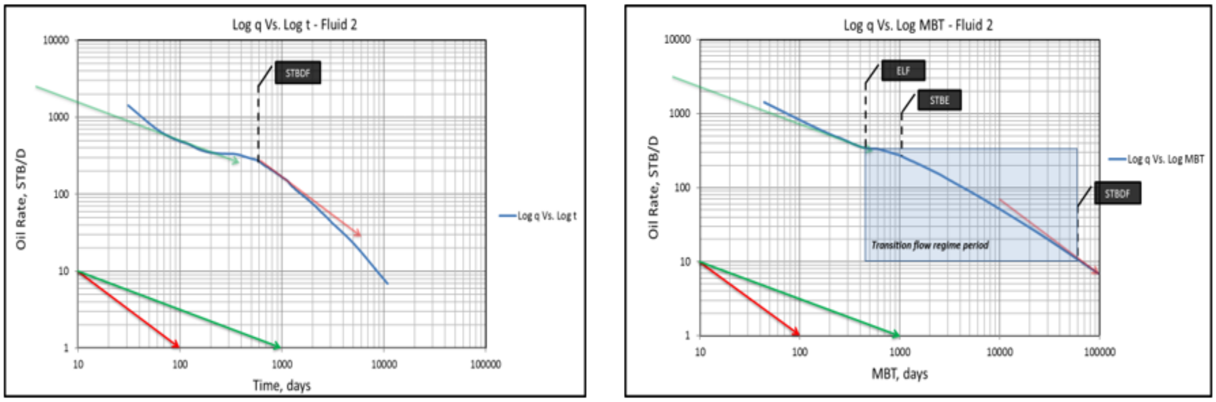

Figure 3-3 Log q vs. Log t and Log q vs. Log MBT – Fluid 2

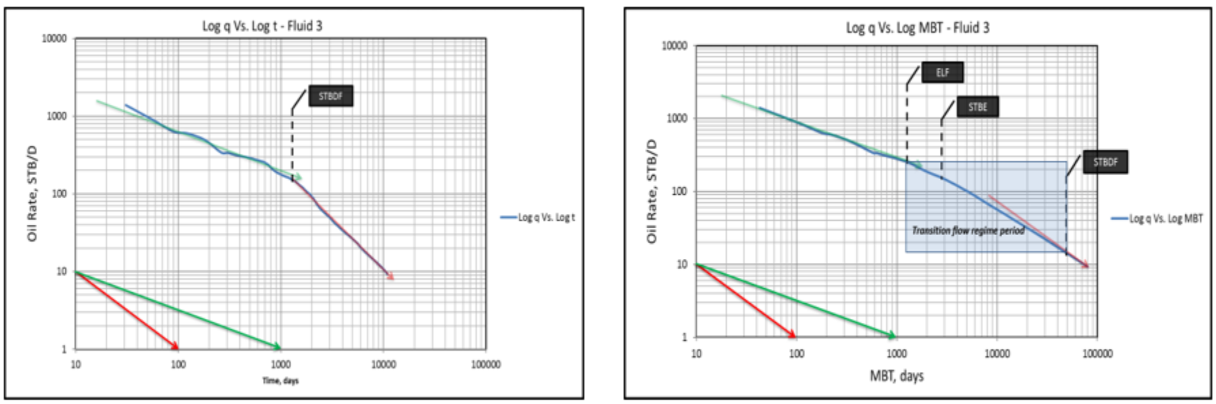

Figure 3-4 Log q vs. Log t and Log q vs. Log MBT – Fluid 3

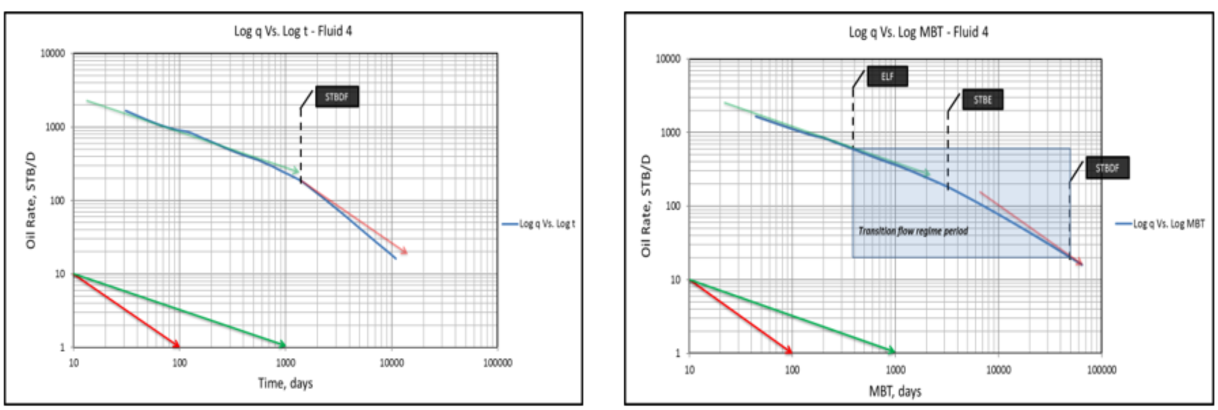

Figure 3-5 Log q vs. Log t and Log q vs. Log MBT – Fluid 4

Diagnostic plots for each fluid sample are shown in Figures 3-2 to 3-5. Prolonged transition periods between transient linear flow and BDF, as indicated in these figures, are common for shale volatile oil reservoirs. The impact of multi-phase flow as the reservoir pressure drops below the bubble point is presumed to be one of the major reasons. This transition period is much shorter in single-phase shale reservoirs as shown in Figure 3-6. The ultra-low permeability of shale reservoirs may also be a contributing factor.

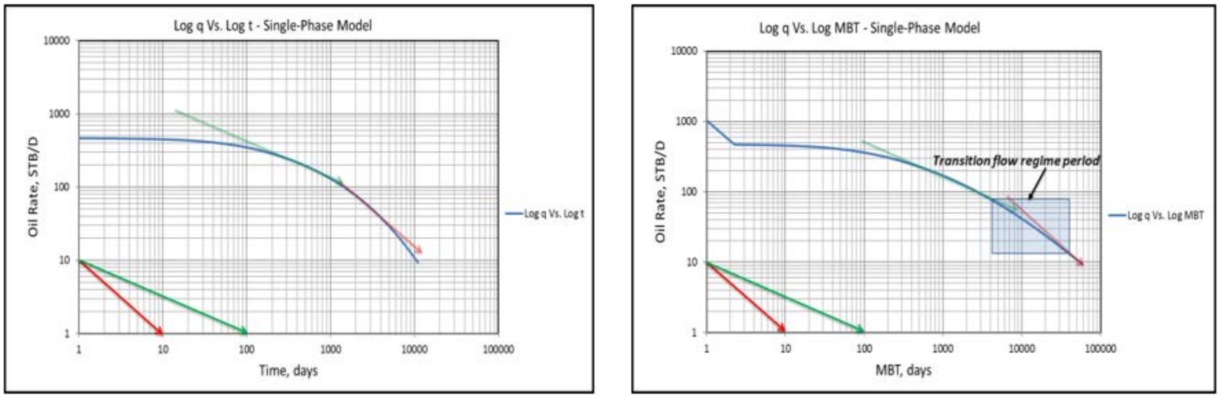

Figure 3-6 Log q vs. Log t and Log q vs. Log MBT – Single-Phase Model

On the log-log rate-time diagnostic plots, we observe that the slopes after the perceived "start of boundary dominated flow" (STBDF) steadily decrease to values more negative than -1. Despite this, we assume that boundary dominated flow regime covers the range from the STBDF till the end of the production period. The STBDF on the log-log rate-time diagnostic plot corresponds with what we call the "start of boundary effects" (STBE) on the log-log rate-MBT diagnostic plot. On the log-log rate-MBT diagnostic plots, the "end of linear flow" (ELF), the "start of boundary effect" (STBE) and the "start of boundary dominated flow" (STBDF) are clearly shown. The regions between the ELF and STBDF are the "transition flow regime periods". The "start of boundary effect" (STBE) is a point on the log-log rate-MBT diagnostic plot where there is a slightly observable change of slope which matches with the STBDF on the log-log rate-time plot. At this point, we assume that the reservoir boundaries have started to affect flow rate.

3.4. Point (Time) of Switch

The application of hybrid (combination) models require a switch from one DCA model to another, depending on the flow regimes identified on the diagnostic plots. Nevertheless, the critical question is, “what is the appropriate point (time) to switch decline models?” Long duration of transition flow between the end of linear flow and the start of boundary dominated flow, as seen on the diagnostic plot, further complicates possible answers to this question. In order to possibly answer this question, the inverse MBT vs. time plot from the Duong model and the Yu plot from the YM-SEPD model were examined. It is observed that there is an evident change of slope at approximately the same point on these plots. The point of this change aligns with the “start of boundary dominated flow” (STBDF) on the log-log rate-time plots and the “start of boundary effects” (STBE) on the log-log rate-MBT plots. This may be the “true” start of boundary dominated flow, thereby providing us with a possible single point to switch to Arps’ model when applying hybrid models for forecasting production. Figures 3-7 to 3-10 show the inverse MBT vs. time plot combined with the Yu plot for each fluid sample. The black dotted line indicates the point of slope change on both plots. The two plots appear almost as inverse replicas of each other.

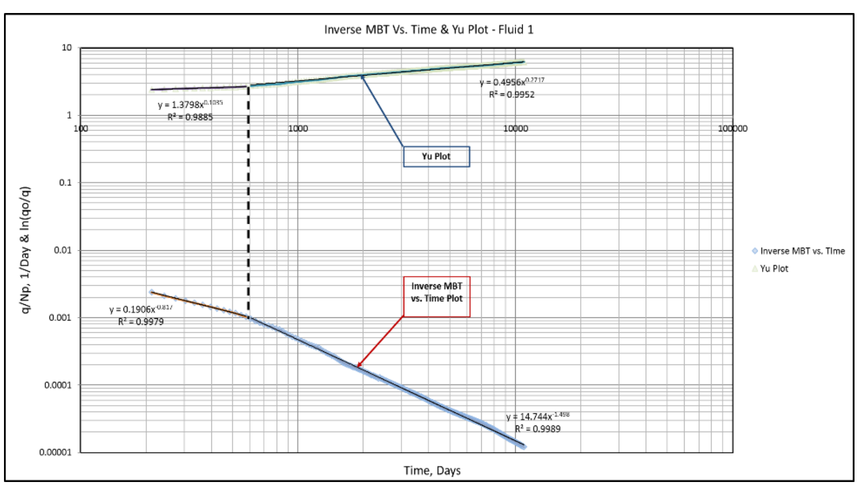

Figure 3-7 Inverse MBT vs. Time and Yu Plot – Fluid 1

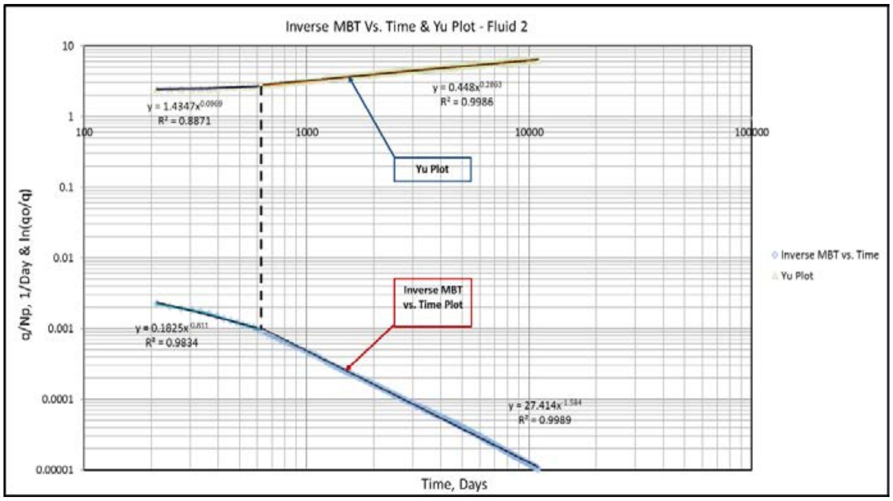

Figure 3-8 Inverse MBT vs. Time and Yu Plot – Fluid 2

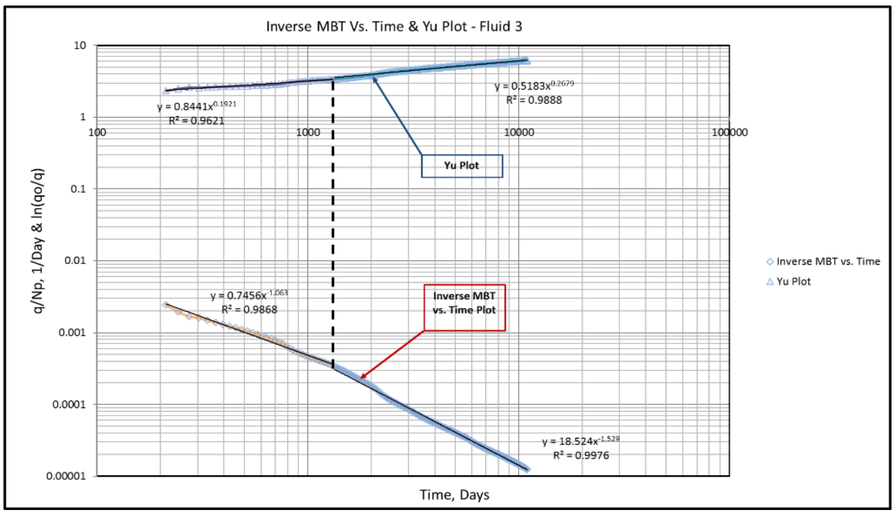

Figure 3-9 Inverse MBT vs. Time and Yu Plot – Fluid 3

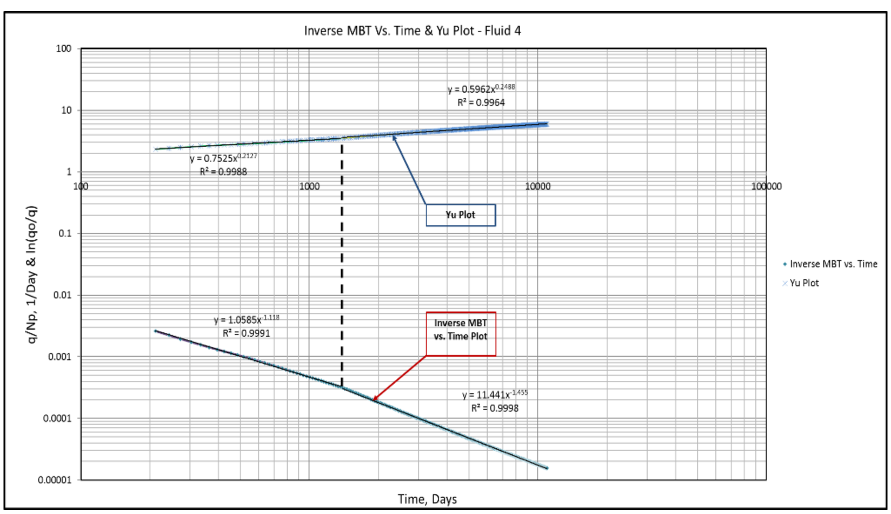

Figure 3-10 Inverse MBT vs. Time and Yu Plot – Fluid 4

In this study, 3 different hybrid models were considered:

a. Duong and YM-SEPD models for transient flow coupled with switch to Arps' model at the end of linear flow (ELF), as indicated on the log-log rate-MBT plot. We refer to these models as Duong + Arps(1) and YM-SEPD + Arps(1) models respectively. "Arps(1)" in this work refers to switch to Arps' model at ELF with an appropriate b value;
b. Duong and YM-SEPD models for transient flow coupled with switch to Arps' models both at the end of linear flow (ELF) and at the start of boundary dominated flow (STBDF), as indicated on the log-log rate-MBT plot. We refer to these models as Duong + Arps(1) + Arps(2) and YM-SEPD + Arps(1) + Arps(2) models respectively. "Arps(1)" and "Arps(2)" refer to a switch to Arps' model at ELF and STBDF, both with suitable b values;
c. Duong and YM-SEPD models for transient flow coupled with switch to Arps' model (with an appropriate b value) at the start of boundary effects (STBE), as indicated on the log-log rate-MBT plot. It should be recalled that this point corresponds to the point of slope change on the 'inverse MBT vs. time" and Yu plots, as well as the STBDF on the log-log rate-time plot. We refer to these models as simply Duong + Arps and YM-SEPD + Arps models respectively.

3.4.1. Sensitivity of Decline Exponents (b values) to Time of Switch

When switching to Arps' model (in this case), it is important to use suitable decline exponents (b values) for proper curve fitting and forecasting production as accurately as possible. Decline exponents (b values) are quite sensitive to times of switch. The later the time of switch, the less sensitive b values are, i.e., the change in b values will cause minimal changes in oil rates. Conversely, the earlier the time of switch, the more sensitive b values are, i.e., the change in b values will cause significant changes in oil rates. These results are graphically shown in Figures 3-11 to 3-13. These outcomes can have a significant effect on production forecasting when using hybrid DCA models. For example, a very late time of switch (as may be the case in this study – at the STBDF of the log-log rate-MBT plots) may make curve fitting difficult, as changes in b values will have little or no effect on changing oil rates. This can lead to problems of discontinuity on the oil rate vs. time semi-log plots, consequently leading to inaccurate production forecasts. This issue can be controlled by switching to Arps' models twice (as we suggested), first at the end of linear flow (ELF) then at the STBDF identified using the log-log rate-MBT diagnostic plots.

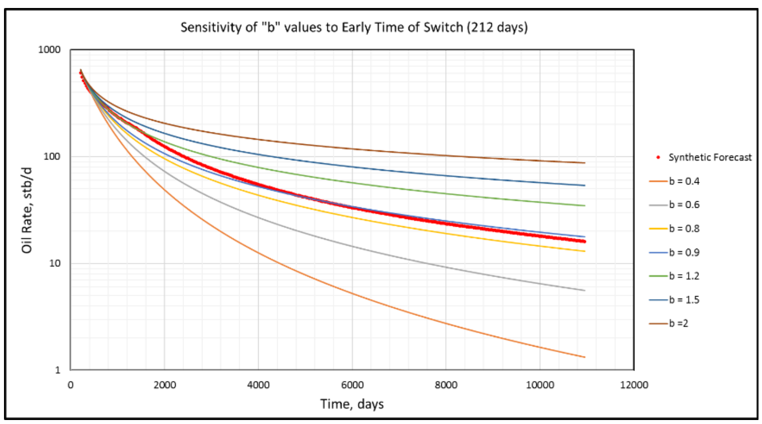

Figure 3-11 Sensitivity of b values to Time of Switch (212 days)

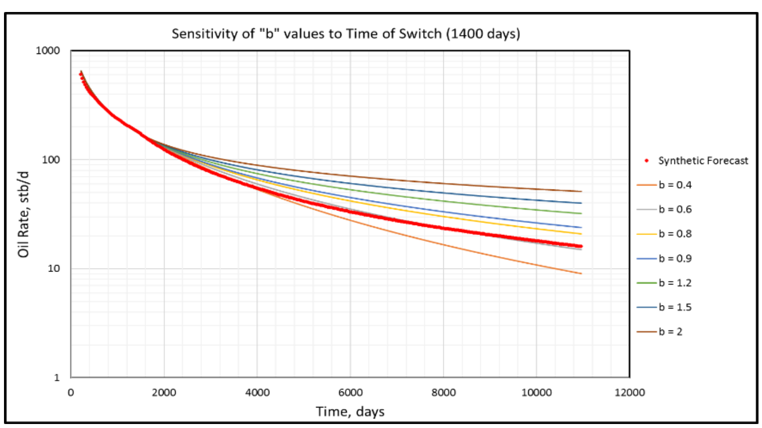

Figure 3-12 Sensitivity of b values to Time of Switch (1400 days)

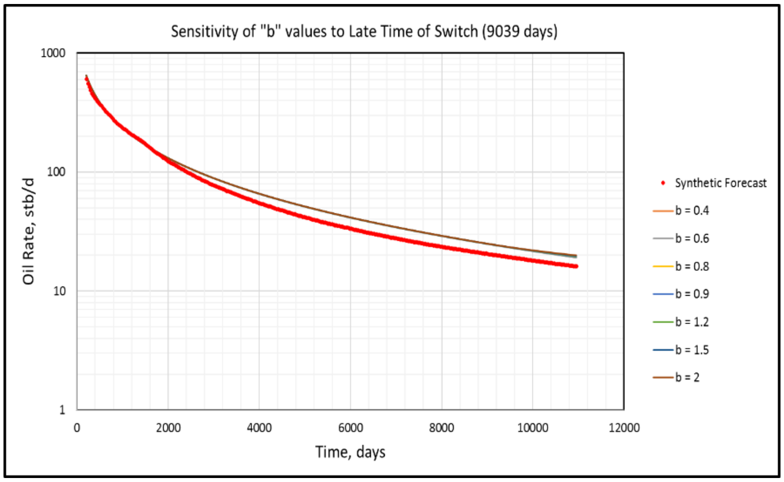

Figure 3-13 Sensitivity of b values to Time of Switch (9039 days)

3.5. Solution Gas Production Forecasting

Unavailability of data and/or incorrect gas measurements can affect the gas-oil ratio (GOR) histories of wells (Yu, 2014). This therefore, makes the task of forecasting solution gas production from shale oil reservoirs difficult. Yu (2014) presented a simple methodology for forecasting solution gas production based on predicted oil production. He suggested a specialized plot based on a linear relationship between the logarithm of a well's cumulative gas-oil ratio (GOR_{cum}) and cumulative oil production (N_p). This relationship was represented with the following expression:

$$(GOR)_{cum} = A_1 exp(N_p B_1)\,, \tag{8}$$

where $(GOR)_{cum} = G_p/N_p$; G_p is the cumulative solution gas production, A_1 is the intercept and B_1 is the slope. Yu (2014) tested his methodology on tight black oil and volatile oil reservoirs. For this study, we were interested in determining how well this methodology works with shale reservoirs containing moderate to highly volatile oil reservoir fluid samples. The procedure used for solution gas forecasting is summarized as follows:

1. Identify the inflection point(s) on the GOR vs. time plot. This point signifies the approximate start of two-phase flow on the GOR vs. time plot (Yu, 2014);
2. Plot a log-log plot of $(GOR)_{cum}$ and N_p from available simulated data;
3. Starting from the inflection point, select data points on the log-log $(GOR)_{cum}$ vs. N_p plot to be used for regression analysis;
4. Solve $(GOR)_{cum} = A_1 {N_p}^{B_1}$ – equation (*) by least squares regression to estimate parameters A_1 and B_1;
5. Obtain cumulative oil production, N_p, for 30 years from simulated data;
6. Forecast cumulative GOR with equation (*);
7. Finally, calculate future solution gas production using the known cumulative oil production;
8. For actual field cases, the analyst can use traditional or hybrid DCA models to forecast oil production from available historical data.

3.6. Examples – Simulated Data

A compositional reservoir simulator was used to simulate 30 years of production with four different reservoir fluids. We then tested different simple and hybrid DCA models on simulated data, after identifying flow regimes on the diagnostic plots for each fluid sample. 0.5 to 3 years of simulated production history were used to estimate model parameters for predicting future production. Production forecasts obtained from a variety of simple and hybrid DCA models were then compared to simulated production data. Further, we attempted to forecast solution gas production for each fluid sample with the procedure outlined above.

Data from the 2nd to 3rd year on the specialized Yu plot (as in all cases in this work) were used to generate model parameters for the YM-SEPD model. For production histories of 2 years and less, Duong's model was used to forecast the 2nd and 3rd year pseudohistorical data, as suggested by Yu and Miocevic (2013) based on simulated production histories of varying time span (from 0.5yr – 2 yrs). The YM-SEPD hybrid models considered here are YM-SEPD + Arps, YM-SEPD + Arps(1) and YM-SEPD + Arps(1) + Arps(2). We also examined the Duong model and its hybrid variants – Duong + Arps, Duong + Arps(1) and Duong +Arps(1) + Arps(2) respectively.

3.6.1. Fluid 1

Fluid 1 is a moderately volatile oil with an initial GOR of 3043 scf/bbl. Results of production forecasts for this case are the following:

3.6.1.1. Using 3 years of Simulated Production History – Fluid 1

1. YM-SEPD and YM-SEPD Hybrid Models – Plots and Parameters:

   The Yu plot and parameters generated both for the YM-SEPD model and Arps' models are shown in Figure 3-14 and Table 3-3. The portion of the Yu plot used to generate n and τ was 2 to 3 years of historical data.

Table 3-3 YM-SEPD and Arps Parameters – Fluid 1 (3yrs History)

YM-SEPD Parameters – Fluid 1 (3yrs history)			
n	0.335		
Intercept	0.310		
τ, days	37.72		
q_o, stb/d	5347		
Arps Parameters – Fluid 1 (3yrs history)			
	Arps	**Arps(1)**	**Arps(2)**
t_{sw}, days	608	212	8279
D_{sw}, 1/days	0.002	0.003	0.005
q_{sw}, stb/d	372.2	822.8	19.33
b	0.7	0.8	0.9

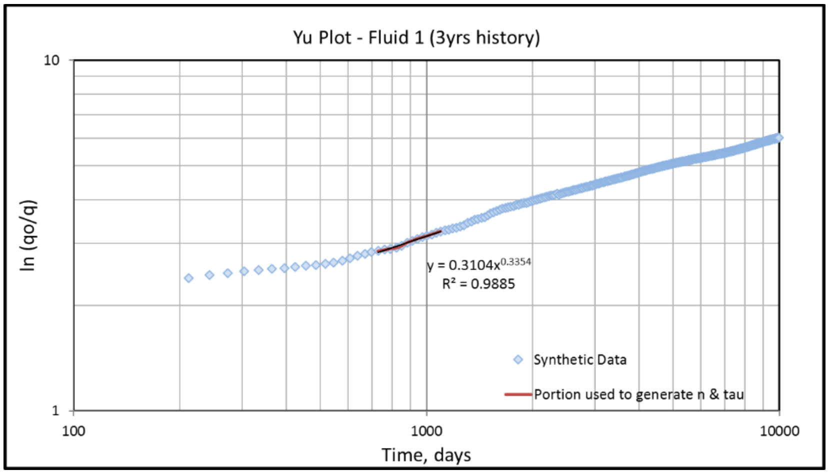

Figure 3-14 Yu Plot – Fluid 1 (3yrs History)

2. Duong and Duong Hybrid Models – Plots and Parameters:

   The inverse MBT vs. time plot, q_1 determination plot and parameters used for the Duong and Arps' models are shown in Table 3-4, Figures 3-15 and 3-16.

Table 3-4 Duong and Arps Parameters – Fluid 1 (3yrs History)

Duong Parameters – Fluid 1 (3yrs history)			
a	1.270		
m	-1.137		
q_1, stb/d	2035		
q_∞, stb/d	0		
Arps Parameters – Fluid 1 (3yrs history)			
	Arps	**Arps(1)**	**Arps(2)**
t_{sw}, days	608	212	8279
D_{sw}, 1/days	0.023	0.050	0.004
q_{sw}, stb/d	313.8	571.6	36.53
b	0.9	0.95	0.9

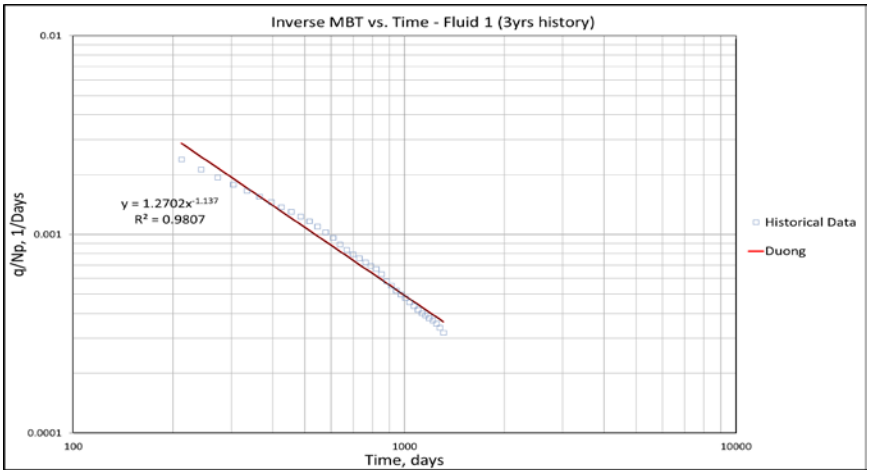

Figure 3-15 Inverse MBT vs. Time – Fluid 1 (3yrs History)

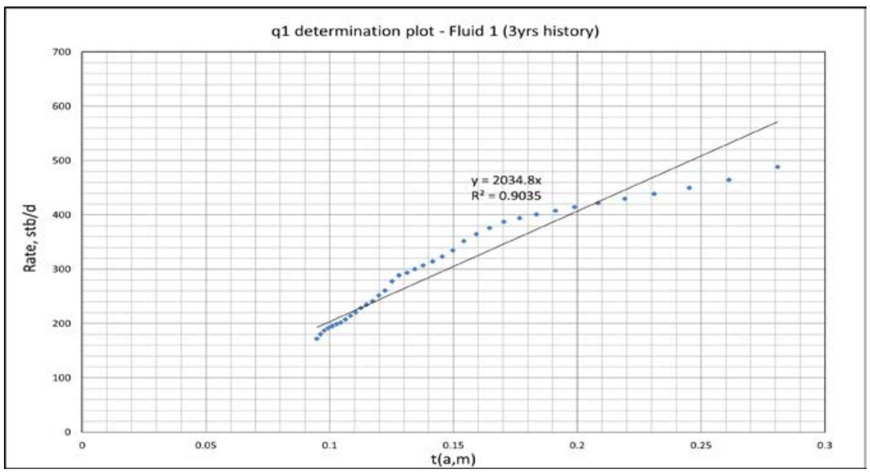

Figure 3-16 q_1 Determination Plot – Fluid 1 (3yrs History)

3.6.1.2. Using 2 years of Simulated Production History – Fluid 1

1. YM-SEPD and YM-SEPD Hybrid Models – Plots and Parameters:

   Figure 3-17 and Table 3-5 show the Yu plot and parameters for the YM-SEPD and Arps' models. In this case, Yu suggests using the Duong model to forecast to the desired 3 years of production history. Therefore, we used the Duong model to generate the 2nd and 3rd year pseudohistorical data based on 2 years of simulated production history.

Table 3-5 YM-SEPD and Arps Parameters – Fluid 1 (2yrs History)

YM-SEPD Parameters – Fluid 1 (2yrs history + Duong pseudohistory)			
n	0.154		
Intercept	1.042		
τ, days	0.764		
q_o, stb/d	5347		
Arps Parameters – Fluid 1 (2yrs history + Duong pseudohistory)			
	Arps	**Arps(1)**	**Arps(2)**
t_{sw}, days	608	212	8279
D_{sw}, 1/days	0.001	0.002	0.005
q_{sw}, stb/d	329.1	499.0	16.89
b	0.4	0.7	0.8

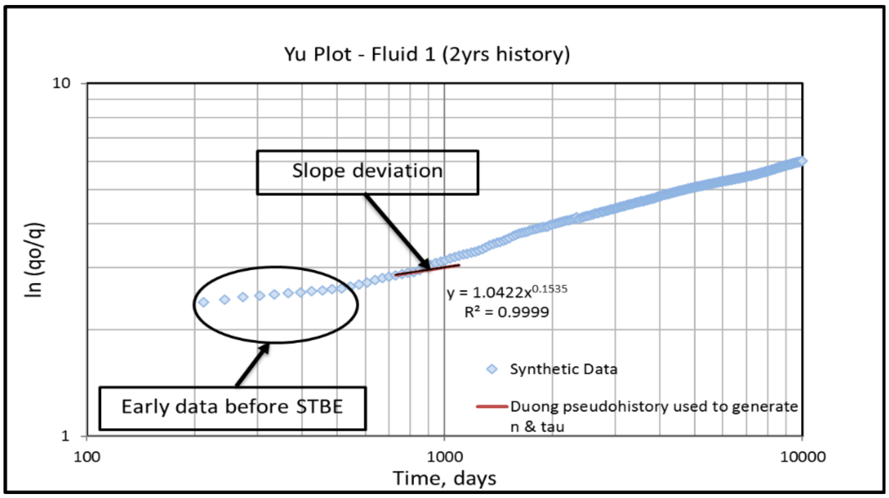

Figure 3-17 Yu Plot – Fluid 1 (2yrs History)

As shown in Figure 3-17, because the Duong pseudohistorical data were generated from data that included early data before the STBE (Start of Boundary Effects), there is a visible slope deviation from the original synthetic data. This led to calculation of “unfavorable” n and τ parameters, thereby making production forecasts more inaccurate. This inaccuracy increases with shorter production histories as shown in Table 3-11 – highlighting the importance of the nature of data particularly when forecasting production from shale volatile oil reservoirs. We lay emphasis on the nature of data because, as observed on the diagnostic plot (Fig. 3-2), there was an early change from linear flow to the transition flow regime (ELF = 212 days). This affected the ability of the Duong model to forecast accurately as it is based on the assumption of long-term linear (or bilinear) flow. The use of YM-SEPD hybrid models significantly improved forecasts. Forecasts are for the most part better when we switch models at an early time [in this case, at the end of linear flow (ELF) – YM-SEPD + Arps(1) and twice at the ELF and STBDF – YM-SEPD + Arps(1) +Arps(2)]. This is as a result of the sensitivity of b values to time of switch as earlier stated. That is, despite the generation of "unfavorable" n and τ parameters, an earlier time of switch to Arps' model enabled us to do better curve fitting than when we use a later time of switch – leading to relatively more reasonable forecasts. It should be noted, however, that when "favorable" n and τ parameters were obtained, the YM-SEPD hybrid model with time (point) of switch at the STBE as observed on the Yu plot, Inverse MBT vs. Time and log-log rate-MBT plots (Figures 3-2 and 3-7), led to the best result (the 3yrs column in Table 3-11).

2. Duong and Duong Hybrid Models – Plots and Parameters:

   The Duong model plots as well as parameters used for the Duong and Arps' models are depicted in Table 3-6, Figures 3-18 and 3-19.

Table 3-6 Duong and Arps Parameters – Fluid 1 (2yrs History)

Duong Parameters – Fluid 1 (2yrs history)			
a	0.575		
m	-1.006		
q_1, stb/d	5631		
q_∞, stb/d	0		
Arps Parameters – Fluid 1 (2yrs history)			
	Arps	**Arps(1)**	**Arps(2)**
t_{sw}, days	608	212	8279
D_{sw}, 1/days	0.018	0.045	0.002
q_{sw}, stb/d	330.4	531.5	81.35
b	1.55	1.6	0.9

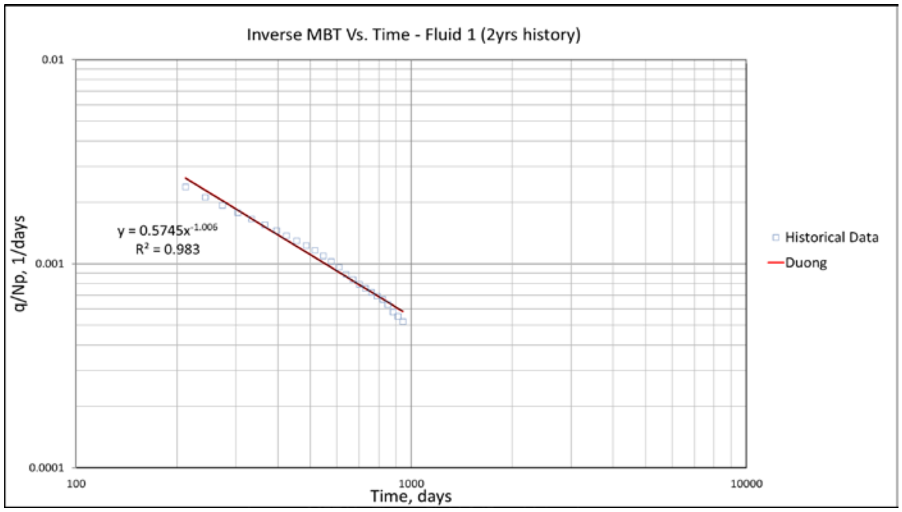

Figure 3-18 Inverse MBT vs. Time – Fluid 1 (2yrs History)

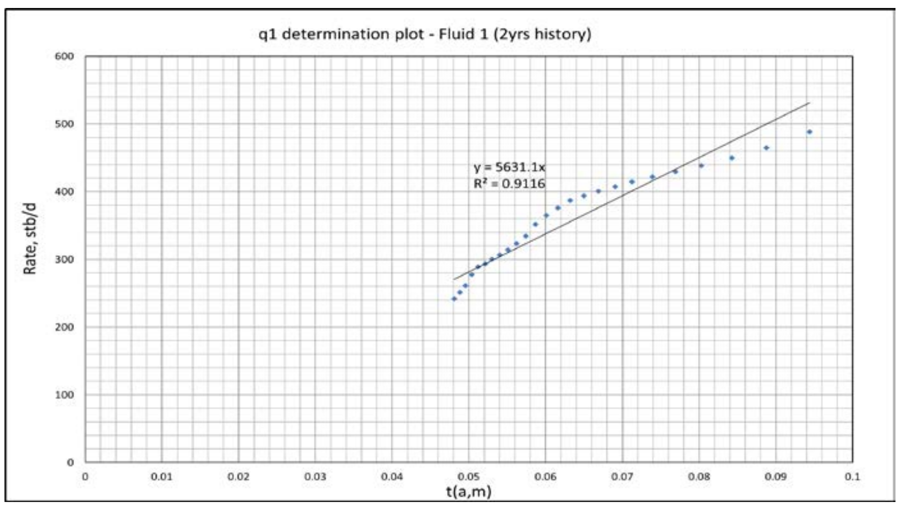

Figure 3-19 q_1 Determination Plot – Fluid 1 (2yrs History)

3.6.1.3. Using 1 year of Simulated Production History – Fluid 1

1. YM-SEPD and YM-SEPD Hybrid Models – Plots and Parameters:

   Figure 3-20 and Table 3-7 show the Yu plot and parameters for the YM-SEPD and Arps' models. Here, Yu suggests using the Duong model to forecast to the desired 3 years of production history. Hence, we used the Duong model to generate the 2nd and 3rd year pseudohistorical data based on 1 year of simulated production history.

Table 3-7 YM-SEPD and Arps Parameters – Fluid 1 (1yr History)

YM-SEPD Parameters – Fluid 1 (1yr history + Duong pseudohistory)			
n	0.057		
Intercept	1.856		
τ, days	2E-05		
q_o, stb/d	5347		
Arps Parameters – Fluid 1 (1yr history + Duong pseudohistory)			
	Arps	**Arps(1)**	**Arps(2)**
t_{sw}, days	608	212	8279
D_{sw}, 1/days	2.5E-04	0.001	0.008
q_{sw}, stb/d	369.1	431.3	19.07
b	0.01	0.33	0.5

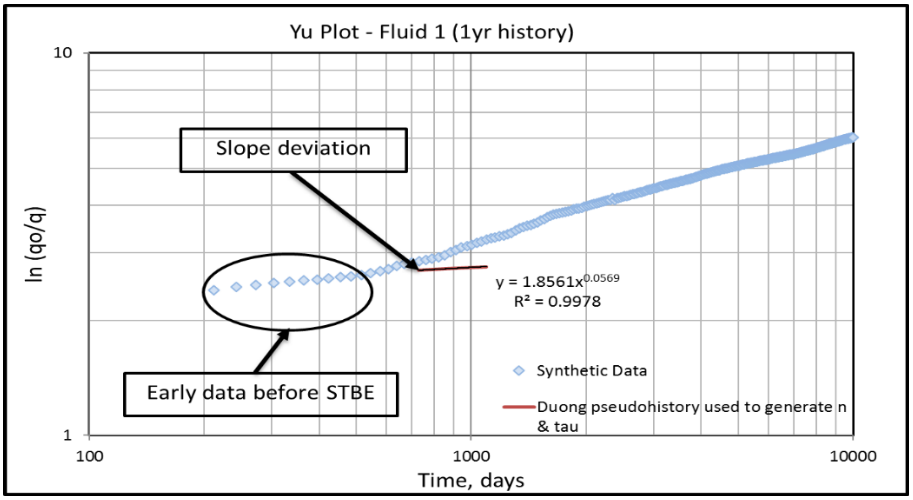

Figure 3-20 Yu Plot – Fluid 1 (1yr History)

Here, as in the cases for 0.5yr (will be shown later) and 2yrs history, the slope deviation from the original synthetic data led to the calculation of "unfavorable" n and τ parameters. This, in turn, led to highly inaccurate forecasts. The use of YM-SEPD hybrid models improved results.

2. Duong and Duong Hybrid Models – Plots and Parameters:

   The Duong model parameters and plots used for the Duong and Arps' models are depicted in Table 3-8, Figures 3-21 and 3-22.

Table 3-8 Duong and Arps Parameters – Fluid 1 (1yr History)

Duong Parameters – Fluid 1 (1yr history)			
a	0.191		
m	-0.817		
q_1, stb/d	6853		
q_∞, stb/d	0		
Arps Parameters – Fluid 1 (1yr history)			
	Arps	**Arps(1)**	**Arps(2)**
t_{sw}, days	608	212	8279
D_{sw}, 1/days	0.010	0.024	0.003
q_{sw}, stb/d	372.4	488.1	80.75
b	1.2	1.2	0.9

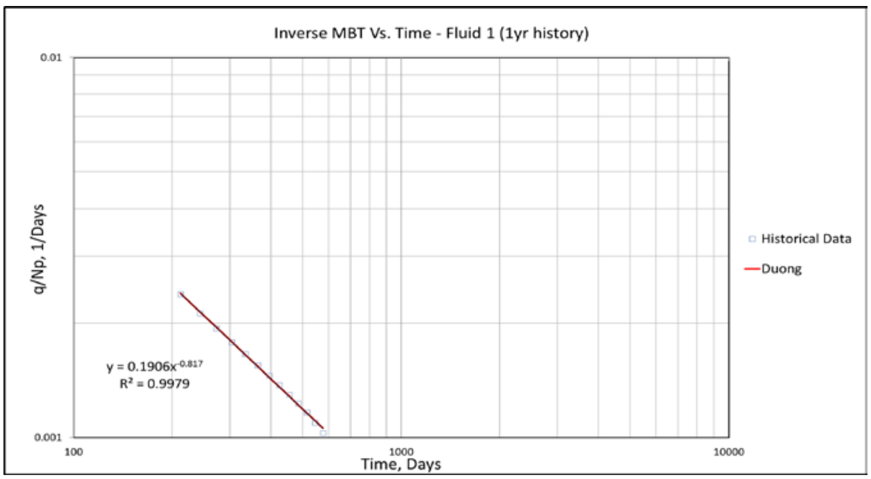

Figure 3-21 Inverse MBT vs. Time – Fluid 1 (1yr History)

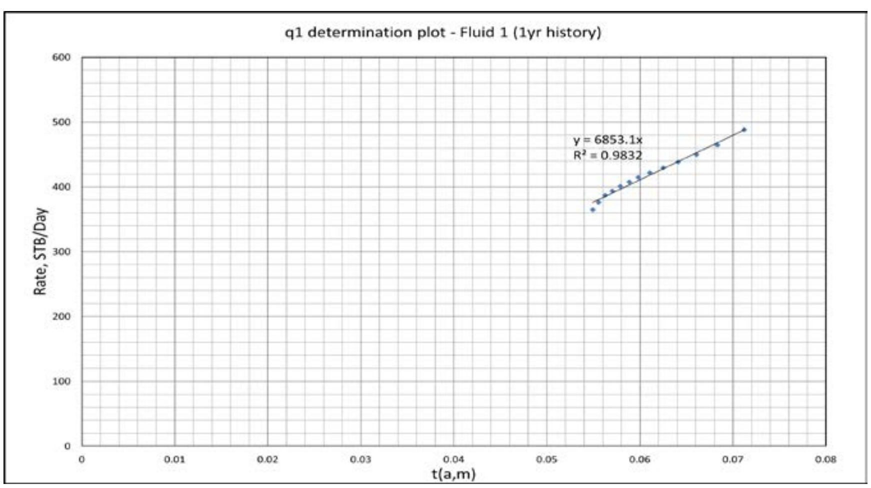

Figure 3-22 q_1 Determination Plot – Fluid 1 (1yr History)

3.6.1.4. Using 6 months of Simulated Production History – Fluid 1

1. YM-SEPD and YM-SEPD Hybrid Models – Plots and Parameters:

   Table 3-9 and Figure 3-23 show the Yu plot and parameters for the YM-SEPD and Arps' models. In this instance, Yu suggests using the Duong model to forecast to the desired 3 years of production history. Thus, we used the Duong model to generate the 2nd and 3rd year pseudohistorical data based on 6 months of simulated production history.

Table 3-9 YM-SEPD and Arps Parameters – Fluid 1 (0.5yr History)

YM-SEPD Parameters – Fluid 1 (0.5yr history + Duong pseudohistory)			
n	0.038		
Intercept	2.071		
τ, days	5.6E-9		
q_o, stb/d	5347		
Arps Parameters – Fluid 1 (0.5yr history + Duong pseudohistory)			
	Arps	Arps(1)	Arps(2)
t_{sw}, days	608	212	8279
D_{sw}, 1/days	1.7E-4	0.001	0.009
q_{sw}, stb/d	378.7	420.5	22.91
b	0.01	0.16	0.3

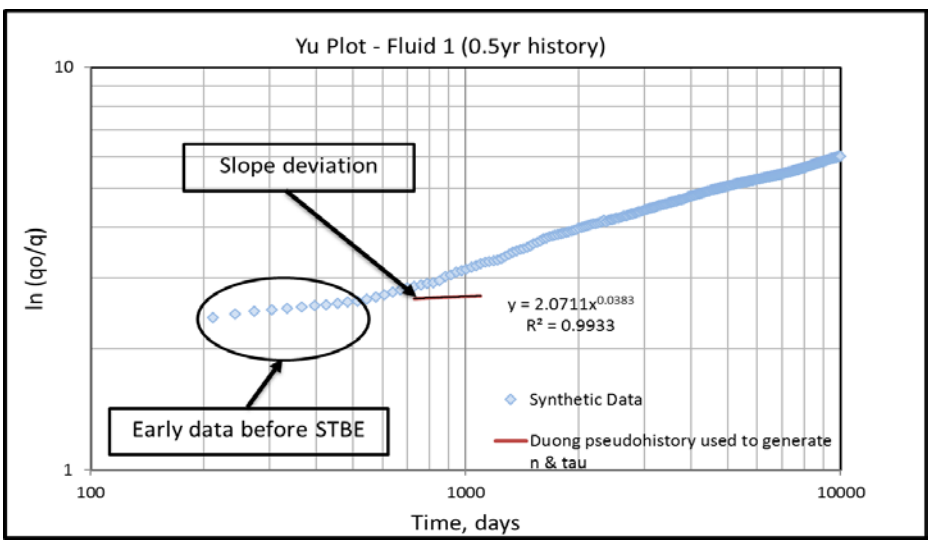

Figure 3-23 Yu Plot – Fluid 1 (0.5yr History)

2. Duong and Duong Hybrid Models – Plots and Parameters:

The Duong model plots and parameters used for the Duong and Arps' models are depicted in Table 3-10, Figures 3-24 and 3-25.

Table 3-10 Duong and Arps Parameters – Fluid 1 (0.5yr History)

Duong Parameters – Fluid 1 (0.5yr history)			
a	0.159		
m	-0.786		
q_1, stb/d	6591		
q_∞, stb/d	0		
Arps Parameters – Fluid 1 (0.5yr history)			
	Arps	**Arps(1)**	**Arps(2)**
t_{sw}, days	608	212	8279
D_{sw}, 1/days	0.010	0.024	0.002
q_{sw}, stb/d	382.5	484.0	130.4
b	0.9	2	0.9

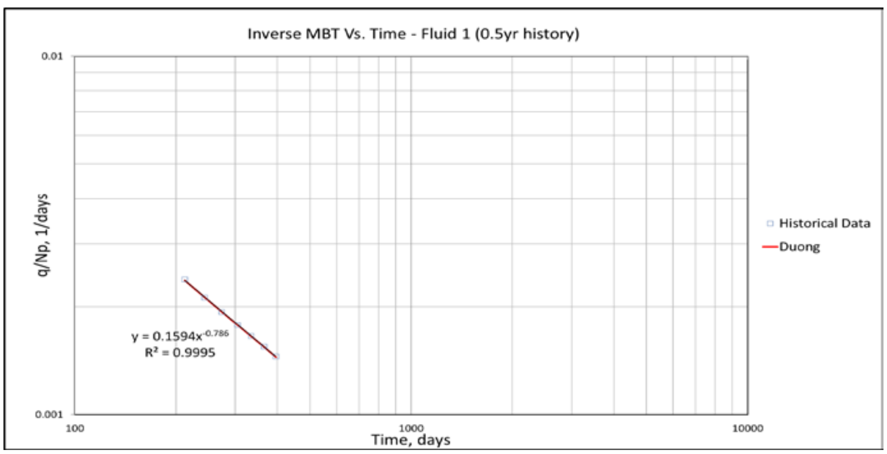

Figure 3-24 Inverse MBT vs. Time – Fluid 1 (0.5yr History)

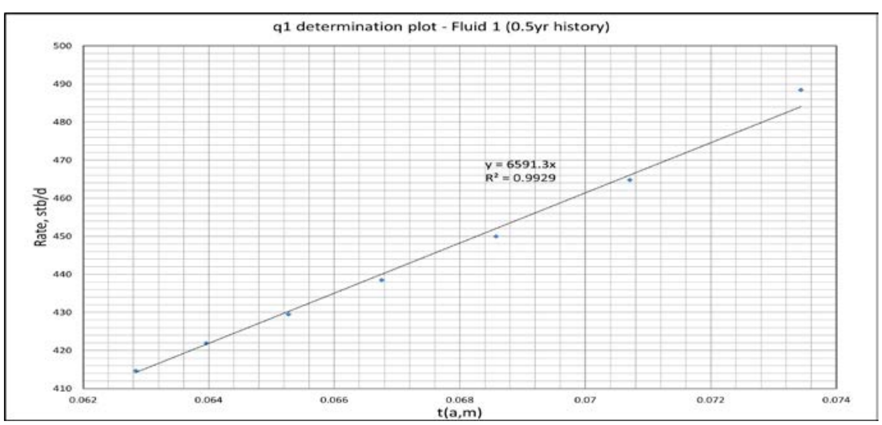

Figure 3-25 q_1 Determination Plot – Fluid 1 (0.5yr History)

Results of production forecasts in comparison to simulated data are shown in Figures 3-26 – 3-29. The YM-SEPD hybrid models led to more accurate forecasts than others. From these graphs, it can be observed that the Duong model and its hybrid alternatives overestimated production in all cases. We assume that the overestimation is due to the imprecise q_1 determination (in comparison to the real first day oil rate) caused by the generation of “unfavorable” a and m parameters, which in turn was a result of the nature of early data before the STBE (Start of Boundary Effects). As mentioned earlier, there was an early deviation from linear flow to the transition flow regime period and since the Duong model assumes long-term linear (or bilinear) flow, it will lead to inaccurate forecasts. This further emphasizes the fact that the complex physics of flow in shale volatile oil reservoirs makes traditional DCA methods quite inappropriate for forecasting their production. It should be noted that our graphs for determining q_1 are based on the least squares best fit of the data going through the origin (zero intercept).

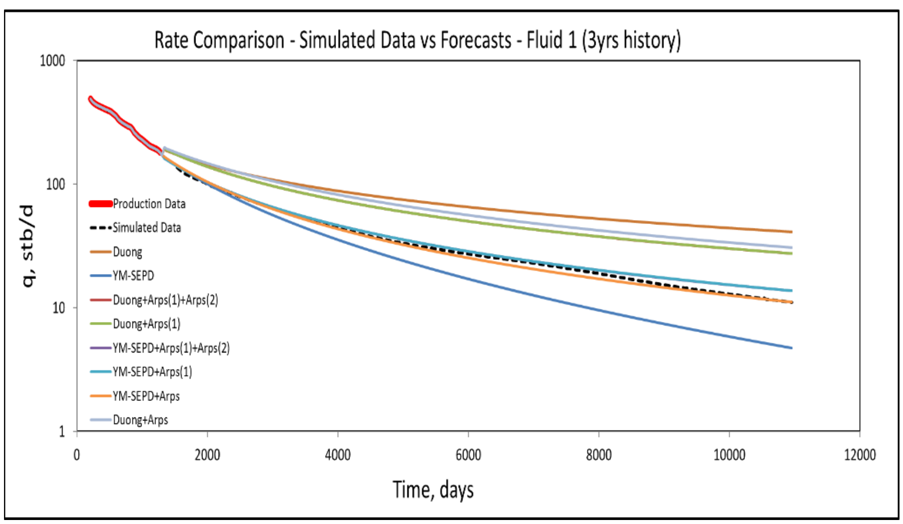

Figure 3-26 Rate Comparisons: Simulated Data vs. Forecasts – Fluid 1 (3yrs History)

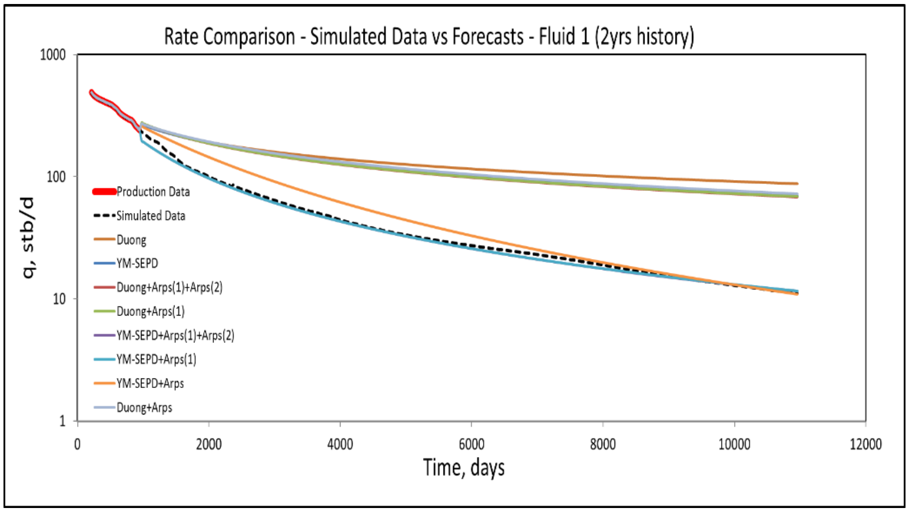

Figure 3-27 Rate Comparisons: Simulated Data vs. Forecasts – Fluid 1 (2yrs History)

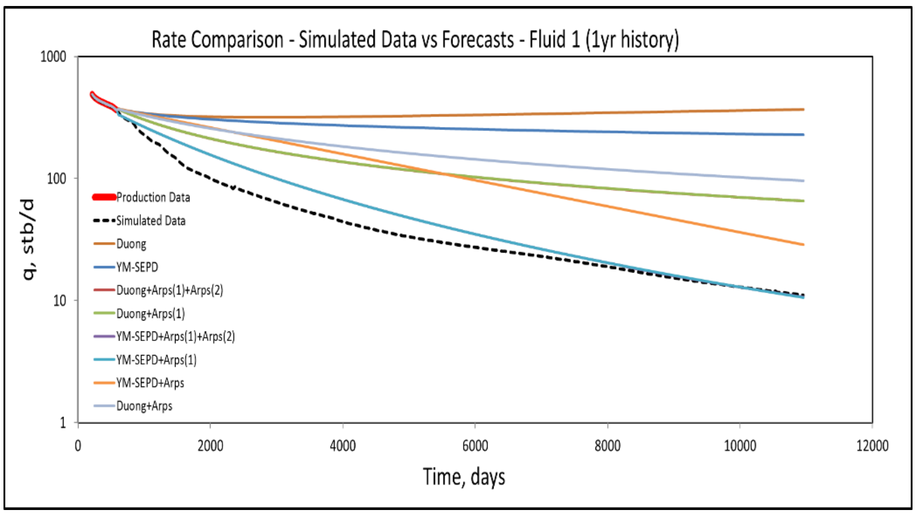

Figure 3-28 Rate Comparisons: Simulated Data vs. Forecasts – Fluid 1 (1yr History)

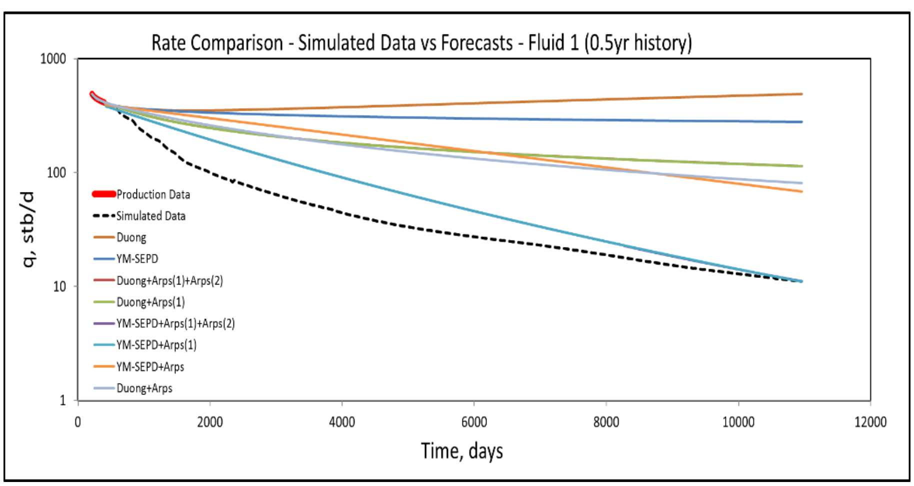

Figure 3-29 Rate Comparisons: Simulated Data vs. Forecasts – Fluid 1 (0.5yr History)

In addition to the graphical displays of results, Table 3-11 shows the comparison of percentage errors, absolute errors and forecasts of all the DCA models applied. In the percentage error columns, the figures in red indicate the lowest percentage errors.

Table 3-11 Forecasts, Errors and Percentage Errors – Fluid 1

Cumulative Oil Production Forecast Errors – Fluid 1	Forecast, STB				Error (absolute value), STB				Percentage Error, %			
Matched Production Data	0.5 yr.	1 yr.	2 yrs.	3 yrs.	0.5 yr.	1 yr.	2 yrs.	3 yrs.	0.5 yr.	1 yr.	2 yrs.	3 yrs.
Simulated Data	20701	18370	14825	12392	0	0	0	0	-	-	-	-
YM-SEPD	106435	90712	38791	9984	+85734	+72342	+23966	-2408	+80.6	+79.8	+61.8	-24.1
YM-SEPD + Arps(1)	31507	23914	13897	12946	+10806	+5544	-928	+554	+34.3	+23.2	-6.7	+4.3
YM-SEPD + Arps(1) +Arps(2)	31498	23910	13894	12942	+10797	+5540	-931	+550	+34.3	+23.2	-6.7	+4.3
Duong	141112	114636	42927	24364	+120411	+96266	+28102	+11972	+85.3	+84.0	+65.5	+49.1
Duong + Arps(1)	62081	44711	38200	20188	+41380	+26341	+23375	+7796	+66.7	+58.9	+61.2	+38.6
Duong + Arps(1) + Arps(2)	62076	44722	38198	20183	+41375	+26352	+23373	+7791	+66.7	+58.9	+61.2	+38.6
YM-SEPD + Arps	64053	45269	18933	12216	+43352	+26899	+4108	-176	+67.7	+59.4	+21.7	-1.4
Duong + Arps	57454	57886	39825	22169	+36753	+39516	+25000	+9777	+64.0	+68.3	+62.8	+44.1

3.6.1.5. Solution Gas Production Forecast – Fluid 1

Following the procedure previously stated, we forecasted solution gas production for Fluid 1 and compared our result to simulated gas production over the period of 30 years. The specialized plot and graphical result are shown in Figures 3-30 and 3-31. The total error in the solution gas forecast was approximately 11.8%.

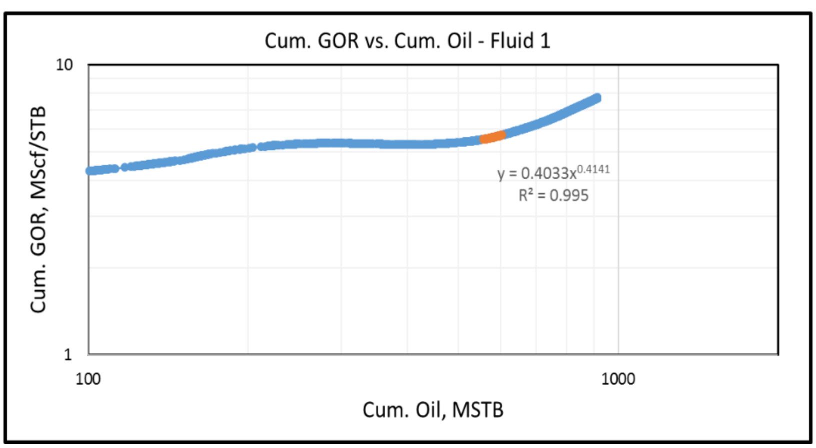

Figure 3-30 Cumulative GOR vs. Cumulative Oil – Fluid 1

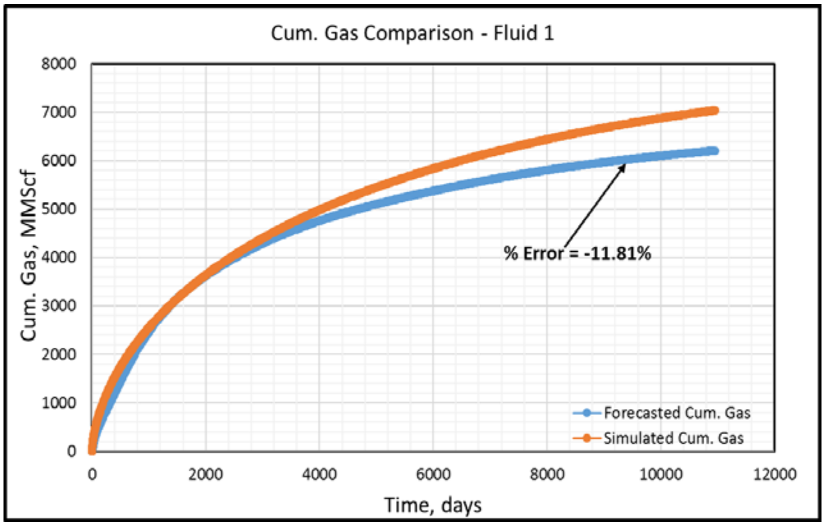

Figure 3-31 Cumulative Gas Comparison – Fluid 1

3.6.2. Fluid 2

Fluid 2 is a highly volatile oil with an initial GOR of about 4081 scf/bbl. Results of production forecasts for this case are the following:

3.6.2.1. Using 3 years of Simulated Production History – Fluid 2

1. YM-SEPD and YM-SEPD Hybrid Models – Plots and Parameters:

   The Yu plot and parameters generated both for the YM-SEPD model and Arps' models are shown in Figure 3-32 and Table 3-12. The portion of the Yu plot used to generate n and τ was 2 to 3 years of historical data.

Table 3-12 YM-SEPD and Arps Parameters – Fluid 2 (3yrs History)

YM-SEPD Parameters – Fluid 2 (3yrs history)			
n	0.299		
Intercept	0.402		
τ, days	21.06		
q_o, stb/d	4015		
Arps Parameters – Fluid 2 (3yrs history)			
	Arps	Arps(1)	Arps(2)
t_{sw}, days	608	212	8248
D_{sw}, 1/days	0.001	0.003	0.005
q_{sw}, stb/d	261.5	546.8	11.65
b	0.65	0.75	0.7

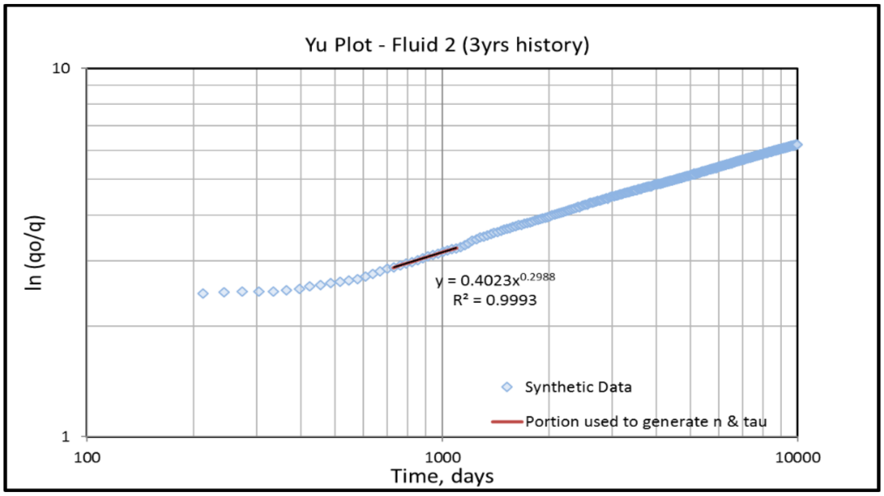

Figure 3-32 Yu Plot – Fluid 2 (3yrs History)

2. Duong and Duong Hybrid Models – Plots and Parameters:

   The Duong model plots and parameters used for the Duong and Arps' models are depicted in Table 3-13, Figures 3-33 and 3-34.

Table 3-13 Duong and Arps Parameters – Fluid 2 (3yrs History)

Duong Parameters – Fluid 2 (3yrs history)			
a	1.482		
m	-1.164		
q_1, stb/d	1129		
q_∞, stb/d	0		
Arps Parameters – Fluid 2 (3yrs history)			
	Arps	**Arps(1)**	**Arps(2)**
t_{sw}, days	608	212	8248
D_{sw}, 1/days	0.025	0.055	0.004
q_{sw}, stb/d	231.4	434.9	45.05
b	0.8	0.95	0.8

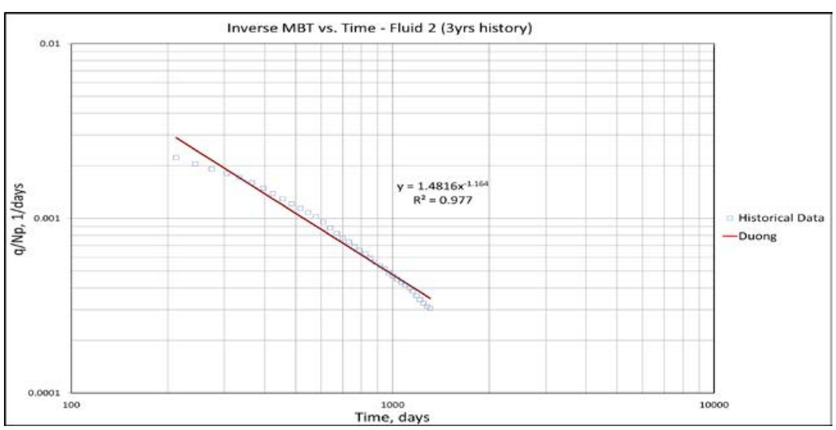

Figure 3-33 Inverse MBT vs. Time – Fluid 2 (3yrs History)

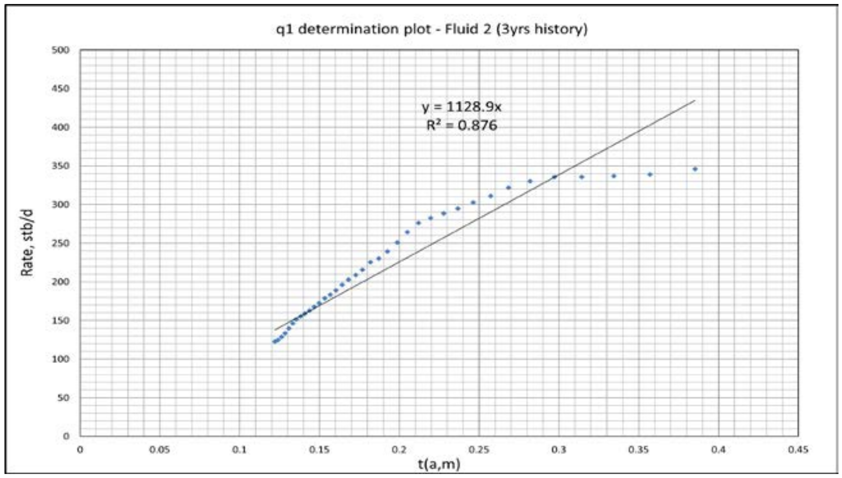

Figure 3-34 q_1 Determination Plot – Fluid 2 (3yrs History)

3.6.2.2. Using 2 years of Simulated Production History – Fluid 2

1. YM-SEPD and YM-SEPD Hybrid Models – Plots and Parameters:

   Figure 3-35 and Table 3-14 show the Yu plot and parameters for the YM-SEPD and Arps' models. In this instance, Yu suggests using the Duong model to forecast to the desired 3 years of production history. Therefore, we used the Duong model to generate the 2nd and 3rd year pseudohistorical data based on 2 years of simulated production history.

Table 3-14 YM-SEPD and Arps Parameters – Fluid 2 (2yrs History)

YM-SEPD Parameters – Fluid 2 (2yrs history + Duong pseudohistory)			
n	0.166		
Intercept	0.967		
τ, days	1.226		
q_o, stb/d	4015		
Arps Parameters – Fluid 2 (2yrs history + Duong pseudohistory)			
	Arps	Arps(1)	Arps(2)
t_{sw}, days	608	212	8248
D_{sw}, 1/days	0.001	0.002	0.005
q_{sw}, stb/d	242.9	381.1	11.81
b	0.4	0.7	0.7

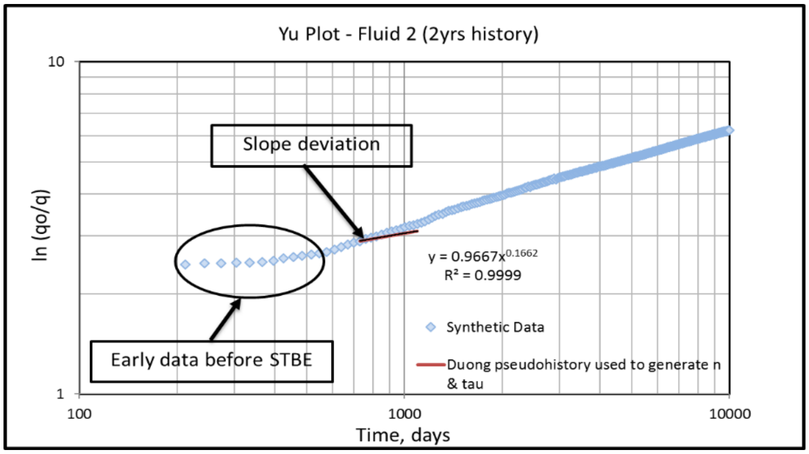

Figure 3-35 Yu Plot – Fluid 2 (2yrs History)

Here, the slope deviation from the original synthetic data (as observed on the Yu plot) also leads to inaccurate forecasts. This is especially the case when short production histories (2years or less) are available. However, the application of YM-SEPD hybrid models improve significantly.

2. Duong and Duong Hybrid Models – Plots and Parameters:

   The Duong plots and parameters used for the Duong and Arps' models are shown in Table 3-15, Figures 3-36 and 3-37.

Table 3-15 Duong and Arps Parameters – Fluid 2 (2yrs History)

Duong Parameters – Fluid 2 (2yrs history)			
a	0.670		
m	-1.033		
q_1, stb/d	3814		
q_∞, stb/d	0		
Arps Parameters – Fluid 2 (2yrs history)			
	Arps	**Arps(1)**	**Arps(2)**
t_{sw}, days	608	212	8248
D_{sw}, 1/days	0.016	0.053	0.002
q_{sw}, stb/d	243.8	404.7	58.71
b	0.9	1.65	0.9

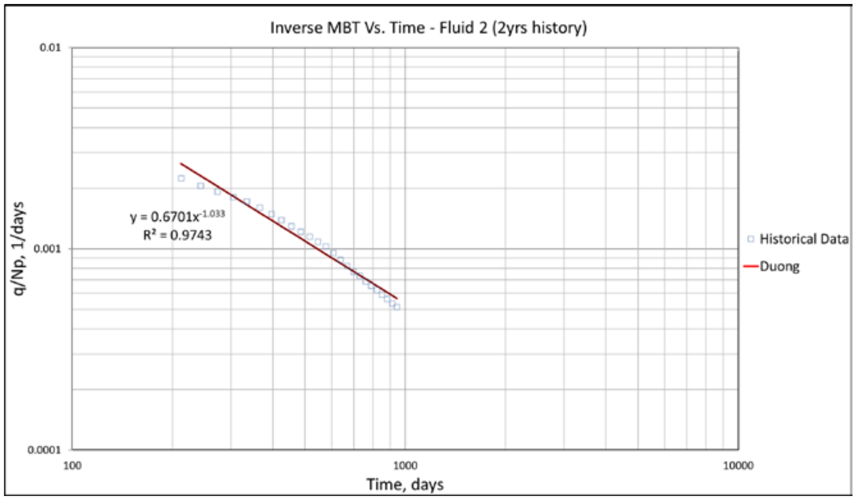

Figure 3-36 Inverse MBT vs. Time – Fluid 2 (2yrs History)

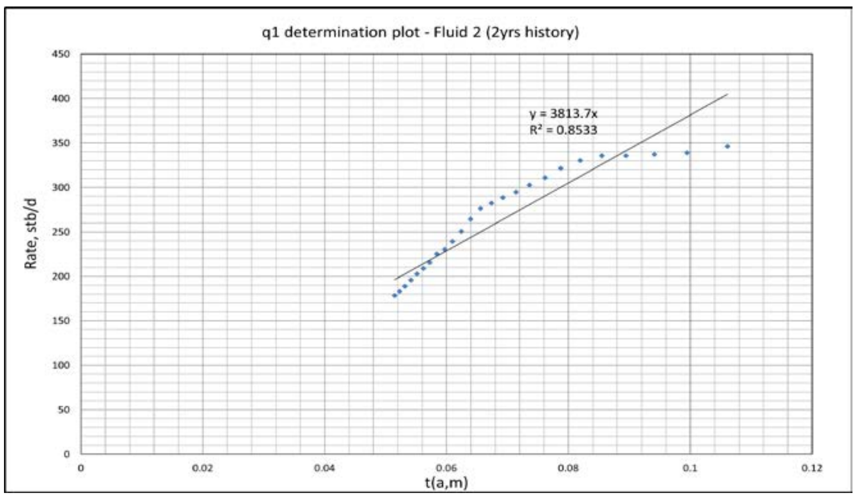

Figure 3-37 q_1 Determination Plot – Fluid 2 (2yrs History)

3.6.2.3. Using 1 year of Simulated Production History – Fluid 2

1. YM-SEPD and YM-SEPD Hybrid Models – Plots and Parameters:

   Figure 3-38 and Table 3-16 show the Yu plot and parameters for the YM-SEPD and Arps' models. In this case, Yu suggests using the Duong model to forecast to the desired 3 years of production history. Therefore, we used the Duong model to generate the 2nd and 3rd year pseudohistorical data based on 1 year of simulated production history.

Table 3-16 YM-SEPD and Arps Parameters – Fluid 2

YM-SEPD Parameters – Fluid 2 (1yr history + Duong pseudohistory)			
n	0.042		
Intercept	2.029		
τ, days	4.8E-8		
q_o, stb/d	4015		
Arps Parameters – Fluid 2 (1yr history + Duong pseudohistory)			
	Arps	**Arps(1)**	**Arps(2)**
t_{sw}, days	608	212	8248
D_{sw}, 1/days	1.8E-4	5E-4	0.009
q_{sw}, stb/d	282.0	316.3	15.14
b	0.1	0.18	0.3

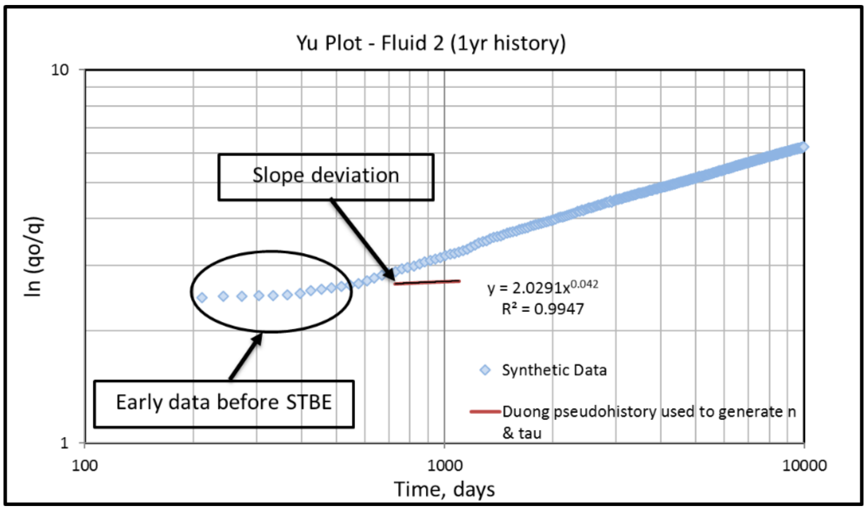

Figure 3-38 Yu Plot – Fluid 2 (1yr History)

2. Duong and Duong Hybrid Models – Plots and Parameters:

   The Duong plots and parameters used for the Duong and Arps' models are shown in Table 3-17, Figures 3-39 and 3-40.

Table 3-17 Duong and Arps Parameters – Fluid 2 (1yr History)

Duong Parameters – Fluid 2 (1yr history)			
a	0.161		
m	-0.789		
q_1, stb/d	5027		
q_∞, stb/d	0		
Arps Parameters – Fluid 2 (1yr history)			
	Arps	**Arps(1)**	**Arps(2)**
t_{sw}, days	608	212	8248
D_{sw}, 1/days	0.010	0.024	0.002
q_{sw}, stb/d	284.7	363.2	75.55
b	0.9	1.5	0.9

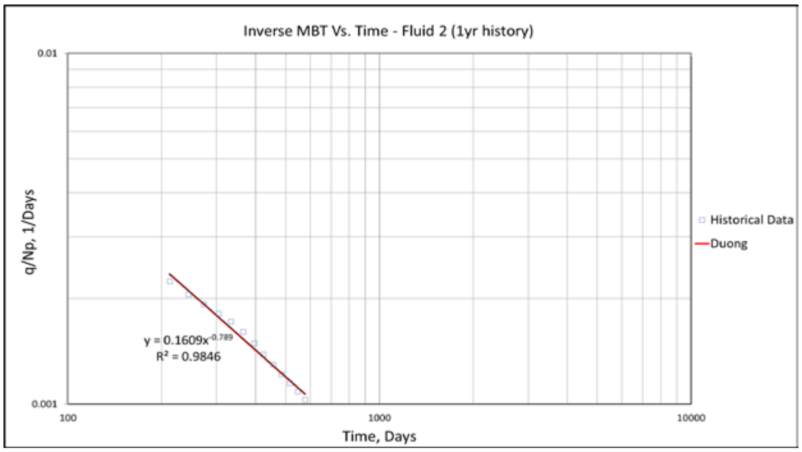

Figure 3-39 Inverse MBT vs. Time – Fluid 2 (1yr History)

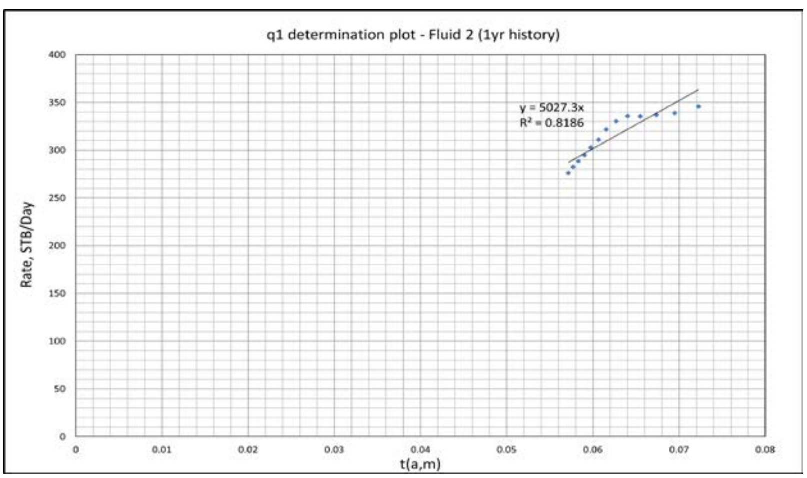

Figure 3-40 q_1 Determination Plot – Fluid 2 (1yr History)

3.6.2.4. Using 6 months of Simulated Production History – Fluid 2

1. YM-SEPD and YM-SEPD Hybrid Models – Plots and Parameters:

   Yu recommends using the Duong model to forecast to the desired 3 years of production history. Therefore, we used the Duong model to generate the 2nd and 3rd year pseudohistorical data based on 6 months of simulated production history. However, the Duong pseudohistorical data obtained from the Duong forecast generated a negative slope (parameter n) on the Yu plot. This made it impossible to forecast with the Yu methodology in this case. This can be seen in Figure 3-41 below.

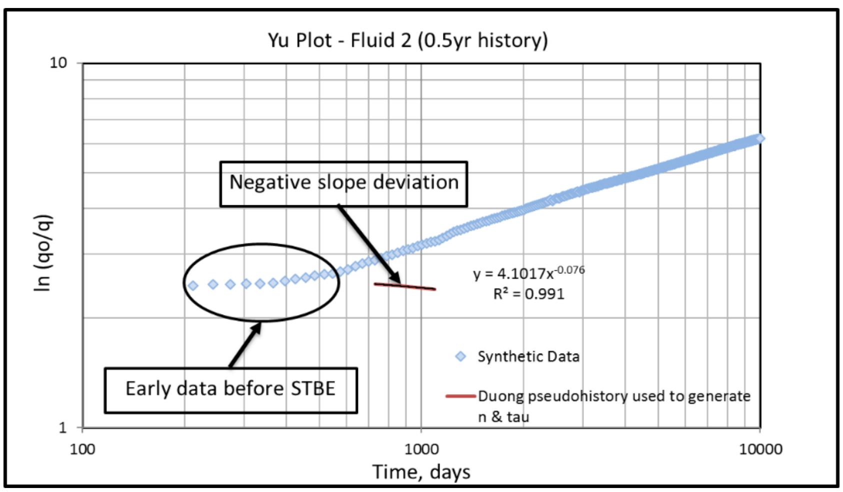

Figure 3-41 Yu Plot – Fluid 2 (0.5yr History)

2. Duong and Duong Hybrid Models – Plots and Parameters:

   Plots and parameters used for the Duong and Arps' models are shown in Table 3-18, Figures 3-42 and 3-43.

Table 3-18 Duong and Arps Parameters – Fluid 2 (0.5yr History)

Duong Parameters – Fluid 2 (0.5yr history)			
a	0.066		
m	-0.630		
q_1, stb/d	3330		
q_∞, stb/d	0		
Arps Parameters – Fluid 2 (0.5yr history)			
	Arps	**Arps(1)**	**Arps(2)**
t_{sw}, days	608	212	8248
D_{sw}, 1/days	0.025	0.024	0.002
q_{sw}, stb/d	331.3	347.4	93.80
b	0.9	2	0.9

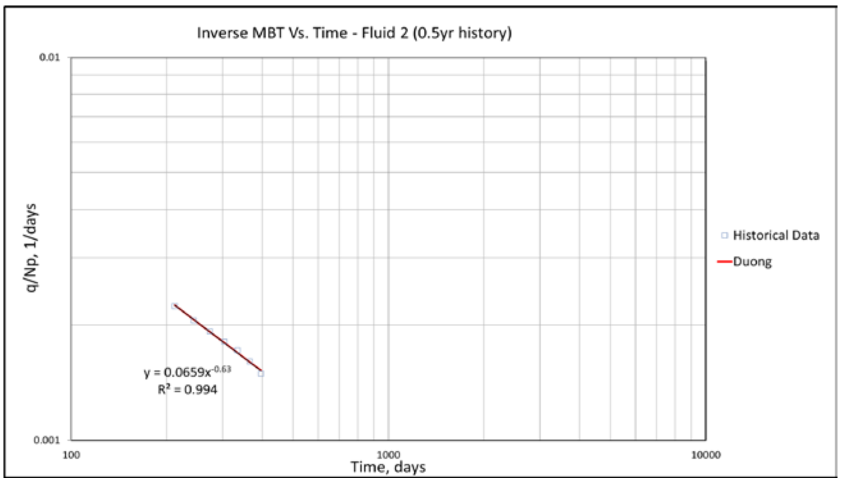

Figure 3-42 Inverse MBT vs. Time – Fluid 2 (0.5yr History)

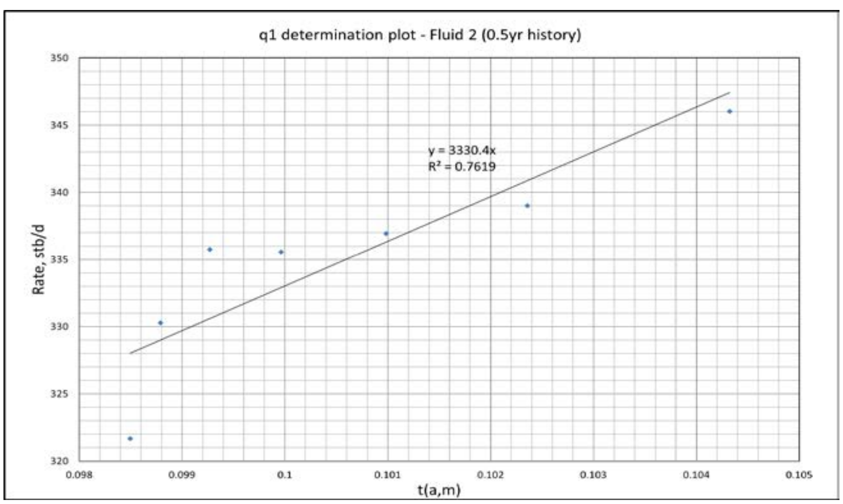

Figure 3-43 q_1 Determination Plot – Fluid 2 (0.5yr History)

Results of production forecasts in comparison to simulated data are shown in Figures 3-44 – 3-47. The YM-SEPD hybrid models led to more accurate forecasts than others in most of the cases. From the graphs, it can be seen that the Duong model and its hybrid variants overestimated production in all instances.

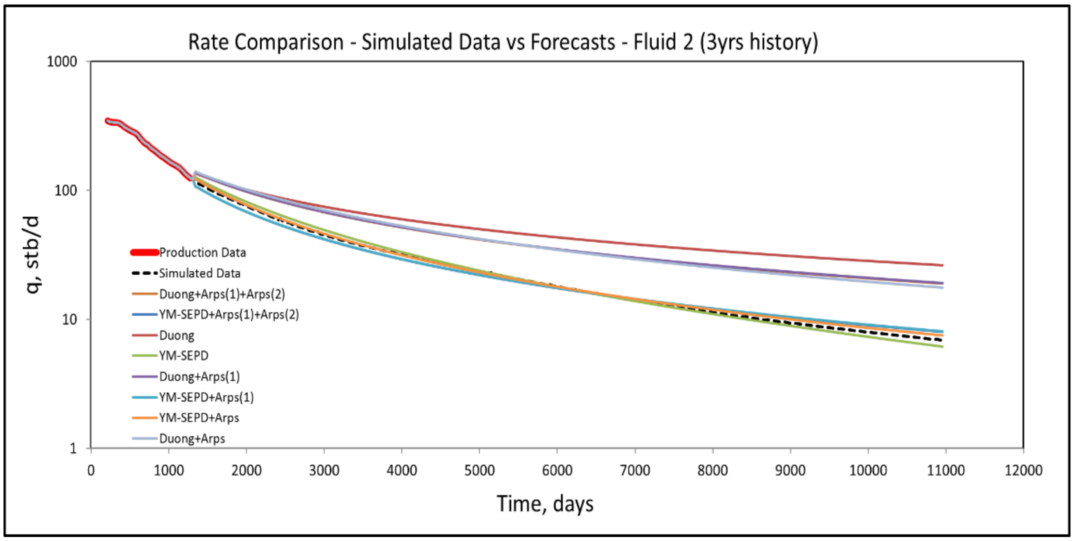

Figure 3-44 Rate Comparisons: Simulated Data vs. Forecasts – Fluid 2 (3yrs History)

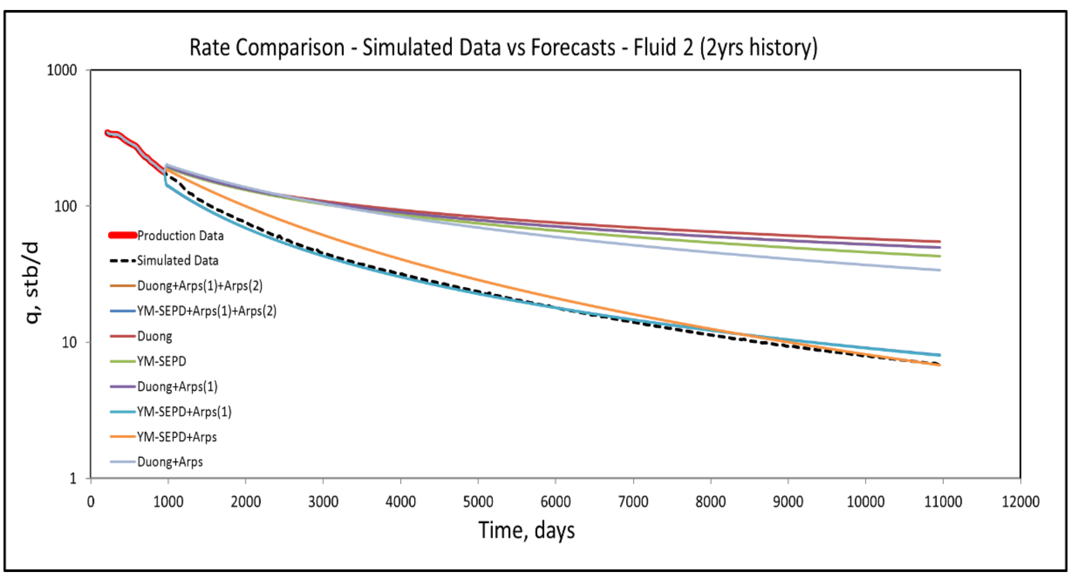

Figure 3-45 Rate Comparisons: Simulated Data vs. Forecasts – Fluid 2 (2yrs History)

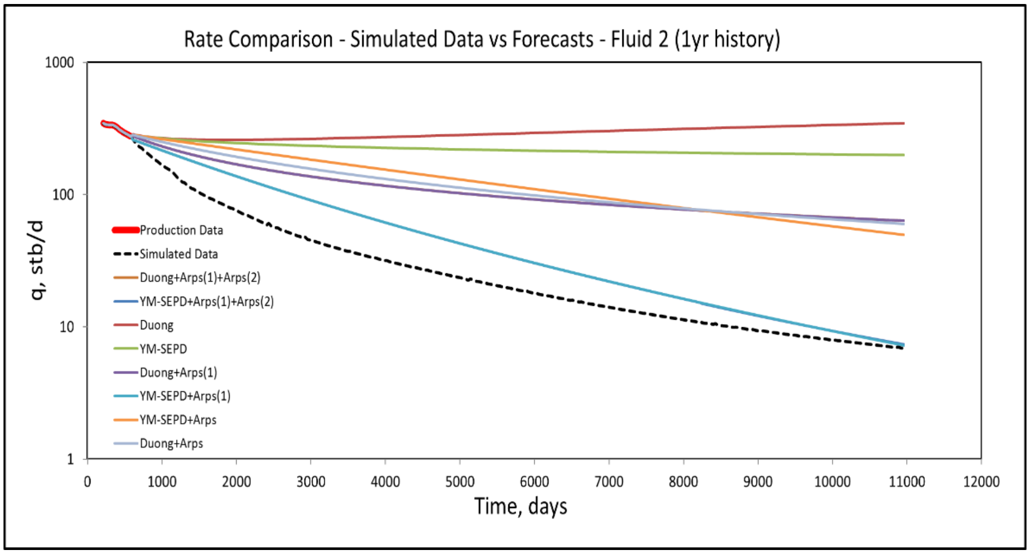

Figure 3-46 Rate Comparisons: Simulated Data vs. Forecasts – Fluid 2 (1yr History)

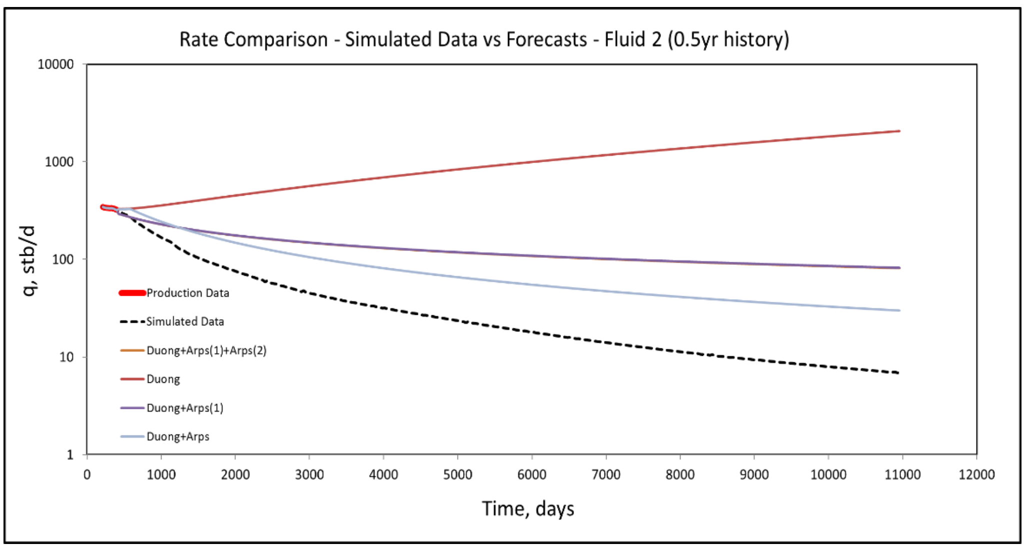

Figure 3-47 Rate Comparisons: Simulated Data vs. Forecasts – Fluid 2 (0.5yr History)

Table 3-19 shows the comparison of percentage errors, absolute errors and forecasts of all the DCA models applied. In the percentage error columns, the figures in red indicate the lowest percentage errors.

Table 3-19 Forecast, Errors and Percentage Errors – Fluid 2

Cumulative Oil Production Forecast Errors – Fluid 2	Forecast, STB				Error (absolute value), STB				Percentage Error, %			
Matched Production Data	0.5 yr.	1 yr.	2 yrs.	3 yrs.	0.5 yr.	1 yr.	2 yrs.	3 yrs.	0.5 yr.	1 yr.	2 yrs.	3 yrs.
Simulated Data	15067	12989	10405	8641	0	0	0	0	-	-	-	-
YM-SEPD	-	73715	25527	9002	-	+60726	+15122	+361	-	+82.4	+59.2	+4.0
YM-SEPD + Arps(1)	-	19477	10076	8199	-	+6488	-329	-442	-	+33.3	-3.3	-5.4
YM-SEPD + Arps(1) +Arps(2)	-	19476	10100	8196	-	+6487	-305	-445	-	+33.3	-3.0	-5.4
Duong	351795	98096	28241	16398	+336728	+85107	+17836	+7757	+95.7	+86.76	+63.2	+47.3
Duong + Arps(1)	43326	36639	26948	14119	+28259	+23650	+16543	+5478	+65.2	+64.6	+61.4	+38.8
Duong + Arps(1) + Arps(2)	43324	36638	26948	14117	+28257	+23649	+16543	+5476	+65.2	+64.5	+61.4	+38.8
YM-SEPD + Arps	-	44534	12852	8804	-	+31545	+2447	+163	-	+70.8	+19.0	+1.9
Duong + Arps	30097	40995	24534	14225	+15030	+28006	+14129	+5584	+49.9	+68.3	+57.6	+39.3

3.6.2.5. Solution Gas Production Forecast – Fluid 2

Solution gas production was forecasted for Fluid 2 and compared our result to simulated gas production over the period of 30 years. The specialized plot and graphical result are shown in Figures 3-48 and 3-49. The total error in the solution gas forecast was approximately 9.6%.

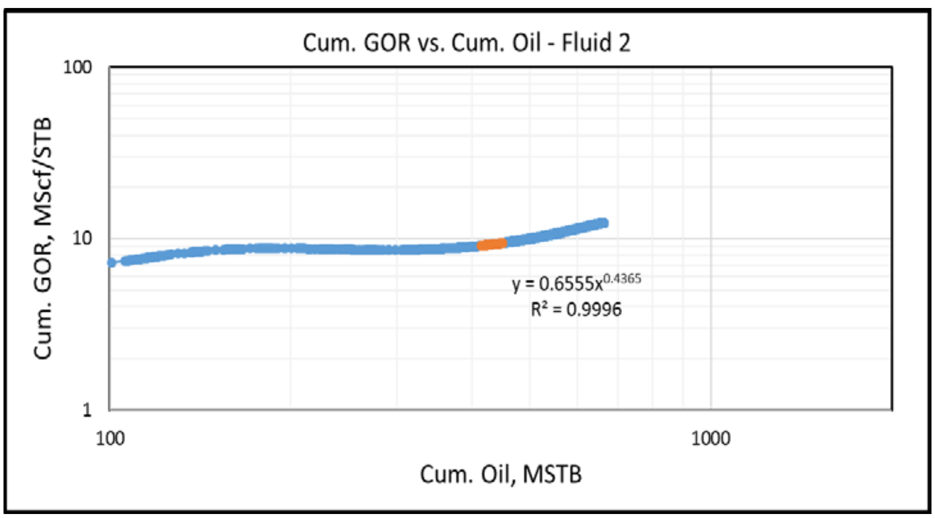

Figure 3-48 Cumulative GOR vs. Cumulative Oil – Fluid 2

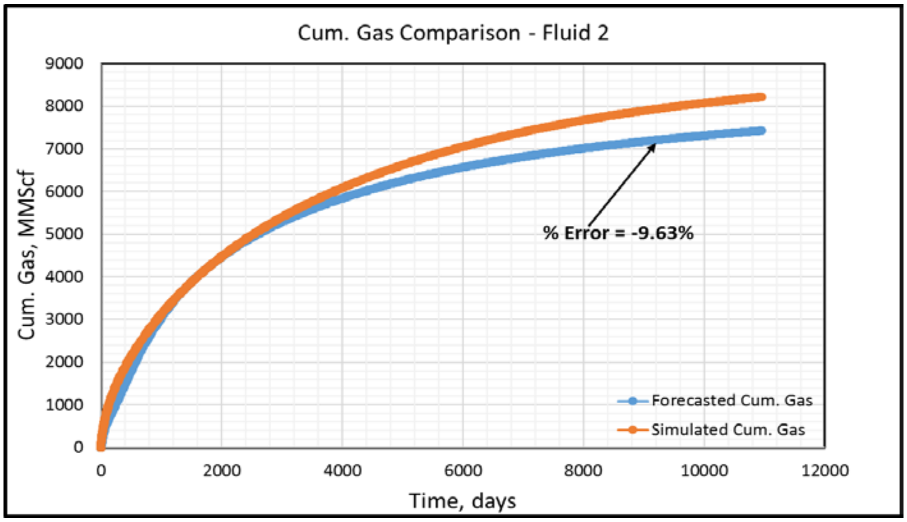

Figure 3-49 Cumulative Gas Comparison – Fluid 2

3.6.3. Fluid 3

Fluid 3 is a highly volatile oil with an initial GOR of about 3967 scf/bbl. Results of production forecasts for this case are the following:

3.6.3.1. Using 3 years of Simulated Production History – Fluid 3

1. YM-SEPD and YM-SEPD Hybrid Models – Plots and Parameters:

   The Yu plot and parameters generated both for the YM-SEPD model and Arps' models are shown in Figure 3-50 and Table 3-20. The portion of the Yu plot used to generate n and τ was 2 to 3 years of historical data.

Table 3-20 YM-SEPD and Arps Parameters – Fluid 3 (3yrs History)

YM-SEPD Parameters – Fluid 3 (3yrs history)			
n	0.296		
Intercept	0.417		
τ, days	19.17		
q_o, stb/d	4462		
Arps Parameters – Fluid 3 (3yrs history)			
	Arps	Arps(1)	Arps(2)
t_{sw}, days	1308	699	7943
D_{sw}, 1/days	0.001	0.001	0.005
q_{sw}, stb/d	136.3	246.0	14.60
b	0.7	0.7	0.8

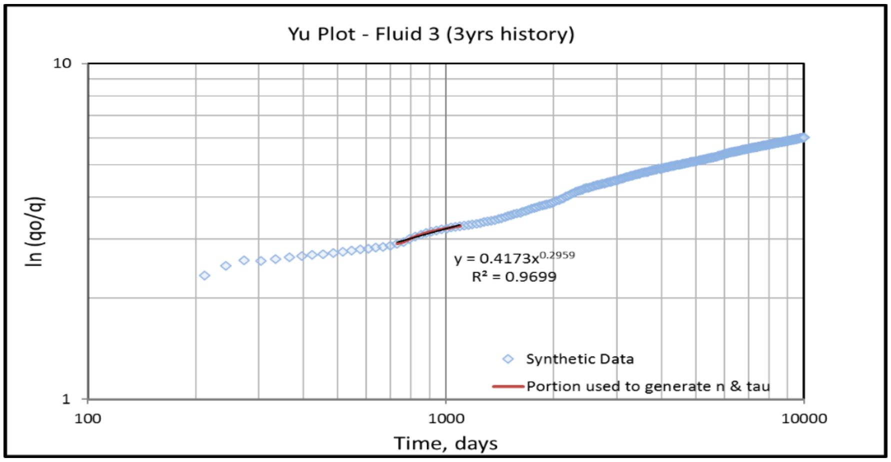

Figure 3-50 Yu Plot – Fluid 3 (3yrs History)

2. Duong and Duong Hybrid Models – Plots and Parameters:

The Duong model plots and parameters used for the Duong and Arps' models are illustrated in Table 3-21, Figures 3-51 and 3-52.

Table 3-21 Duong and Arps Parameters – Fluid 3 (3yrs History)

Duong Parameters – Fluid 3 (3yrs history)			
a	0.746		
m	-1.063		
q_1, stb/d	4348		
q_∞, stb/d	0		
Arps Parameters – Fluid 3 (3yrs history)			
	Arps	Arps(1)	Arps(2)
t_{sw}, days	1308	699	7943
D_{sw}, 1/days	0.010	0.018	0.004
q_{sw}, stb/d	156.6	225.1	38.75
b	0.5	0.9	0.5

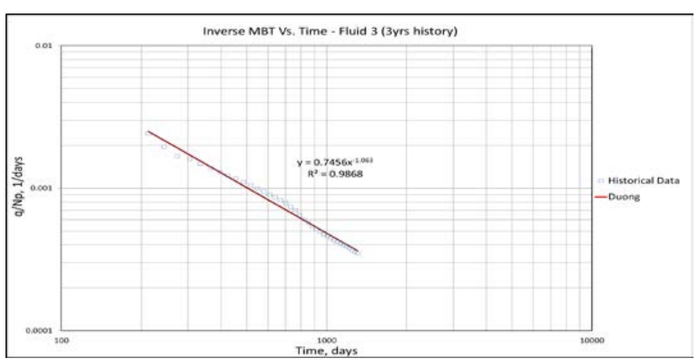

Figure 3-51 Inverse MBT vs. Time – Fluid 3 (3yrs History)

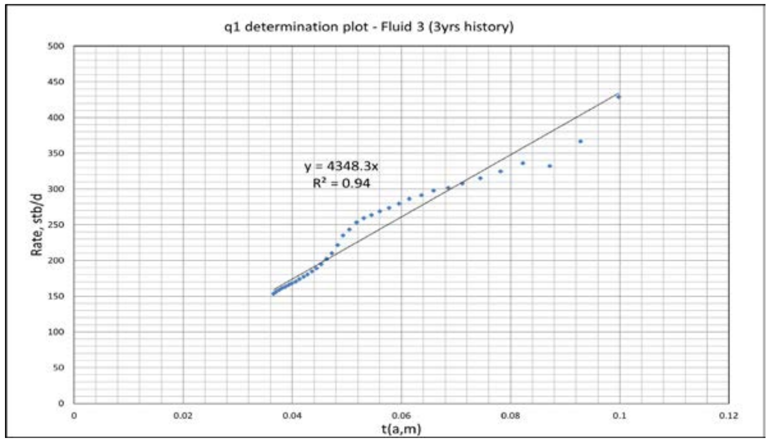

Figure 3-52 q_1 Determination Plot – Fluid 3 (3yrs History)

3.6.3.2. Using 2 years of Simulated Production History – Fluid 3 (2yrs History)

1. YM-SEPD and YM-SEPD Hybrid Models – Plots and Parameters:

   Figure 3-53 and Table 3-22 show the Yu plot and parameters for the YM-SEPD and Arps' models. In this instance, Yu suggests using the Duong model to forecast to the desired 3 years of production history. Therefore, we used the Duong model to generate the 2nd and 3rd year pseudohistorical data based on 2 years of simulated production history.

Table 3-22 YM-SEPD and Arps – Fluid 3 (2yrs History)

YM-SEPD Parameters – Fluid 3 (2yrs history + Duong pseudohistory)			
n	0.153		
Intercept	1.081		
τ, days	0.600		
q_o, stb/d	4462		
Arps Parameters – Fluid 3 (2yrs history + Duong pseudohistory)			
	Arps	Arps(1)	Arps(2)
t_{sw}, days	1308	699	7943
D_{sw}, 1/days	3.7E-4	0.001	0.007
q_{sw}, stb/d	174.9	235.1	16.92
b	0.15	0.4	0.8

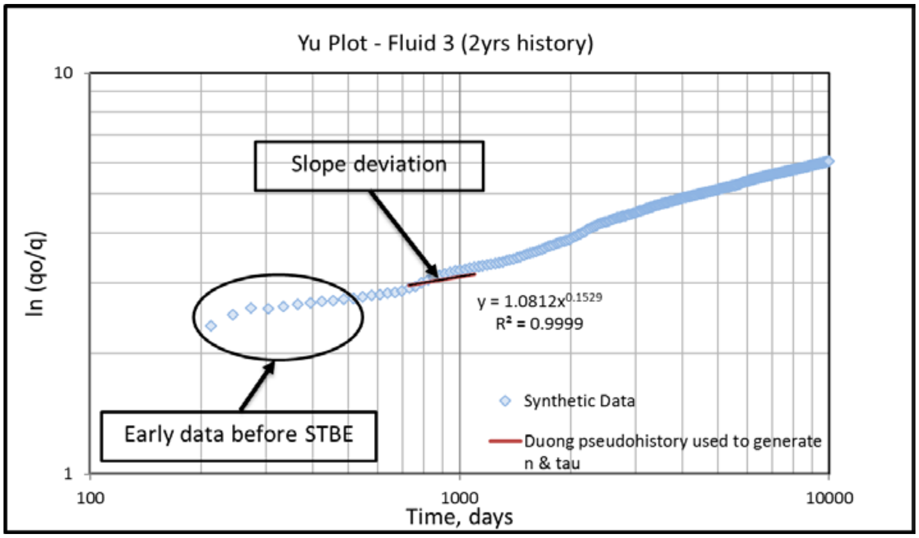

Figure 3-53 Yu Plot – Fluid 3 (2yrs History)

The slope deviation of the Duong pseudohistorical data in comparison to the original data as observed in Figure 3-53 led to the calculation of n and τ parameters that are not entirely favorable for obtaining good forecasts (especially with the availability of short production histories). The use of YM-SEPD hybrid models improved forecasts considerably.

2. Duong and Duong Hybrid Models – Plots and Parameters:

   The Duong model plots and parameters used for the Duong and Arps' models are shown in Table 3-23, Figures 3-54 and 3-55.

Table 3-23 Duong and Arps Parameters – Fluid 3 (2yrs History)

Duong Parameters – Fluid 3 (2yrs history)			
a	0.463		
m	-0.984		
q_1, stb/d	6050		
q_∞, stb/d	0		
Arps Parameters – Fluid 3 (2yrs history)			
	Arps	**Arps(1)**	**Arps(2)**
t_{sw}, days	1308	699	7943
D_{sw}, 1/days	0.008	0.016	0.002
q_{sw}, stb/d	175.8	235.6	66.05
b	0.9	1.5	0.9

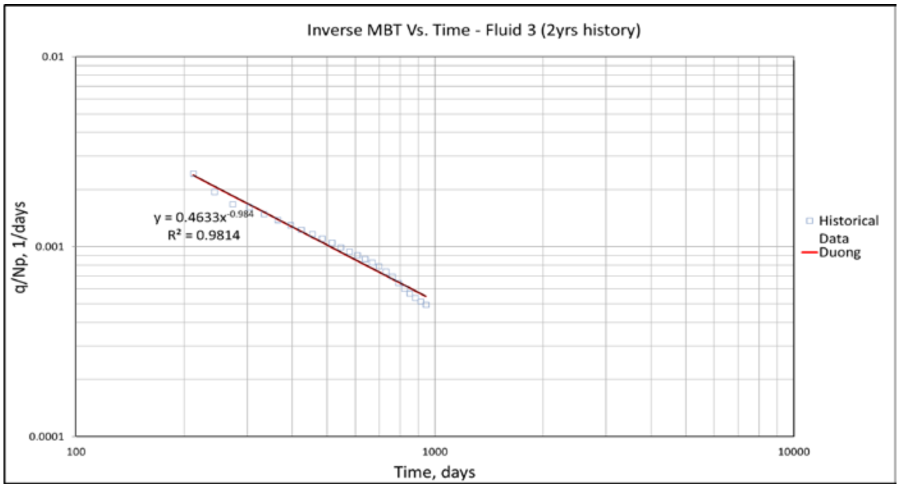

Figure 3-54 Inverse MBT vs. Time – Fluid 3 (2yrs History)

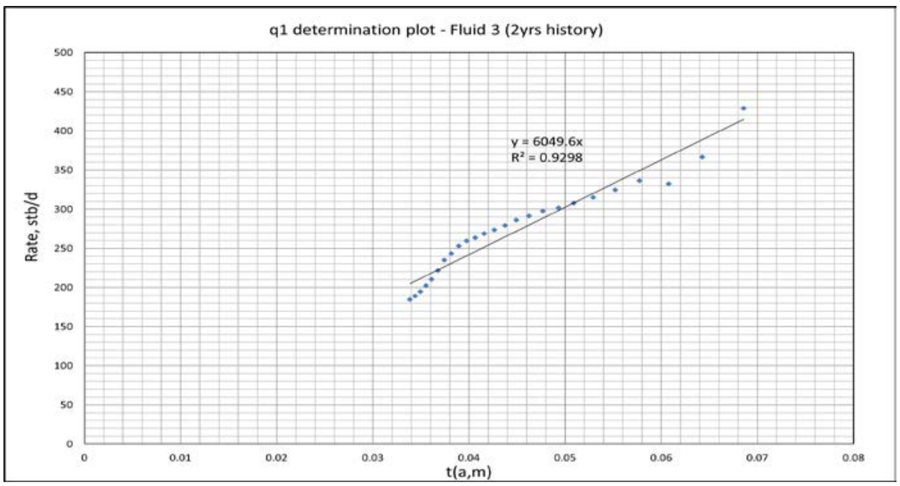

Figure 3-55 q_1 Determination Plot – Fluid 3 (2yrs History)

3.6.3.3. Using 1 year of Simulated Production History – Fluid 3

1. YM-SEPD and YM-SEPD Hybrid Models – Plots and Parameters:

   Table 3-24 and Figure 3-56 show the Yu plot and parameters for the YM-SEPD and Arps' models. In this instance, Yu suggests using the Duong model to forecast to the desired 3 years of production history. Then, we used the Duong model to generate the 2nd and 3rd year pseudohistorical data based on 1 year of simulated production history.

Table 3-24 YM-SEPD and Arps Parameters – Fluid 3 (1yr History)

YM-SEPD Parameters – Fluid 3 (1yr history + Duong pseudohistory)			
n	0.099		
Intercept	1.490		
τ, days	0.018		
q_o, stb/d	4462		
Arps Parameters – Fluid 3 (1yr history + Duong pseudohistory)			
	Arps	Arps(1)	Arps(2)
t_{sw}, days	1308	699	7943
D_{sw}, 1/days	2.3E-4	4E-4	0.009
q_{sw}, stb/d	213.8	256.8	22.50
b	0.1	0.15	0.5

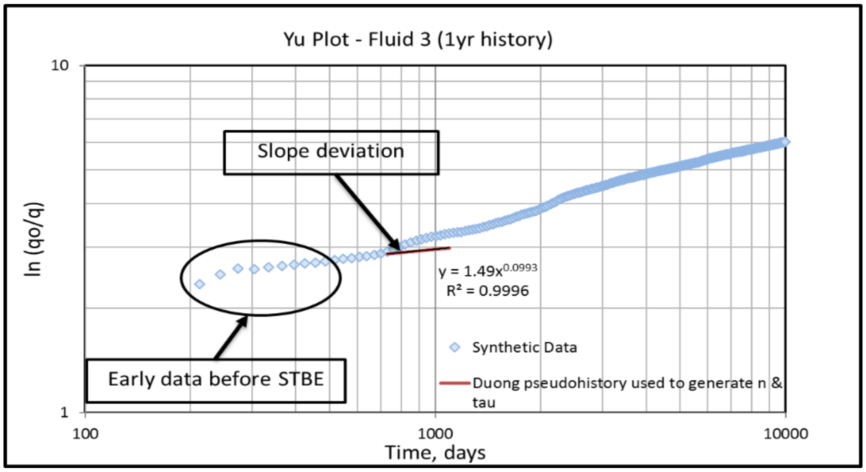

Figure 3-56 Yu Plot – Fluid 3 (1yr History)

2. Duong and Duong Hybrid Models – Plots and Parameters:

   The Duong model plots and parameters used for the Duong and Arps' models are illustrated in Table 3-25, Figures 3-57 and 3-58.

Table 3-25 Duong and Arps Parameters – Fluid 3 (1yr History)

Duong Parameters – Fluid 3 (1yr history)			
a	0.229		
m	-0.865		
q_1, stb/d	6644		
q_∞, stb/d	0		
Arps Parameters – Fluid 3 (1yr history)			
	Arps	Arps(1)	Arps(2)
t_{sw}, days	1308	699	7943
D_{sw}, 1/days	0.004	0.007	0.002
q_{sw}, stb/d	215.3	257.5	111.5
b	1.5	1.5	0.9

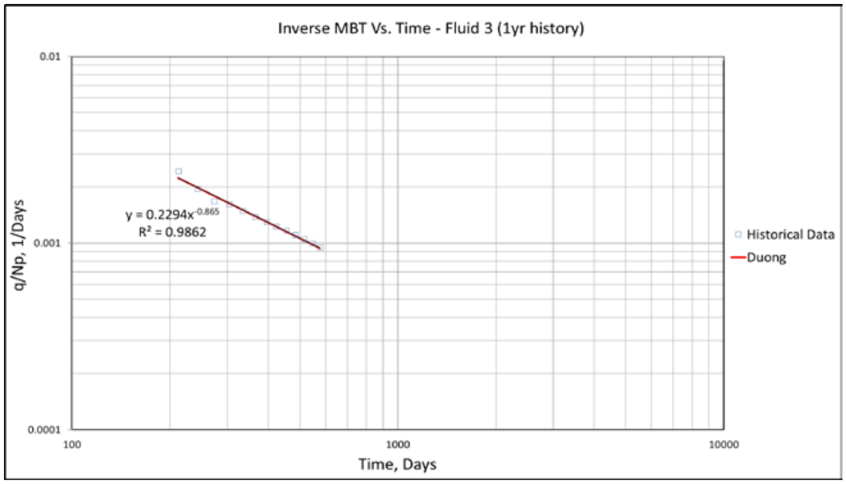

Figure 3-57 Inverse MBT vs. Time – Fluid 3 (1yr History)

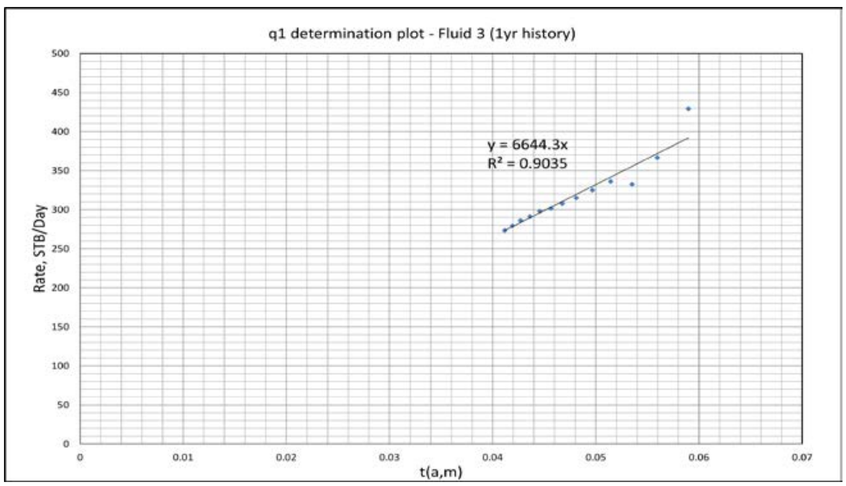

Figure 3-58 q_1 Determination Plot – Fluid 3 (1yr History)

3.6.3.4. Using 6 months of Simulated Production History – Fluid 3

1. YM-SEPD and YM-SEPD Hybrid Models – Plots and Parameters:

   Figure 3-59 and Table 3-26 show the Yu plot and parameters for the YM-SEPD and Arps' models. In this instance, Yu suggests using the Duong model to forecast to the desired 3 years of production history. Further, we used the Duong model to generate the 2nd and 3rd year pseudohistorical data based on 6 months of simulated production history.

Table 3-26 YM-SEPD and Arps Parameters – Fluid 3 (0.5yr History)

YM-SEPD Parameters – Fluid 3 (0.5yr history + Duong pseudohistory)			
n	0.139		
Intercept	1.188		
τ, days	0.289		
q_o, stb/d	4462		
Arps Parameters – Fluid 3 (0.5yr history + Duong pseudohistory)			
	Arps	**Arps(1)**	**Arps(2)**
t_{sw}, days	1308	699	7943
D_{sw}, 1/days	3.4E-4	0.001	0.008
q_{sw}, stb/d	179.7	234.7	17.51
b	0.1	0.35	0.9

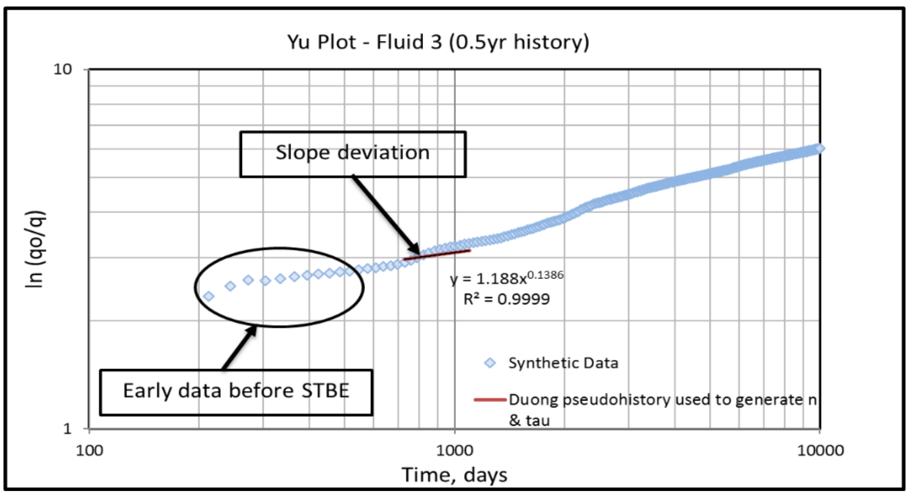

Figure 3-59 Yu Plot – Fluid 3 (0.5yr History)

2. Duong and Duong Hybrid Models – Plots and Parameters:

   The Duong model plots and parameters used for the Duong and Arps' models are illustrated in Table 3-27, Figures 3-60 and 3-61.

Table 3-27 Duong and Arps Parameters – Fluid 3 (0.5yr History)

Duong Parameters – Fluid 3 (0.5yr history)			
a	0.360		
m	-0.945		
q_1, stb/d	6735		
q_∞, stb/d	0		
Arps Parameters – Fluid 3 (0.5yr history)			
	Arps	**Arps(1)**	**Arps(2)**
t_{sw}, days	1308	699	7943
D_{sw}, 1/days	0.007	0.011	0.003
q_{sw}, stb/d	180.8	235.3	61.10
b	0.9	0.9	0.9

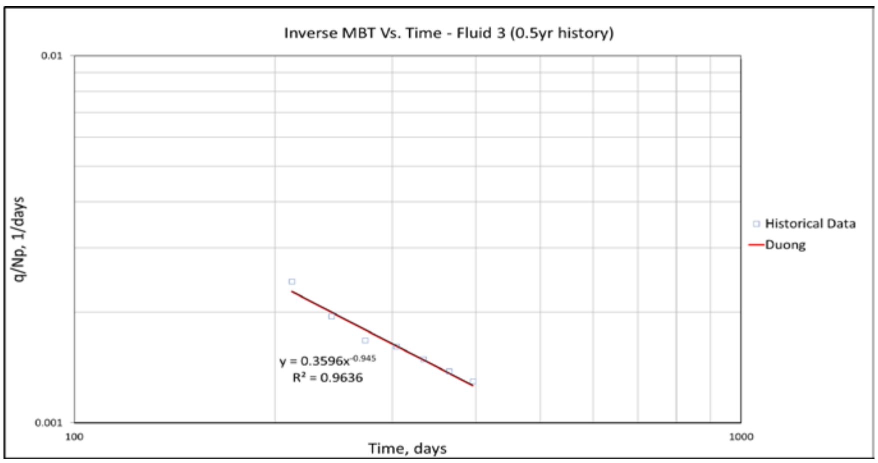

Figure 3-60 Inverse MBT vs. Time – Fluid 3 (0.5yr History)

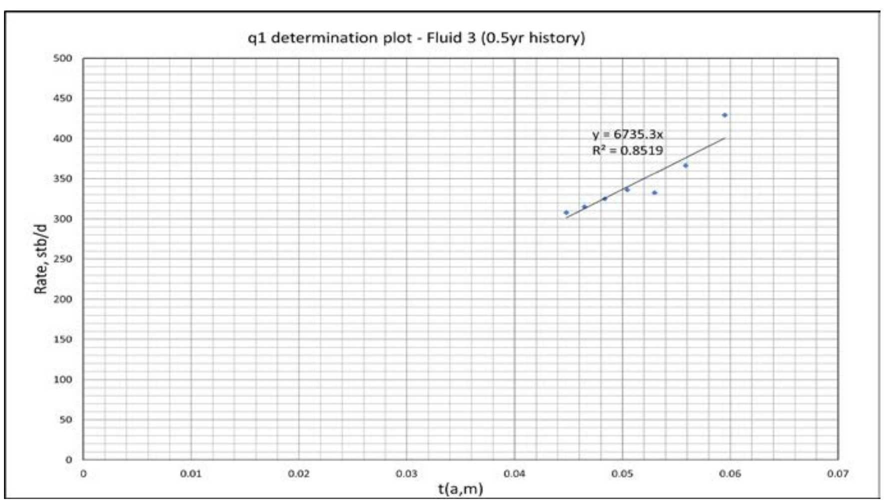

Figure 3-61 q_1 Determination Plot – Fluid 3 (0.5yr History)

Results of production forecasts in comparison to simulated data are shown in Figures 3-62 – 3-65. The YM-SEPD hybrid models led to more accurate forecasts than others in most of the cases. From the plots, it can be seen that the Duong model and its hybrid modifications overestimated production in all instances.

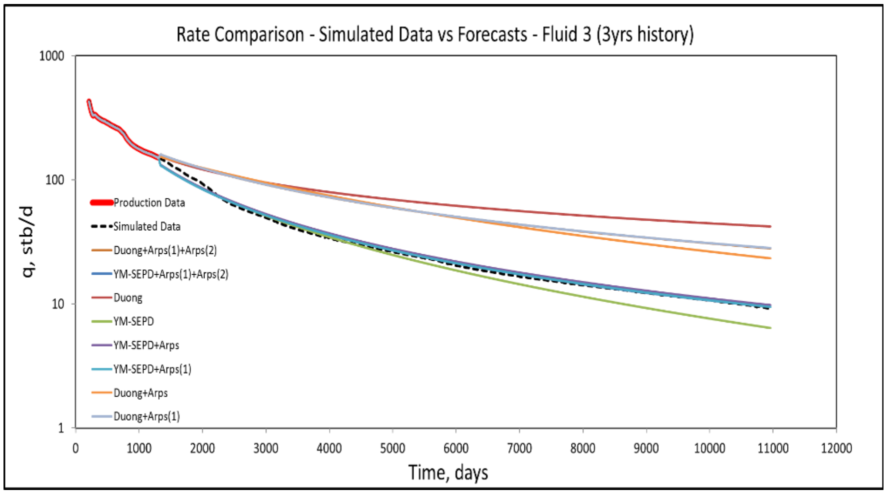

Figure 3-62 Rate Comparisons: Simulated Data vs. Forecasts – Fluid 3 (3yrs History)

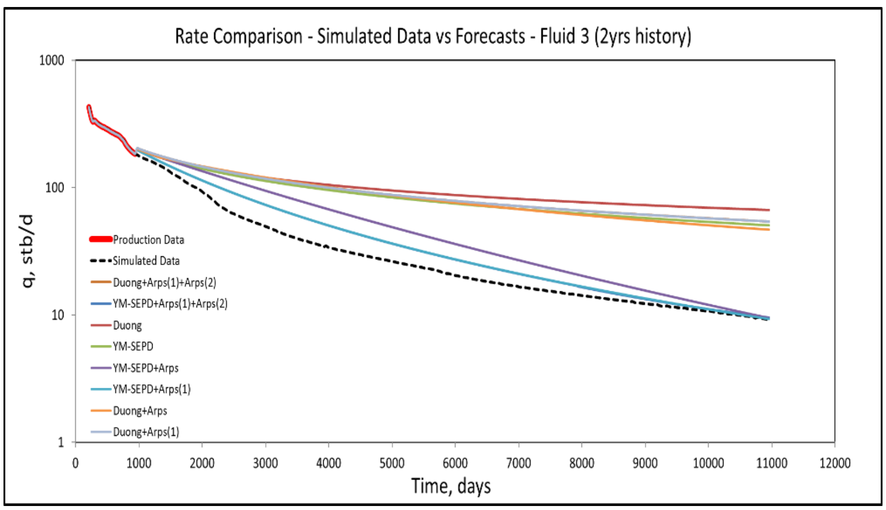

Figure 3-63 Rate Comparisons: Simulated Data vs. Forecasts – Fluid 3 (2yrs History)

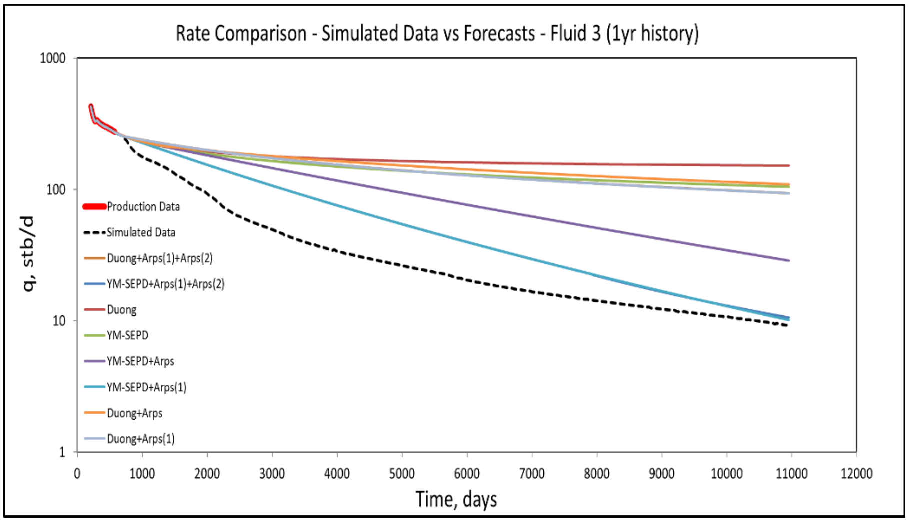

Figure 3-64 Rate Comparisons: Simulated Data vs. Forecasts – Fluid 3 (1yr History)

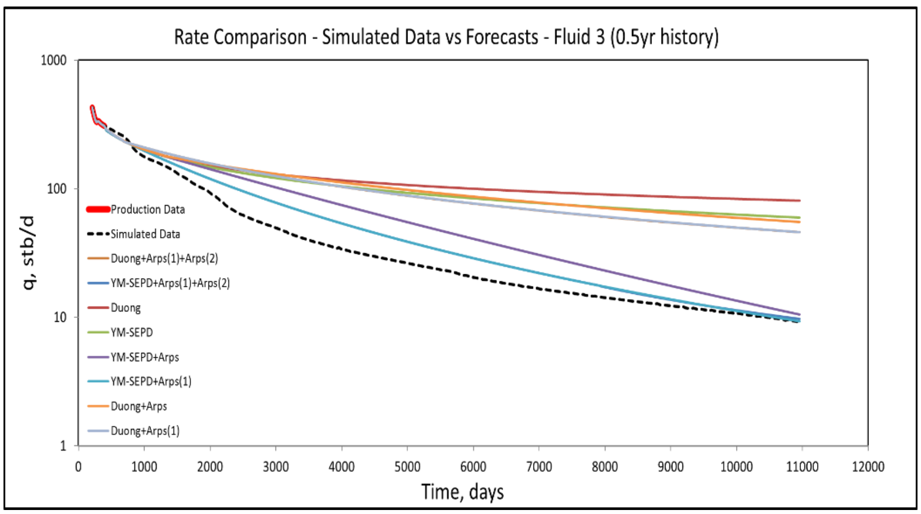

Figure 3-65 Rate Comparisons: Simulated Data vs. Forecasts – Fluid 3 (0.5yr History)

Table 3-28 shows the comparison of percentage errors, absolute errors and forecasts of all the DCA models applied. In the percentage error columns, the figures in red indicate the lowest percentage errors.

Table 3-28 Forecasts, Errors and Percentage Errors – Fluid 3

Cumulative Oil Production Forecast Errors – Fluid 3	Forecast, STB				Error (absolute value), STB				Percentage Error, %			
Matched Production Data	0.5 yr.	1 yr.	2 yrs.	3 yrs.	0.5 yr.	1 yr.	2 yrs.	3 yrs.	0.5 yr.	1 yr.	2 yrs.	3 yrs.
Simulated Data	16572	14842	12115	10135	0	0	0	0	-	-	-	-
YM-SEPD	35957	49056	28695	9429	+19385	+34214	+16580	-706	+53.9	+69.7	+57.8	-7.5
YM-SEPD + Arps(1)	20294	23821	15278	10018	+3722	+8979	+3163	-117	+18.3	+37.7	+20.7	-1.2
YM-SEPD + Arps(1) +Arps(2)	20296	23818	15279	10015	+3724	+8976	+3164	-120	+18.4	+37.7	+20.7	-1.2
Duong	40548	58127	32380	22208	+23976	+43285	+20265	+12073	+59.1	+74.5	+62.6	+54.4
Duong + Arps(1)	34505	49034	29999	19370	+17933	+34192	+17884	+9235	+52.0	+69.7	+59.6	+47.7
Duong + Arps(1) + Arps(2)	34504	49024	30007	19364	+17932	+34182	+17892	+9229	+52.0	+69.7	+59.6	+47.7
YM-SEPD + Arps	24316	33867	18520	10273	+7744	+19025	+6405	+138	+31.9	+56.2	+34.6	+1.3
Duong + Arps	36689	52382	29251	19006	+20117	+37540	17136	+8871	+54.8	+71.7	+58.6	+46.7

3.6.3.5. Solution Gas Production Forecast – Fluid 3

We forecasted solution gas production for Fluid 3 and compared our result to simulated gas production over the period of 30 years. The specialized plot and graphical result are shown in Figures 3-66 and 3-67. The total error in the solution gas forecast was approximately 17.6%.

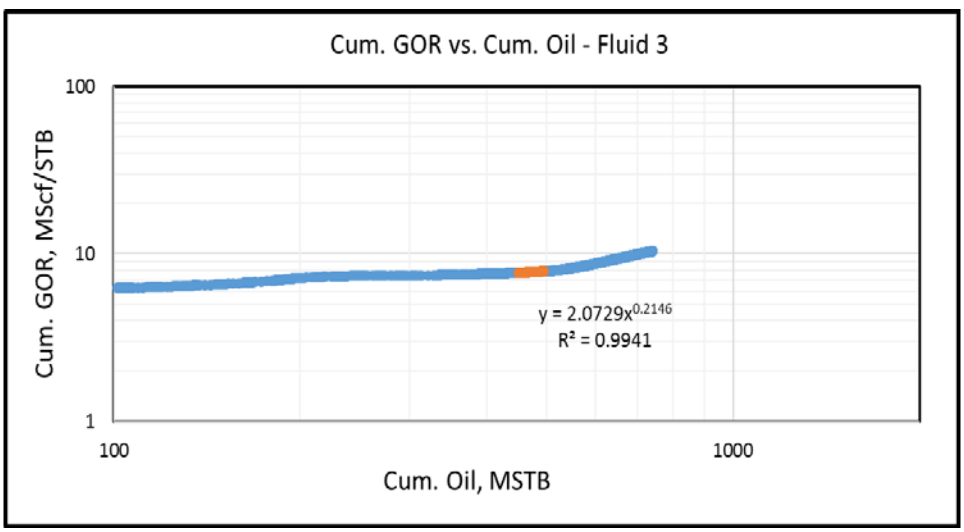

Figure 3-66 Cumulative GOR vs. Cumulative Oil – Fluid 3

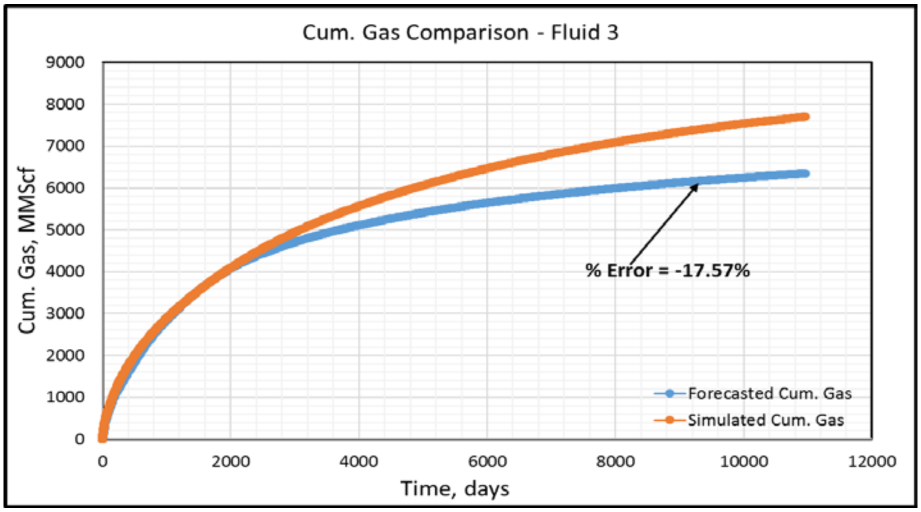

Figure 3-67 Cumulative Gas Comparison – Fluid 3

3.6.4. Fluid 4

Fluid 4 is volatile oil sample with an initial GOR of 2561 scf/bbl. Results of oil and solution gas production forecasts for this case are the following:

3.6.4.1. Using 3 years of Simulated Production History – Fluid 4

1. YM-SEPD and YM-SEPD Hybrid Models – Plots and Parameters:

   Yu plot and parameters generated both for the YM-SEPD model and Arps' models are displayed in Figure 3-68 and Table 3-29. The portion of the Yu plot used to generate n and τ was 2 to 3 years of historical data.

Table 3-29 YM-SEPD and Arps Parameters – Fluid 4 (3yrs History)

YM-SEPD Parameters – Fluid 4 (3yrs history)			
n	0.226		
Intercept	0.688		
τ, days	5.230		
q_o, stb/d	6245		
Arps Parameters – Fluid 4 (3yrs history)			
	Arps	Arps(1)	Arps(2)
t_{sw}, days	1400	212	9039
D_{sw}, 1/days	0.001	0.003	0.004
q_{sw}, stb/d	182.8	622.2	21.69
b	0.55	0.9	0.9

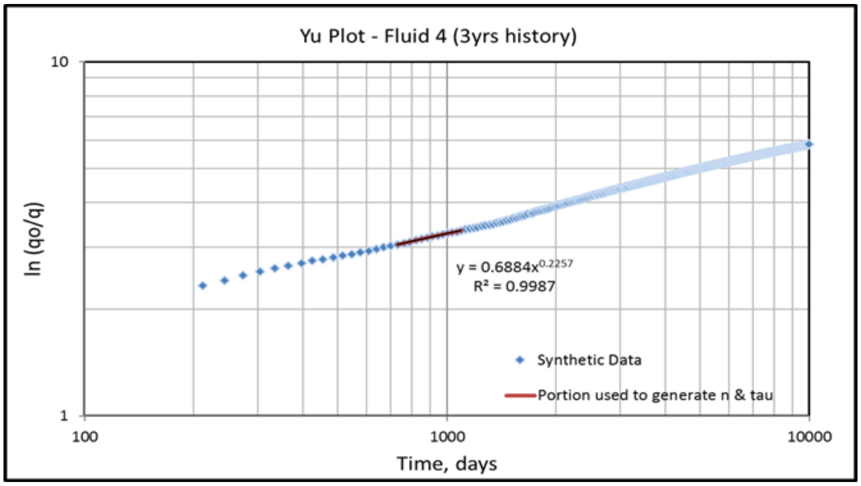

Figure 3-68 Yu Plot – Fluid 4 (3yrs History)

2. Duong and Duong Hybrid Models – Plots and Parameters:

   The inverse MBT vs. time plot, q_1 determination plot and parameters used for the Duong and Arps' models are shown in Table 3-30 as well as Figures 3-69 and 3-70.

Table 3-30 Duong and Arps Parameters – Fluid 4 (3yrs History)

Duong Parameters – Fluid 4 (3yrs history)			
a	1.039		
m	-1.115		
q_1, stb/d	3724		
q_∞, stb/d	0		
Arps Parameters – Fluid 4 (3yrs history)			
	Arps	**Arps(1)**	**Arps(2)**
t_{sw}, days	1400	212	9039
D_{sw}, 1/days	0.012	0.050	0.004
q_{sw}, stb/d	191.0	604.7	31.98
b	0.8	0.9	0.9

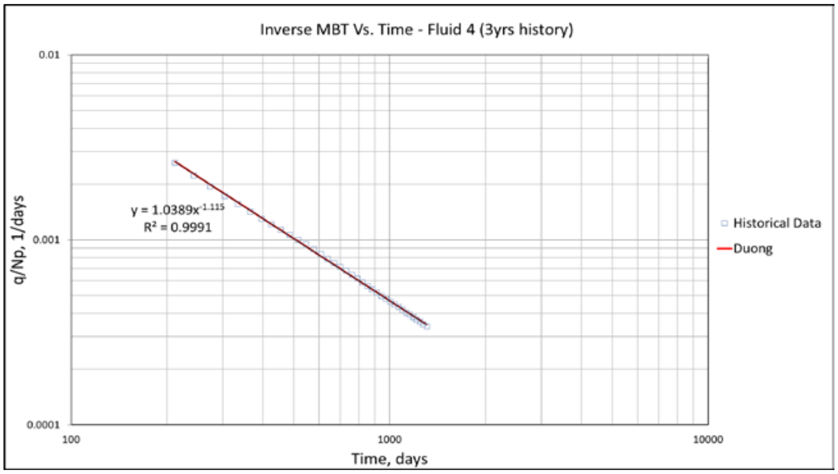

Figure 3-69 Inverse MBT vs. Time – Fluid 4 (3yrs History)

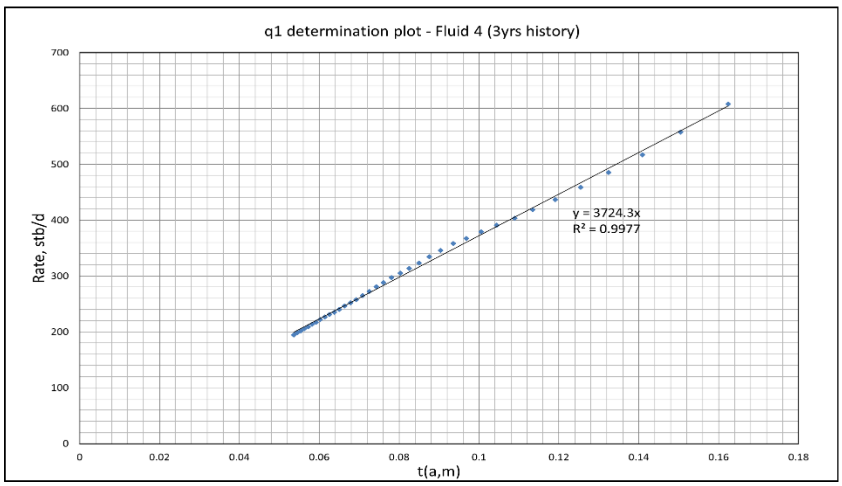

Figure 3-70 q1 Determination Plot – Fluid 4 (3yrs History)

3.6.4.2. Using 2 years of Simulated Production History – Fluid 4

1. YM-SEPD and YM-SEPD Hybrid Models – Plots and Parameters:

   Figure 3-71 and Table 3-31 show the Yu plot and parameters for the YM-SEPD and Arps' models. In this instance, Yu suggests using the Duong model to forecast to the desired 3 years of production history. We then used the Duong model to generate the 2nd and 3rd year pseudohistorical data based on 2 years of simulated production history.

Table 3-31 YM-SEPD and Arps Parameters – Fluid 4 (2yrs History)

YM-SEPD Parameters – Fluid 4 (2yrs history + Duong pseudohistory)			
n	0.191		
Intercept	0.868		
τ, days	2.100		
q_o, stb/d	6245		
Arps Parameters – Fluid 4 (2yrs history + Duong pseudohistory)			
	Arps	**Arps(1)**	**Arps(2)**
t_{sw}, days	1400	212	9039
D_{sw}, 1/days	0.001	0.002	0.004
q_{sw}, stb/d	197.6	561.0	22.31
b	0.43	0.9	0.9

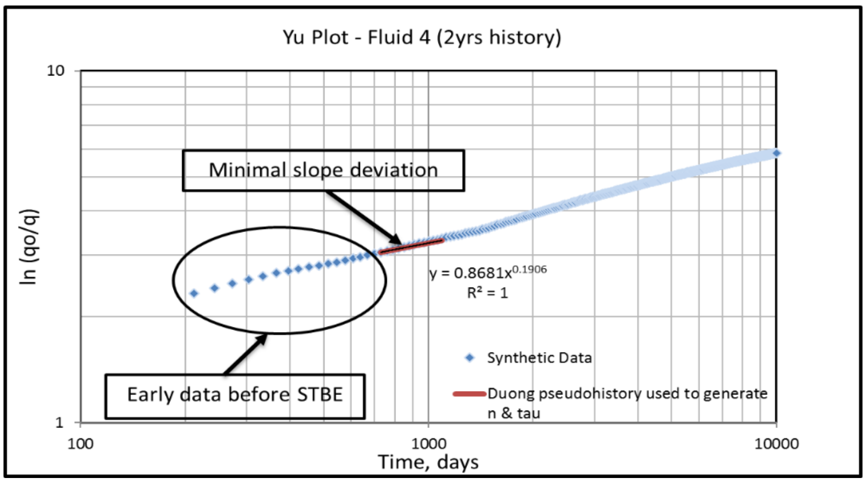

Figure 3-71 Yu Plot – Fluid 4 (2yrs History)

In Figure 3-71 above, there is minimal slope deviation of the Duong pseudohistorical data in comparison to the synthetic data. Therefore, more "favorable" n and τ parameters were generated in this case. The minimal slope deviation of the Duong pseudohistorical data was because after the end of linear flow, a "near-linear" flow regime (though still in the transition flow regime period) continued for some time (Fig. 3-5). Due to this, the Duong model was able to calculate a reasonably good forecast for the 2nd and 3rd year of production.

2. Duong and Duong Hybrid Models – Plots and Parameters:

The Duong model plots as well as parameters used for the Duong and Arps' models are shown in Table 3-32, Figures 3-72 and 3-73.

Table 3-32 Duong and Arps Parameters – Fluid 4 (2yrs History)

Duong Parameters – Fluid 4 (2yrs history)			
a	0.895		
m	-1.090		
q_1, stb/d	4569		
q_∞, stb/d	0		
Arps Parameters – Fluid 4 (2yrs history)			
	Arps	**Arps(1)**	**Arps(2)**
t_{sw}, days	1400	212	9039
D_{sw}, 1/days	0.011	0.060	0.002
q_{sw}, stb/d	198.9	596.6	52.27
b	0.8	1.3	0.9

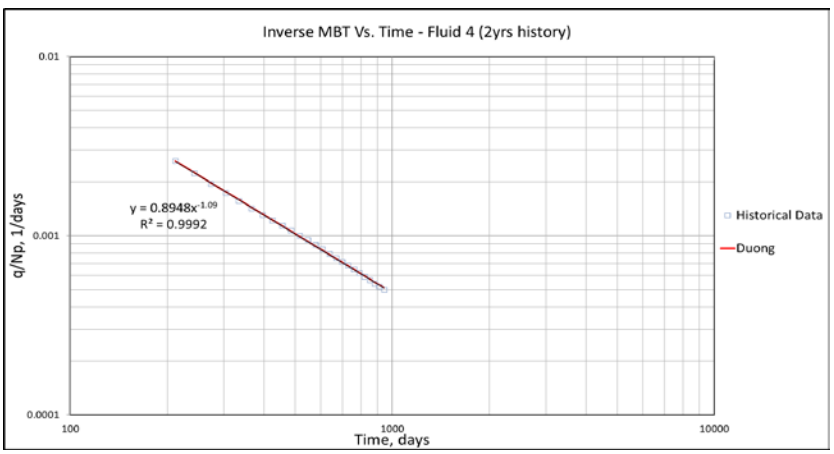

Figure 3-72 Inverse MBT vs. Time – Fluid 4 (2yrs History)

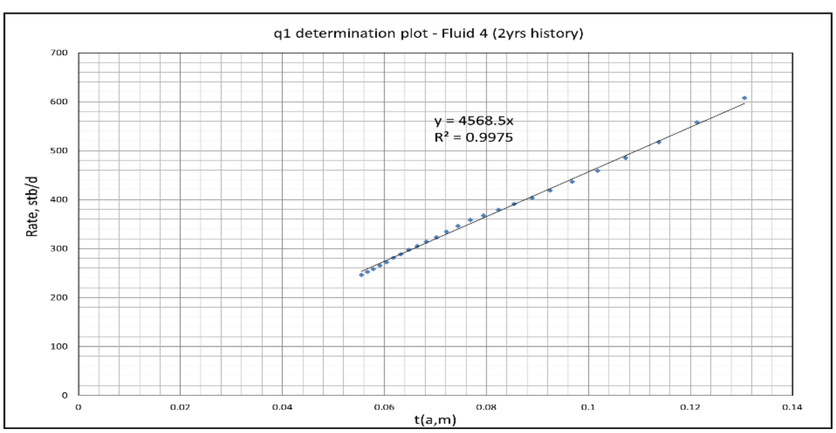

Figure 3-73 q_1 Determination Plot – Fluid 4 (2yrs History)

3.6.4.3. Using 1 year of Simulated Production History – Fluid 4

1. YM-SEPD and YM-SEPD Hybrid Models – Plots and Parameters:

   Figure 3-74 and Table 3-33 show the Yu plot and parameters for the YM-SEPD and Arps' models. Here, Yu proposes using the Duong model to forecast to the desired 3 years of production history. Hence, we used the Duong model to generate the 2nd and 3rd year pseudohistorical data based on 1 year of simulated production history.

Table 3-33 YM-SEPD and Arps Parameters – Fluid 4 (1yr History)

YM-SEPD Parameters – Fluid 4 (1yr history + Duong pseudohistory)			
n	0.180		
Intercept	0.922		
τ, days	1.574		
q_o, stb/d	6245		
Arps Parameters – Fluid 4 (1yr history + Duong pseudohistory)			
	Arps	**Arps(1)**	**Arps(2)**
t_{sw}, days	1400	212	9039
D_{sw}, 1/days	4E-4	0.002	0.004
q_{sw}, stb/d	208.0	554.9	22.19
b	0.35	0.88	0.9

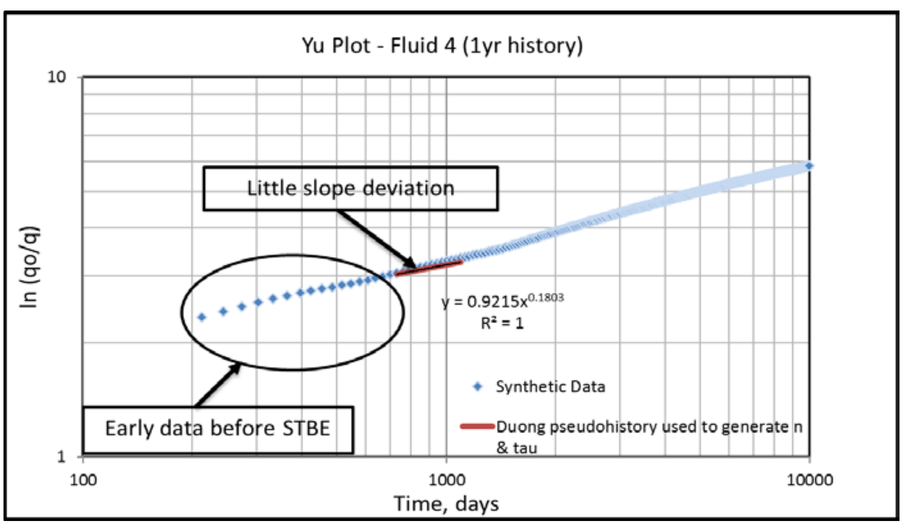

Figure 3-74 Yu Plot – Fluid 4 (1yr History)

2. Duong and Duong Hybrid Models – Plots and Parameters:

The Duong model plots as well as parameters used for the Duong and Arps' models are shown in Table 3-34, Figures 3-75 and 3-76.

Table 3-34 Duong and Arps Parameters – Fluid 4 (1yr History)

Duong Parameters – Fluid 4 (1yr history)			
a	0.762		
m	-1.063		
q_1, stb/d	5490		
q_∞, stb/d	0		
Arps Parameters – Fluid 4 (1yr history)			
	Arps	**Arps(1)**	**Arps(2)**
t_{sw}, days	1400	212	9039
D_{sw}, 1/days	0.011	0.061	0.002
q_{sw}, stb/d	209.2	591.0	64.67
b	0.95	1.5	0.9

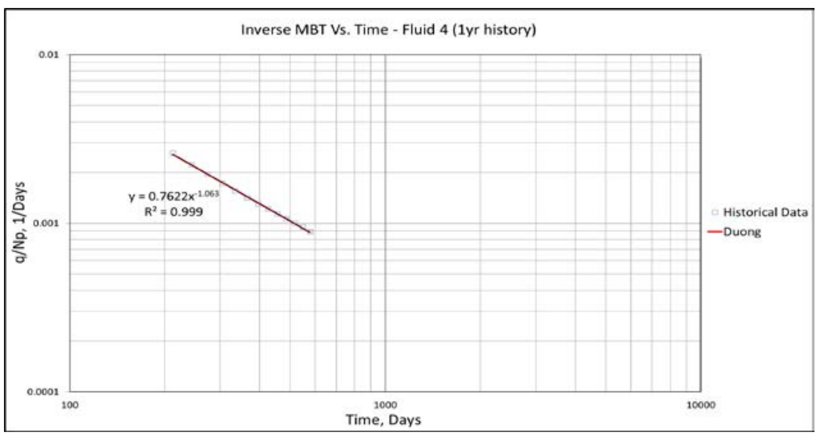

Figure 3-75 Inverse MBT vs. Time – Fluid 4 (1yr History)

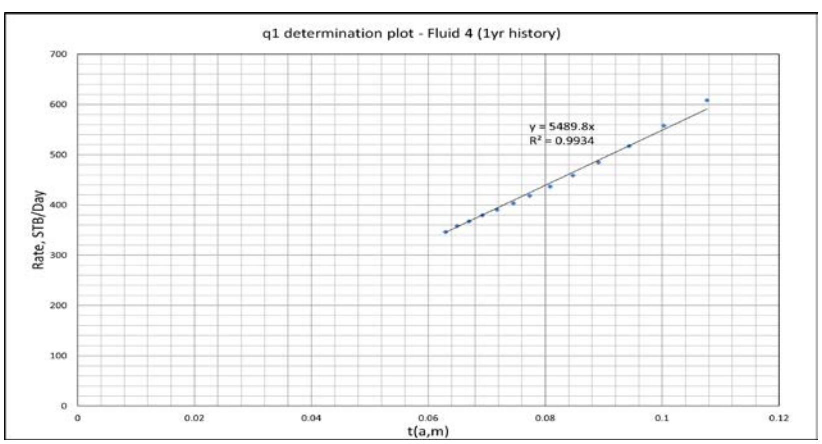

Figure 3-76 q_1 Determination Plot – Fluid 4 (1yr History)

3.6.4.4. Using 6 months of Simulated Production History – Fluid 4

1. YM-SEPD and YM-SEPD Hybrid Models – Plots and Parameters:

   Figure 3-77 and Table 3-35 show the Yu plot and parameters for the YM-SEPD and Arps' models. Yu proposes using the Duong model to forecast to the desired 3 years of production history. Therefore, we used the Duong model to generate the 2nd and 3rd year pseudohistorical data based on 6 months of simulated production history.

Table 3-35 YM-SEPD and Arps Parameters – Fluid 4 (0.5yr History)

YM-SEPD Parameters – Fluid 4 (0.5yr history)			
n	0.201		
Intercept	0.819		
τ, days	2.697		
q_o, stb/d	6245		
Arps Parameters – Fluid 4 (0.5yr history)			
	Arps	Arps(1)	Arps(2)
t_{sw}, days	1400	212	9039
D_{sw}, 1/days	0.001	0.002	0.004
q_{sw}, stb/d	185.6	563.5	22.28
b	0.5	0.92	0.9

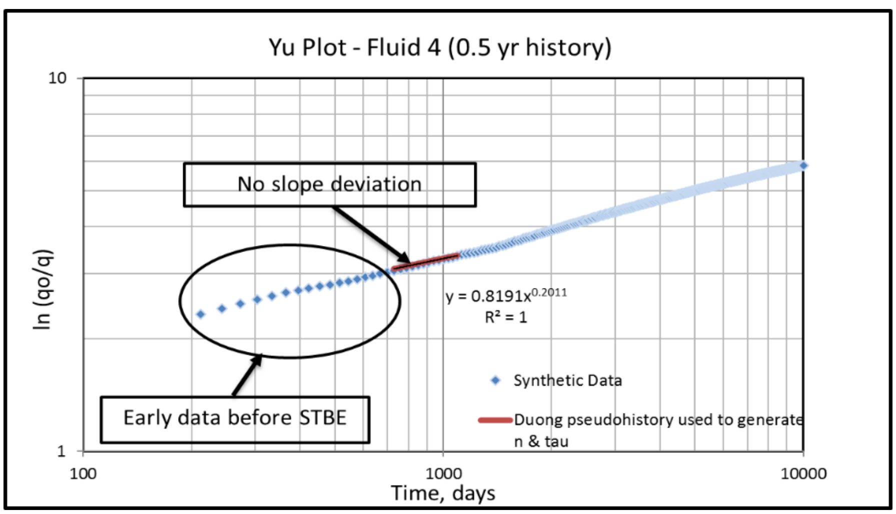

Figure 3-77 Yu Plot – Fluid 4 (0.5yr History)

2. Duong and Duong Hybrid Models – Plots and Parameters:

The Duong model plots as well as parameters used for the Duong and Arps' models are shown in Table 3-36, Figures 3-78 and 3-79.

Table 3-36 Duong and Arps Parameters – Fluid 4 (0.5yr History)

Duong Parameters – Fluid 4 (0.5yr history)			
a	1.015		
m	-1.114		
q_1, stb/d	4015		
q_∞, stb/d	0		
Arps Parameters – Fluid 4 (0.5yr history)			
	Arps	**Arps(1)**	**Arps(2)**
t_{sw}, days	1400	212	9039
D_{sw}, 1/days	0.012	0.060	0.003
q_{sw}, stb/d	187.0	591.0	45.05
b	0.8	1.2	0.9

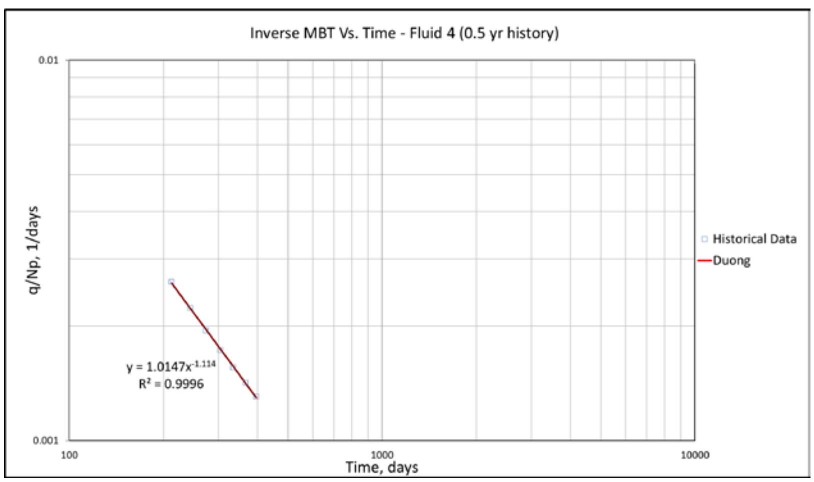

Figure 3-78 Inverse MBT vs. Time – Fluid 4 (0.5yr History)

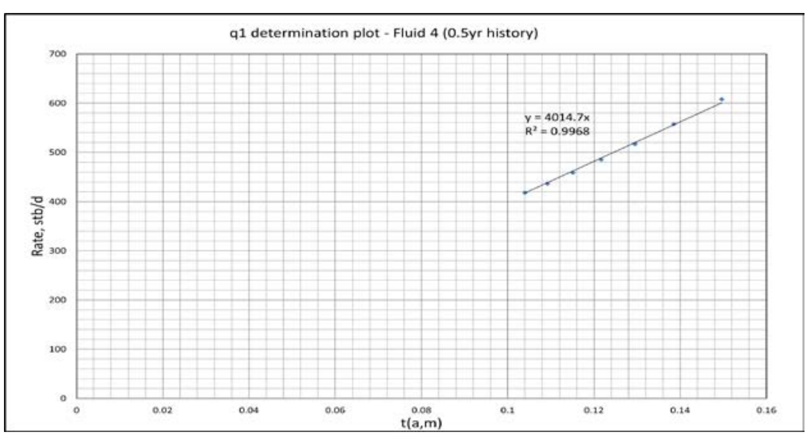

Figure 3-79 q_1 Determination Plot – Fluid 4 (0.5yr History)

Simulated data were compared to production forecasts as shown in Figures 3-80 – 3-83. It can be observed in all cases, that the Duong model and its hybrid alternatives overestimated production (overestimation relatively less than in fluid 1 cases). The simple YM-SEPD model led to better forecasts than the Duong models, whereas the YM-SEPD hybrid models led to the most accurate forecasts.

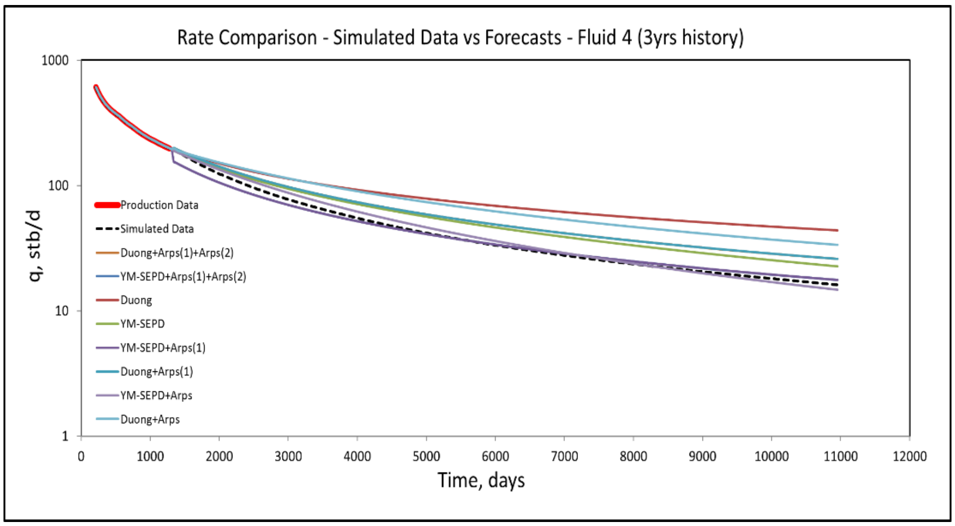

Figure 3-80 Rate Comparisons: Simulated Data vs. Forecasts – Fluid 4 (3yrs History)

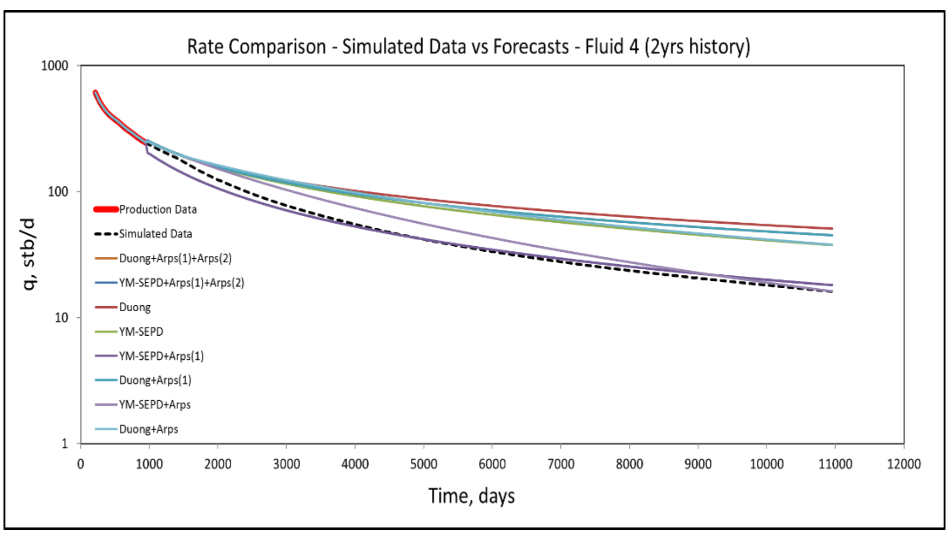

Figure 3-81 Rate Comparisons: Simulated Data vs. Forecasts – Fluid 4 (2yrs History)

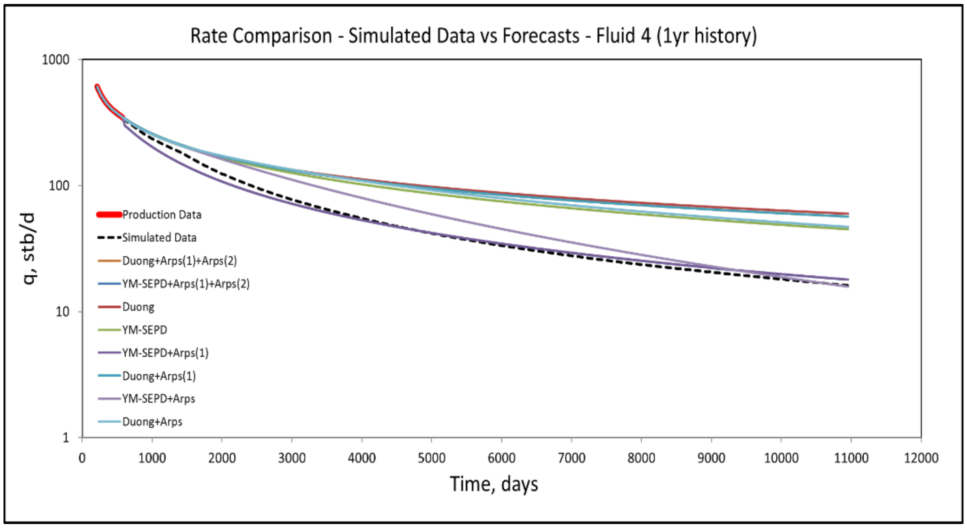

Figure 3-82 Rate Comparisons: Simulated Data vs. Forecasts – Fluid 4 (1yr History)

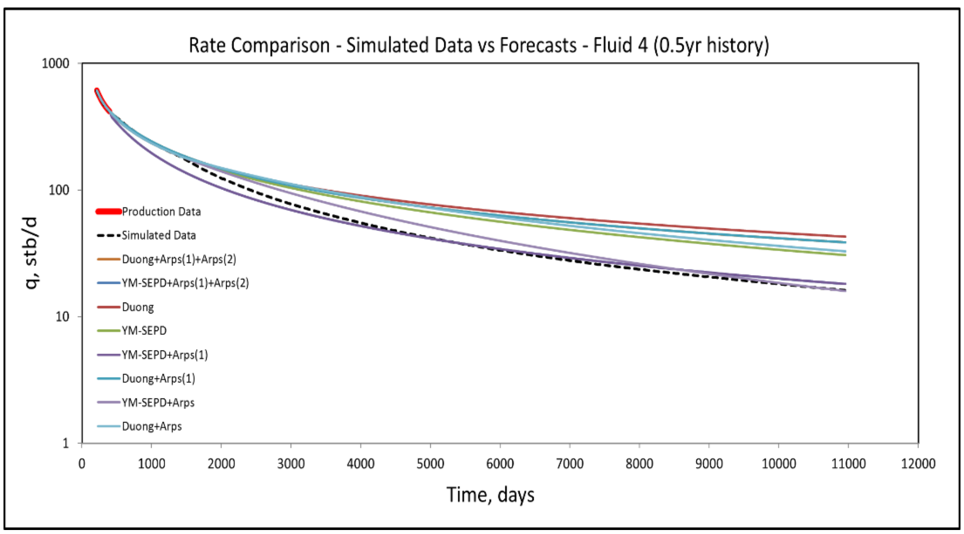

Figure 3-83 Rate Comparisons: Simulated Data vs. Forecasts – Fluid 4 (0.5yr History)

Also, Table 3-37 shows the comparison of percentage errors, absolute errors and forecasts of all the DCA models applied. In the percentage error columns, the figures in red indicate the lowest percentage errors.

Table 3-37 Forecast, Errors and Percentage Errors – Fluid 4

Cumulative Oil Production Forecast Errors – Fluid 4	Forecast, STB				Error (absolute value), STB				Percentage Error, %			
Matched Production Data	0.5 yr.	1 yr.	2 yrs.	3 yrs.	0.5 yr.	1 yr.	2 yrs.	3 yrs.	0.5 yr.	1 yr.	2 yrs.	3 yrs.
Simulated Data	23613	21368	17932	15336	0	0	0	0	-	-	-	-
YM-SEPD	29862	34138	27512	18967	+6249	+12770	+9580	+3631	+20.9	+37.4	+34.8	+19.1
YM-SEPD + Arps(1)	21355	19816	16644	14261	-2258	-1552	-1288	-1075	-10.6	-7.8	-7.7	-7.5
YM-SEPD + Arps(1) +Arps(2)	21352	19815	16641	14258	-2261	-1553	-1291	-1078	-10.6	-7.8	-7.8	-7.6
Duong	32973	37618	30741	25554	+9360	+16250	+12809	+10218	+28.4	+43.2	+41.7	+39.9
Duong + Arps(1)	32127	37091	29219	20054	+8514	+15723	+11287	+4718	+26.5	+42.4	+38.6	+23.5
Duong + Arps(1) + Arps(2)	32125	37089	29216	20050	+8512	+15721	+11284	+4714	+26.5	+42.4	+38.6	+23.5
YM-SEPD + Arps	25626	26421	21637	16367	+2013	+3253	+3705	+1031	+7.9	+12.3	+17.1	+6.3
Duong + Arps	31311	35445	28585	23702	7698	+14077	+10653	+8366	+24.6	+39.7	+37.3	+35.3

3.6.4.5. Solution Gas Production Forecast – Fluid 4

We forecasted solution gas production for Fluid 4 and compared our result to simulated gas production over the period of 30 years. The specialized plot and graphical result are shown in Figures 3-84 and 3-85. The total error in the solution gas forecast was approximately 16.9%.

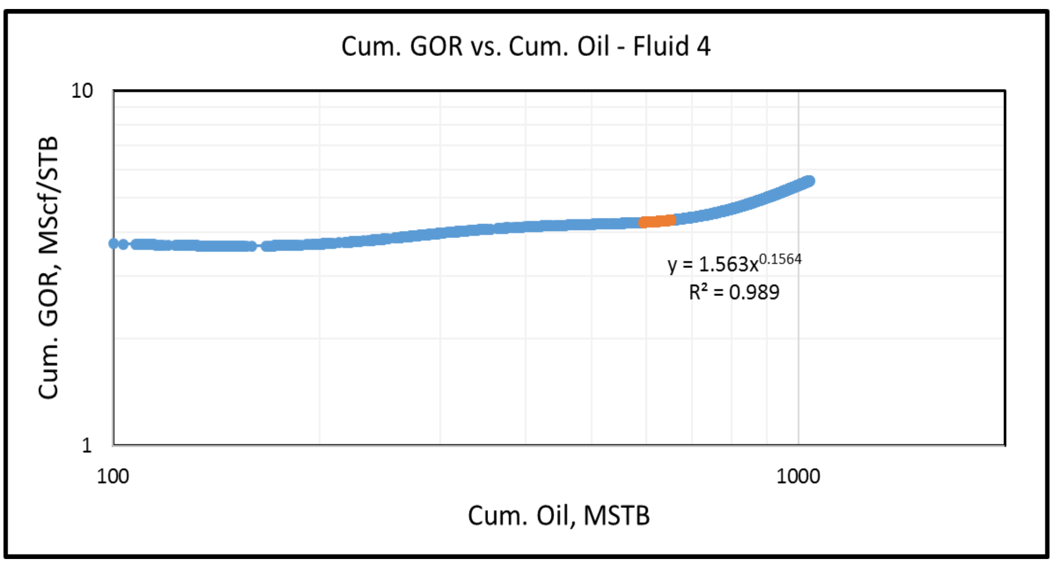

Figure 3-84 Cumulative GOR vs. Cumulative Oil – Fluid 4

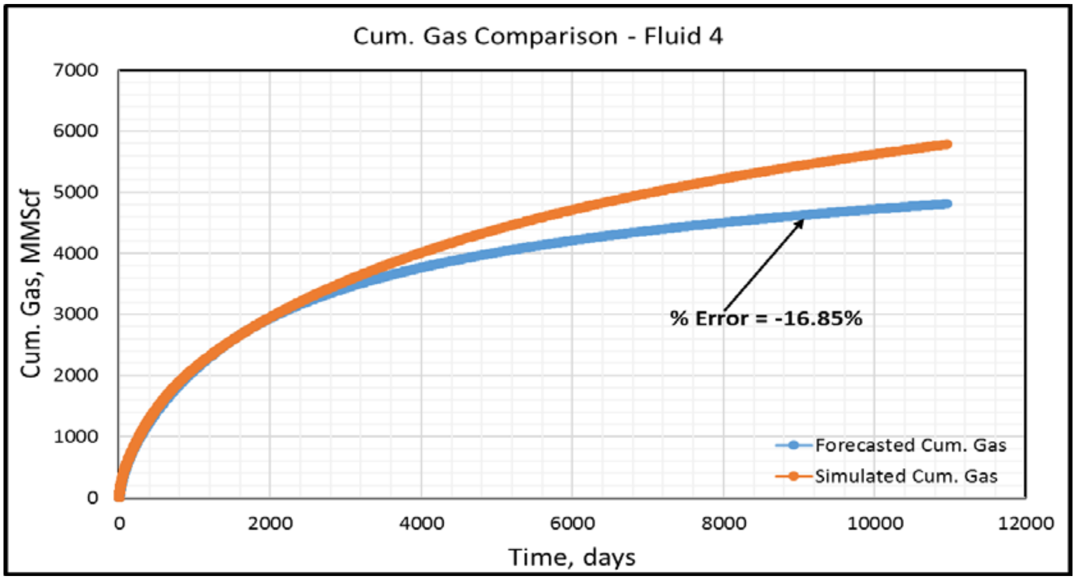

Figure 3-85 Cumulative Gas Comparison – Fluid 4

3.7. Example – Field Data

YM-SEPD and YM-SEPD + Arps(1) DCA models were tested on field data from a well (in a shale volatile oil reservoir) with a short production history. The reservoir fluid has an initial GOR of approximately 2633 scf/bbl. From the diagnostic plot in Figure 3-86, the well exhibits linear flow to about 200 days, perhaps followed by a transition region. Figures 3-87 and 3-88 show the Yu plot and oil rate vs. time forecasts.

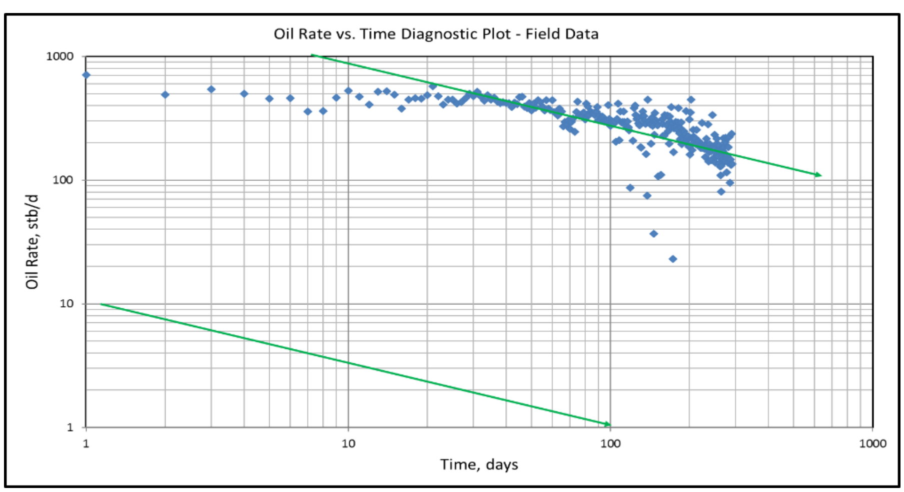

Figure 3-86 Oil Rate vs. Time Diagnostic Plot – Field Data

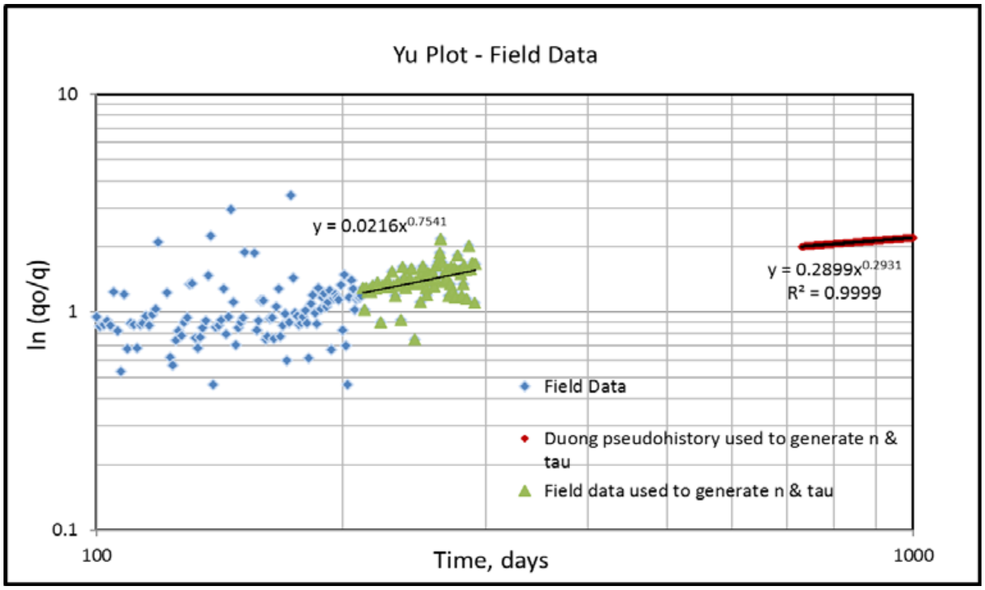

Figure 3-87 Yu Plot – Field Data

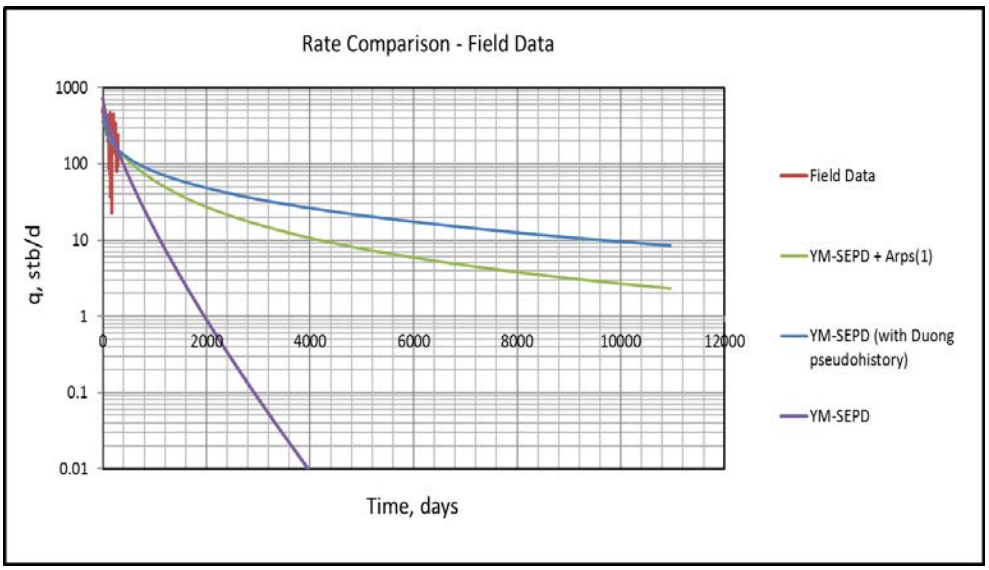

Figure 3-88 Rate Comparisons – Field Data

The Duong model was used to forecast the 2nd and 3rd year data based on the field data. The Duong forecast was then used to generate the parameters n and τ. In another case, we calculated parameters n and τ directly using the field data. The results were compared to the YM-SEPD +Arps(1) hybrid model. We can observe that simple YM-SEPD model almost certainly seriously underestimated future production. Using the Duong 2nd and 3rd year pseudohistorical data and the YM-SEPD + Arps(1) hybrid model led to more reasonable-looking forecasts. It should be noted that the hybrid model forecast in this case can vary depending on the decline exponent (b value) used. Here, the b value was 0.6.

3.8. Modified Duong Model

Due to the importance of the nature of data used to generate model parameters, we examined the idea of selecting a suitable set of historical data to calculate parameters, a and m, to reduce the overestimates of future production by the original Duong model (Makinde and Lee, 2016). In other words, we eliminated early "bad" data and chose data on a straight (or nearly straight) line on the Inverse MBT vs. Time plot, to compute parameters, a and m. We considered the case of 3 years' production history and modified the Duong model by using historical data from the 2nd to 3rd year on the Inverse MBT vs. Time plot; that are on a straight (or nearly straight) line. These historical data enabled us to generate parameters, a and m, that led to a straight (or nearly straight) line on the rate – t(a,m) plot.

3.8.1. Fluid 1 – Modified Duong Model

Figures 3-89 – 3-91 show the plots for Fluid 1. The small value of the slope of the rate – t(a,m) plot in this case, is as a result of the large value of parameter "a" calculated from the Inverse MBT vs Time plot. However, the values of t(a,m) obtained (with equation 5), compensated for this small value and led to a good forecast. Table 3-38 shows the results of the Modified Duong forecast in comparison to the original Duong model forecast and the simulated data. For Fluid 1, the percentage error in the forecast was reduced from 49% (original Duong model) to approximately 2%.

Table 3-38 Forecasts, Errors and Percentage Errors – Fluid 1 (Modified Duong)

Cumulative Oil Production Forecast Errors – Fluid 1	Forecast, STB	Error (absolute value), STB	Percentage Error, %
Matched Production Data	3 yrs.	3 yrs.	3 yrs.
Simulated Data	12392	0	-
Duong	24364	+11972	+49.2
Modified Duong	12598	+206	+1.6

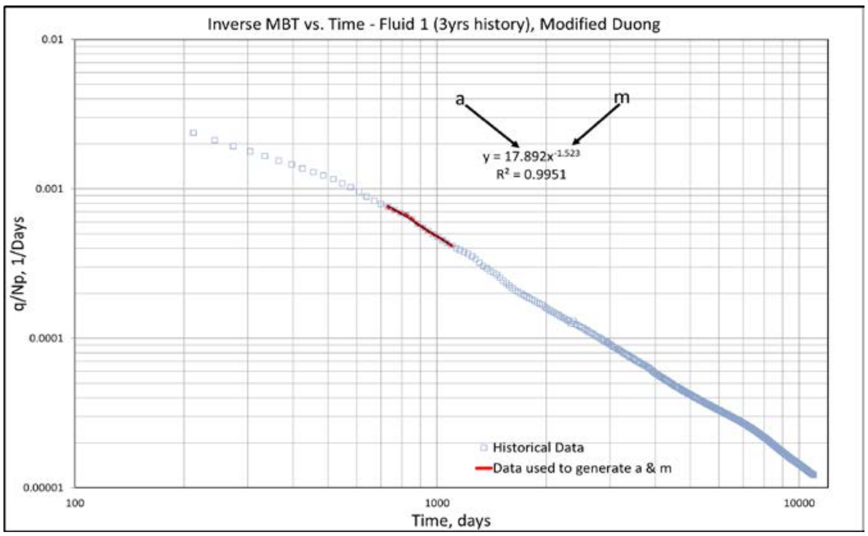

Figure 3-89 Inverse MBT vs. Time – Fluid 1 (Modified Duong)

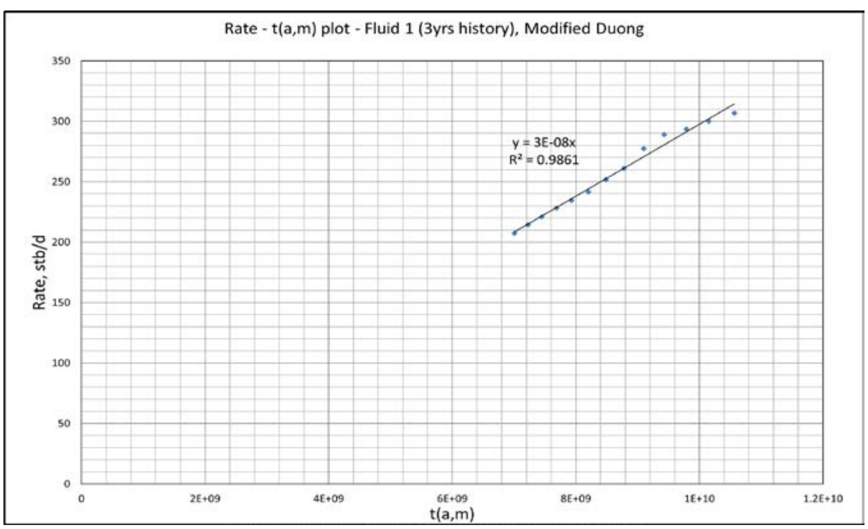

Figure 3-90 Rate - t(a,m) Plot – Fluid 1 (Modified Duong)

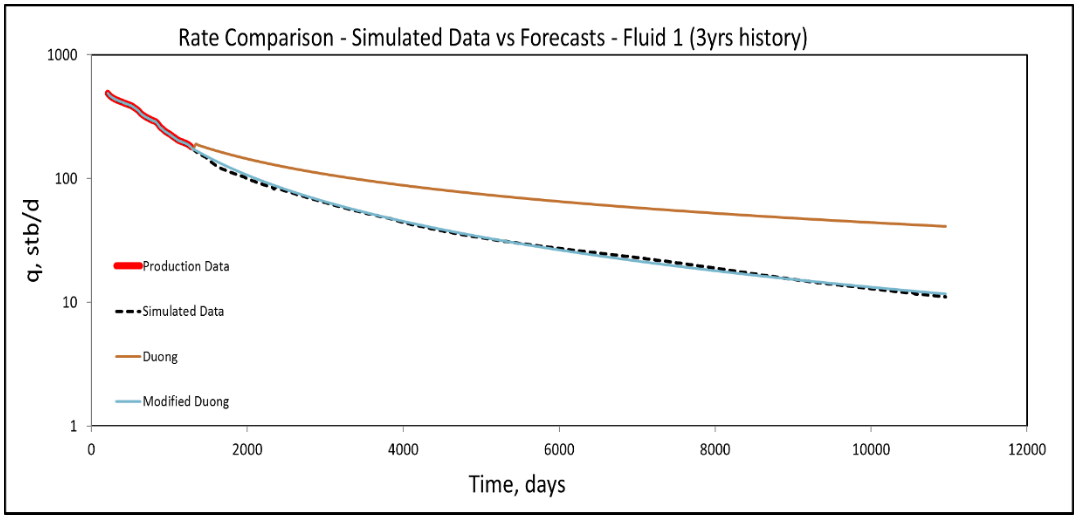

Figure 3-91 Rate Comparisons: Simulated Data vs. Forecasts – Fluid 1 (Modified Duong)

3.8.2. Fluid 2 – Modified Duong Model

The plots for Fluid 2 are shown in Figures 3-92 to 3-94. Table 3-39 shows the results of the Modified Duong forecast in comparison to the original Duong model forecast and the simulated data. For Fluid 2, the percentage error in the forecast was reduced from 47% (original Duong model) to approximately 21%.

Table 3-39 Forecasts, Errors and Percentage Errors – Fluid 2 (Modified Duong)

Cumulative Oil Production Forecast Errors – Fluid 2	Forecast, STB	Error (absolute value), STB	Percentage Error, %
Matched Production Data	3 yrs.	3 yrs.	3 yrs.
Simulated Data	8641	0	-
Duong	16398	+7757	+47.3
Modified Duong	10939	+2298	+21.0

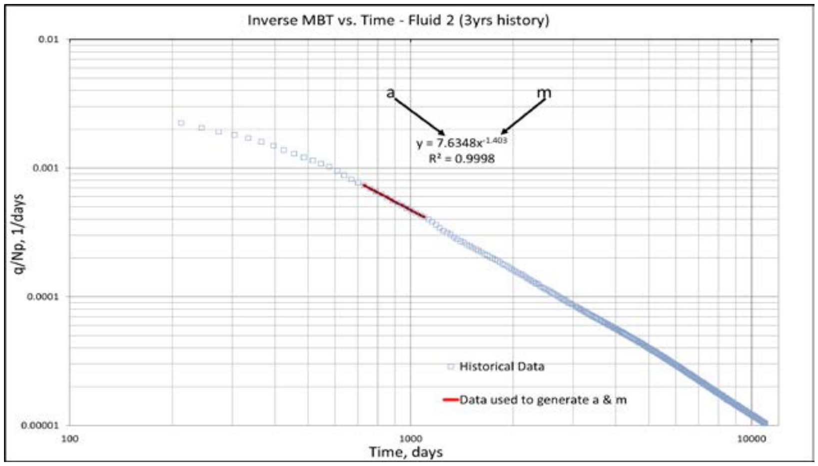

Figure 3-92 Inverse MBT vs. Time – Fluid 2 (Modified Duong)

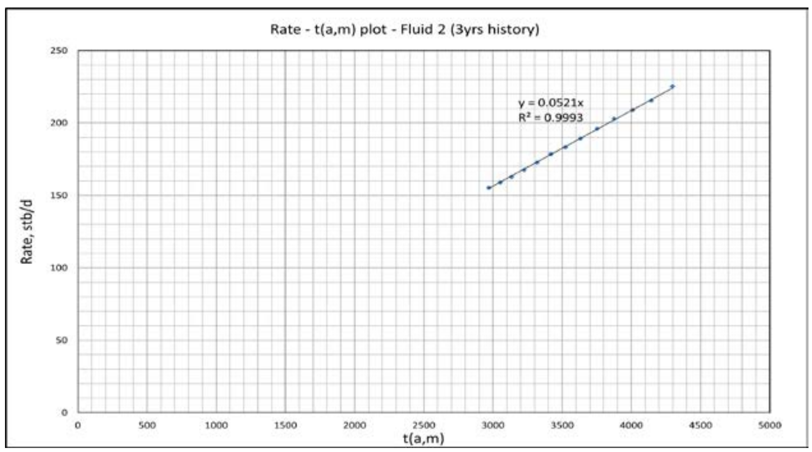

Figure 3-93 Rate - t(a,m) Plot – Fluid 2 (Modified Duong)

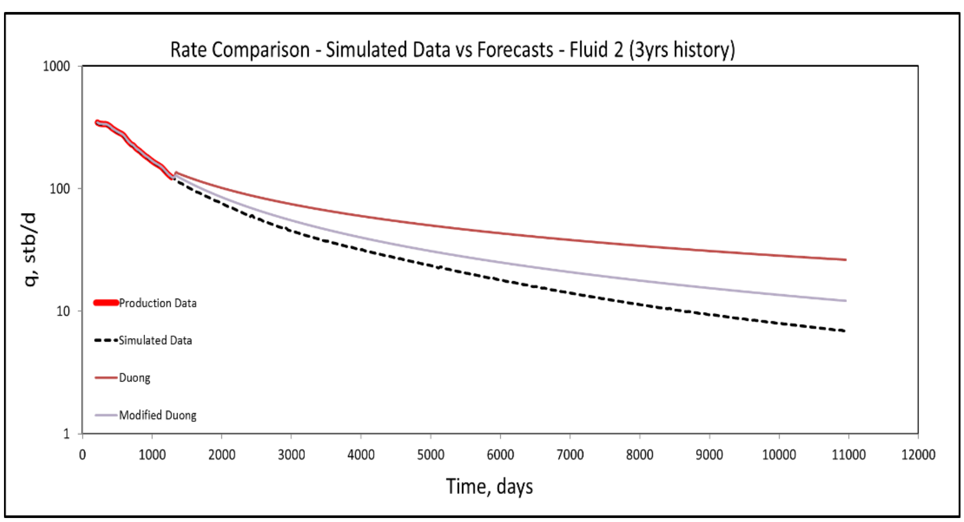

Figure 3-94 Rate Comparisons: Simulated Data vs. Forecasts – Fluid 2 (Modified Duong)

3.8.3. Fluid 3 – Modified Duong Model

Figures 3-95 – 3-97 show the plots for Fluid 3. Table 3-40 shows the results of the Modified Duong forecast in comparison to the original Duong model forecast and the simulated data. For Fluid 3, the percentage error in the forecast was reduced from 54% (original Duong model) to approximately 13%.

Table 3-40 Forecasts, Errors and Percentage Errors – Fluid 3 (Modified Duong)

Cumulative Oil Production Forecast Errors – Fluid 3	Forecast, STB	Error (absolute value), STB	Percentage Error, %
Matched Production Data	3 yrs.	3 yrs.	3 yrs.
Simulated Data	10135	0	-
Duong	22208	+12073	+54.4
Modified Duong	11676	+1541	+13.2

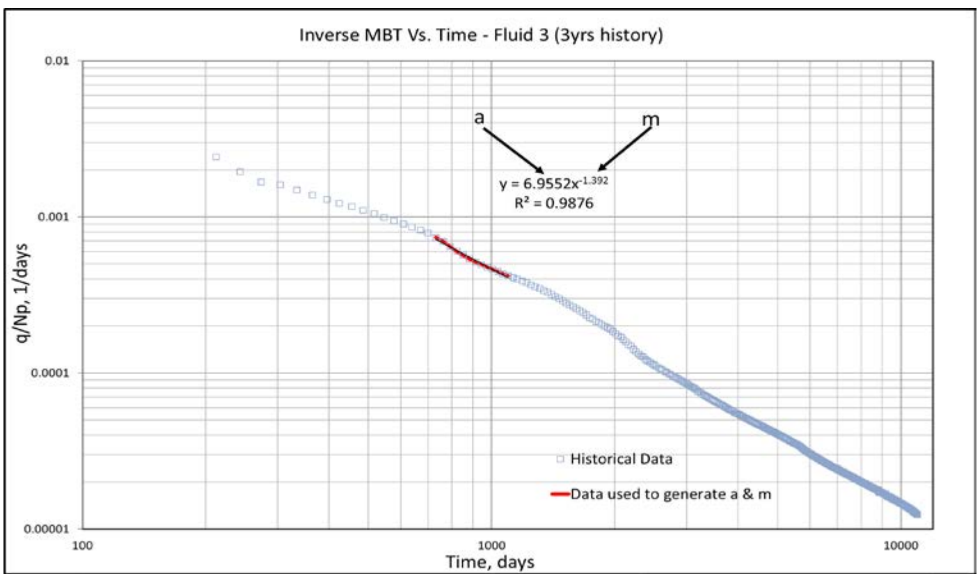

Figure 3-95 Inverse MBT vs. Time – Fluid 3 (Modified Duong)

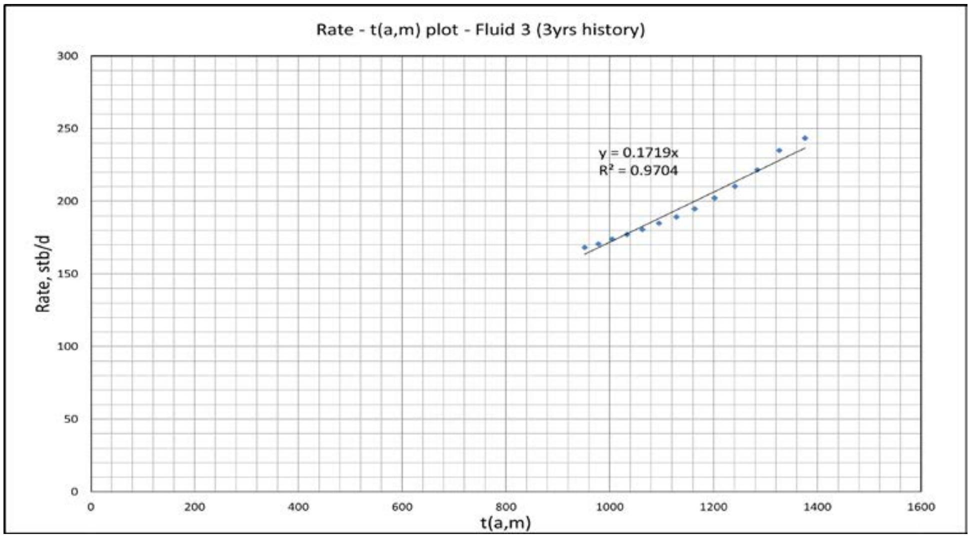

Figure 3-96 Rate - t(a,m) Plot – Fluid 3 (Modified Duong)

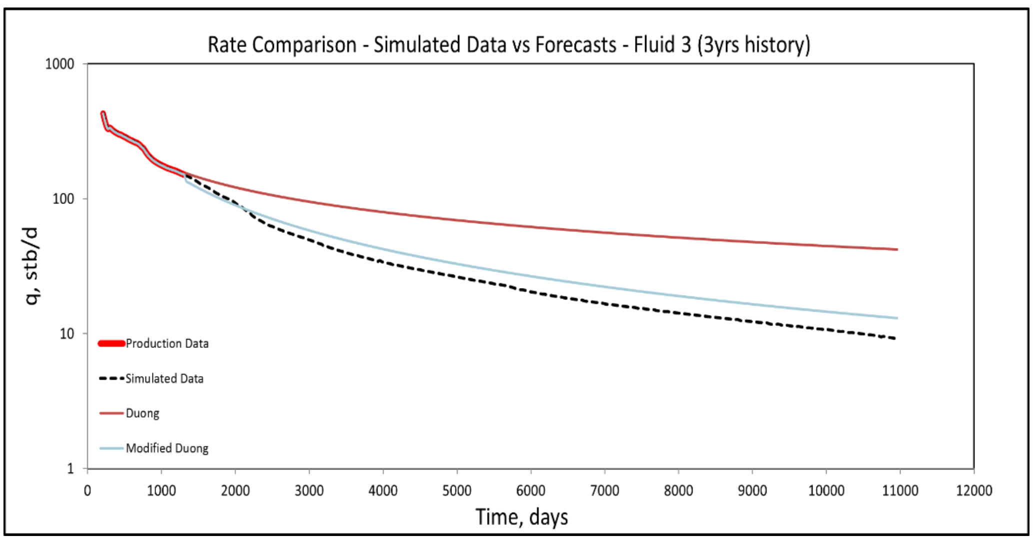

Figure 3-97 Rate Comparisons: Simulated Data vs. Forecasts – Fluid 3 (Modified Duong)

3.8.4. Fluid 4 – Modified Duong Model

The plots for Fluid 4 are shown in Figures 3-98 to 3-100. Table 3-41 shows the results of the Modified Duong forecast in comparison to the original Duong model forecast and the simulated data. For Fluid 4, the percentage error in the forecast was reduced from 40% (original Duong model) to approximately 30%.

Table 3-41 Forecasts, Errors and Percentage Errors – Fluid 4 (Modified Duong)

Cumulative Oil Production Forecast Errors – Fluid 4	Forecast, STB	Error (absolute value), STB	Percentage Error, %
Matched Production Data	3 yrs.	3 yrs.	3 yrs.
Simulated Data	15336	0	-
Duong	25554	+10218	+40.0
Modified Duong	21917	+6581	+30.0

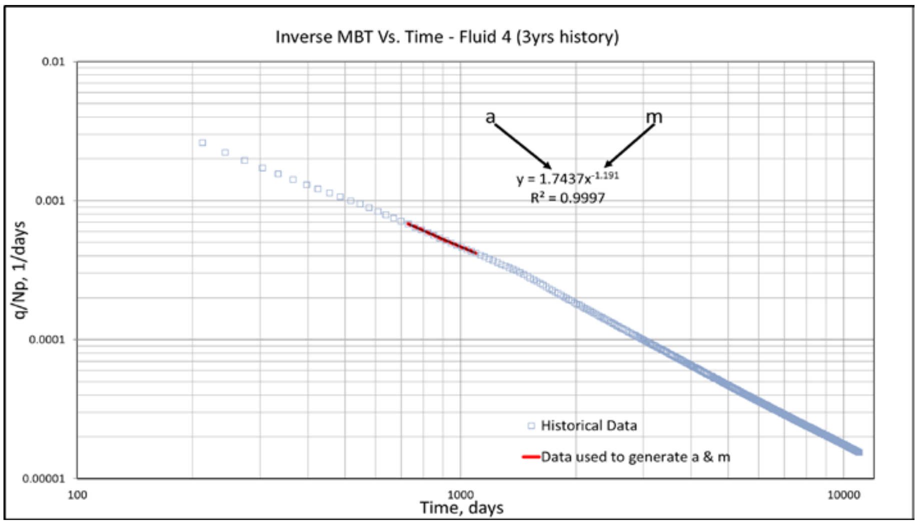

Figure 3-98 Inverse MBT vs. Time – Fluid 4 (Modified Duong)

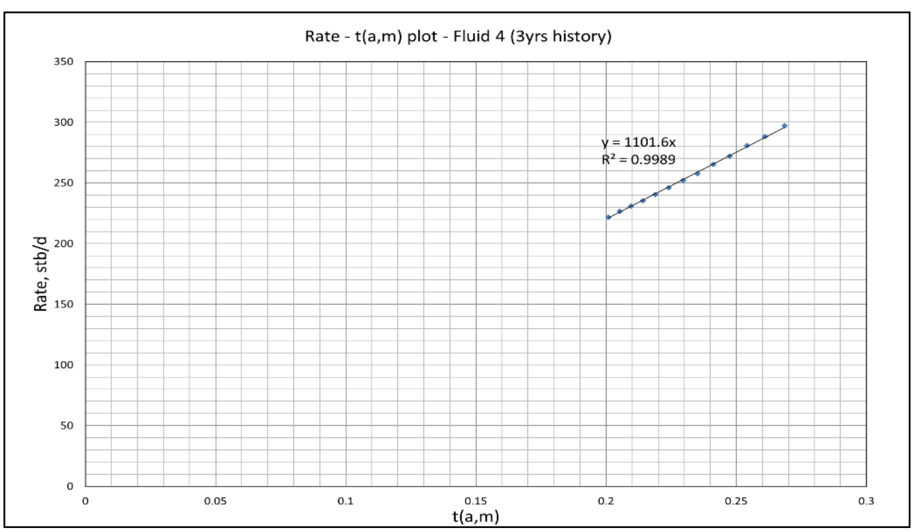

Figure 3-99 Rate - t(a,m) Plot – Fluid 4 (Modified Duong)

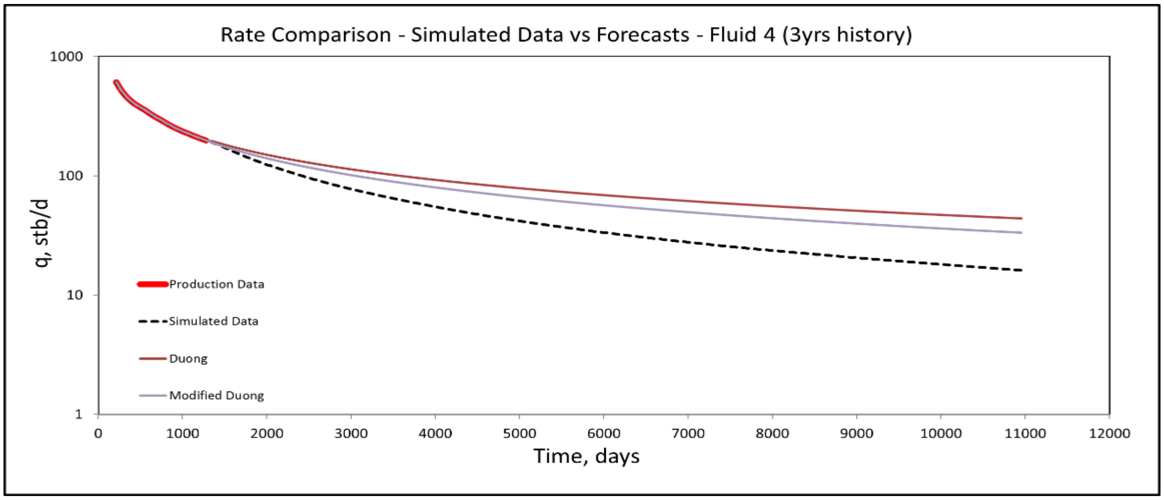

Figure 3-100 Rate Comparisons: Simulated Data vs. Forecasts – Fluid 4 (Modified Duong)

3.9. Inferences

1. Traditional decline curve analysis (DCA) models are not entirely satisfactory for shale volatile oil reservoirs;
2. Due to lengthy transition flow and multiphase flow effects in shale volatile oil reservoirs, hybrid DCA models are better alternatives than traditional DCA models;
3. Diagnostic plots are important prerequisites prior to applying DCA techniques to production data for forecasting;
4. When applying hybrid models, the time of switch to an Arps model determines the sensitivity of production data to changes in Arps' decline exponents (b values);
5. It is possible to determine the time (point) of switch to Arps after careful analyses of the inverse MBT vs. time plot, the Yu plot and corresponding diagnostic plots – this time of switch may be the "true" start of boundary dominated flow;
6. The Duong model and its hybrid alternatives overestimate production in shale volatile oil reservoirs – overestimation increases with shorter production histories. These inaccuracies are a result of the nature of data due to early change from linear

flow to transition flow regime, which contradicts the assumption of long-term linear (or bilinear) flow in the original Duong model;

7. The Duong hybrid models led to better forecasts than the original Duong model but still overestimate production (in most cases) in comparison to results from the YM-SEPD and its hybrid models;
8. The YM-SEPD hybrid models led to better production forecasts in all cases, but were limited by lack of production data beyond the minimum of 2-3 years required for best application of the YM-SEPD model.
9. Even though further research is needed in the area of solution gas production forecasting, it is possible to forecast solution gas production from shale volatile oil reservoirs with some measure of accuracy, provided there are sufficient data available;
10. A proposed Modified Duong model helps to alleviate the problem of serious overestimate of future production by the original Duong model.

Chapter 4 – Production Mechanisms and Behavior of Shale Volatile Oil Reservoirs

A good understanding of shale volatile oil reservoir production mechanisms is essential to properly estimate reserves and improve oil recovery. Also, it is important to know how various factors can affect the behavior and performance of shale volatile oil reservoirs. A broad range of volatile oil fluid compositions from moderately volatile to highly volatile (near-critical) oils were considered. The fluid compositions are shown in Table 4-1. Compositional simulations were run on a basecase multi-fractured horizontal well (MFHW) model, as in Figure 4-1. Reservoir data and conditions were the same as in the previous chapter.

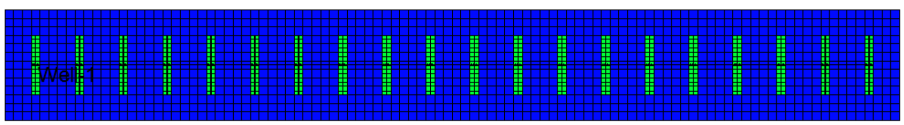

Figure 4-1 Basecase Multi-Fractured Horizontal Well (MFHW) Model

Table 4-1 Fluid Compositions

	Fluid 1	Fluid 2	Fluid 3	Fluid 4	Fluid 5	Fluid 6	Fluid 7	Fluid 8	Fluid 9	Fluid 10
Components	Composition (%)	Composition (%)	Composition (%)	Composition (%)	Composition (%)	Composition (%)	Composition (%)	Composition (%)	Composition (%)	Composition (%)
CH_4	58.77	58.07	61.82	53.47	49.43	49.96	48.78	51.93	44.42	41.52
C_2H_6	7.57	7.43	7.91	11.46	7.28	6.44	6.24	6.64	9.52	6.12
C_3H_8	4.09	4.16	4.42	8.79	8.02	3.48	3.49	3.71	7.30	6.74
I-C_4H_{10}	0.91	0.96	1.02	-	2.31	0.77	0.81	0.86	-	1.94
N-C_4H_{10}	2.09	1.63	1.74	4.56	3.61	1.78	1.37	1.46	3.79	3.03
I-C_5H_{12}	0.77	0.75	0.80	-	1.80	0.66	0.63	0.67	-	1.51
N-C_5H_{12}	1.15	0.80	0.86	2.09	1.79	0.98	0.67	0.72	1.74	1.50
C_6H_{14}	1.75	1.14	1.21	1.51	2.32	1.49	0.96	1.02	1.26	1.95
C_{7+}	21.76	22.59	17.59	16.92	22.41	33.50	34.98	30.78	30.98	34.82
CO_2	0.93	2.32	2.47	0.90	0.16	0.79	1.95	2.08	0.75	0.13
N_2	0.21	0.15	0.16	0.30	0.87	0.18	0.13	0.13	0.25	0.73
	Highly Volatile Oils					Moderately Volatile Oils				
GOR, scf/bbl	3,024	3,043	4,081	3,967	2,561	1,806	1,755	2,128	1,873	1,513
API	63.5	63.0	63.5	64.9	65.2	49.2	49.1	46.8	49.7	50.6
Oil FVF, bbl/stb	3.56	3.55	-	4.81	3.26	2.23	2.19	2.42	2.32	2.10

Figures 4-2 – 4-5 show the P-T diagrams for each of the different fluid compositions. The curves represent the two-phase boundaries; the straight chain lines going through the curves are the isothermal pressure decrease paths during production and the red arrows point to the critical points on the curves. CMG Winprop software was used to generate the P-T diagrams. Here, the straight chain lines indicate the positions of the reservoir temperature (250 F) compared to the critical points.

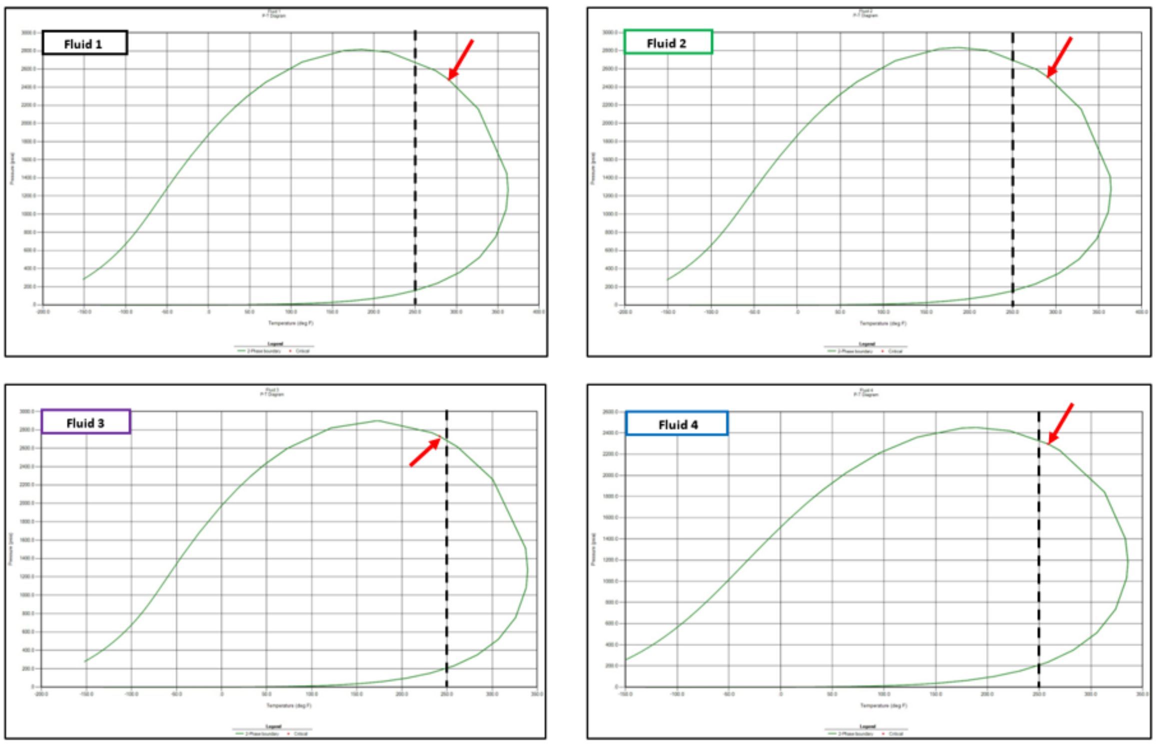

Figure 4-2 P-T Diagrams: Fluids 1-4

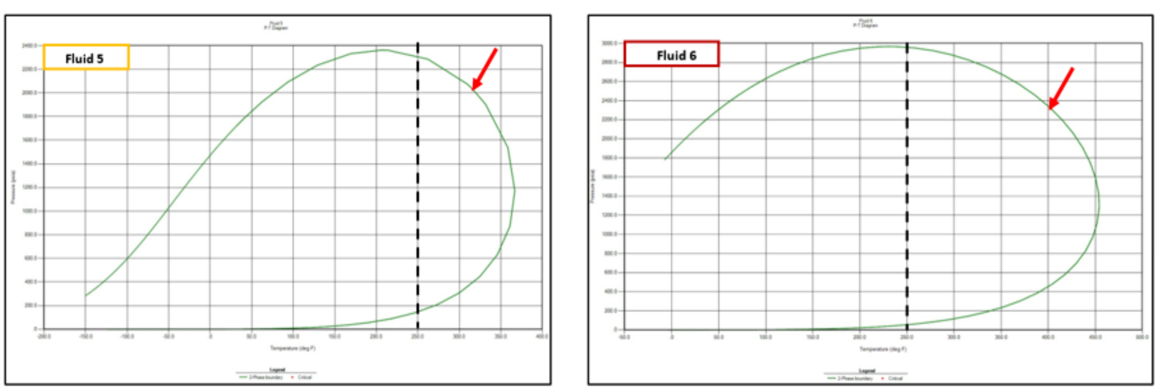

Figure 4-3 P-T Diagrams: Fluids 5 and 6

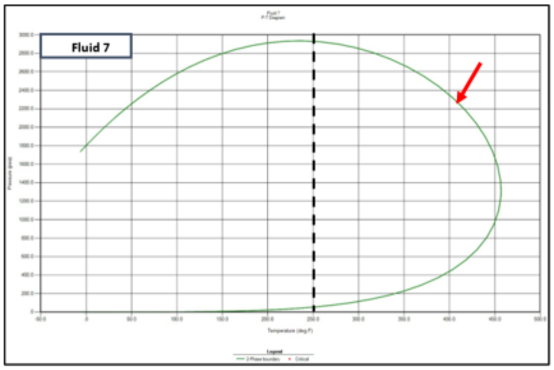

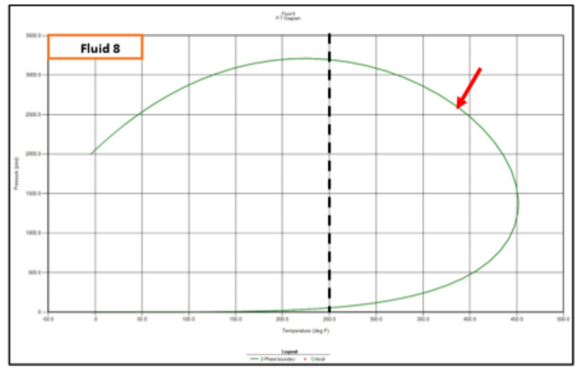

Figure 4-4 P-T Diagrams: Fluids 7 and 8

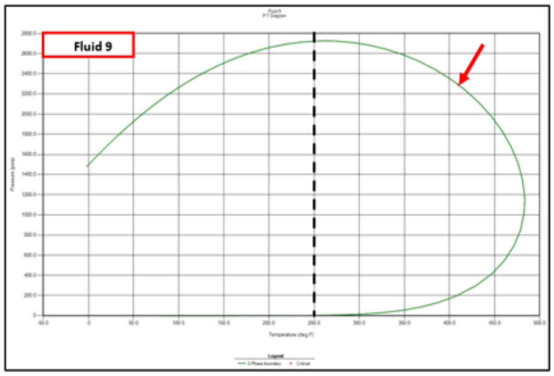

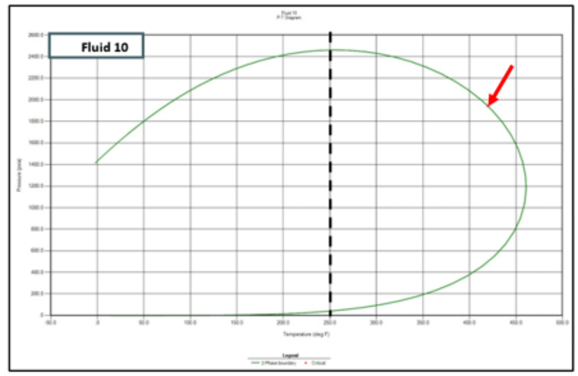

Figure 4-5 P-T Diagrams: Fluid 9 and 10

The reservoir temperature is close to the critical point for highly volatile oils and vice versa for moderately volatile oils. Fluids 3 and 4 are near-critical fluids.

4.1. Solution Gas Drive Mechanism

Solution gas drive is the primary drive mechanism in shale volatile oil reservoirs. In this study, the reservoir is initially undersaturated i.e., the initial reservoir pressure is greater than the saturation pressure (bubble point pressure). At this time, production is mainly driven by the bulk expansion of reservoir rock and oil. When reservoir pressure drops below the bubble point, expansion of gases dissolved in oil provide most of the reservoir drive energy. Illustrations of gas-oil ratio history, reservoir pressure and gas saturation with time for one of the fluid samples in the basecase scenario are shown in Figures 4-6, 4-7 and 4-8. Figure 4-7 is a semi-log plot of the gas-oil ratio history to enable proper visibility of the various critical points of production mechanism of shale volatile oil reservoirs.

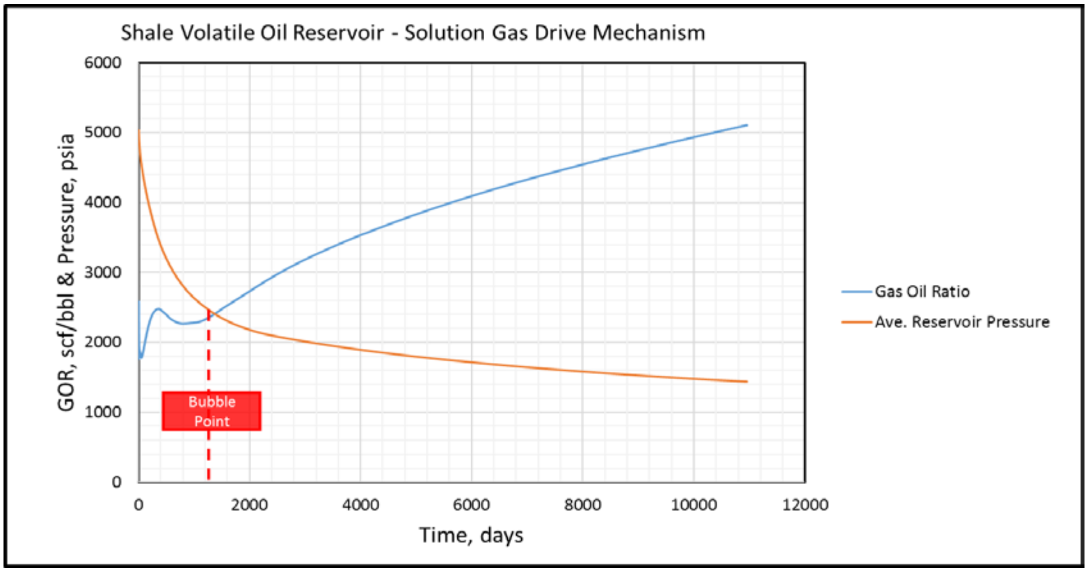

Figure 4-6 Shale Volatile Oil Reservoir – Solution Gas Drive Mechanism

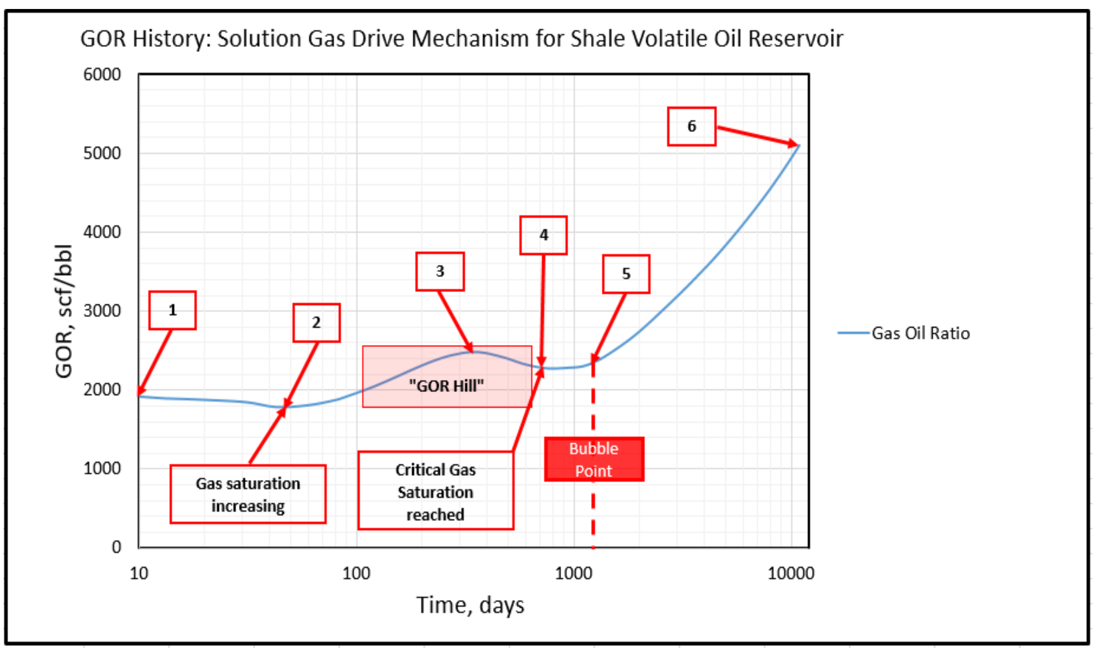

Figure 4-7 GOR History: Solution Gas Drive Mechanism for Shale Volatile Oil Reservoir

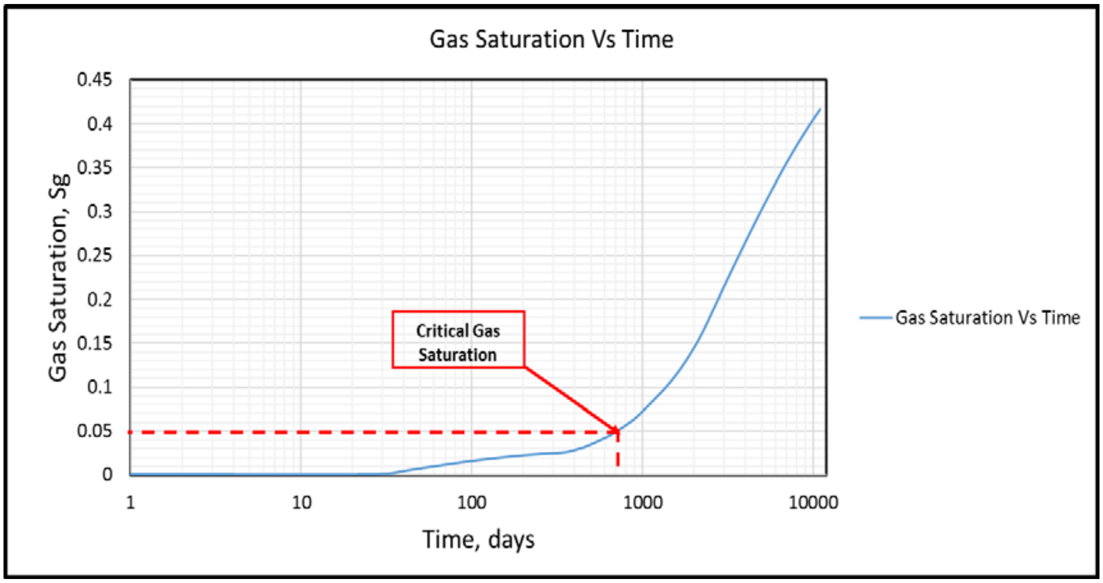

Figure 4-8 Gas Saturation vs. Time

In Figure 4-6, it is evident that the reservoir pressure declines rapidly before reaching the bubble point. Beyond the bubble point, the rate of decline slows due to the evolution of gas. The six critical stages of the GOR history of a well in a shale volatile oil reservoir driven by solution gas drive mechanism shown in Figure 4-7 are briefly explained below:

1. Reservoir pressure is greater than the saturation pressure (bubble point pressure). Here, no free gas exists in the formation and the producing GOR is approximately equal to the initial solution GOR (i.e., approximately constant GOR);
2. The gas saturation starts to increase forming a “GOR hill”. Though gas is not mobile yet, there is an increase in the amount of gas released from oil from point 2 to 3 and an increasing gas saturation;
3. Due to the continuous rapid decline in pressure above the bubble point, gas solubility decreases from point 3 to 4;
4. The critical gas saturation is reached and gas can flow;

5. At this point, the reservoir pressure decreases below the bubble point, gas evolution accelerates and producing GOR starts to increase rapidly;
6. Producing GOR is still increasing after 30 years. For shale oil reservoirs, the producing GOR may continue to increase for even longer due to ultra-low permeability of shales and other contributing factors.

The producing GOR for all the fluid samples (basecases) are compared and shown in Figure 4-9. They all have a similar trend but generally, the more volatile the fluid, the higher the producing GOR throughout the production period.

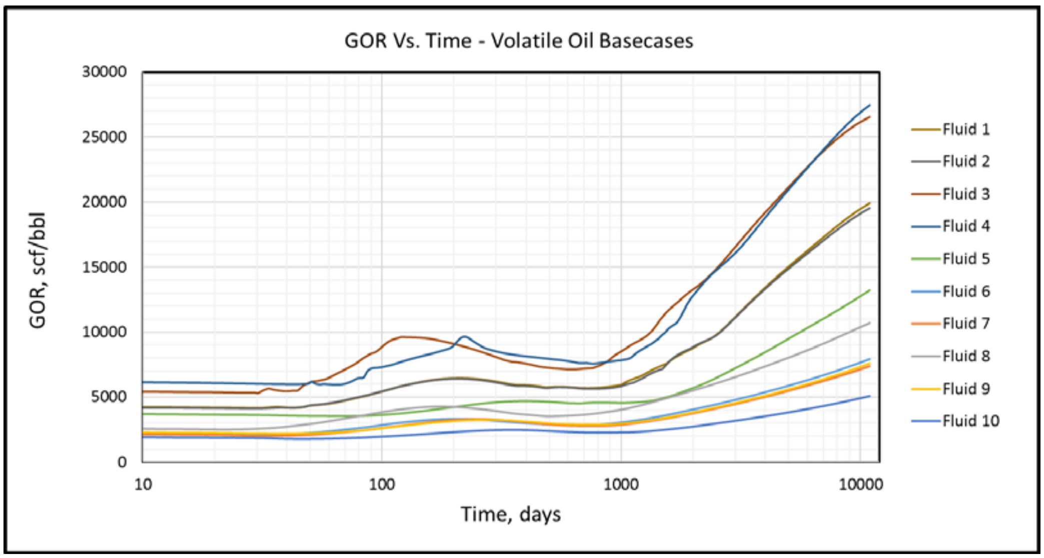

Figure 4-9 GOR vs. Time – Volatile Oil Basecases

Next, we investigated the effect of several factors on gas-oil ratio (GOR) behavior and production performance of multi-fractured horizontal wells (MFHW) in shale volatile oil reservoirs.

4.2. Critical Gas Saturation

The gas produced when reservoir pressure drops below the saturation pressure in an oil reservoir remains immobile until it reaches a certain threshold. This threshold is called the critical gas saturation. At and above the critical gas saturation, gas become mobile and begin to flow towards the wellbore. Critical gas saturations of 5% (basecase), 10%, 15% and 20% were considered to determine the impact on the performance of MFHW in shale volatile oil reservoirs. Figures 4-10 to 4-29 illustrate the impacts of critical gas saturation on producing GOR (semi-log plots) and cumulative oil production for all the fluid samples. Generally, the higher the critical gas saturation, the larger the cumulative oil production and the lower the producing GOR with time. There is also a delay in the rise of producing GOR with time, as critical gas saturation increases. With increasing critical gas saturation, there is a slight dip in producing GOR after the period of constant GOR. The further away the fluid is from the critical point, the more pronounced the dip is. Fluids 3 and 4 are near-critical fluids, therefore, the dip in producing GOR after the constant GOR period, is nearly absent in these cases. This can be observed in Figures 4-14 and 4-16.

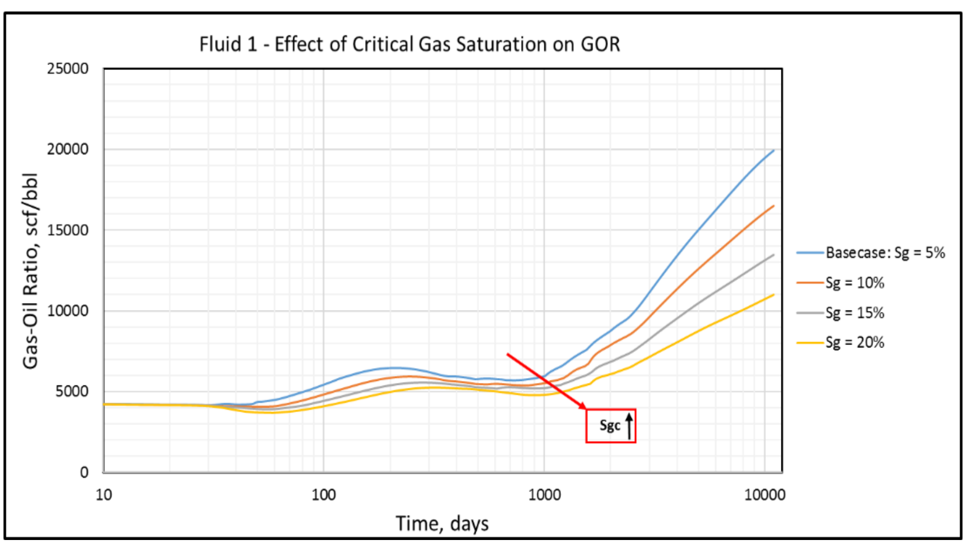

Figure 4-10 Fluid 1 – Effect of Critical Gas Saturation on GOR

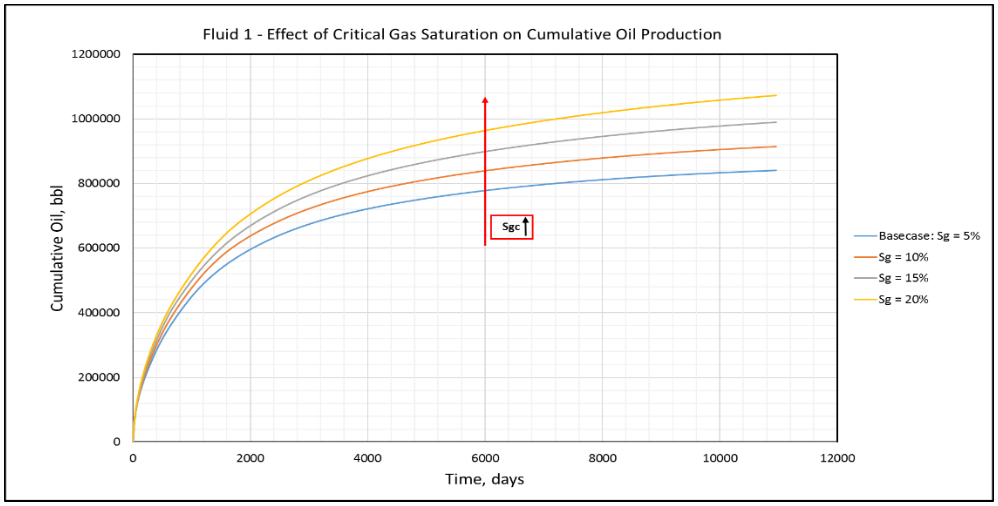

Figure 4-11 Fluid 1 – Effect of Critical Gas Saturation on Cumulative Oil Production

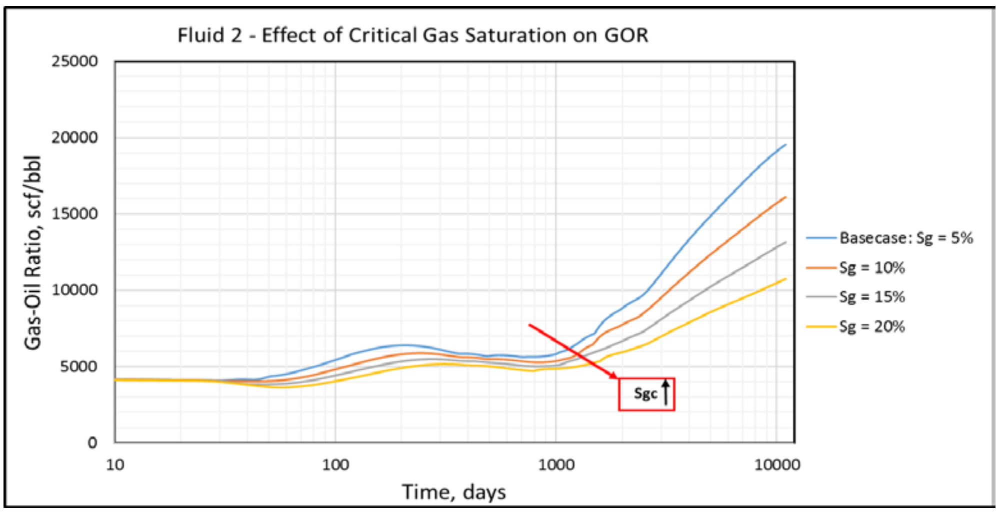

Figure 4-12 Fluid 2 – Effect of Critical Gas Saturation on GOR

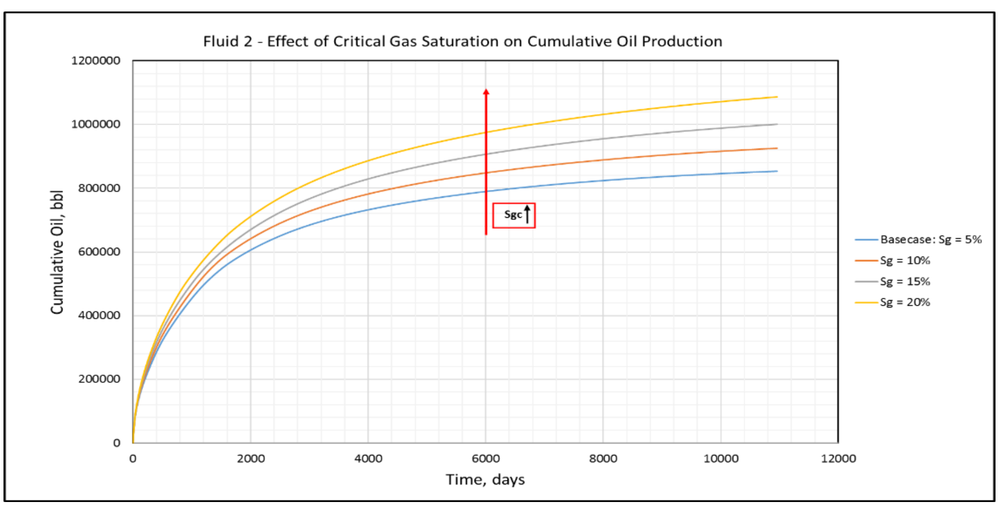

Figure 4-13 Fluid 2 – Effect of Critical Gas Saturation on Cumulative Oil Production

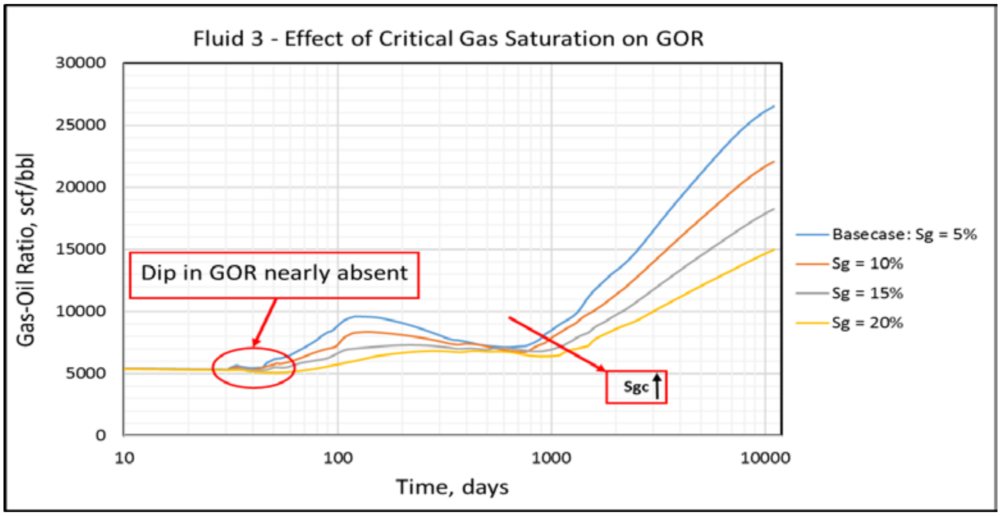

Figure 4-14 Fluid 3 – Effect of Critical Gas Saturation on GOR

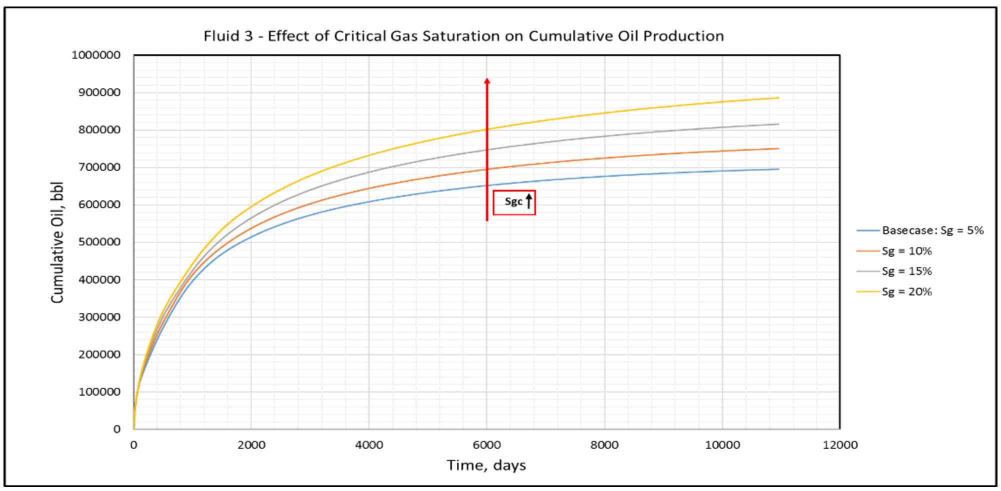

Figure 4-15 Fluid 3 – Effect of Critical Gas Saturation on Cumulative Oil Production

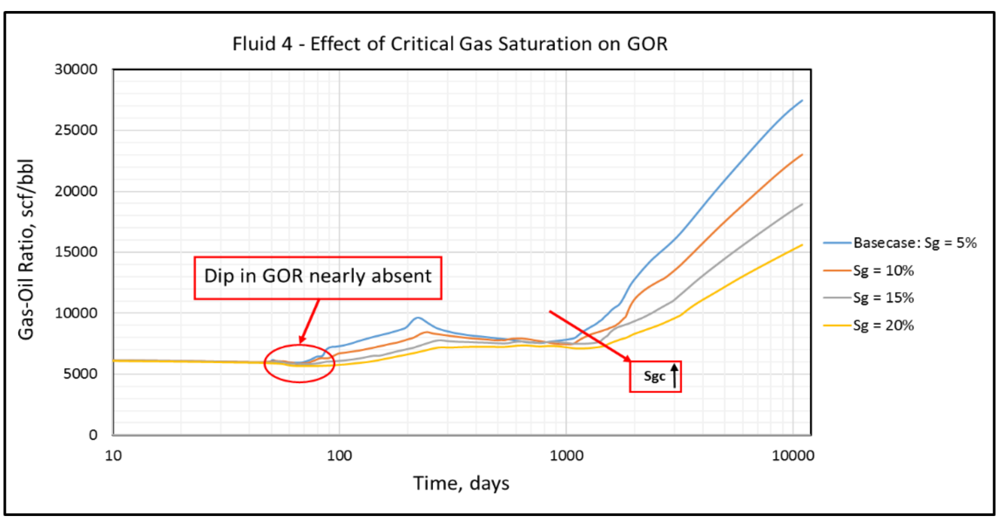

Figure 4-16 Fluid 4 – Effect of Critical Gas Saturation on GOR

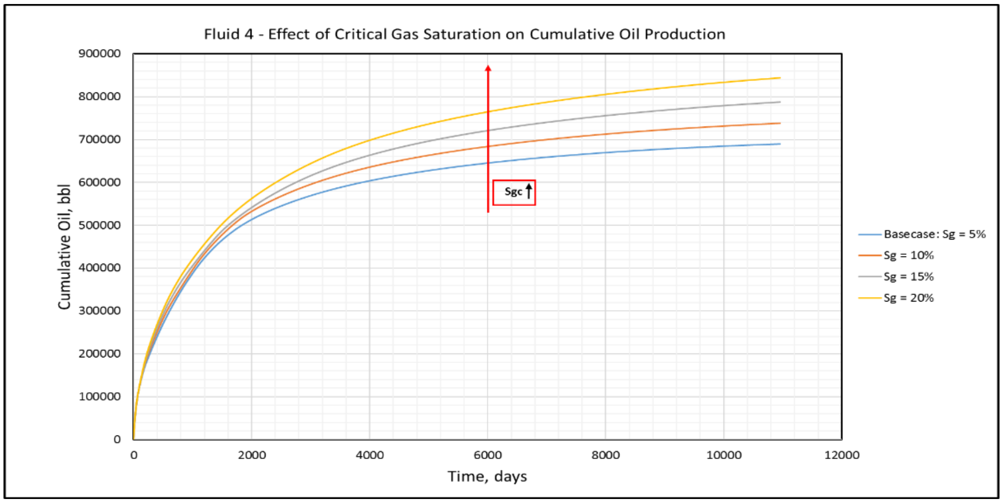

Figure 4-17 Fluid 4 – Effect of Critical Gas Saturation on Cumulative Oil Production

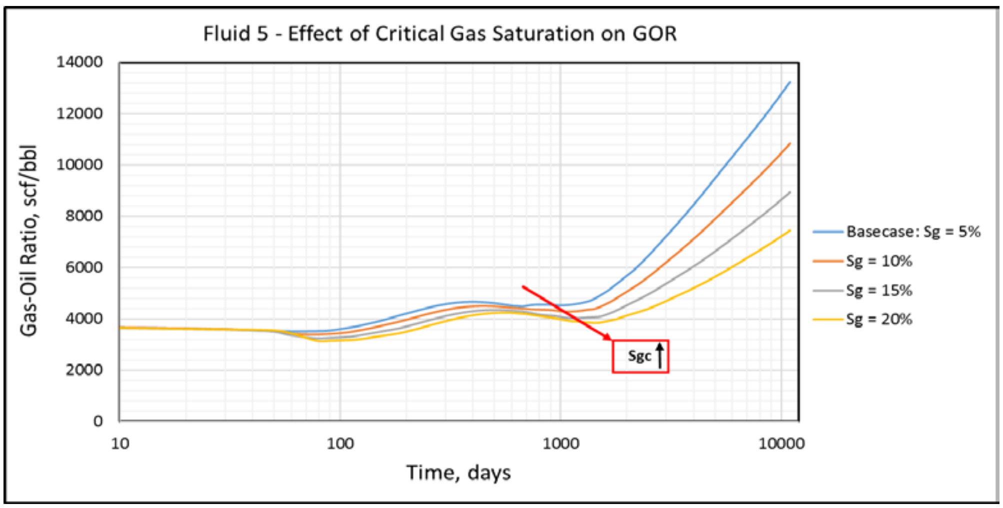

Figure 4-18 Fluid 5 – Effect of Critical Gas Saturation on GOR

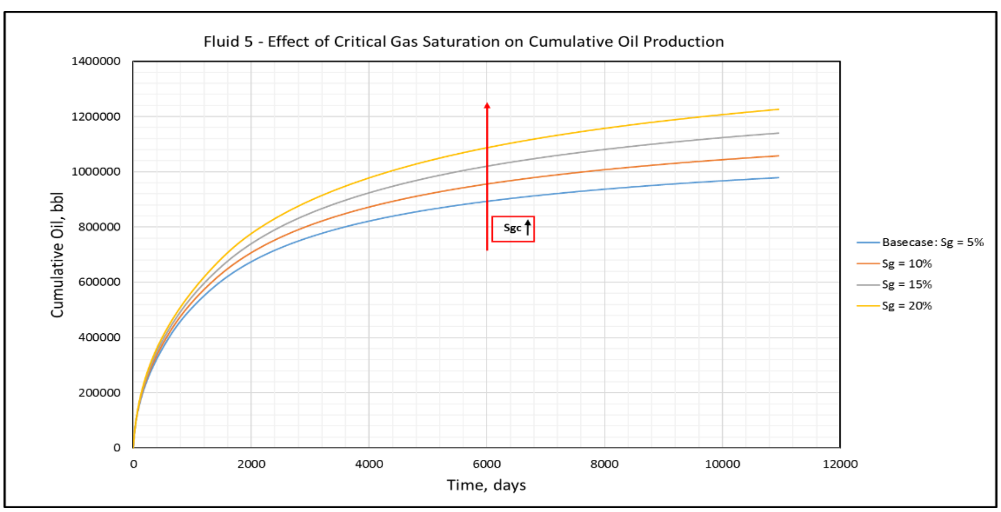

Figure 4-19 Fluid 5 – Effect of Critical Gas Saturation on Cumulative Oil Production

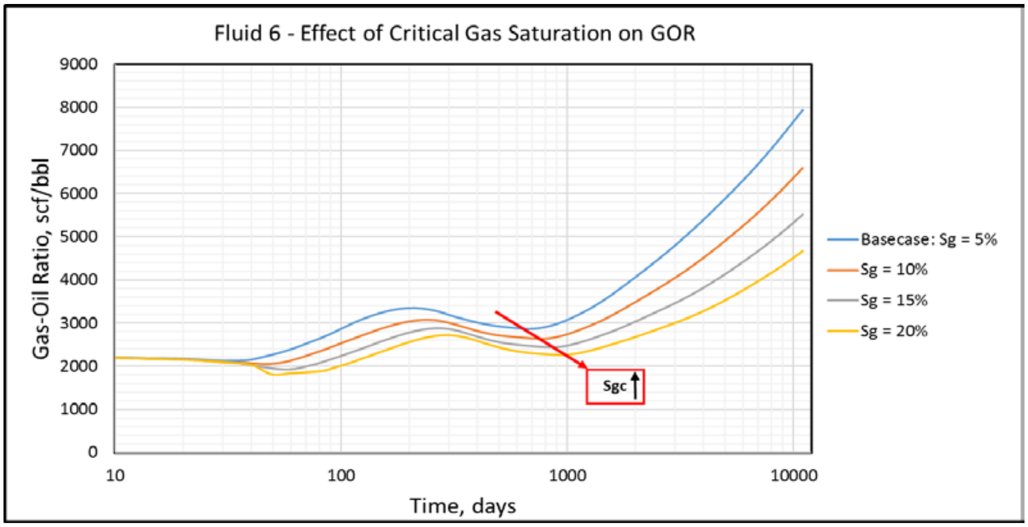

Figure 4-20 Fluid 6 – Effect of Critical Gas Saturation on GOR

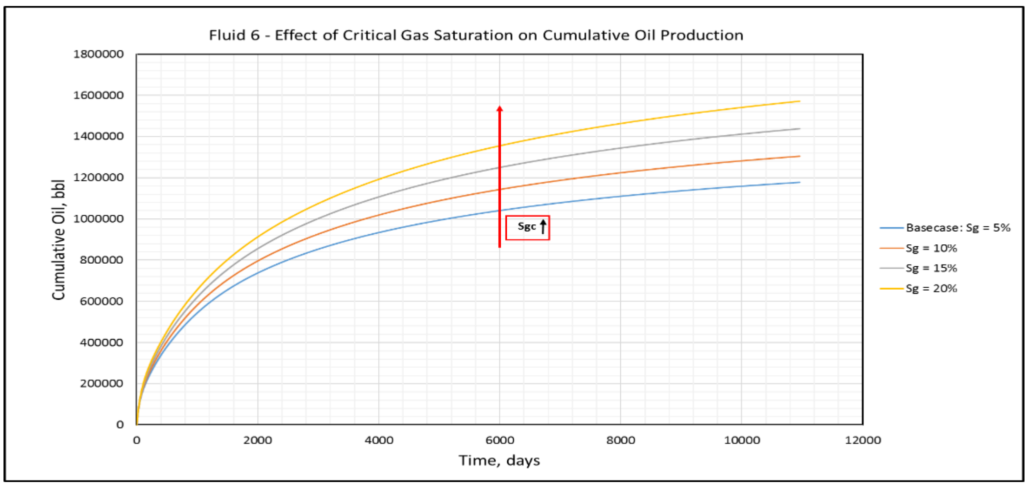

Figure 4-21 Fluid 6 – Effect of Critical Gas Saturation on Cumulative Oil Production

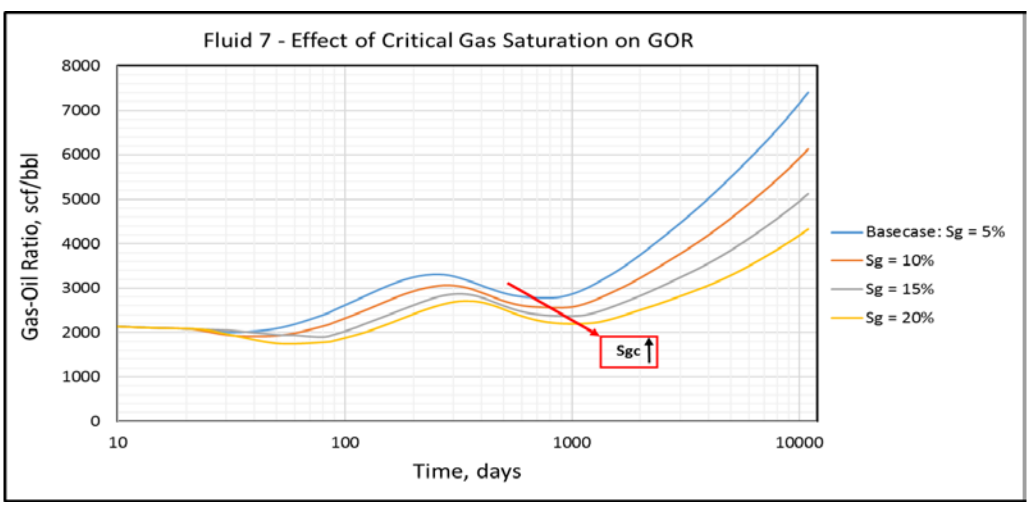

Figure 4-22 Fluid 7 – Effect of Critical Gas Saturation on GOR

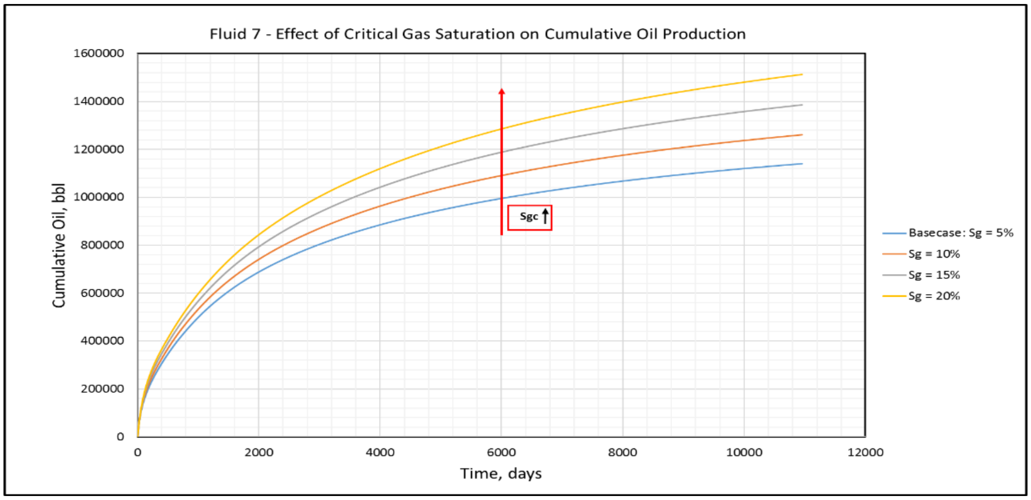

Figure 4-23 Fluid 7 – Effect of Critical Gas Saturation on Cumulative Oil Production

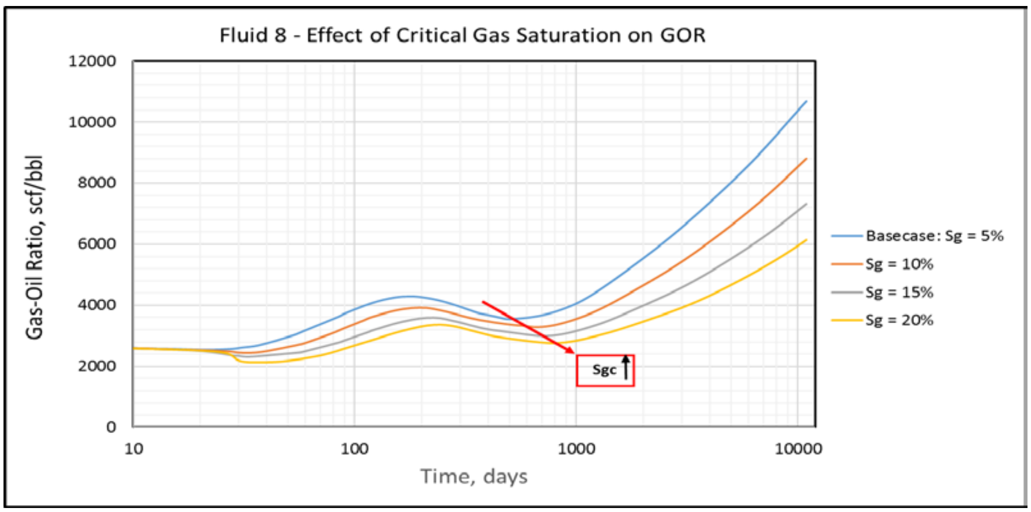

Figure 4-24 Fluid 8 – Effect of Critical Gas Saturation on GOR

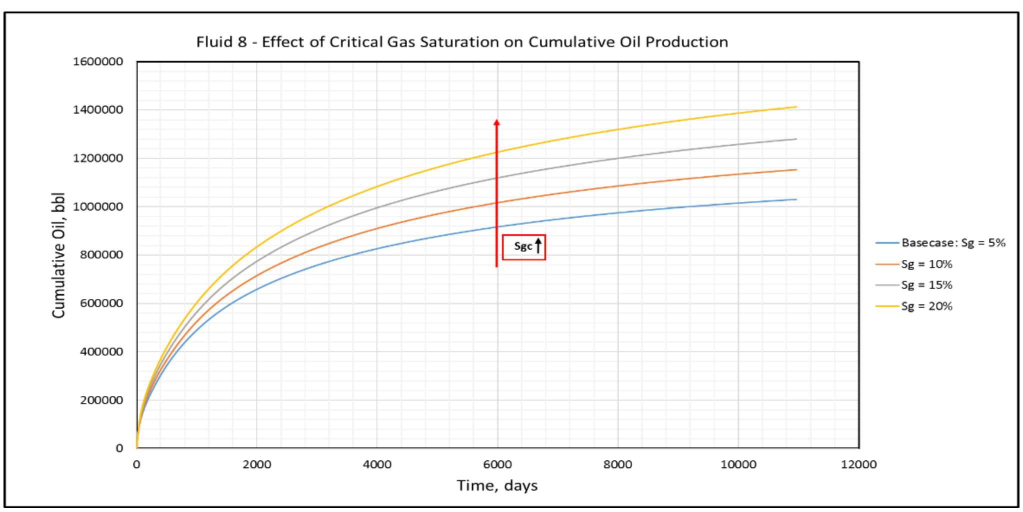

Figure 4-25 Fluid 8 – Effect of Critical Gas Saturation on Cumulative Oil Production

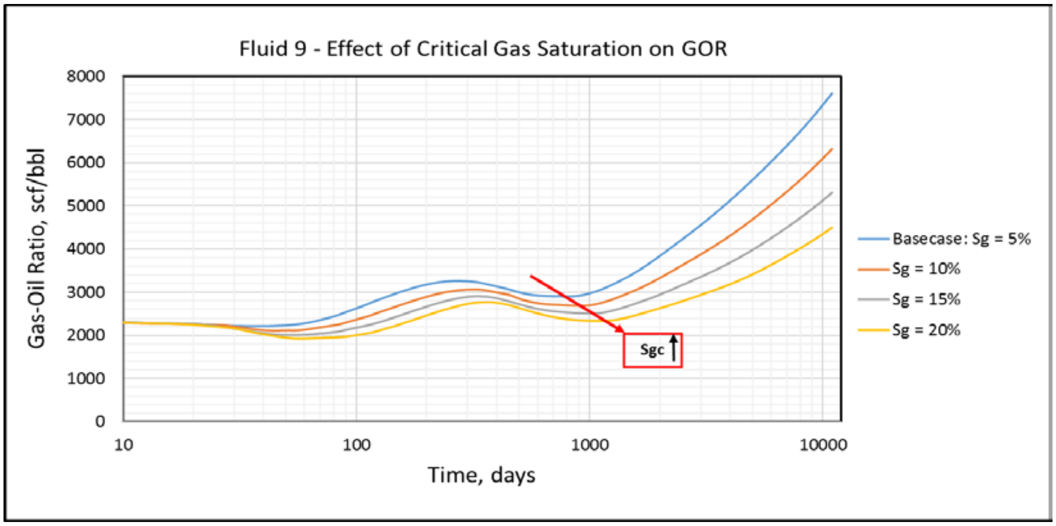

Figure 4-26 Fluid 9 – Effect of Critical Gas Saturation on GOR

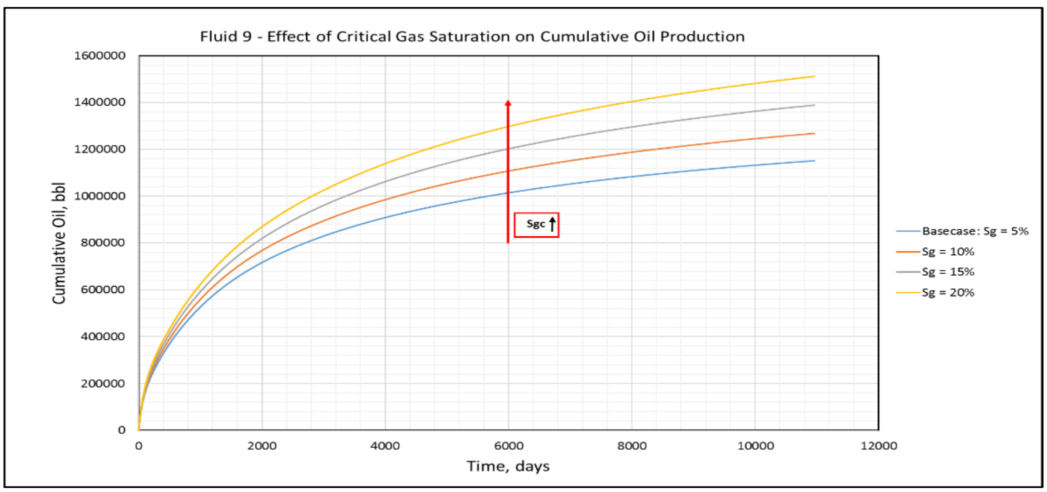

Figure 4-27 Fluid 9 – Effect of Critical Gas Saturation on Cumulative Oil Production

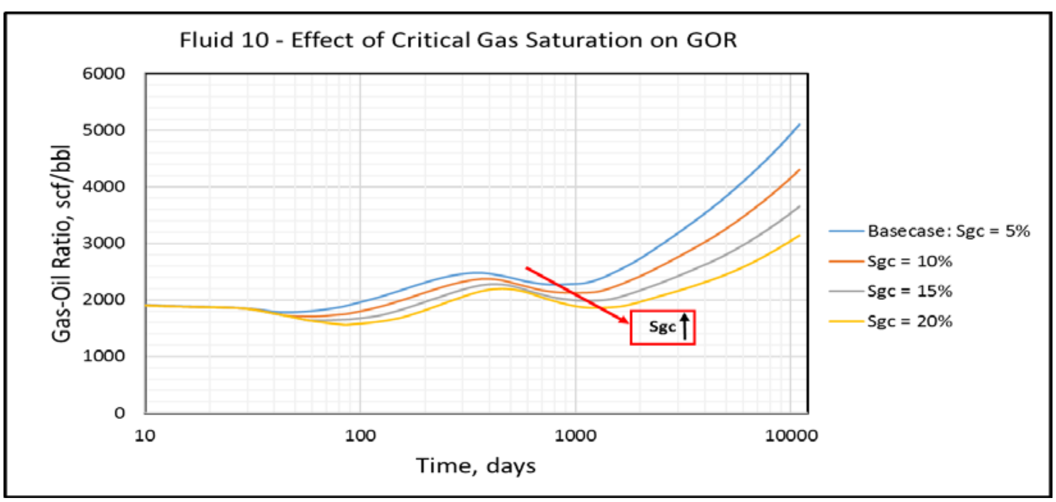

Figure 4-28 Fluid 10 – Effect of Critical Gas Saturation on GOR

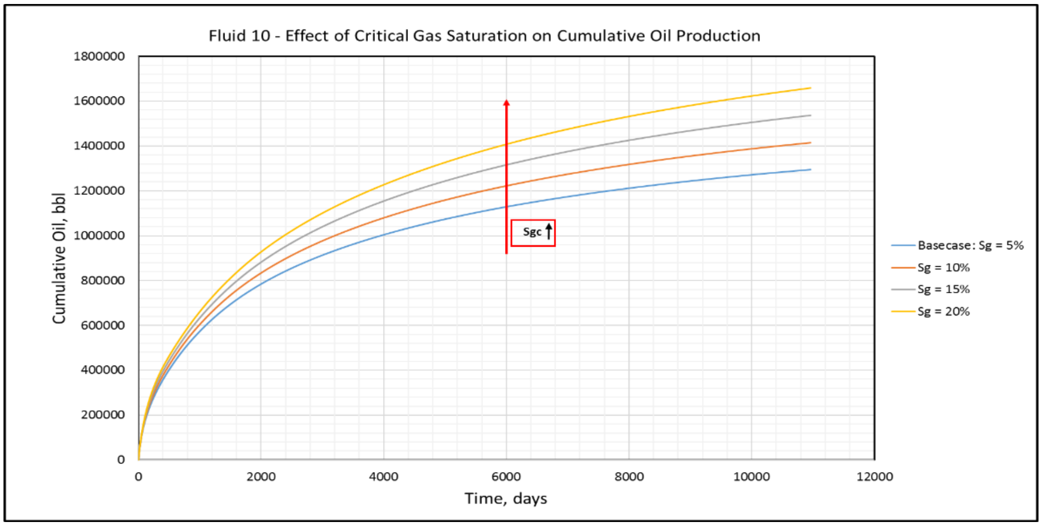

Figure 4-29 Fluid 10 – Effect of Critical Gas Saturation on Cumulative Oil Production

4.3. Bottomhole Pressure (BHP)

The wells under consideration here produce at constant flowing bottomhole pressure (BHP). The lower the BHP below the saturation pressure, the more the drawdown. Cases of different constant flowing BHPs were considered including when the BHP is equal to the bubble point pressure. The basecase is a constant flowing BHP of 1000 psi. The lower the constant flowing BHP, the higher the producing GOR except for the cases of 100 psi and below for the least volatile oil – Fluid 10, 250 psi and below for other moderately volatile oils and from 500 psi and below for highly volatile oils. In these cases, the producing GOR towards the end of the production time decreases with lesser constant flowing BHP due to the large drawdown which led to the production of gas reaching a peak quickly and declining with time till the end. The more volatile the fluid, the quicker the producing GOR reaches a peak and starts to decline even at higher flowing bottomhole pressures. When the constant flowing BHP is equal to the bubble point pressure, the producing GOR remains constant throughout the production. There is a mild increase in producing GOR with time for the case of BHP equal to 2000 psi (slightly lower than the saturation pressure in most of the cases). As for oil production, the lesser the constant flowing BHP, the larger the cumulative oil production. This is generally the case, especially for highly volatile oils. Highly volatile oils have more gas phase contribution that drives oil production with lower and lower flowing bottomhole pressures. At constant flowing BHP of 100 psi and less, there is little effect on the quantity of oil produced or no significant increase in cumulative oil production for moderately volatile oils. The least oil is produced when the constant BHP is equal to the saturation pressure because there is no gas evolution to propel further production of oil i.e., the pressure never drops below the bubble point in these cases. Only single phase oil production takes place in these instances. Figures 4-30 to 4-59 show the effects of bottomhole pressure (BHP) on producing gas-oil ratio (semi-log plots), cumulative oil production and average reservoir pressure.

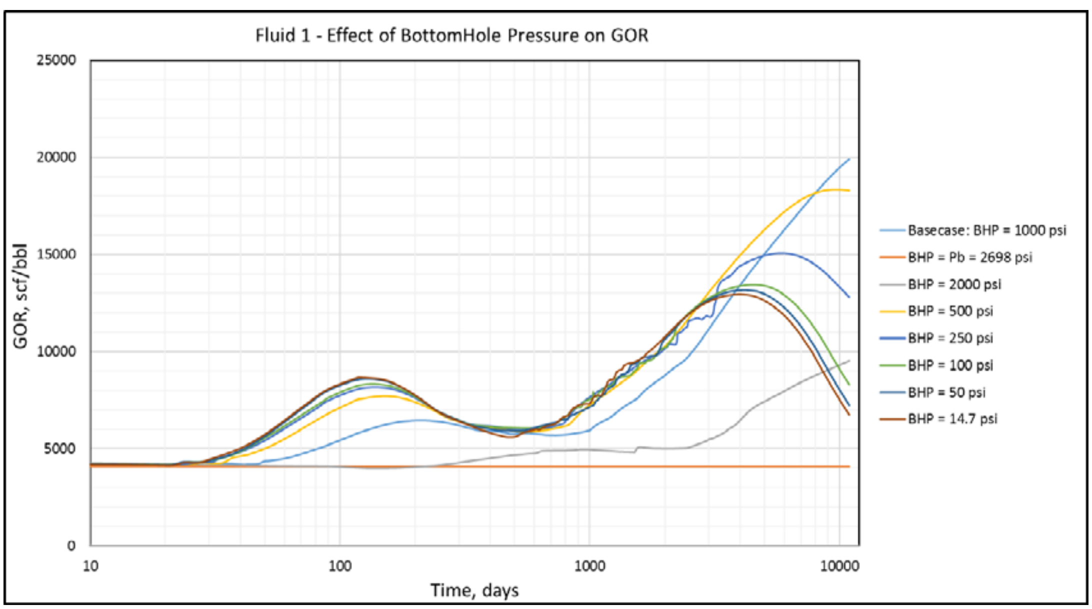

Figure 4-30 Fluid 1 – Effect of Bottomhole Pressure on GOR

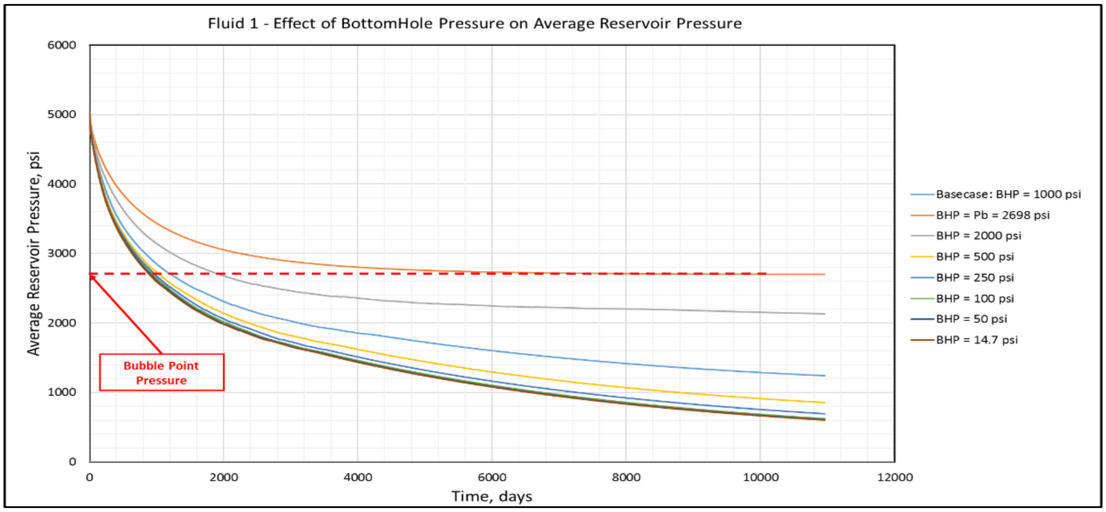

Figure 4-31 Fluid 1 – Effect of Bottomhole Pressure on Average Reservoir Pressure

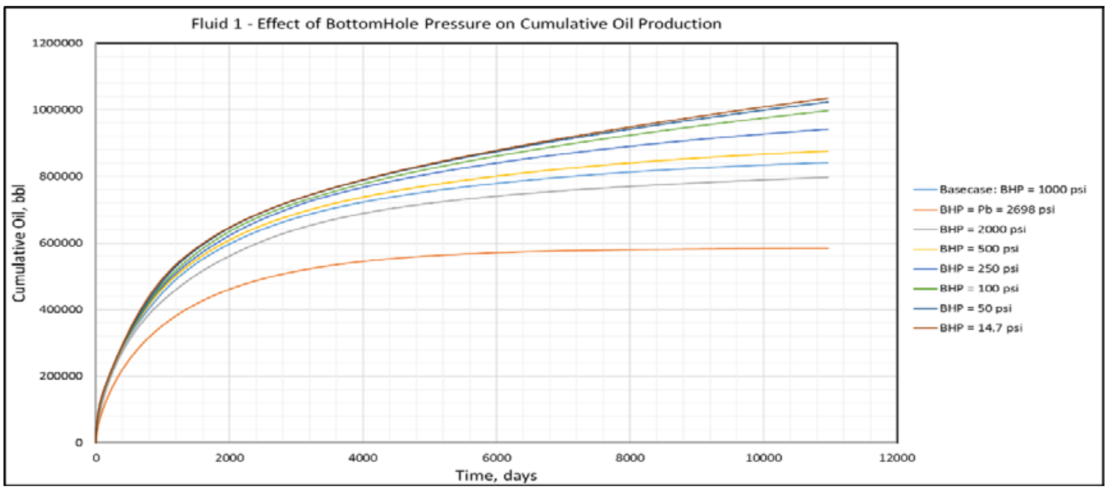

Figure 4-32 Fluid 1 – Effect of Bottomhole Pressure on Cumulative Oil Production

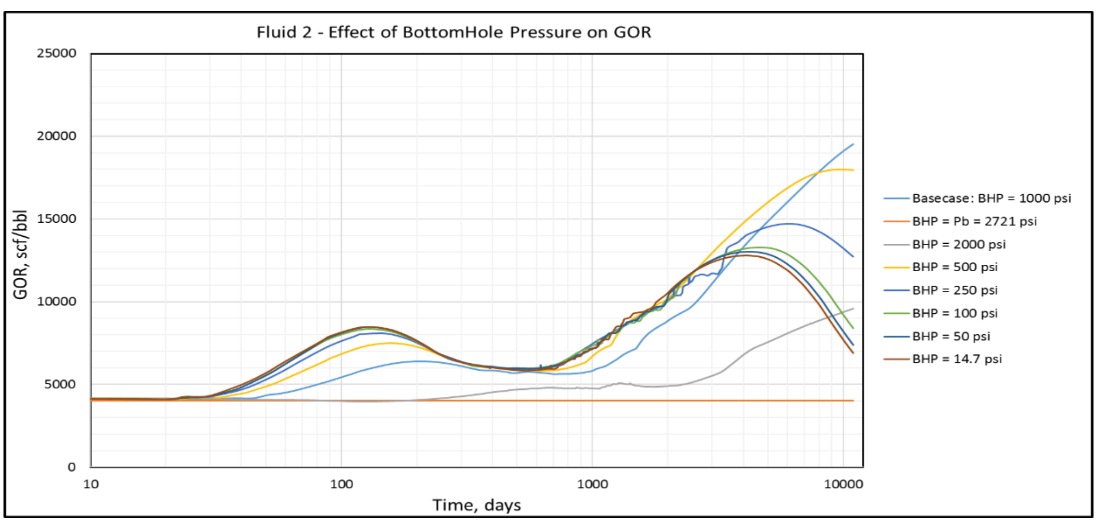

Figure 4-33 Fluid 2 – Effect of Bottomhole Pressure on GOR

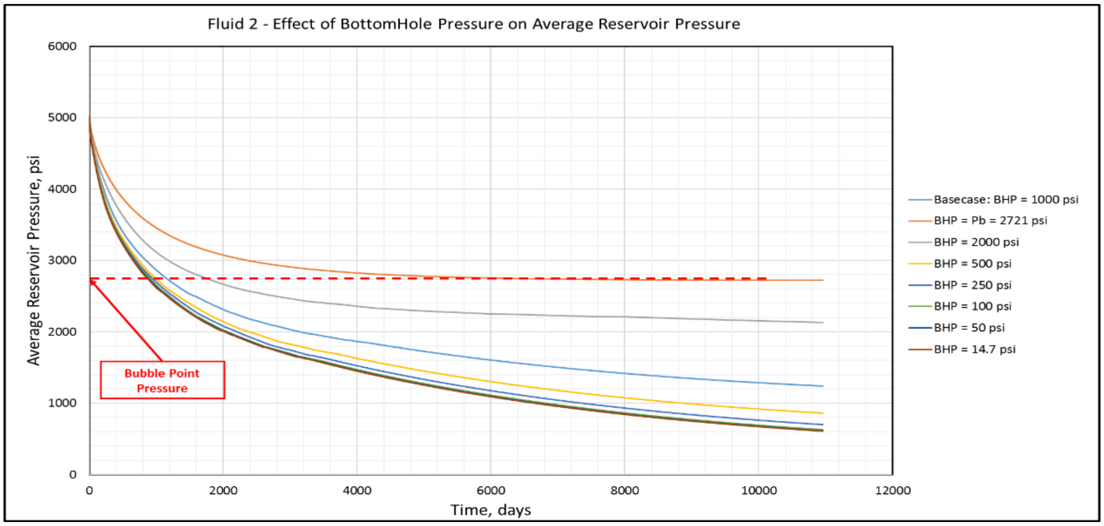

Figure 4-34 Fluid 2 – Effect of Bottomhole Pressure on Average Reservoir Pressure

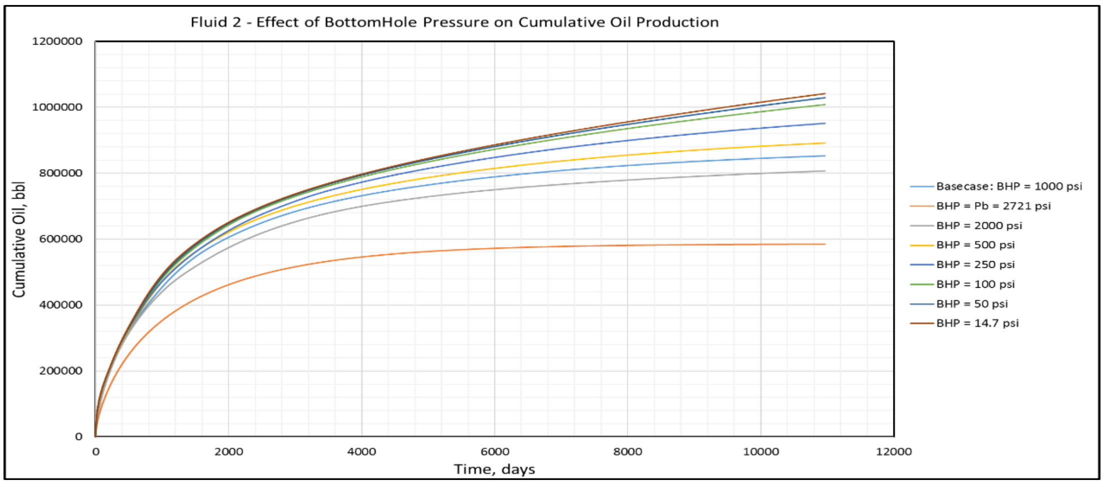

Figure 4-35 Fluid 2 – Effect of Bottomhole Pressure on Cumulative Oil Production

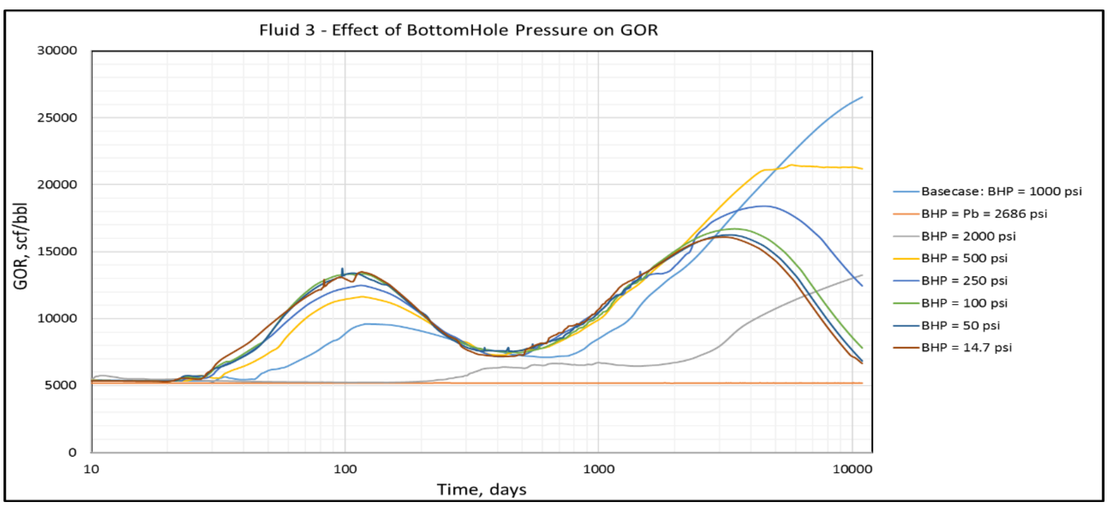

Figure 4-36 Fluid 3 – Effect of Bottomhole Pressure on GOR

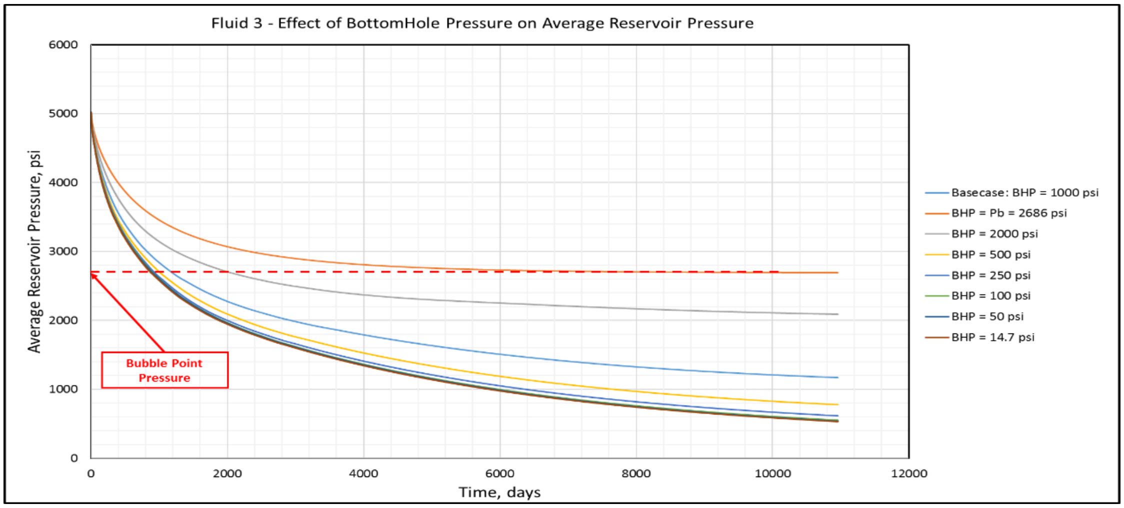

Figure 4-37 Fluid 3 – Effect of Bottomhole Pressure on Average Reservoir Pressure

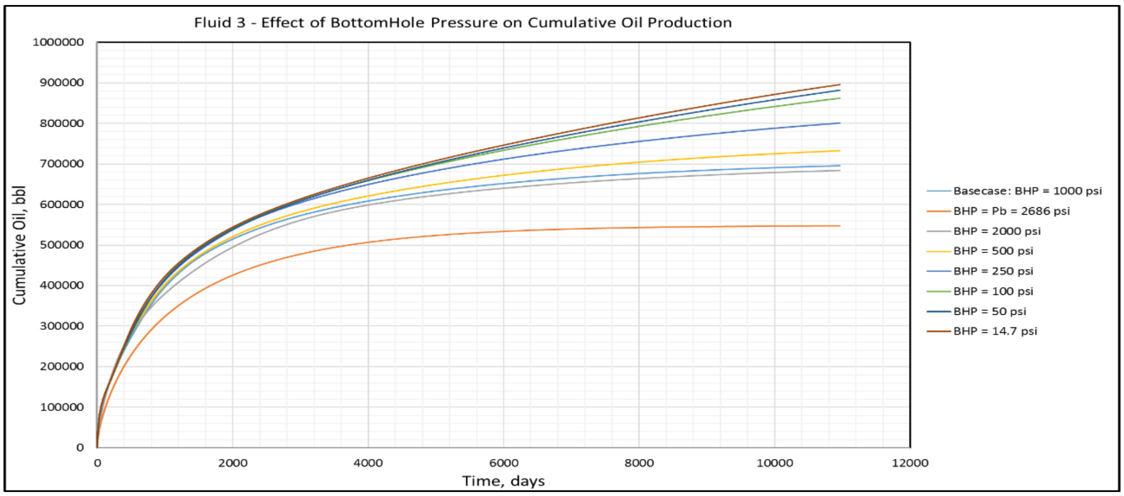

Figure 4-38 Fluid 3 – Effect of Bottomhole Pressure on Cumulative Oil Production

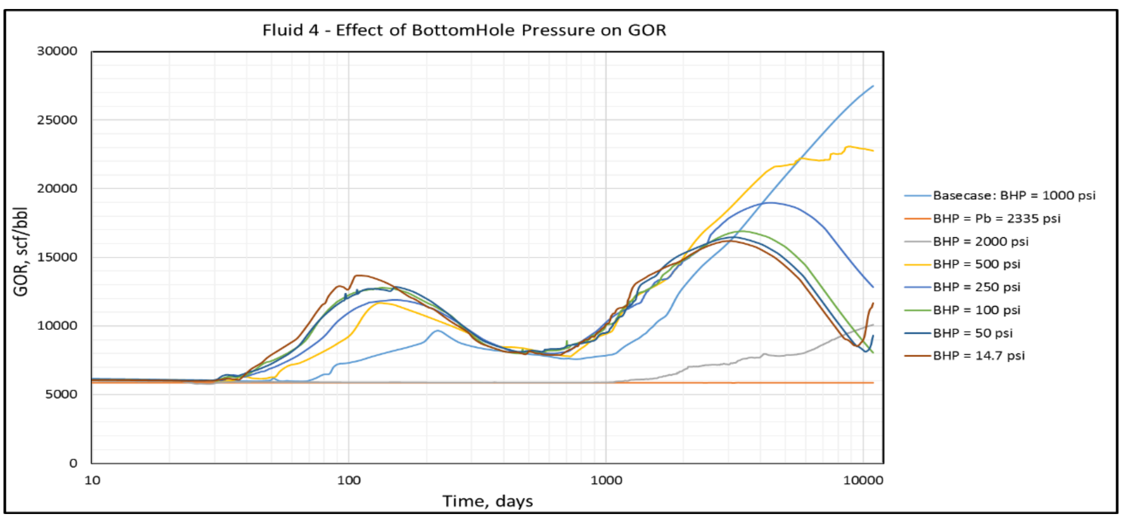

Figure 4-39 Fluid 4 – Effect of Bottomhole Pressure on GOR

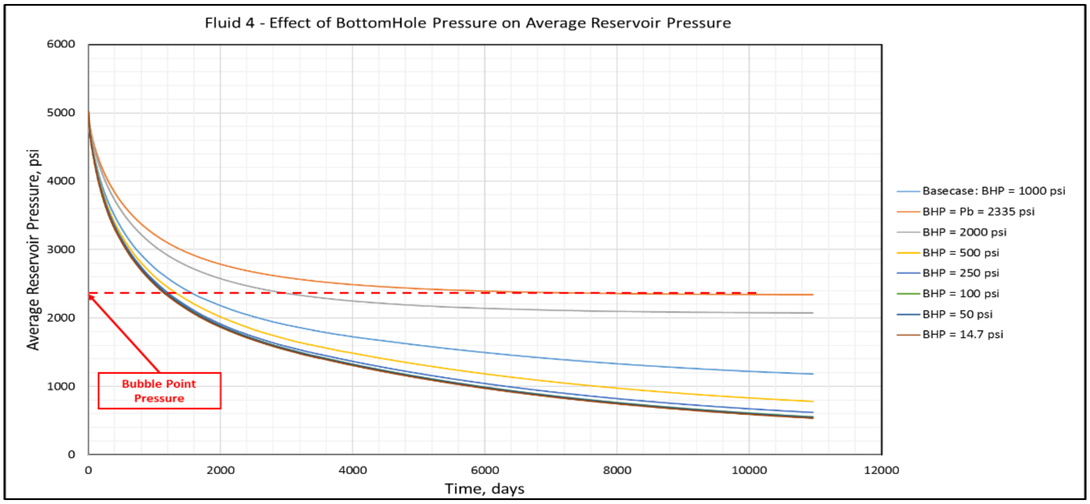

Figure 4-40 Fluid 4 - Effect of Bottomhole Pressure on Average Reservoir Pressure

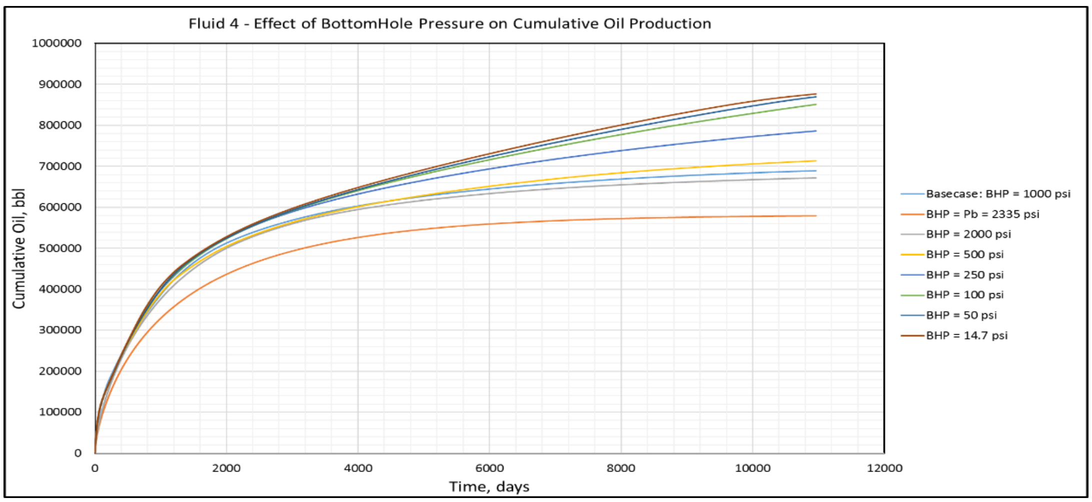

Figure 4-41 Fluid 4 – Effect of Bottomhole Pressure on Cumulative Oil Production

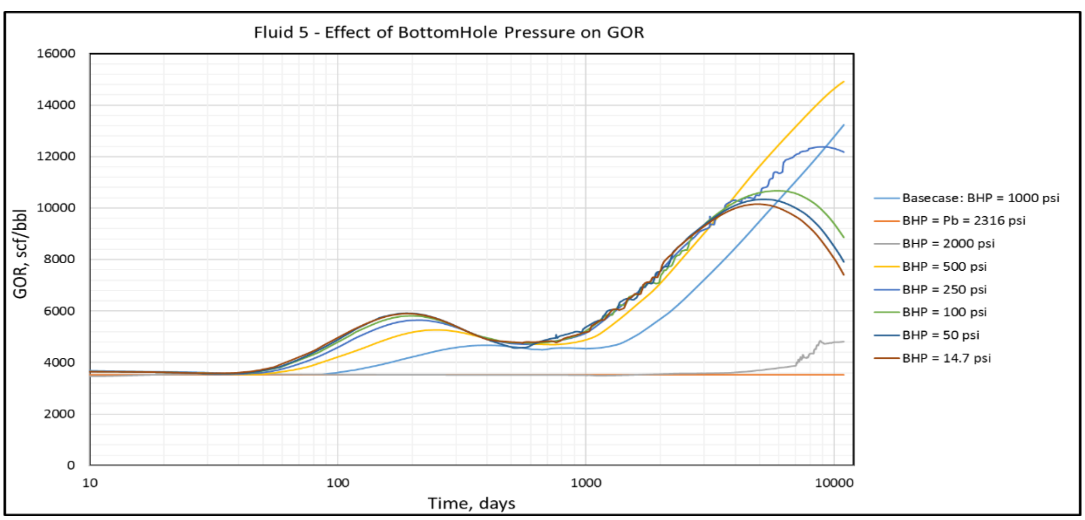

Figure 4-42 Fluid 5 – Effect of Bottomhole Pressure on GOR

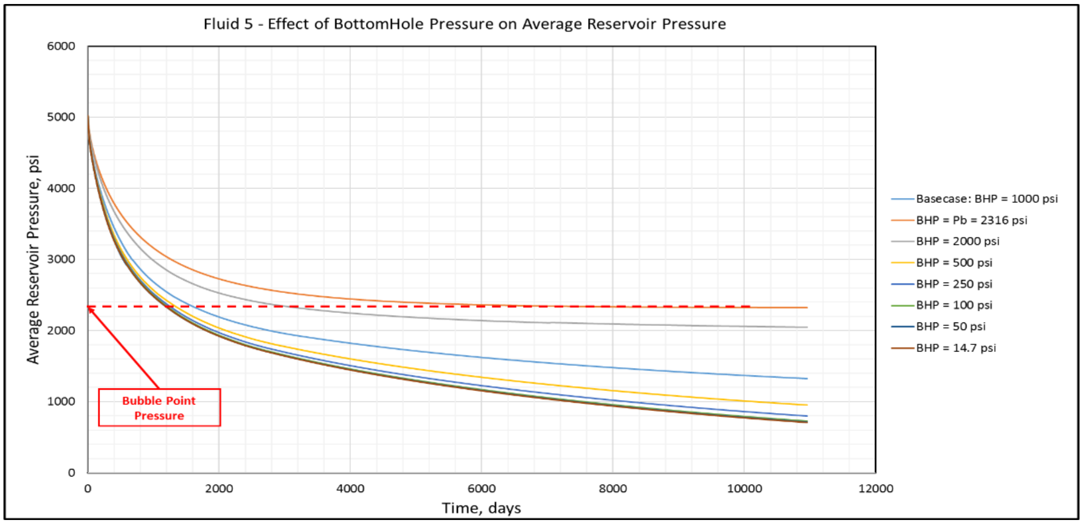

Figure 4-43 Fluid 5 – Effect of Bottomhole Pressure on Average Reservoir Pressure

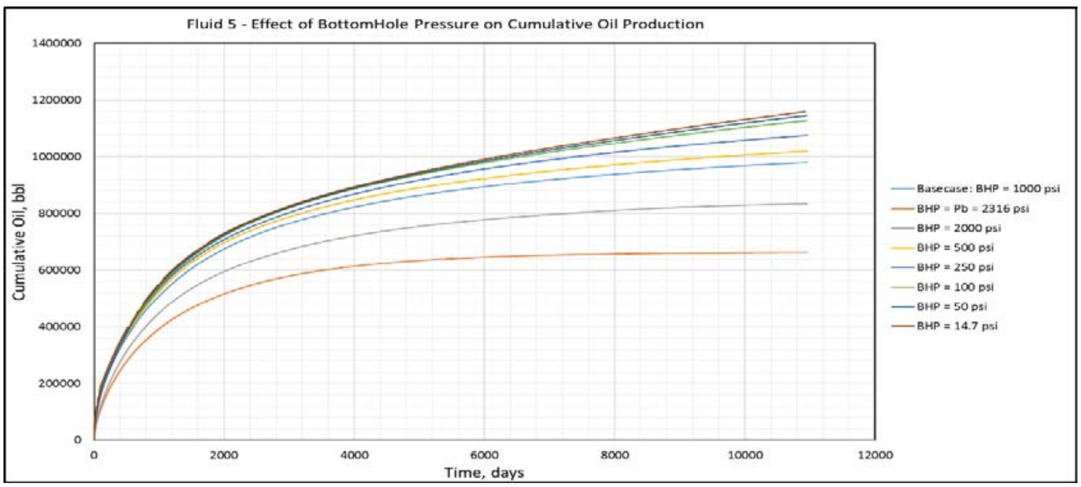

Figure 4-44 Fluid 5 – Effect of Bottomhole Pressure on Cumulative Oil Production

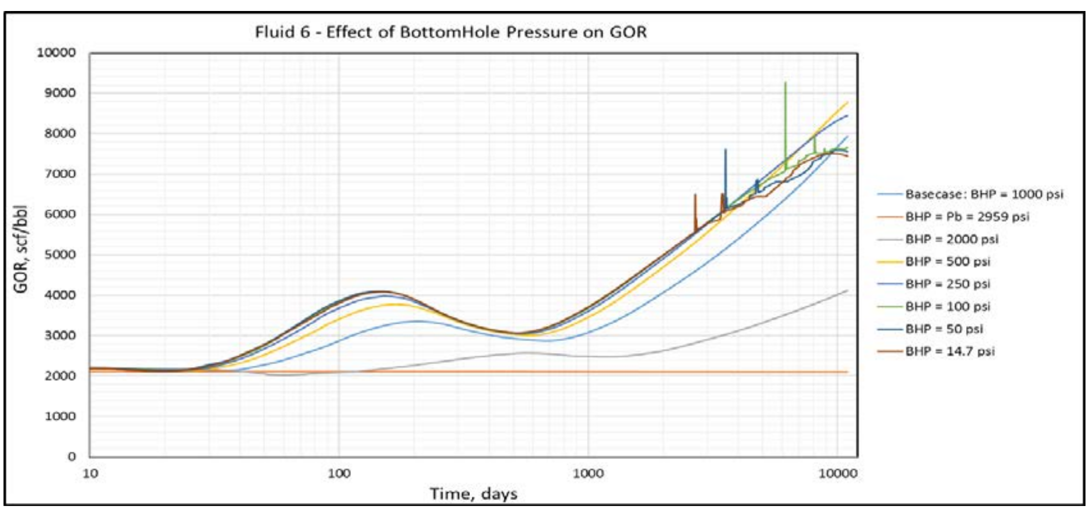

Figure 4-45 Fluid 6 – Effect of Bottomhole Pressure on GOR

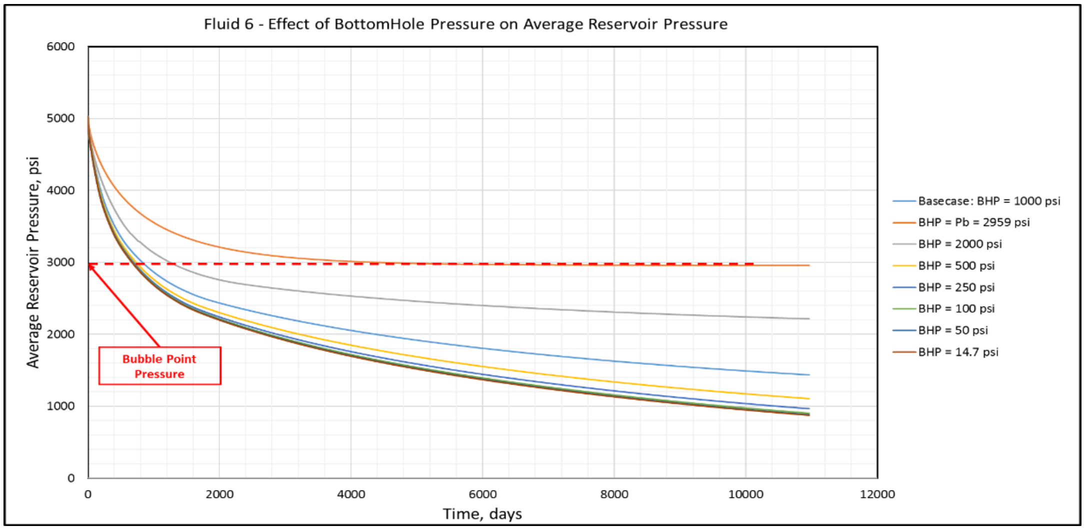

Figure 4-46 Fluid 6 – Effect of Bottomhole Pressure on Average Reservoir Pressure

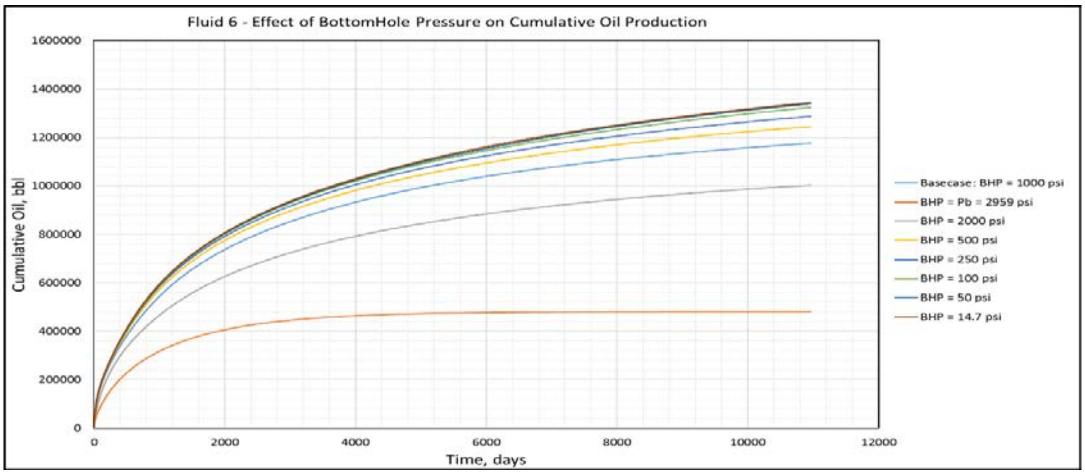

Figure 4-47 Fluid 6 – Effect of Bottomhole Pressure on Cumulative Oil Production

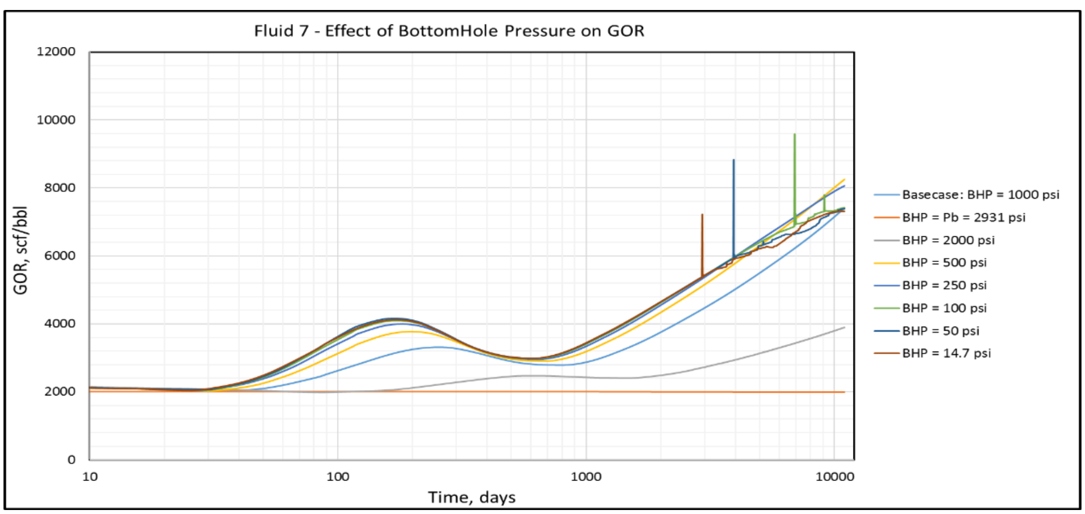

Figure 4-48 Fluid 7 – Effect of Bottomhole Pressure on GOR

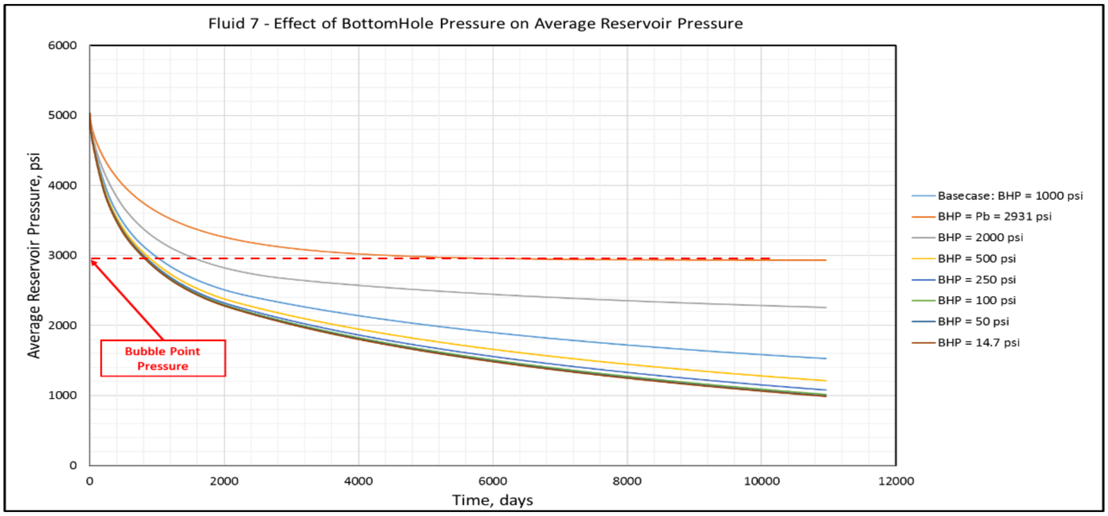

Figure 4-49 Fluid 7 – Effect of Bottomhole Pressure on Average Reservoir Pressure

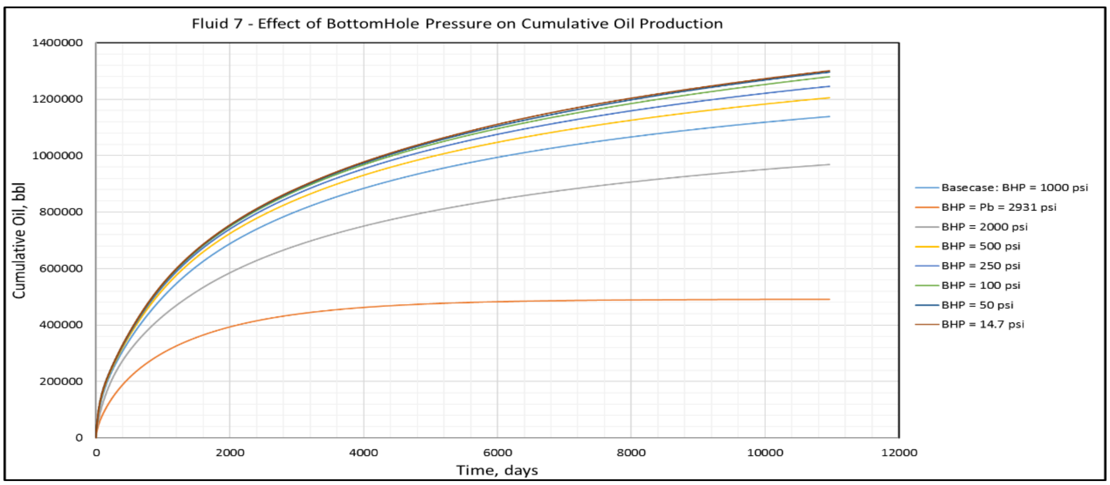

Figure 4-50 Fluid 7 – Effect of Bottomhole Pressure on Cumulative Oil Production

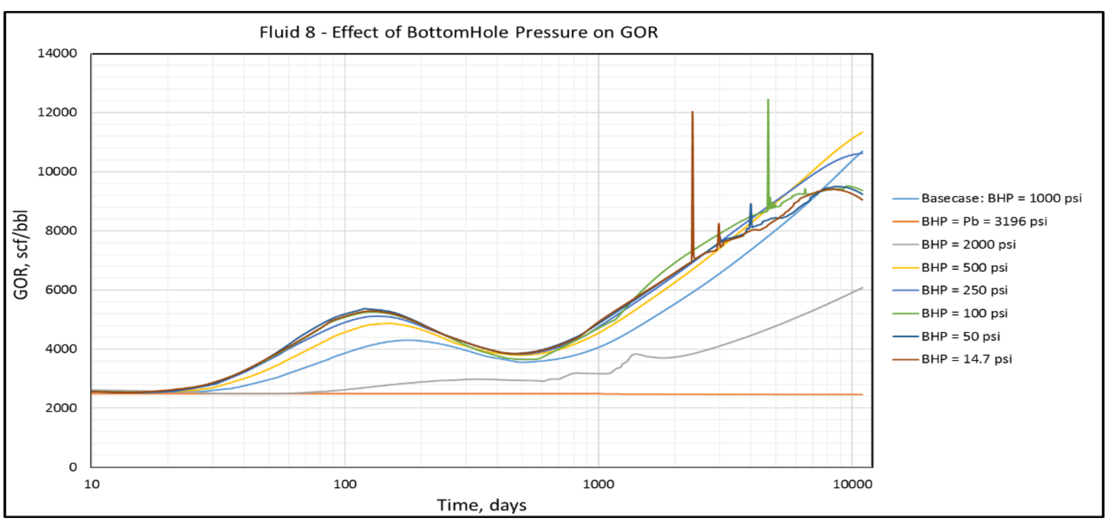

Figure 4-51 Fluid 8 – Effect of Bottomhole Pressure on GOR

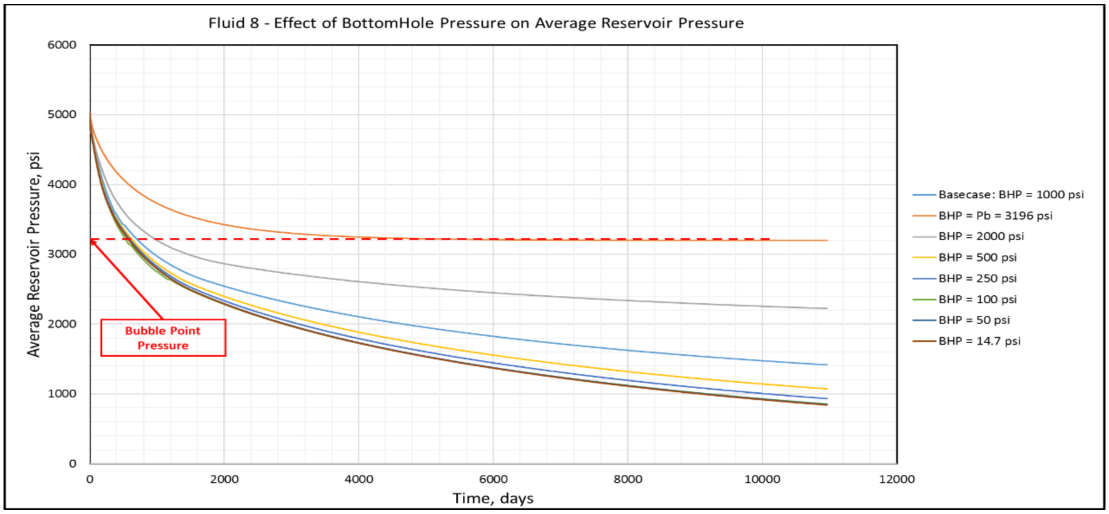

Figure 4-52 Fluid 8 – Effect of Bottomhole Pressure on Average Reservoir Pressure

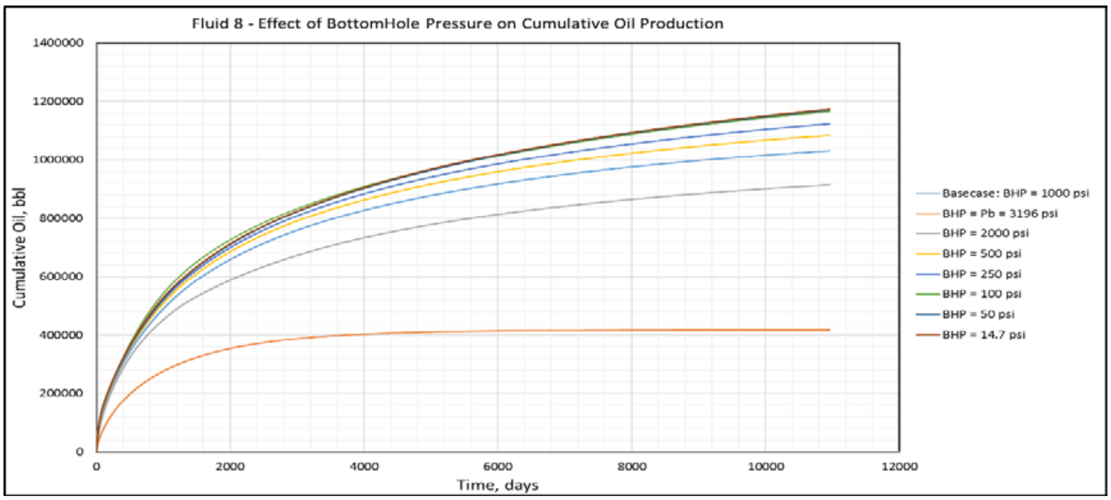

Figure 4-53 Fluid 8 – Effect of Bottomhole Pressure on Cumulative Oil Production

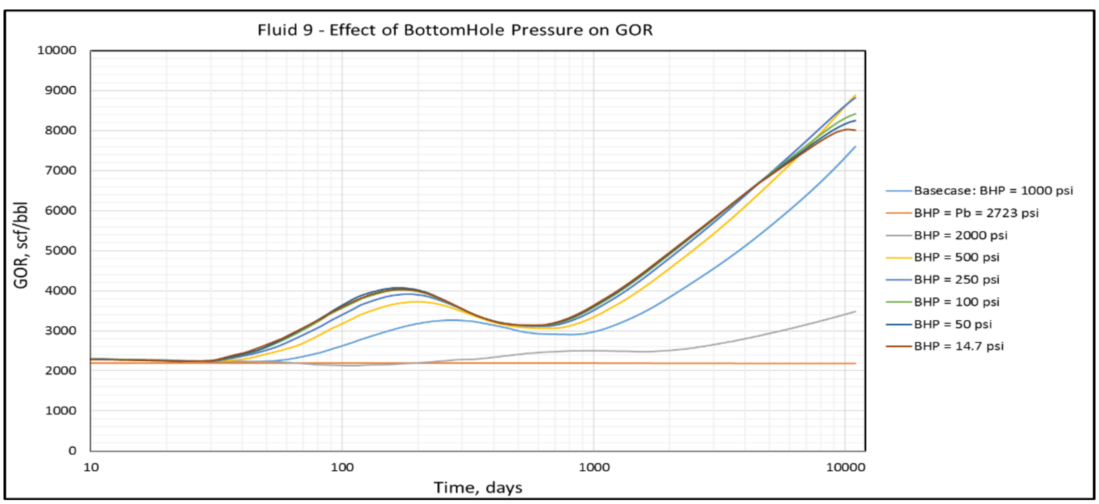

Figure 4-54 Fluid 9 – Effect of Bottomhole Pressure on GOR

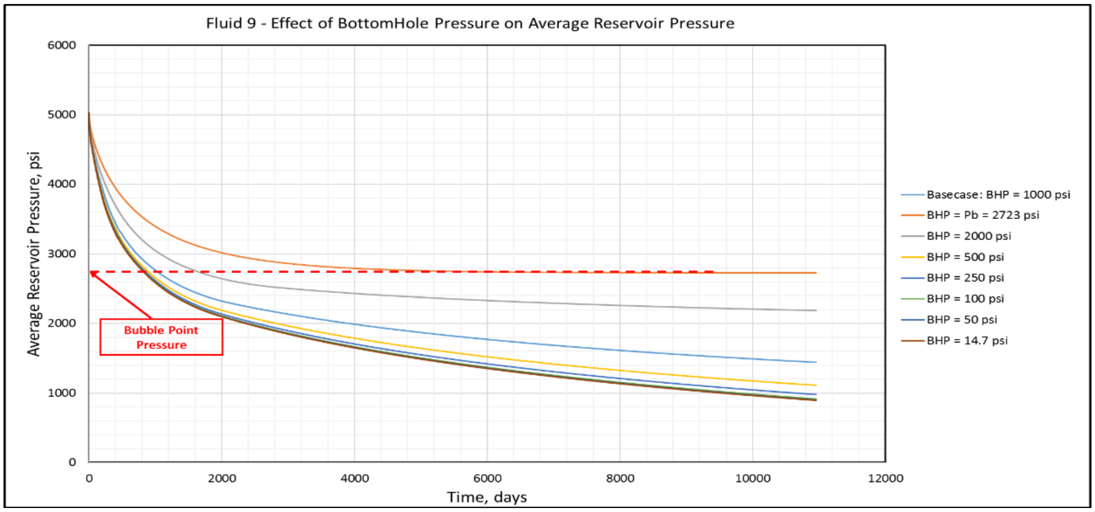

Figure 4-55 Fluid 9 – Effect of Bottomhole Pressure on Average Reservoir Pressure

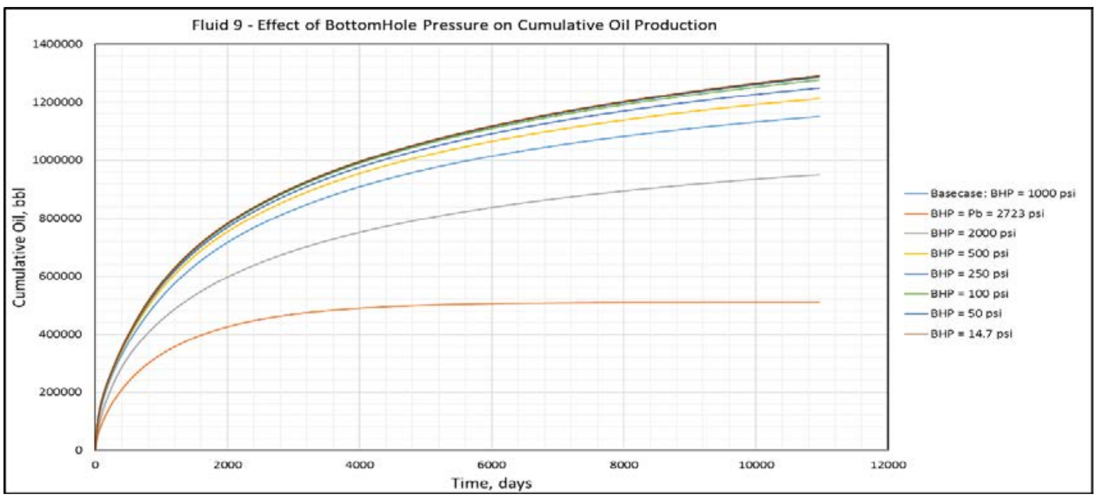

Figure 4-56 Fluid 9 – Effect of Bottomhole Pressure on Cumulative Oil Production

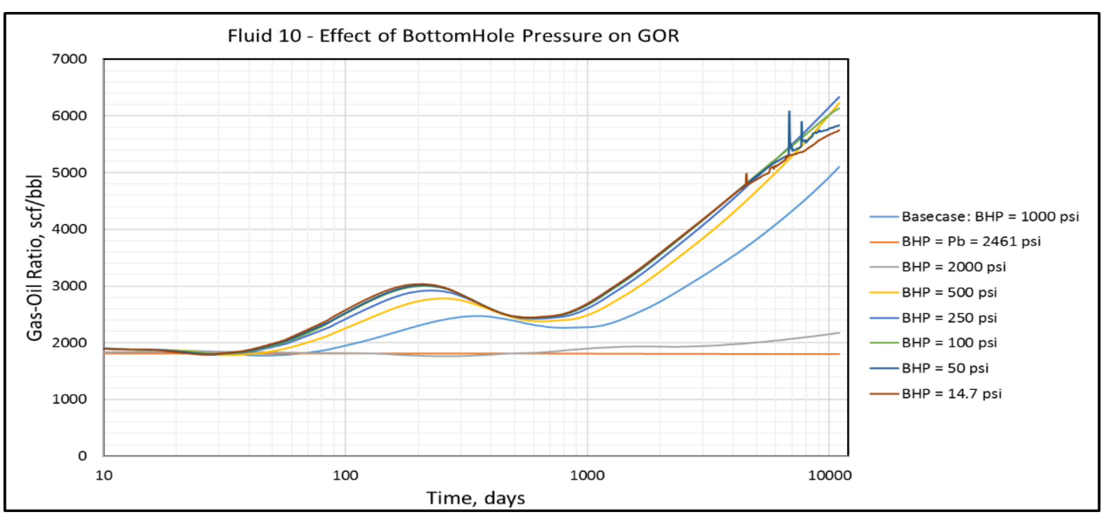

Figure 4-57 Fluid 10 – Effect of Bottomhole Pressure on GOR

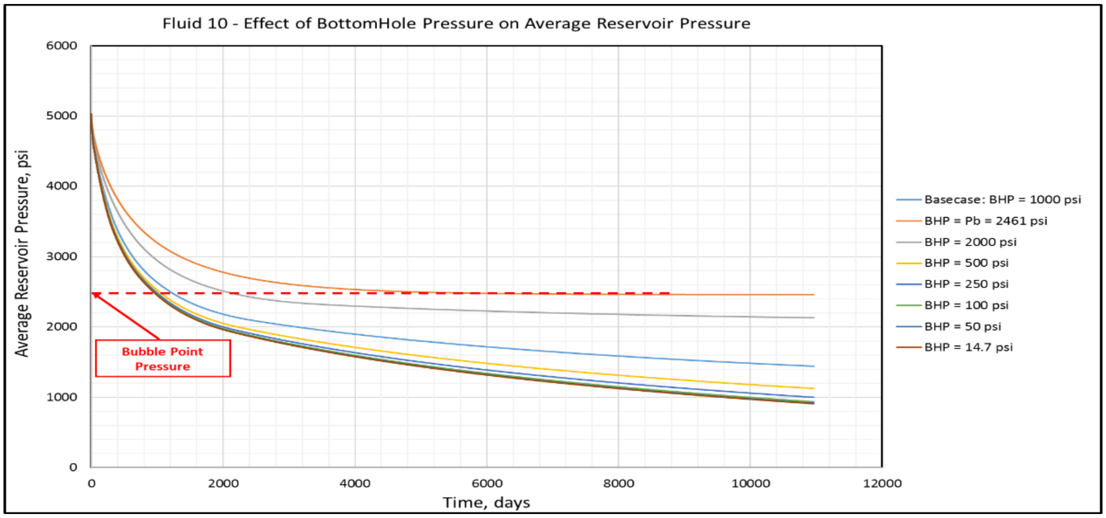

Figure 4-58 Fluid 10 – Effect of Bottomhole Pressure on Average Reservoir Pressure

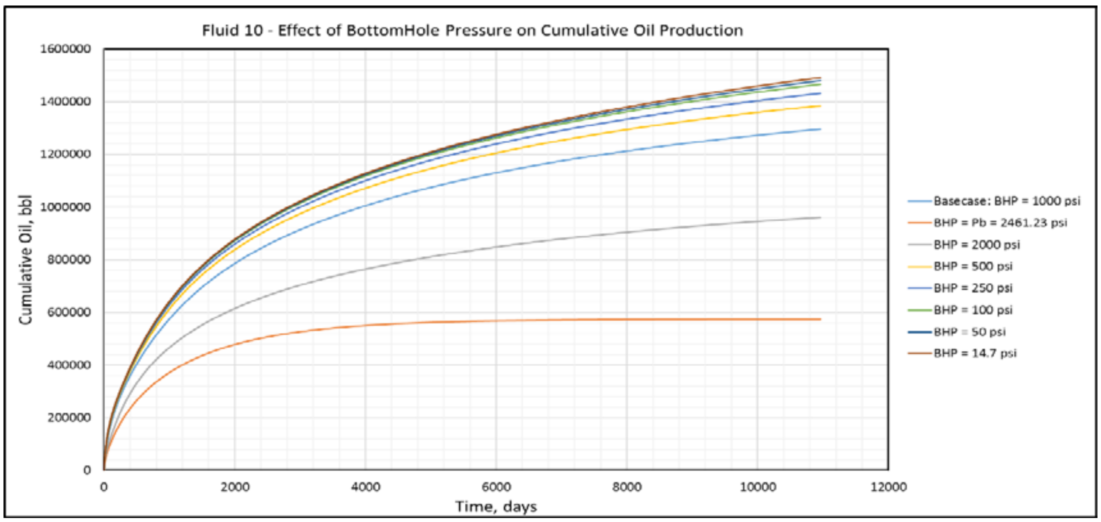

Figure 4-59 Fluid 10 – Effect of Bottomhole Pressure on Cumulative Oil Production

4.4. Degree of Undersaturation

The degree of undersaturation is the difference between the initial reservoir pressure and the saturation (bubble point) pressure. Cases with initial reservoir pressures of 5000 psi (basecase), 4500 psi, 4000 psi and 3500 psi were studied. The lower the degree of undersaturation, the quicker the reservoir pressure will reach the saturation pressure. Therefore, with decreasing degree of undersaturation, the producing GOR increases with time and vice versa. Correspondingly, there is a delay in the initial rise of producing GOR with increasing degree of undersaturation and vice versa. Likewise, the higher the degree of undersaturation, the lesser the height of the "GOR hill". Moreover, the higher the degree of undersaturation, the longer the period (at the start of production) where the producing GOR remains constant i.e., the period where the producing GOR is approximately equal to the initial solution GOR. Also, oil production increases with increasing degree of undersaturation. With higher degree of undersaturation, there is more time for single phase oil production before the reservoir pressure reaches the bubble point and the evolution of gas starts to aid further production of oil. Figures 4-60 to 4-89 show the effects of the degree of undersaturation on the producing GOR (semi-log plots), cumulative oil production and average reservoir pressure. Generally, the trends are similar in all cases regardless of the volatility of the volatile oil fluid sample considered.

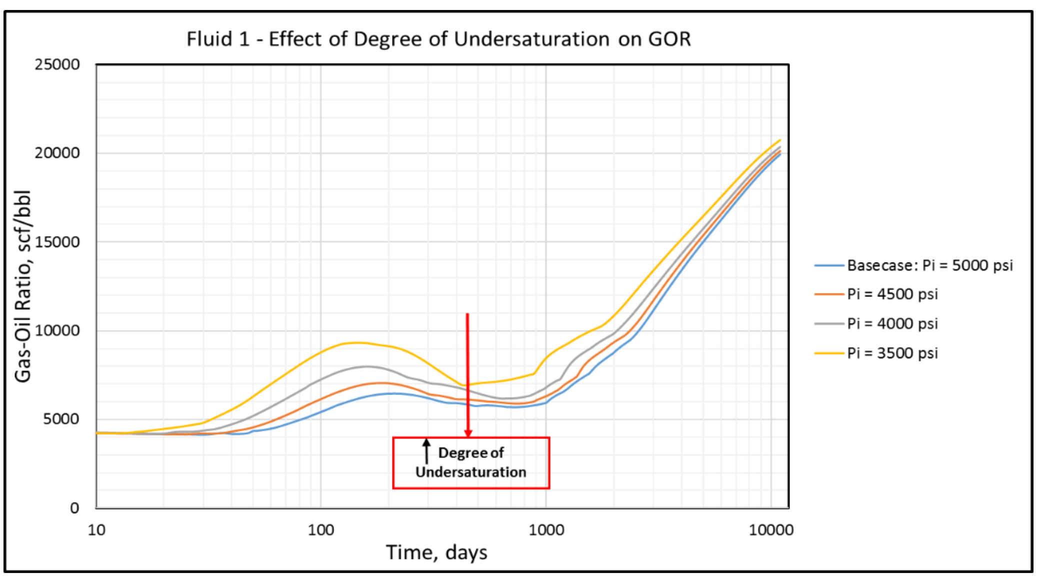

Figure 4-60 Fluid 1 – Effect of Degree of Undersaturation on GOR

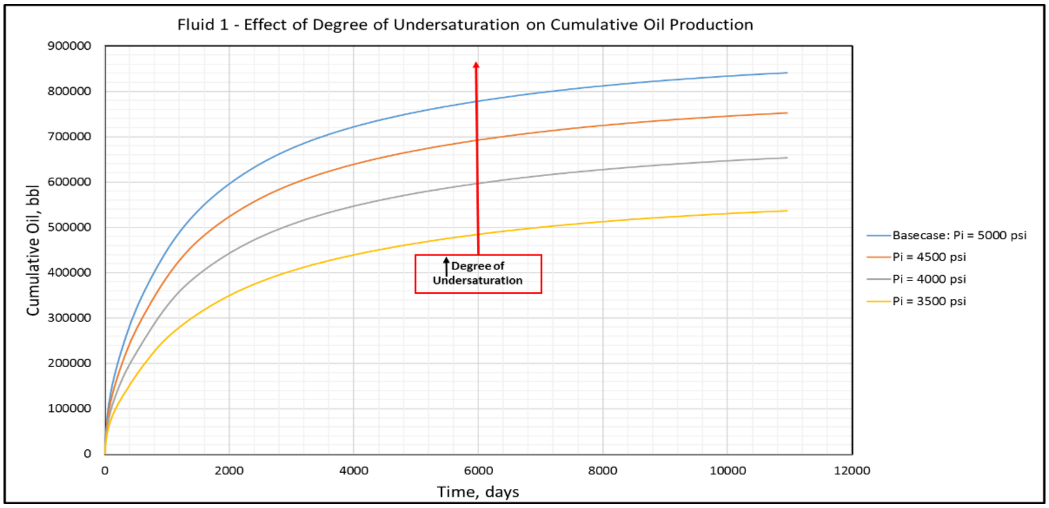

Figure 4-61 Fluid 1 – Effect of Degree of Undersaturation on Cumulative Oil Production

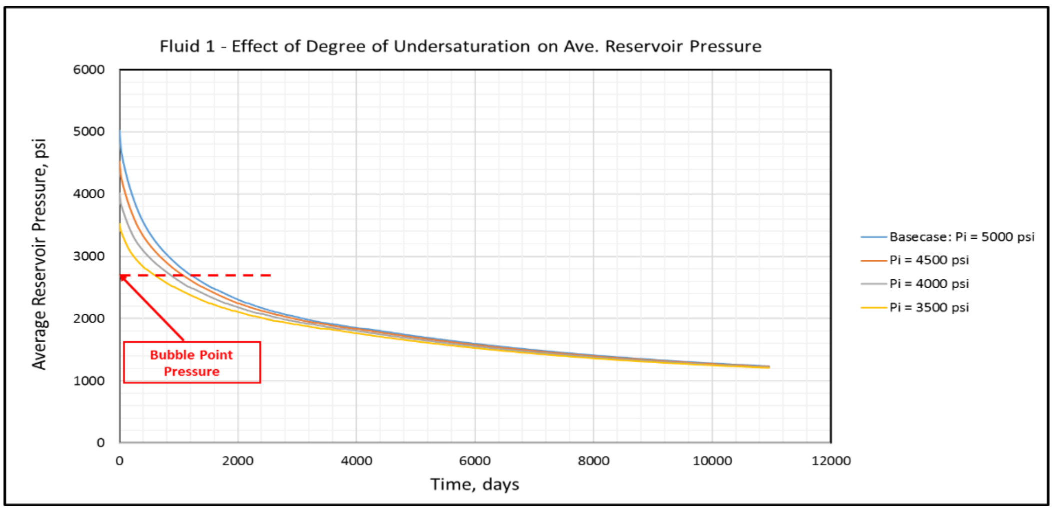

Figure 4-62 Fluid 1 – Effect of Degree of Undersaturation on Average Reservoir Pressure

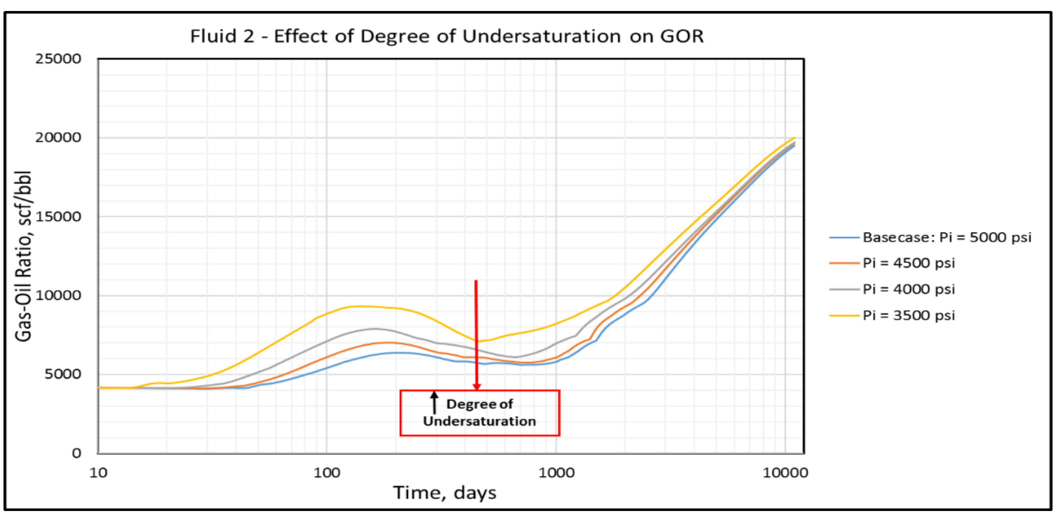

Figure 4-63 Fluid 2 – Effect of Degree of Undersaturation on GOR

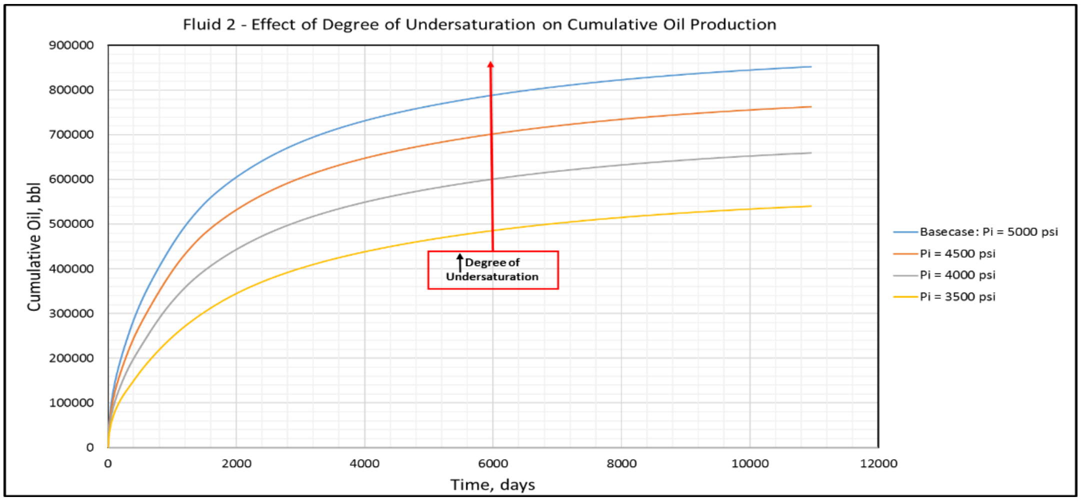

Figure 4-64 Fluid 2 – Effect of Degree of Undersaturation on Cumulative Oil Production

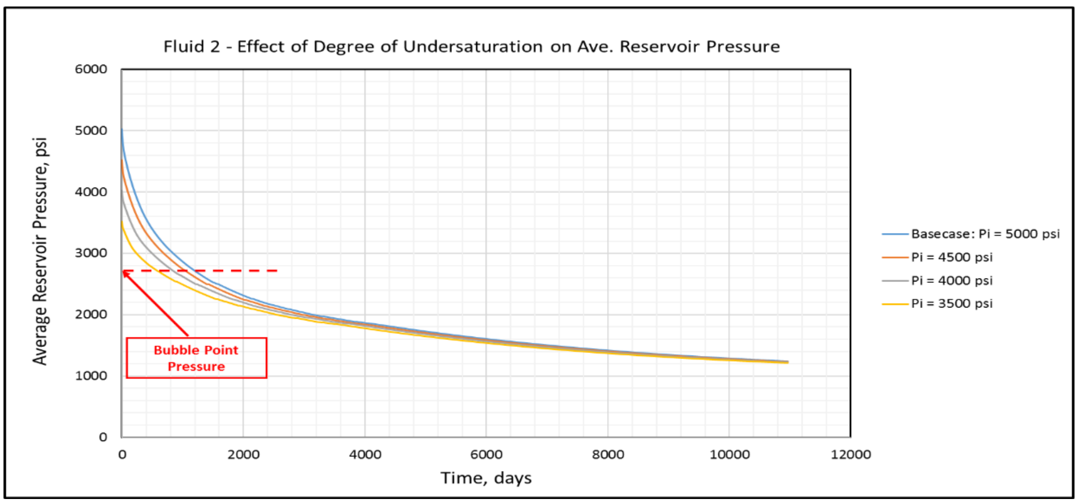

Figure 4-65 Fluid 2 – Effect of Degree of Undersaturation on Average Reservoir Pressure

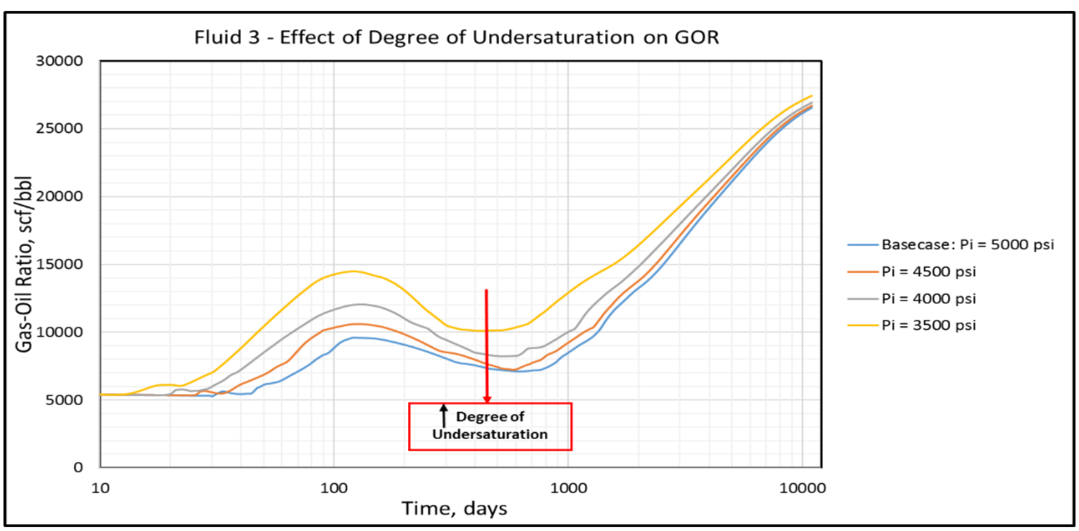

Figure 4-66 Fluid 3 – Effect of Degree of Undersaturation on GOR

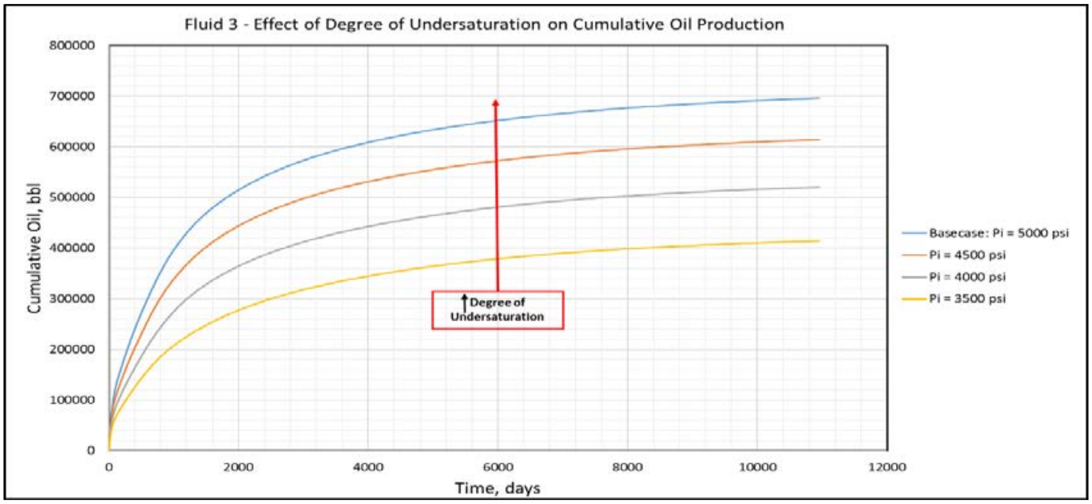

Figure 4-67 Fluid 3 – Effect of Degree of Undersaturation on Cumulative Oil Production

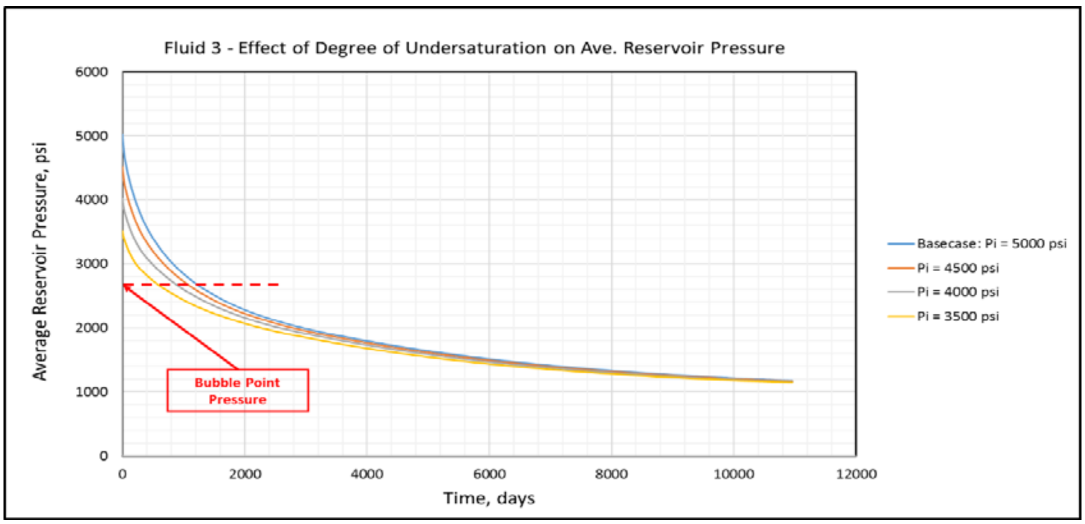

Figure 4-68 Fluid 3 – Effect of Degree of Undersaturation on Average Reservoir Pressure

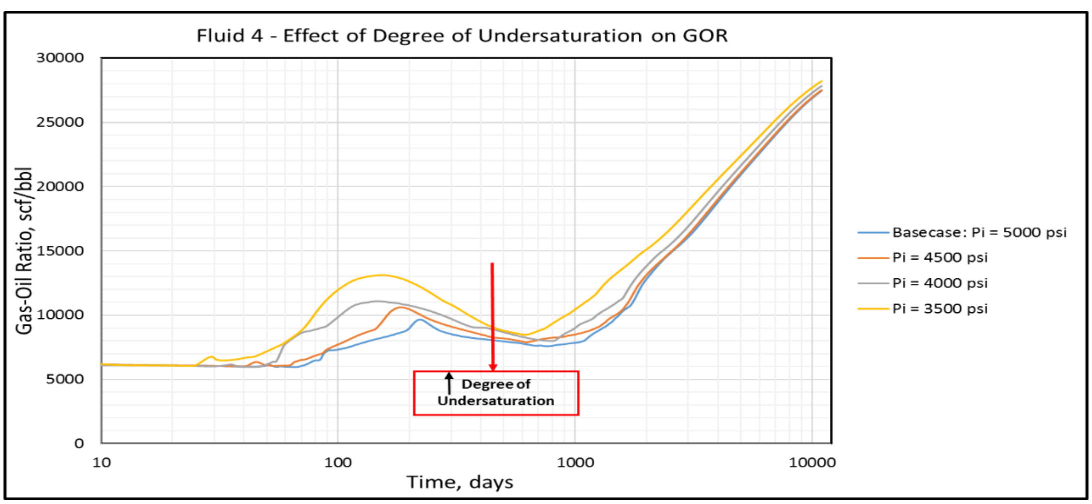

Figure 4-69 Fluid 4 – Effect of Degree of Undersaturation on GOR

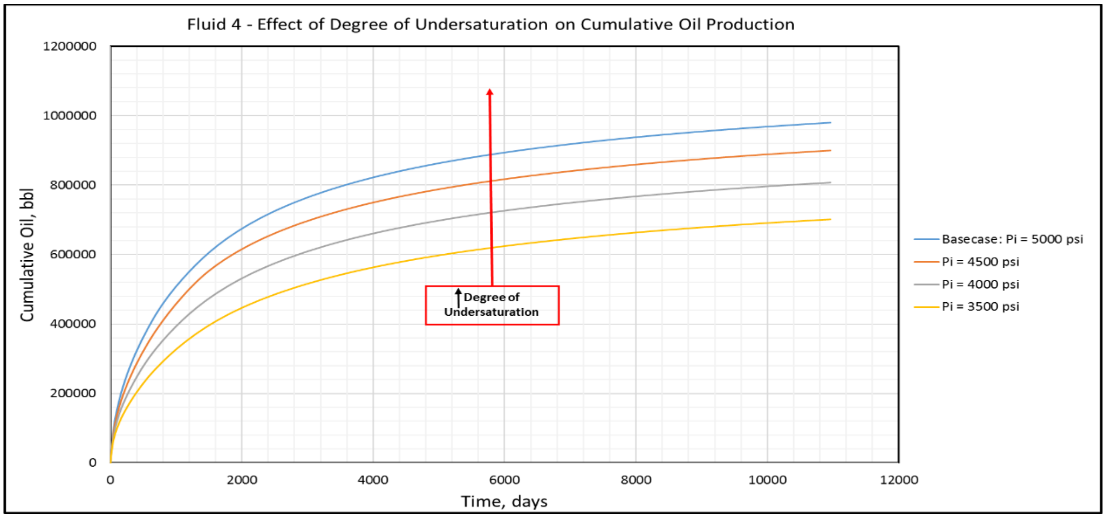

Figure 4-70 Fluid 4 – Effect of Degree of Undersaturation on Cumulative Oil Production

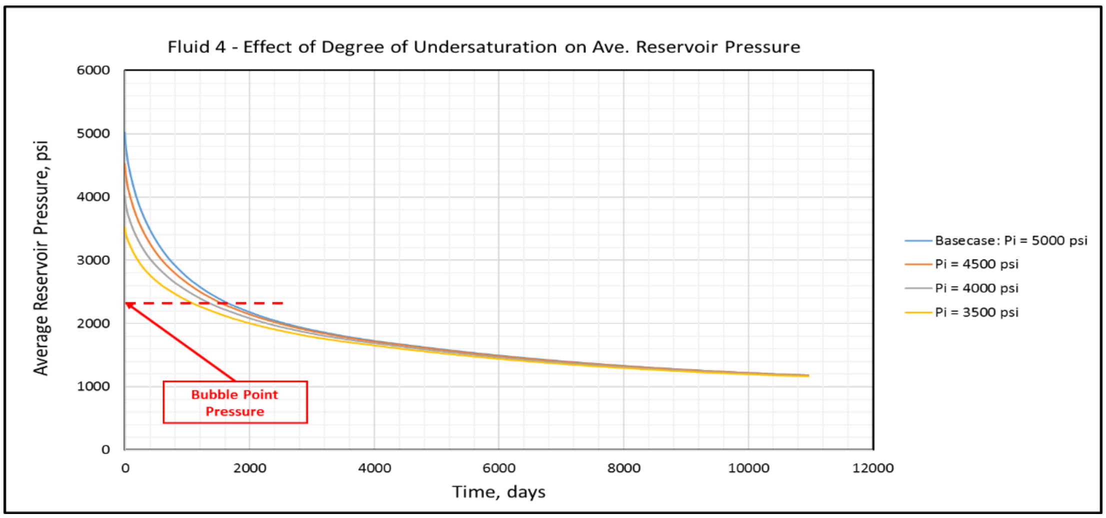

Figure 4-71 Fluid 4 – Effect of Degree of Undersaturation on Average Reservoir Pressure

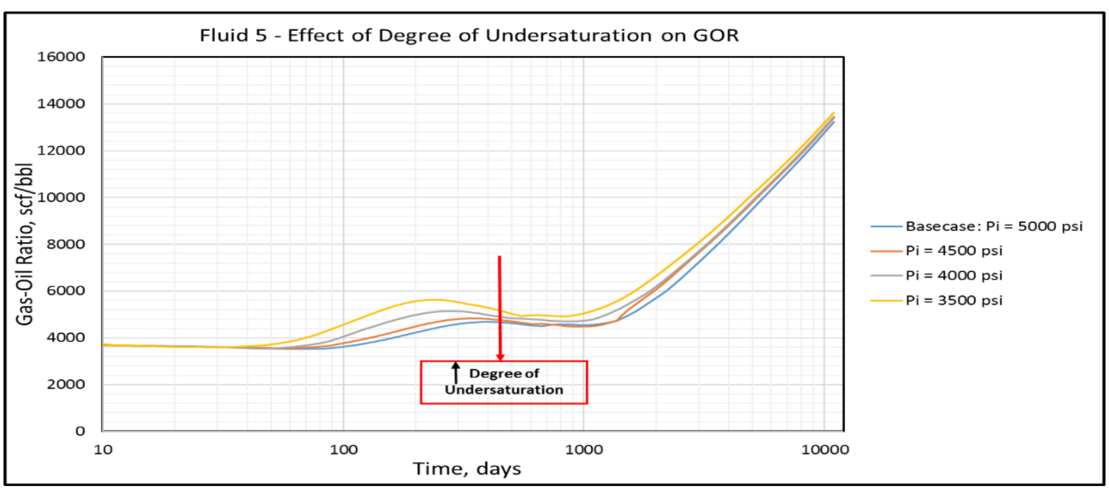

Figure 4-72 Fluid 5 – Effect of Degree of Undersaturation on GOR

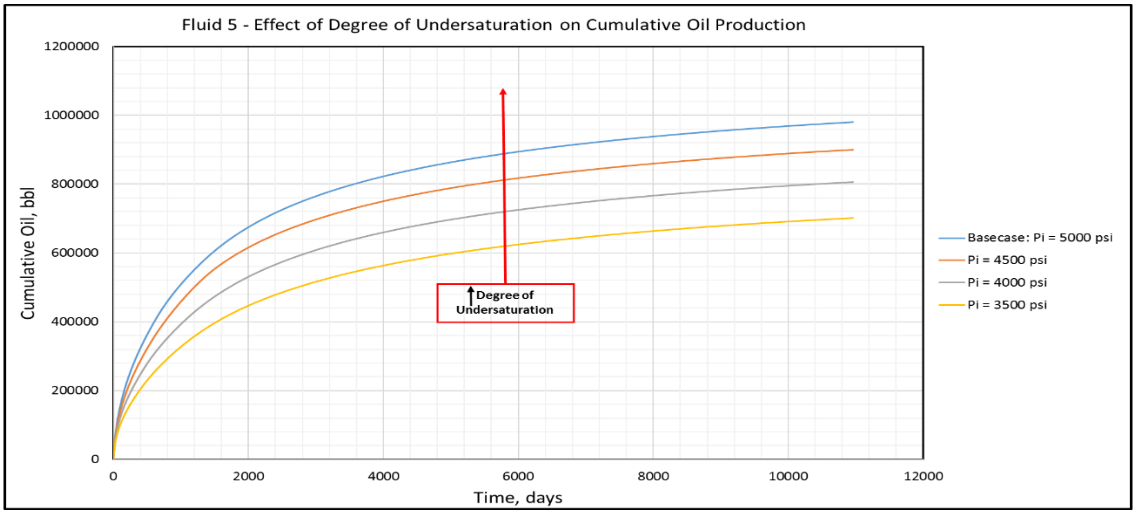

Figure 4-73 Fluid 5 – Effect of Degree of Undersaturation on Cumulative Oil Production

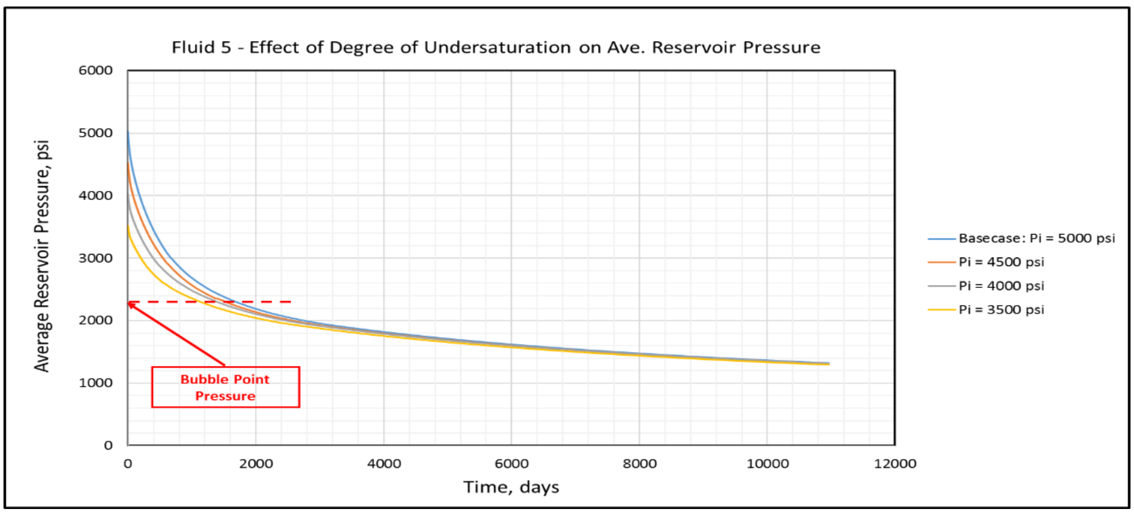

Figure 4-74 Fluid 5 – Effect of Degree of Undersaturation on Average Reservoir Pressure

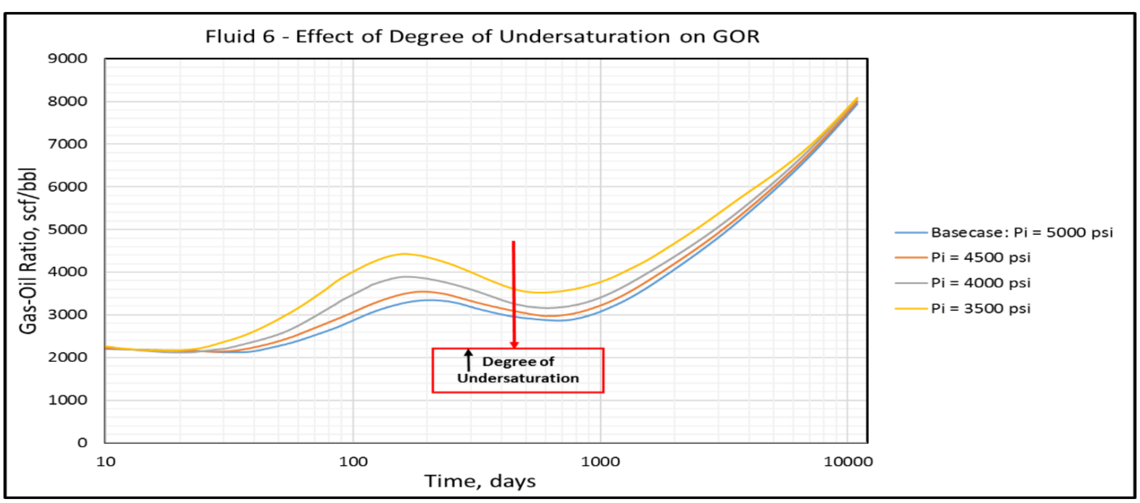

Figure 4-75 Fluid 6 – Effect of Degree of Undersaturation on GOR

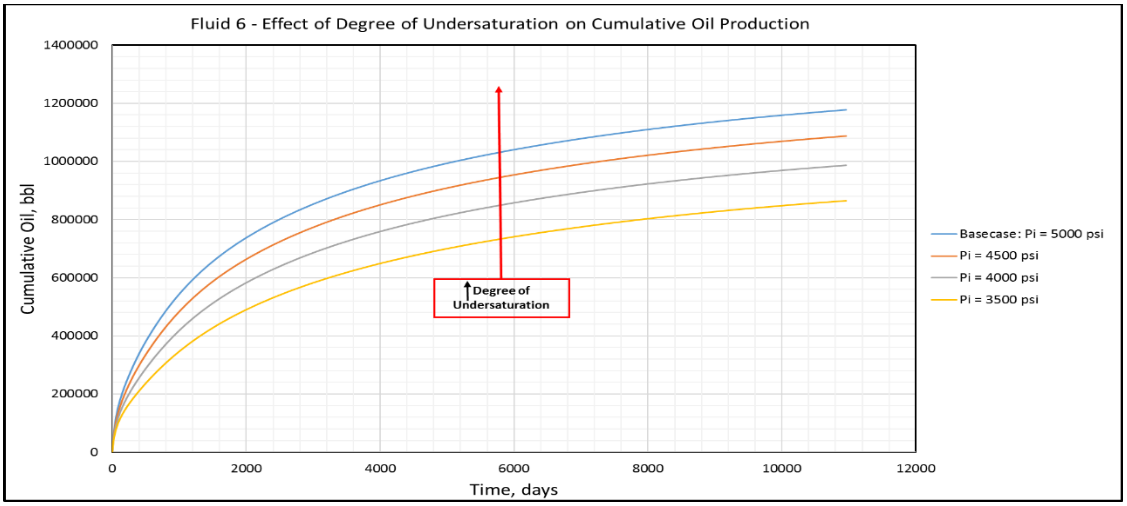

Figure 4-76 Fluid 6 – Effect of Degree of Undersaturation on Cumulative Oil Production

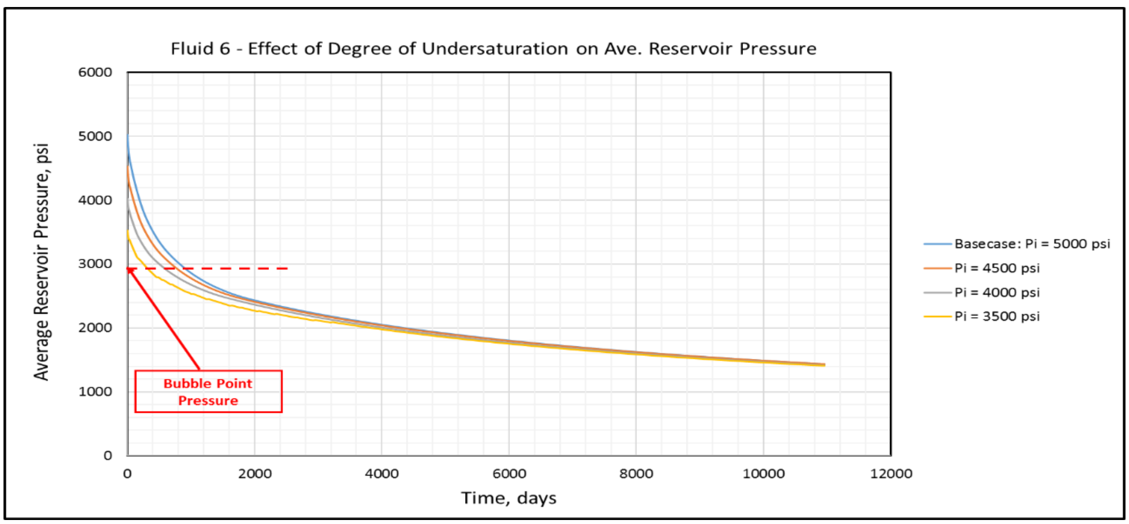

Figure 4-77 Fluid 6 – Effect of Degree of Undersaturation on Average Reservoir Pressure

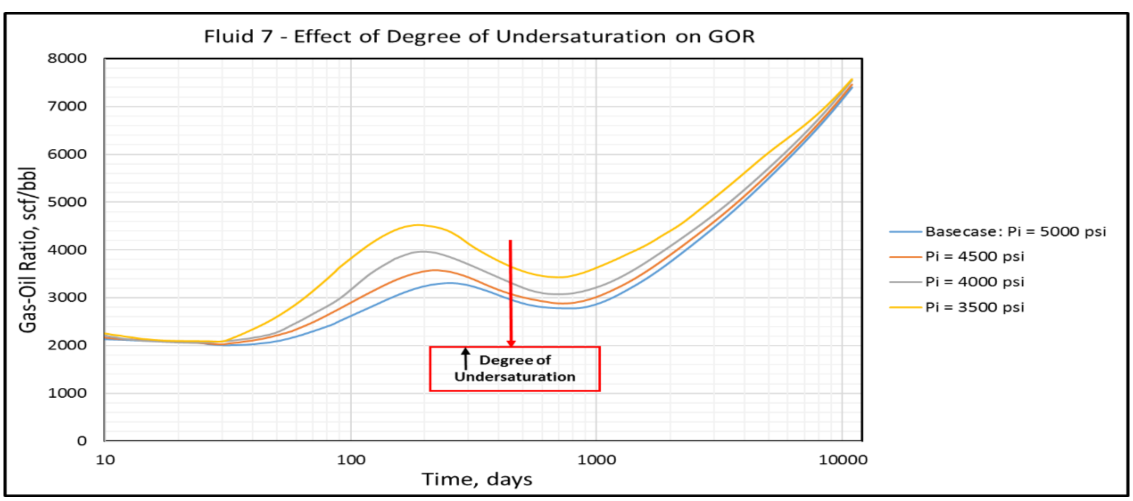

Figure 4-78 Fluid 7 – Effect of Degree of Undersaturation on GOR

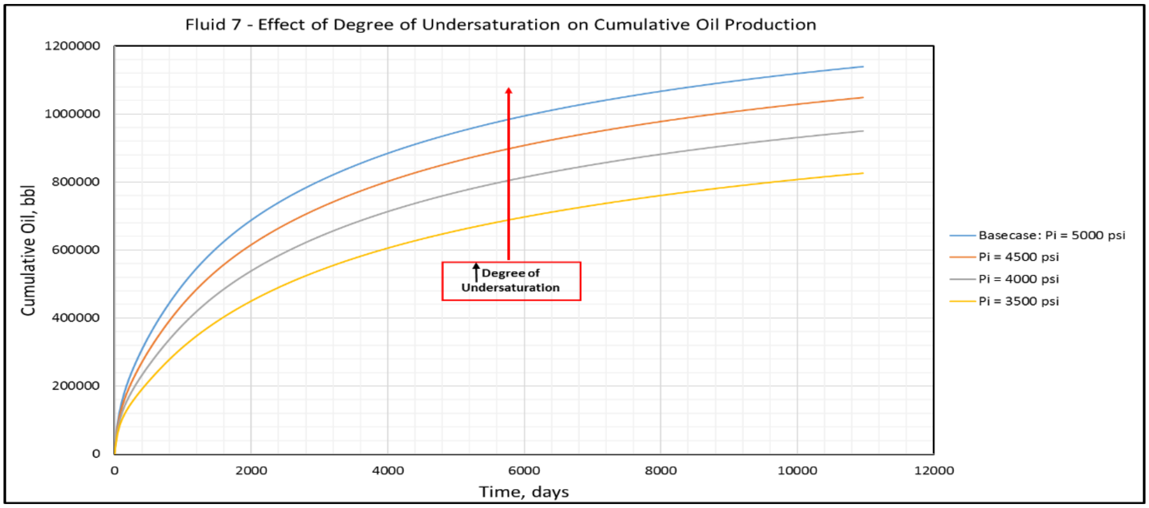

Figure 4-79 Fluid 7 – Effect of Degree of Undersaturation on Cumulative Oil Production

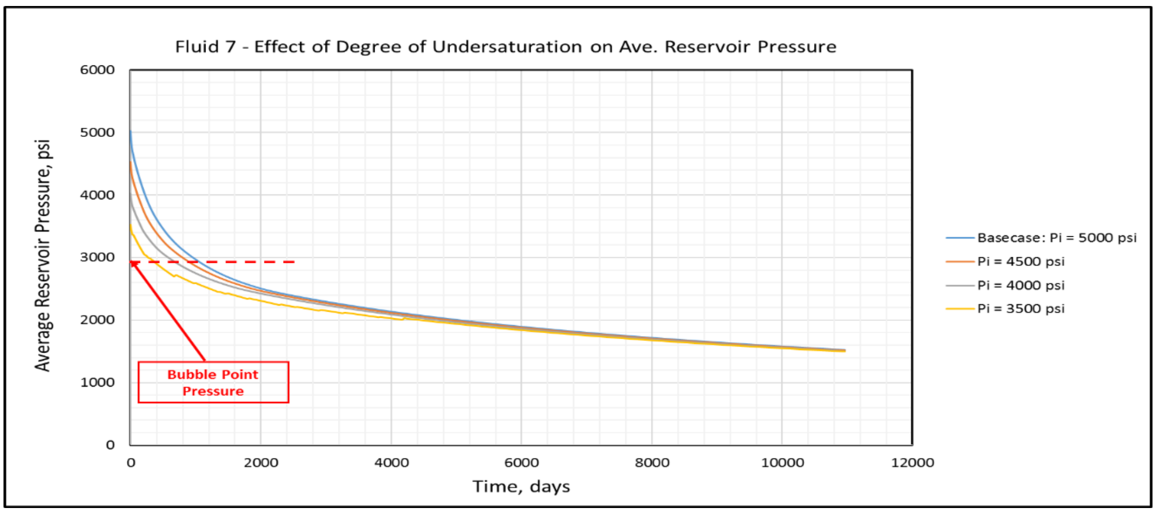

Figure 4-80 Fluid 7 – Effect of Degree of Undersaturation on Average Reservoir Pressure

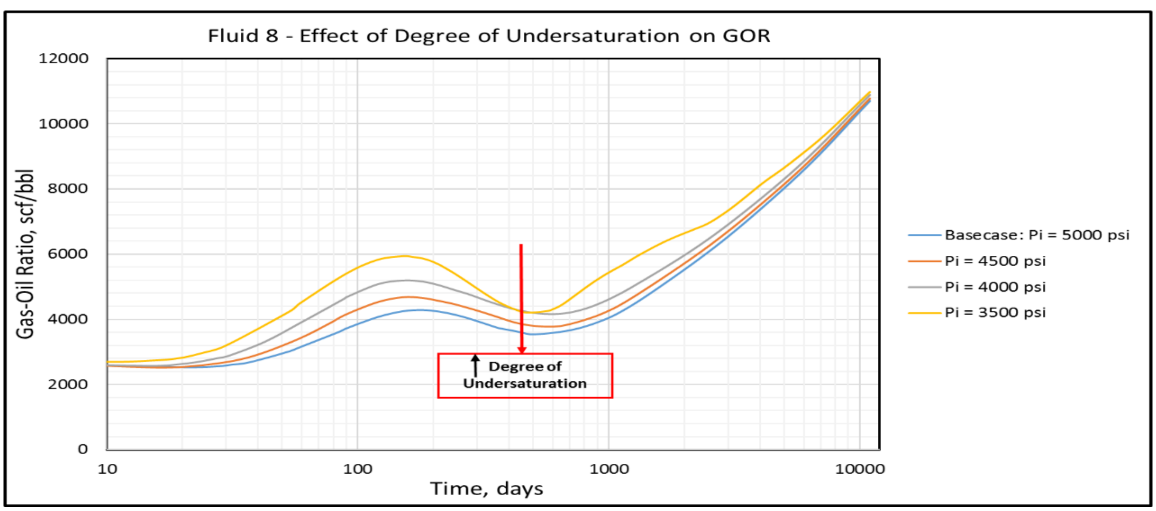

Figure 4-81 Fluid 8 – Effect of Degree of Undersaturation on GOR

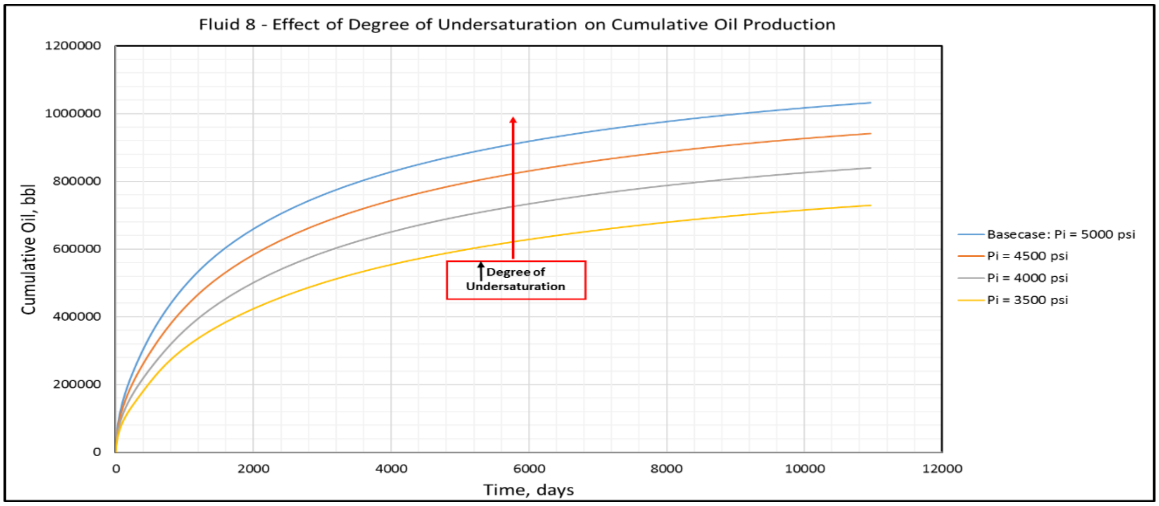

Figure 4-82 Fluid 8 – Effect of Degree of Undersaturation on Cumulative Oil Production

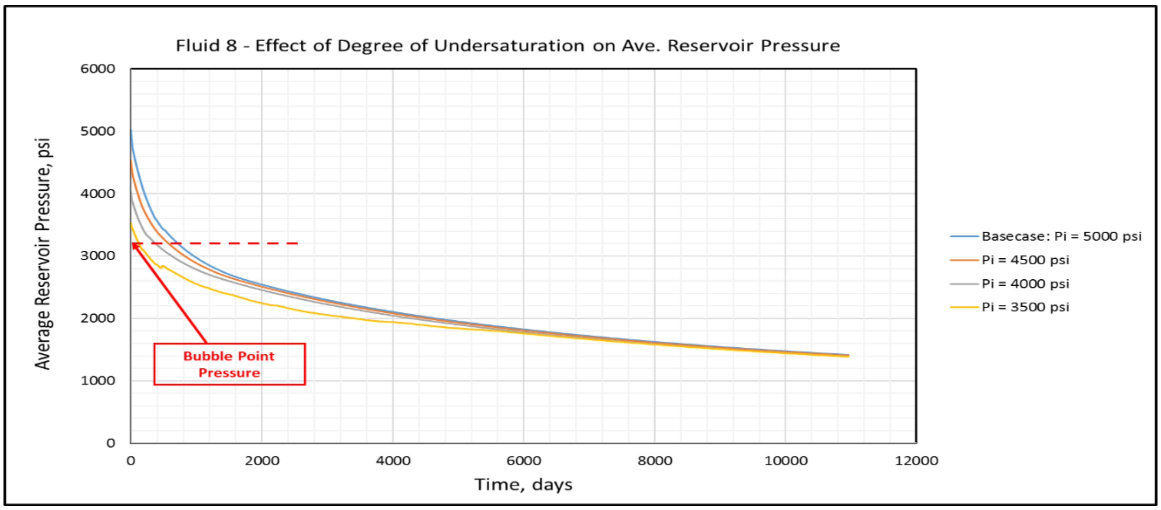

Figure 4-83 Fluid 8 – Effect of Degree of Undersaturation on Average Reservoir Pressure

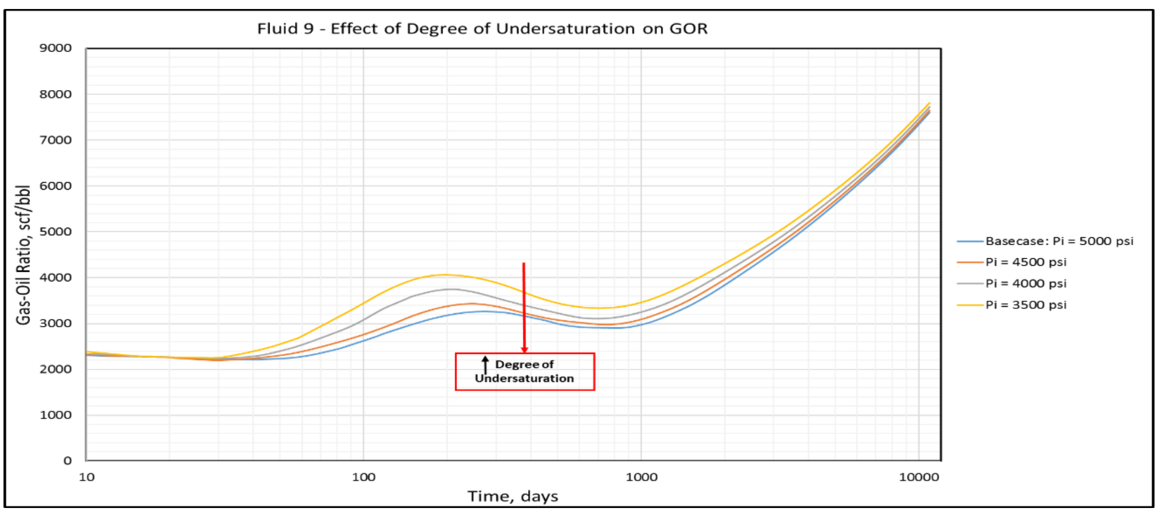

Figure 4-84 Fluid 9 – Effect of Degree of Undersaturation on GOR

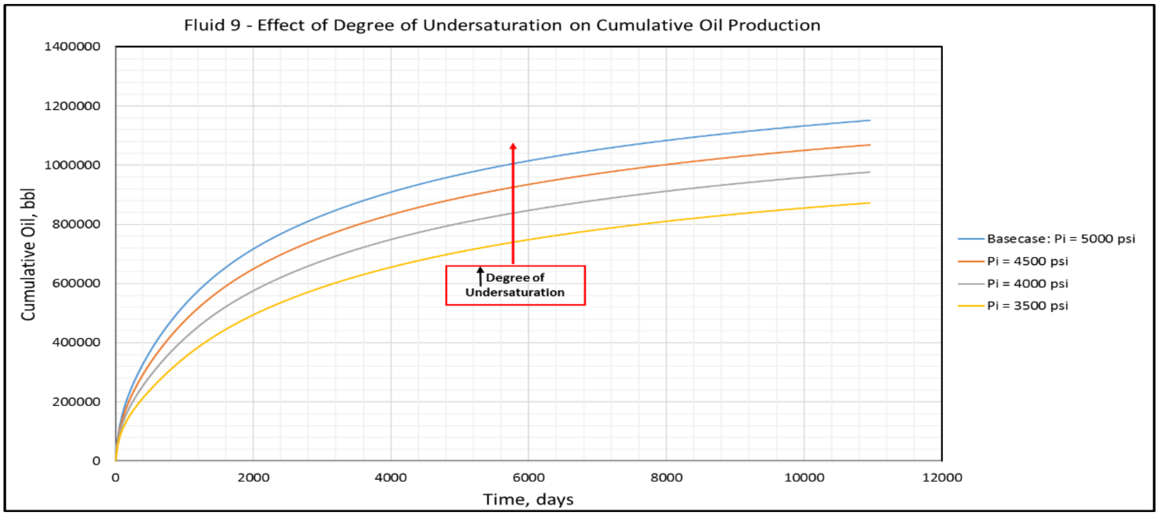

Figure 4-85 Fluid 9 – Effect of Degree of Undersaturation on Cumulative Oil Production

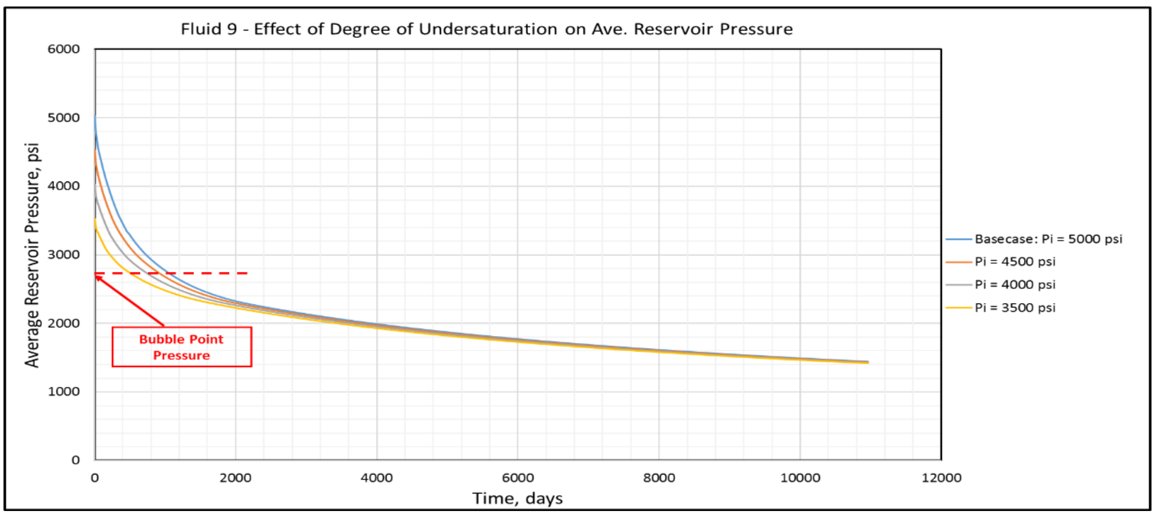

Figure 4-86 Fluid 9 – Effect of Degree of Undersaturation on Average Reservoir Pressure

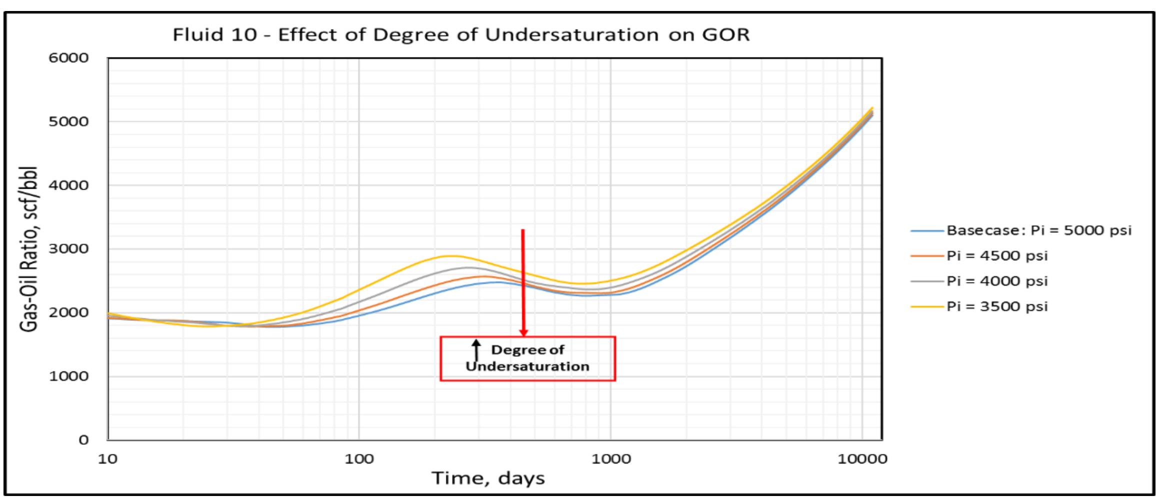

Figure 4-87 Fluid 10 – Effect of Degree of Undersaturation on GOR

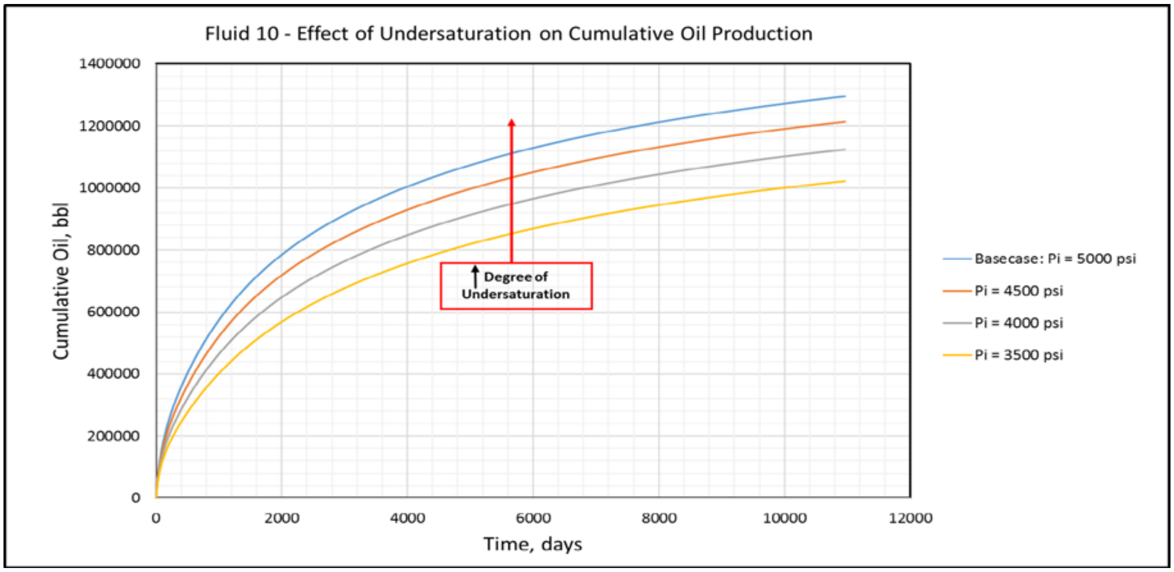

Figure 4-88 Fluid 10 – Effect of Undersaturation on Cumulative Oil Production

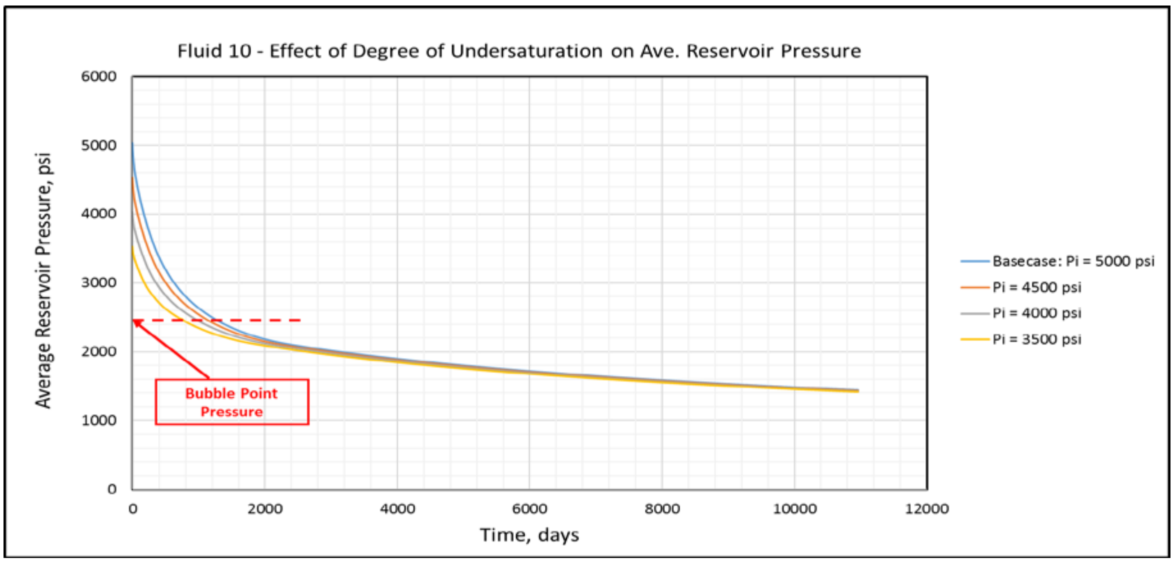

Figure 4-89 Fluid 10 – Effect of Degree of Undersaturation on Average Reservoir Pressure

4.5. Drainage Area

Drainage area is the reservoir area drained by the well. We varied the drainage area to investigate the effect it has on well performance in shale volatile oil reservoirs. Apart from the basecase that has an approximate drainage area of 76 acres, we considered to two other different cases – drainage area 1 (approximately 104 acres) and drainage area 2 (approximately 275 acres). Figures 4-90 to 4-92 show the pictorial description of each drainage area.

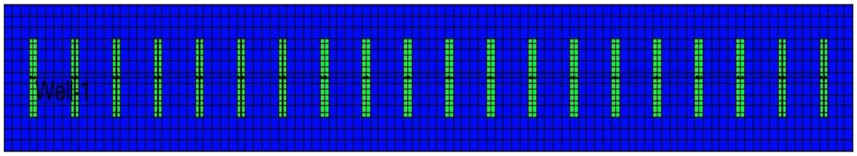

Figure 4-90 Basecase Drainage Area (Approx. 76 acres)

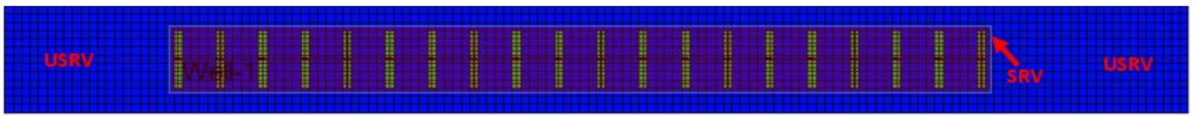

Figure 4-91 Drainage Area 1 (Approx. 104 acres)

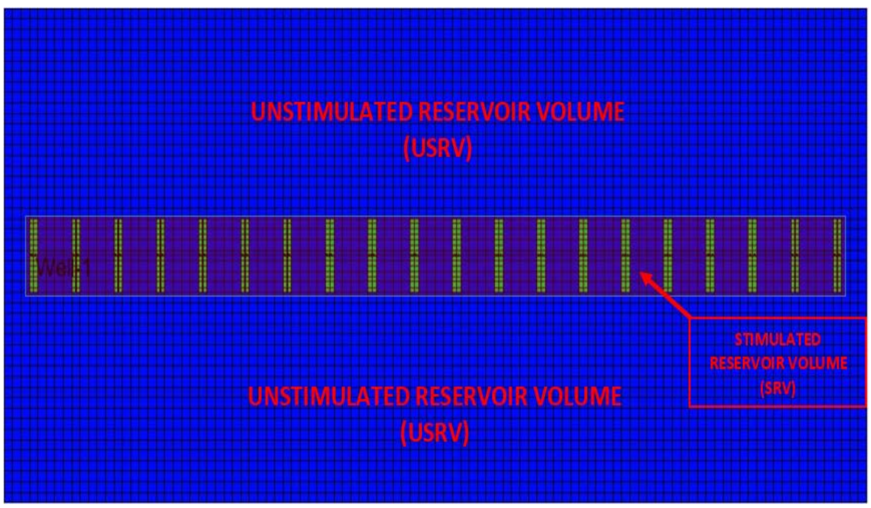

Figure 4-92 Drainage Area 2 (Approx. 275 acres)

With increasing reservoir drainage area, cumulative oil production increases. However, oil recovery increases with decreasing reservoir drainage area. This result is similar to that obtained in a study by Permadi (1998).

For the case with drainage area of approximately 275 acres (drainage area 2 – Figure 4-92), boundary-dominated flow (BDF) is not reached in some instances due to low permeability and the relatively large unstimulated reservoir volume (USRV). This is the situation especially when moderately volatile oil reservoir fluids are present. For highly volatile oils, BDF is observed because of higher oil mobility (less viscosity in comparison to less volatile oils) towards the regions close to the stimulated reservoir volume (SRV). This BDF is followed by a late linear (or compound linear) flow when production from the unstimulated reservoir volume (USRV) dominates.

The trend of producing GOR is generally the same till boundary-dominated flow (as observed on the rate-time diagnostic plots) is reached. According to Jones (2016), for multi-fractured horizontal wells (MFHW), producing GOR rises during BDF because of declining pressures at the midpoint between fractures and corresponding increase in average gas saturation in the drainage area. This phenomenon is observable in our results. After boundary-dominated flow, there is a steeper rise in producing GOR with reducing reservoir drainage area. With increasing reservoir drainage area, it takes longer to reach boundary-dominated flow (BDF is not even observed in some cases depending on the volatility of the reservoir fluid). Therefore, the larger the reservoir area, the milder the rise in producing GOR with time. Due to the higher mobility of highly volatile oils, production may later be dominated by the regions beyond the SRV (for larger reservoir drainage areas), leading to the decline of producing GOR towards the end of the production period (30 years in our cases). Figures 4-93 to 4-132 show the impacts of drainage area on cumulative oil production, oil recovery factor, rate-time diagnostic plots and producing GOR (semi-log plots).

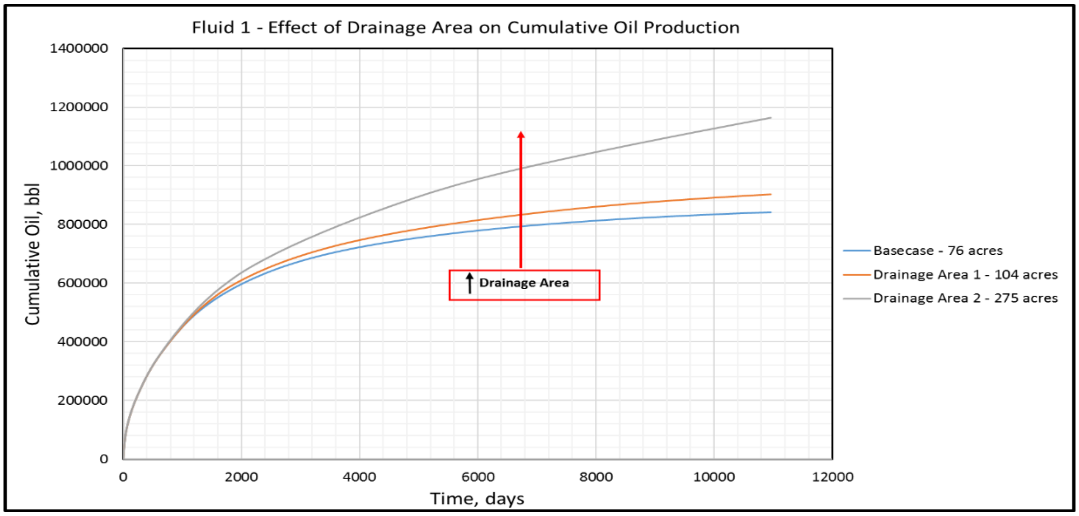

Figure 4-93 Fluid 1 – Effect of Drainage Area on Cumulative Oil Production

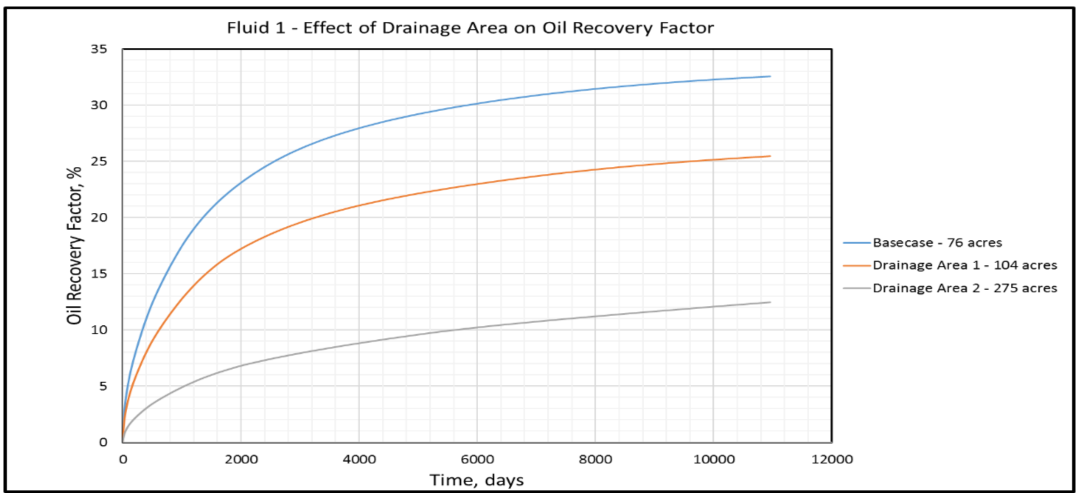

Figure 4-94 Fluid 1 – Effect of Drainage Area on Oil Recovery Factor

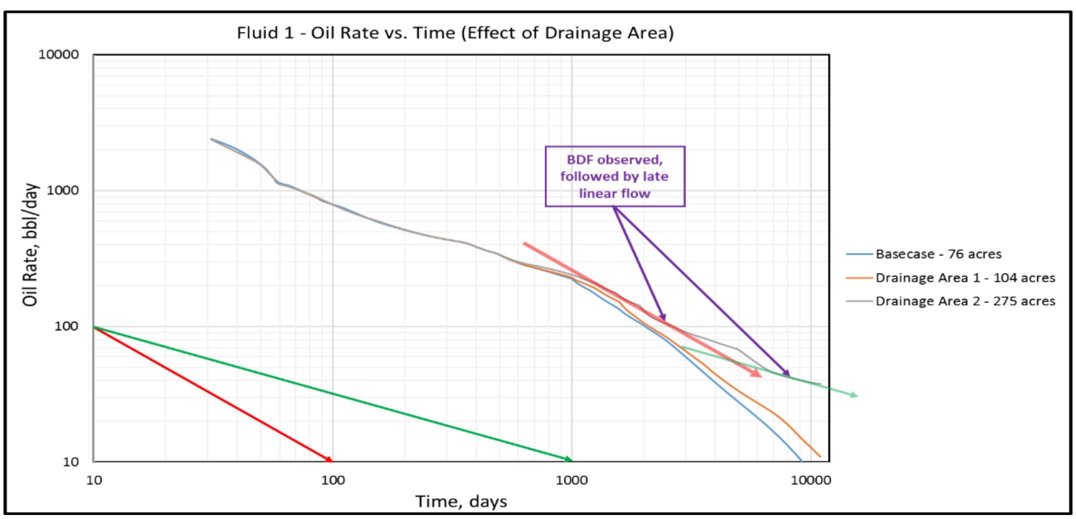

Figure 4-95 Fluid 1 – Effect of Drainage Area on Rate-Time Diagnostic Plots

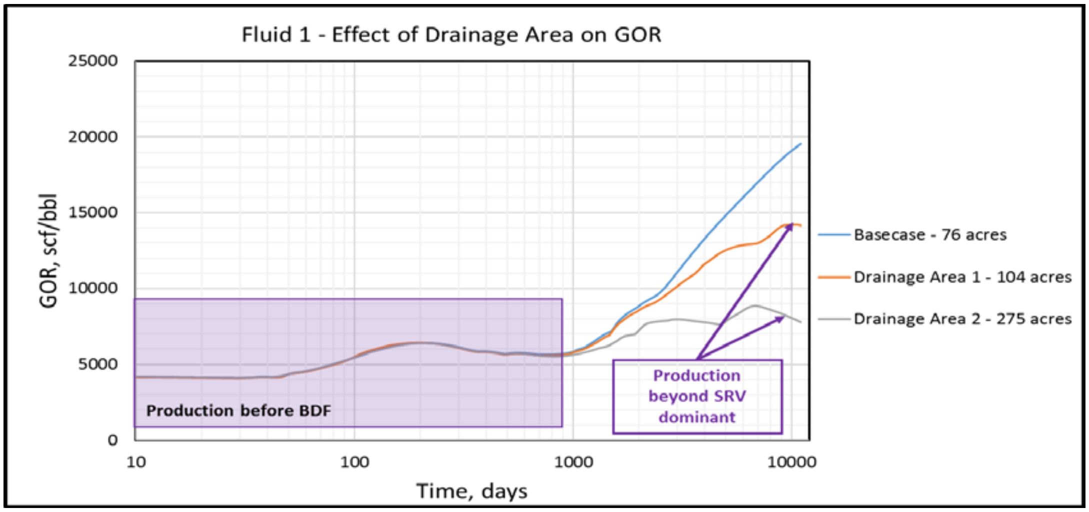

Figure 4-96 Fluid 1 – Effect of Drainage Area on GOR

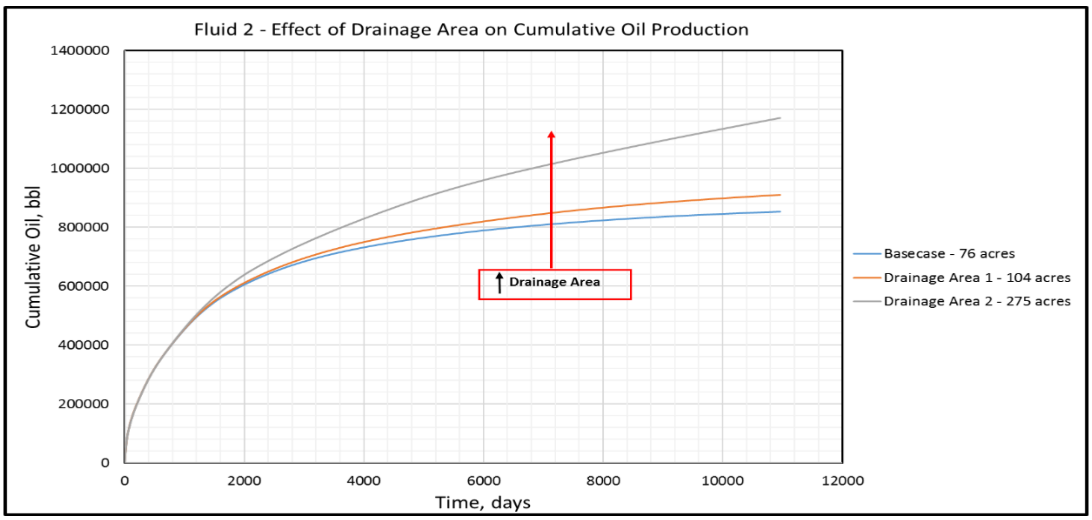

Figure 4-97 Fluid 2 – Effect of Drainage Area on Cumulative Oil Production

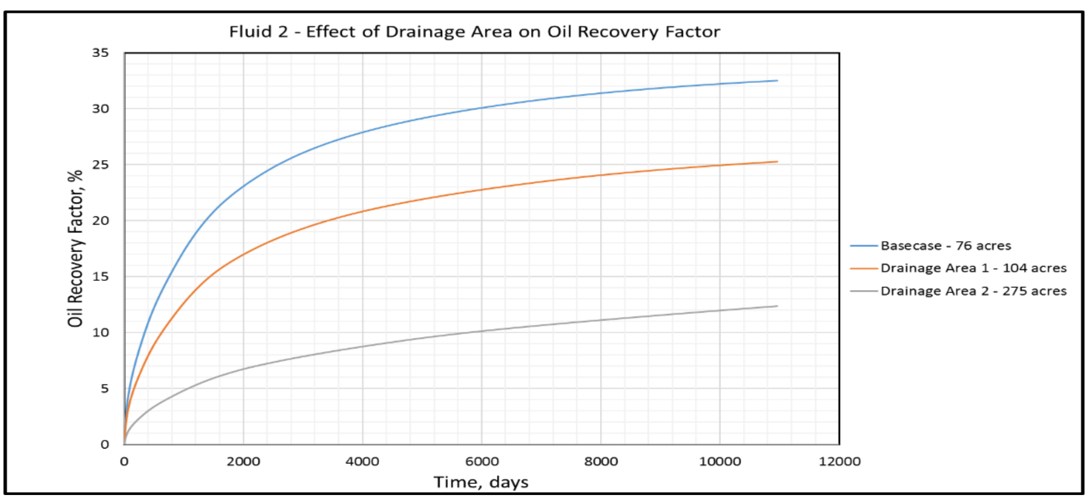

Figure 4-98 Fluid 2 – Effect of Drainage Area on Oil Recovery Factor

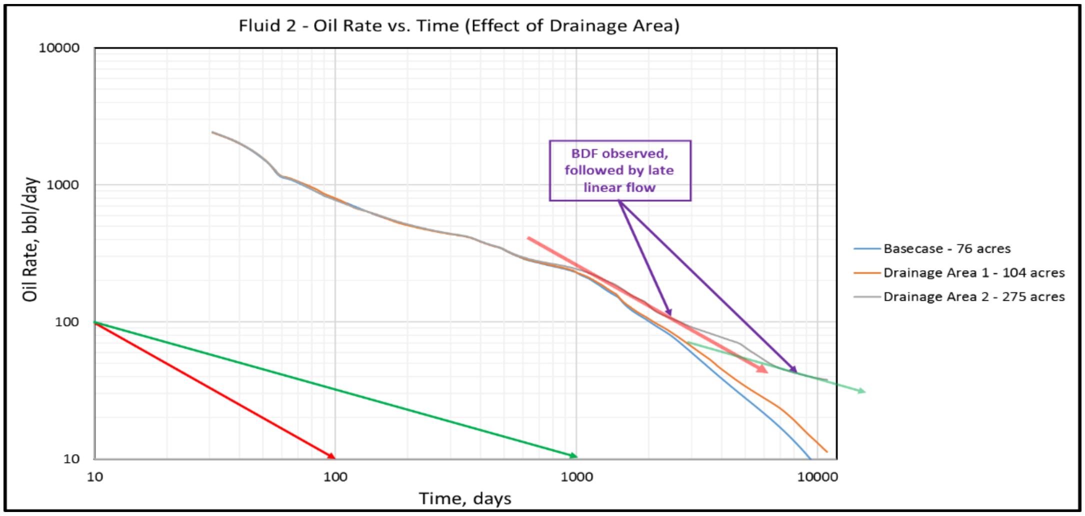

Figure 4-99 Fluid 2 – Effect of Drainage Area on Rate-Time Diagnostic Plots

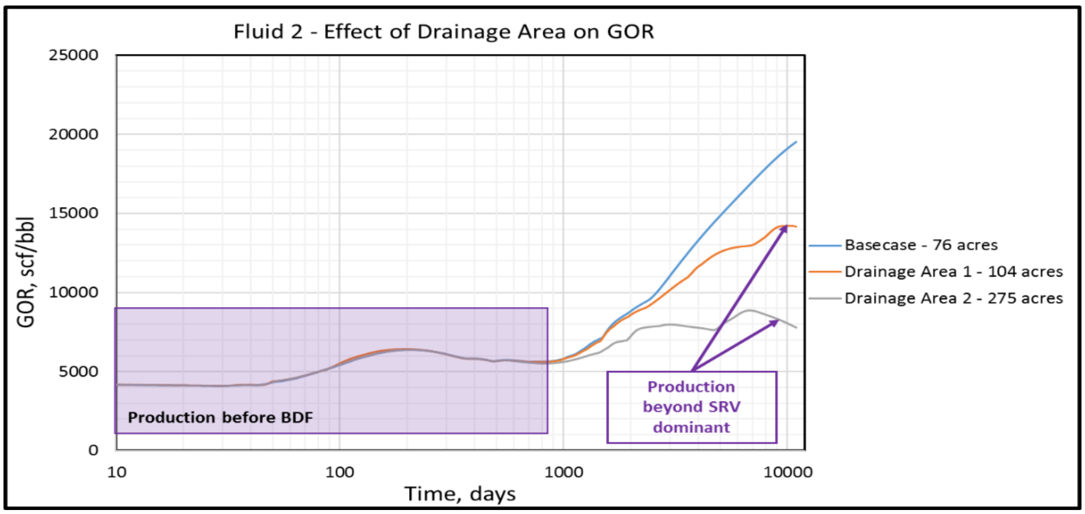

Figure 4-100 Fluid 2 – Effect on Drainage Area on GOR

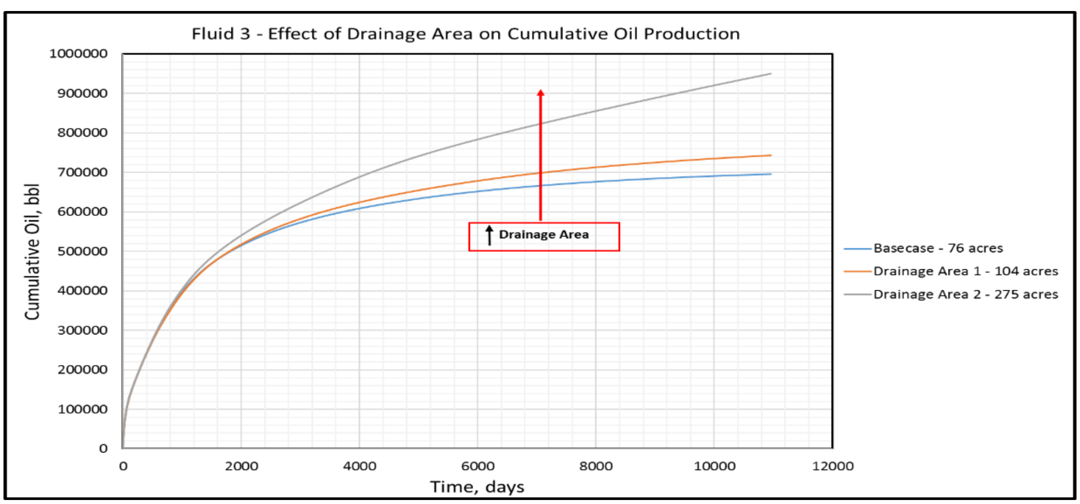

Figure 4-101 Fluid 3 – Effect of Drainage Area on Cumulative Oil Production

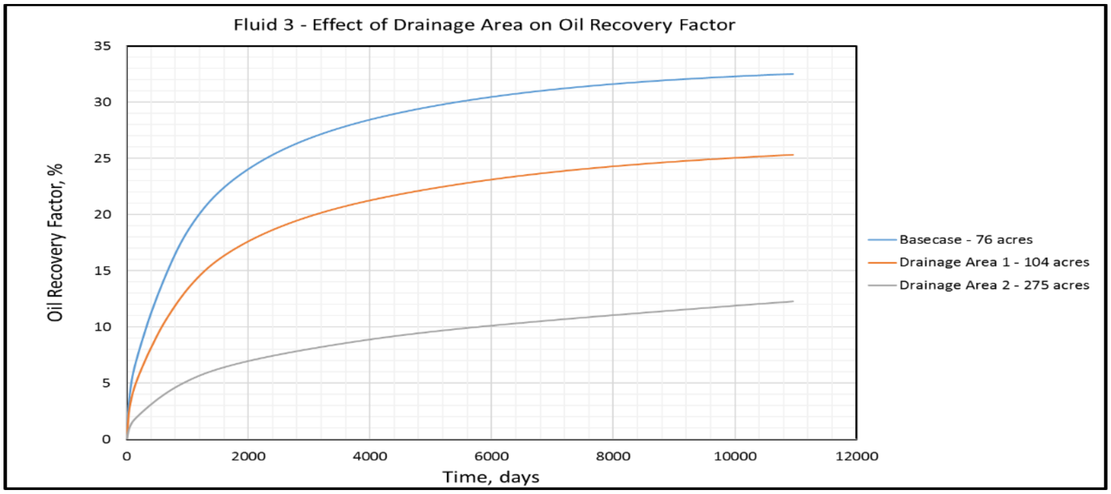

Figure 4-102 Fluid 3 – Effect of Drainage Area on Oil Recovery Factor

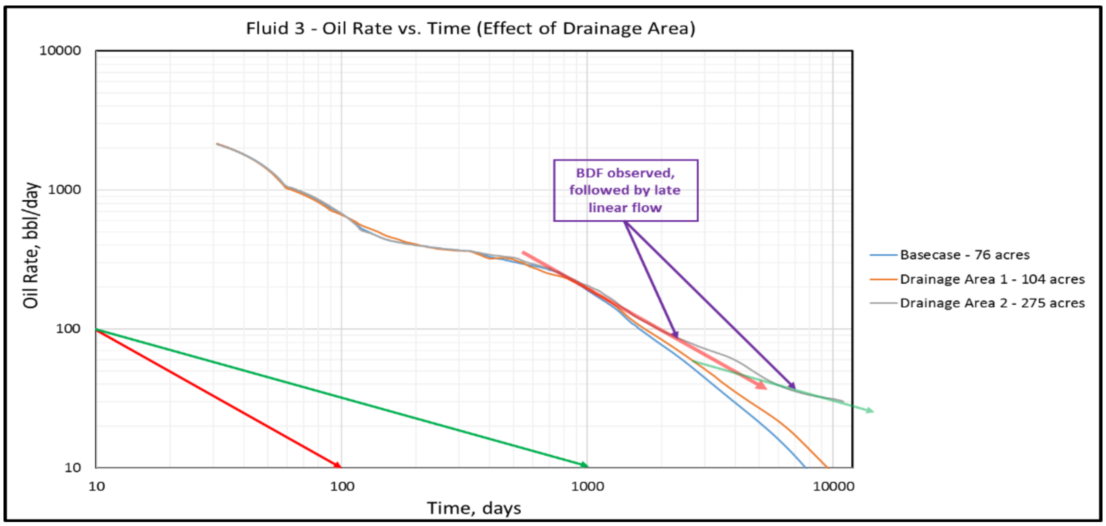

Figure 4-103 Fluid 3 – Effect of Drainage Area on Rate-Time Diagnostic Plots

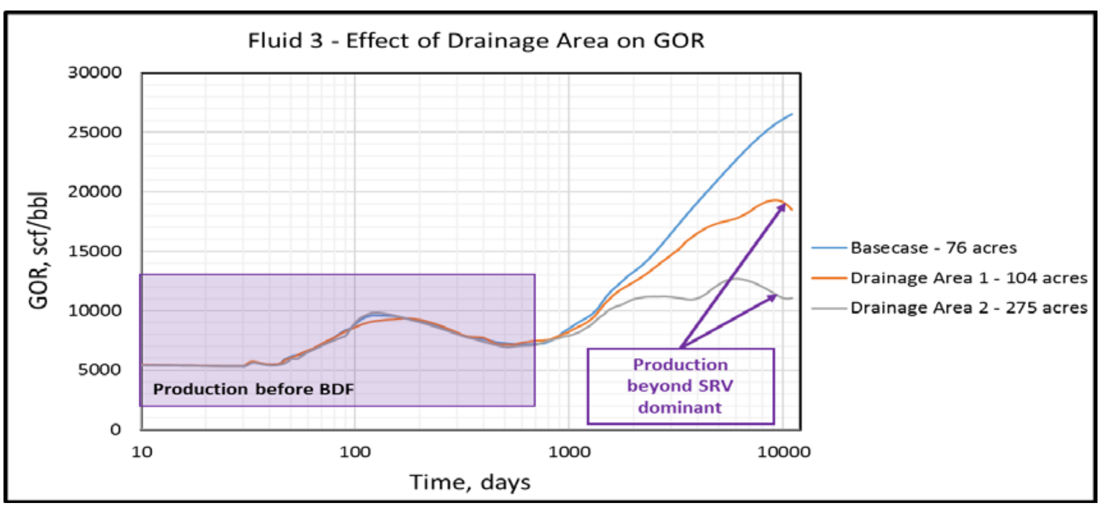

Figure 4-104 Fluid 3 – Effect of Drainage Area on GOR

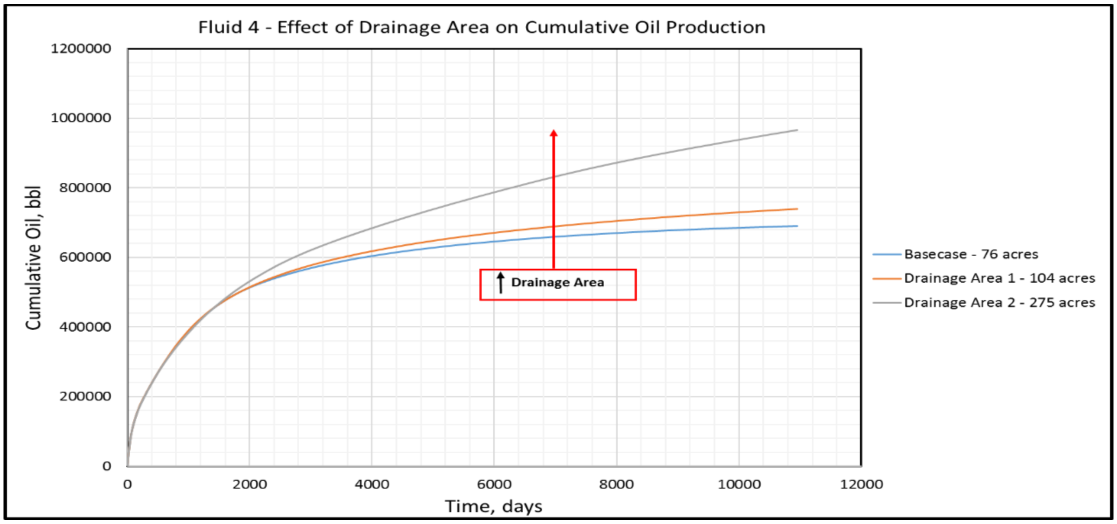

Figure 4-105 Fluid 4 – Effect of Drainage Area on Cumulative Oil Production

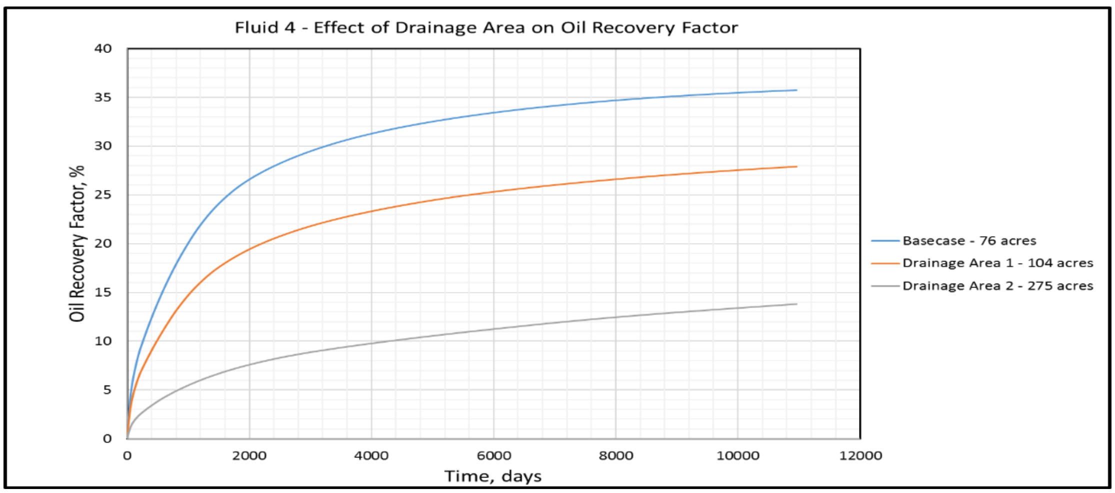

Figure 4-106 Fluid 4 – Effect of Drainage Area on Oil Recovery Factor

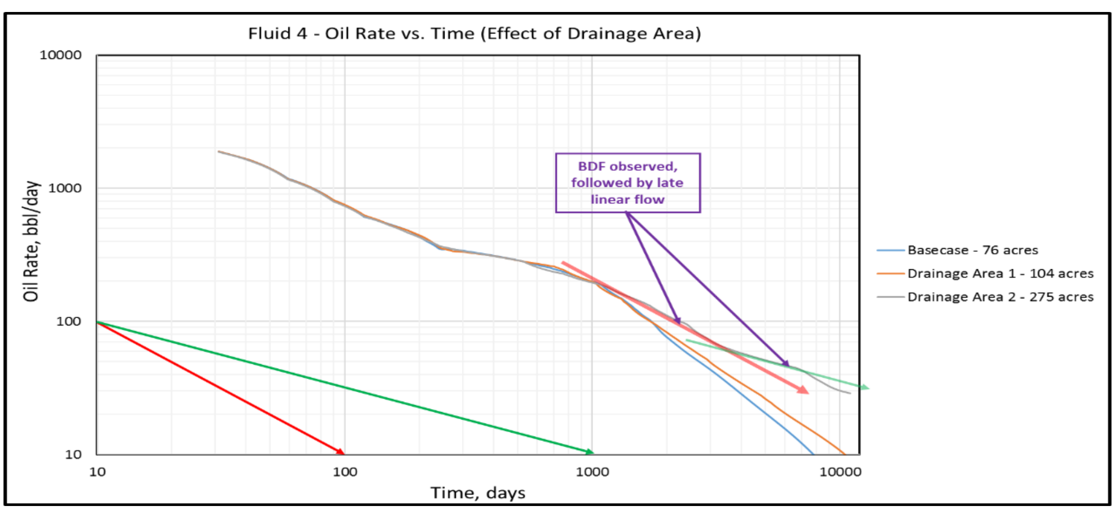

Figure 4-107 Fluid 4 – Effect of Drainage Area on Rate-Time Diagnostic Plots

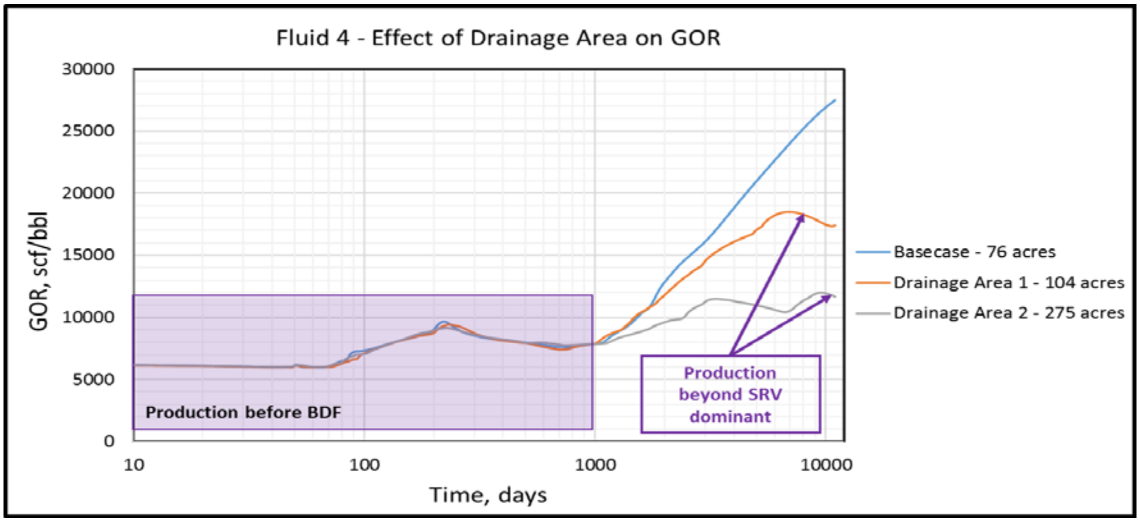

Figure 4-108 Fluid 4 – Effect of Drainage Area on GOR

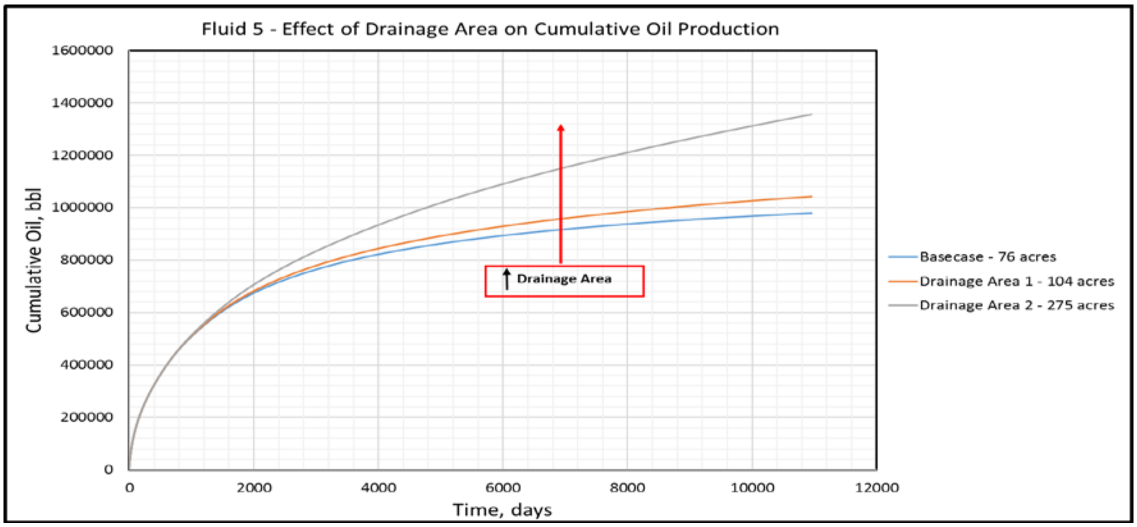

Figure 4-109 Fluid 5 – Effect of Drainage Area on Cumulative Oil Production

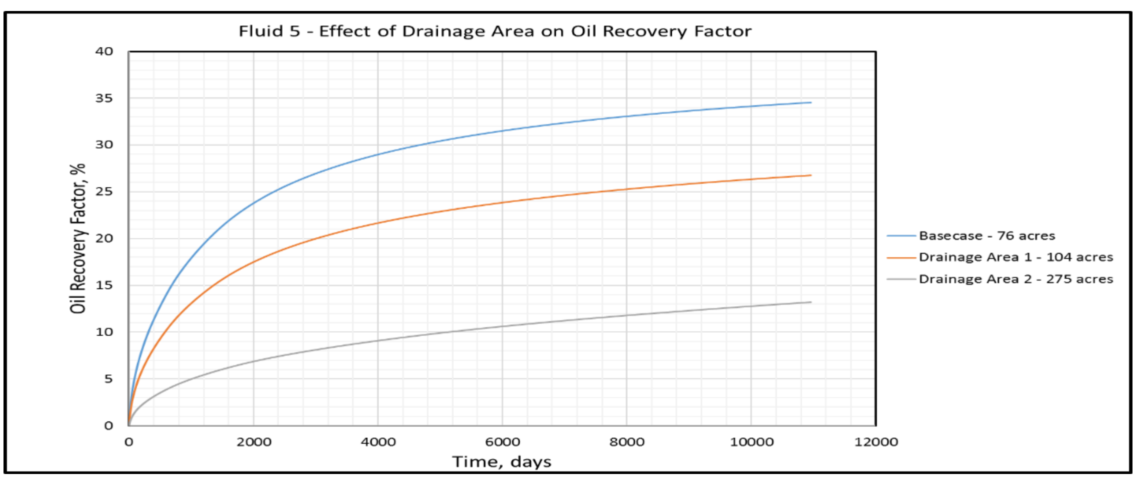

Figure 4-110 Fluid 5 – Effect of Drainage Area on Oil Recovery Factor

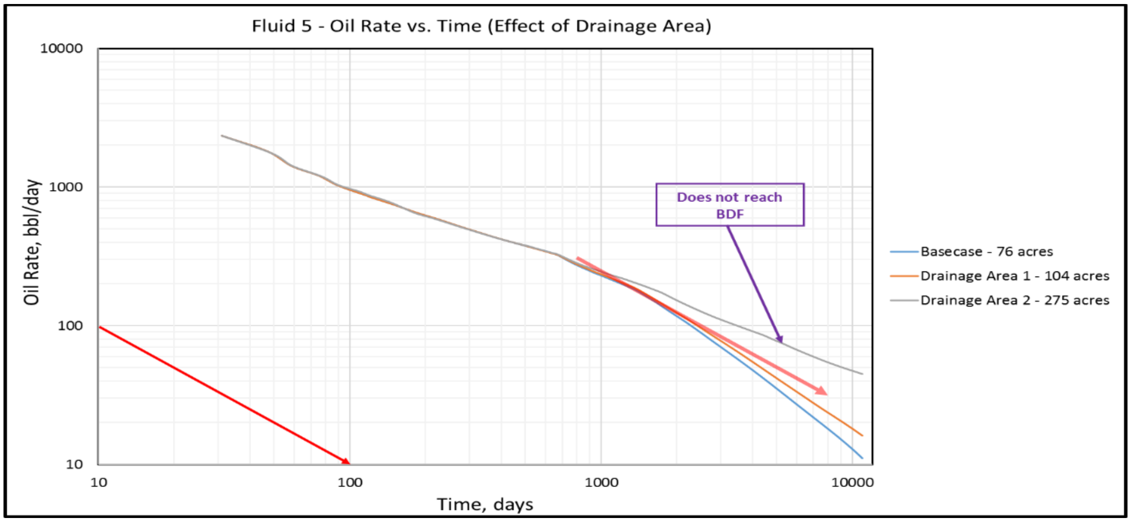

Figure 4-111 Fluid 5 – Effect of Drainage Area on Rate-Time Diagnostic Plots

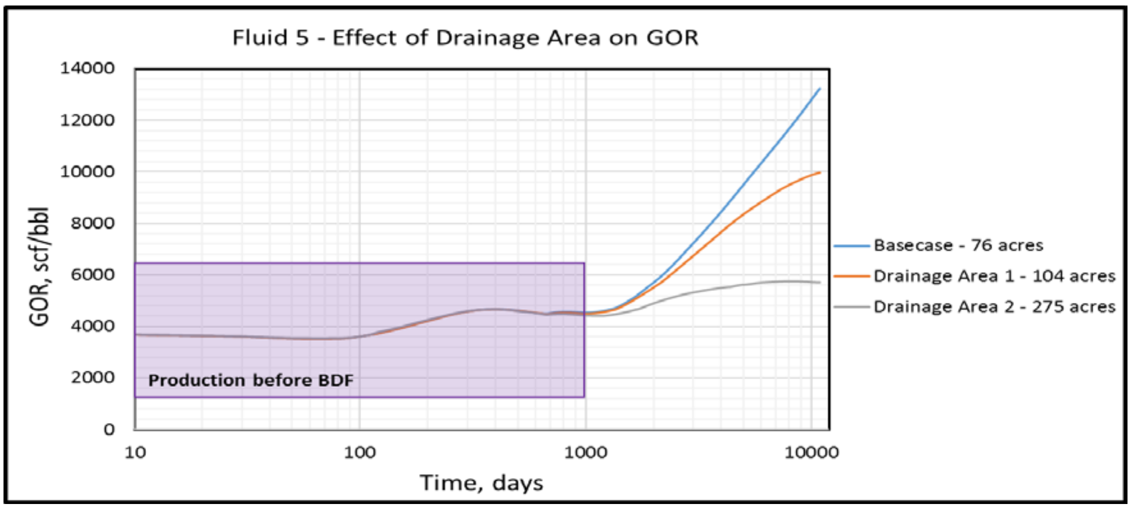

Figure 4-112 Fluid 5 – Effect of Drainage Area on GOR

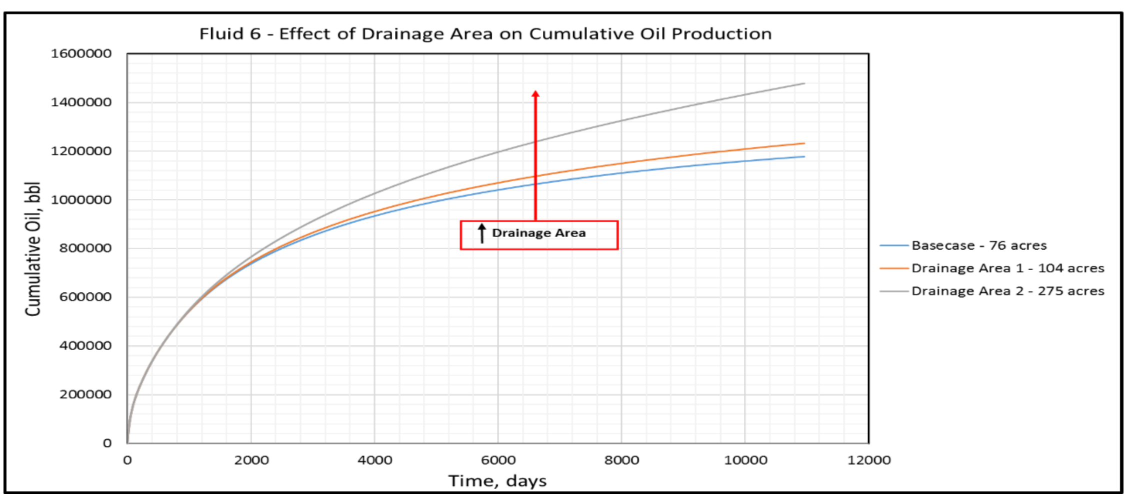

Figure 4-113 Fluid 6 – Effect of Drainage Area on Cumulative Oil Production

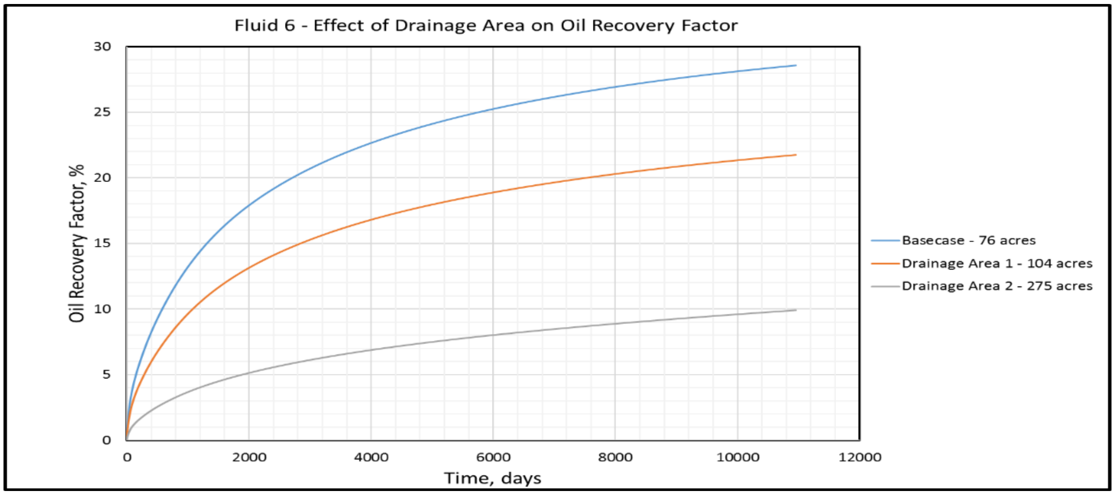

Figure 4-114 Fluid 6 – Effect of Drainage Area on Oil Recovery Factor

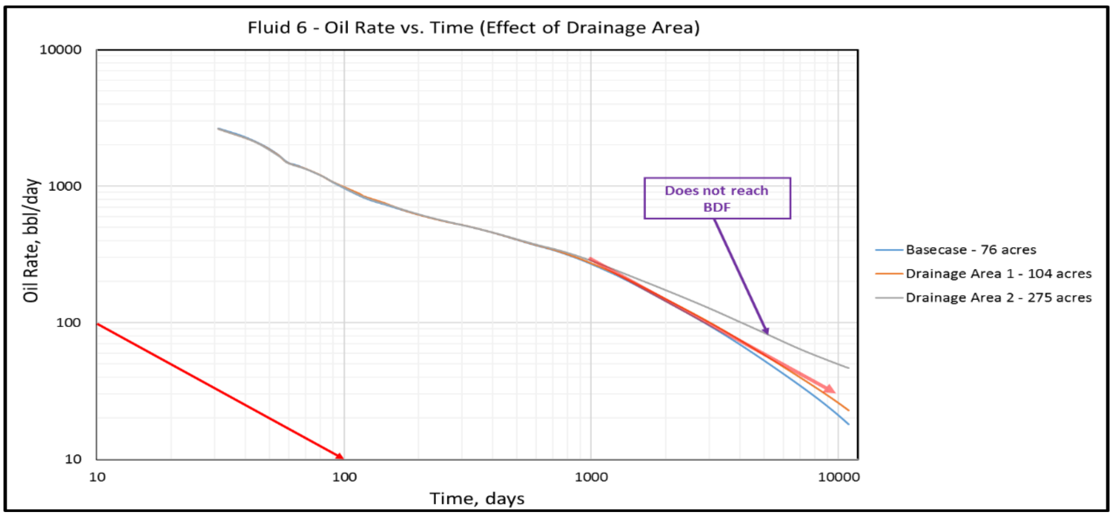

Figure 4-115 Fluid 6 – Effect of Drainage Area on Rate-Time Diagnostic Plots

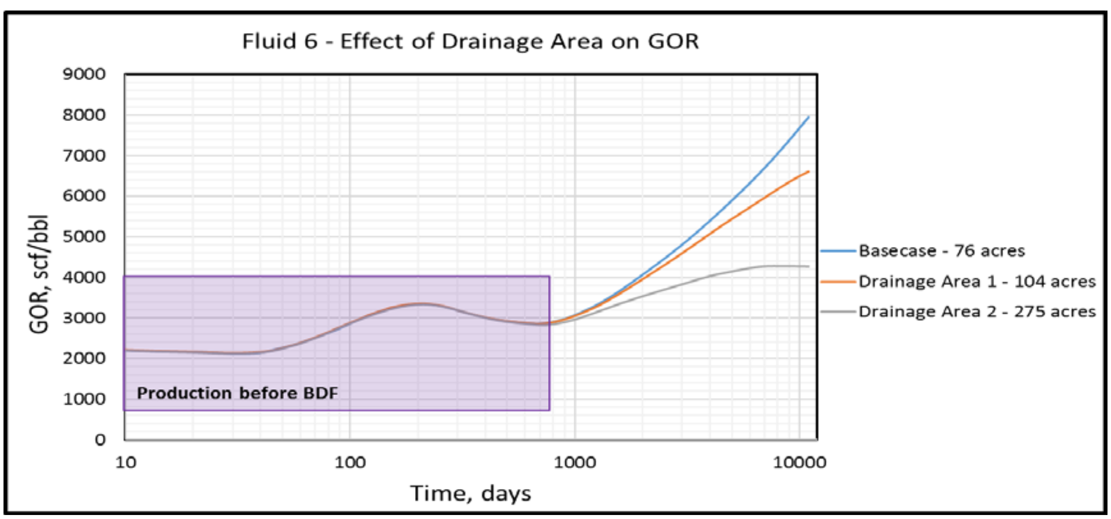

Figure 4-116 Fluid 6 – Effect of Drainage Area on GOR

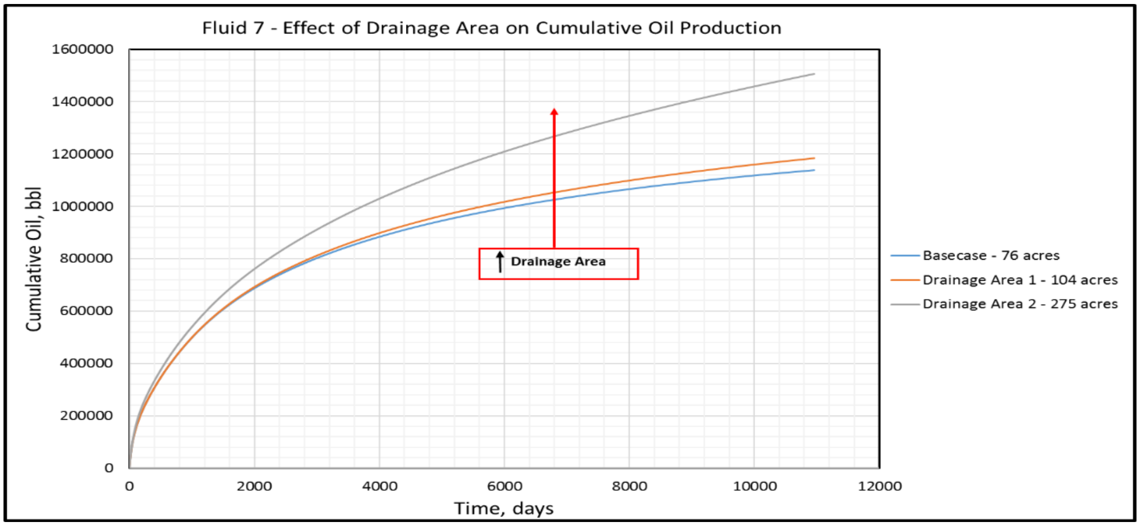

Figure 4-117 Fluid 7 – Effect of Drainage Area on Cumulative Oil Production

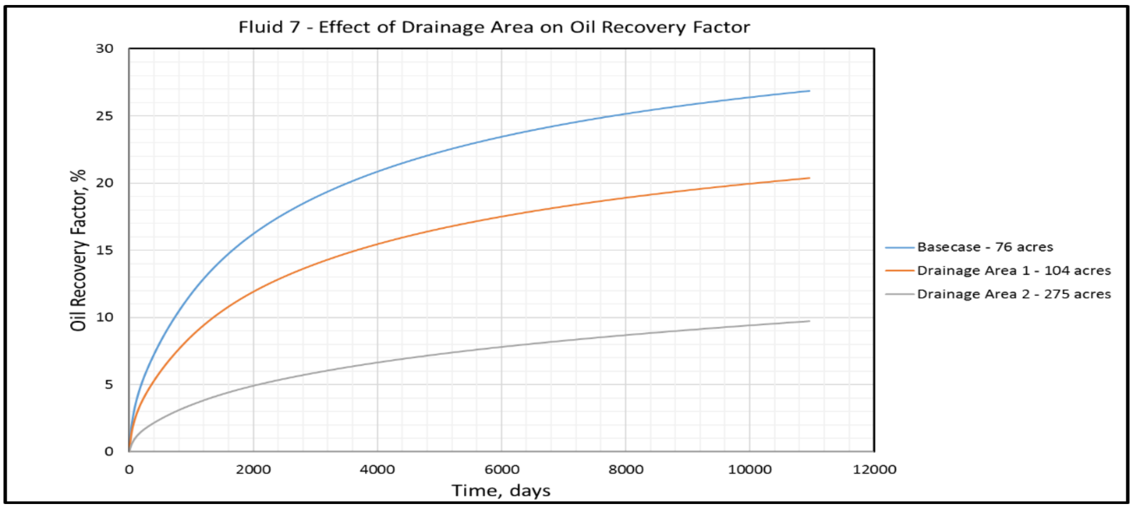

Figure 4-118 Fluid 7 – Effect of Drainage Area on Oil Recovery Factor

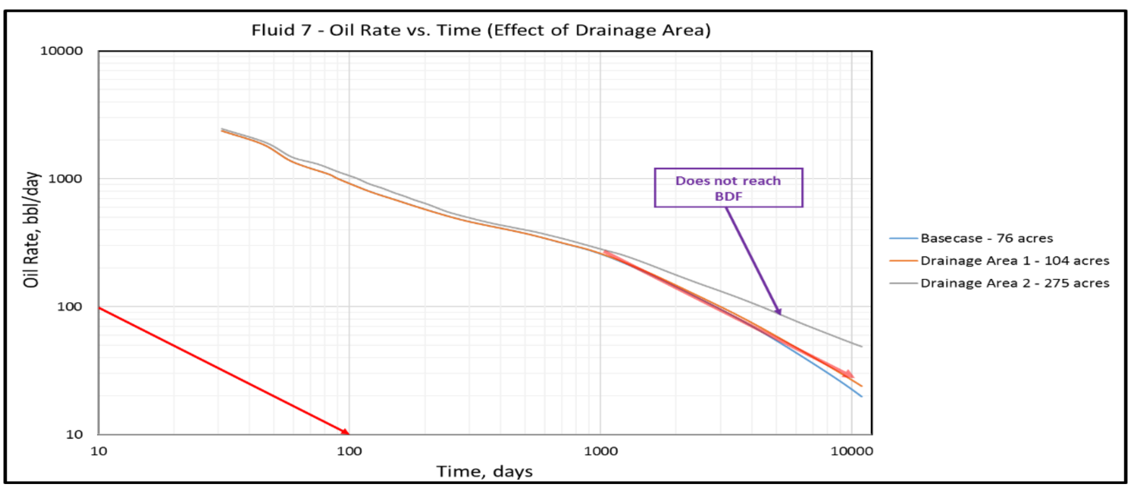

Figure 4-119 Fluid 7 – Effect of Drainage Area on Rate-Time Diagnostic Plots

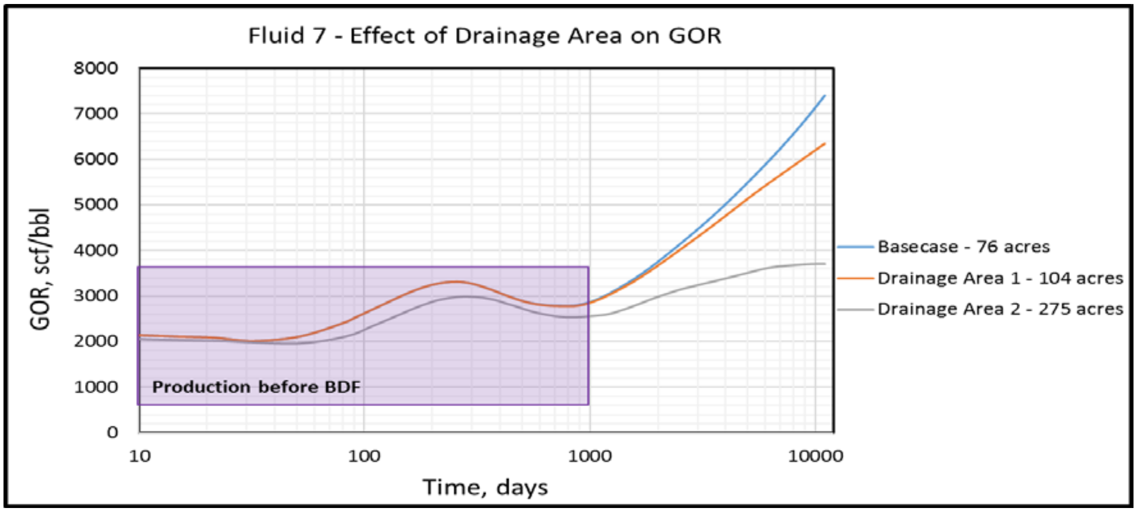

Figure 4-120 Fluid 7 – Effect of Drainage Area on GOR

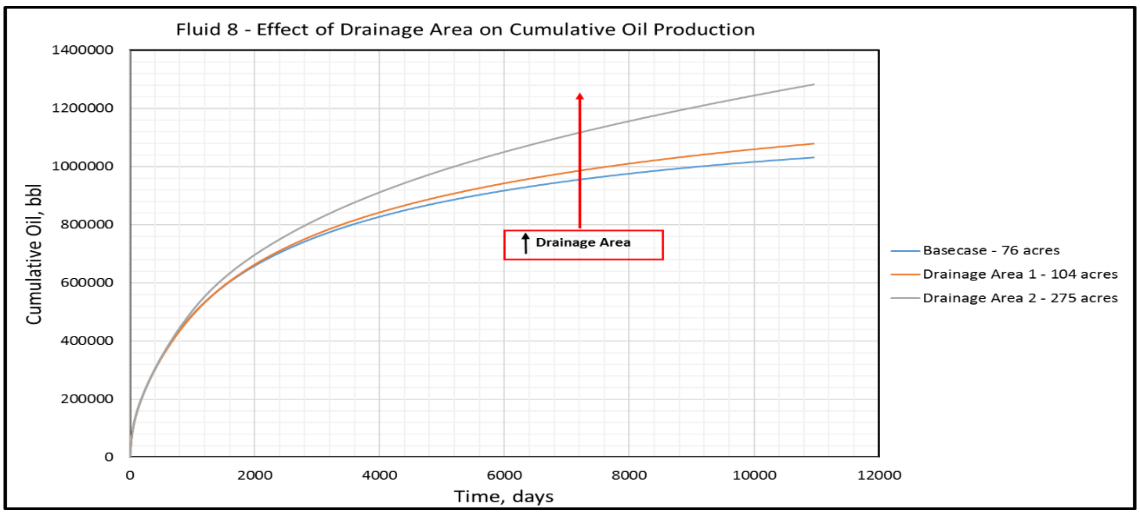

Figure 4-121 Fluid 8 – Effect of Drainage Area on Cumulative Oil Production

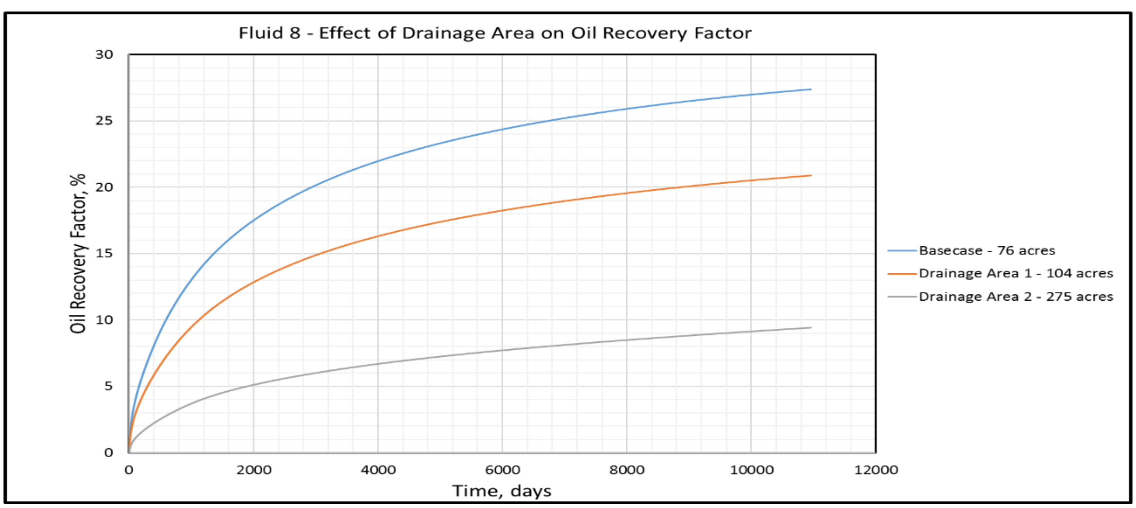

Figure 4-122 Fluid 8 – Effect of Drainage Area on Oil Recovery Factor

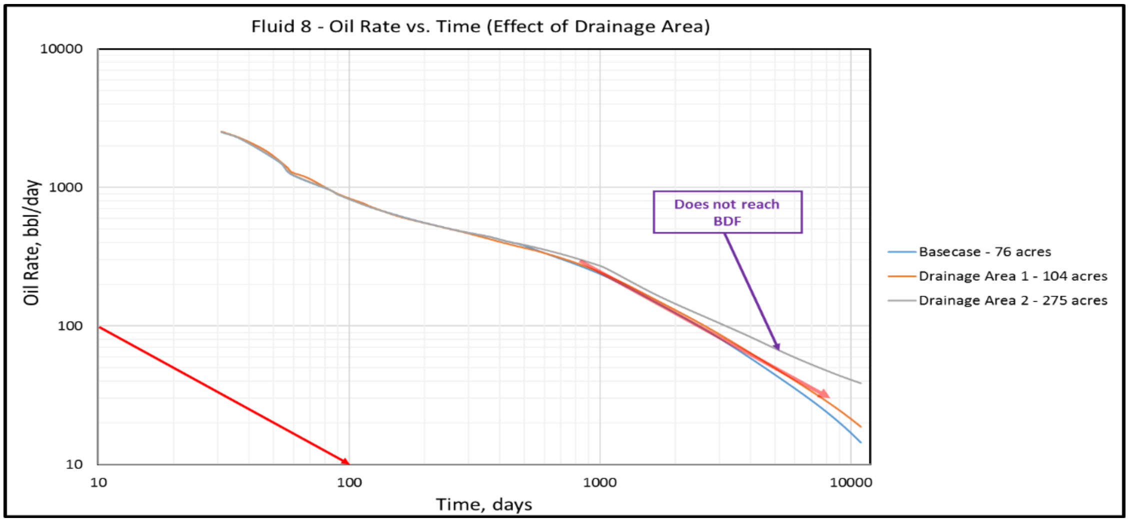

Figure 4-123 Fluid 8 – Effect of Drainage Area on Rate-Time Diagnostic Plots

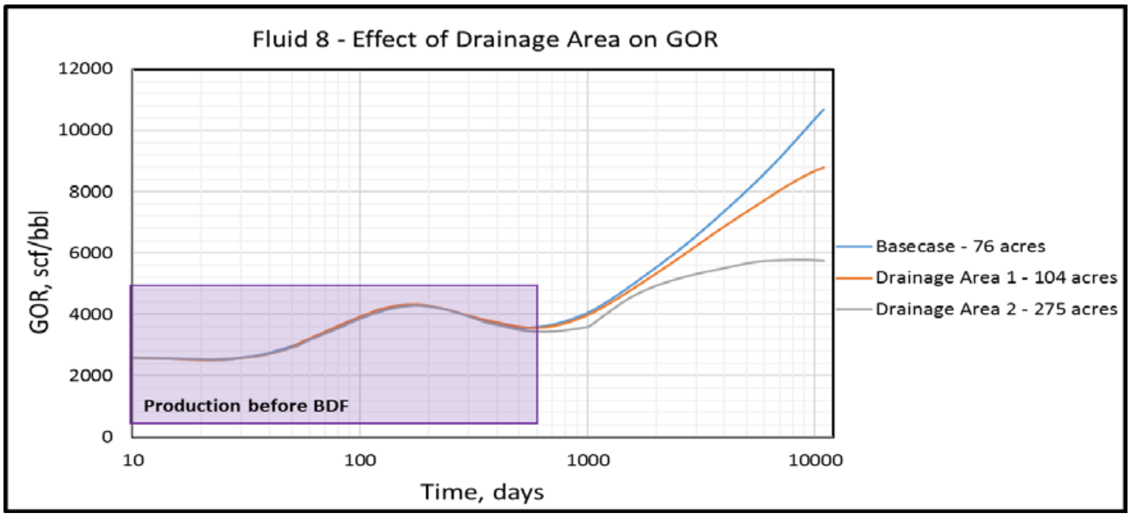

Figure 4-124 Fluid 8 – Effect of Drainage Area on GOR

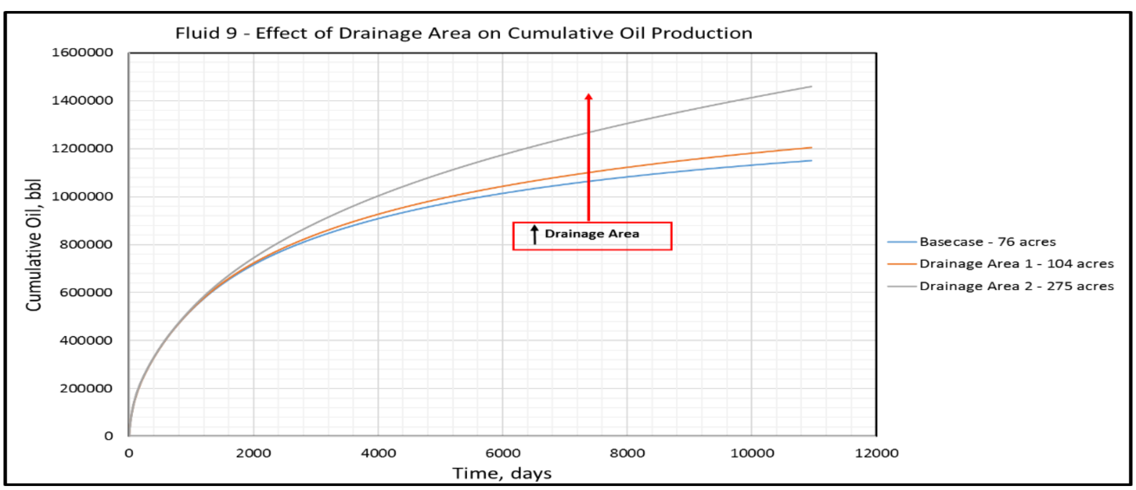

Figure 4-125 Fluid 9 – Effect of Drainage Area on Cumulative Oil Production

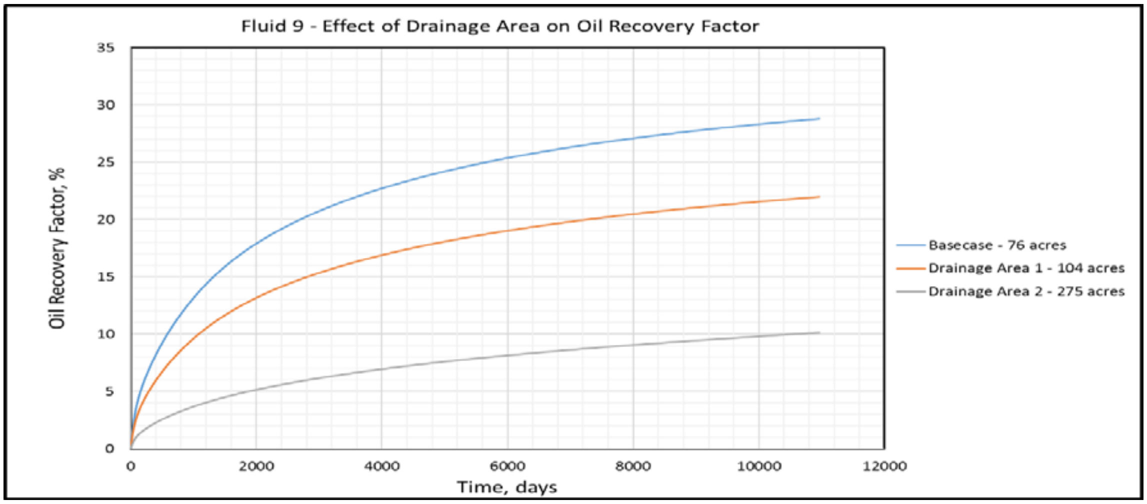

Figure 4-126 Fluid 9 – Effect of Drainage Area on Oil Recovery Factor

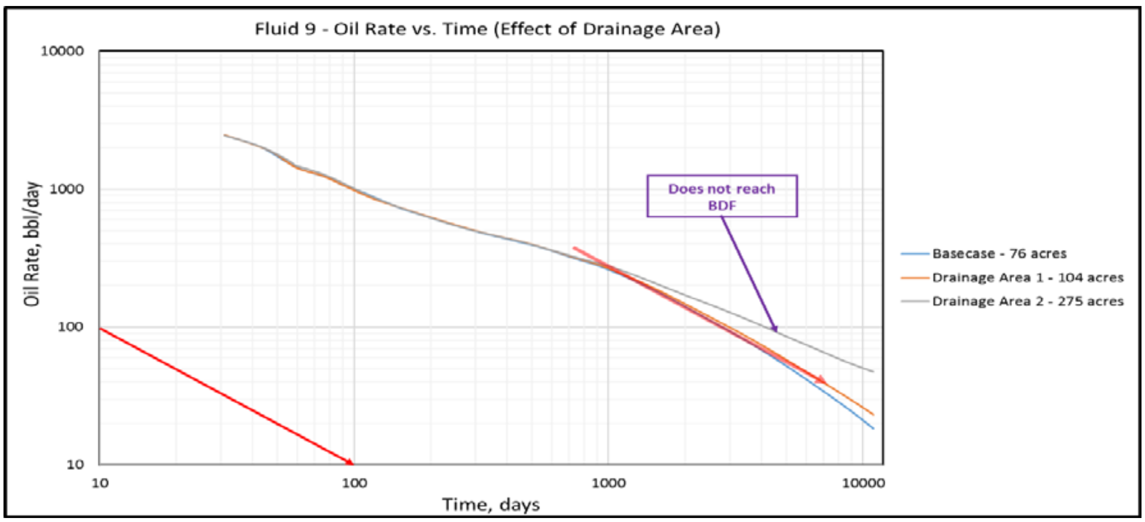

Figure 4-127 Fluid 9 – Effect of Drainage Area on Rate-Time Diagnostic Plots

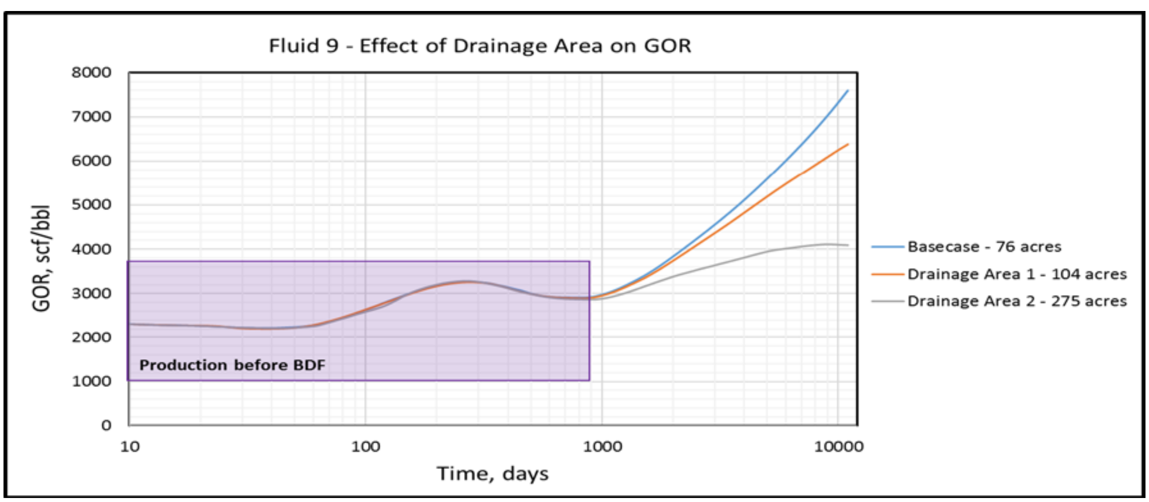

Figure 4-128 Fluid 9 – Effect of Drainage Area on GOR

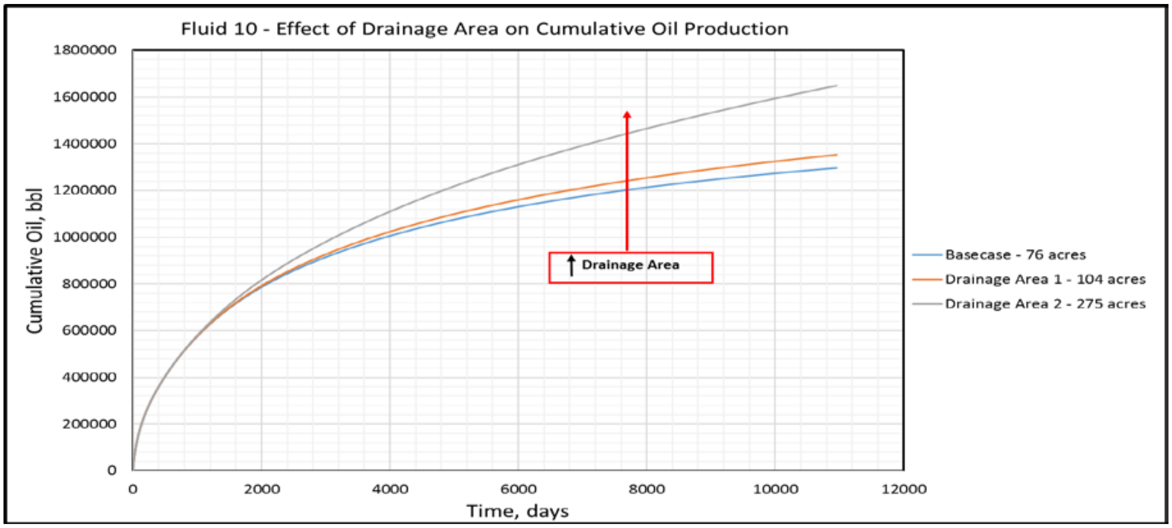

Figure 4-129 Fluid 10 – Effect of Drainage Area on Cumulative Oil Production

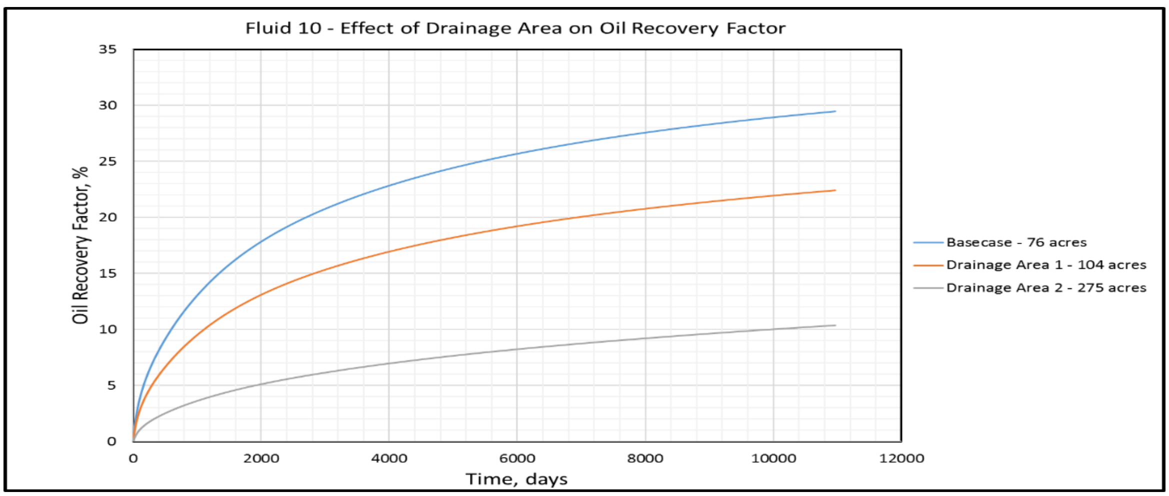

Figure 4-130 Fluid 10 – Effect of Drainage Area on Oil Recovery Factor

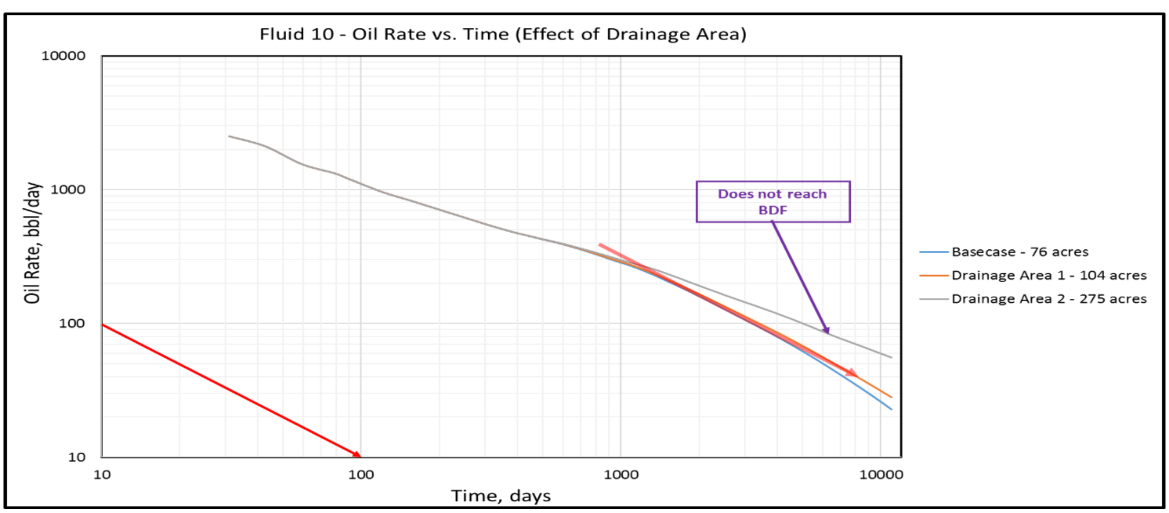

Figure 4-131 Fluid 10 – Effect of Drainage Area on Rate-Time Diagnostic Plots

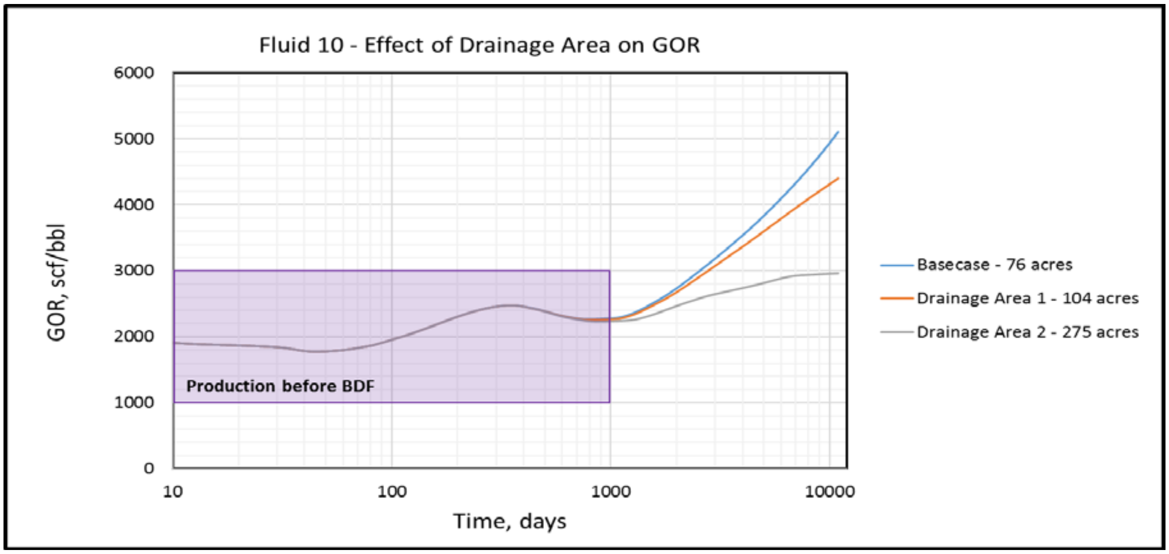

Figure 4-132 Fluid 10 – Effect of Drainage Area on GOR

4.6. Fracture Half-Length

Fracture half-length is the distance from the wellbore to the outer tip of a fracture propagated from the well by hydraulic fracturing or penetrated by the well. It is an important completion parameter for shale reservoirs. For these analyses, we considered fracture half-lengths of 50 ft, 100 ft, 150 ft (basecase), 200 ft, 250 ft, 300 ft and two other cases where the fracture half-lengths are of different lengths, i.e. uneven configuration of fracture lengths. These two special cases were compared separately to the basecase to determine their impact on production performance. Figures 4-133 to 4-139 show the pictorial representations of each case apart from the basecase (already shown in Figure 4-1).

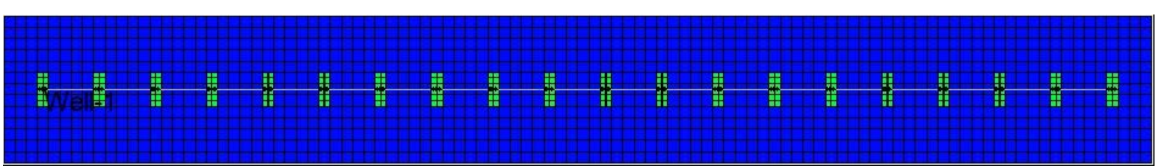

Figure 4-133 Reservoir Model – 50 ft Fracture Half-Lengths

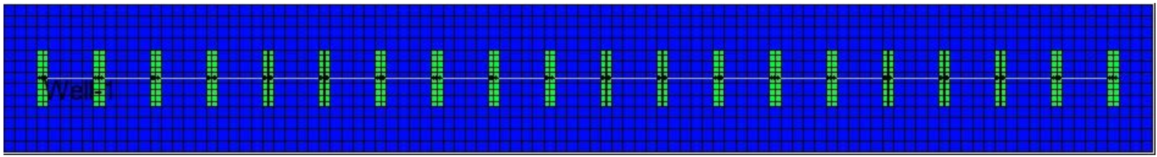

Figure 4-134 Reservoir Model – 100 ft Fracture Half-Lengths

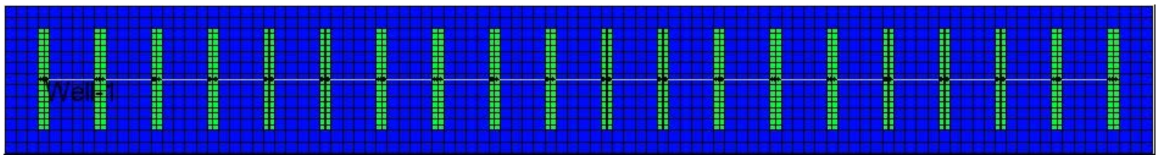

Figure 4-135 Reservoir Model – 200 ft Fracture Half-Lengths

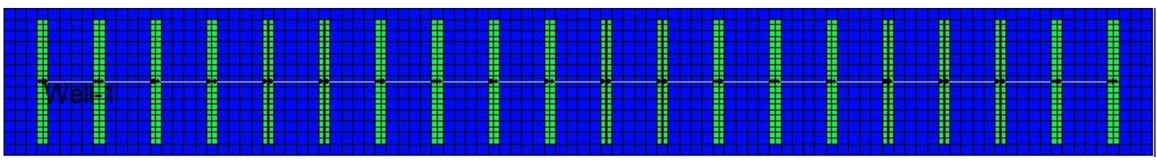

Figure 4-136 Reservoir Model – 250 ft Fracture Half-Lengths

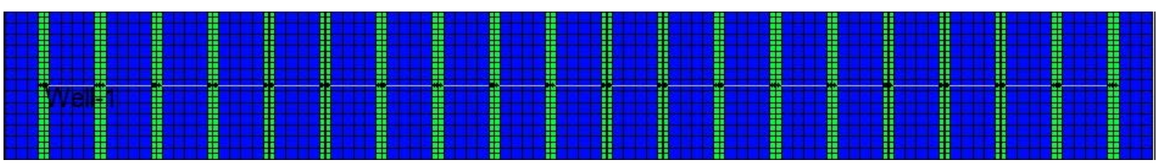

Figure 4-137 Reservoir Model – 300 ft Fracture Half-Lengths

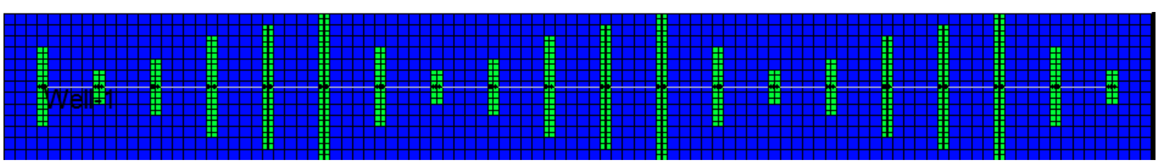

Figure 4-138 Reservoir Model – Uneven Configuration 1 (Fracture Half-Lengths)

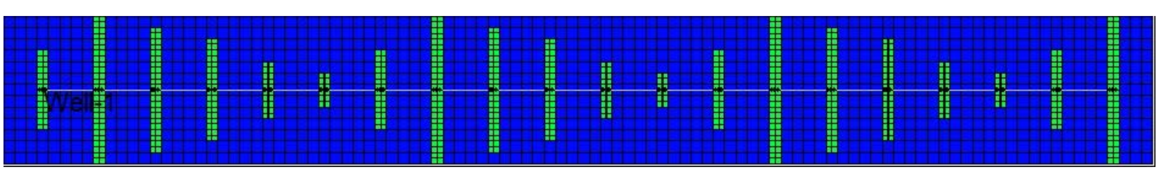

Figure 4-139 Reservoir Model – Uneven Configuration 2 (Fracture Half-Lengths)

The longer the fracture half-lengths, the larger the cumulative oil production. The well can drain more volume of the reservoir with larger fracture half-lengths. However, for the highly volatile oils, when fracture half-lengths are 300 ft, rapid drainage of the reservoir volume and high gas saturation at the fracture faces, cause slight reduction in cumulative oil production towards the end of the production period.

There is a delay in the rise of producing GOR with reducing fracture half-lengths. The shorter the fracture half-length, the lesser the gas saturation at the fracture faces. Also, the further away the bubble point of the volatile oil is from the initial reservoir pressure (degree of undersaturation), the lower the height of the “GOR hill”. This is more noticeable for cases with highly volatile oils. Therefore, the higher the degree of undersaturation and the shorter the fracture half-lengths, the lower the height of the “GOR hill”. The highly volatile oils are closer to the critical point (two fluids are near-critical), therefore in most of these instances, the “GOR hill” is very low or absent during the production period.

Reservoir model with uneven configuration 1 has three of its fractures with half-lengths of 300 ft whereas the reservoir model with uneven configuration 2 has four of its fractures with half-lengths of 300ft. Therefore, the well with uneven configuration 2 generally produce more oil than the well with uneven configuration 1. They both produce more oil than the well with the basecase configuration (uniform fracture half-lengths of 150 ft). The producing GOR generally follows the same trend as already discussed in the previous paragraph. Figures 4-140 to 4-179 illustrate the effects of fracture half-lengths on cumulative oil production and producing GOR (semi-log plots) with time.

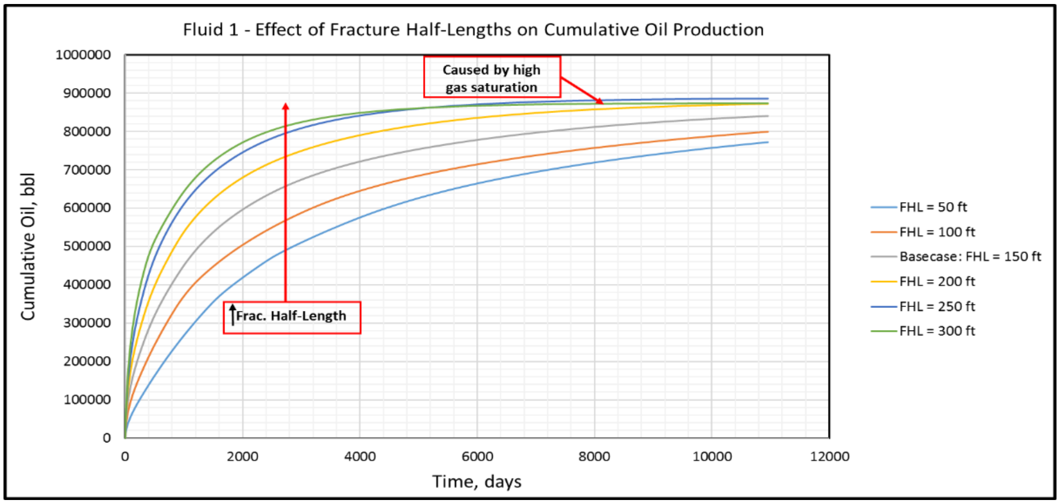

Figure 4-140 Fluid 1 – Effect of Fracture Half-Lengths on Cumulative Oil Production

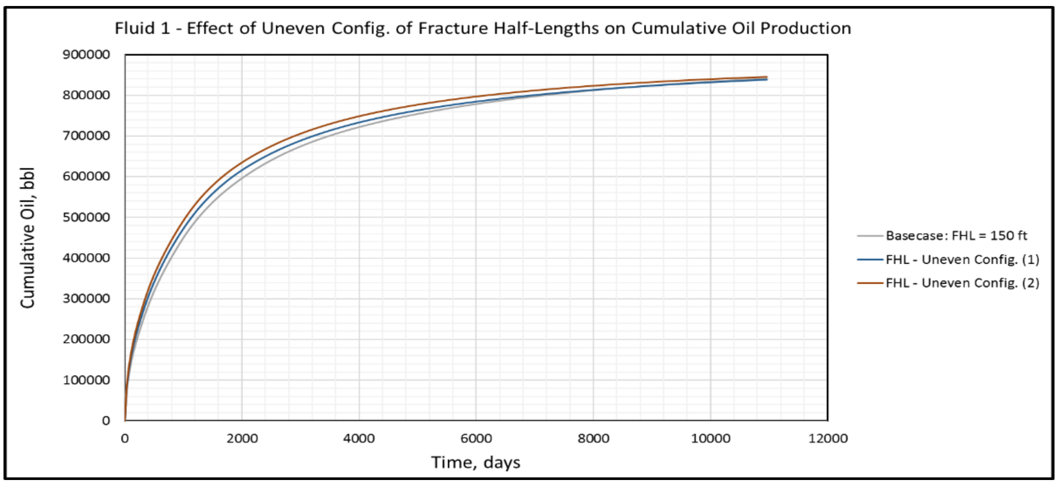

Figure 4-141 Fluid 1 – Effect of Uneven Configuration of Fracture Half-Lengths on Cumulative Oil Production

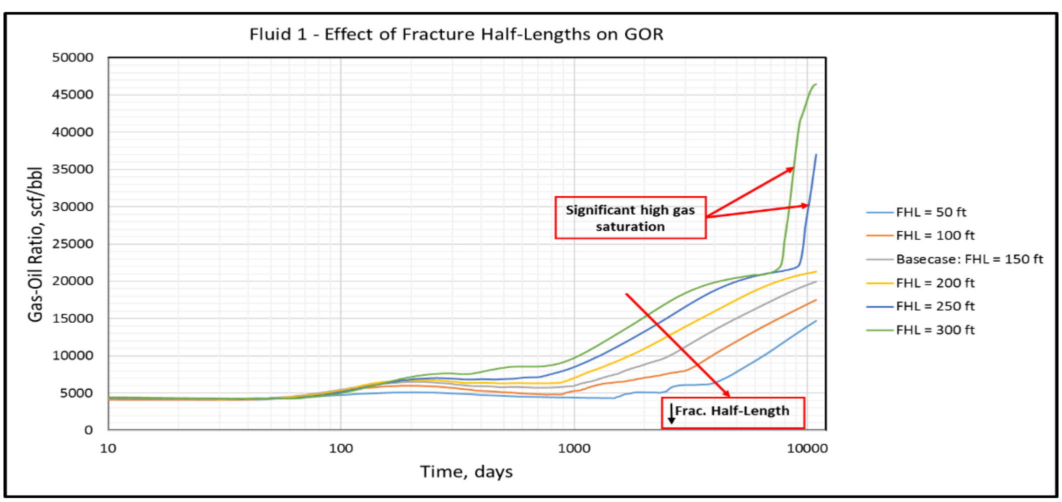

Figure 4-142 Fluid 1 – Effect of Fracture Half-Lengths on GOR

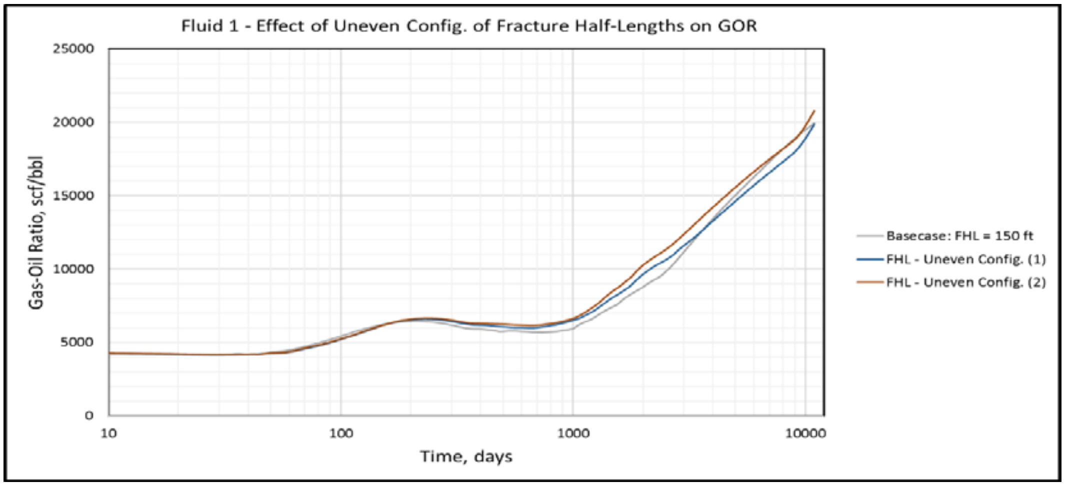

Figure 4-143 Fluid 1 – Effect of Uneven Configuration of Fracture Half-Lengths on GOR

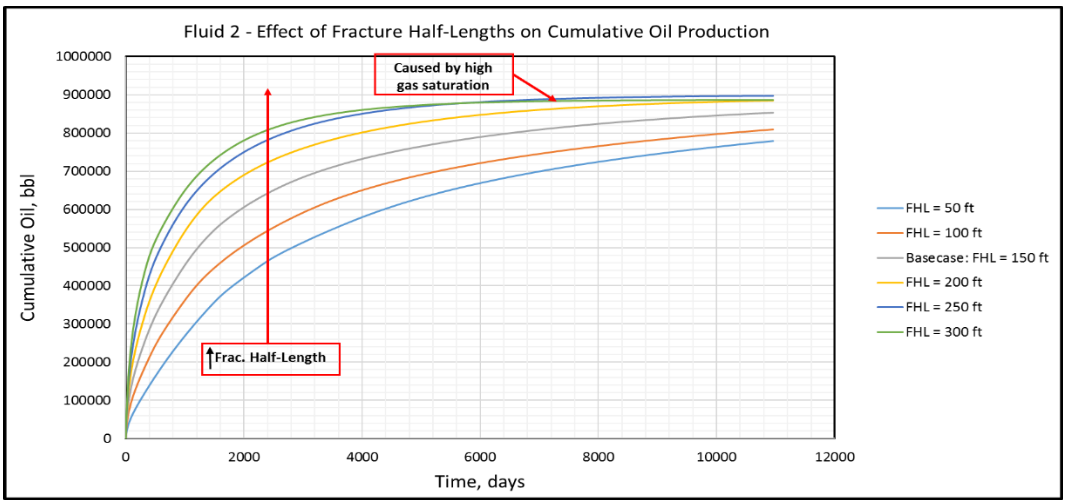

Figure 4-144 Fluid 2 – Effect of Fracture Half-Lengths on Cumulative Oil Production

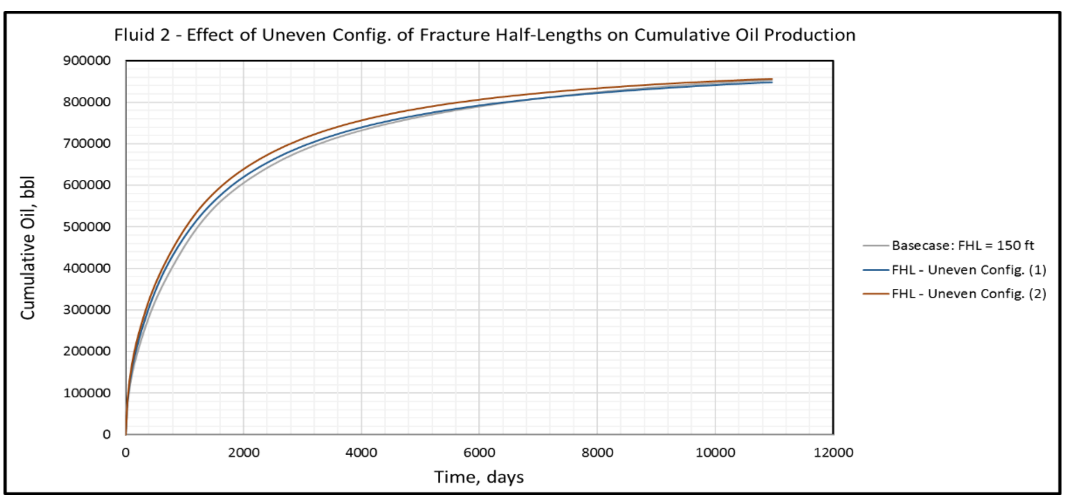

Figure 4-145 Fluid 2 – Effect of Uneven Configuration of Fracture Half-Lengths on Cumulative Oil Production

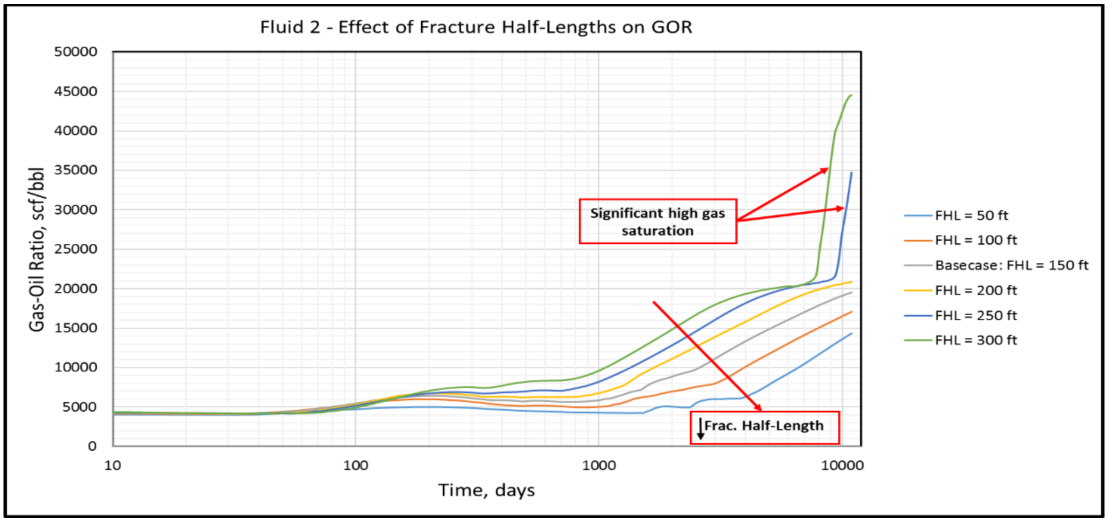

Figure 4-146 Fluid 2 – Effect of Fracture Half-Lengths on GOR

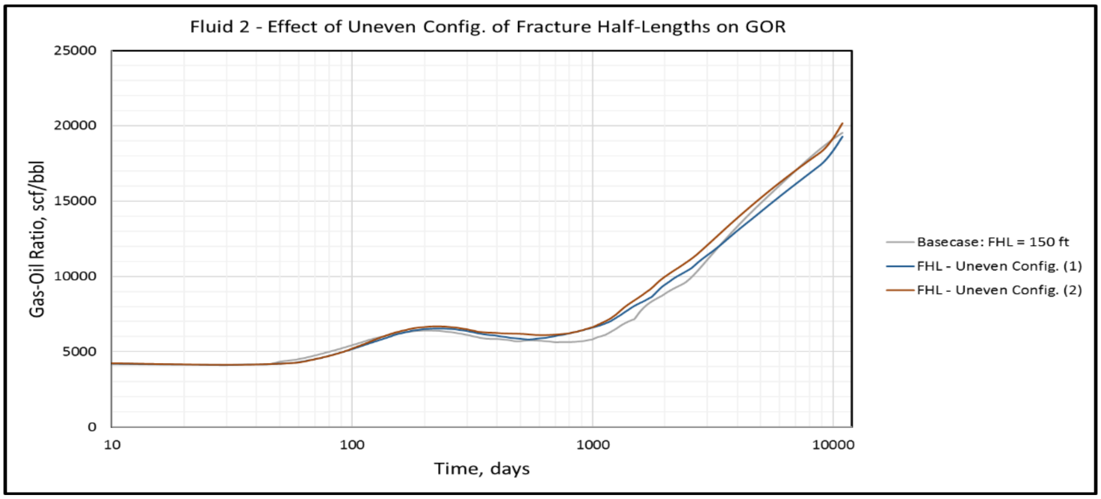

Figure 4-147 Fluid 2 – Effect of Uneven Configuration of Fracture Half-Lengths on GOR

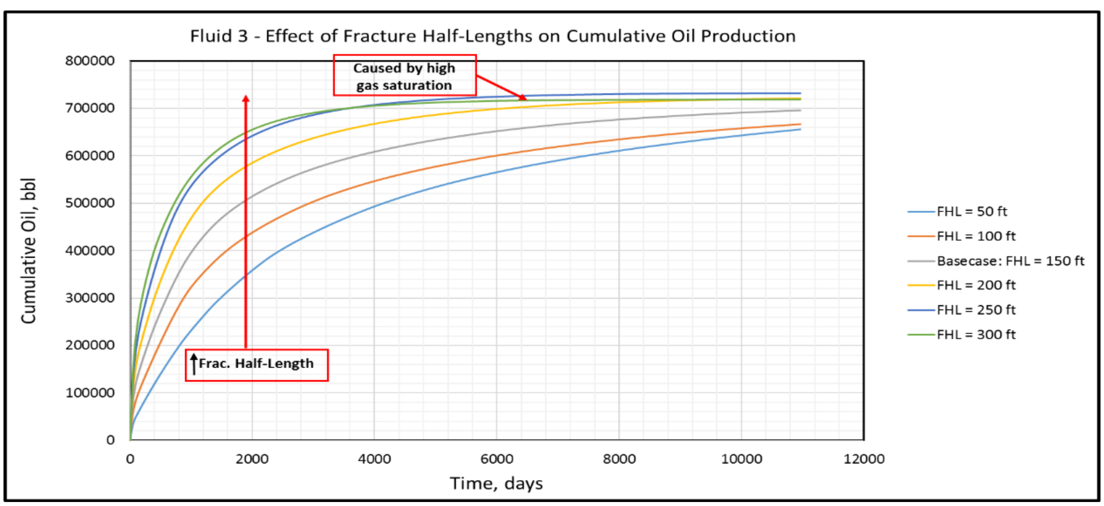

Figure 4-148 Fluid 3 – Effect of Fracture Half-Lengths on Cumulative Oil Production

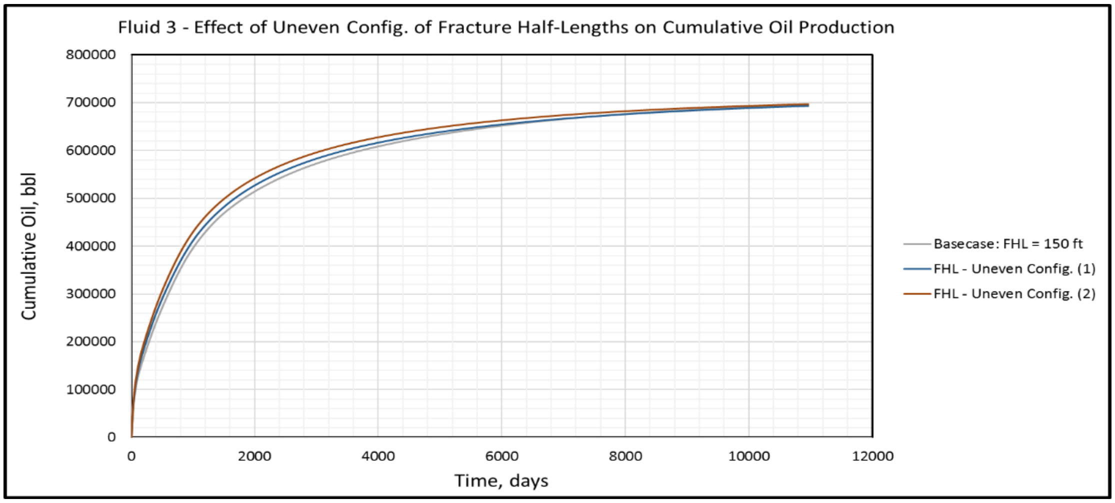

Figure 4-149 Fluid 3 – Effect of Uneven Configuration of Fracture Half-Lengths on Cumulative Oil Production

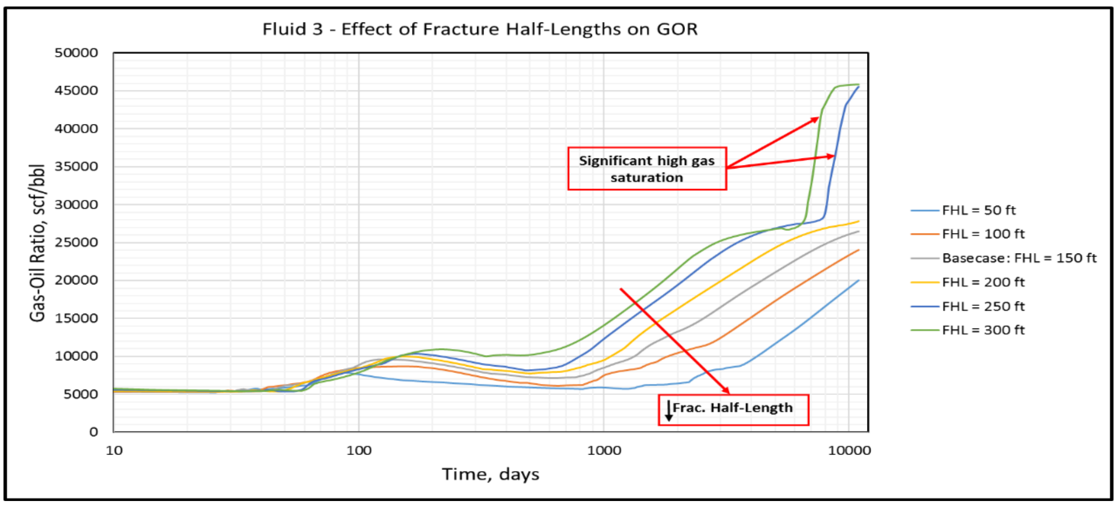

Figure 4-150 Fluid 3 – Effect of Fracture Half-Lengths on GOR

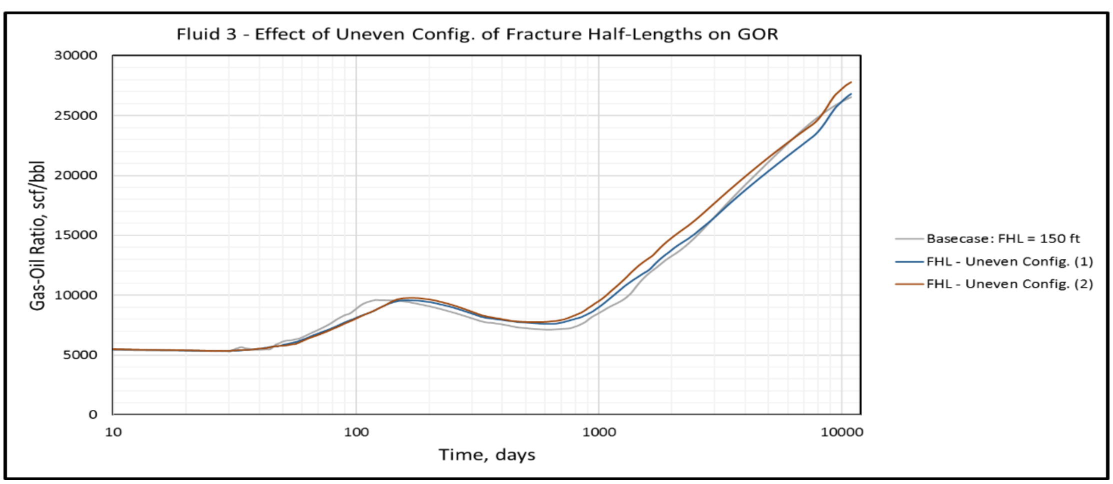

Figure 4-151 Fluid 3 – Effect of Uneven Configuration of Fracture Half-Lengths on GOR

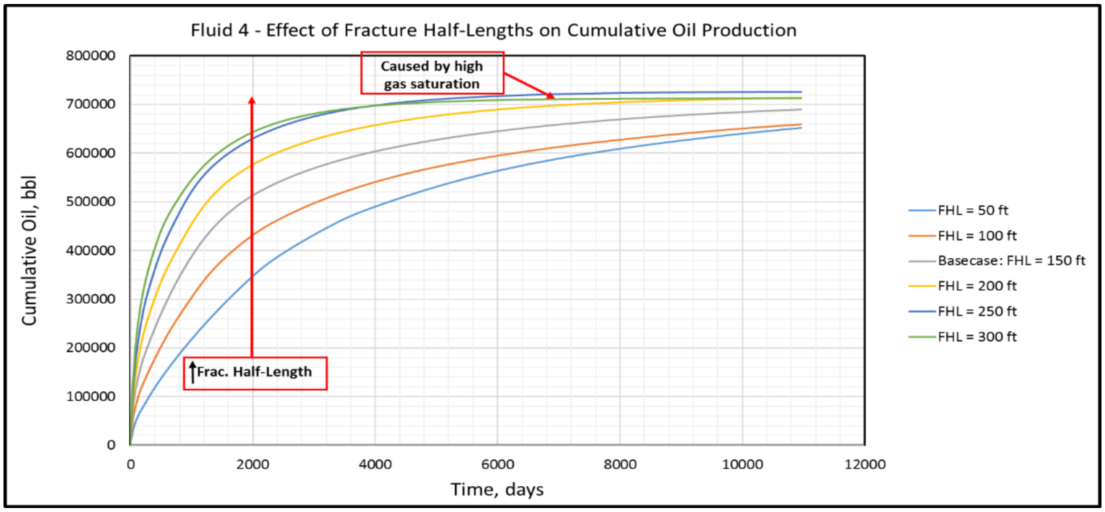

Figure 4-152 Fluid 4 – Effect of Fracture Half-Lengths on Cumulative Oil Production

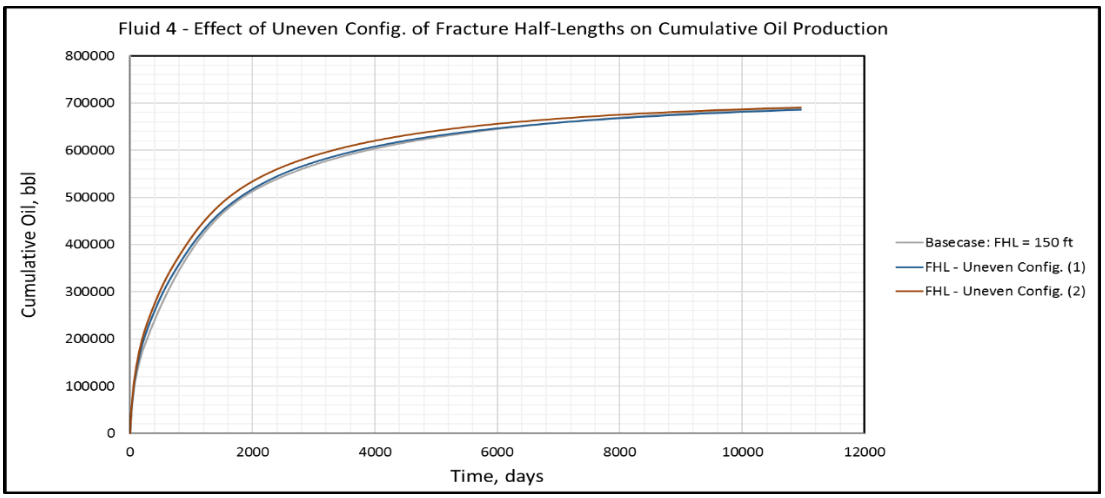

Figure 4-153 Fluid 4 – Effect of Uneven Configuration of Fracture Half-Lengths on Cumulative Oil Production

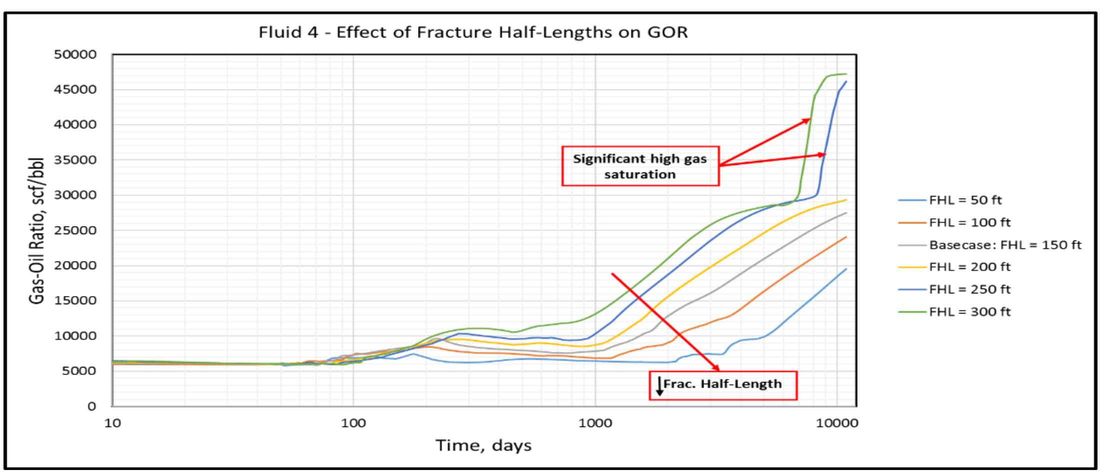

Figure 4-154 Fluid 4 – Effect of Fracture Half-Lengths on GOR

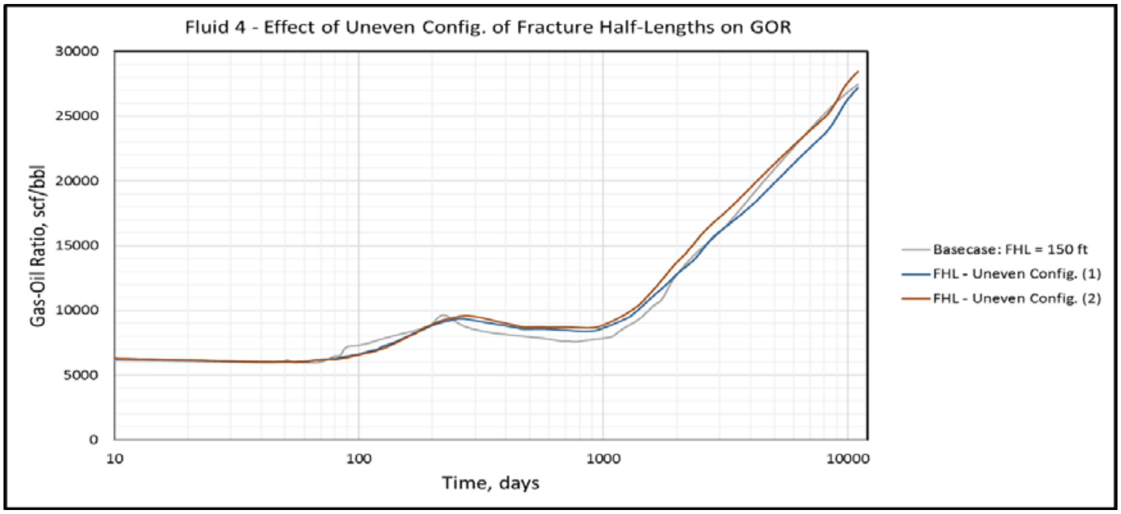

Figure 4-155 Fluid 4 – Effect of Uneven Configuration of Fracture Half-Lengths on GOR

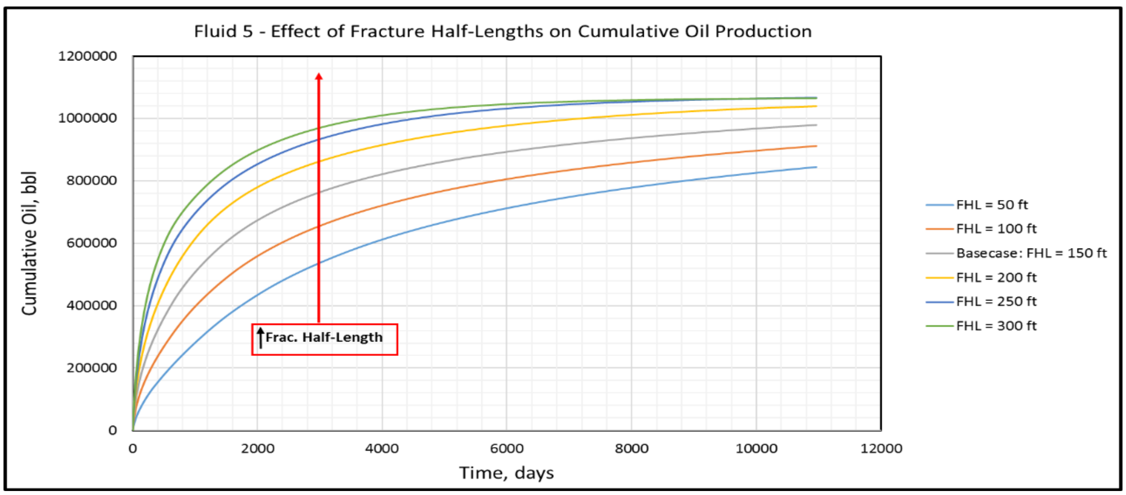

Figure 4-156 Fluid 5 – Effect of Fracture Half-Lengths on Cumulative Oil Production

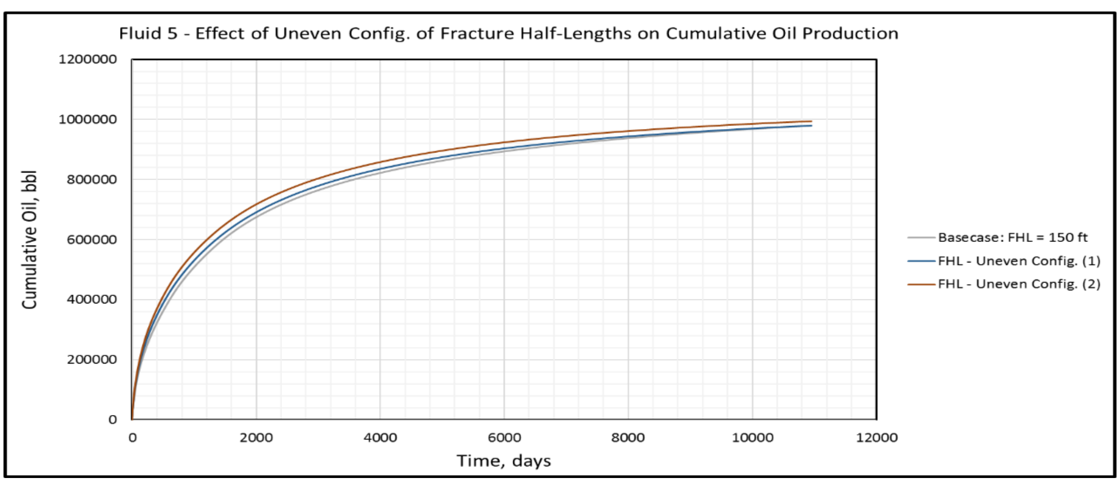

Figure 4-157 Fluid 5 – Effect of Uneven Configuration of Fracture Half-Lengths on Cumulative Oil Production

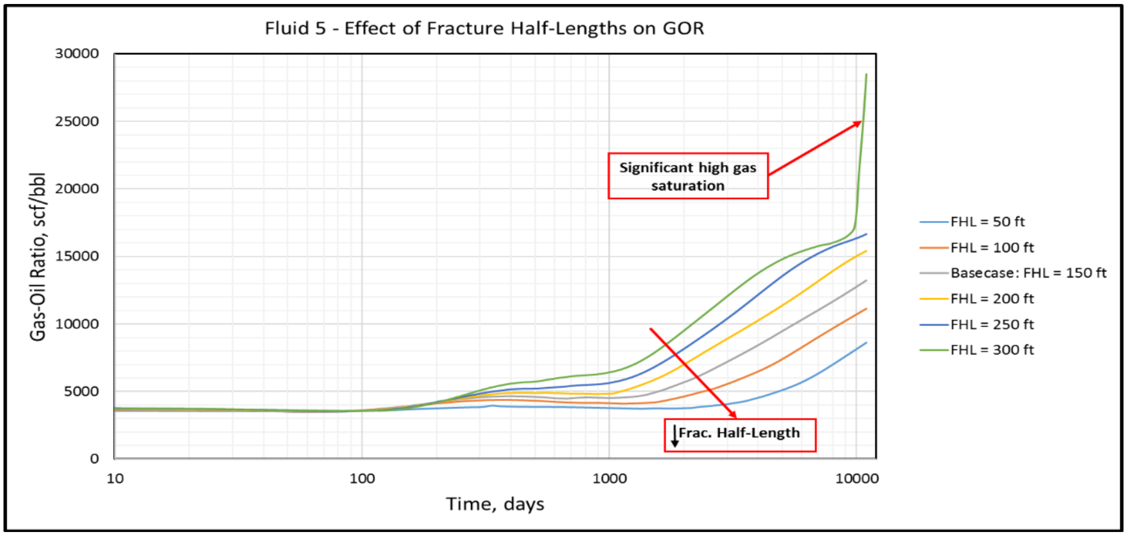

Figure 4-158 Fluid 5 – Effect of Fracture Half-Lengths on GOR

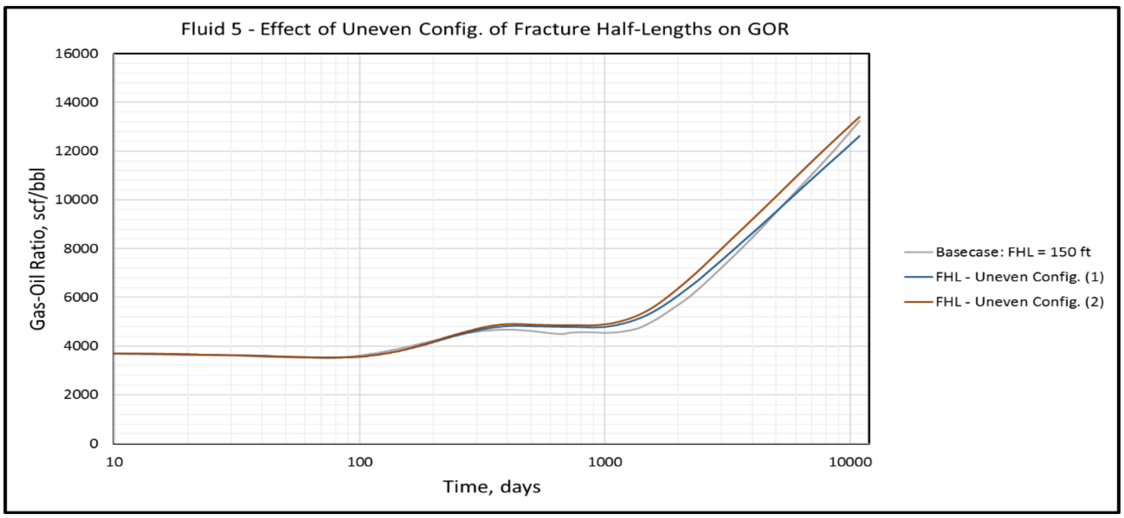

Figure 4-159 Fluid 5 – Effect of Uneven Configuration of Fracture Half-Lengths on GOR

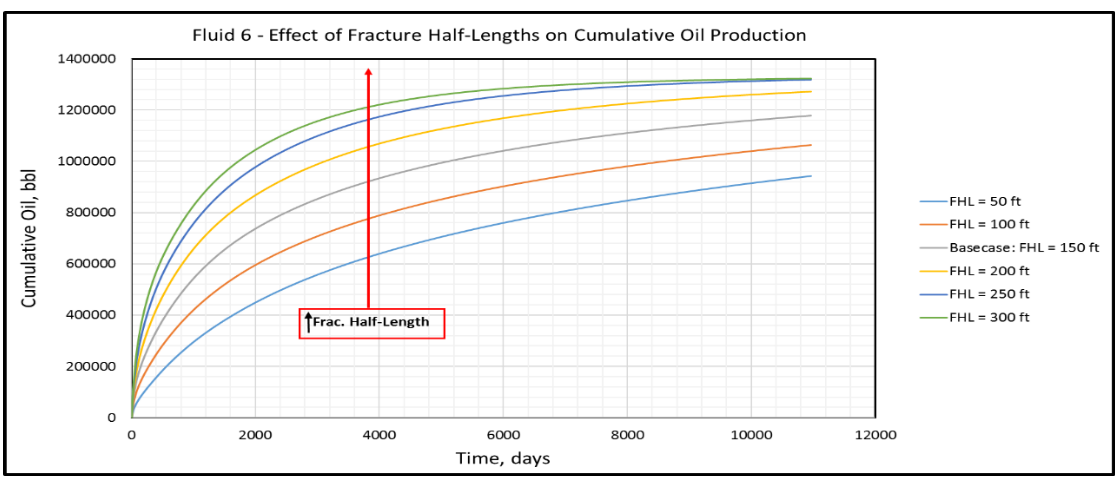

Figure 4-160 Fluid 6 – Effect of Fracture Half-Lengths on Cumulative Oil Production

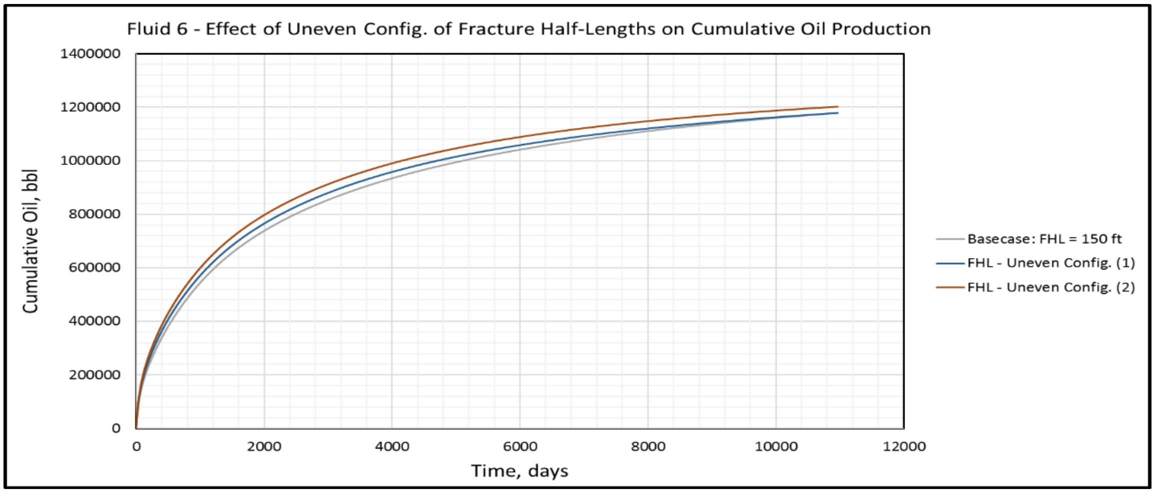

Figure 4-161 Fluid 6 – Effect of Uneven Configuration of Fracture Half-Lengths on Cumulative Oil Production

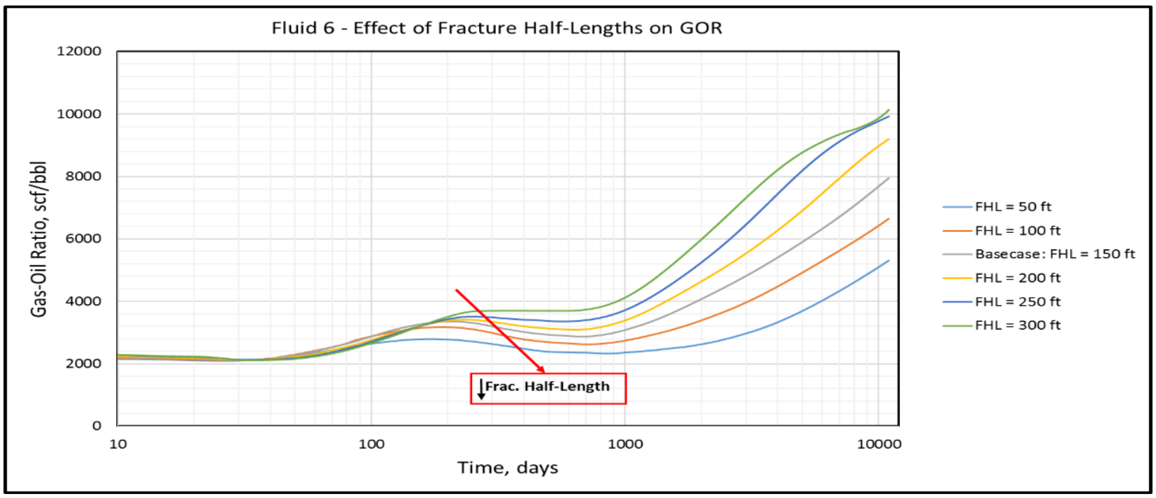

Figure 4-162 Fluid 6 – Effect of Fracture Half-Lengths on GOR

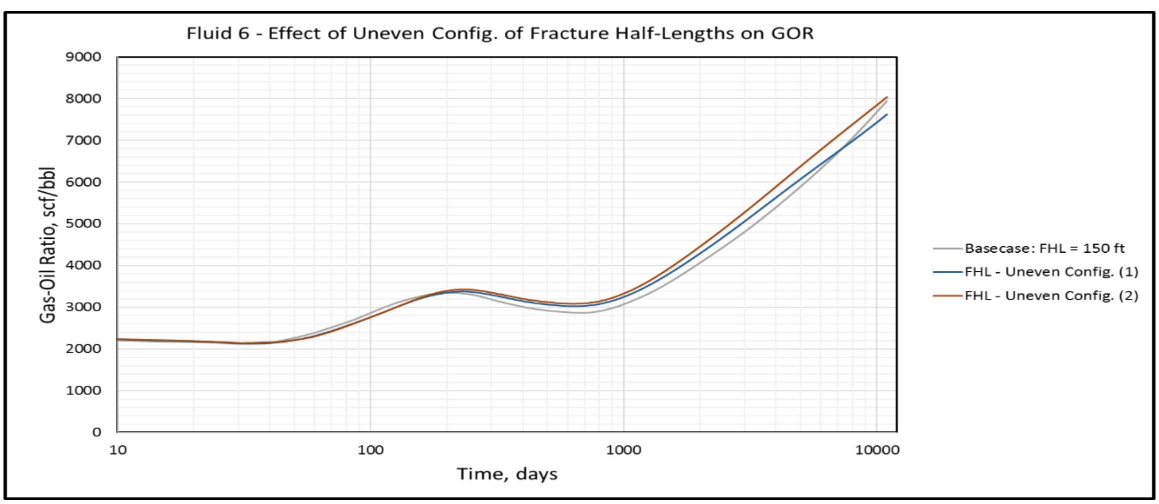

Figure 4-163 Fluid 6 – Effect of Uneven Configuration of Fracture Half-Lengths on GOR

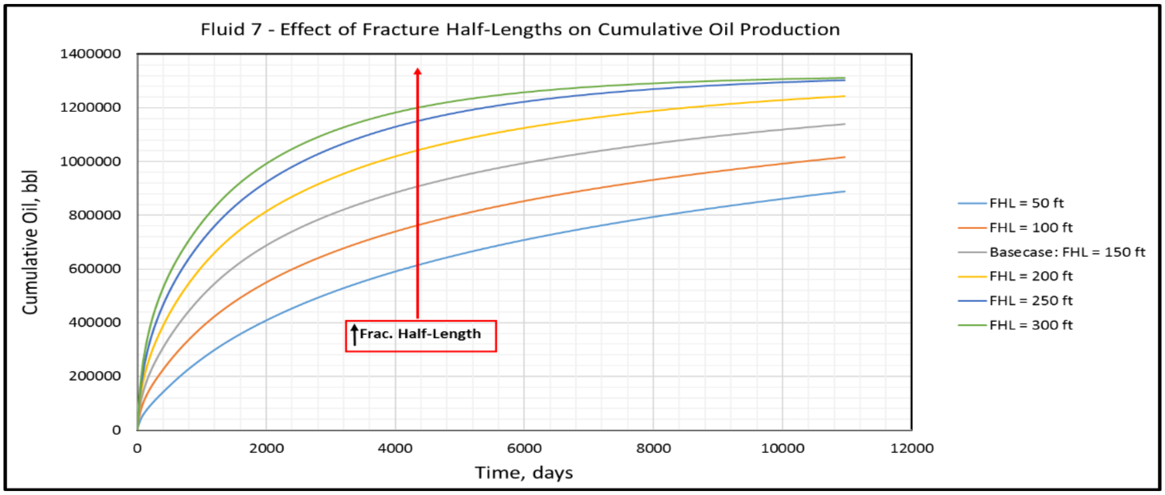

Figure 4-164 Fluid 7 – Effect of Fracture Half-Lengths on Cumulative Oil Production

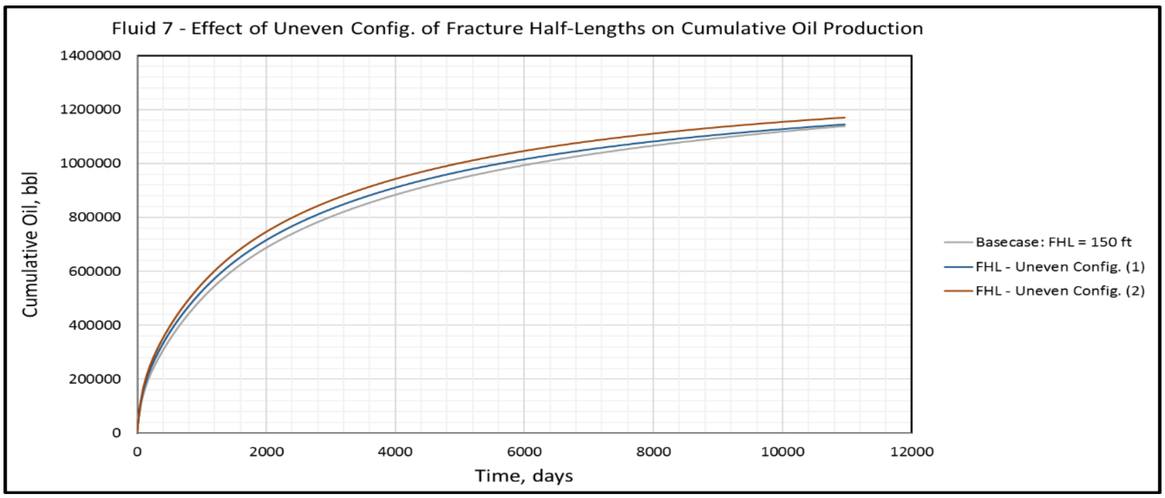

Figure 4-165 Fluid 7 – Effect of Uneven Configuration of Fracture Half-Lengths on Cumulative Oil Production

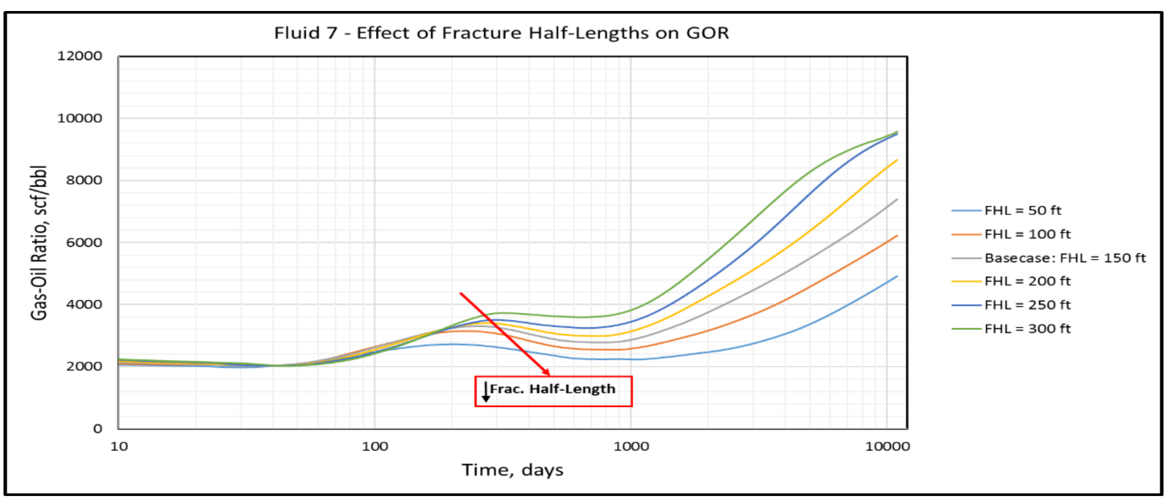

Figure 4-166 Fluid 7 – Effect of Fracture Half-Lengths on GOR

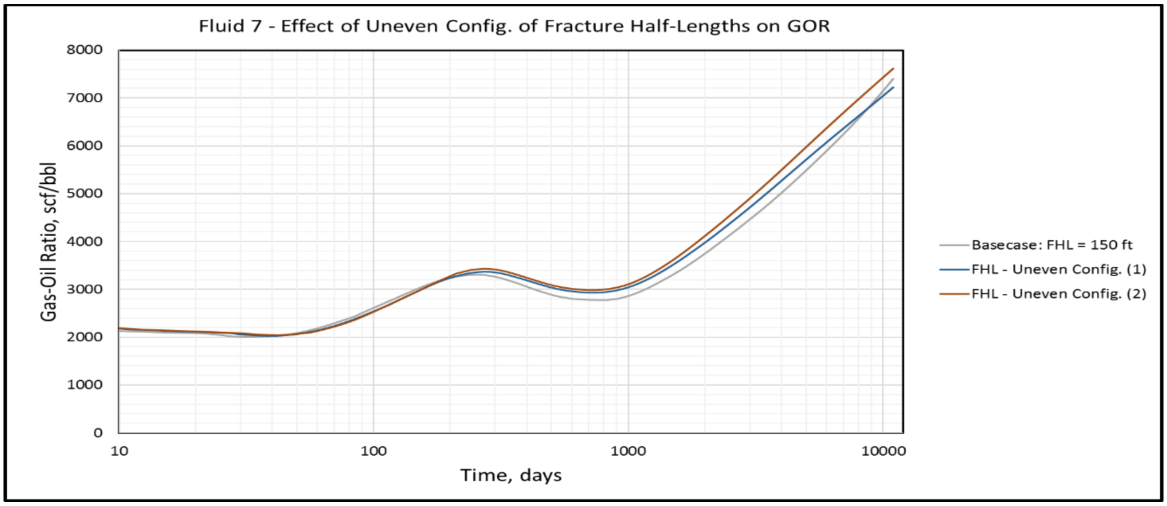

Figure 4-167 Fluid 7 – Effect of Uneven Configuration of Fracture Half-Lengths on GOR

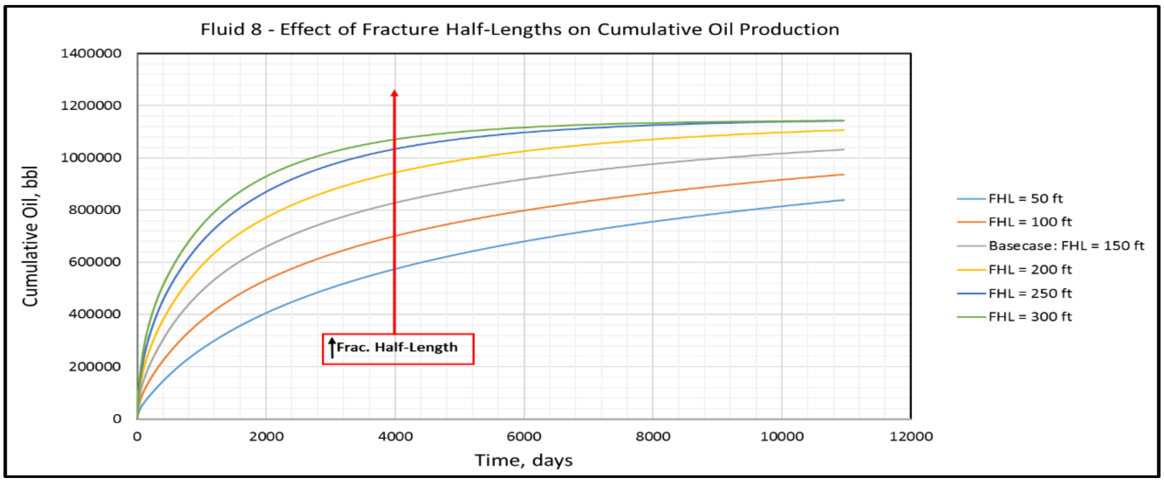

Figure 4-168 Fluid 8 – Effect of Fracture Half-Lengths on Cumulative Oil Production

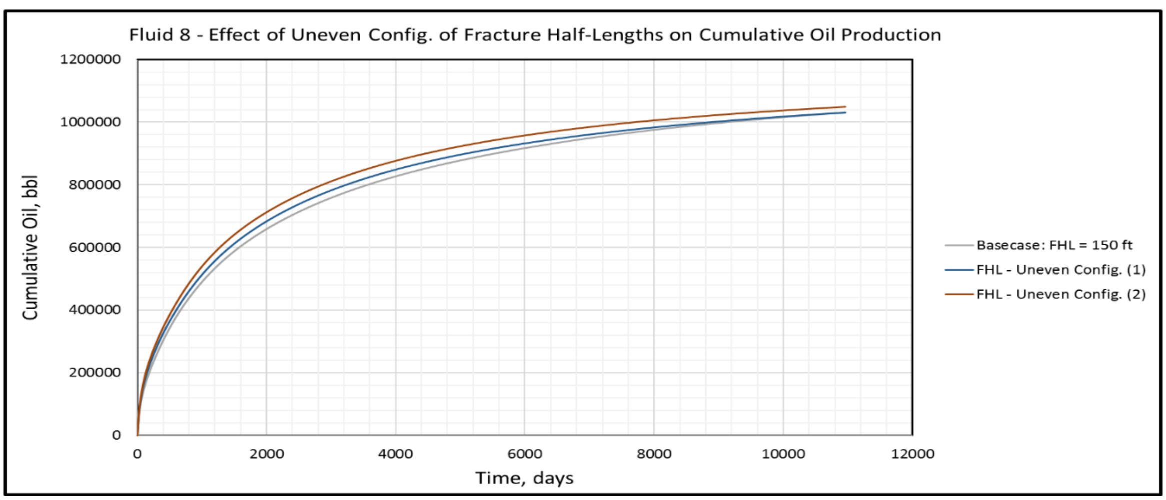

Figure 4-169 Fluid 8 – Effect of Uneven Configuration of Fracture Half-Lengths on Cumulative Oil Production

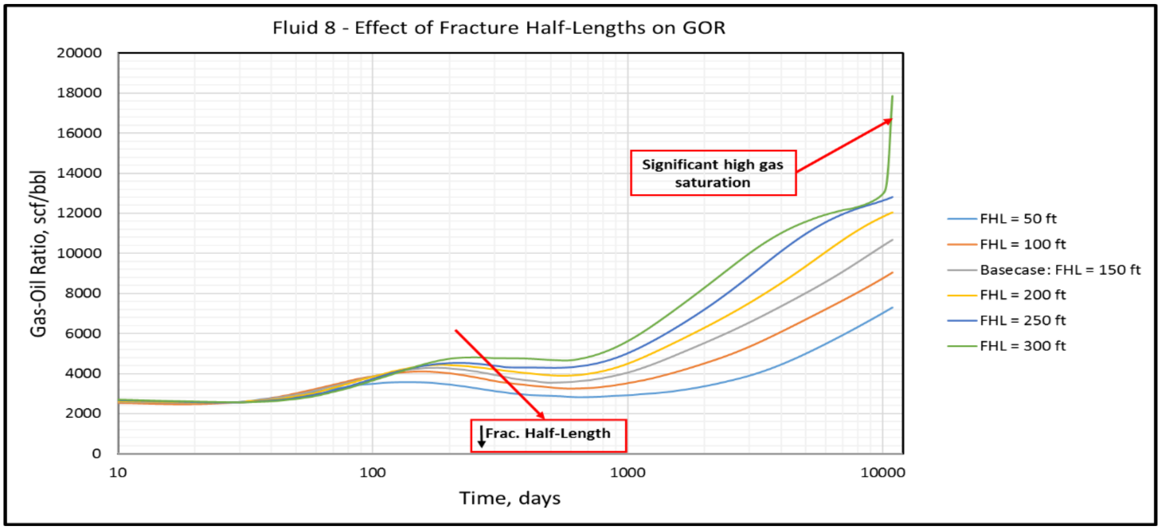

Figure 4-170 Fluid 8 – Effect of Fracture Half-Lengths on GOR

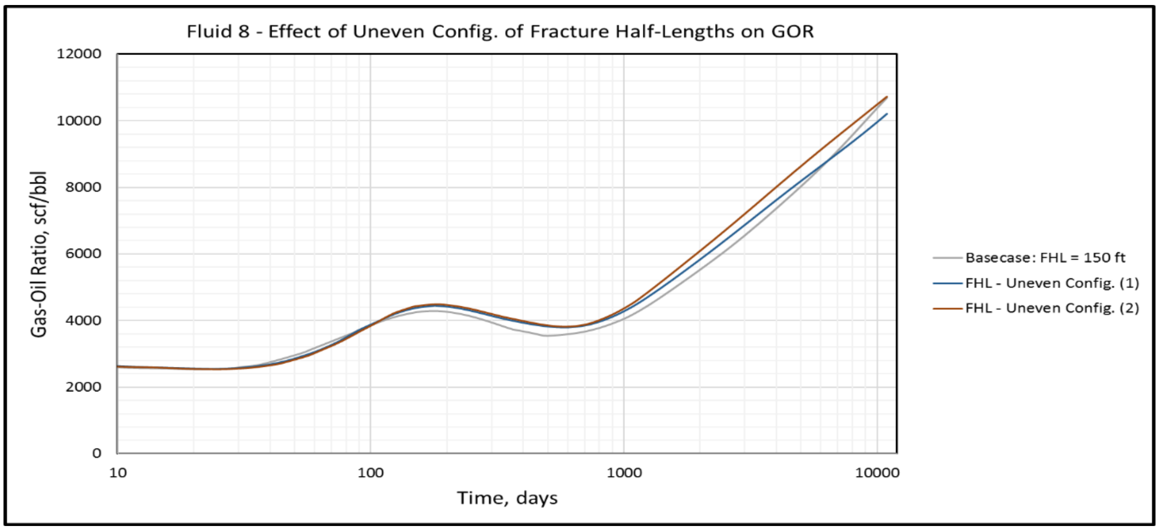

Figure 4-171 Fluid 8 – Effect of Uneven Configuration of Fracture Half-Lengths on GOR

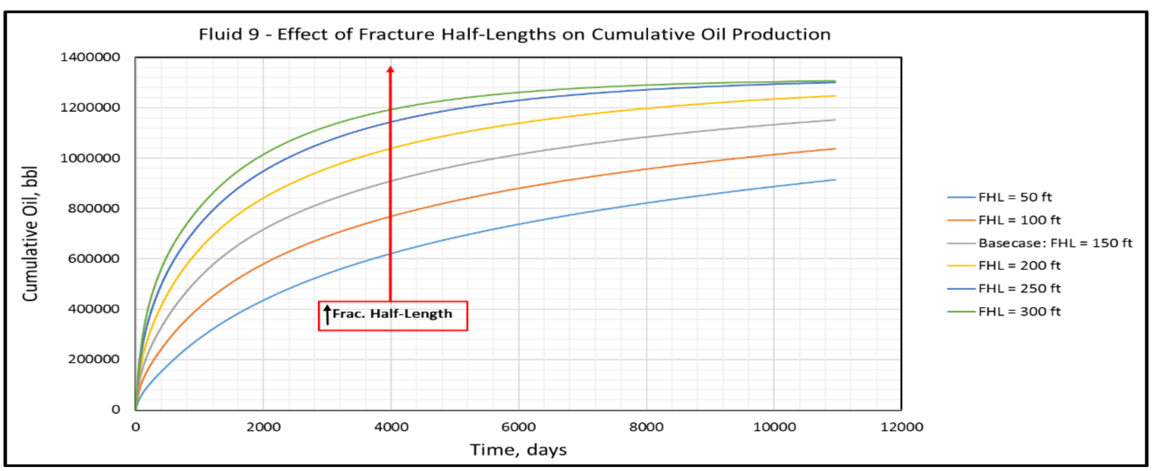

Figure 4-172 Fluid 9 – Effect of Fracture Half-Lengths on Cumulative Oil Production

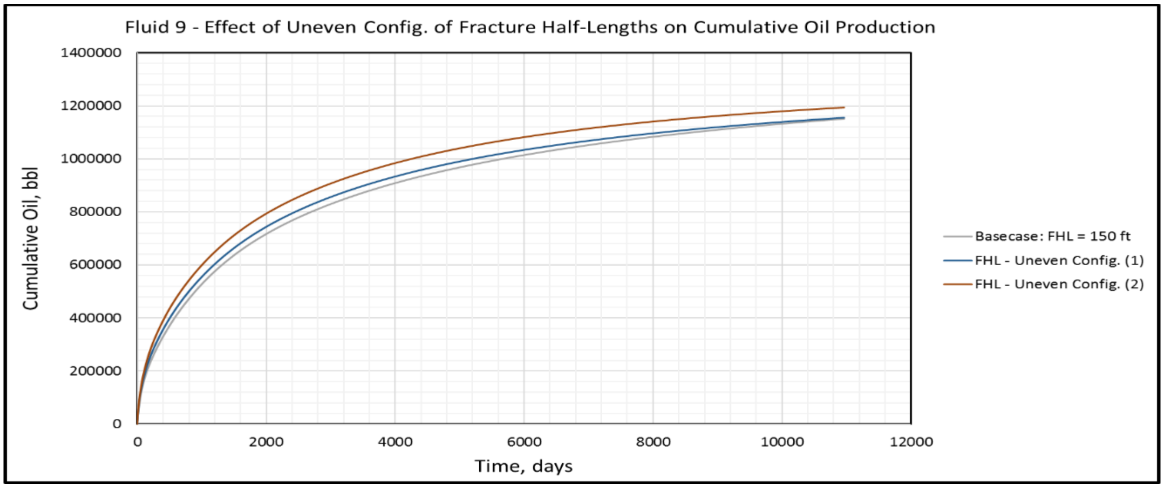

Figure 4-173 Fluid 9 – Effect of Uneven Configuration of Fracture Half-Lengths on Cumulative Oil Production

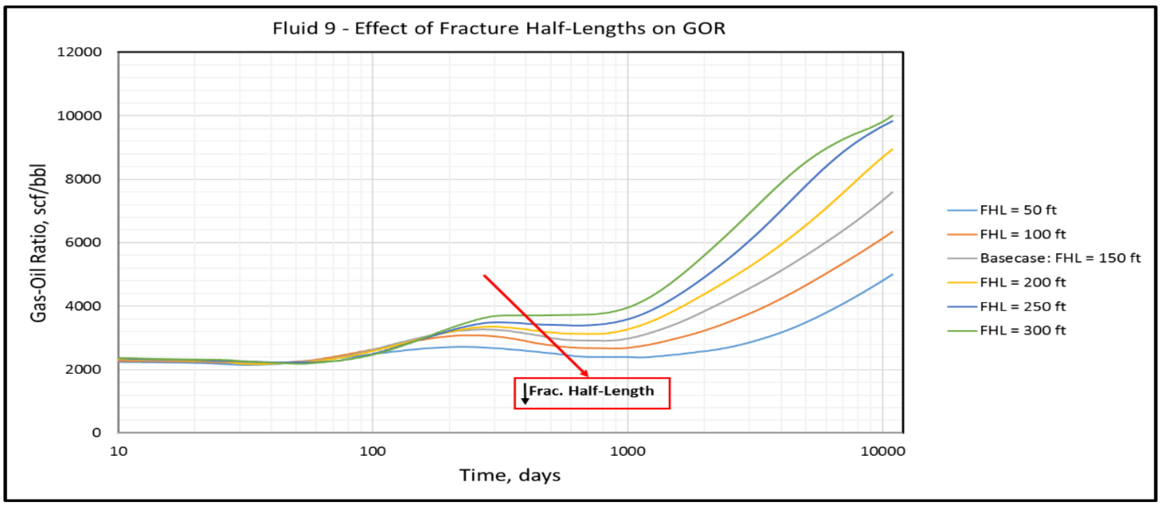

Figure 4-174 Fluid 9 – Effect of Fracture Half-Lengths on GOR

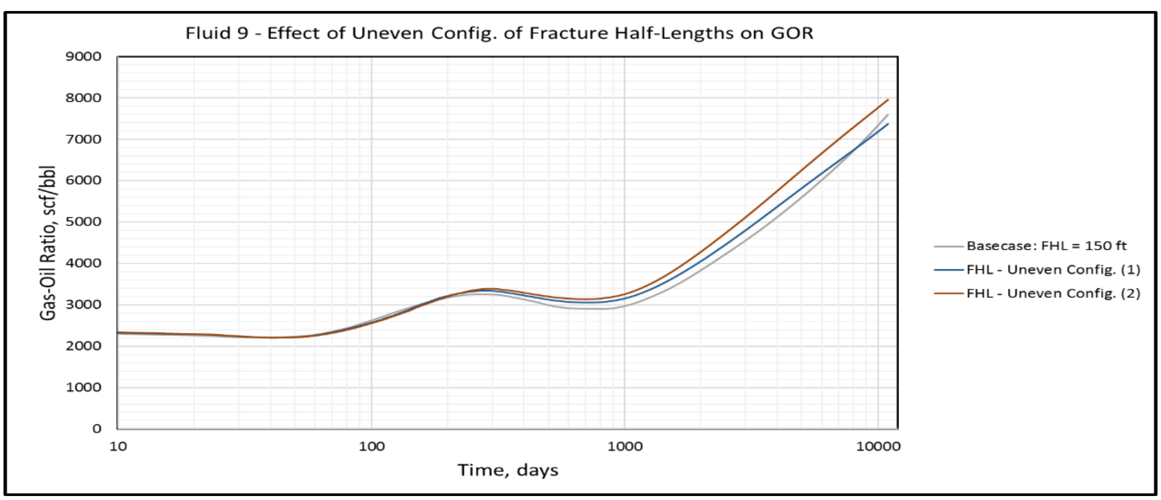

Figure 4-175 Fluid 9 – Effect of Uneven Configuration of Fracture Half-Lengths on GOR

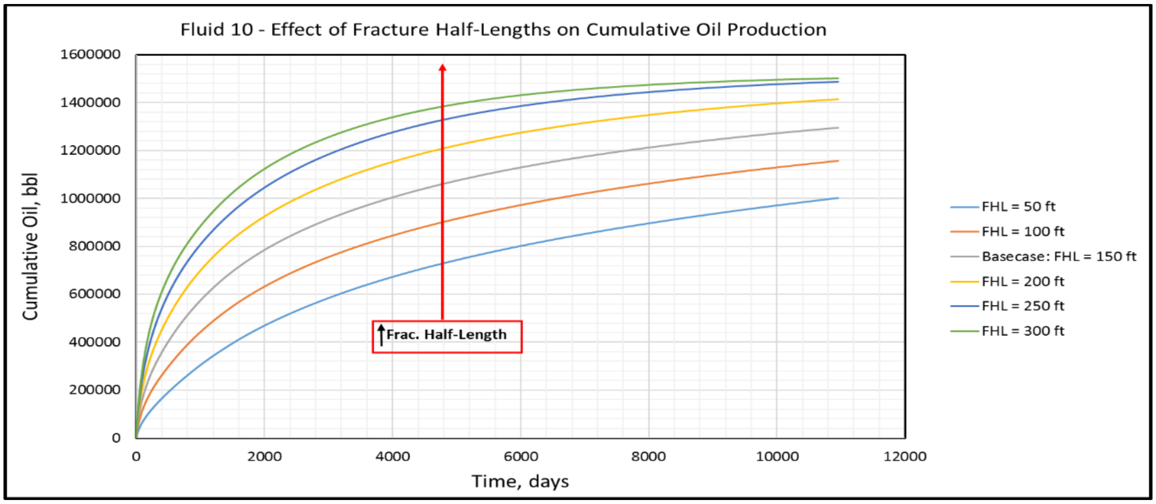

Figure 4-176 Fluid 10 – Effect of Fracture Half-Lengths on Cumulative Oil Production

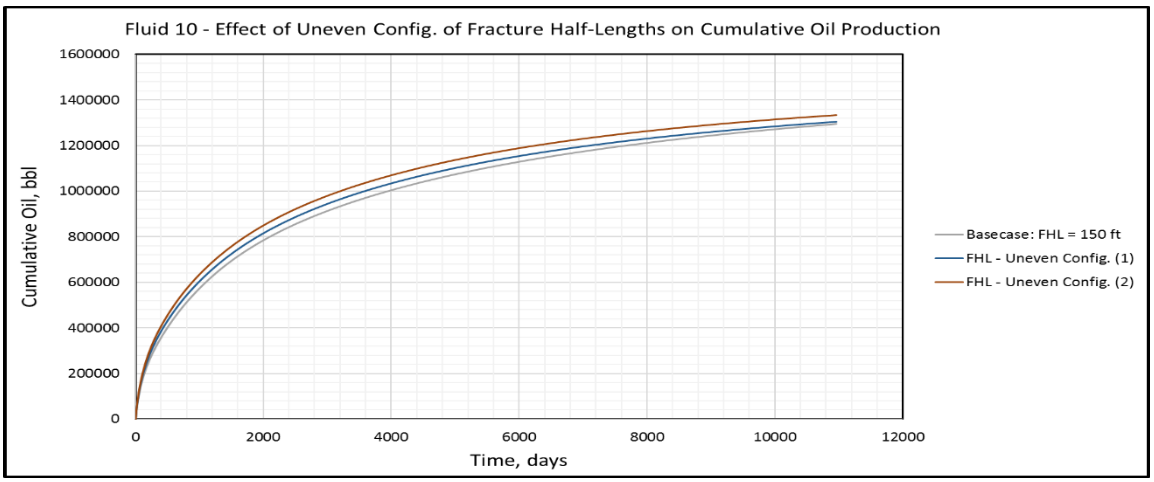

Figure 4-177 Fluid 10 – Effect of Uneven Configuration of Fracture Half-Lengths on Cumulative Oil Production

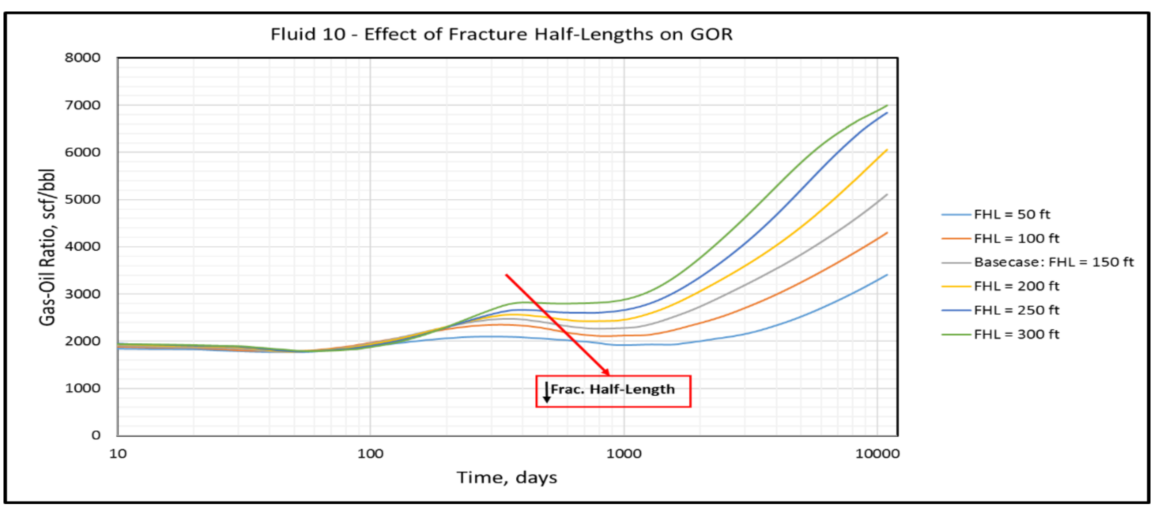

Figure 4-178 Fluid 10 – Effect of Fracture Half-Lengths on GOR

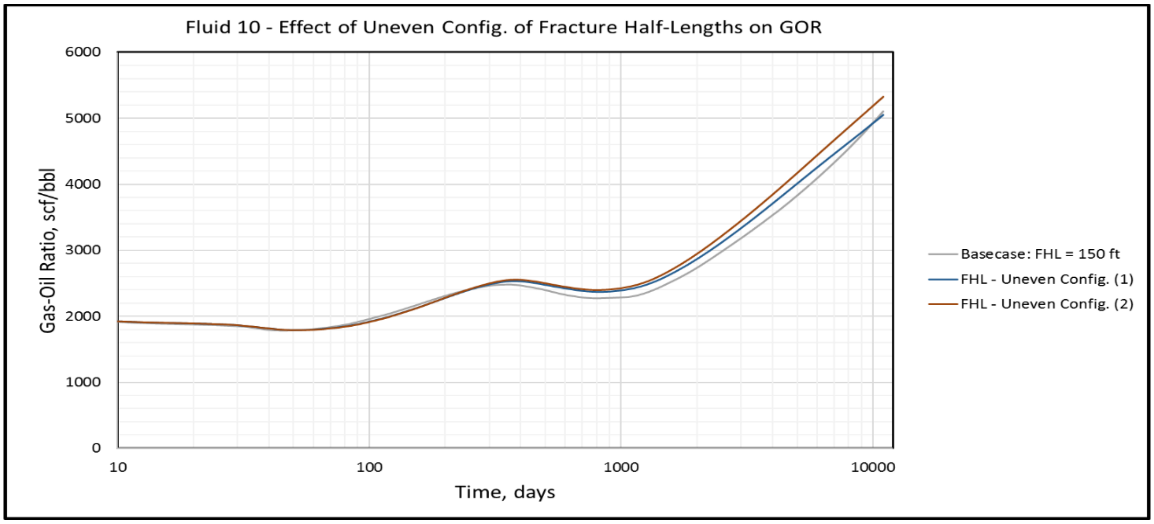

Figure 4-179 Fluid 10 – Effect of Uneven Configuration of Fracture Half-Lengths on GOR

4.7. Fracture Permeability

Fracture permeability is a measure of the ease with which fluids flow through the connecting pore spaces of fractured rocks. In other words, it is a measure of the ability of fractured rocks to transmit fluids. Fracture permeability is directly proportional to the dimensionless fracture conductivity, as seen in Equation 9 below.

$$F_{CD} = \frac{k_f w_f}{k x_f}, \tag{9}$$

where F_{CD} is the dimensionless fracture conductivity, k_f is the fracture permeability, w_f is the fracture width, k is the formation permeability and x_f is the fracture half-length. In our analyses of the impacts of fracture permeability on well performance, we considered fracture permeabilities of 5 md, 10 md, 20 md, 60 md, 80 md and the basecase – 41.65 md.

The impact of fracture permeability on cumulative oil production is not substantial, as there are no huge differences in the quantities of oil produced for each case. However, the common trend is that the higher the fracture permeability, the larger the cumulative oil production. Nevertheless, for highly volatile oils, high gas saturation later impedes oil production and cumulative oil production reduces with increase in fracture permeability after a while.

With reducing fracture permeability, there is a delay in the increase of gas saturation at the fracture faces. Consequently, there is a delay in the formation of the "GOR hill" (delay in the initial rise of producing GOR) and longer period of constant GOR. The reverse is the case with increasing fracture permeability. Figures 4-180 to 4-199 show the impacts of fracture permeability on cumulative oil production and producing GOR (semi-log plots).

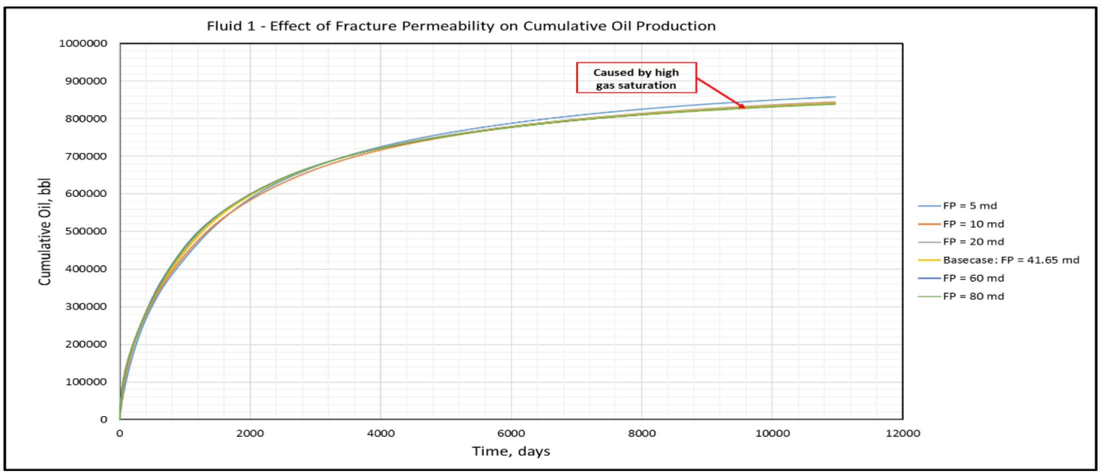

Figure 4-180 Fluid 1 – Effect of Fracture Permeability on Cumulative Oil Production

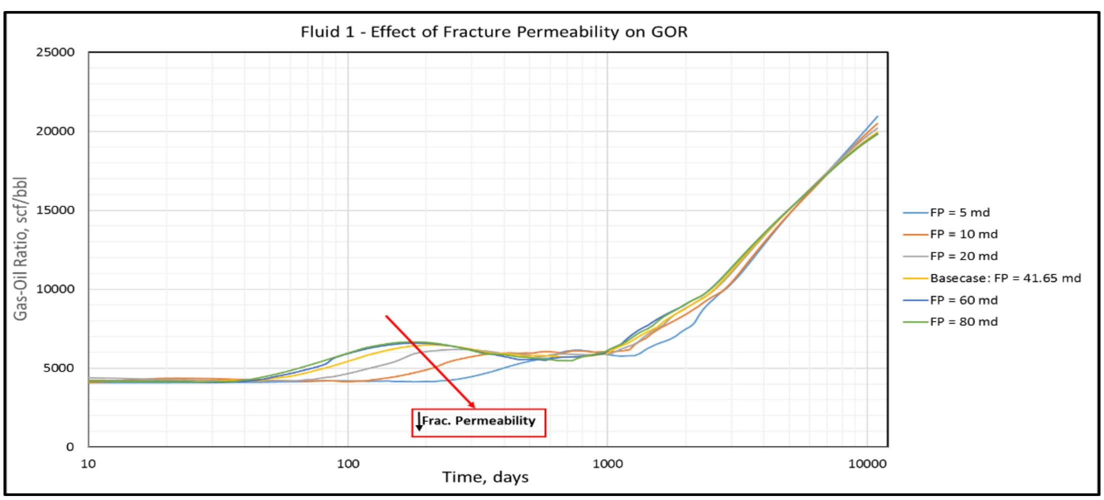

Figure 4-181 Fluid 1 – Effect of Fracture Permeability on GOR

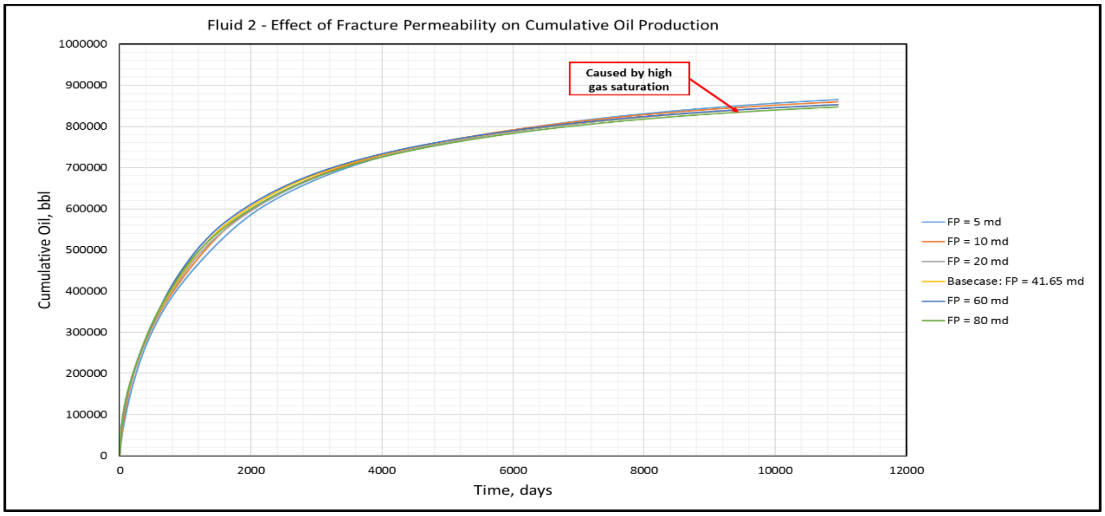

Figure 4-182 Fluid 2 – Effect of Fracture Permeability on Cumulative Oil Production

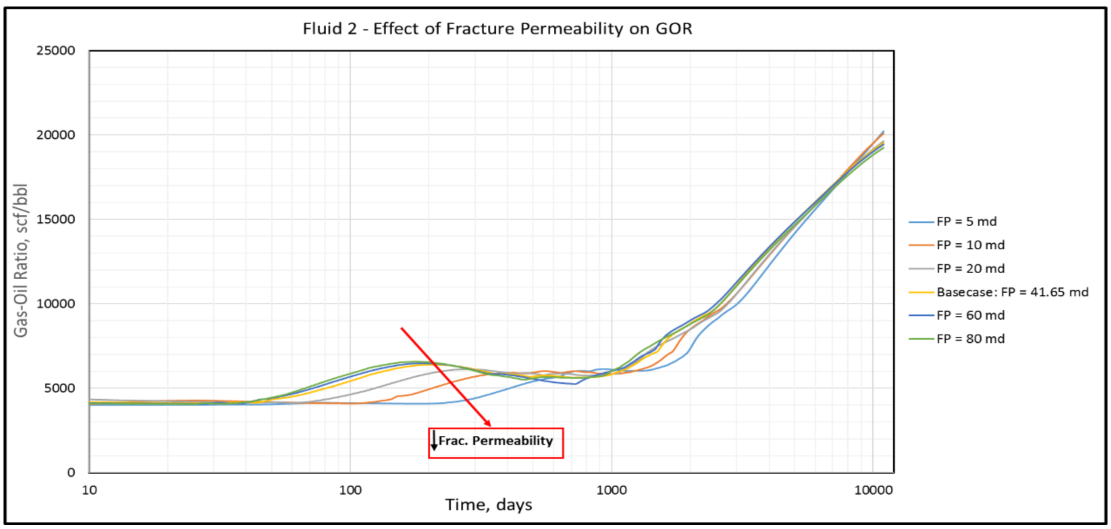

Figure 4-183 Fluid 2 – Effect of Fracture Permeability on GOR

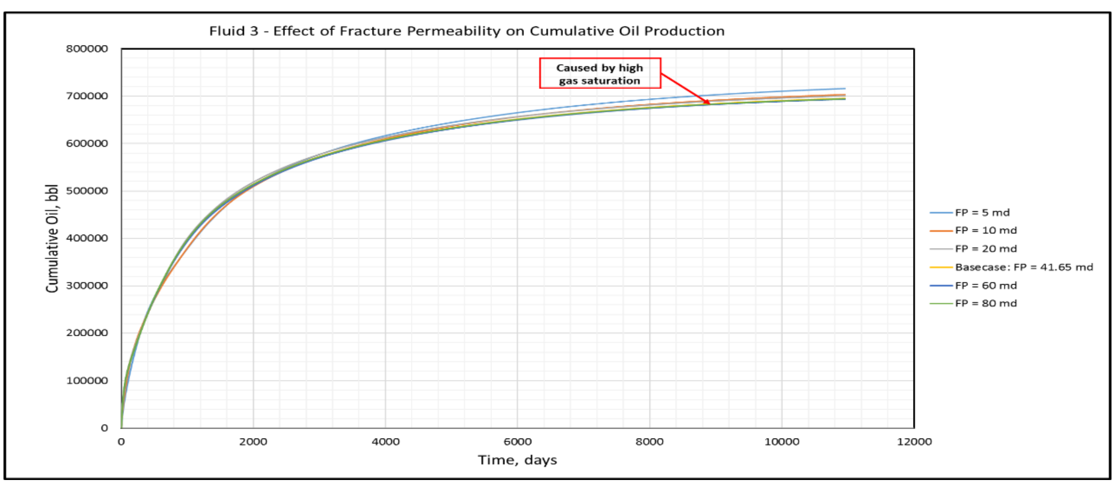

Figure 4-184 Fluid 3 – Effect of Fracture Permeability on Cumulative Oil Production

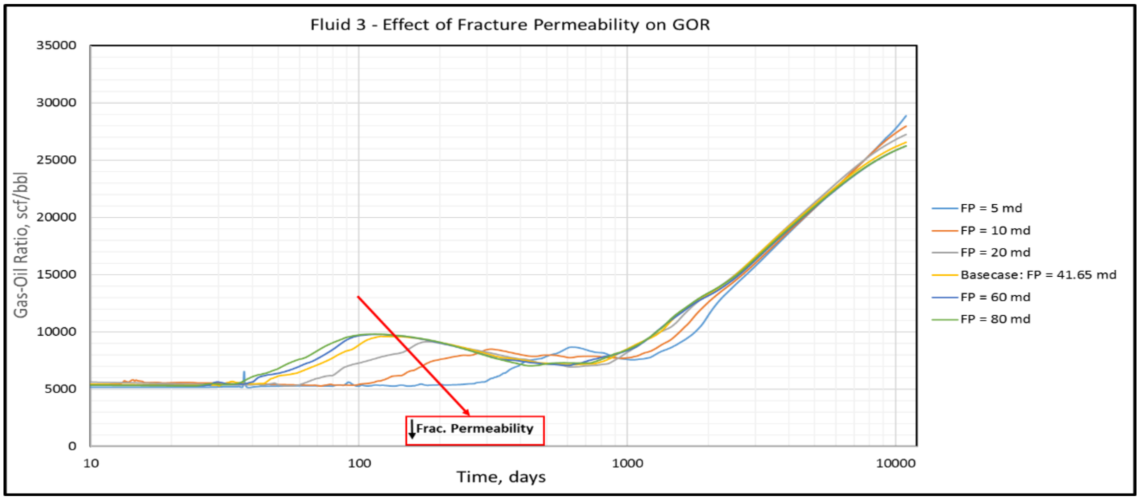

Figure 4-185 Fluid 3 – Effect of Fracture Permeability on GOR

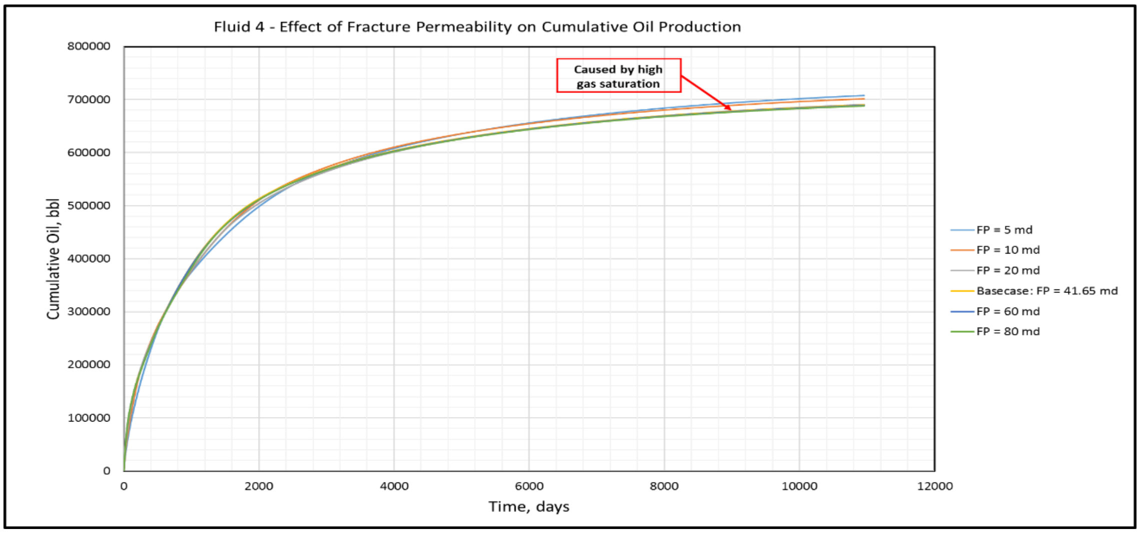

Figure 4-186 Fluid 4 – Effect of Fracture Permeability on Cumulative Oil Production

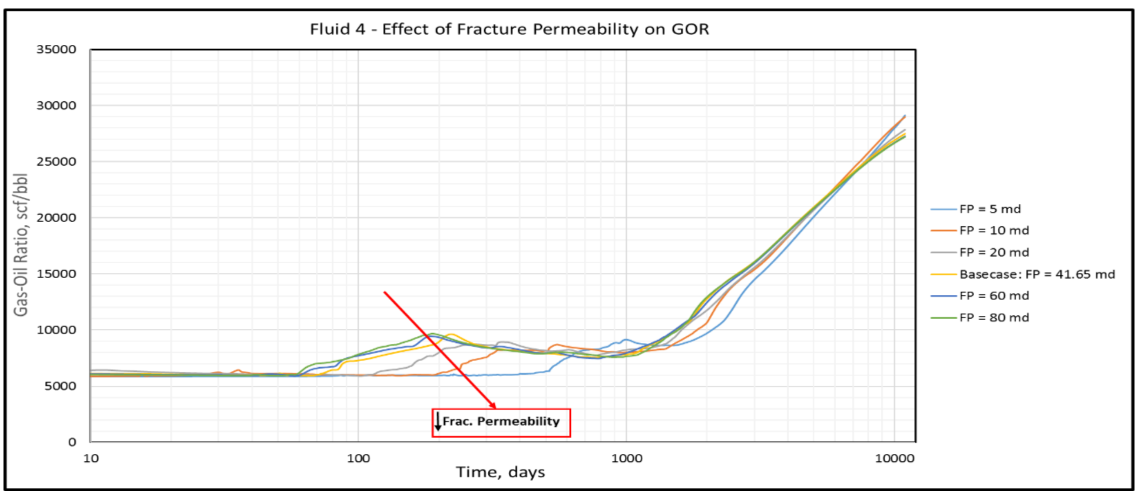

Figure 4-187 Fluid 4 – Effect of Fracture Permeability on GOR

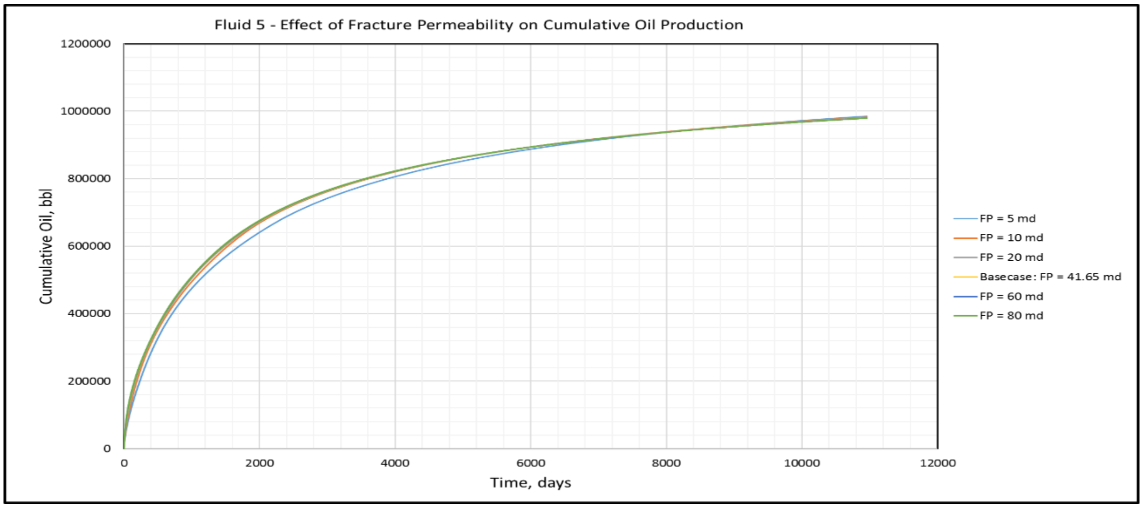

Figure 4-188 Fluid 5 – Effect of Fracture Permeability on Cumulative Oil Production

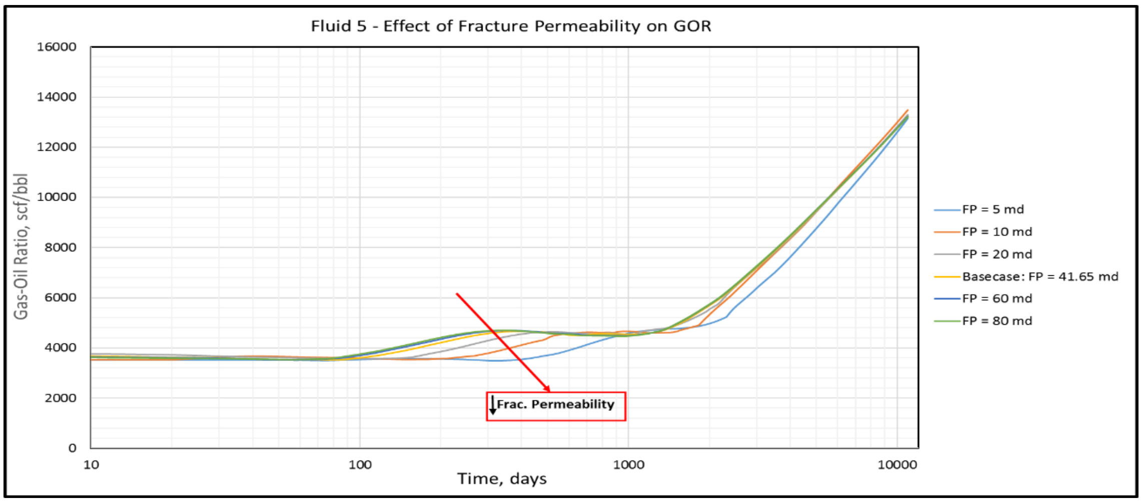

Figure 4-189 Fluid 5 – Effect of Fracture Permeability on GOR

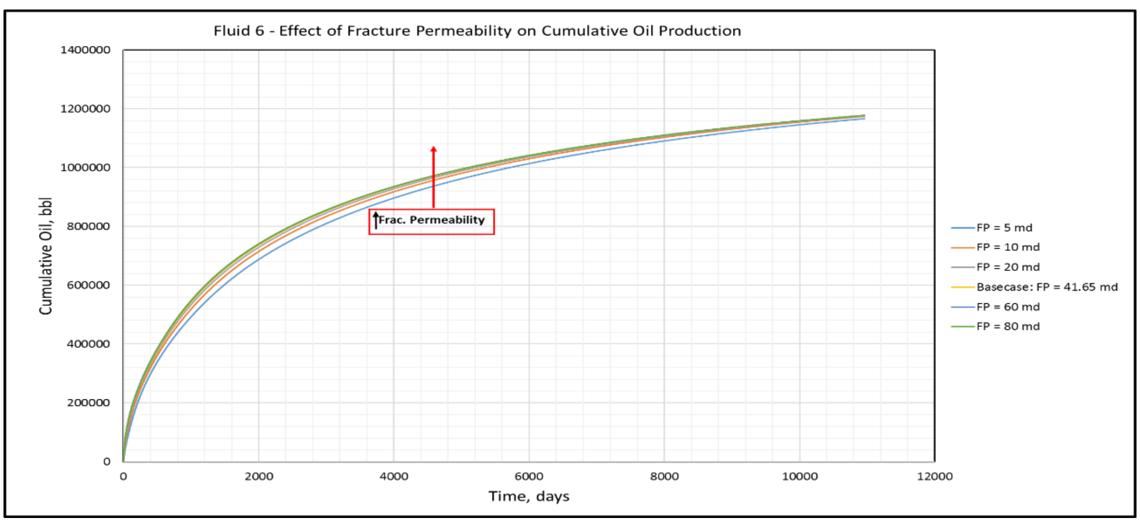

Figure 4-190 Fluid 6 – Effect of Fracture Permeability on Cumulative Oil Production

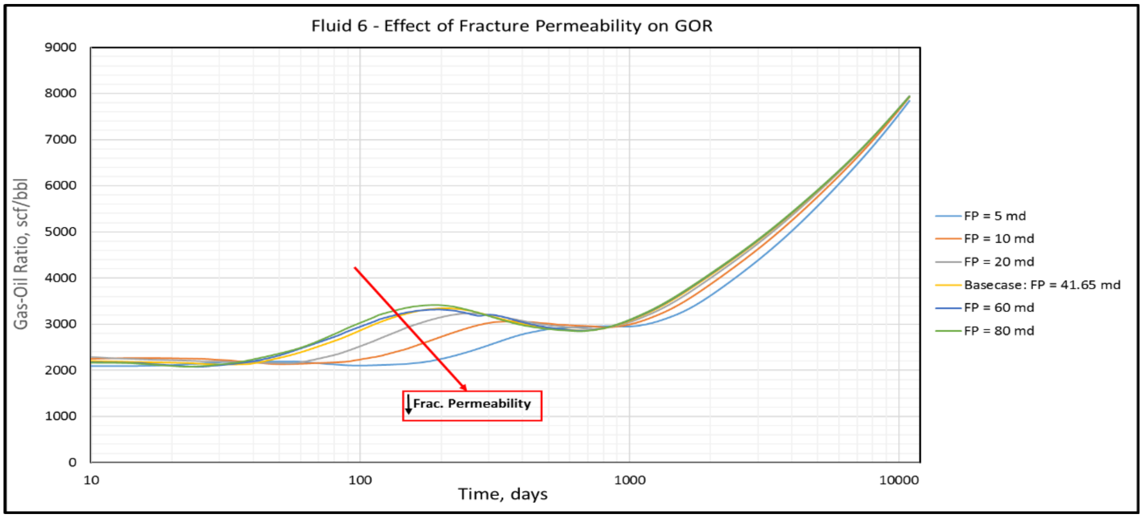

Figure 4-191 Fluid 6 – Effect of Fracture Permeability on GOR

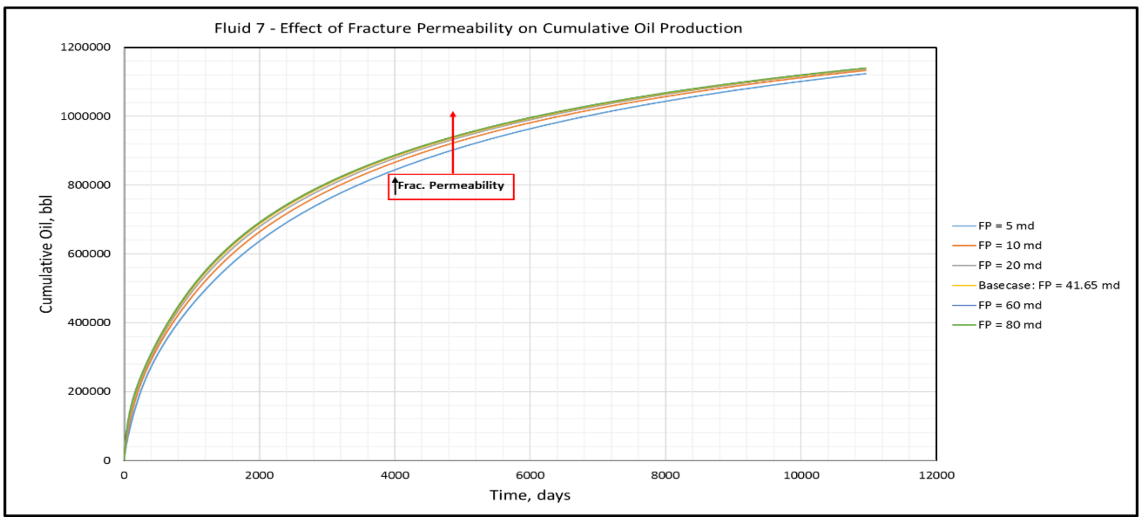

Figure 4-192 Fluid 7 – Effect of Fracture Permeability on Cumulative Oil Production

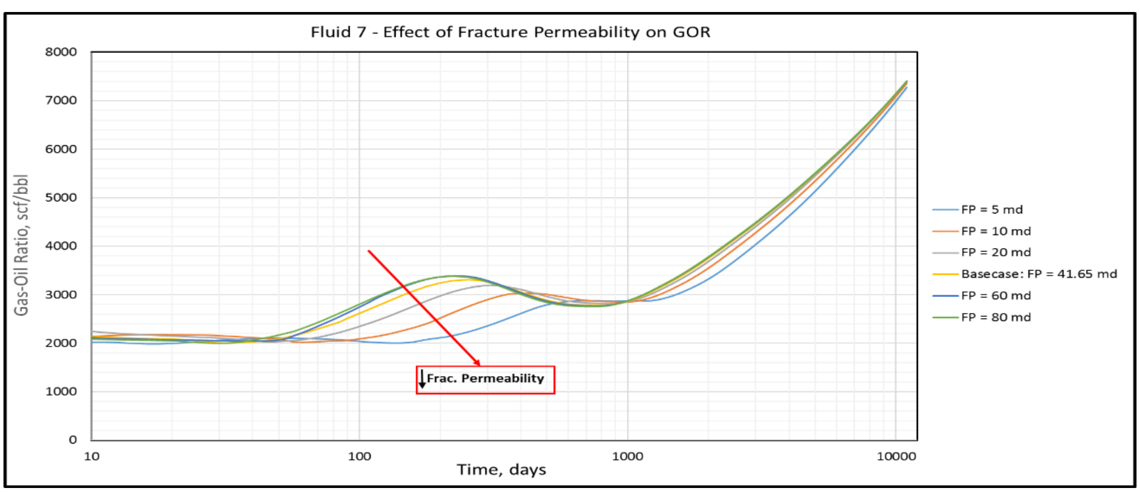

Figure 4-193 Fluid 7 – Effect of Fracture Permeability on GOR

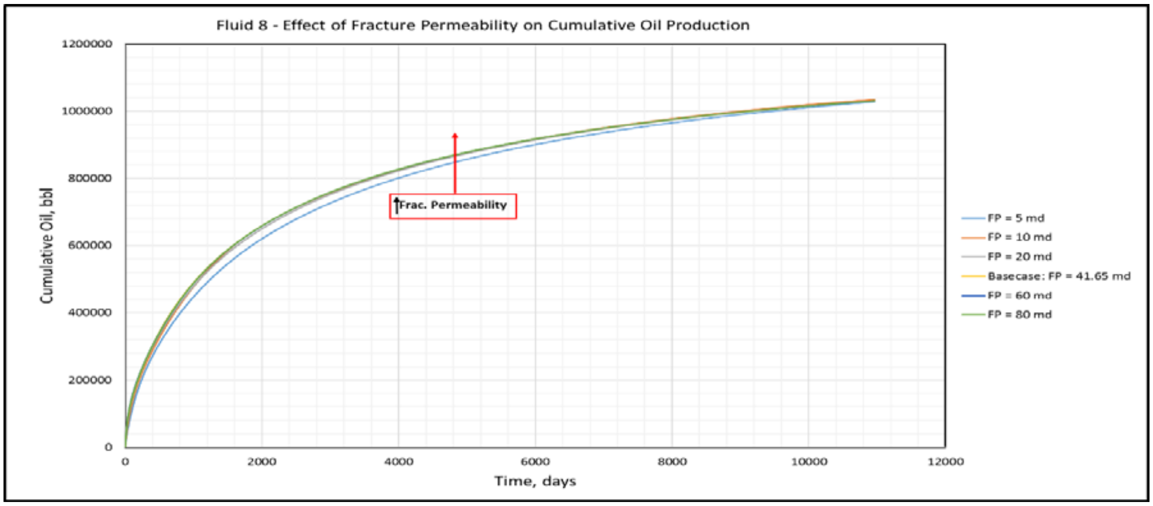

Figure 4-194 Fluid 8 – Effect of Fracture Permeability on Cumulative Oil Production

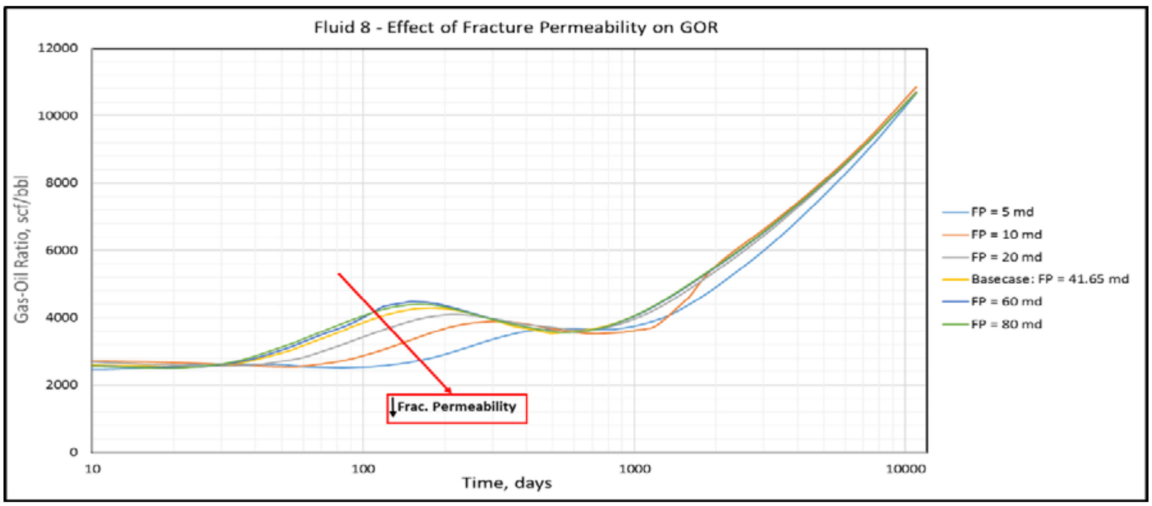

Figure 4-195 Fluid 8 – Effect of Fracture Permeability on GOR

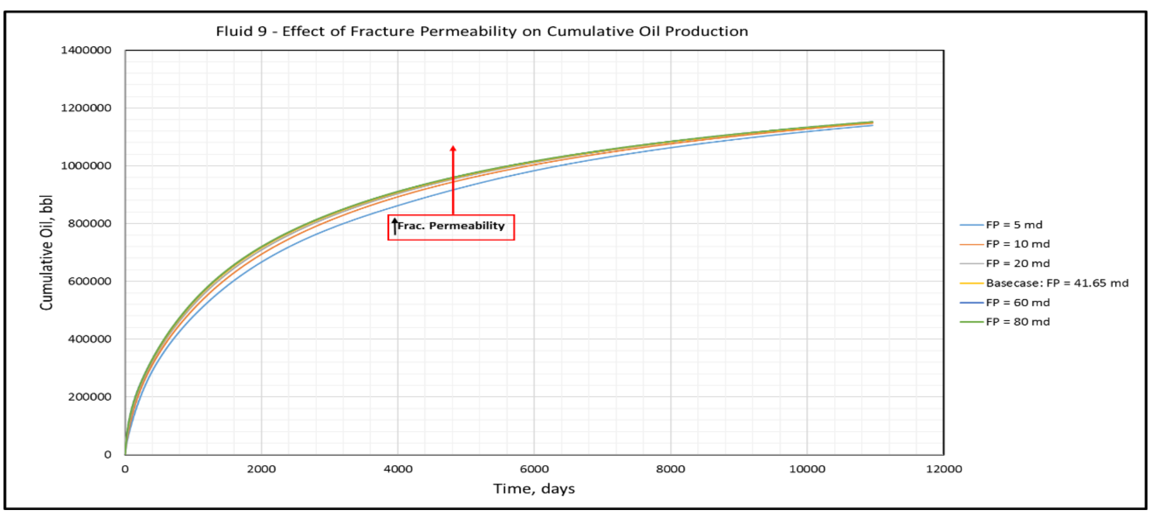

Figure 4-196 Fluid 9 – Effect of Fracture Permeability on Cumulative Oil Production

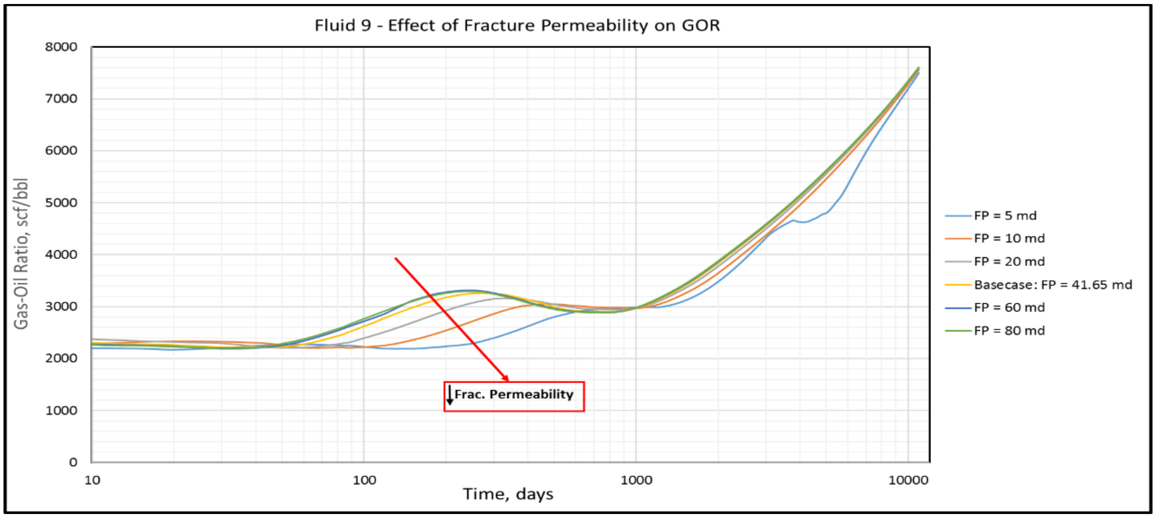

Figure 4-197 Fluid 9 – Effect of Fracture Permeability on GOR

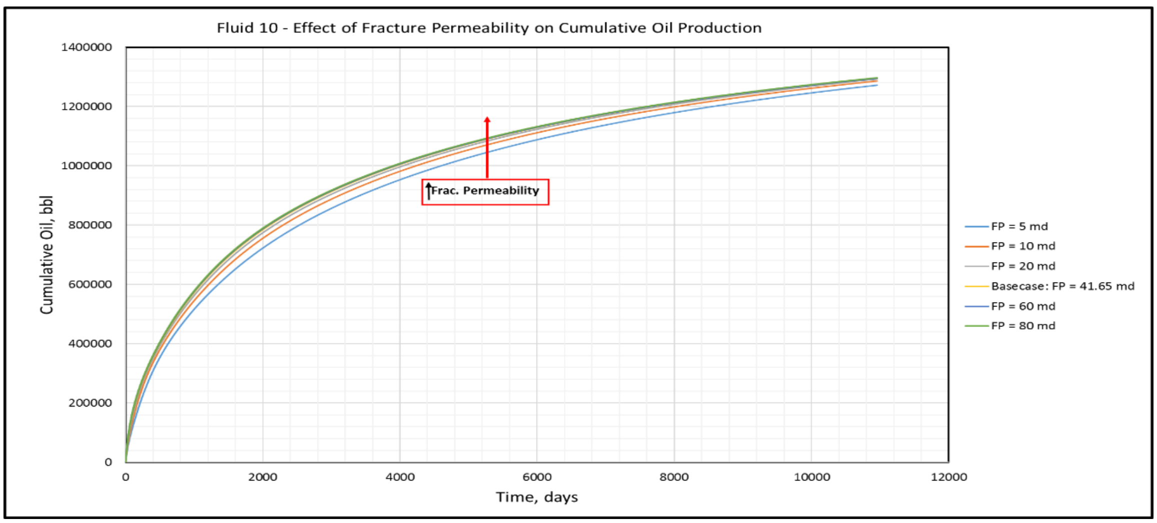

Figure 4-198 Fluid 10 – Effect of Fracture Permeability on Cumulative Oil Production

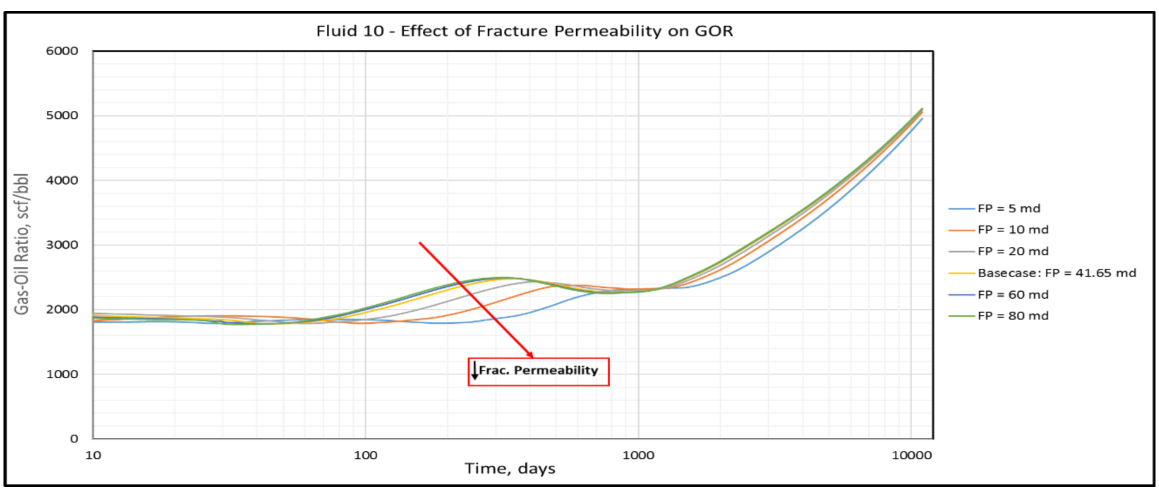

Figure 4-199 Fluid 10 – Effect of Fracture Permeability on GOR

4.8. Fracture Spacing

Fracture spacing is a vital parameter to consider during well completions. It is possible for reservoir engineers to generate different scenarios that can help completion engineers find the optimum spacing necessary for their operations. Apart from the basecase – fracture spacing of 250 ft (20 fracture stages), four other cases were considered in this study – 100 ft (50 fracture stages), 500 ft (10 fracture stages) and two different scenarios with uneven fracture spacing. The cases with uneven fracture spacing are compared to the basecase separately to investigate the impact of non-uniform fracture spacing on shale volatile oil well production performance. Figures 4-200 to 4-203 show the reservoir models for the different instances apart from the basecase (already shown in Figure 4-1).

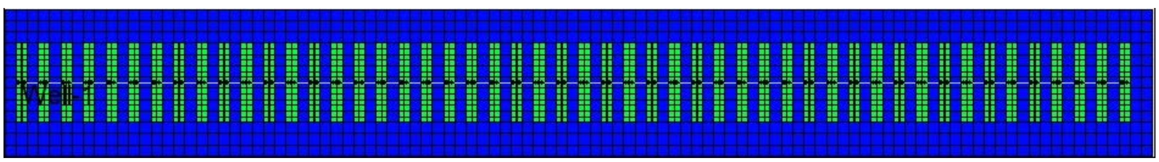

Figure 4-200 Reservoir Model – 100 ft Fracture Spacing (50 Fracture Stages)

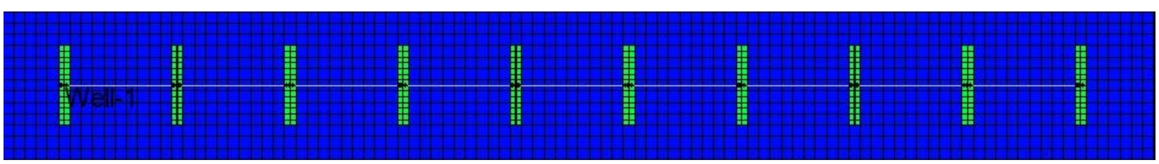

Figure 4-201 Reservoir Model – 500 ft Fracture Spacing (10 Fracture Stages)

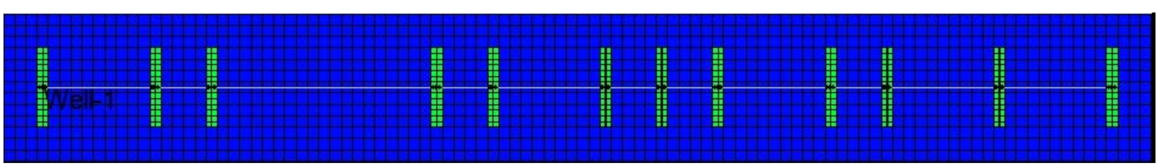

Figure 4-202 Reservoir Model – Uneven Configuration 1 (Fracture Spacing)

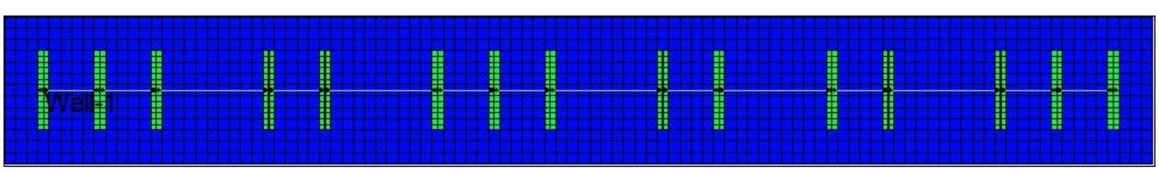

Figure 4-203 Reservoir Model – Uneven Configuration 2 (Fracture Spacing)

Even though closer fracture spacing (more fracture stages) requires a higher completion cost per well, it eventually means better drainage of the SRV within a shorter period of time (Makinde, 2014). The closer the fracture spacing, the larger the cumulative oil production. For highly volatile oils, cumulative oil production starts to reduce with closer fracture spacing later on during production because of high gas saturation.

The effect of fracture spacing on producing GOR is quite significant. The closer the fracture spacing, the more rapid the critical gas saturation is reached. This therefore results in higher producing GOR with time as fracture spacing reduces. For highly volatile oils, high gas saturation can result in very high producing GOR towards the end of the production period.

For the special cases with uneven fracture spacing, the well with uneven configuration 2 (15 fracture stages) has closer fracture spacing in comparison with the well with uneven configuration 1 (12 fracture stages). This can be observed in Figures 4-202 and 4-203. Therefore, though fracture spacing is non-uniform and since the well with uneven configuration 2 generally has closer fracture spacing than that with uneven configuration 1, it produces more oil (larger cumulative oil production). Oil produced in both cases is lower than the oil produced from the well with basecase configuration (Figure 4-1). This is because they both have lesser fracture stages than the basecase (20 fracture stages). The impact on producing GOR is similar to earlier discussed scenarios. The closer the fracture spacing, the higher the producing GOR with time. Figures 4-204 to 4-243 show the effects of fracture spacing on cumulative oil production and producing GOR (semi-log plots).

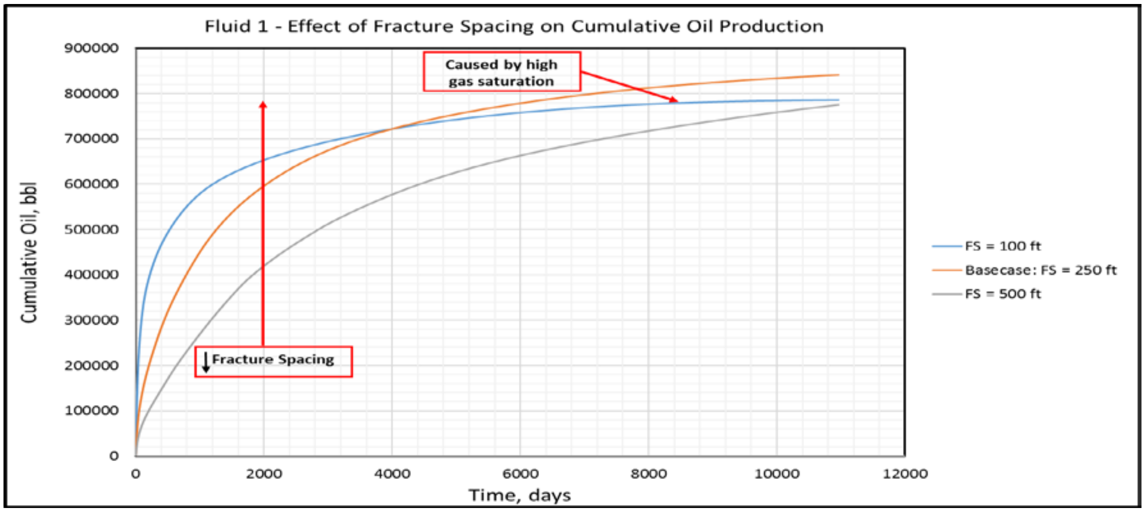

Figure 4-204 Fluid 1 – Effect of Fracture Spacing on Cumulative Oil Production

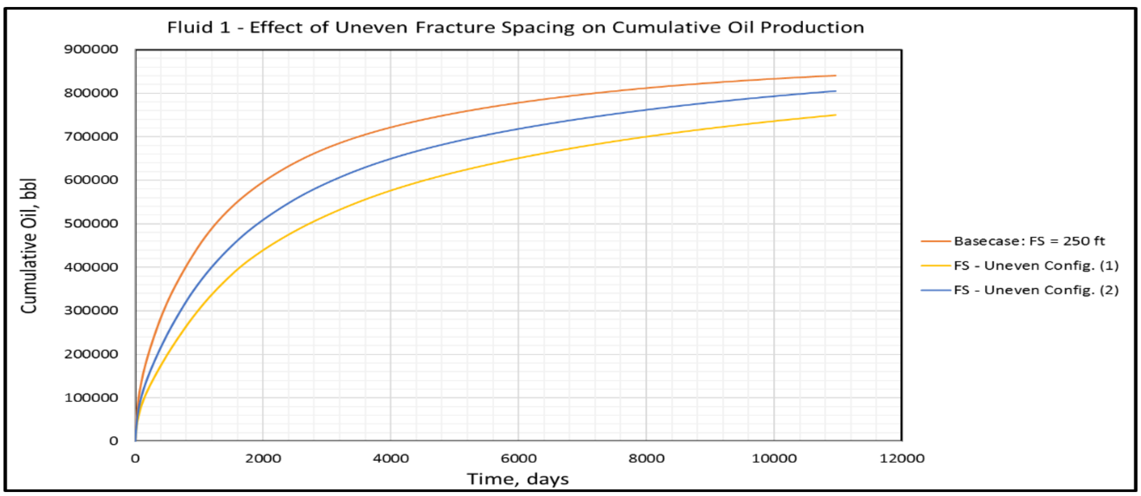

Figure 4-205 Fluid 1 – Effect of Uneven Fracture Spacing on Cumulative Oil Production

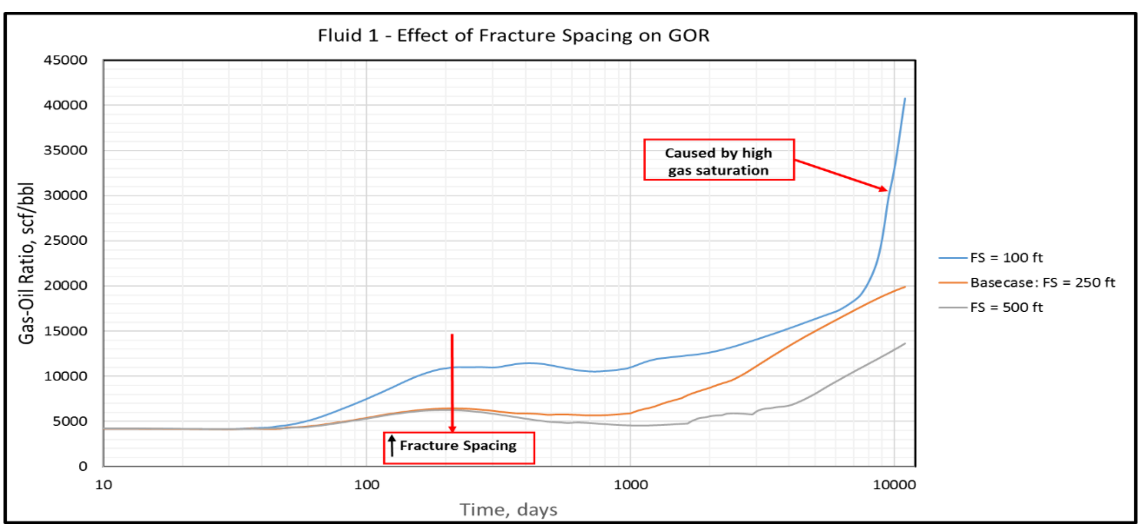

Figure 4-206 Fluid 1 – Effect of Fracture Spacing on GOR

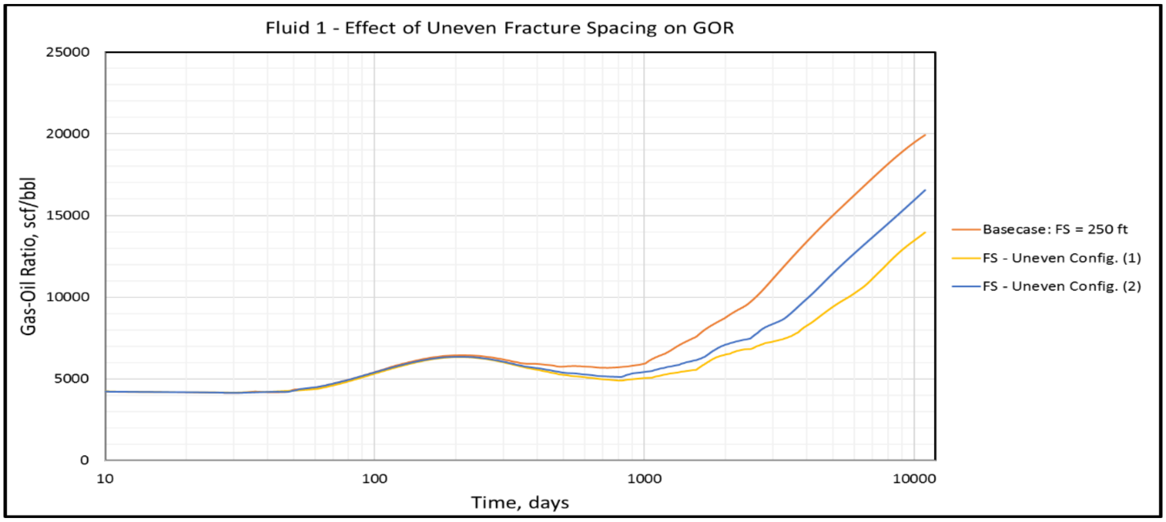

Figure 4-207 Fluid 1 – Effect of Uneven Fracture Spacing on GOR

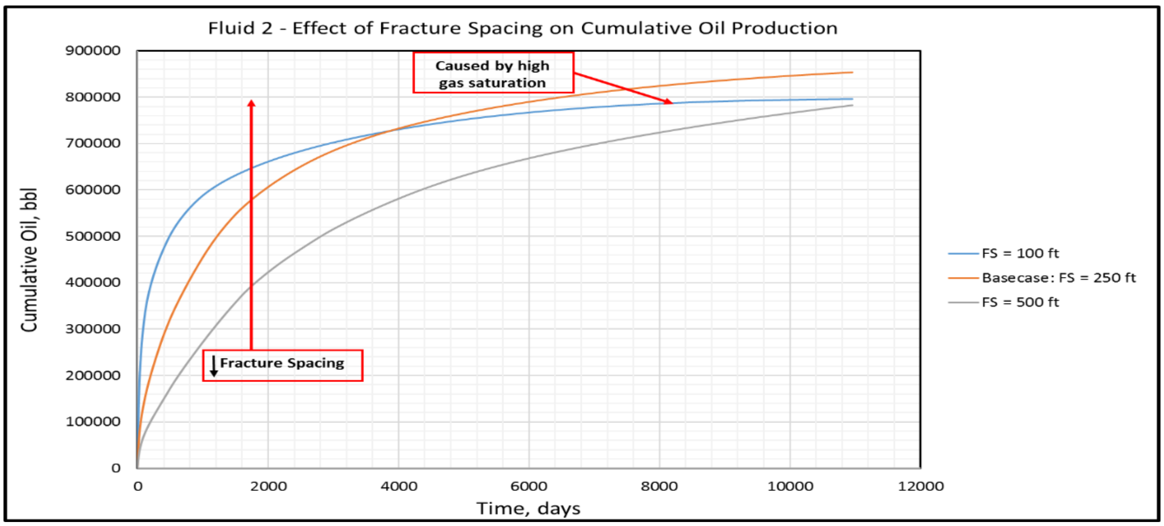

Figure 4-208 Fluid 2 – Effect of Fracture Spacing on Cumulative Oil Production

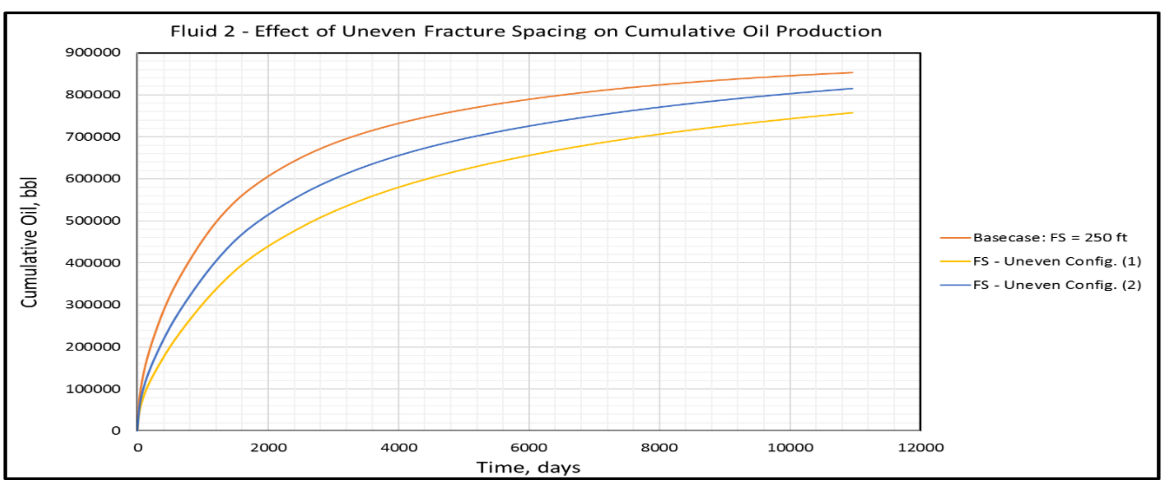

Figure 4-209 Fluid 2 – Effect of Uneven Fracture Spacing on Cumulative Oil Production

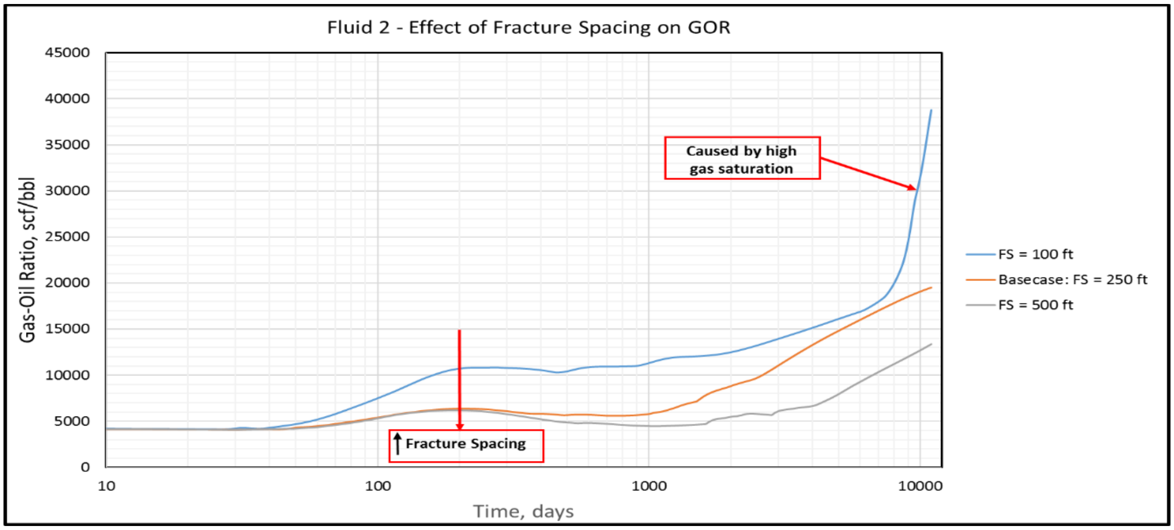

Figure 4-210 Fluid 2 – Effect of Fracture Spacing on GOR

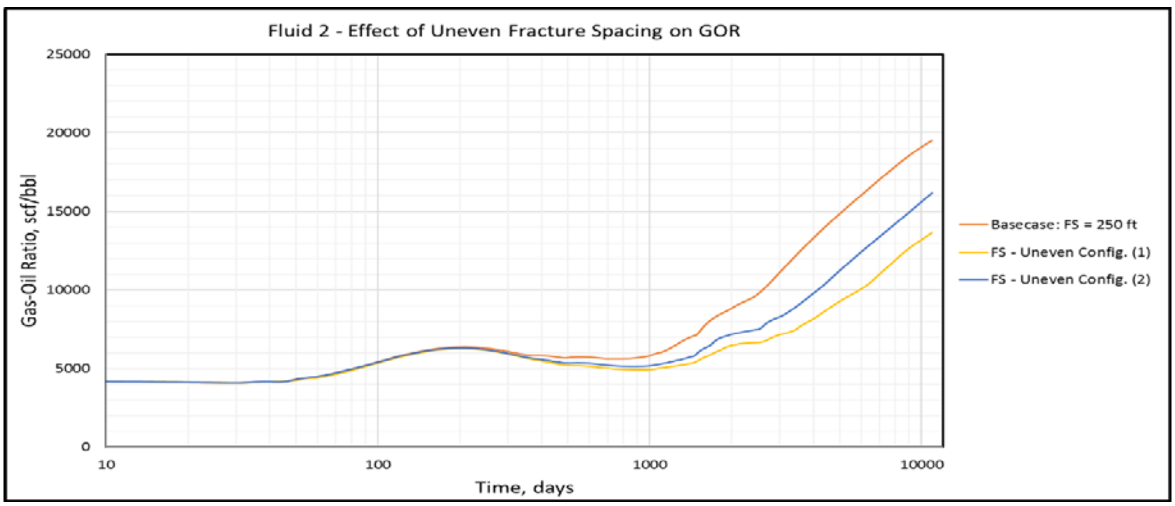

Figure 4-211 Fluid 2 – Effect of Uneven Fracture Spacing on GOR

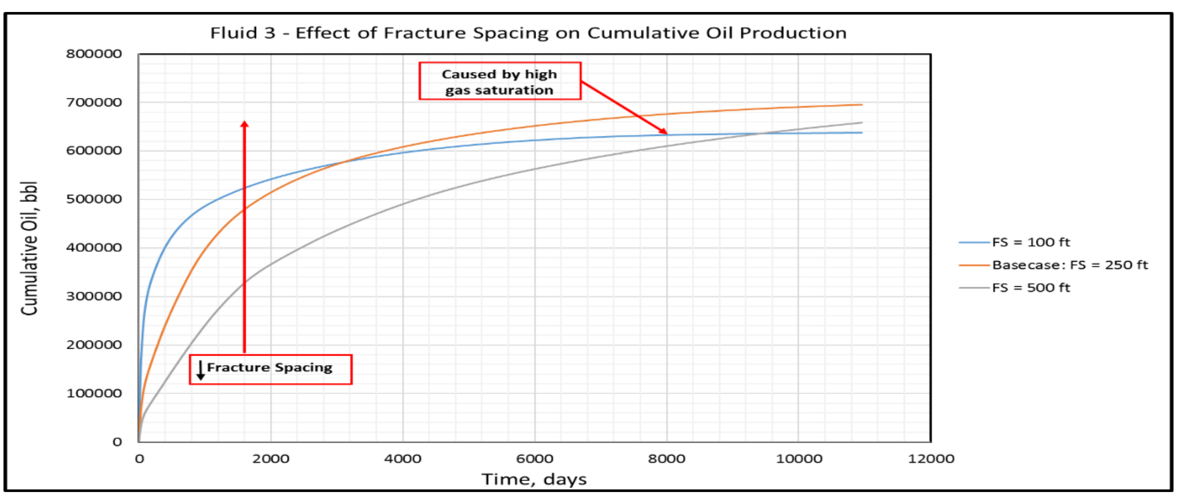

Figure 4-212 Fluid 3 – Effect of Fracture Spacing on Cumulative Oil Production

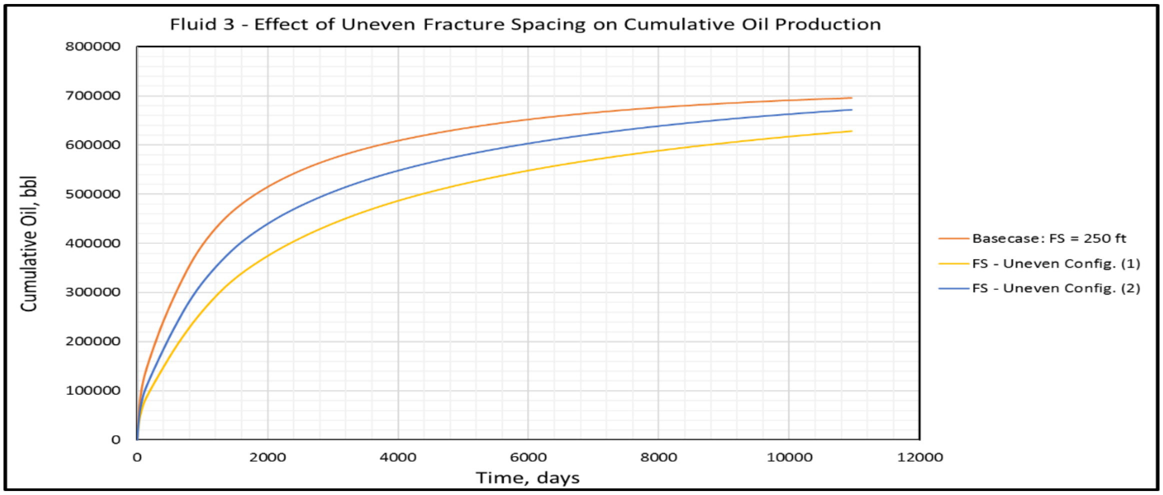

Figure 4-213 Fluid 3 – Effect of Uneven Fracture Spacing on Cumulative Oil Production

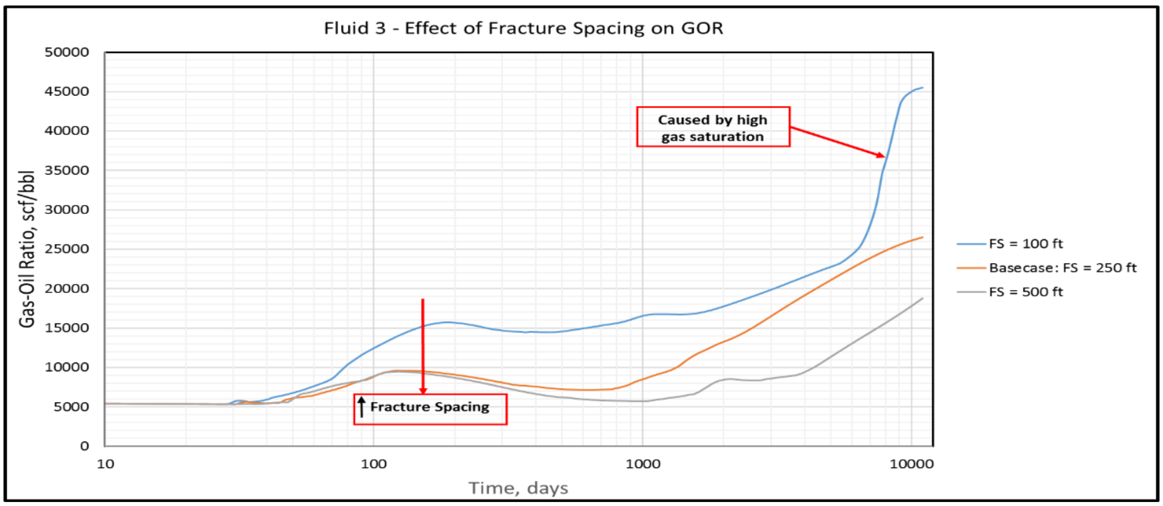

Figure 4-214 Fluid 3 – Effect of Fracture Spacing on GOR

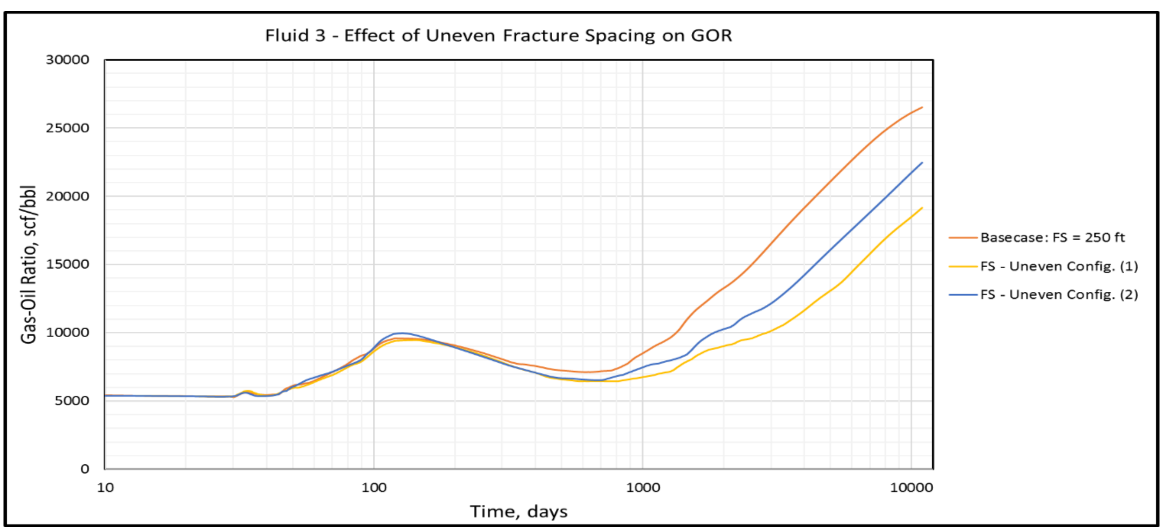

Figure 4-215 Fluid 3 – Effect of Uneven Fracture Spacing on GOR

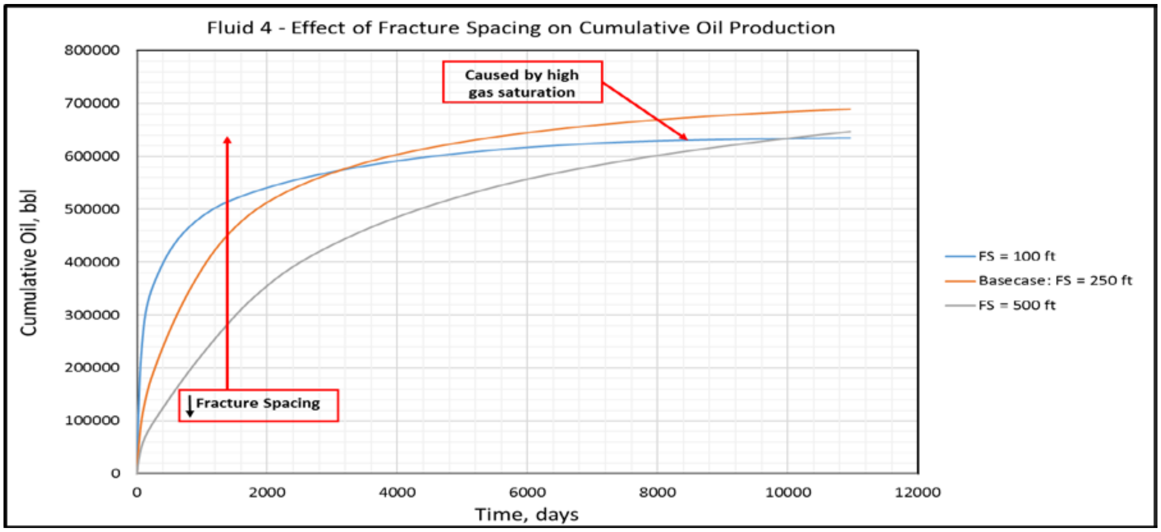

Figure 4-216 Fluid 4 – Effect of Fracture Spacing on Cumulative Oil Production

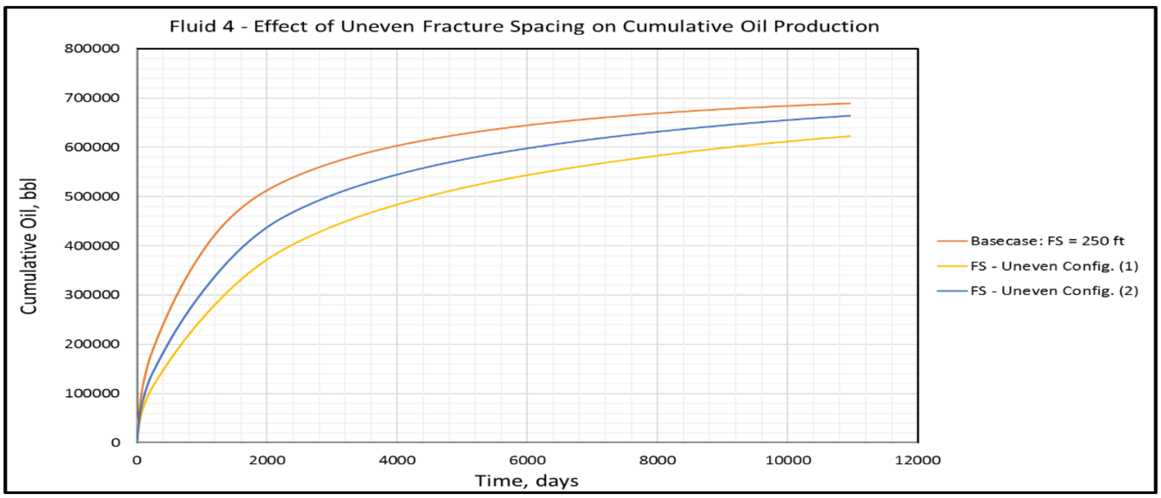

Figure 4-217 Fluid 4 – Effect of Uneven Fracture Spacing on Cumulative Oil Production

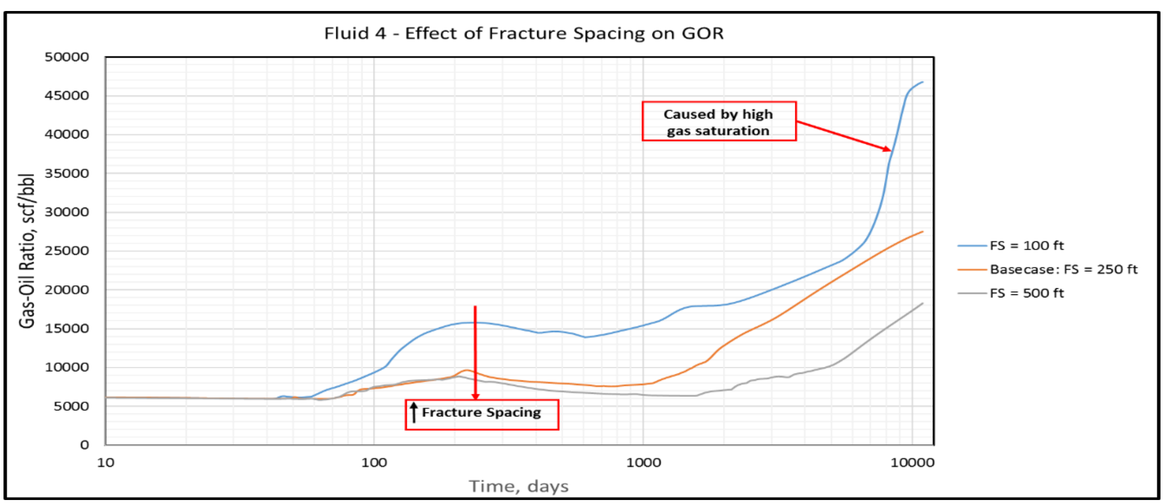

Figure 4-218 Fluid 4 – Effect of Fracture Spacing on GOR

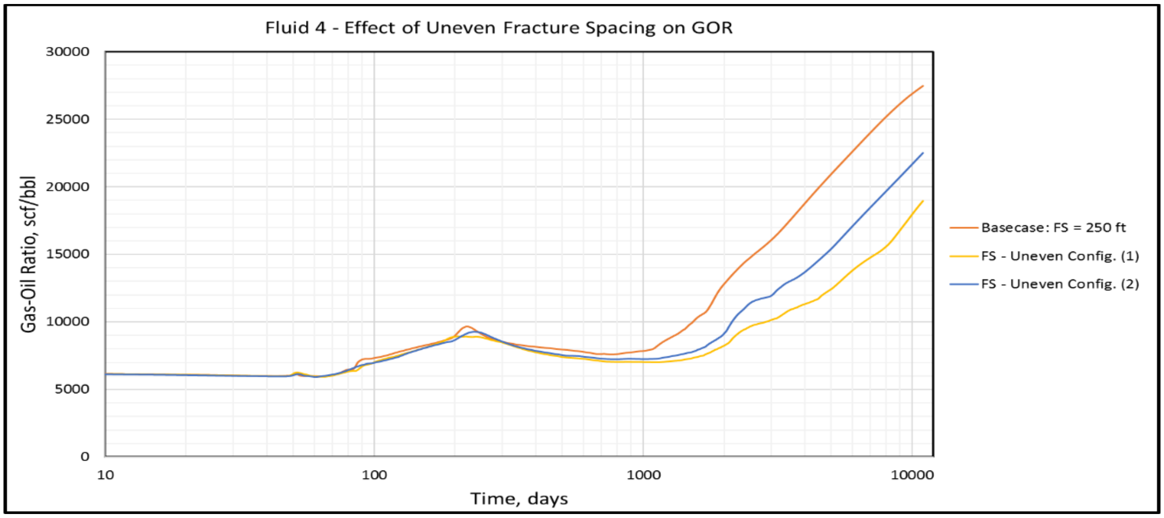

Figure 4-219 Fluid 4 – Effect of Uneven Fracture Spacing on GOR

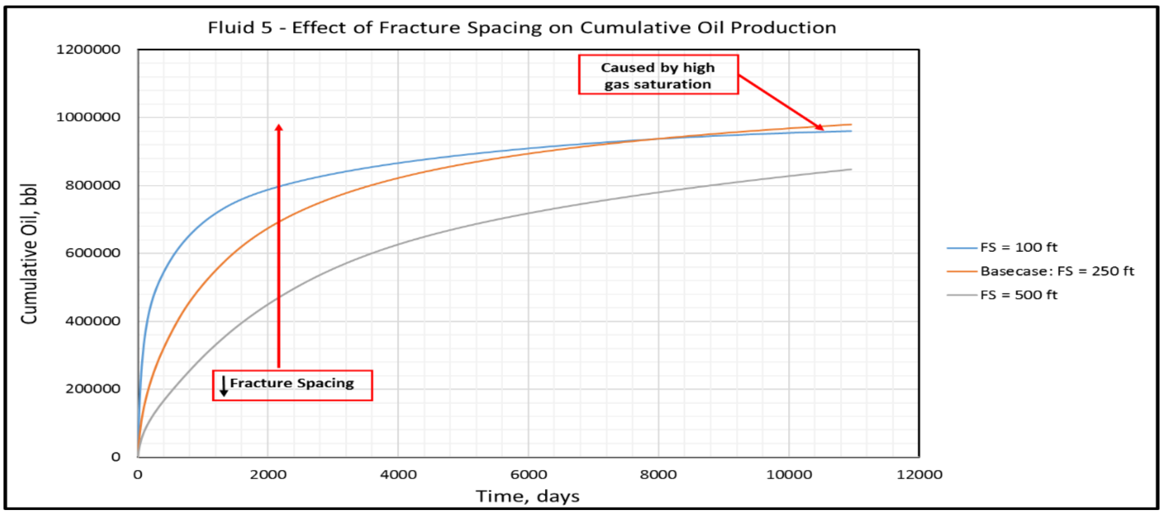

Figure 4-220 Fluid 5 – Effect of Fracture Spacing on Cumulative Oil Production

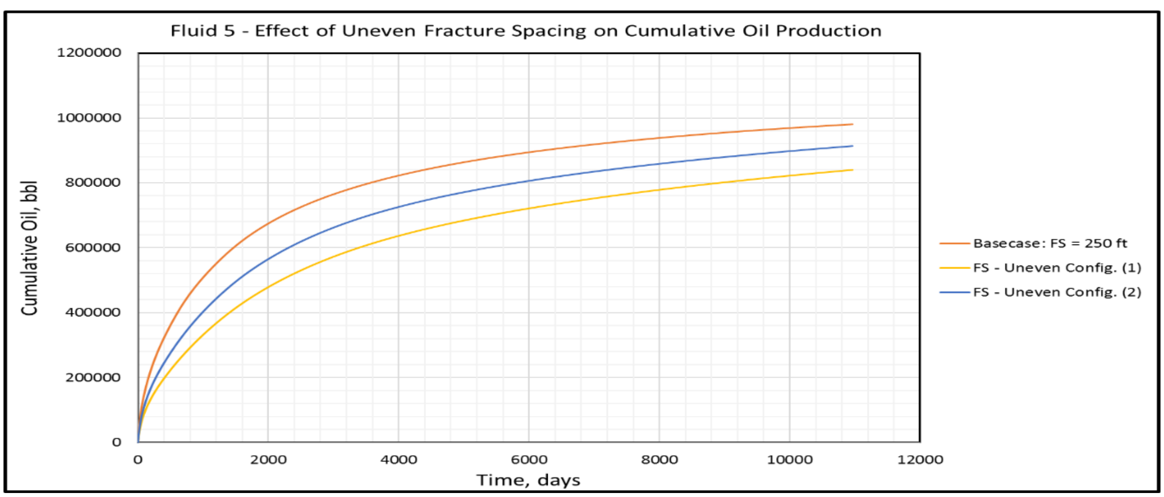

Figure 4-221 Fluid 5 – Effect of Uneven Fracture Spacing on Cumulative Oil Production

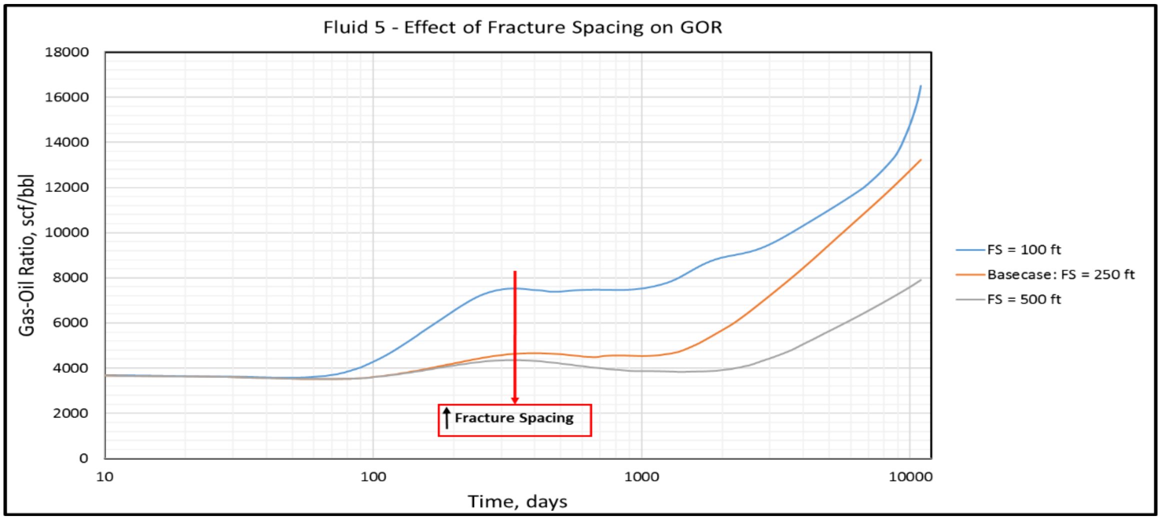

Figure 4-222 Fluid 5 – Effect of Fracture Spacing on GOR

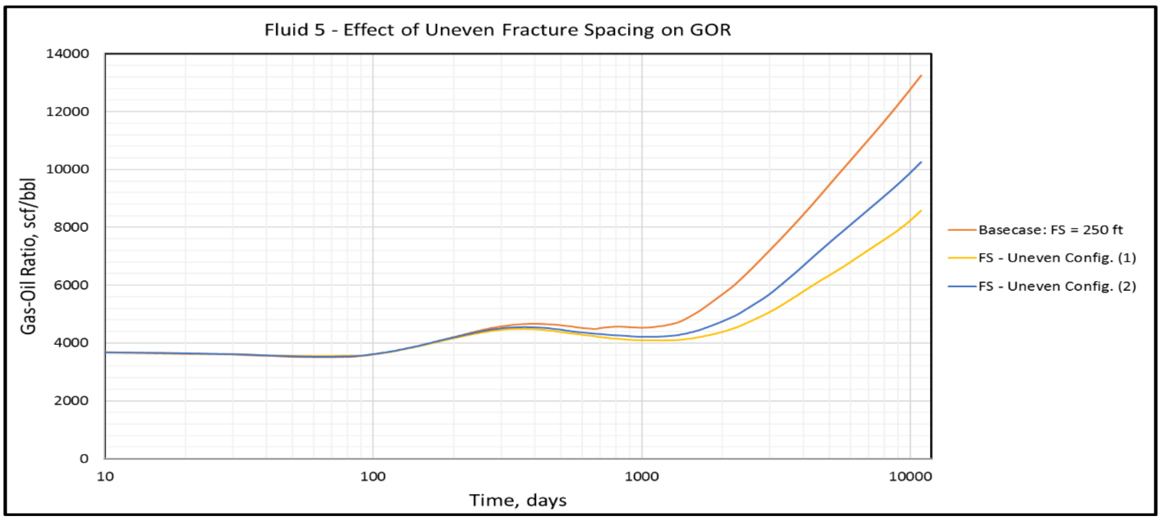

Figure 4-223 Fluid 5 – Effect of Uneven Fracture Spacing on GOR

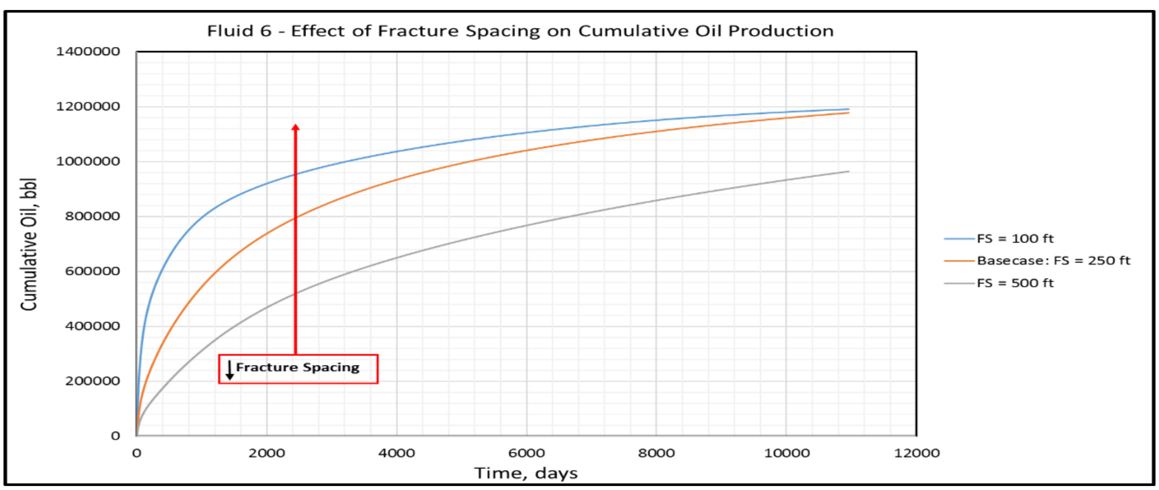

Figure 4-224 Fluid 6 – Effect of Fracture Spacing on Cumulative Oil Production

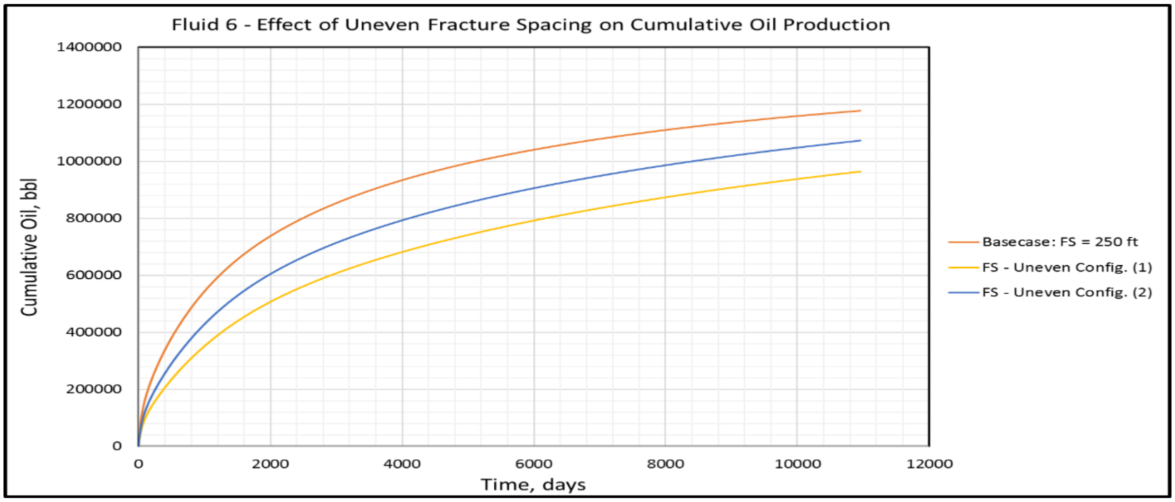

Figure 4-225 Fluid 6 – Effect of Uneven Fracture Spacing on Cumulative Oil Production

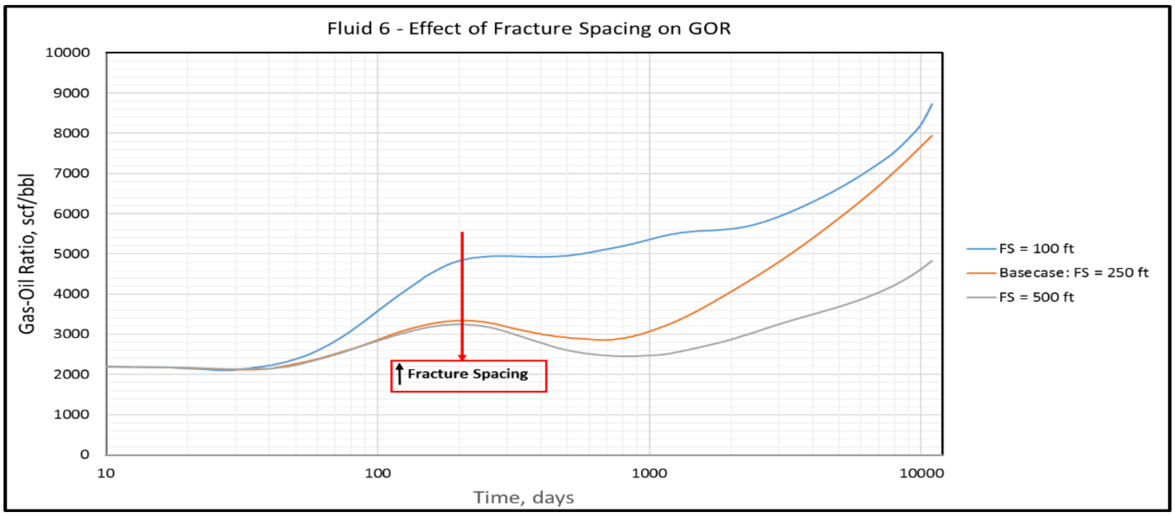

Figure 4-226 Fluid 6 – Effect of Fracture Spacing on GOR

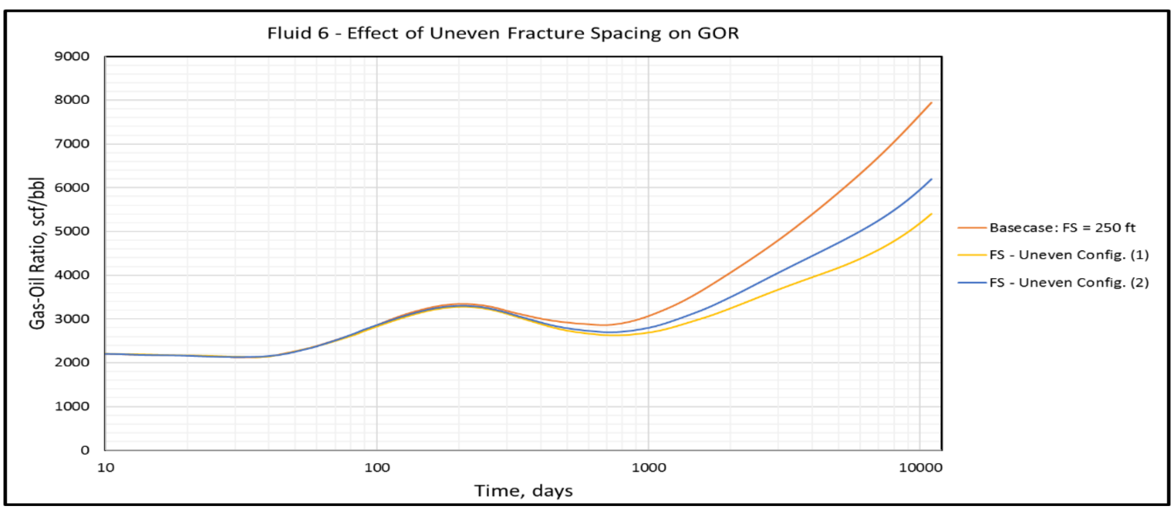

Figure 4-227 Fluid 6 – Effect of Uneven Fracture Spacing on GOR

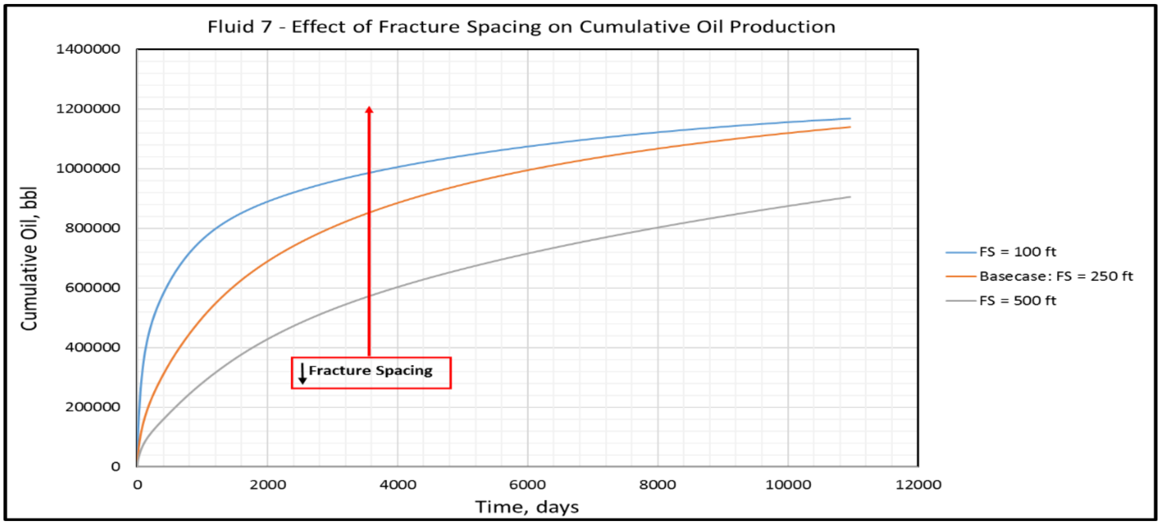

Figure 4-228 Fluid 7 – Effect of Fracture Spacing on Cumulative Oil Production

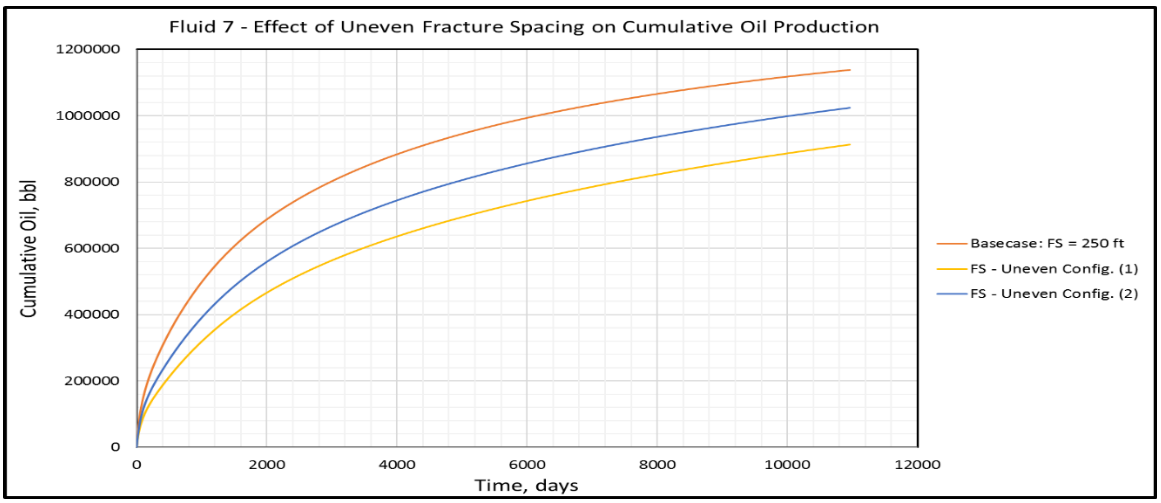

Figure 4-229 Fluid 7 – Effect of Uneven Fracture Spacing on Cumulative Oil Production

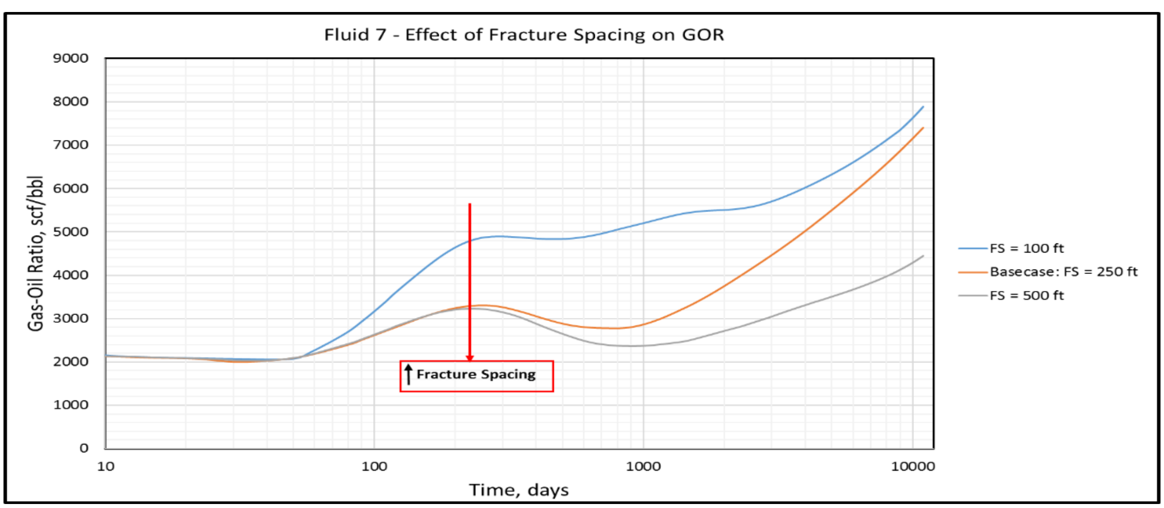

Figure 4-230 Fluid 7 – Effect of Fracture Spacing on GOR

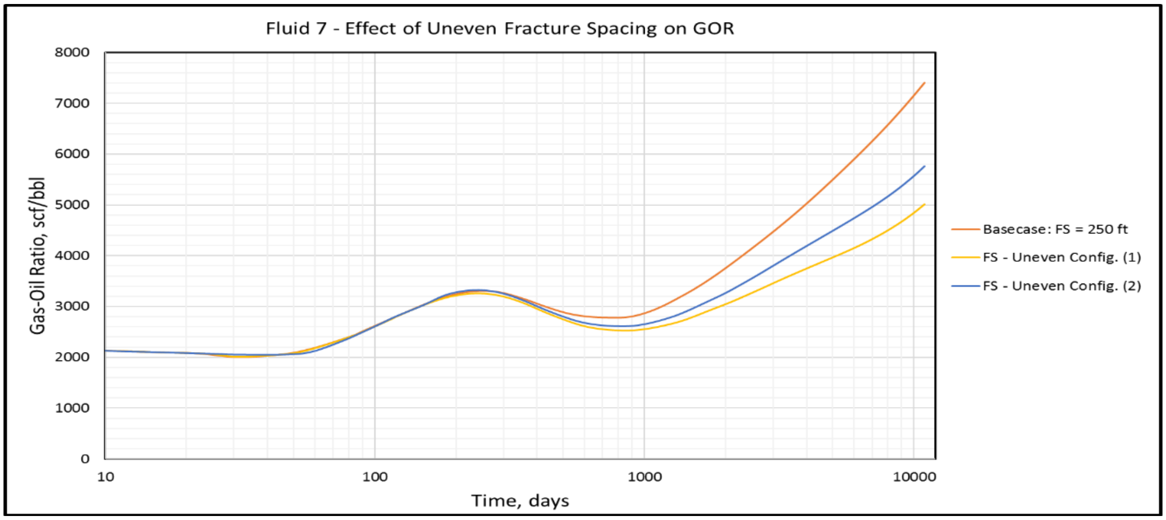

Figure 4-231 Fluid 7 – Effect of Uneven Fracture Spacing on GOR

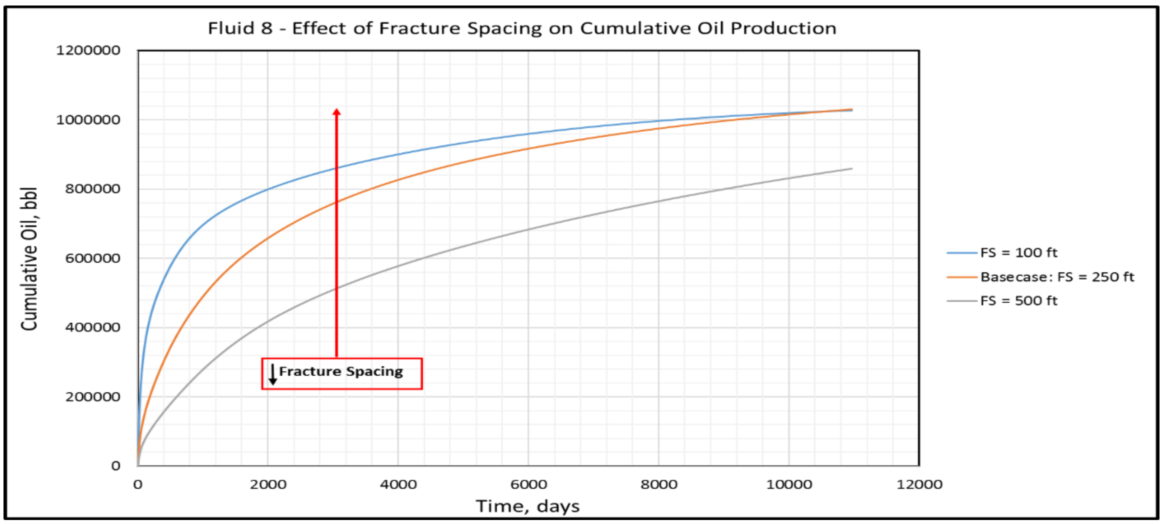

Figure 4-232 Fluid 8 – Effect of Fracture Spacing on Cumulative Oil Production

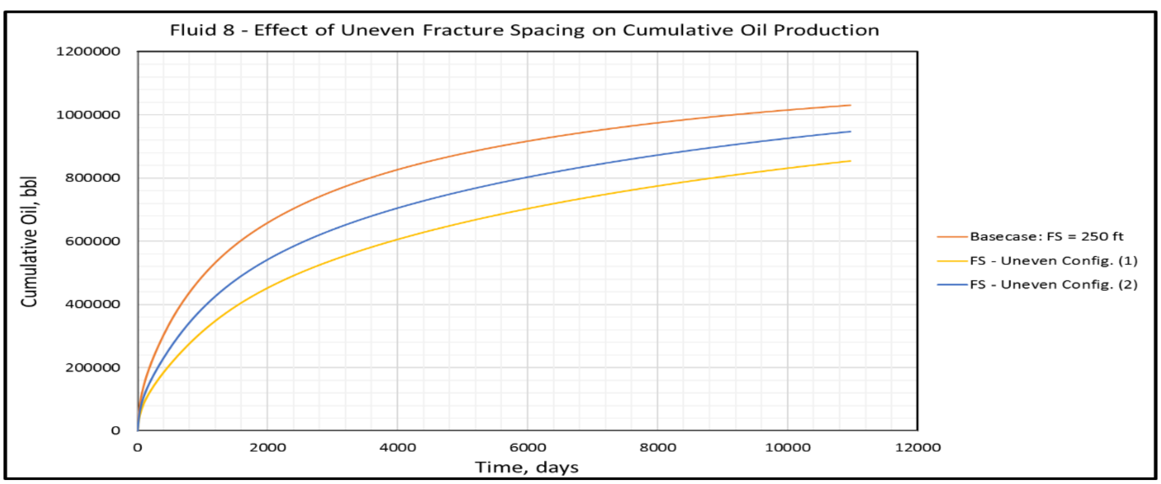

Figure 4-233 Fluid 8 – Effect of Uneven Fracture Spacing on Cumulative Oil Production

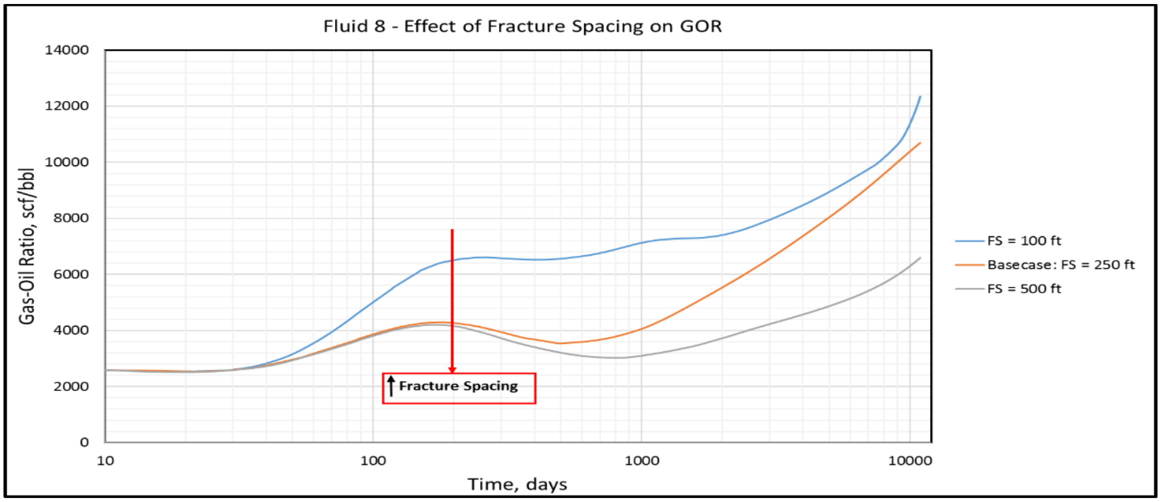

Figure 4-234 Fluid 8 – Effect of Fracture Spacing on GOR

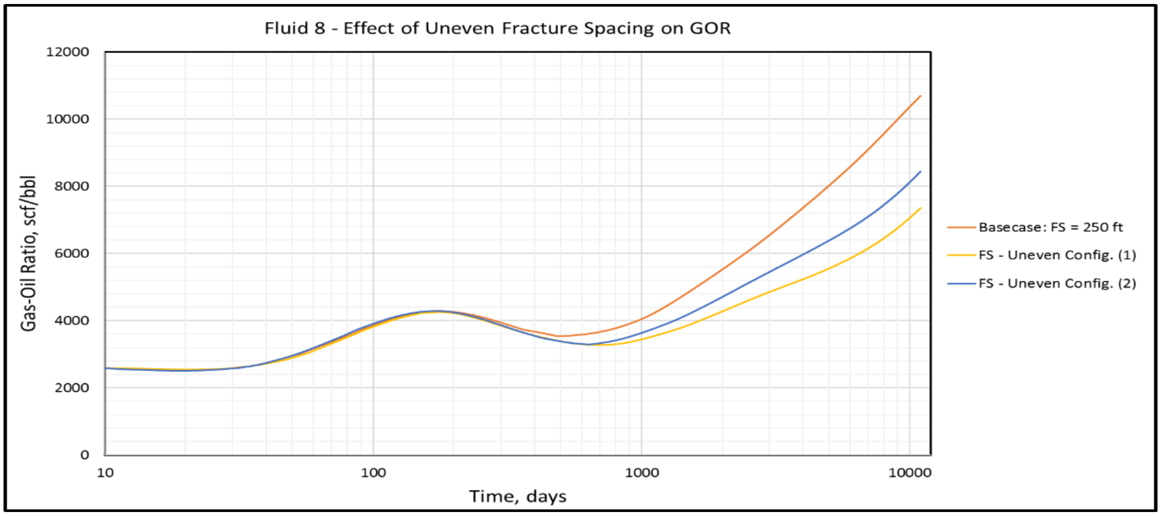

Figure 4-235 Fluid 8 – Effect of Uneven Fracture Spacing on GOR

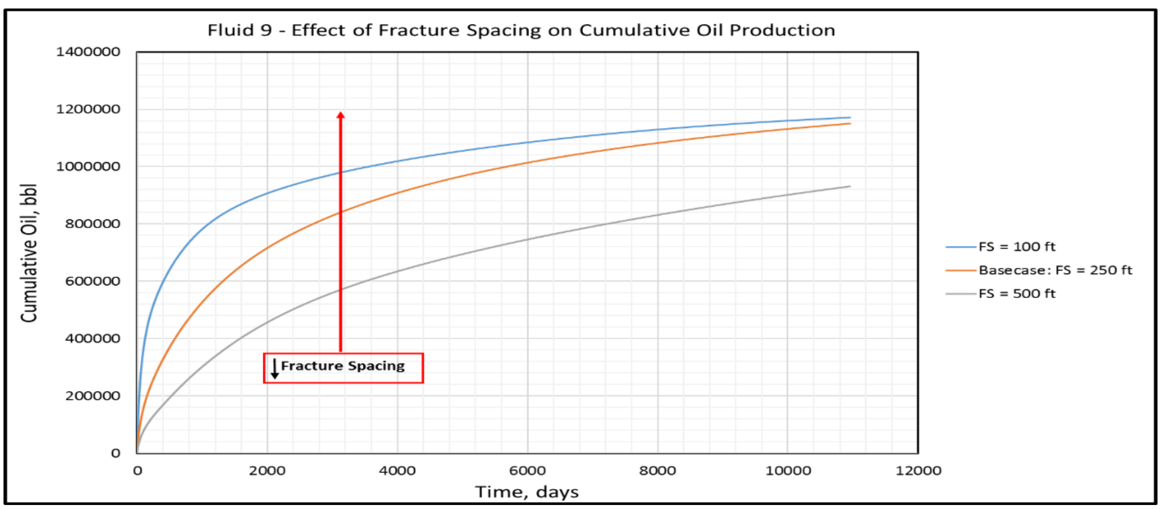

Figure 4-236 Fluid 8 – Effect of Fracture Spacing on Cumulative Oil Production

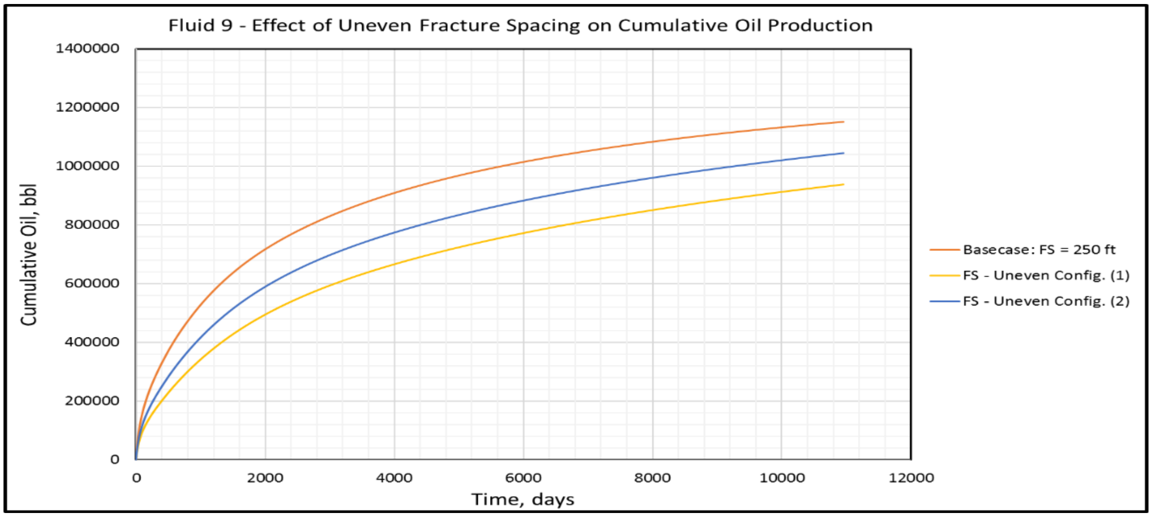

Figure 4-237 Fluid 9 – Effect of Uneven Fracture Spacing on Cumulative Oil Production

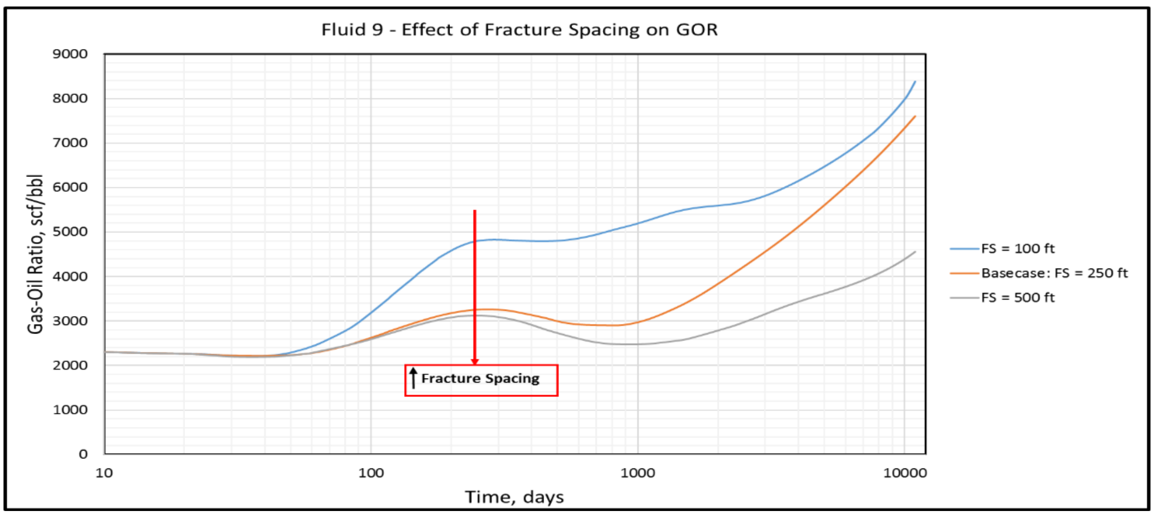

Figure 4-238 Fluid 9 – Effect of Fracture Spacing on GOR

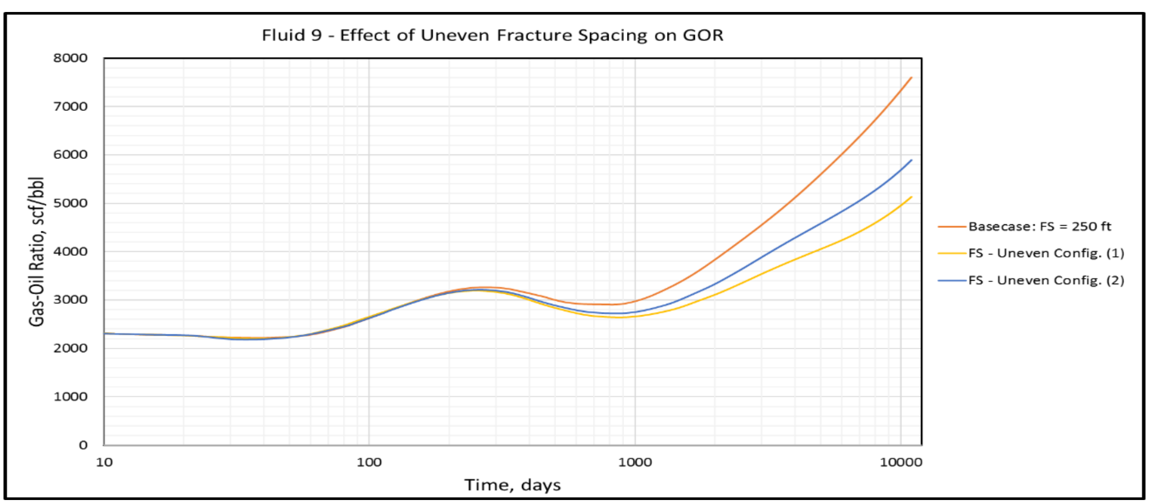

Figure 4-239 Fluid 9 – Effect of Uneven Fracture Spacing on GOR

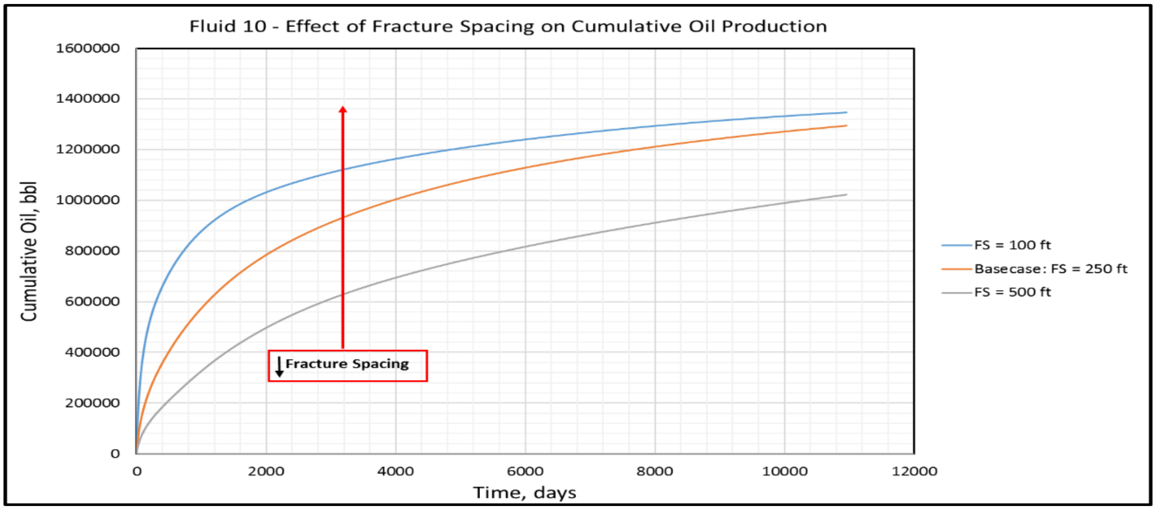

Figure 4-240 Fluid 10 – Effect of Fracture Spacing on Cumulative Oil Production

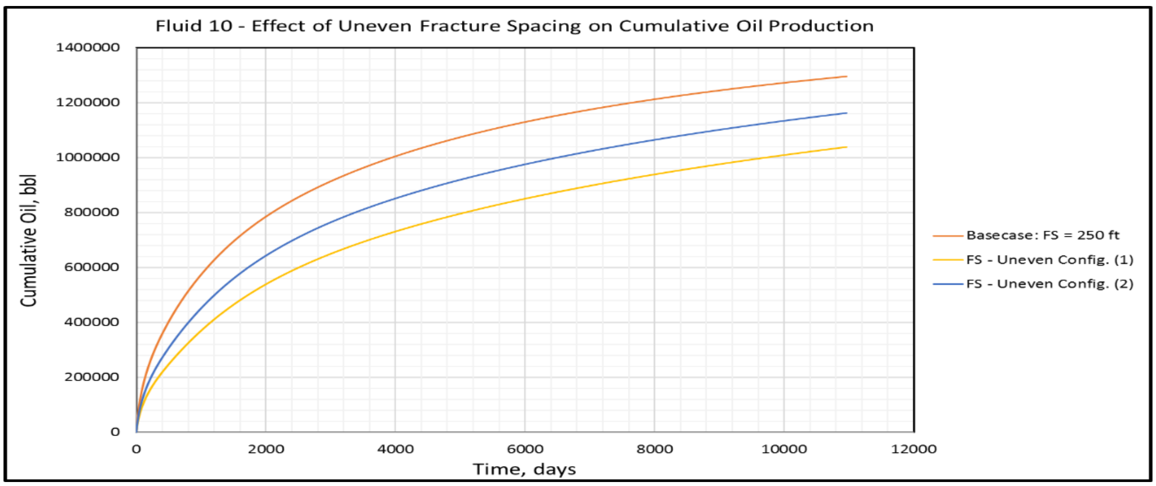

Figure 4-241 Fluid 10 – Effect of Uneven Fracture Spacing on Cumulative Oil Production

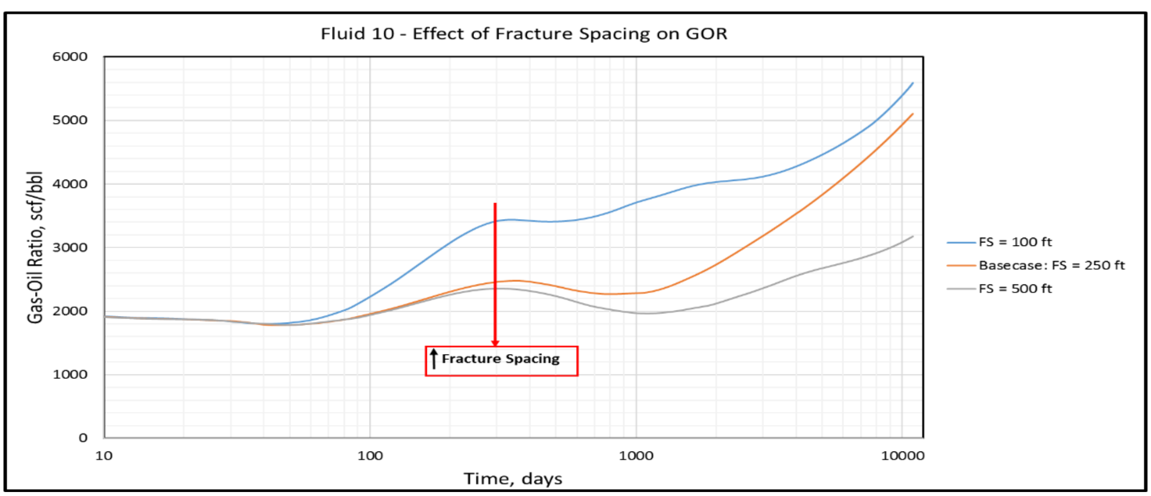

Figure 4-242 Fluid 10 – Effect of Fracture Spacing on GOR

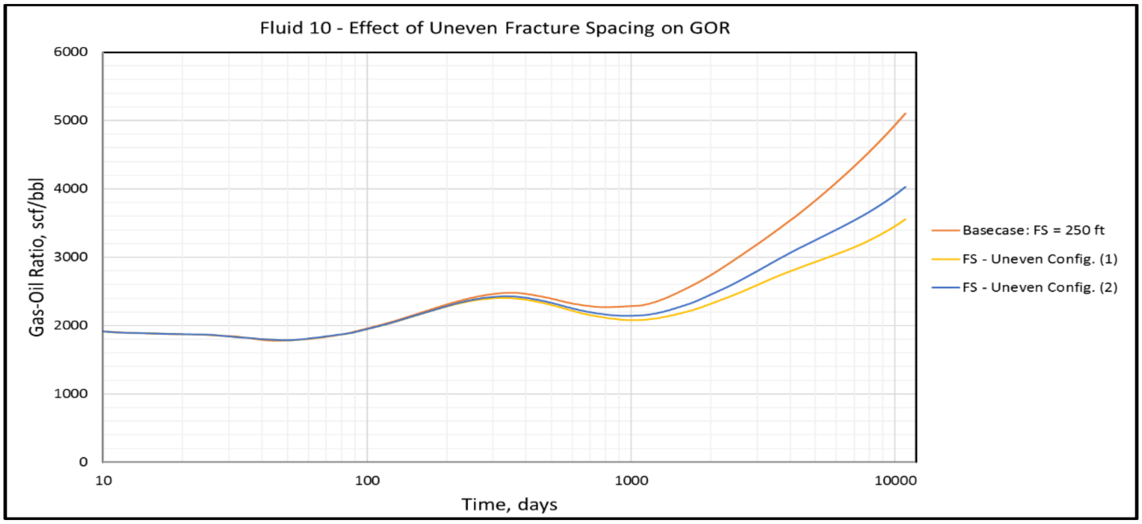

Figure 4-243 Fluid 10 – Effect of Uneven Fracture Spacing on GOR

4.9. Rock Compressibility

Rock compressibility is the isothermal change in rock volume per unit volume per unit change in pressure. For these analyses, we considered rock compressibility with the following values – $2*10^{-6}$ psi^{-1}, $6*10^{-6}$ psi^{-1}, $8*10^{-6}$ psi^{-1} and $4*10^{-6}$ psi^{-1} (basecase). The depletion of reservoir pressure during production causes the volume of reservoir rocks to expand. Therefore, the higher the rock compressibility, the larger the cumulative oil production and vice versa. At much higher rock compressibility values, there is a possibility that high gas saturation may impede oil production later on during production, especially for highly volatile oils.

The effect of rock compressibility on producing GOR (for the values we considered) is not really significant. The trends are generally similar and the higher the rock compressibility, the lower the producing GOR with time. It is likely that the impact of high gas saturation may alter the pattern of producing GOR at much higher rock compressibility values. Figures 4-244 to 4-263 show the effects of rock compressibility on producing GOR (semi-log plots) and cumulative oil production.

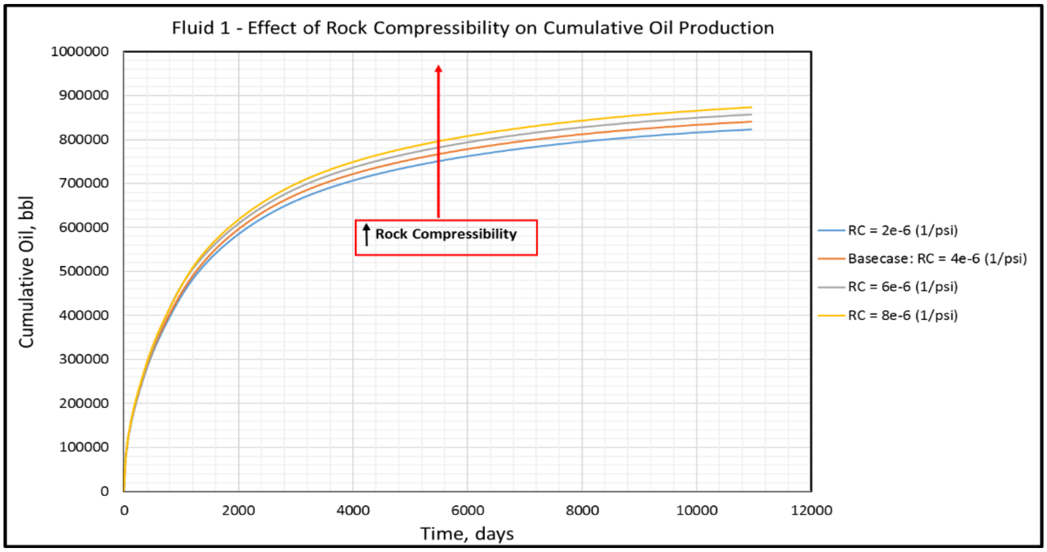

Figure 4-244 Fluid 1 – Effect of Rock Compressibility on Cumulative Oil Production

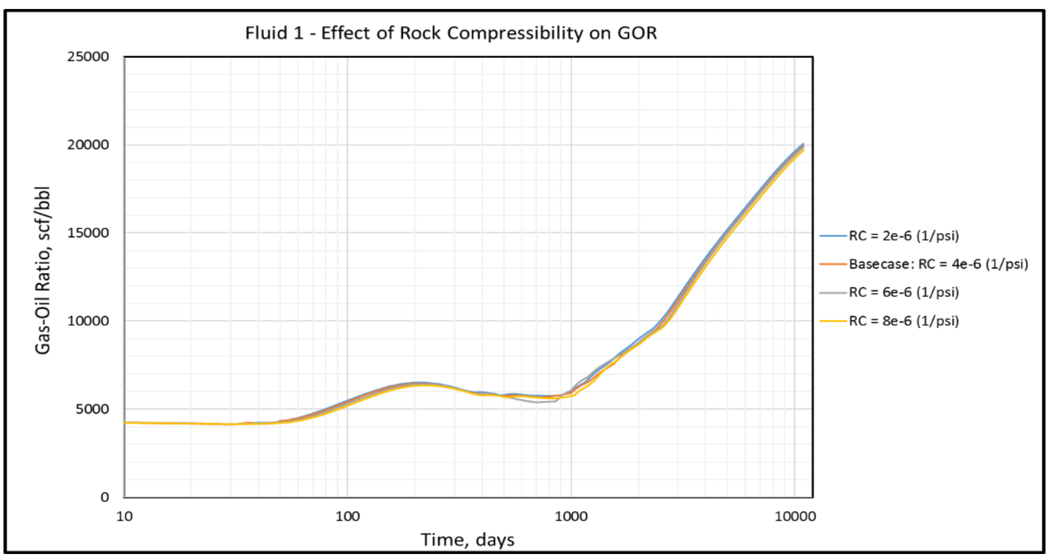

Figure 4-245 Fluid 1 – Effect of Rock Compressibility on GOR

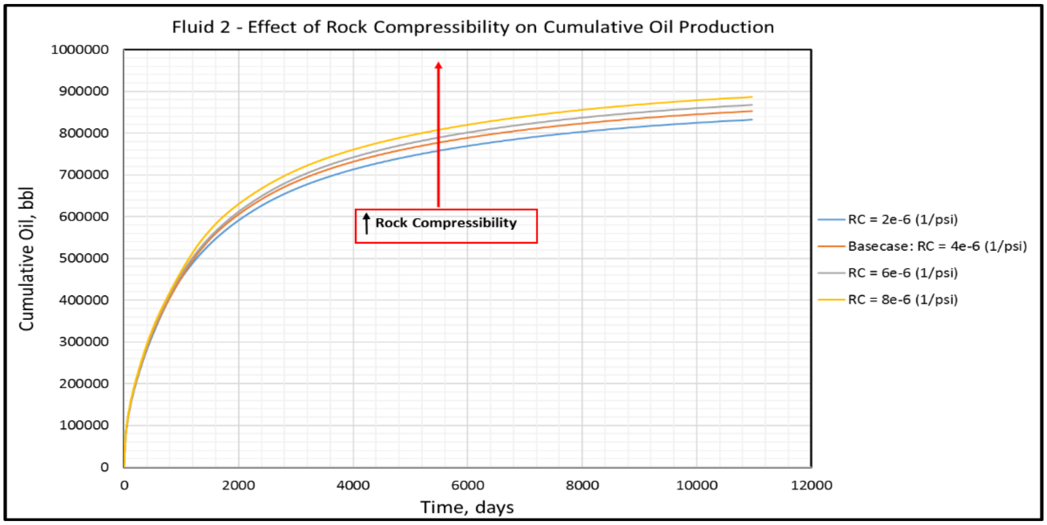

Figure 4-246 Fluid 2 – Effect of Rock Compressibility on Cumulative Oil Production

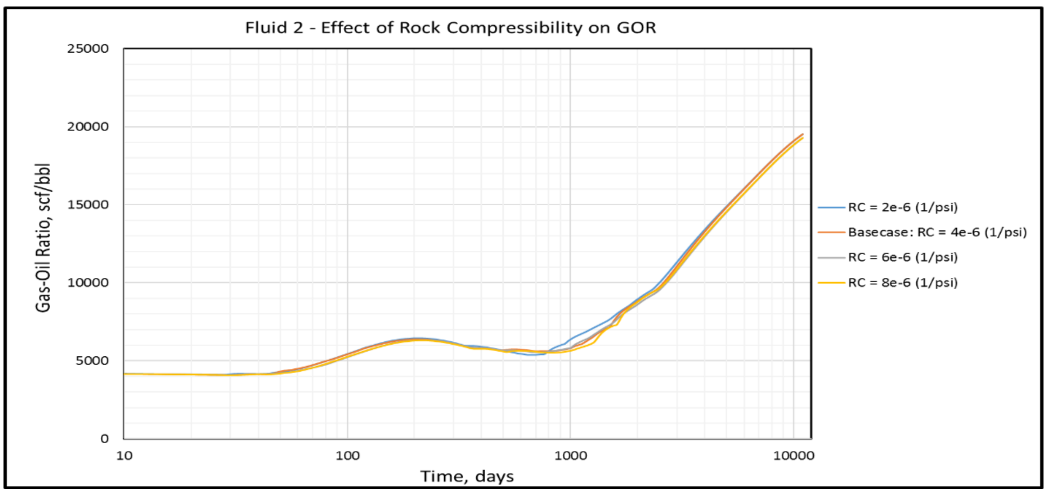

Figure 4-247 Fluid 2 – Effect of Rock Compressibility on GOR

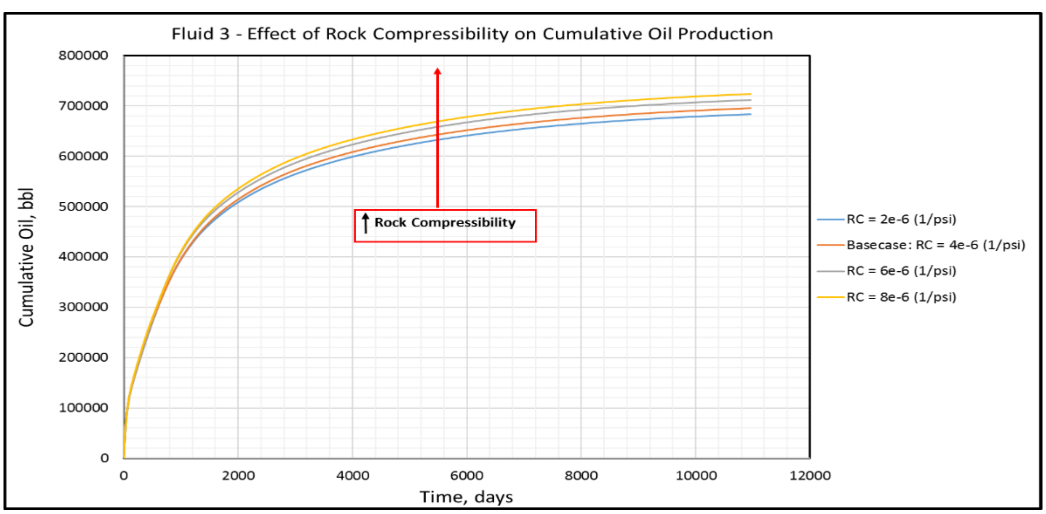

Figure 4-248 Fluid 3 – Effect of Rock Compressibility on Cumulative Oil Production

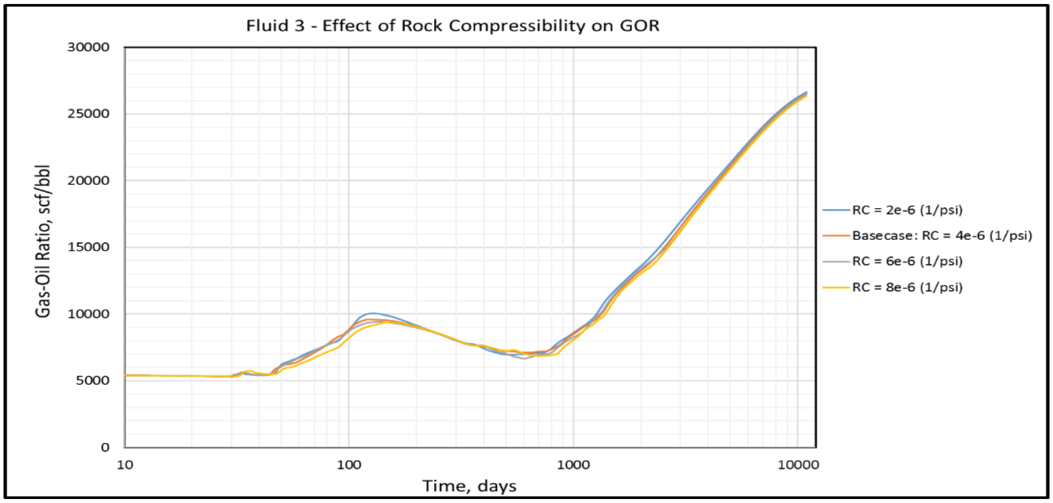

Figure 4-249 Fluid 3 – Effect of Rock Compressibility on GOR

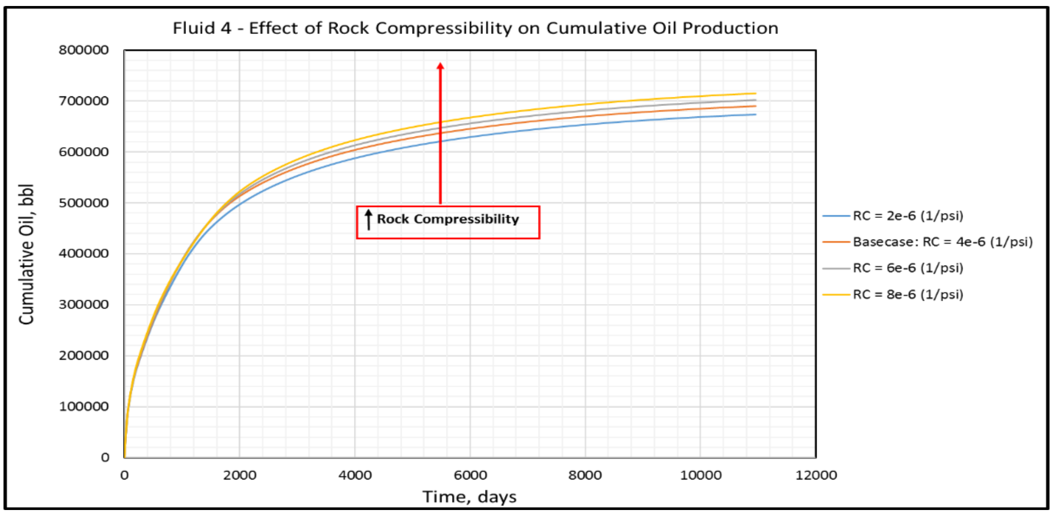

Figure 4-250 Fluid 4 – Effect of Rock Compressibility on Cumulative Oil Production

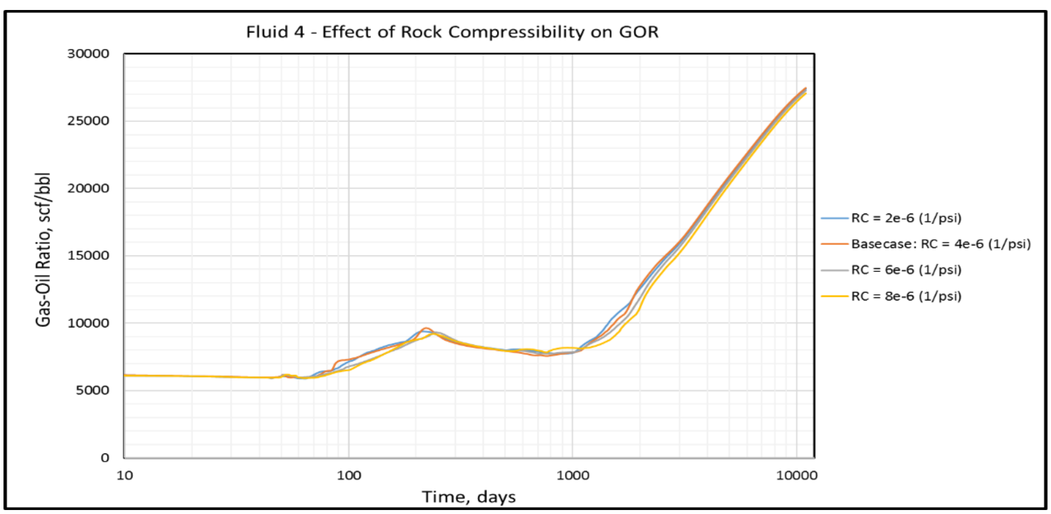

Figure 4-251 Fluid 4 – Effect of Rock Compressibility on GOR

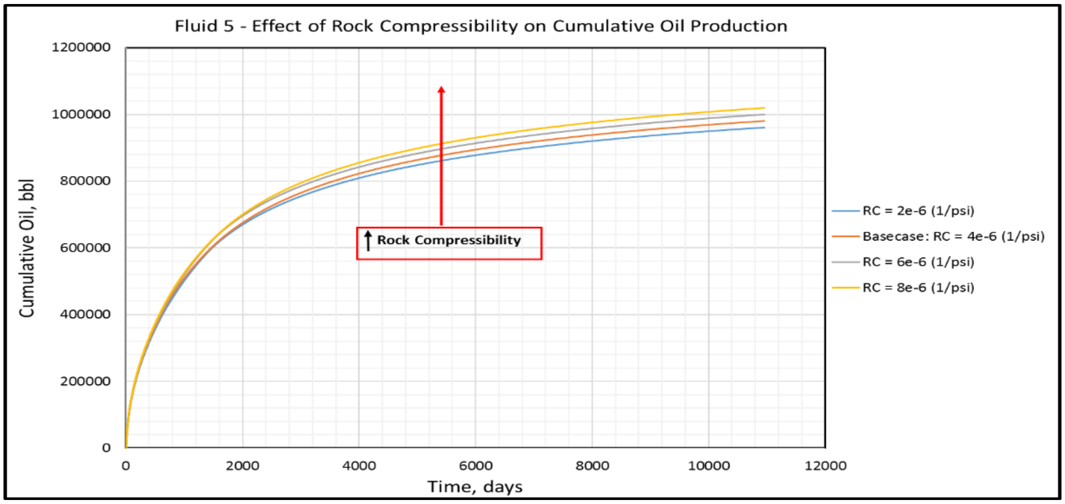

Figure 4-252 Fluid 5 – Effect of Rock Compressibility on Cumulative Oil Production

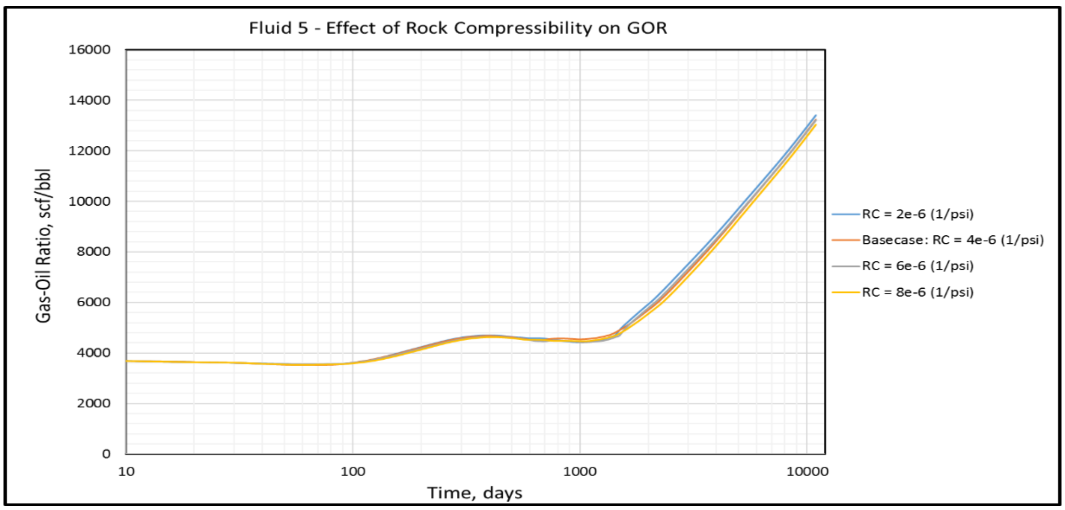

Figure 4-253 Fluid 5 – Effect of Rock Compressibility on GOR

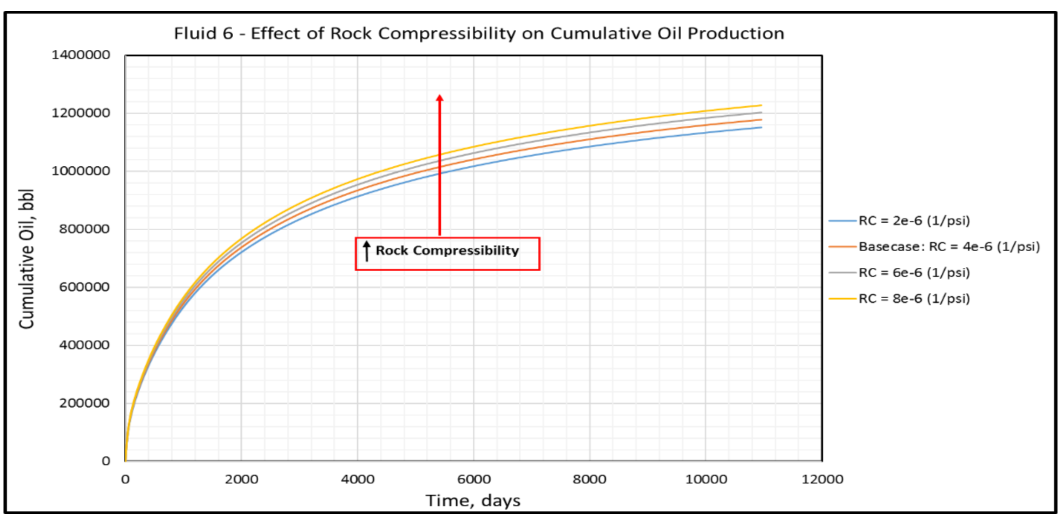

Figure 4-254 Fluid 6 – Effect of Rock Compressibility on Cumulative Oil Production

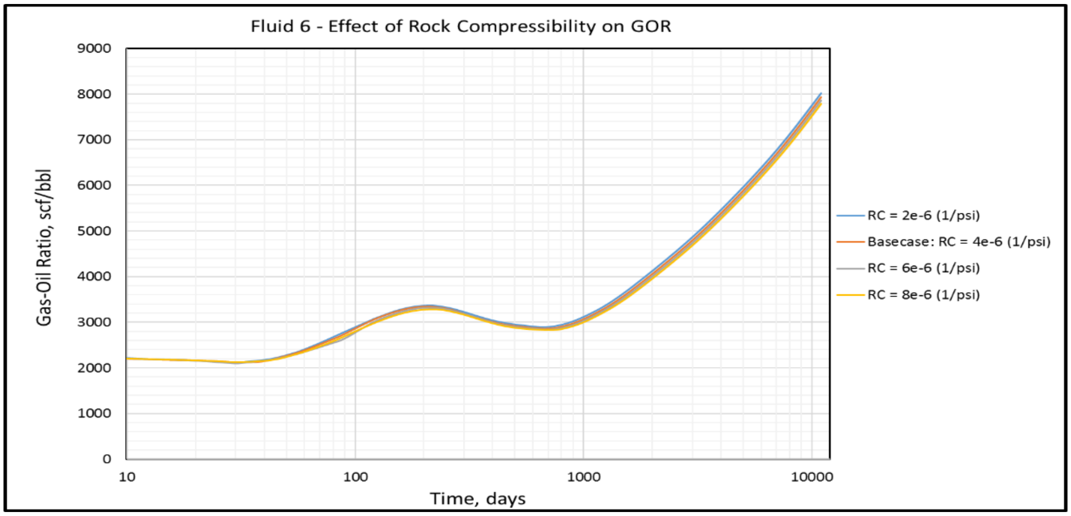

Figure 4-255 Fluid 6 – Effect of Rock Compressibility on GOR

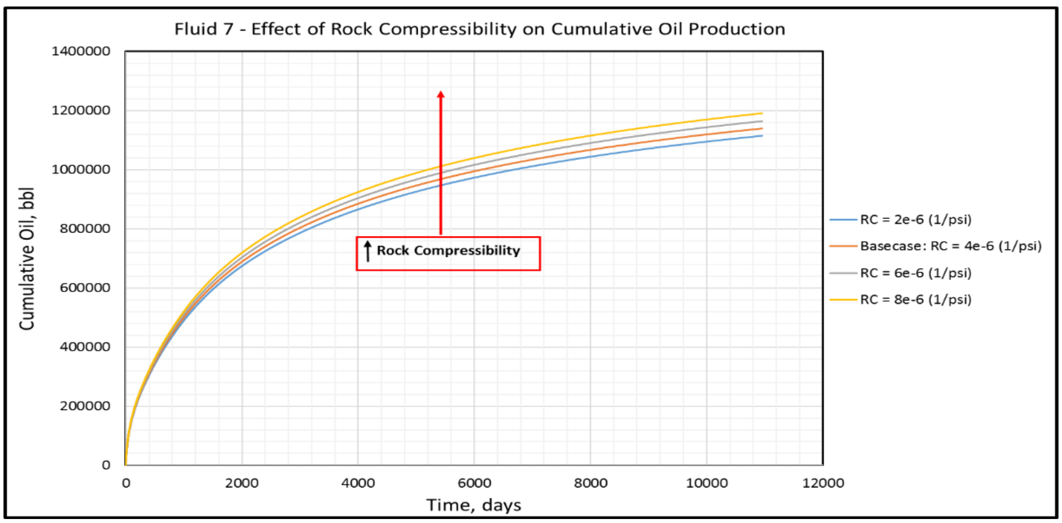

Figure 4-256 Fluid 7 – Effect of Rock Compressibility on Cumulative Oil Production

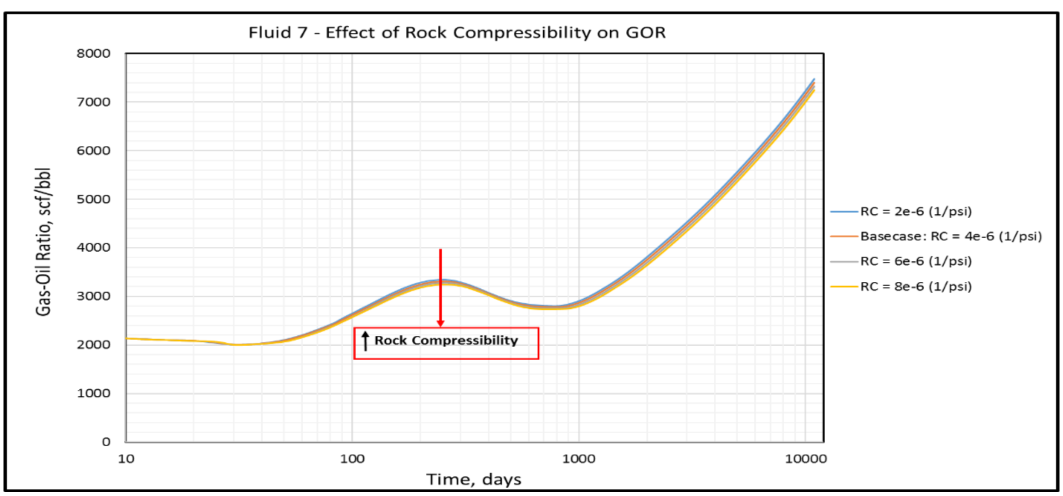

Figure 4-257 Fluid 7 – Effect of Rock Compressibility on GOR

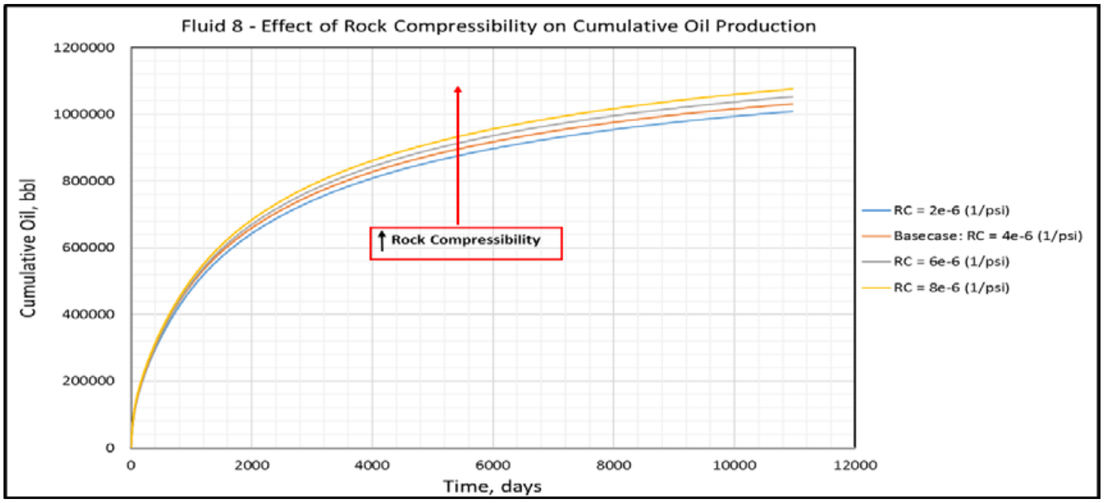

Figure 4-258 Fluid 8 – Effect of Rock Compressibility on Cumulative Oil Production

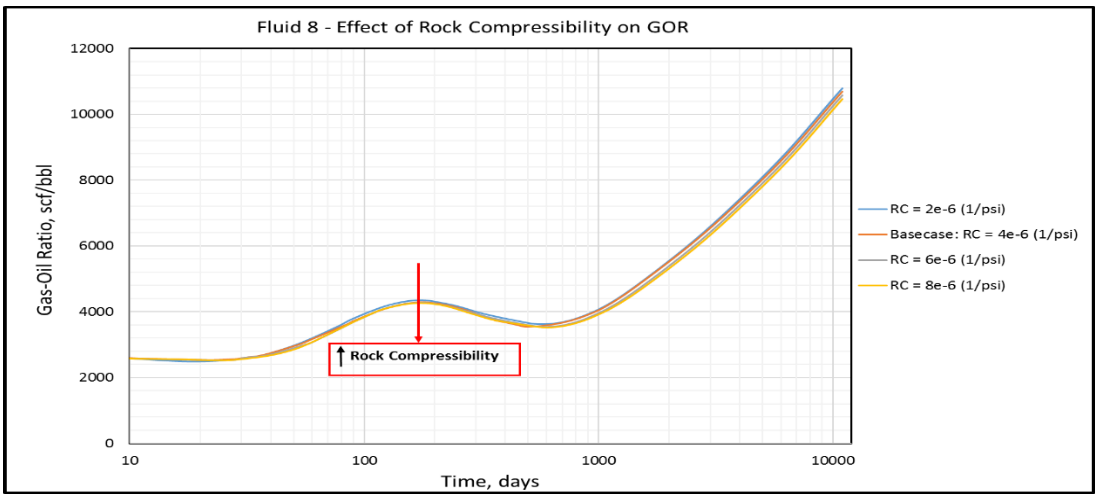

Figure 4-259 Fluid 8 – Effect of Rock Compressibility on GOR

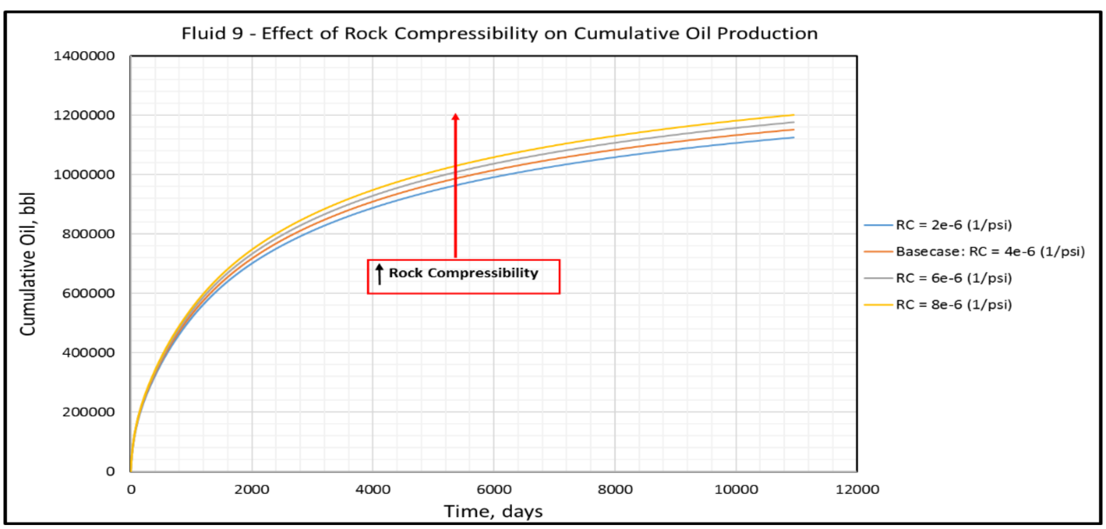

Figure 4-260 Fluid 9 – Effect of Rock Compressibility on Cumulative Oil Production

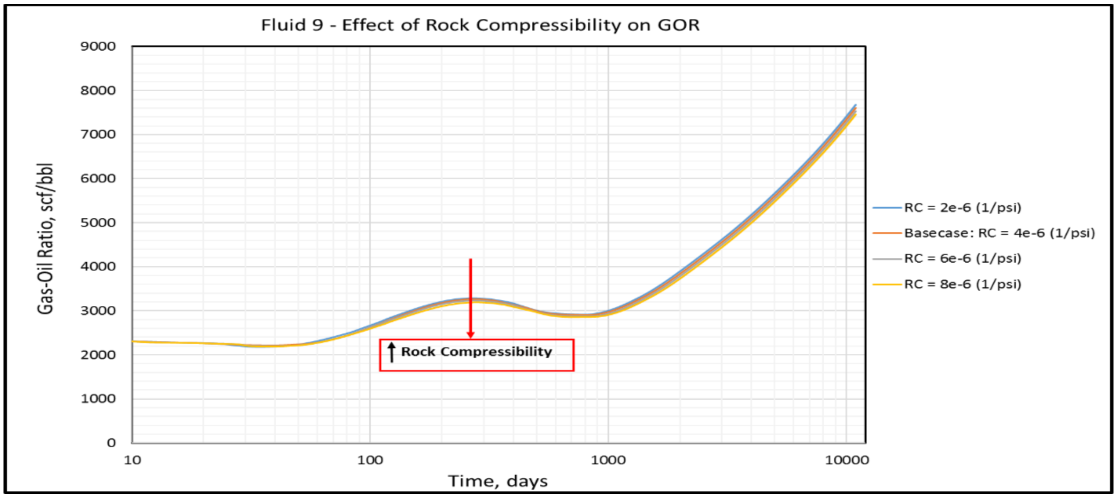

Figure 4-261 Fluid 9 – Effect of Rock Compressibility on GOR

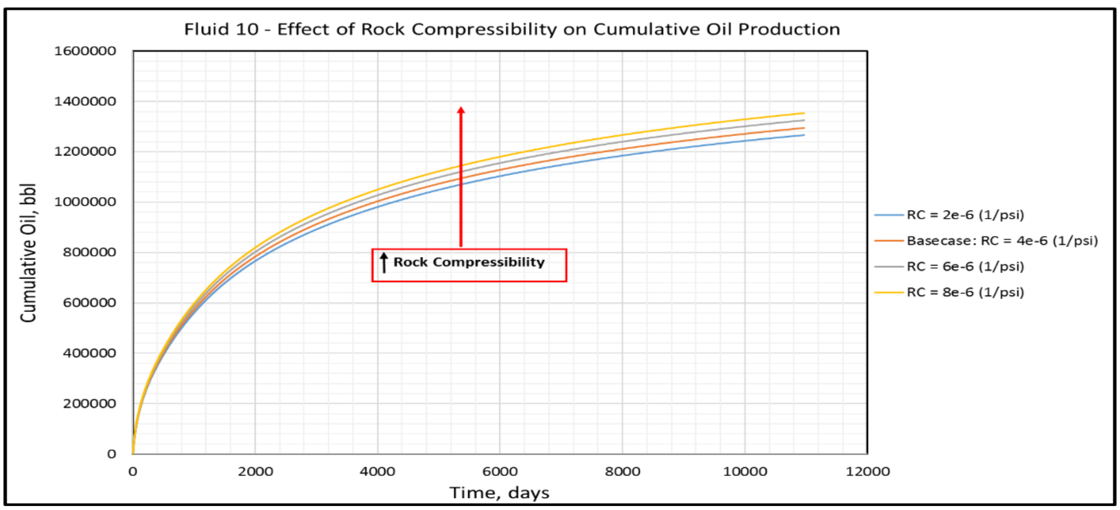

Figure 4-262 Fluid 10 – Effect of Rock Compressibility on Cumulative Oil Production

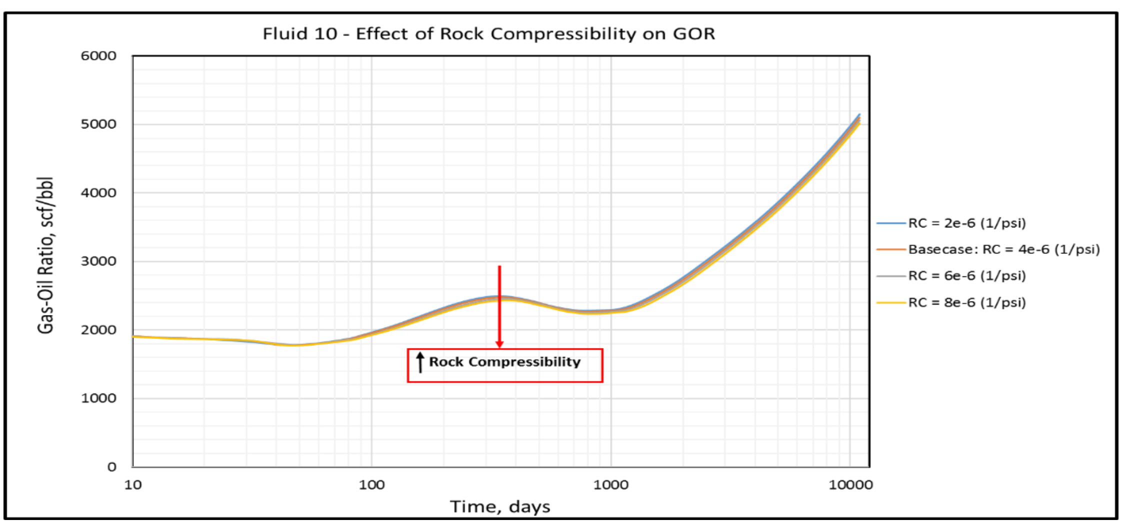

Figure 4-263 Fluid 10 – Effect of Rock Compressibility on GOR

4.10. Compaction

Compaction is the consolidation of sediments that results in the cementing or packing together of grains. Compaction may lead to subsidence i.e. sediment loading and removal of fluids from the reservoir. It can have a tremendous impact on well performance. For our basecase, we did not consider compaction. However, here, we investigated the effects of compaction on shale volatile oil well production performance. We studied the cases where weak compaction (constant rock compressibility of $4*10^{-6}$ psi^{-1}), mild compaction (constant rock compressibility of $20*10^{-6}$ psi^{-1}) and strong compaction (with the use of pressure-dependent compaction table shown in Table 4-2) were included in our reservoir model. All the results were compared together with the basecase (no compaction) results.

Table 4-2 Pressure-Dependent Compaction Table

Reservoir Pressure, psi	Porosity Multiplier	Horizontal Permeability Multiplier	Vertical Permeability Multiplier
1,000	0.2	0.2	0.2
1,500	0.2	0.2	0.2
2,000	0.2	0.2	0.2
2,500	0.2	0.2	0.2
3,000	0.4	0.4	0.4
3,500	0.6	0.6	0.6
4,000	0.8	0.8	0.8
4,500	0.9	0.9	0.9
5,000	1.0	1.0	1.0

As reservoir pressure depletion occurs during production, compaction increases the pressure on the rocks (net confining pressure) due to the weight of the overlying sediments (overburden) and the pore fluid pressure decreases. This increase in net confining pressure can lead to collapse of pore spaces and as a result, efficient expulsion of hydrocarbons can take place. Though compaction leads to reduction of porosity and permeability, strong compaction can enhance oil recovery significantly. The stronger the compaction, the larger the cumulative oil production. Weak compaction may lead to slight reduction in cumulative oil production as in our cases (slightly smaller oil production than the basecases). This is because the slight reduction in porosity and permeability caused by weak compaction overrides the major compaction effect already discussed earlier. Mild compaction leads to more oil production than the basecases and strong compaction results in the largest cumulative oil production. A similar result was obtained by Khoshghadam *et al.* (2015) in their study of the impact of confined pore spaces on liquid rich shale reservoir performance.

Weak compaction has little or no effect on producing GOR with time. For most cases, it is approximately identical to our basecases (no compaction). Mild compaction results in the reduction of producing GOR with time as more oil is produced in this case. For the cases with strong compaction, producing GOR remains approximately constant throughout the production period. This is because strong compaction keeps the average reservoir pressure so high that it never depletes beyond the saturation pressure. Also, large quantities of oil were produced due to strong compaction. Figures 4-264 to 4-293 portray the impacts of compaction on cumulative oil production, producing GOR (semi-log plots) and average reservoir pressure.

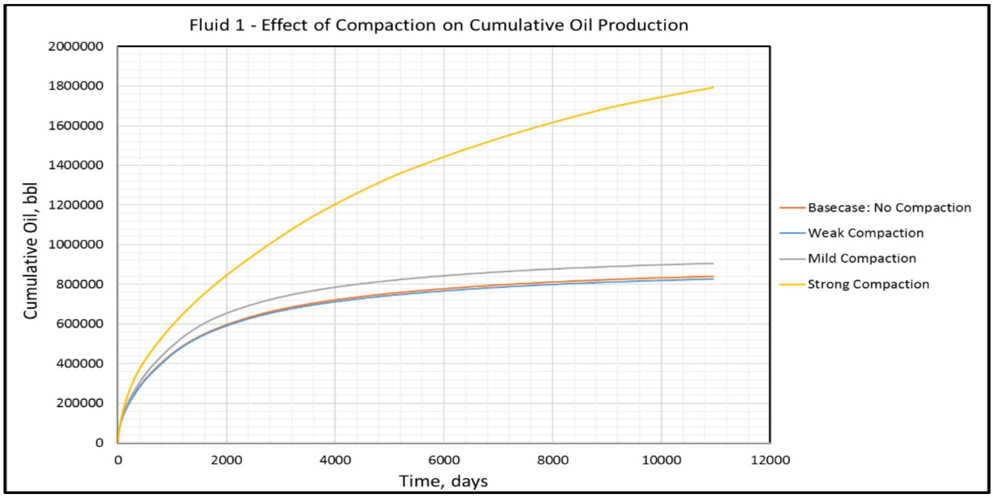

Figure 4-264 Fluid 1 – Effect of Compaction on Cumulative Oil Production

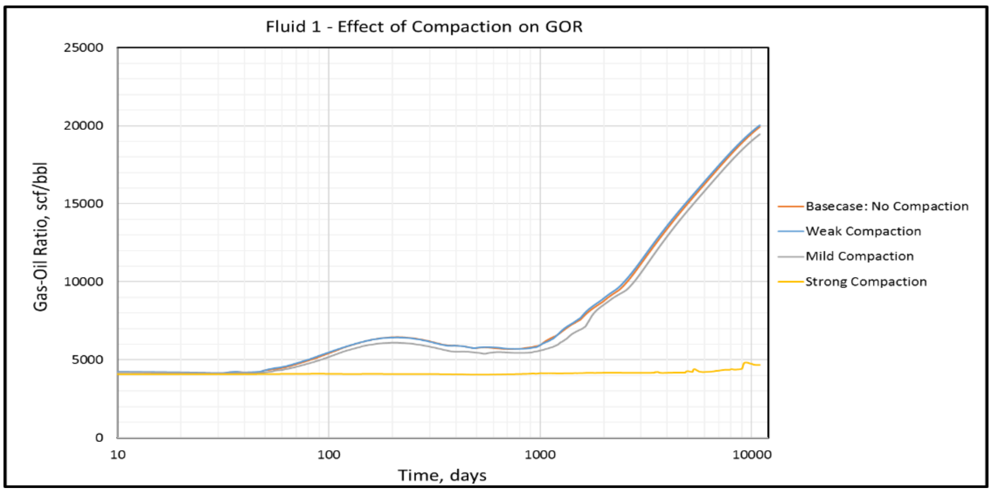

Figure 4-265 Fluid 1 – Effect of Compaction on GOR

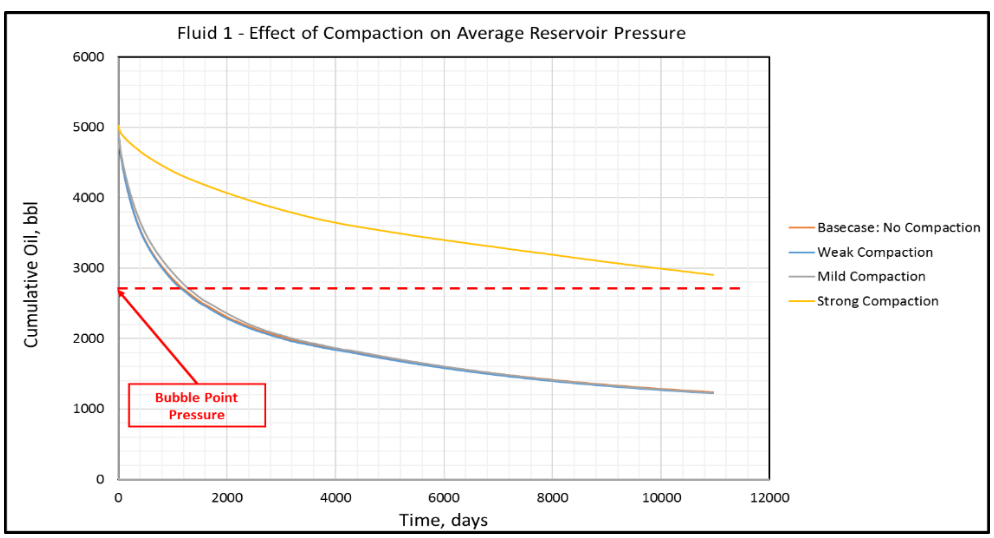

Figure 4-266 Fluid 1 – Effect of Compaction on Average Reservoir Pressure

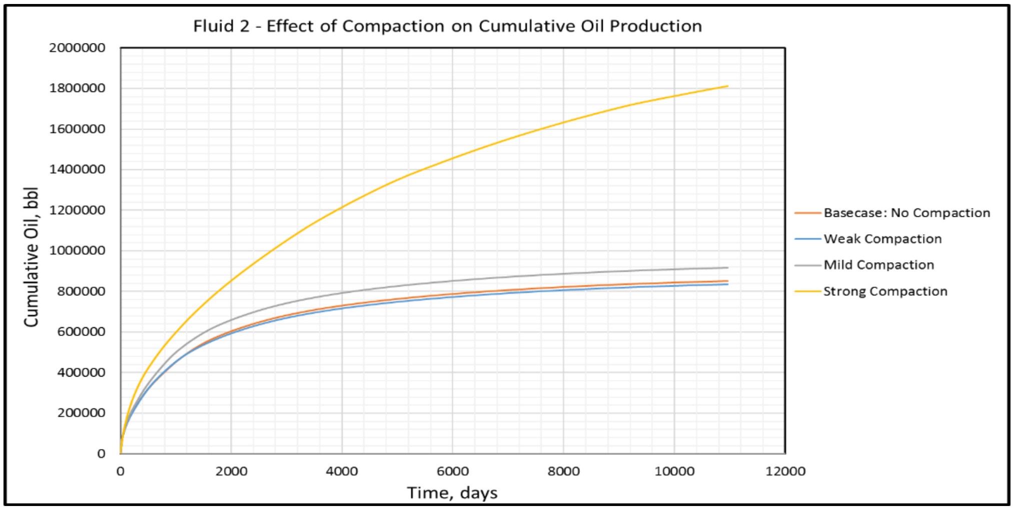

Figure 4-267 Fluid 2 – Effect of Compaction on Cumulative Oil Production

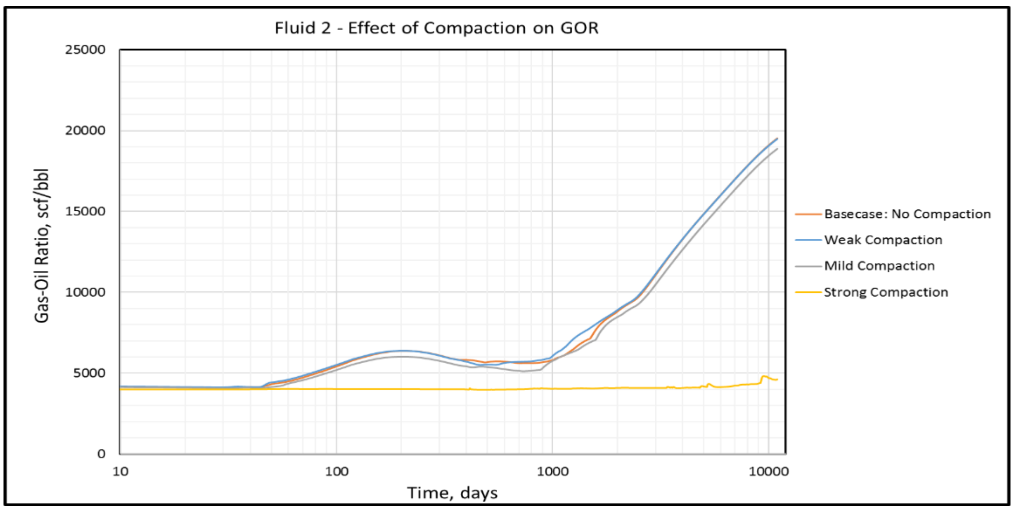

Figure 4-268 Fluid 2 – Effect of Compaction on GOR

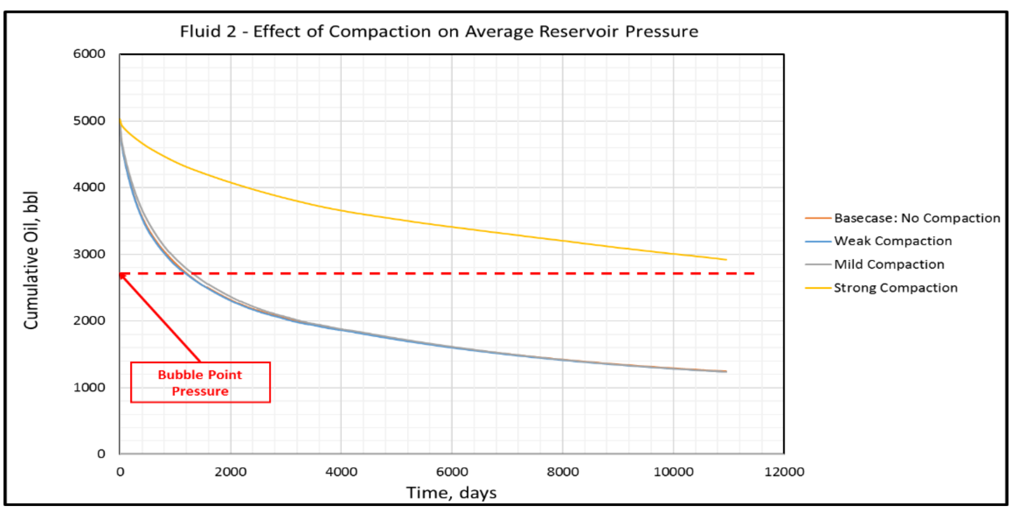

Figure 4-269 Fluid 2 – Effect of Compaction on Average Reservoir Pressure

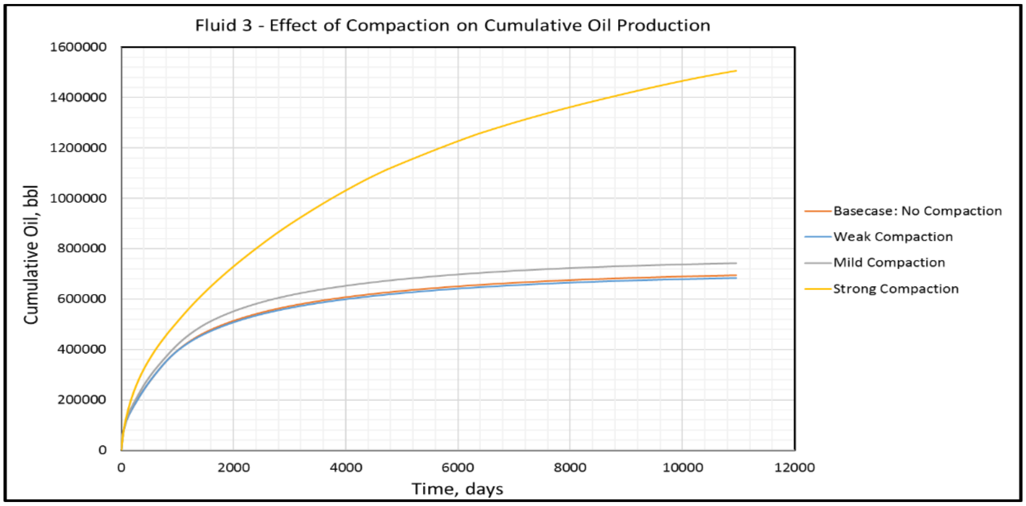

Figure 4-270 Fluid 3 – Effect of Compaction on Cumulative Oil Production

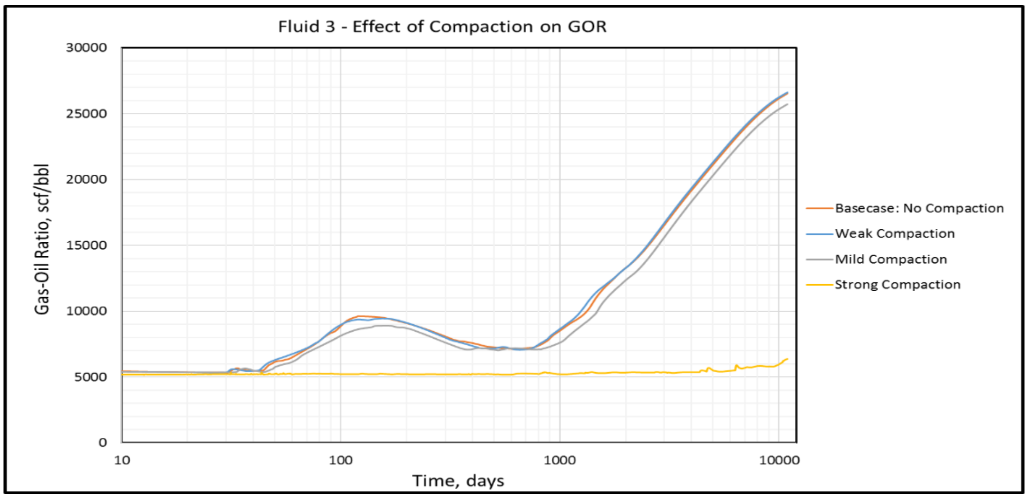

Figure 4-271 Fluid 3 – Effect of Compaction on GOR

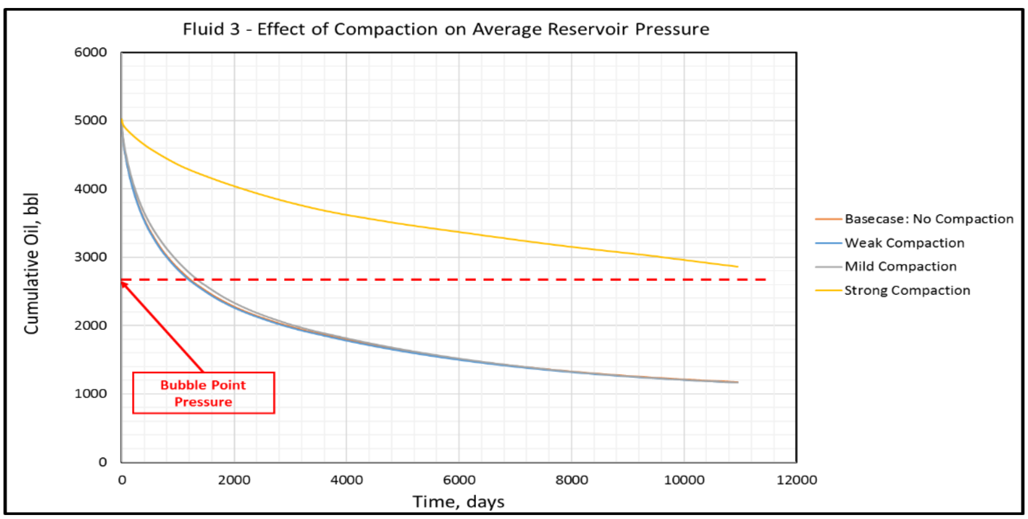

Figure 4-272 Fluid 3 – Effect of Compaction on Average Reservoir Pressure

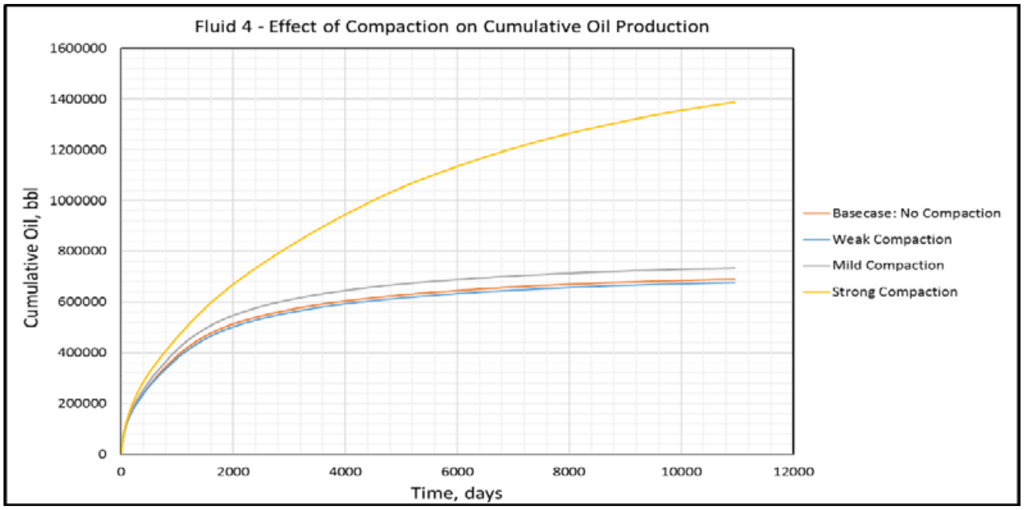

Figure 4-273 Fluid 4 – Effect of Compaction on Cumulative Oil Production

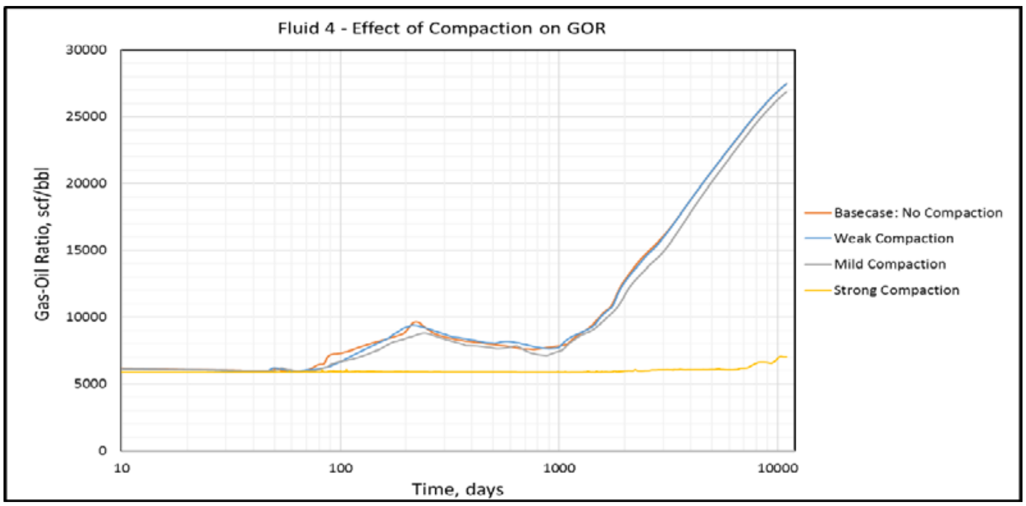

Figure 4-274 Fluid 4 – Effect of Compaction on GOR

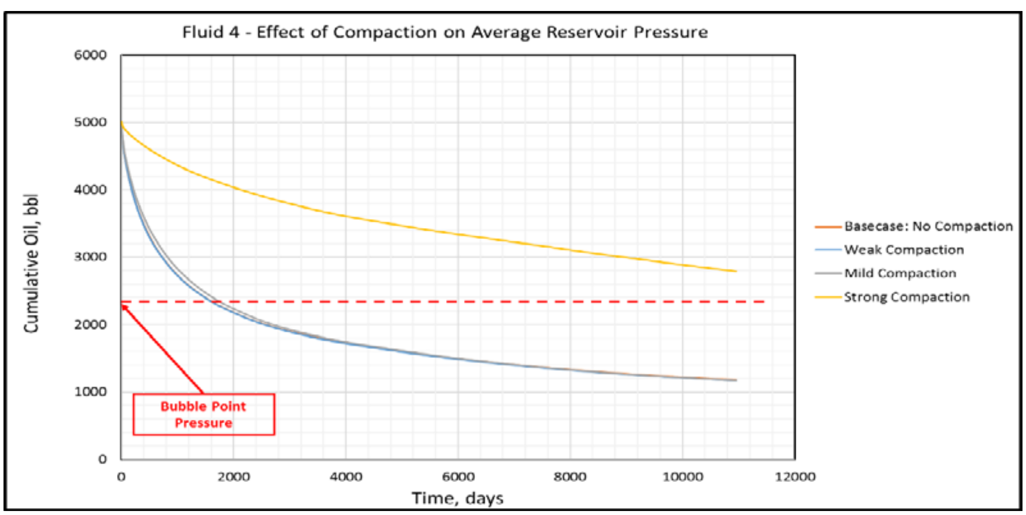

Figure 4-275 Fluid 4 – Effect of Compaction on Average Reservoir Pressure

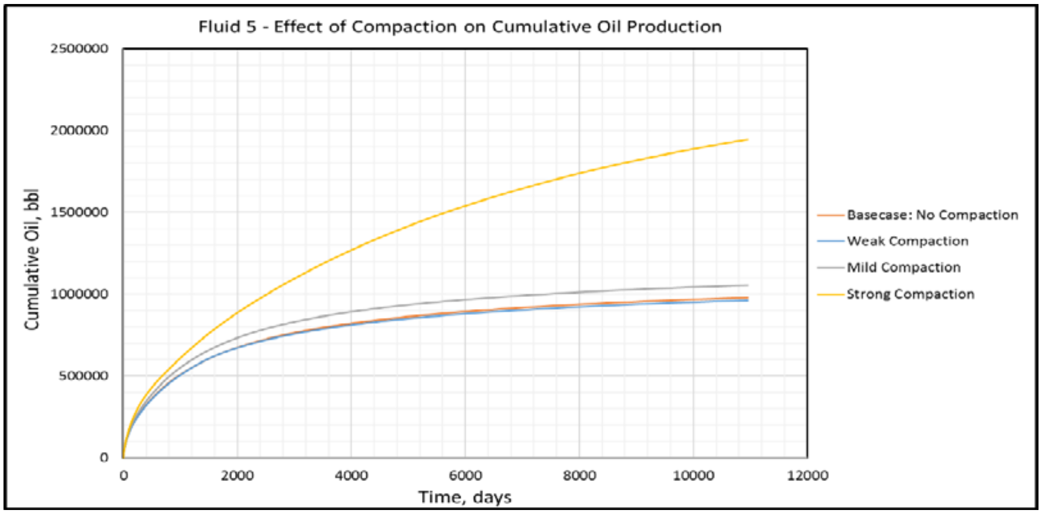

Figure 4-276 Fluid 5 – Effect of Compaction on Cumulative Oil Production

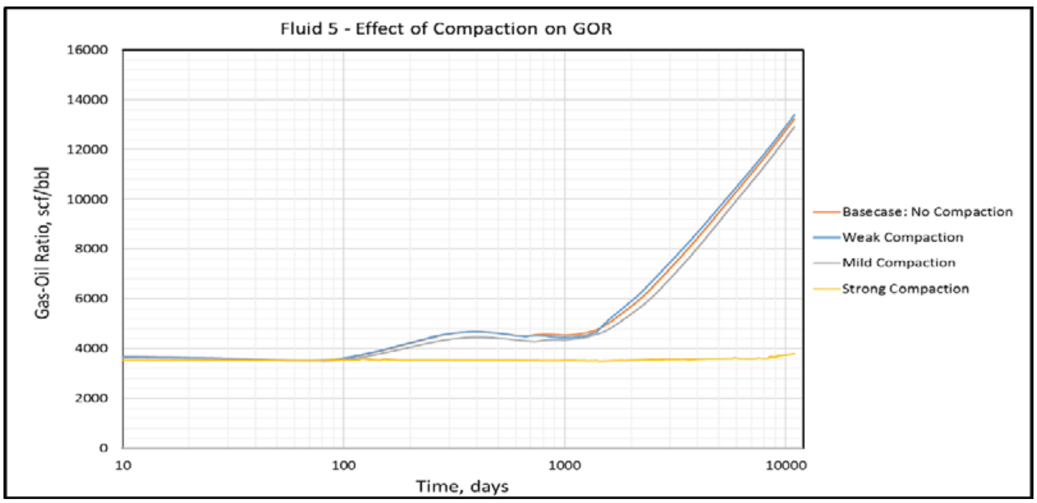

Figure 4-277 Fluid 5 – Effect of Compaction on GOR

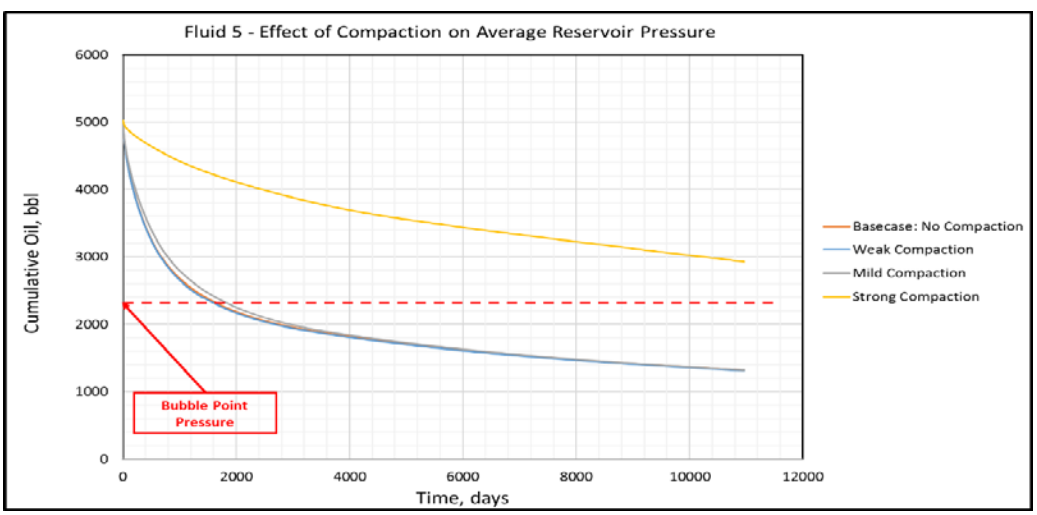

Figure 4-278 Fluid 5 – Effect of Compaction on Average Reservoir Pressure

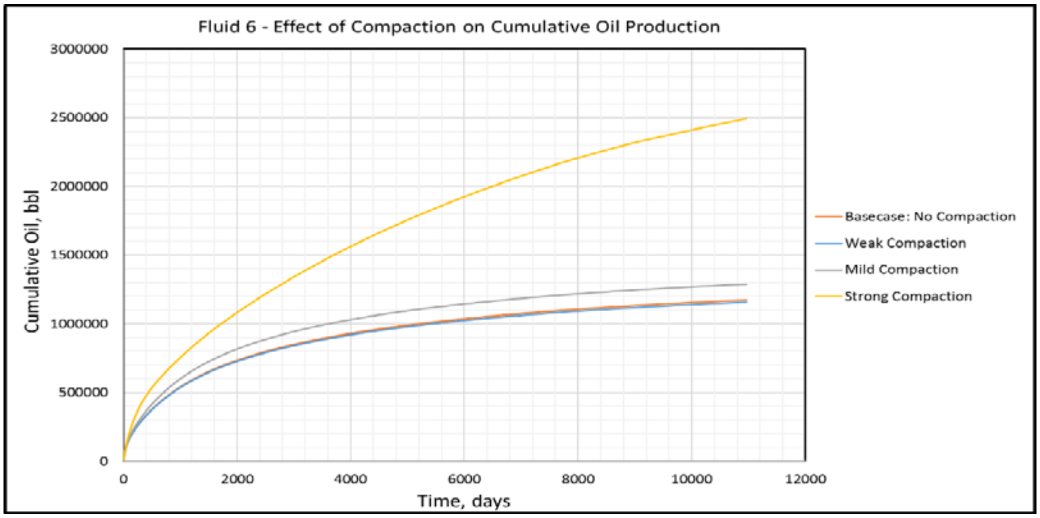

Figure 4-279 Fluid 6 – Effect of Compaction on Cumulative Oil Production

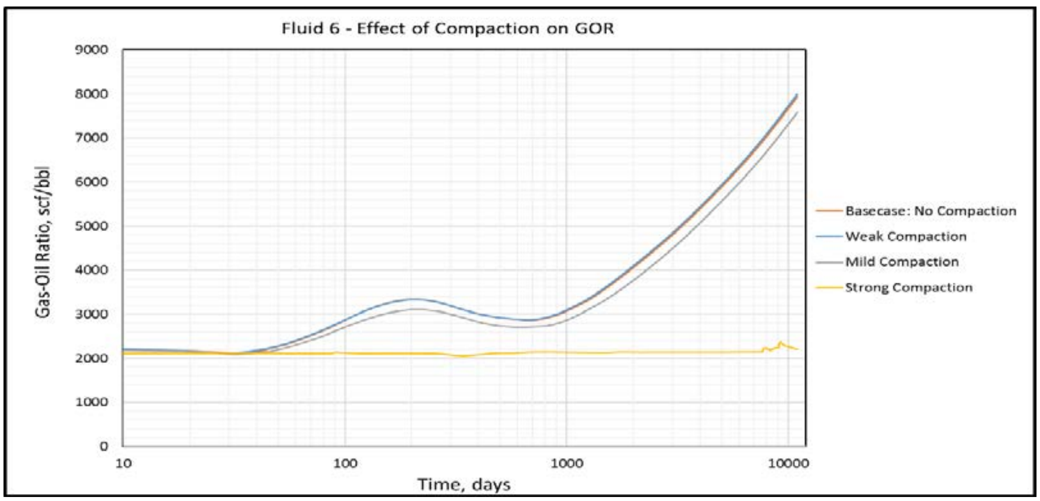

Figure 4-280 Fluid 6 – Effect of Compaction on GOR

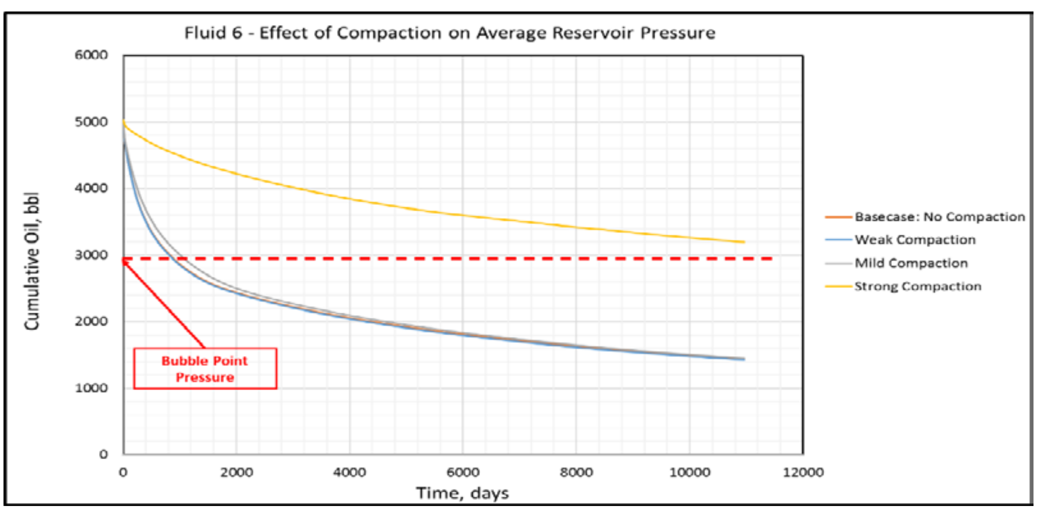

Figure 4-281 Fluid 6 – Effect of Compaction on Average Reservoir Pressure

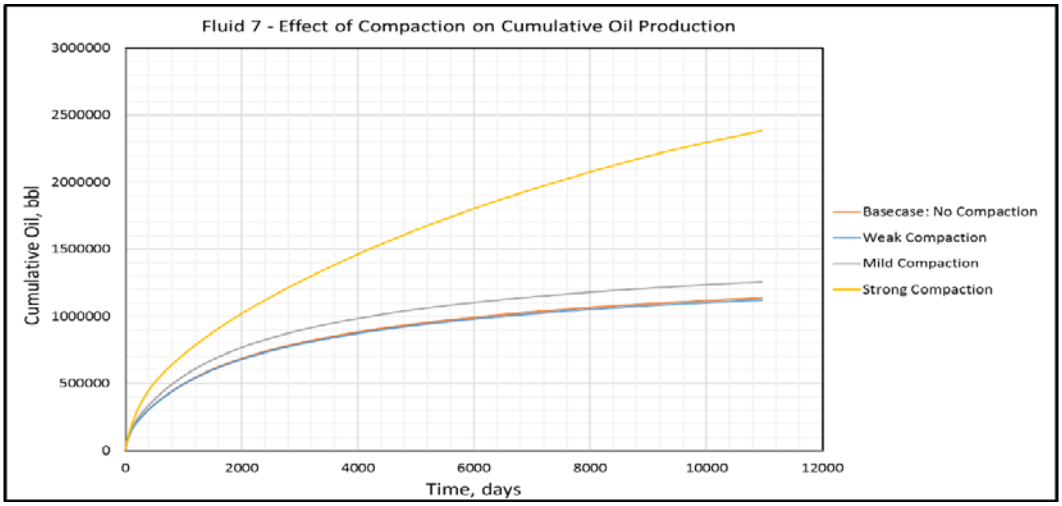

Figure 4-282 Fluid 7 – Effect of Compaction on Cumulative Oil Production

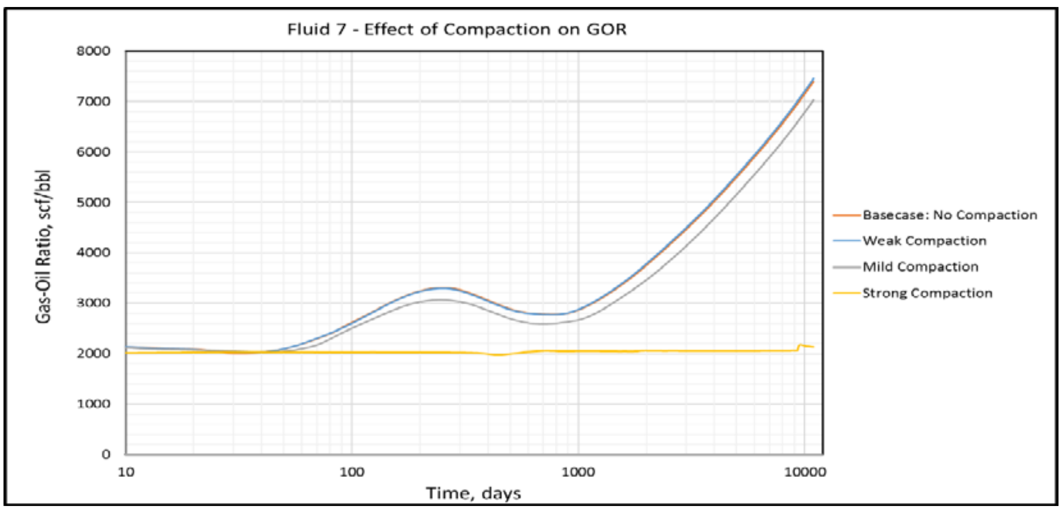

Figure 4-283 Fluid 7 – Effect of Compaction on GOR

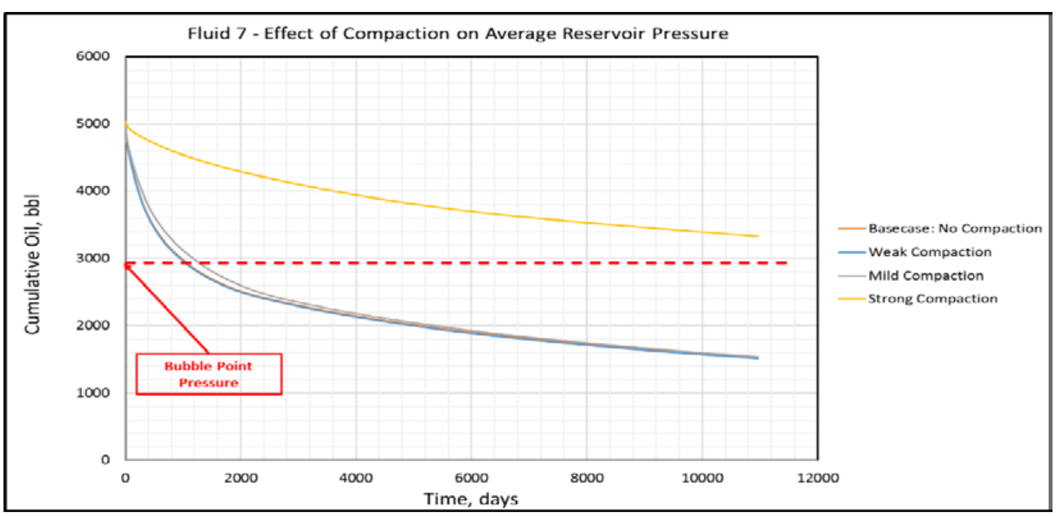

Figure 4-284 Fluid 7 – Effect of Compaction on Average Reservoir Pressure

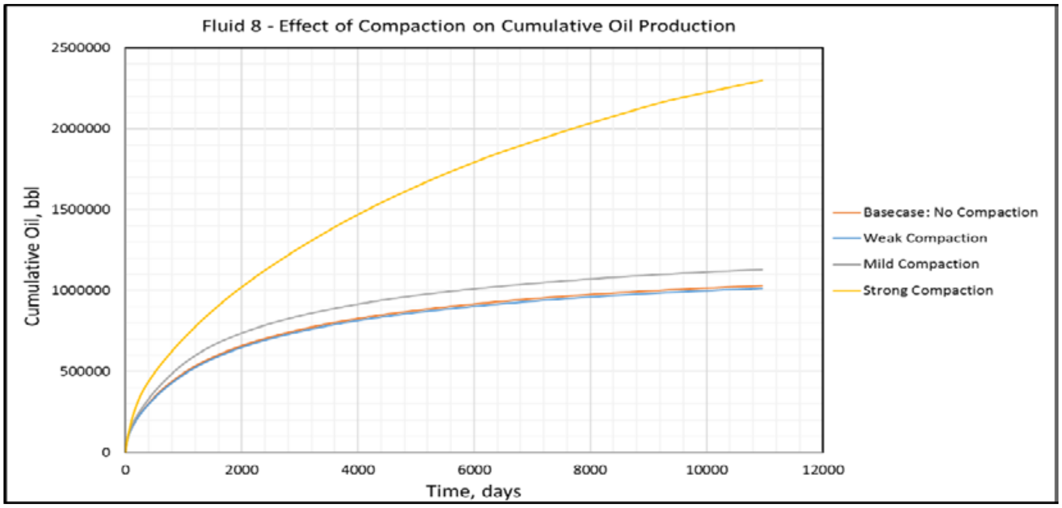

Figure 4-285 Fluid 8 – Effect of Compaction on Cumulative Oil Production

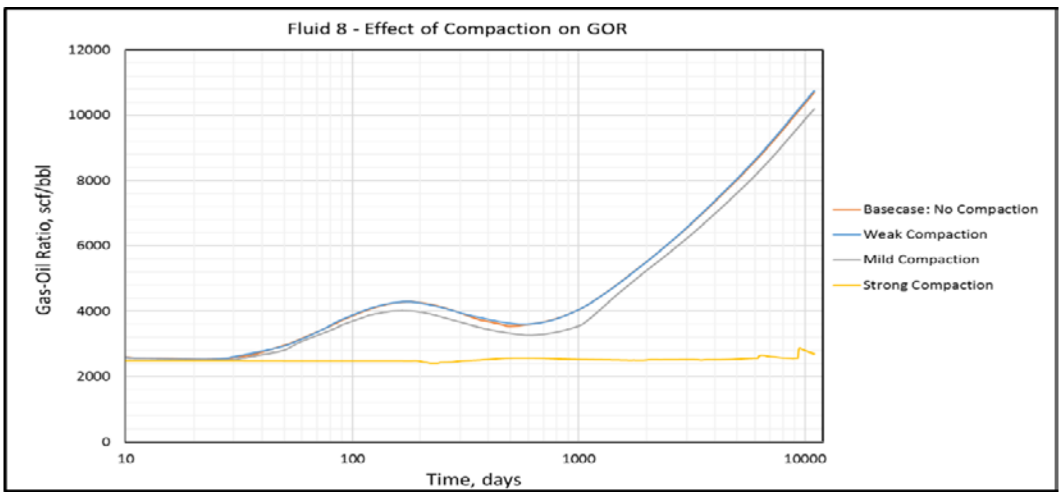

Figure 4-286 Fluid 8 – Effect of Compaction on GOR

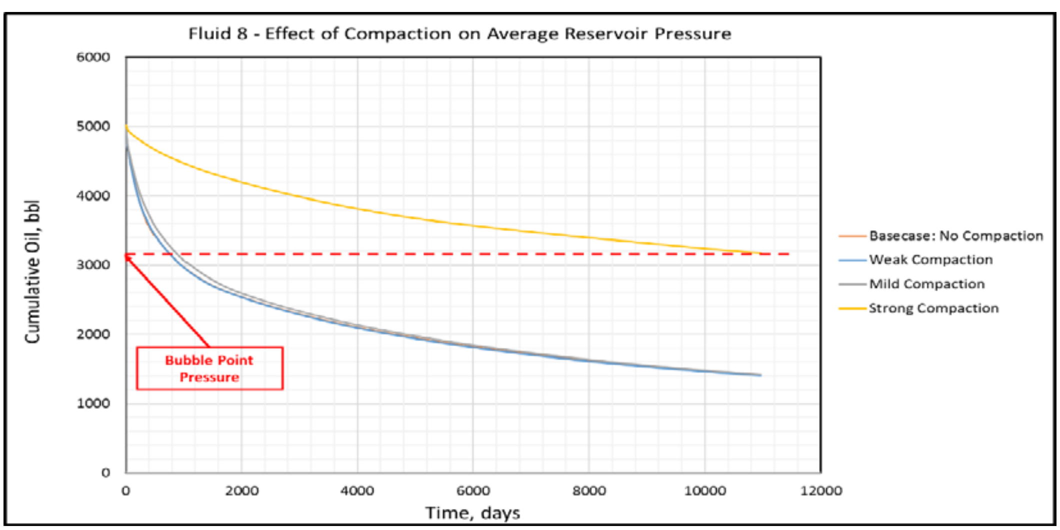

Figure 4-287 Fluid 8 – Effect of Compaction on Average Reservoir Pressure

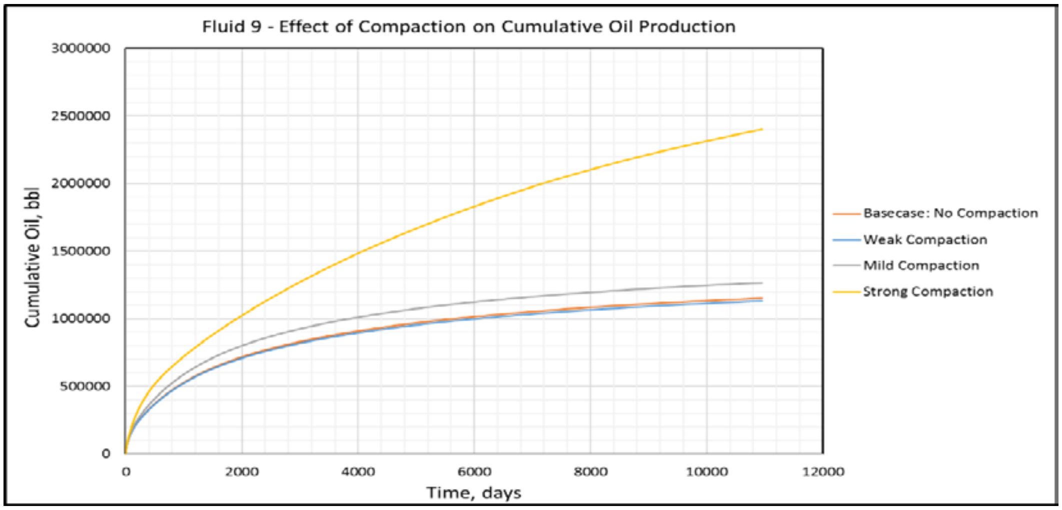

Figure 4-288 Fluid 9 – Effect of Compaction on Cumulative Oil Production

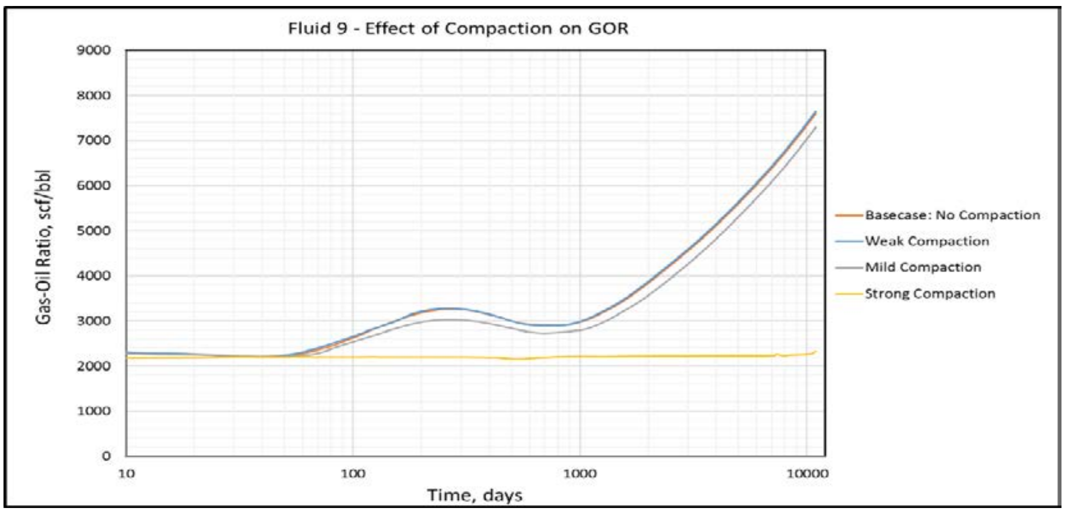

Figure 4-289 Fluid 9 – Effect of Compaction on GOR

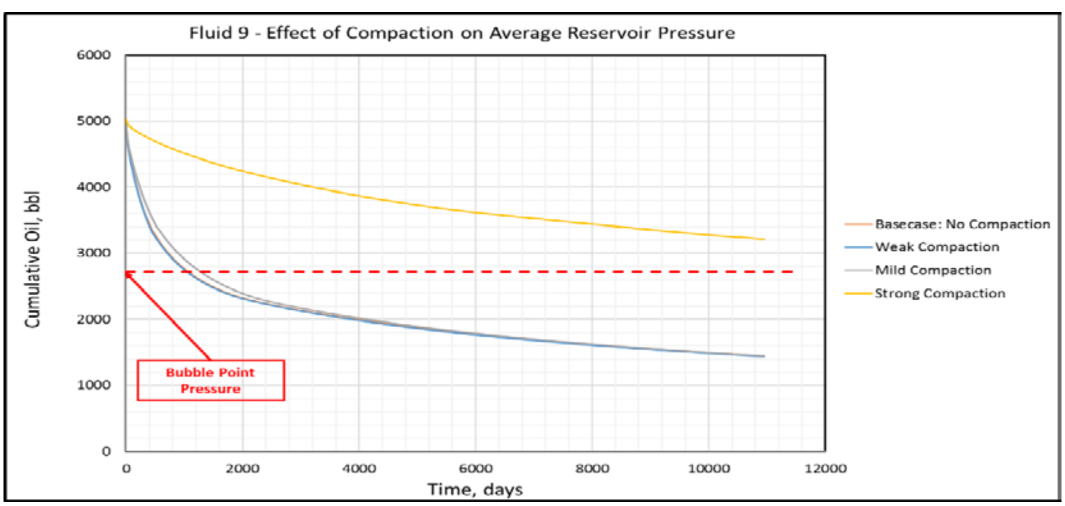

Figure 4-290 Fluid 9 – Effect of Compaction on Average Reservoir Pressure

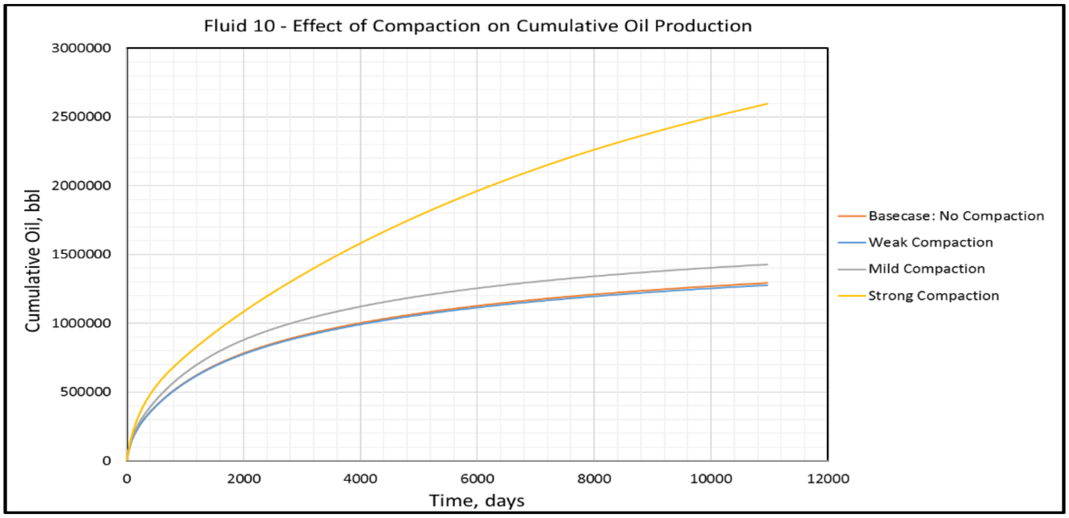

Figure 4-291 Fluid 10 – Effect of Compaction on Cumulative Oil Production

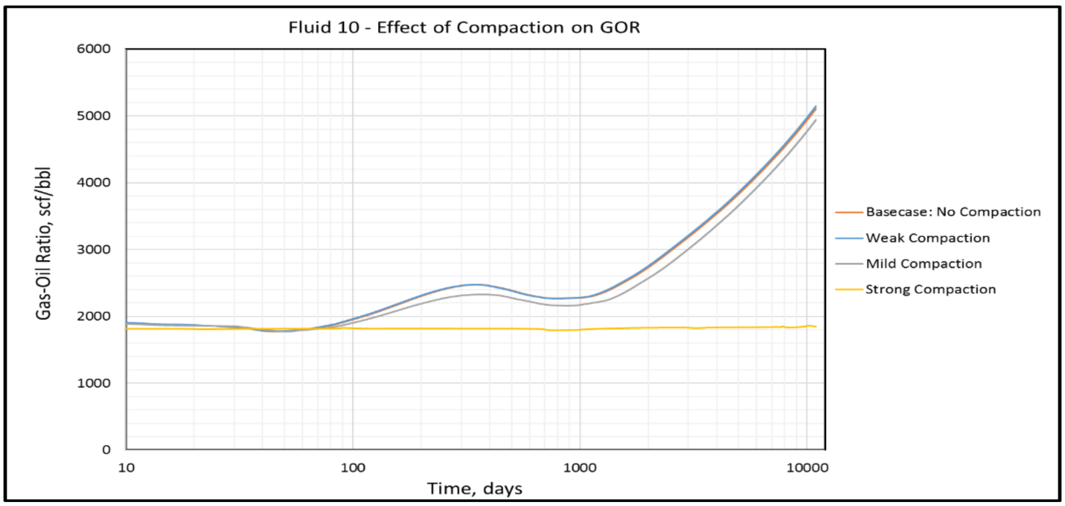

Figure 4-292 Fluid 10 – Effect of Compaction on GOR

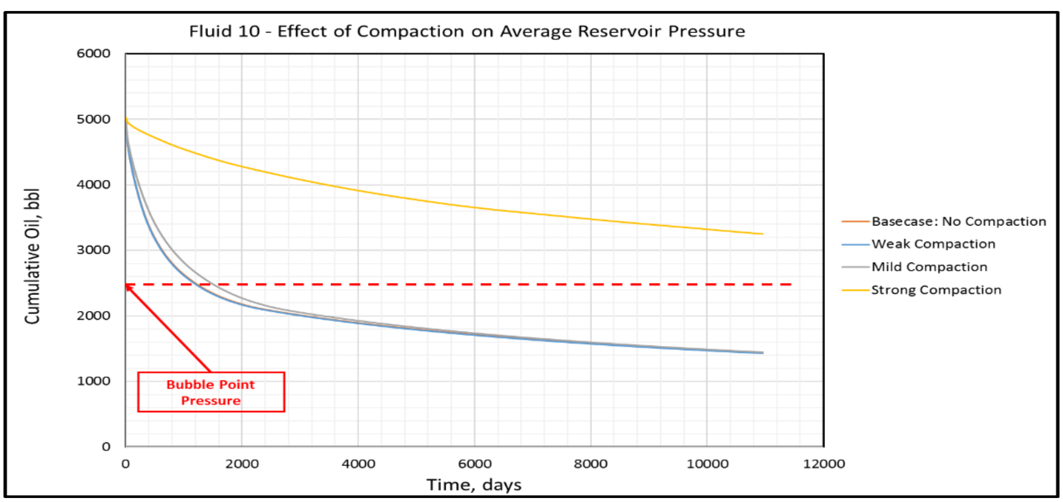

Figure 4-293 Fluid 10 – Effect of Compaction on Average Reservoir Pressure

4.11. Inferences

1. Shale volatile oil reservoir production mechanisms may be influenced by factors or combination of factors that include reservoir and fluid characteristics, as well as vital completion parameters;
2. Six critical stages in the GOR history of shale volatile oil reservoirs producing by solution gas drive mechanism were identified;
3. The degree of volatility of volatile oils can have substantial impact on production performance of shale volatile oil reservoirs;
4. Gas saturation is a critical factor that influences production performance of shale volatile oil reservoirs;
5. Sensitivity analyses have proven that the flowing bottomhole pressure, rock compressibility, fracture half-length, fracture spacing and fracture permeability are important parameters that affect shale volatile oil reservoir performance;
6. The degree of undersaturation of shale volatile oil reservoirs is a major factor that impacts oil recovery. The higher the degree of undersaturation, the more oil is produced and vice versa;
7. Production performance of multi-fractured horizontal wells in a shale volatile oil reservoir is hugely influenced by the drainage area. Increasing drainage area results in larger cumulative oil production, lower oil recovery factors and vice versa;
8. The presence of compaction can play a significant role in the production mechanisms of shale volatile oil reservoirs. Strong compaction may lead to considerably enhanced oil recovery;

9. The following factors or combination of these factors may lead to constant GOR or prolonged periods of constant GOR during production of shale volatile oil reservoirs:

- High degree of undersaturation;
- Flowing bottomhole pressure equal to or approximately equal to the fluid saturation pressure;
- Closeness of the reservoir fluids to the critical point;
- Short fracture half-lengths;
- The presence of strong compaction.

Chapter 5 – Principal Components Methodology (PCM)

Existing traditional decline curve analysis (DCA) methods have been limited in their ability to satisfactorily forecast production from liquid rich shale reservoirs. This is due to several causes ranging from the complicated production mechanisms to the ultra-low permeability of shale as mentioned in previous chapters. The use of hybrid (combination) DCA models have been able to improve results significantly. However, complexities associated with these techniques can still make their application quite tedious without proper diagnostic plots, correct use of model parameters and some knowledge of the production mechanisms involved. Therefore, the Principal Components Methodology (PCM) provides us with a way to bypass a lot of these difficulties. It involves the application of a well-established statistical approach called the principal components analysis (PCA) to forecasting production and gas-oil ratio from liquid rich shale reservoirs. Bhattacharya and Nikolaou (2013) used PCA for analysis and history matching in unconventional gas reservoirs but did not forecast future production. Makinde and Lee (2016) used the Principal Components Methodology (PCM) to forecast production from shale volatile oil reservoirs and compared the results to compositionally simulated data and production estimates from different decline curve analysis (DCA) models.

5.1. Singular Value Decomposition (SVD)

Singular value decomposition (SVD) is a mathematical method of breaking a matrix into simpler and more meaningful parts. In the Principal Components Methodology, principal components analysis is done with SVD. It can be represented with the formula below:

$$\mathbf{Z} = \mathbf{uSv^T}, \tag{10}$$

where $\mathbf{Z}$ is a m × t matrix of well data (m – number of wells and t – production time steps), $\mathbf{u}$ is a m × m matrix whose m columns are the normalized eigenvectors of $\mathbf{ZZ^T}$, $\mathbf{S}$ is a diagonal matrix whose diagonal elements are the singular values of $\mathbf{Z}$ (the singular values of $\mathbf{Z}$ are the positive square roots of the eigenvalues of $\mathbf{Z^TZ}$) and $\mathbf{v}$ is a t × t matrix whose t columns are the normalized eigenvectors of $\mathbf{Z^TZ}$. After singular value decomposition, we obtain $\mathbf{Z} = \sum_{k=1}^{m} \sigma_k \mathbf{u}_k \mathbf{v}_k^T$, which can be approximated as $\mathbf{Z} = \sum_{k=1}^{R} \sigma_k \mathbf{u}_k \mathbf{v}_k^T$, where $R \ll m$. σ_k are the singular values of Z (diagonal elements of $\mathbf{S}$) and $\sigma_1 > \sigma_2 > \ldots > \sigma_R$. The eigenvectors, $\mathbf{v}_k^T = [v_k(t_1) \ldots v_k(t_{max})]$ with the largest singular values are the principal components – PCs (Smith, L., 2002). The principal components provide production pattern that best captures the variance in the representative data considered. The parameters $\sigma_k u_k$ can be lumped up as β_k. Therefore, $\mathbf{Z} = \sum_{k=1}^{R} \beta_k \mathbf{v}_k^T$.

5.2. Forecasting Production and Gas-Oil Ratios (GOR) Using Principal Components Methodology (PCM)

The Principal Components Methodology (PCM) introduces a new and different way of forecasting production based on the statistical approach of principal components analysis. The procedure for forecasting production or GOR using PCM consists of the following steps:

1. Generate representative collection of well production/GOR data through simulation for time $t_{\max}$ (e.g., 30 years in our case) and construct a m × t matrix Z from the representative data. The rows m are the number of wells and the columns t are the production time steps as shown below:

$$\boldsymbol{Z} = \begin{bmatrix} d_1(t_1) & \cdots & d_1(t_{max}) \\ \vdots & \ddots & \vdots \\ d_m(t_1) & \cdots & d_m(t_{max}) \end{bmatrix}, \tag{11}$$

where d_i (i = 1…m) are the oil/gas rates or GOR data of well i over time.

2. Apply principal components analysis to the representative well data through the use of singular value decomposition to obtain the principal components.
3. Given wells with limited production history (in cases here, ranging from 0.5 to 3 years), use the least squares regression method to identify best estimates for β_k (PC multiplier), which would be $\hat{\beta}_k$, with the following formula:

$$\min_{\beta_1 \ldots \beta_R} \left\| \left[d(t_1) \ldots d\left(t_{history}\right)\right]^T - \sum_{k=1}^{R} \beta_k \left[v_k(t_1) \ldots\ v_k\left(t_{history}\right)\right]^T \right\|_2^2, \tag{12}$$

where d can be oil/gas rates or GOR data and $\mathbf{v}_k^T$ are the principal components.

4. Production/GOR can then be forecasted using the formula below:

$$Forecast = \sum_{k=1}^{R} \hat{\beta}_k \left[v_k\left(t_{history}\right) \ldots\ v_k(t_{max})\right]^T. \tag{13}$$

In many cases, the first set of principal components ($\mathbf{v}_1^T$ with the highest singular value) capture enough variance in the representative data that there is no need to consider using the other principal components. Figure 5-1 shows a simple pictorial depiction of the basic workflow of the Principal Components Methodology (PCM).

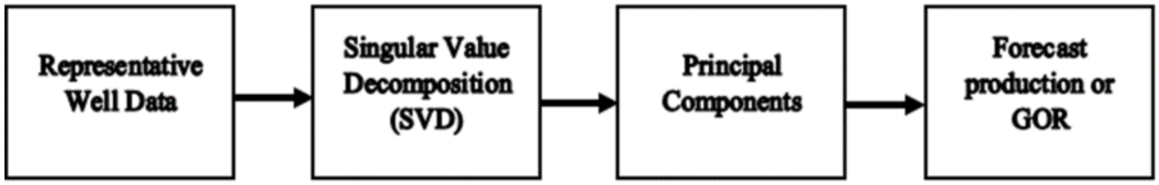

Figure 5-1 Basic Workflow for Principal Components Methodology (PCM)

5.2.1. Principal Components Methodology (PCM) vs. Hybrid Decline Curve Analysis (DCA) Models

Empirical methods such as Decline Curve Analysis (DCA) are commonly used in the industry due to their relative simplicity. Nevertheless, traditional DCA models such Arps' hyperbolic decline model, Duong's model, Stretched Exponential Production Decline (SEPD) model, etc. are not completely suitable for production forecasting in shale volatile oil reservoirs. Long transition periods between the end of linear flow (ELF) and the start of boundary-dominated flow (STBDF) are a common feature of liquid rich shale (LRS) reservoirs mainly due to multiphase flow effects and ultra-low permeability of shales among other possible factors. These factors create limitations for the application of traditional DCA techniques for analysis of production from LRS reservoirs. For example, the Arps' hyperbolic decline model (Arps, 1945) assumes boundary-dominated flow (BDF) and most shale reservoirs reach BDF only after many years – making the use of this model not entirely appropriate in this case. Also, Duong's model (Duong, 2011) assumes long-term linear flow which can lead to serious overestimation of production from LRS reservoirs. The SEPD model (Valko and Lee, 2010) can often underestimate reserves especially with short production histories. YM-SEPD, a modified form of the SEPD model proposed by Yu and Miocevic (2013) can also be severely limited by the nature of production data, short production histories and an uncertain initial production rate. In a bid to find empirical forecasting methods that can be proper for LRS reservoirs, there has been more research into the use of hybrid (combination) DCA models. The application of hybrid DCA models, in most cases, have been found to improve forecast results considerably (Makinde and Lee, 2016).

Analytical models are alternative modes of forecasting production. Models such as the tri-linear flow model (Ozkan *et al*., 2010) and its extended version by Stalgorova and Mattar (2013) consider multi-fractured horizontal wells (MFHWs) with appropriate boundary conditions. Clarkson and Qanbari (2015) also proposed a semi-analytical model that incorporates empirical and analytical forecasting techniques. However, all these methods assume single-phase flow which makes them possibly inaccurate and not quite appropriate for shale volatile oil reservoirs, especially when the reservoir pressure drops below the bubble-point.

Here, a study was undertaken to compare production forecast results from hybrid decline curve analysis (DCA) models with those obtained using the Principal Components Methodology (PCM). A 5,000 ft multi-fractured horizontal well (MFHW) was modeled. The well has 20 uniform hydraulic fractures with fracture spacing of 250 ft. All the fractures are infinitely conductive with half lengths of 150 ft. A commercial compositional simulator was used to simulate production with four different reservoir fluids (volatile oils). 30 years of production was simulated at a minimum bottomhole pressure constraint of 1000 psia. Pressure drop and fluid flow were modeled using the logarithmically-spaced local grid refinement (LS-LGR) and the Peng-Robinson equation of state was used for the PVT. Figure 5-2 shows the MFHW model. Table 5-1 and 5-2 show the reservoir data and the reservoir fluid compositions used.

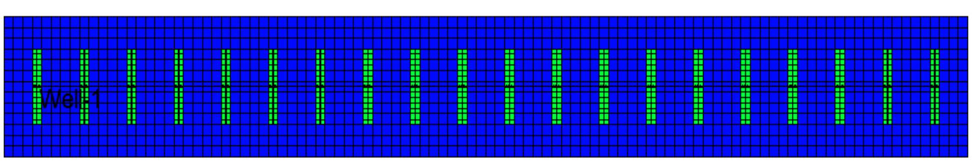

Figure 5-2 Multi-Fractured Horizontal (MFHW) Well

Table 5-1 Reservoir Data (1)

Permeability	0.001 md
Porosity	0.06
Reservoir Temperature	250°F
Initial Reservoir Pressure	5,000 psia
Depth to top of formation	10,000 ft
Reservoir Thickness	250 ft
Corey Relative Permeability Exponent	2.5
Critical gas saturation, S_{gc}	0.05
Residual saturation of oil (gas/oil displacement), S_{org}	0.2

Table 5-2 Fluid Compositions (1)

	Fluid A	Fluid B	Fluid C	Fluid D
Components	Composition (%)	Composition (%)	Composition (%)	Composition (%)
CH_4	58.77	58.07	53.47	49.43
C_2H_6	7.57	7.43	11.46	7.28
C_3H_8	4.09	4.16	8.79	8.02
I-C_4H_{10}	0.91	0.96	-	2.31
N-C_4H_{10}	2.09	1.63	4.56	3.61
I-C_5H_{12}	0.77	0.75	-	1.80
N-C_5H_{12}	1.15	0.80	2.09	1.79
C_6H_{14}	1.75	1.14	1.51	2.32
C_{7+}	21.76	22.59	16.92	22.41
CO_2	0.93	2.32	0.90	0.16
N_2	0.21	0.15	0.30	0.87

We simulated production with four different reservoir fluids (volatile oils) using a commercial compositional reservoir simulator. Then, we tested a variety of traditional and hybrid DCA models (i.e., a model such as the SEPD model for transient flow combined with a different model like the Arps hyperbolic model with a fitting value of the parameter "b") on simulated data for each fluid sample. Further, we also used PCM to forecast production and finally, we compared all the results.

5.2.1.1. YM-SEPD and Modified Duong Models

The YM-SEPD model (earlier described in Chapter 3) was introduced by Yu and Miocevic (2013). It is based on the SEPD model proposed by Valko and Lee (2010). Points on the Yu plot used to generate parameters n and τ should normally be on a straight (or nearly straight line) for this model to be effective. This constitutes a major limitation as slopes of data on the Yu plot for most cases with less than 2 years of production history are not always favorable for calculating appropriate n and τ parameters for reliable prediction of production. In many of these cases, the YM-SEPD model seriously underestimates production. In these situations, Yu and Miocevic (2013) suggested using Duong's model (Duong, 2011) to forecast pseudohistorical data in order to generate "good" n and τ parameters necessary for the YM-SEPD model. However, this does not always guarantee a reliable forecast. Makinde and Lee (2016) observed that the assumptions inherent in the creation of the Duong model can limit its ability to forecast "good" pseudohistorical data needed by the YM-SEPD model for cases of short production histories (less than 2 years). This is because of early deviation from linear flow and correspondingly early start of lengthy transition flow periods observed in some liquid rich shale reservoirs. This was thoroughly investigated in Chapter 3. Therefore, despite this apparent limitation, we have not used the Duong's model to generate pseudohistory for the YM-SEPD model in this study. Here, we investigated the application of the YM-SEPD model individually and in form of hybrid models (for example, YM-SEPD for transient flow combined with Arps' model at BDF).

The Modified Duong model (earlier described in Chapter 3) was proposed by Makinde and Lee (2016) to reduce the overestimation of forecasts by the Duong model. This modified form of the Duong model may however have limitations with short production histories. As in the YM-SEPD model, early production data (2 years or less) may not always be suitable for calculating “good” a and m parameters for the Duong model. In this work, we studied the use of the Modified Duong individually and in form of hybrid models (for example, Modified Duong for transient flow and the Arps model at BDF). Selected data used for the application of YM-SEPD and Modified Duong models in this study are shown in the table below.

Table 5-3 Production Histories and Selected Data

Production History, years	Selected Data, years
3	2 – 3
2	1 – 2
1	0 – 1
0.5	0 – 0.5

5.2.1.2. Diagnostic Plots

For proper flow regime identification, diagnostic plots are important. They are also necessary before application of empirical DCA models to production data. A slope of -1 characterizes the boundary-dominated flow (BDF) regime. Slopes of -1/2 and -1/4 characterize the transient linear and bilinear flow regimes respectively. Data in BDF on the log-log rate-time plot will eventually have a slope more negative than -1 but the point at which the slope reaches a value of -1 is the start of boundary-dominated flow (STBDF). The diagnostic plots for each of the fluid samples are shown in Figures 5-3 and 5-4.

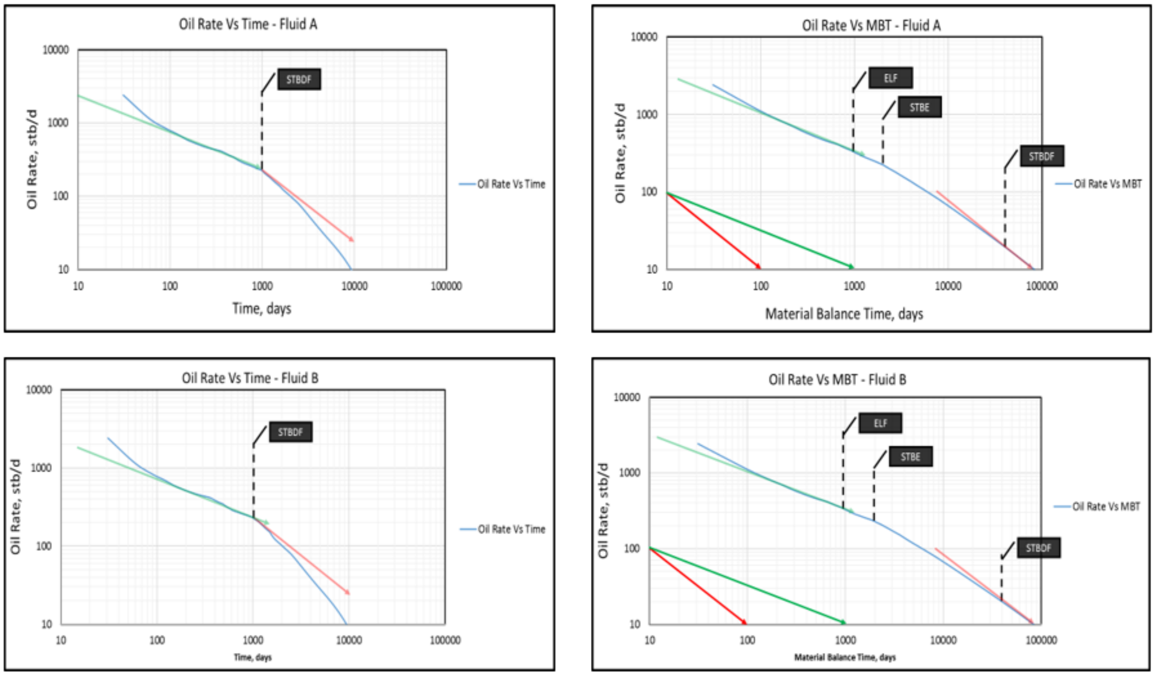

Figure 5-3 Diagnostic Plots for Fluids A and B

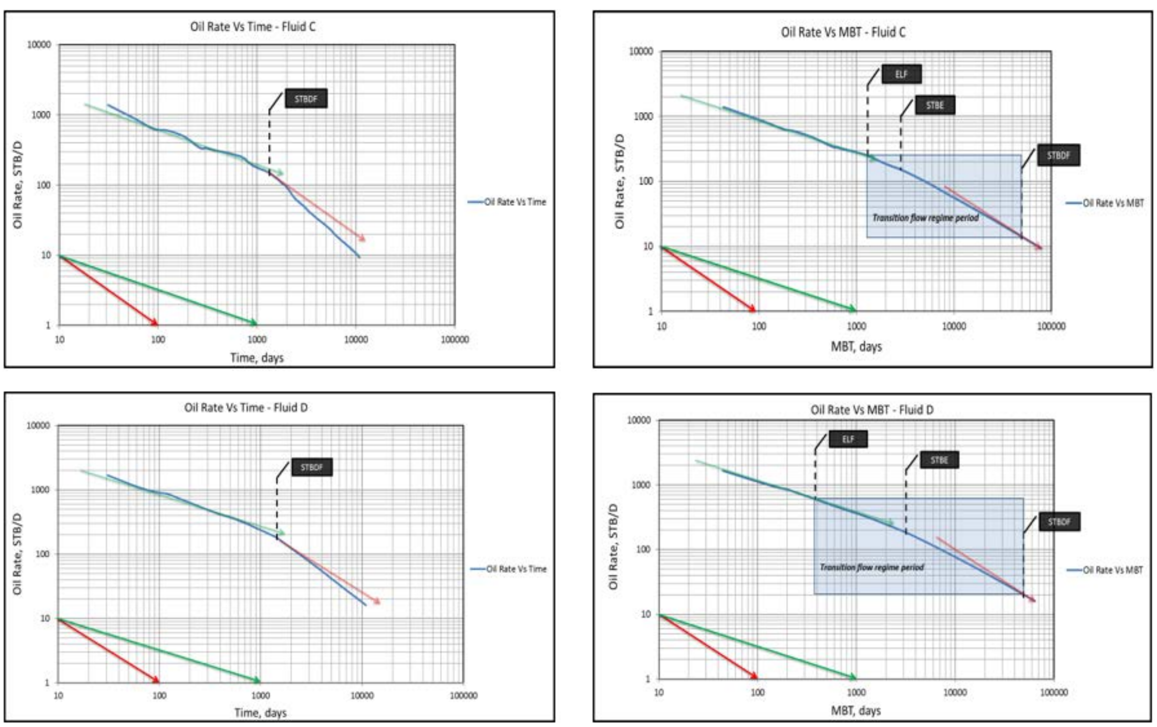

Figure 5-4 Diagnostic Plots for Fluids C and D

5.2.1.3. Inverse MBT vs. Time and Yu Plots

On careful scrutiny of the inverse MBT vs. time and Yu plots, we observe that there is a detectable change of slope at approximately the same time on both plots. This point may be the “true” start of boundary-dominated flow (Makinde and Lee, 2016). Figure 5-5 shows both plots for each fluid. The black dotted lines indicate the approximate time at which the change of slope occurs on both plots. This time corresponds with the start of boundary-dominated flow (STBDF) on the log-log rate-time plots and the start of boundary effects (STBE) on the log-log rate-MBT plots.

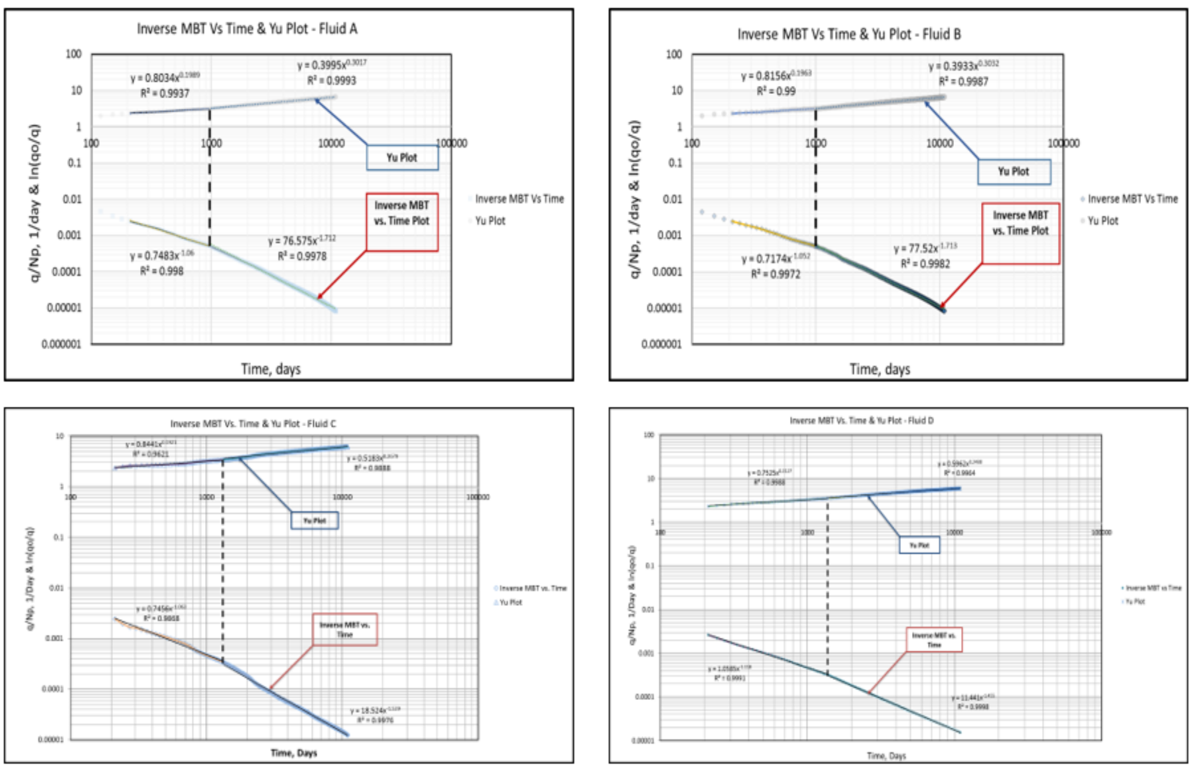

Figure 5-5 Inverse MBT vs. Time and Yu Plots - Fluids A to D

5.2.1.4. Hybrid Decline Curve Analysis (DCA) Models

The two variations of hybrid models considered in these analyses are:

1. YM-SEPD and Modified Duong models for transient flow coupled with switch to Arps' model at the end of linear flow (ELF), as indicated on the log-log rate-MBT plots. These models are referred to as YM-SEPD + Arps(1) and Modified Duong + Arps(1) respectively;
2. YM-SEPD and Modified Duong models for transient flow and a switch to Arps' model at the start of boundary effects (STBE), as indicated on the log-log rate-MBT plots. These models are referred to as YM-SEPD + Arps and Modified Duong + Arps.

5.2.1.5. Application of Principal Components Methodology (PCM)

The basic procedure of Principal Components Methodology (earlier enumerated) was applied to representative data from four wells with the four different reservoir fluids under consideration. Here, one set of principal components (PCs) was found to adequately capture the variance in the representative well data considered. A plot of the principal components with time is shown in Figure 5-6. These principal components were applicable for all cases in this study irrespective of the production history available.

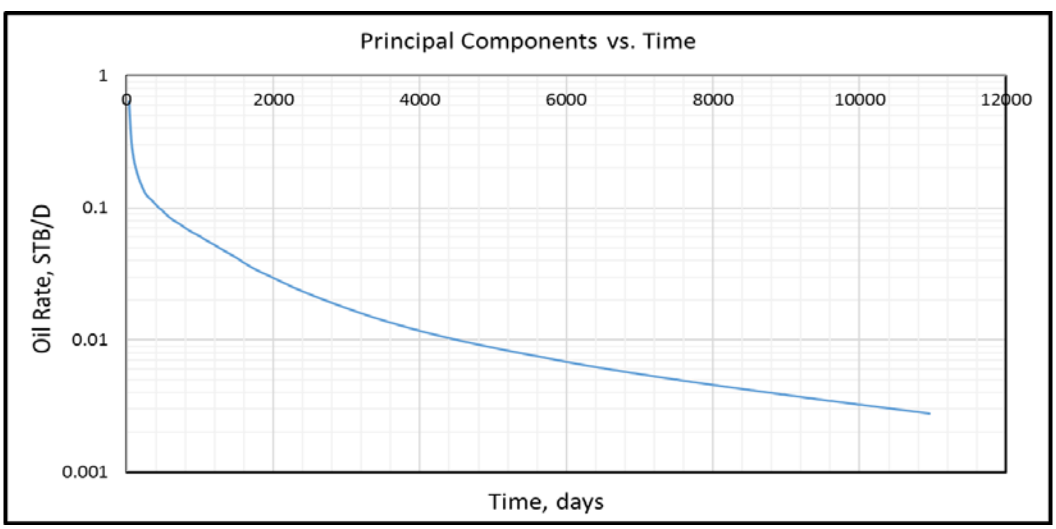

Figure 5-6 Principal Components vs. Time

5.2.1.6. Results – Fluid A Case

Decline curve analysis models and PCM were applied to Fluid A cases for wells with production histories ranging from 0.5 to 3 yrs. The production forecasts obtained were then compared to simulated data. The results for this case are the following:

5.2.1.6.1. 6 months of Production History – Fluid A

The first six months of historical data were used to generate the n and τ parameters for the YM-SEPD model. The same range of historical data were also used to generate the a and m parameters for the Modified Duong model. The results obtained are the following:

1. Plots and Parameters for YM-SEPD and YM-SEPD Hybrid Models: Figure 5-7 shows the Yu plot and Table 5-4 displays the parameters for the YM-SEPD and Arps' models.

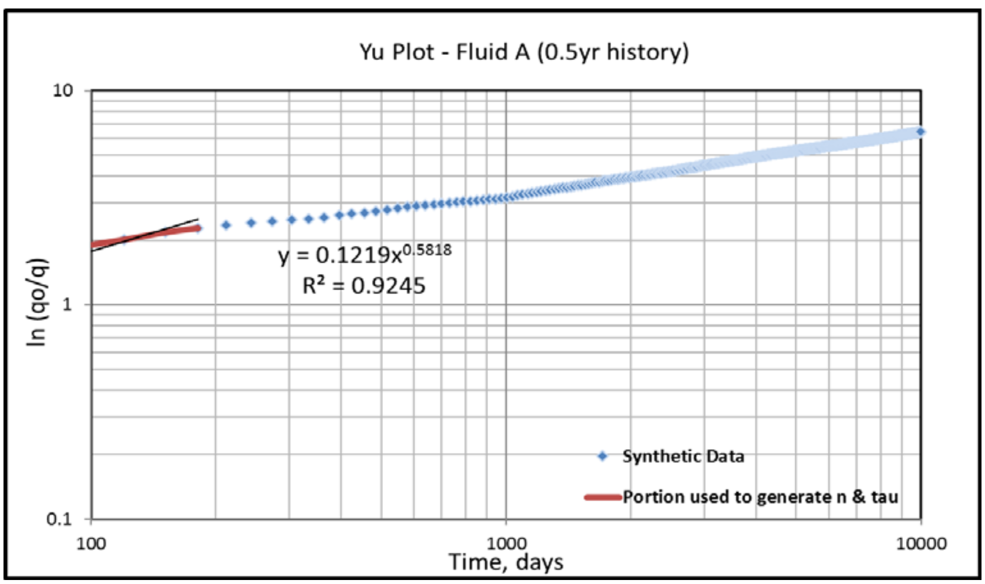

Figure 5-7 Yu Plot – Fluid A (0.5yr History)

Table 5-4 YM-SEPD and Arps Parameters – Fluid A (0.5yr History)

YM-SEPD Parameters – Fluid A (0.5yr history)		
n	0.582	
Intercept	0.122	
τ, days	37.24	
q_o, stb/d	5273	
Arps Parameters – Fluid A (0.5yr history)		
	Arps	**Arps(1)**
t_{sw}, days	1,004	517
D_{sw}, 1/days	0.004	0.005
q_{sw}, stb/d	5.882	51.92
b	2	2.3

2. Plots and Parameters for Modified Duong and Modified Duong Hybrid Models:

   Figure 5-8 and Table 5-5 show the inverse MBT vs. time plot, oil rate vs. t(a,m) plot and parameters for the Modified Duong and Arps' models.

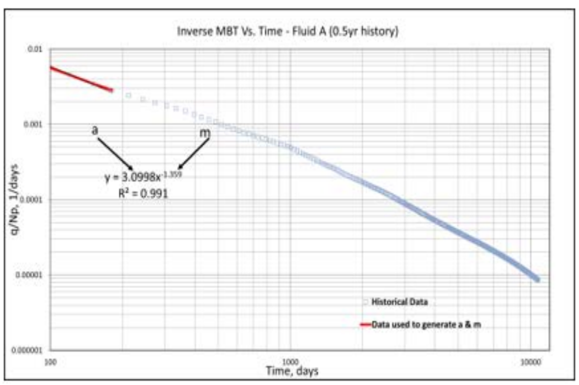

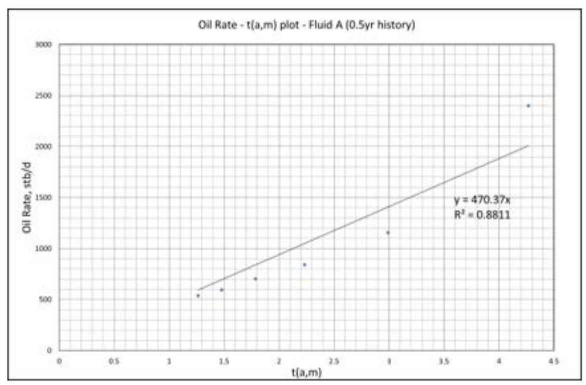

Figure 5-8 Inverse MBT vs. Time and Oil Rate vs. t(a,m) – Fluid A (0.5yr History)

Table 5-5 Modified Duong and Arps Parameters – Fluid A (0.5yr History)

Modified Duong Parameters – Fluid A (0.5yr history)		
a	3.100	
m	-1.359	
q_1, stb/d	470.4	
q_∞, stb/d	0	
Arps Parameters – Fluid A (0.5yr history)		
	Arps	**Arps(1)**
t_{sw}, days	1,004	517
D_{sw}, 1/days	0.034	0.06
q_{sw}, stb/d	107.0	217.1
b	0.9	0.85

5.2.1.6.2. 1 year of Production History – Fluid A

The first year of historical production data were used to generate the n and τ parameters for the YM-SEPD model. The same range of historical data were also used to generate the a and m parameters for the Modified Duong model. The results obtained are the following:

1. Plots and Parameters for YM-SEPD and YM-SEPD Hybrid Models: Figure 5-9 and Table 5-6 display the Yu plot and the parameters for the YM-SEPD and Arps' models.

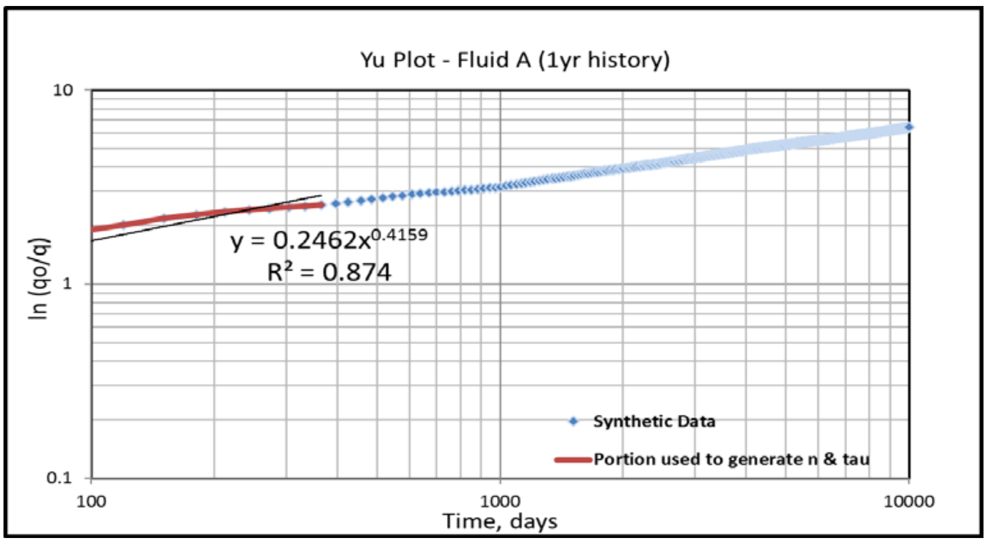

Figure 5-9 Yu Plot – Fluid A (1yr History)

Table 5-6 YM-SEPD and Arps Parameters – Fluid A (1yr History)

YM-SEPD Parameters – Fluid A (1yr history)		
n	0.416	
Intercept	0.246	
τ, days	29.08	
q_o, stb/d	5,273	
Arps Parameters – Fluid A (1yr history)		
	Arps	**Arps(1)**
t_{sw}, days	1,004	517
D_{sw}, 1/days	0.002	0.003
q_{sw}, stb/d	67.23	192.6
b	1.4	1

2. Plots and Parameters for Modified Duong and Modified Duong Hybrid Models: Figure 5-10 and Table 5-7 show the inverse MBT vs. time plot, oil rate vs. t(a,m) plot and parameters for the Modified Duong and Arps' models.

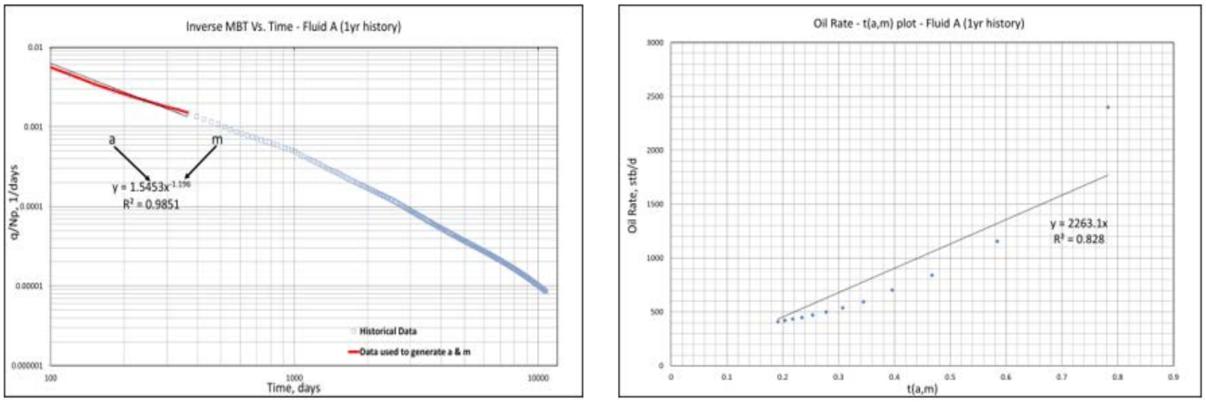

Figure 5-10 Inverse MBT vs. Time and Oil Rate vs. t(a,m) – Fluid A (1yr History)

Table 5-7 Modified Duong and Arps Parameters – Fluid A (1yr History)

Modified Duong Parameters – Fluid A (1yr history)		
a	1.545	
m	-1.196	
q_1, stb/d	2,263	
q_∞, stb/d	0	
Arps Parameters – Fluid A (1yr history)		
	Arps	**Arps(1)**
t_{sw}, days	1,004	517
D_{sw}, 1/days	0.021	0.037
q_{sw}, stb/d	201.9	336.7
b	0.85	0.9

5.2.1.6.3. 2 years of Production History – Fluid A

The first to second year of historical data were used to generate the n and τ parameters for the YM-SEPD model. The same range of historical data were also used to generate the a and m parameters for the Modified Duong model. The results obtained are the following:

1. Plots and Parameters for YM-SEPD and YM-SEPD Hybrid Models: Figure 5-11 and Table 5-8 show the Yu plot and the parameters for the YM-SEPD and Arps' models.

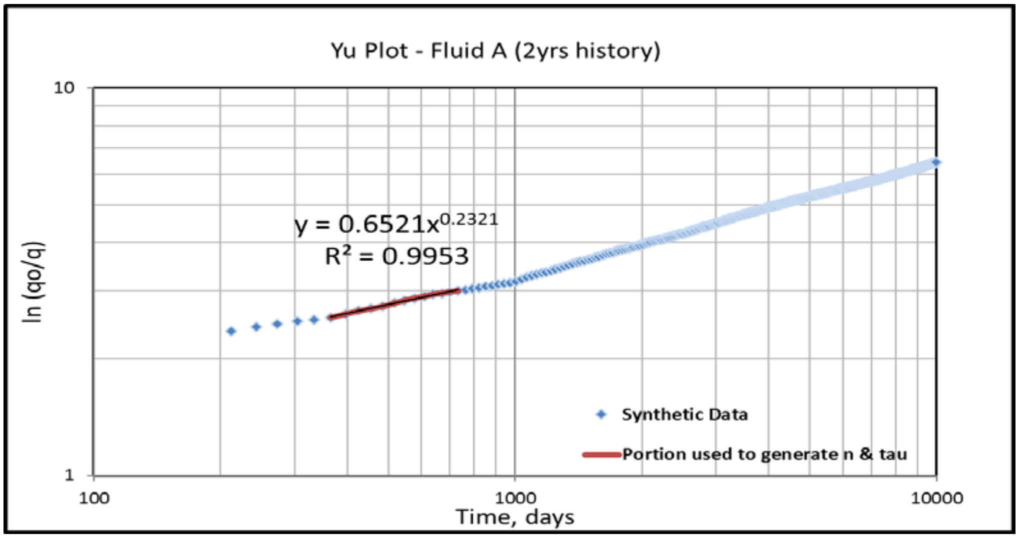

Figure 5-11 Yu Plot – Fluid A (2yrs History)

Table 5-8 YM-SEPD and Arps Parameters – Fluid A (2yrs History)

YM-SEPD Parameters – Fluid A (2yrs history)		
n	0.232	
Intercept	0.652	
τ, days	6.310	
q_o, stb/d	5,273	
Arps Parameters – Fluid A (2yrs history)		
	Arps	Arps(1)
t_{sw}, days	1,004	517
D_{sw}, 1/days	0.001	0.001
q_{sw}, stb/d	205.8	327.0
b	0.42	0.57

2. Plots and Parameters for Modified Duong and Modified Duong Hybrid Models: Figure 5-12 and Table 5-9 show the inverse MBT vs. time plot, oil rate vs. t(a,m) plot and parameters for the Modified Duong and Arps' models.

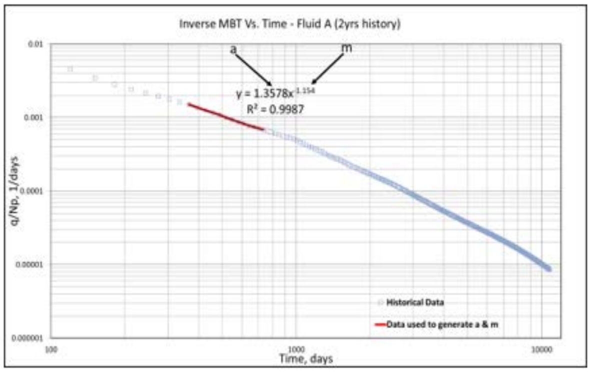

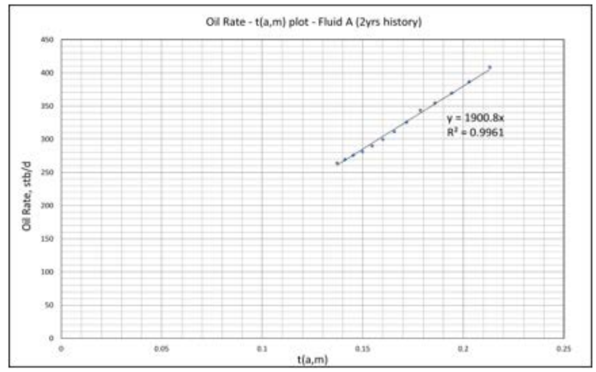

Figure 5-12 Inverse MBT vs. Time and Oil Rate vs. Time – Fluid A (2yrs History)

Table 5-9 Modified Duong and Arps Parameters – Fluid A (2yrs History)

Modified Duong Parameters – Fluid A (2yrs history)		
a	1.358	
m	-1.154	
q_1, stb/d	1,901	
q_∞, stb/d	0	
Arps Parameters – Fluid A (2yrs history)		
	Arps	**Arps(1)**
t_{sw}, days	1,004	517
D_{sw}, 1/days	0.018	0.029
q_{sw}, stb/d	210.5	326.4
b	0.92	0.9

5.2.1.6.4. 3 years of Production History – Fluid A

The second to third year of historical data were used to generate the n and τ parameters for the YM-SEPD model. The same range of historical data were also used to generate the a and m parameters for the Modified Duong model. The results obtained are the following:

1. Plots and Parameters for YM-SEPD and YM-SEPD Hybrid Models: Figure 5-13 and Table 5-10 show the Yu plot and the parameters for the YM-SEPD and Arps' models.

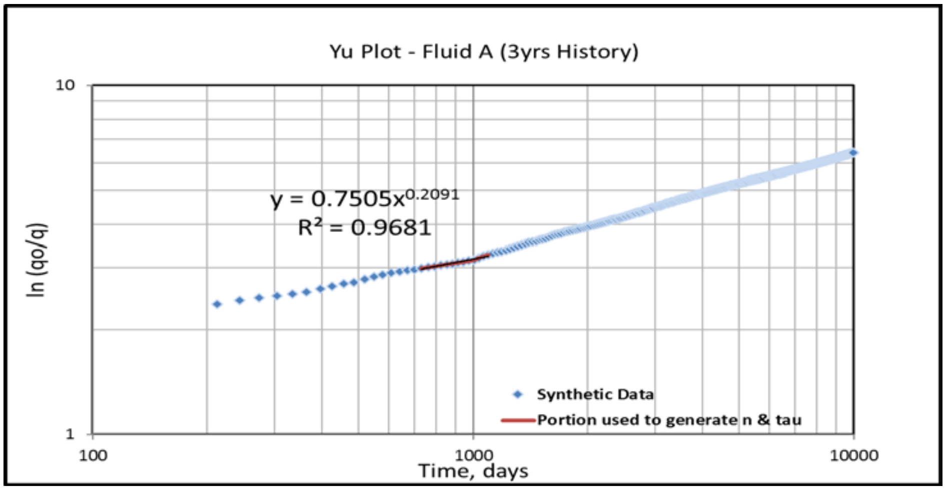

Figure 5-13 Yu Plot – Fluid A (3yrs History)

Table 5-10 YM-SEPD and Arps Parameters – Fluid A (3yrs History)

YM-SEPD Parameters – Fluid A (3yrs history)		
n	0.209	
Intercept	0.751	
τ, days	3.946	
q_o, stb/d	5,273	
Arps Parameters – Fluid A (3yrs history)		
	Arps	**Arps(1)**
t_{sw}, days	1,004	517
D_{sw}, 1/days	0.001	0.001
q_{sw}, stb/d	218.3	329.9
b	0.35	0.5

2. Plots and Parameters for Modified Duong and Modified Duong Hybrid Models: Figure 5-14 and Table 5-11 display the inverse MBT vs. time plot, oil rate vs. t(a,m) plot and parameters for the Modified Duong and Arps' models.

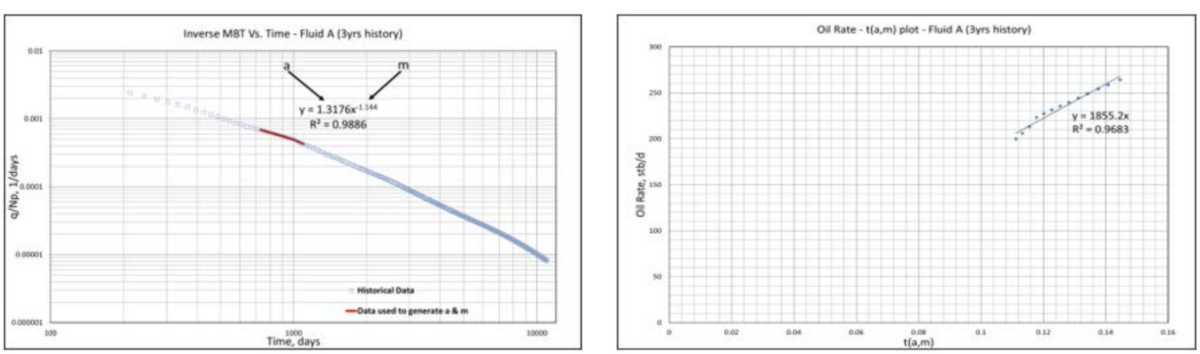

Figure 5-14 Inverse MBT vs. Time and Oil Rate vs. t(a,m) – Fluid A (3yrs History)

Table 5-11 Modified Duong and Arps Parameters – Fluid A (3yrs History)

Modified Duong Parameters – Fluid A (3yrs history)		
a	1.318	
m	-1.144	
q_1, stb/d	1,855	
q_∞, stb/d	0	
Arps Parameters – Fluid A (3yrs history)		
	Arps	**Arps(1)**
t_{sw}, days	1,004	517
D_{sw}, 1/days	0.016	0.027
q_{sw}, stb/d	218.5	332.6
b	0.8	0.9

Graphical production forecast results for all Fluid A cases are shown in Figure 5-15. From the graphs, we can observe that the YM-SEPD hybrid models provide reasonable results with production histories of 2 years or more. However, YM-SEPD and its hybrid models severely underestimate production with availability of less than 2 years of historical data. The Modified Duong and its hybrid variants overestimated production in most cases, whereas the Principal Components Methodology (PCM) provided reasonable forecasts in all cases.

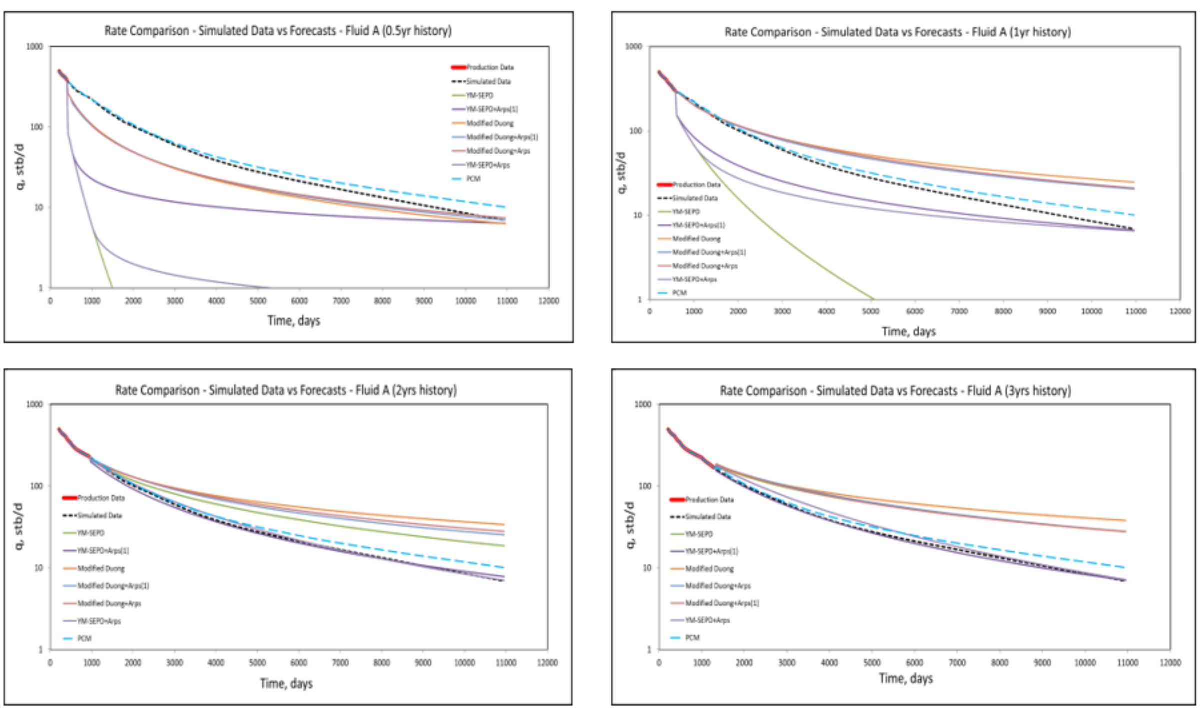

Figure 5-15 Rate Comparisons: Simulated Data vs. Forecasts – Fluid A (All Cases)

Table 5-12 shows the absolute errors, percentage errors and forecasts for all the models. Figures in red indicate the lowest percentage errors.

Table 5-12 Forecast, Errors and Percentage Errors – Fluid A

Cumulative Oil Production Forecast Errors – Fluid A	Forecast, STB				Error (absolute value), STB				Percentage Error, %			
Matched Production Data	0.5 yr.	1 yr.	2 yrs.	3 yrs.	0.5 yr.	1 yr.	2 yrs.	3 yrs.	0.5 yr.	1 yr.	2 yrs.	3 yrs.
Simulated Data	18,350	16,346	13,252	10,925	0	0	0	0	-	-	-	-
YM-SEPD	621	3,050	18,332	20,116	-17,729	-13,296	+5,080	+9,191	-2855	-436.0	+27.7	+45.7
YM-SEPD + Arps(1)	3,876	7,548	12,284	10,498	-14,474	-8,798	-968	-427	-373.4	-116.6	-7.9	-4.1
YM-SEPD + Arps	956	6,119	13,675	12,773	-17,394	-10,227	+423	+1,848	-1820	-167.1	+3.1	+14.5
Modified Duong	10,283	22,372	23,333	22,753	-8,067	+6,026	+10,081	+11,828	-78.5	+26.9	+43.2	+52.0
Modified Duong + Arps(1)	10,355	21,140	21,230	20,305	-7,995	+4,794	+7,978	+9,380	-77.2	+22.7	+37.6	+46.2
Modified Duong + Arps	10,523	21,588	21,968	20,769	-7,827	+5,242	+8,716	+9,844	-74.4	+24.3	+39.7	+47.4
PCM	19,730	17,675	14,497	12,117	+1,380	+1,329	+1,245	+1192	+7.0	+7.5	+8.6	+9.8

5.2.1.7. Results – Fluid B Case

PCM and hybrid DCA models were applied to Fluid B cases for wells with production histories ranging from 0.5 to 3 yrs. The production forecasts obtained were then compared to simulated data. The results for this case are the following:

5.2.1.7.1. 6 months of Production History – Fluid B

The first six months of historical data were used to generate the n and τ parameters for the YM-SEPD model. The same range of historical data were also used to generate the a and m parameters for the Modified Duong model. The results obtained are the following:

1. Plots and Parameters for YM-SEPD and YM-SEPD Hybrid Models: Figure 5-16 shows the Yu plot and Table 5-13 displays the parameters for the YM-SEPD and Arps' models.

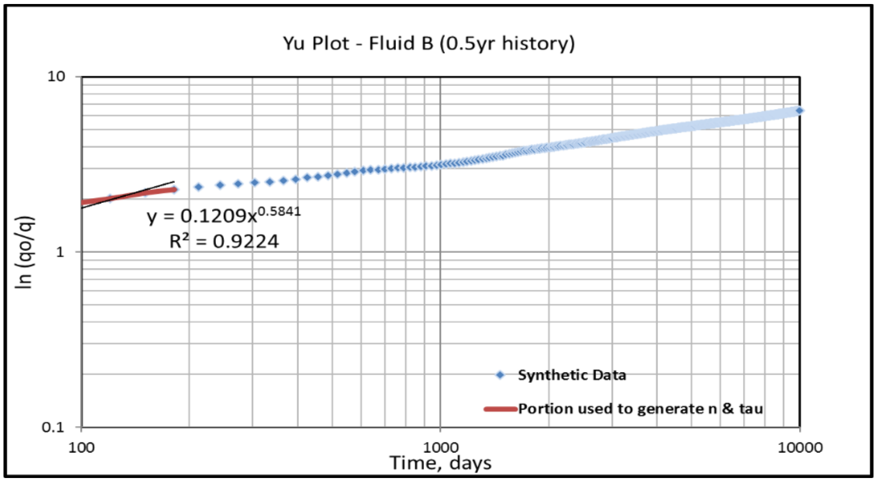

Figure 5-16 Yu Plot – Fluid B (0.5yr History)

Table 5-13 YM-SEPD and Arps Parameters – Fluid B (0.5yr History)

YM-SEPD Parameters – Fluid B (0.5yr history)		
n	0.584	
Intercept	0.121	
τ, days	37.23	
q_o, stb/d	5,306	
Arps Parameters – Fluid B (0.5yr history)		
	Arps	**Arps(1)**
t_{sw}, days	1,004	517
D_{sw}, 1/days	0.004	0.005
q_{sw}, stb/d	5.618	50.78
b	2.5	2.5

2. Plots and Parameters for Modified Duong and Modified Duong Hybrid Models: Figure 5-17 and Table 5-14 display the inverse MBT vs. time plot, oil rate vs. t(a,m) plot and parameters for the Modified Duong and Arps' models.

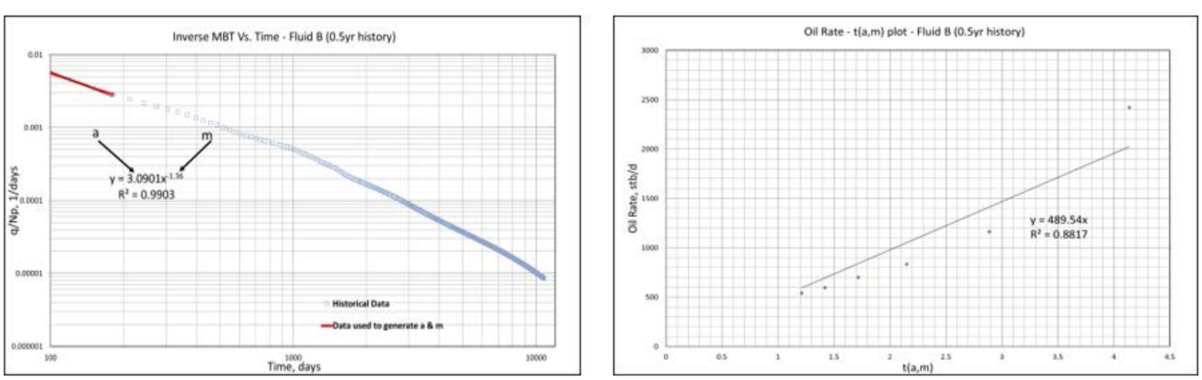

Figure 5-17 Inverse MBT vs. Time and Oil Rate vs. t(a,m) – Fluid B (0.5yr History)

Table 5-14 Modified Duong and Arps Parameters – Fluid B (0.5yr History)

Modified Duong Parameters – Fluid B (0.5yr history)		
a	3.090	
m	-1.360	
q_1, stb/d	489.5	
q_∞, stb/d	0	
Arps Parameters – Fluid B (0.5yr history)		
	Arps	**Arps(1)**
t_{sw}, days	1,004	517
D_{sw}, 1/days	0.035	0.06
q_{sw}, stb/d	106.1	215.8
b	0.9	0.85

5.2.1.7.2. 1 year of Production History – Fluid B

The first year of historical production data were used to generate the n and τ parameters for the YM-SEPD model. The same range of historical data were also used to generate the a and m parameters for the Modified Duong model. The results obtained are the following:

1. Plots and Parameters for YM-SEPD and YM-SEPD Hybrid Models: Figure 5-18 and Table 5-15 display the Yu plot and the parameters for the YM-SEPD and Arps' models.

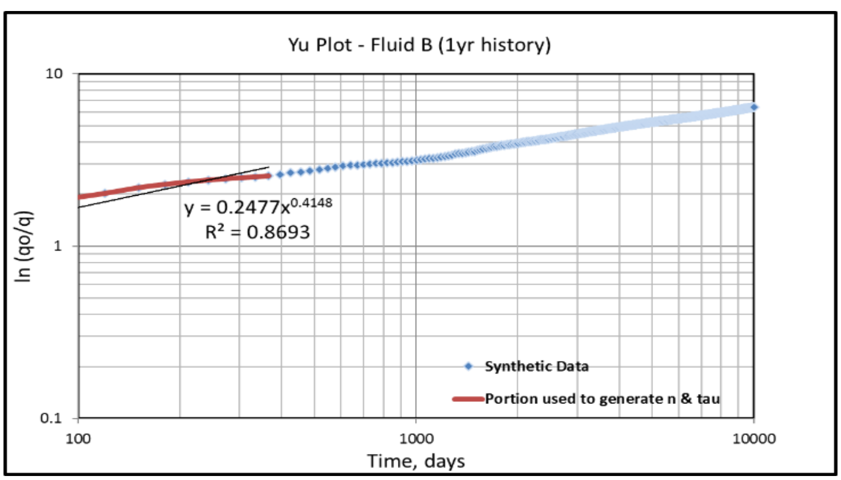

Figure 5-18 Yu Plot – Fluid B (1yr History)

Table 5-15 YM-SEPD and Arps Parameters – Fluid B (1yr History)

YM-SEPD Parameters – Fluid B (1yr history)		
n	0.415	
Intercept	0.248	
τ, days	28.92	
q_o, stb/d	5,306	
Arps Parameters – Fluid B (1yr history)		
	Arps	**Arps(1)**
t_{sw}, days	1,004	517
D_{sw}, 1/days	0.002	0.003
q_{sw}, stb/d	68.10	194.3
b	1.5	1.04

2. Plots and Parameters for Modified Duong and Modified Duong Hybrid Models: Figure 5-19 and Table 5-16 show the inverse MBT vs. time plot, oil rate vs. t(a,m) plot and parameters for the Modified Duong and Arps' models.

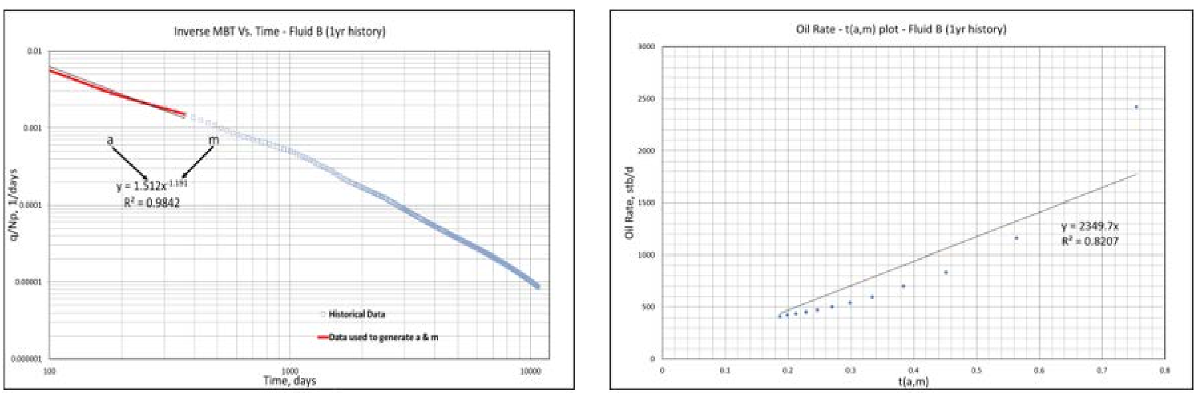

Figure 5-19 Inverse MBT vs. Time and Oil Rate vs. t(a,m) – Fluid B (1yr History)

Table 5-16 Modified Duong and Arps Parameters – Fluid B (1yr History)

Modified Duong Parameters – Fluid B (1yr history)		
a	1.512	
m	-1.191	
q_1, stb/d	2,350	
q_∞, stb/d	0	
Arps Parameters – Fluid B (1yr history)		
	Arps	**Arps(1)**
t_{sw}, days	1,004	517
D_{sw}, 1/days	0.021	0.035
q_{sw}, stb/d	206.9	342.6
b	0.85	0.9

5.2.1.7.3. 2 years of Production History – Fluid B

The first to second year of historical data were used to generate the n and τ parameters for the YM-SEPD model. The same range of historical data were also used to generate the a and m parameters for the Modified Duong model. The results obtained are the following:

1. Plots and Parameters for YM-SEPD and YM-SEPD Hybrid Models: Figure 5-20 and Table 5-17 show the Yu plot and the parameters for the YM-SEPD and Arps' models.

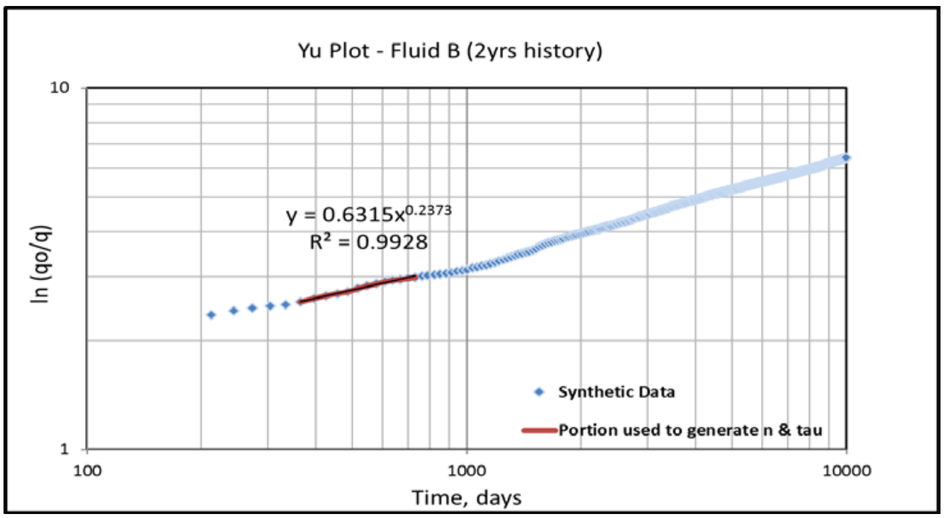

Figure 5-20 Yu Plot – Fluid B (2yrs History)

Table 5-17 YM-SEPD and Arps Parameters – Fluid B (2yrs History)

YM-SEPD Parameters – Fluid B (2yrs history)		
n	0.237	
Intercept	0.632	
τ, days	6.938	
q_o, stb/d	5,306	
Arps Parameters – Fluid B (2yrs history)		
	Arps	Arps(1)
t_{sw}, days	1,004	517
D_{sw}, 1/days	0.001	0.001
q_{sw}, stb/d	204.5	328.7
b	0.44	0.59

2. Plots and Parameters for Modified Duong and Modified Duong Hybrid Models: Figure 5-21 and Table 5-18 show the inverse MBT vs. time plot, oil rate vs. t(a,m) plot and parameters for the Modified Duong and Arps' models.

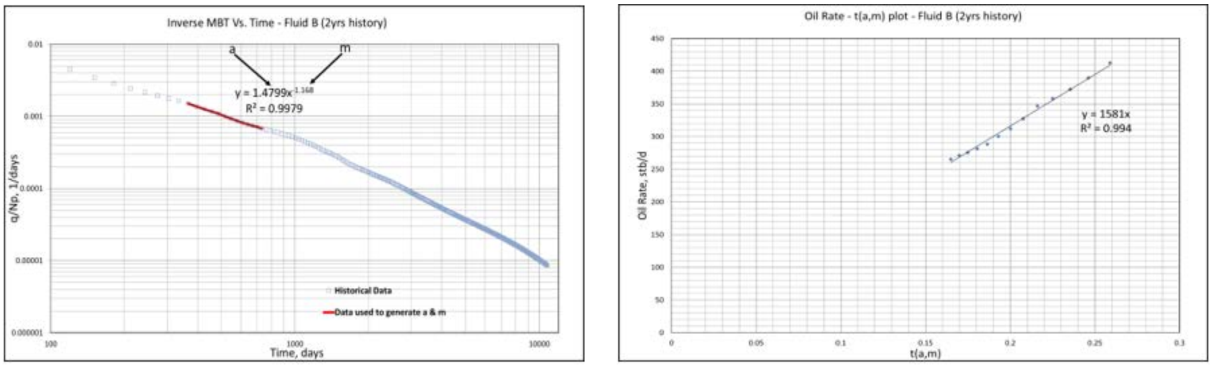

Figure 5-21 Inverse MBT vs. Time and Oil Rate vs. t(a,m) – Fluid B (2yrs History)

Table 5-18 Modified Duong and Arps Parameters – Fluid B (2yrs History)

Modified Duong Parameters – Fluid B (2yrs history)		
a	1.480	
m	-1.168	
q_1, stb/d	1,581	
q_∞, stb/d	0	
Arps Parameters – Fluid B (2yrs history)		
	Arps	Arps(1)
t_{sw}, days	1,004	517
D_{sw}, 1/days	0.018	0.03
q_{sw}, stb/d	209.3	328.1
b	0.85	0.9

5.2.1.7.4. 3 years of Production History – Fluid B

The second to third year of historical data were used to generate the n and τ parameters for the YM-SEPD model. The same range of historical data were also used to generate the a and m parameters for the Modified Duong model. The results obtained are the following:

1. Plots and Parameters for YM-SEPD and YM-SEPD Hybrid Models: Figure 5-22 and Table 5-19 show the Yu plot and the parameters for the YM-SEPD and Arps' models.

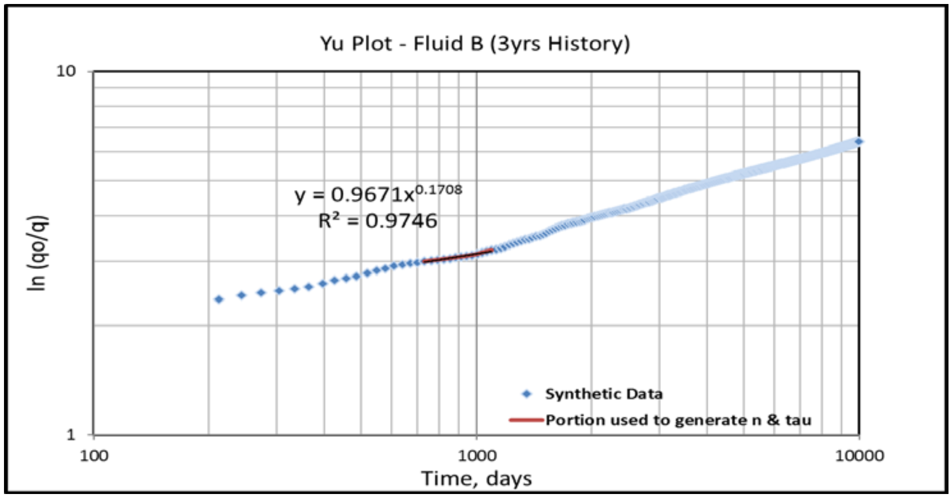

Figure 5-22 Yu Plot – Fluid B (3yrs History)

Table 5-19 YM-SEPD and Arps Parameters – Fluid B (3yrs History)

YM-SEPD Parameters – Fluid B (3yrs history)		
n	0.171	
Intercept	0.967	
τ, days	1.216	
q_o, stb/d	5,306	
Arps Parameters – Fluid B (3yrs history)		
	Arps	**Arps(1)**
t_{sw}, days	1,004	517
D_{sw}, 1/days	0.001	0.001
q_{sw}, stb/d	227.6	319.0
b	0.24	0.45

2. Plots and Parameters for Modified Duong and Modified Duong Hybrid Models: Figure 5-23 and Table 5-20 display the inverse MBT vs. time plot, oil rate vs. t(a,m) plot and parameters for the Modified Duong and Arps' models.

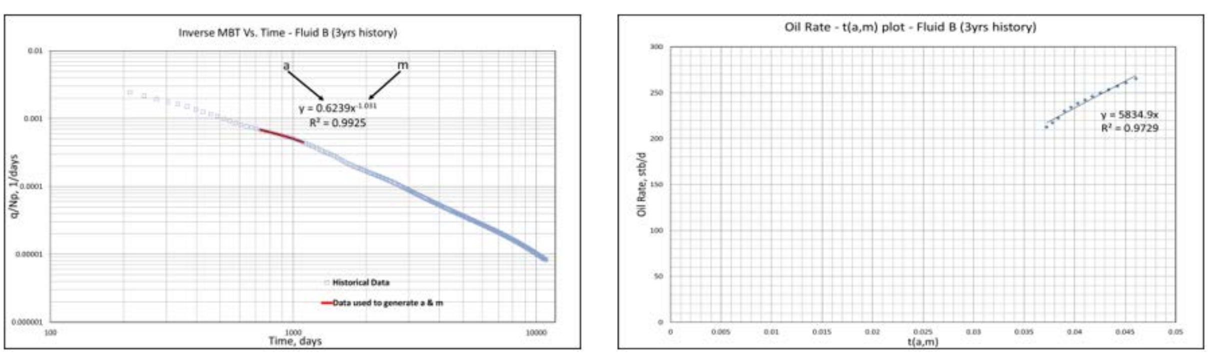

Figure 5-23 Inverse MBT vs. Time and Oil Rate vs. t(a,m) – Fluid B (3yrs History)

Table 5-20 Modified Duong and Arps Parameters – Fluid B (3yrs History)

Modified Duong Parameters – Fluid B (3yrs history)		
a	0.624	
m	-1.031	
q_1, stb/d	5,835	
q_∞, stb/d	0	
Arps Parameters – Fluid B (3yrs history)		
	Arps	**Arps(1)**
t_{sw}, days	1,004	517
D_{sw}, 1/days	0.012	0.021
q_{sw}, stb/d	227.5	321.7
b	0.8	0.95

Graphical production forecast results for all Fluid B cases are shown in Figure 5-24. It can be seen from the graphs that the YM-SEPD hybrid models provide reasonable results with production histories of 2 years or more and seriously underestimate production with availability of less than 2 years of historical data. The Modified Duong and its hybrid variants overestimated production in most cases, whereas the Principal Components Methodology (PCM) provided consistently good forecasts in all cases.

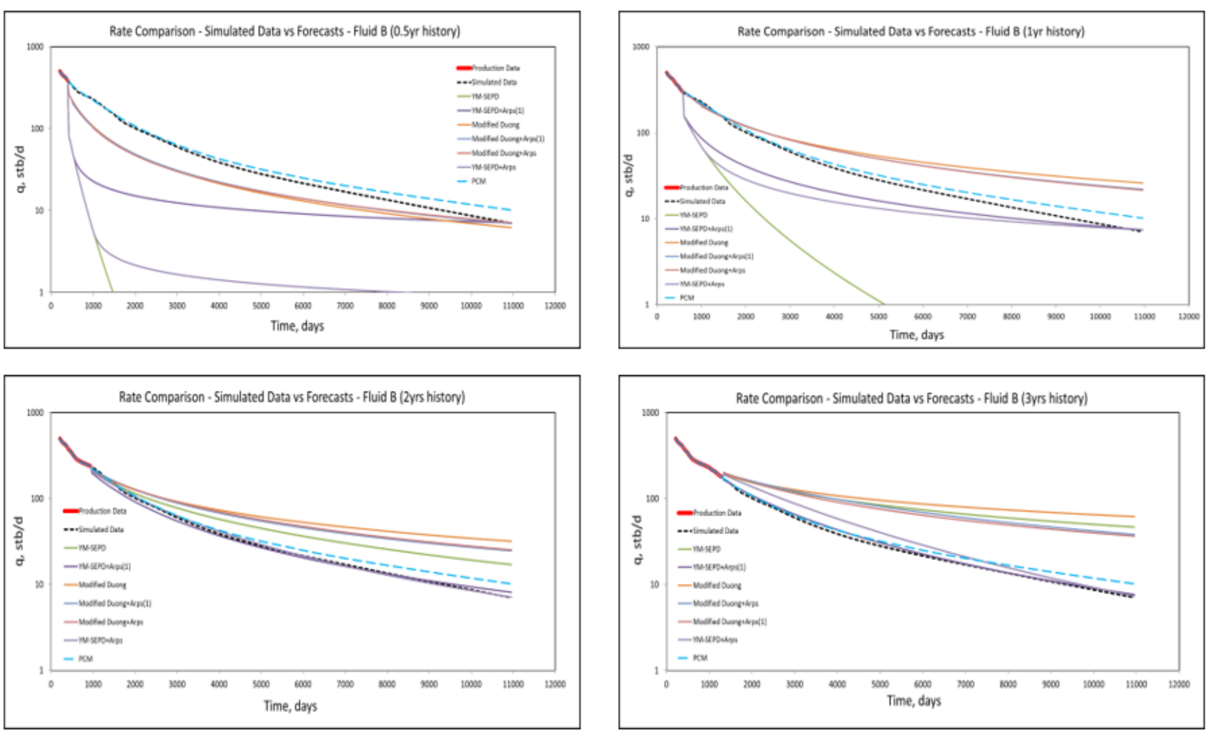

Figure 5-24 Rate Comparisons: Simulated Data vs. Forecasts – Fluid B (All Cases)

Table 5-21 shows the absolute errors, percentage errors and forecasts for all the models. Figures in red indicate the lowest percentage errors.

Table 5-21 Forecasts, Errors and Percentage Errors – Fluid B

Cumulative Oil Production Forecast Errors – Fluid B	Forecast, STB				Error (absolute value), STB				Percentage Error, %			
Matched Production Data	0.5 yr.	1 yr.	2 yrs.	3 yrs.	0.5 yr.	1 yr.	2 yrs.	3 yrs.	0.5 yr.	1 yr.	2 yrs.	3 yrs.
Simulated Data	18,690	16,674	13,545	11,088	0	0	0	0	-	-	-	-
YM-SEPD	604	3,097	17,629	26,866	-18,086	-13,577	+4,084	+15,778	-2,994	-438.4	+23.2	+58.7
YM-SEPD + Arps(1)	4,105	7,948	12,376	11,755	-14,585	-8,726	-1,169	+667	-355.3	-109.8	-9.5	+5.7
YM-SEPD + Arps	1,012	6,477	13,522	14,822	-17,678	-10,197	-23	+3,734	-1,747	-157.4	-0.2	+25.2
Modified Duong	10,175	23,172	22,526	30,453	-8,515	+6,498	+8,981	+19,365	-83.7	+28.0	+39.9	+63.6
Modified Duong + Arps(1)	10,292	22,385	20,802	24,561	-8,398	+5,711	+7,257	+13,473	-81.6	+25.5	+34.9	+54.9
Modified Duong + Arps	10,297	22,101	21,163	25,943	-8,393	+5,427	+7,618	+14,855	-81.5	+24.6	+36.0	+57.3
PCM	19,839	17,781	14,582	12,202	+1,149	+1,107	+1,037	+1,114	+5.8	+6.2	+7.1	+9.1

5.2.1.8. Results – Fluid C Case

Hybrid DCA models and PCM were applied to Fluid C cases for wells with production histories ranging from 0.5 to 3 yrs. The production forecasts obtained were then compared to simulated data. The results for this case are the following:

5.2.1.8.1. 6 months of Production History – Fluid C

The first six months of historical data were used to generate the n and τ parameters for the YM-SEPD model. The same range of historical data were also used to generate the a and m parameters for the Modified Duong model. The results obtained are the following:

1. Plots and Parameters for YM-SEPD and YM-SEPD Hybrid Models: Figure 5-25 shows the Yu plot and Table 5-22 shows the parameters for the YM-SEPD and Arps' models.

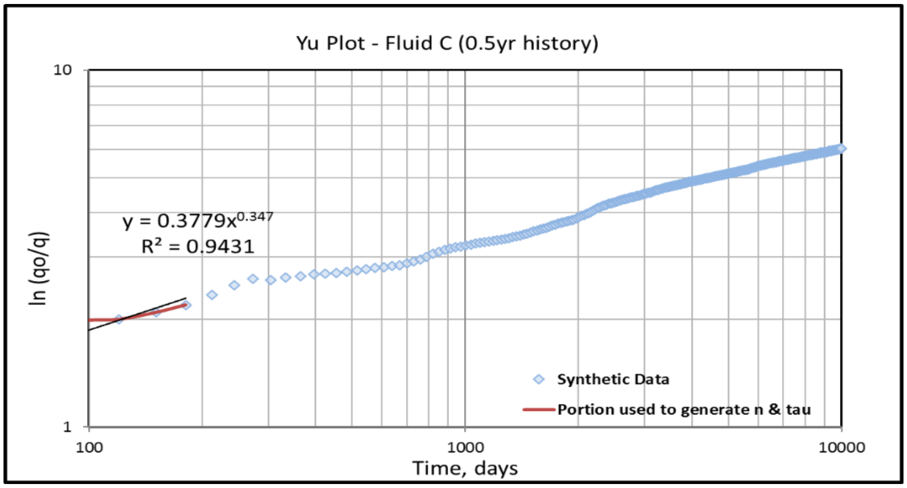

Figure 5-25 Yu Plot – Fluid C (0.5yr History)

Table 5-22 YM-SEPD and Arps Parameters – Fluid C (0.5yr History)

YM-SEPD Parameters – Fluid C (0.5yr history)		
n	0.347	
Intercept	0.378	
τ, days	16.52	
q_o, stb/d	4,462	
Arps Parameters – Fluid C (0.5yr history)		
	Arps	Arps(1)
t_{sw}, days	1,308	699
D_{sw}, 1/days	0.001	0.002
q_{sw}, stb/d	46.74	113.9
b	1.9	0.9

2. Plots and Parameters for Modified Duong and Modified Duong Hybrid Models: Figure 5-26 and Table 5-23 display the inverse MBT vs. time plot, oil rate vs. t(a,m) plot and parameters for the Modified Duong and Arps' models.

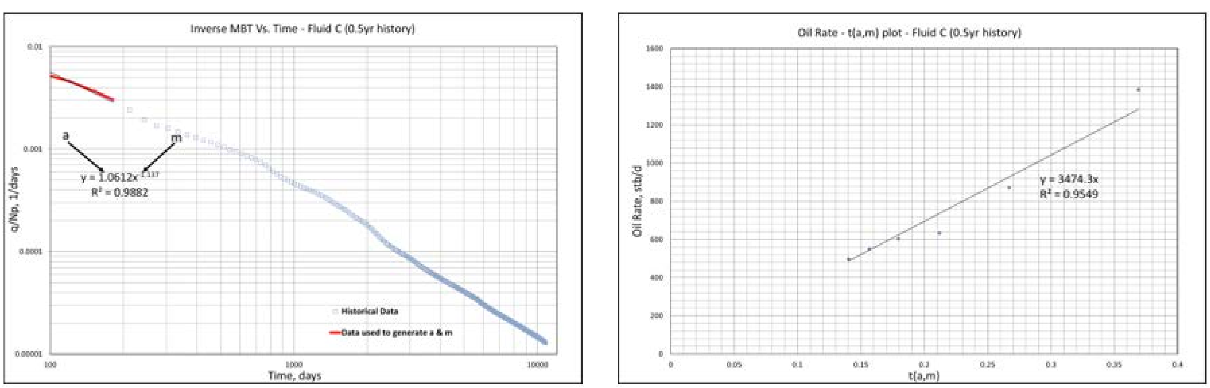

Figure 5-26 Inverse MBT vs. Time and Oil Rate vs. t(a,m) – Fluid C (0.5yr History)

Table 5-23 Modified Duong and Arps Parameters – Fluid C (0.5yr History)

Modified Duong Parameters – Fluid C (0.5yr history)		
a	1.061	
m	-1.137	
q_1, stb/d	3,474	
q_∞, stb/d	0	
Arps Parameters – Fluid C (0.5yr history)		
	Arps	**Arps(1)**
t_{sw}, days	1,308	699
D_{sw}, 1/days	0.013	0.026
q_{sw}, stb/d	126.7	199.2
b	0.5	0.98

5.2.1.8.2. 1 year of Production History – Fluid C

The first year of historical production data were used to generate the n and τ parameters for the YM-SEPD model. The same range of historical data were also used to generate the a and m parameters for the Modified Duong model. The results obtained are the following:

1. Plots and Parameters for YM-SEPD and YM-SEPD Hybrid Models: Figure 5-26 and Table 5-24 show the Yu plot and the parameters for the YM-SEPD and Arps' models.

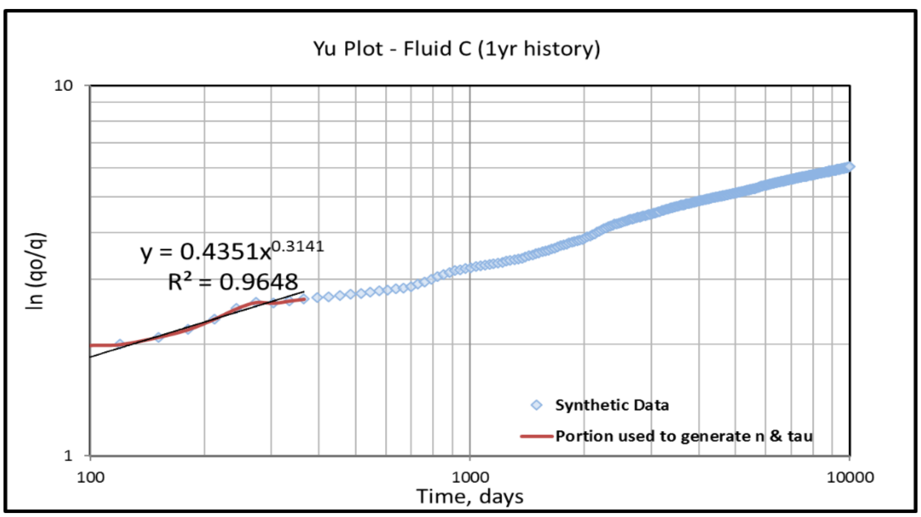

Figure 5-27 Yu Plot – Fluid C (1yr History)

Table 5-24 YM-SEPD and Arps Parameters – Fluid C (1yr History)

YM-SEPD Parameters – Fluid C (1yr history)		
n	0.314	
Intercept	0.435	
τ, days	14.15	
q_o, stb/d	4,462	
Arps Parameters – Fluid C (1yr history)		
	Arps	**Arps(1)**
t_{sw}, days	1,308	699
D_{sw}, 1/days	0.001	0.002
q_{sw}, stb/d	70.70	148.3
b	1.25	1.05

2. Plots and Parameters for Modified Duong and Modified Duong Hybrid Models: Figure 5-28 and Table 5-25 display the inverse MBT vs. time plot, oil rate vs. t(a,m) plot and parameters for the Modified Duong and Arps' models.

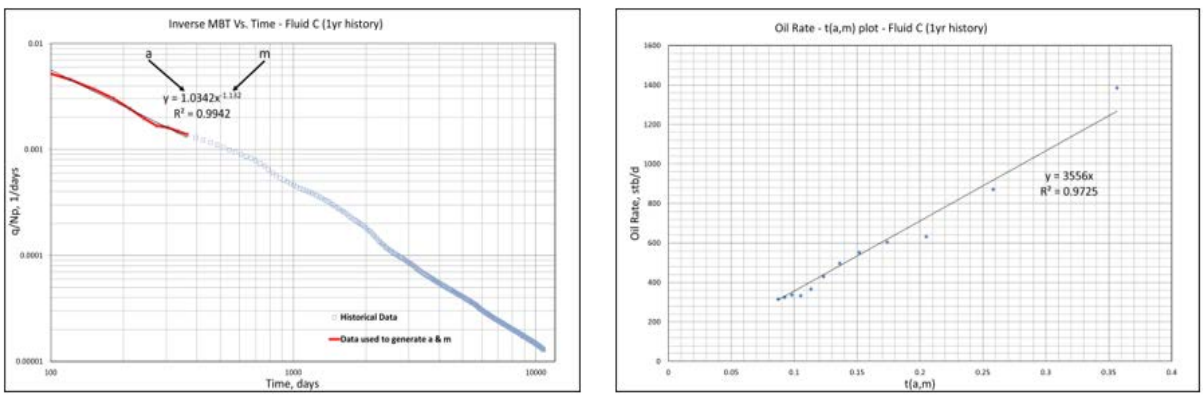

Figure 5-28 Inverse MBT vs. Time and Oil Rate vs. t(a,m) – Fluid C (1yr History)

Table 5-25 Modified Duong and Arps Parameters – Fluid C (1yr History)

Modified Duong Parameters – Fluid C (1yr history)		
a	1.034	
m	-1.132	
q_1, stb/d	3,556	
q_∞, stb/d	0	
Arps Parameters – Fluid C (1yr history)		
	Arps	**Arps(1)**
t_{sw}, days	1,308	699
D_{sw}, 1/days	0.013	0.025
q_{sw}, stb/d	127.7	199.7
b	0.5	0.98

5.2.1.8.3. 2 years of Production History – Fluid C

The first to second year of historical data were used to generate the n and τ parameters for the YM-SEPD model. The same range of historical data were also used to generate the a and m parameters for the Modified Duong model. The results obtained are the following:

1. Plots and Parameters for YM-SEPD and YM-SEPD Hybrid Models: Figure 5-29 and Table 5-26 show the Yu plot and the parameters for the YM-SEPD and Arps' models.

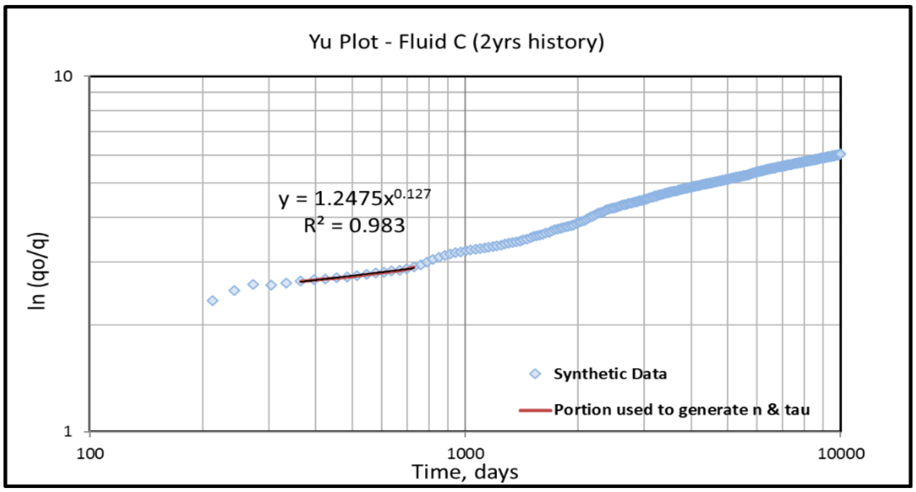

Figure 5-29 Yu Plot – Fluid C (2yrs History)

Table 5-26 YM-SEPD and Arps Parameters – Fluid C (2yrs History)

YM-SEPD Parameters – Fluid C (2yrs history)		
n	0.127	
Intercept	1.248	
τ, days	0.175	
q_o, stb/d	4,462	
Arps Parameters – Fluid C (2yrs history)		
	Arps	Arps(1)
t_{sw}, days	1,308	699
D_{sw}, 1/days	0.0003	0.001
q_{sw}, stb/d	200.3	254.0
b	0.01	0.3

2. Plots and Parameters for Modified Duong and Modified Duong Hybrid Models: Figure 5-30 and Table 5-27 display the inverse MBT vs. time plot, oil rate vs. t(a,m) plot and parameters for the Modified Duong and Arps' models.

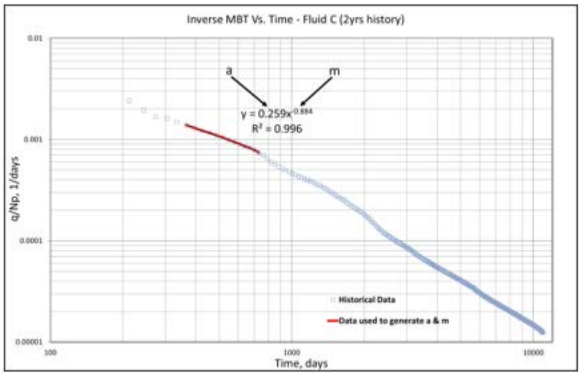

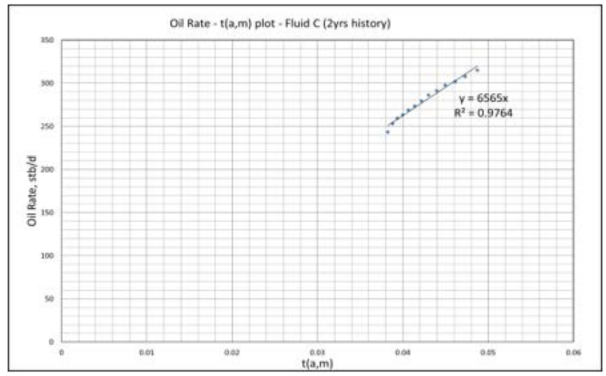

Figure 5-30 Inverse MBT vs. Time and Oil Rate vs. t(a,m) – Fluid C (2yrs History)

Table 5-27 Modified Duong and Arps Parameters – Fluid C (2yrs History)

Modified Duong Parameters – Fluid C (2yrs history)		
a	0.259	
m	-0.884	
q_1, stb/d	6,565	
q_∞, stb/d	0	
Arps Parameters – Fluid C (2yrs history)		
	Arps	**Arps(1)**
t_{sw}, days	1,308	699
D_{sw}, 1/days	0.004	0.008
q_{sw}, stb/d	209.8	254.7
b	0.5	0.98

5.2.1.8.4. 3 years of Production History – Fluid C

The second to third year of historical data were used to generate the n and τ parameters for the YM-SEPD model. The same range of historical data were also used to generate the a and m parameters for the Modified Duong model. The results obtained are the following:

1. Plots and Parameters for YM-SEPD and YM-SEPD Hybrid Models: Figure 5-31 and Table 5-28 show the Yu plot and the parameters for the YM-SEPD and Arps' models.

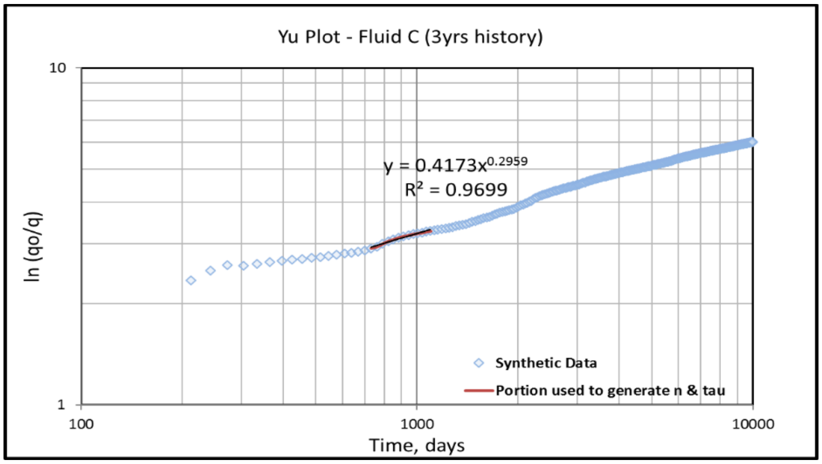

Figure 5-31 Yu Plot – Fluid C (3yrs History)

Table 5-28 YM-SEPD and Arps Parameters – Fluid C (3yrs History)

YM-SEPD Parameters – Fluid C (3yrs history)		
n	0.296	
Intercept	0.417	
τ, days	19.17	
q_o, stb/d	4,462	
Arps Parameters – Fluid C (3yrs history)		
	Arps	**Arps(1)**
t_{sw}, days	1,308	699
D_{sw}, 1/days	0.001	0.001
q_{sw}, stb/d	136.3	246.0
b	0.7	0.7

2. Plots and Parameters for Modified Duong and Modified Duong Hybrid Models: Figure 5-32 and Table 5-29 show the inverse MBT vs. time plot, oil rate vs. t(a,m) plot and parameters for the Modified Duong and Arps' models.

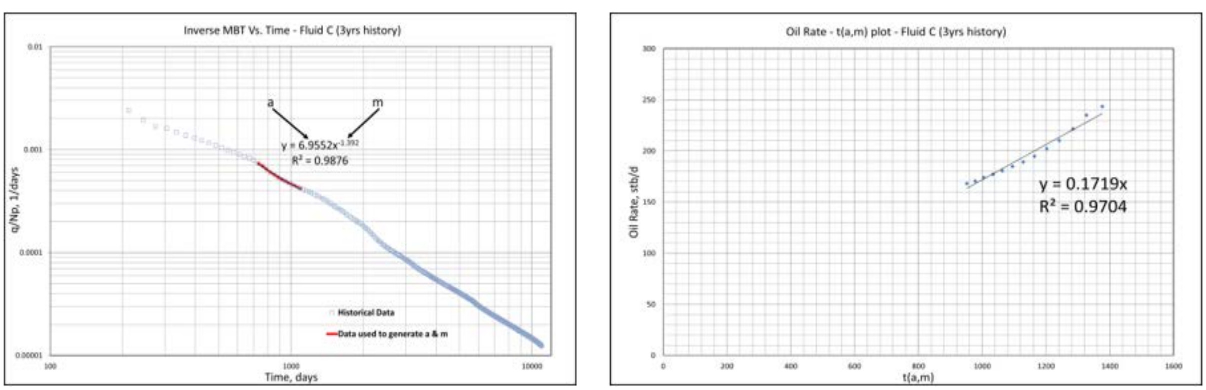

Figure 5-32 Inverse MBT vs. Time and Oil Rate vs. t(a,m) – Fluid C (3yrs History)

Table 5-29 Modified Duong and Arps Parameters – Fluid C (3yrs History)

Modified Duong Parameters – Fluid C (3yrs history)		
a	6.955	
m	-1.392	
q_1, stb/d	0.172	
q_∞, stb/d	0	
Arps Parameters – Fluid C (3yrs history)		
	Arps	**Arps(1)**
t_{sw}, days	1,308	699
D_{sw}, 1/days	0.02	0.04
q_{sw}, stb/d	138.1	245.6
b	0.65	0.98

Graphical production forecast results for all Fluid C cases are shown in Figure 5-33. Here, the YM-SEPD hybrid models provide reasonable results with 3 years of production history and underestimates production or forecasts inaccurately with availability of less than 3 years of historical data. The Modified Duong and its hybrid variants seriously overestimated production with less than 3 years of production history. Forecasts were however reasonable with 3 years of historical data. The PCM provided consistently good forecasts in all cases.

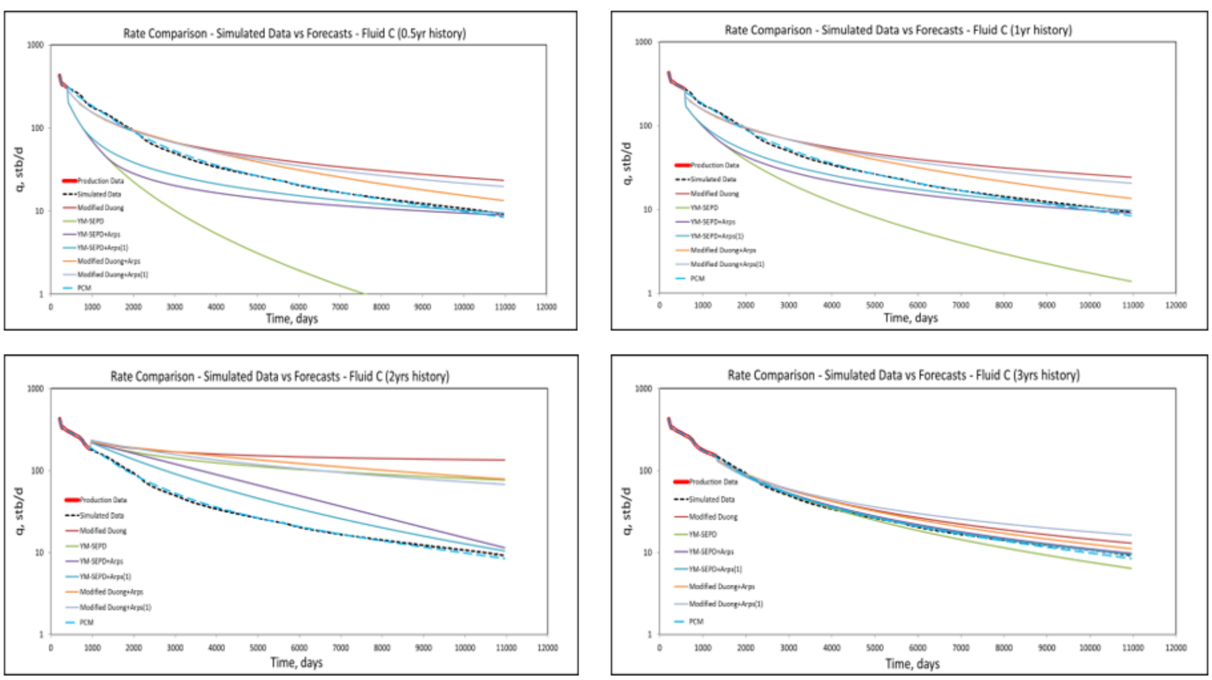

Figure 5-33 Rate Comparisons: Simulated Data vs. Forecasts – Fluid C (All Cases)

Table 5-30 displays the absolute errors, percentage errors and forecasts for all the models. Figures in red indicate the lowest percentage errors.

Table 5-30 Forecasts, Errors and Percentage Errors – Fluid C

Cumulative Oil Production Forecast Errors – Fluid C	Forecast, STB				Error (absolute value), STB				Percentage Error, %			
Matched Production Data	0.5 yr.	1 yr.	2 yrs.	3 yrs.	0.5 yr.	1 yr.	2 yrs.	3 yrs.	0.5 yr.	1 yr.	2 yrs.	3 yrs.
Simulated Data	16,572	14,842	12,115	10,135	0	0	0	0	-	-	-	-
YM-SEPD	4,787	6,276	37,841	9,428	-11,785	-8,566	+25,726	-707	-246.2	-136.5	+68.0	-7.5
YM-SEPD + Arps(1)	9,064	9,862	18,416	10,018	-7,508	-4,980	+6,301	-117	-82.8	-50.4	+34.2	-1.2
YM-SEPD + Arps	7,782	8,867	23,214	10,273	-8,790	-5,975	+11,099	+138	-113.0	-67.4	+47.8	+1.3
Modified Duong	20,202	18,987	51,037	11,676	+3,630	+4,145	+38,922	+1,541	+18.0	+21.8	+76.3	+13.2
Modified Duong + Arps(1)	19,356	18,301	39,208	12,401	+2,784	+3,459	+27,093	+2,266	+14.4	+18.9	+69.1	+18.3
Modified Duong + Arps	18,404	17,005	43,120	11,351	+1,832	+2,163	+31,005	+1,216	+10.0	+12.7	+71.9	+10.7
PCM	16,619	14,771	12,179	10,173	+47	-71	+64	+38	+0.3	-0.5	+0.5	+0.4

5.2.1.9. Results – Fluid D Case

PCM and hybrid (combination) DCA models were applied to Fluid D cases for wells with production histories ranging from 0.5 to 3 yrs. The production forecasts obtained were then compared to simulated data. The results for this case are the following:

5.2.1.9.1. 6 months of Production History – Fluid D

The first six months of historical data were used to generate the n and τ parameters for the YM-SEPD model. The same range of historical data were also used to generate the a and m parameters for the Modified Duong model. The results obtained are the following:

1. Plots and Parameters for YM-SEPD and YM-SEPD Hybrid Models: Figure 5-34 and Table 5-31 display the Yu plot and the parameters for the YM-SEPD and Arps' models.

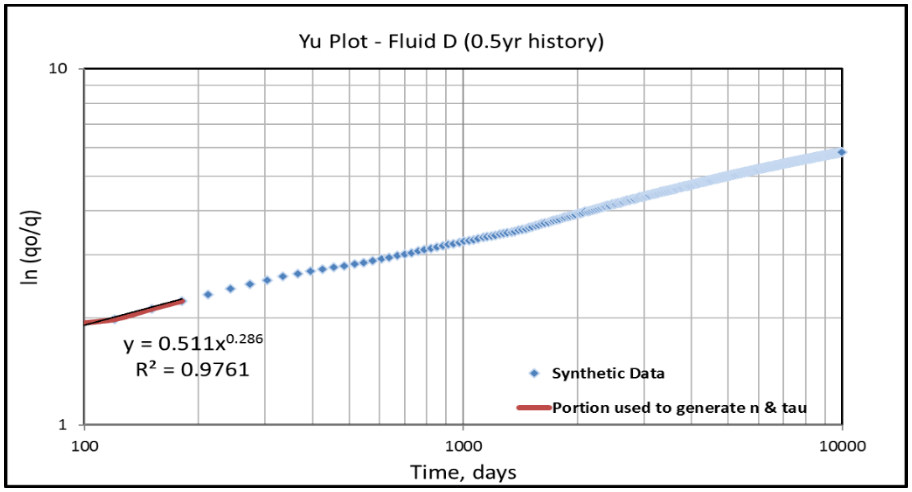

Figure 5-34 Yu Plot – Fluid D (0.5yr History)

Table 5-31 YM-SEPD and Arps Parameters – Fluid D (0.5yr History)

YM-SEPD Parameters – Fluid D (0.5yr history)		
n	0.286	
Intercept	0.511	
τ, days	10.46	
q_o, stb/d	6,244	
Arps Parameters – Fluid D (0.5yr history)		
	Arps	**Arps(1)**
t_{sw}, days	1,400	212
D_{sw}, 1/days	0.001	0.003
q_{sw}, stb/d	108.0	586.9
b	1.3	1

2. Plots and Parameters for Modified Duong and Modified Duong Hybrid Models: Figure 5-35 and Table 5-32 show the inverse MBT vs. time plot, oil rate vs. t(a,m) plot and parameters for the Modified Duong and Arps' models.

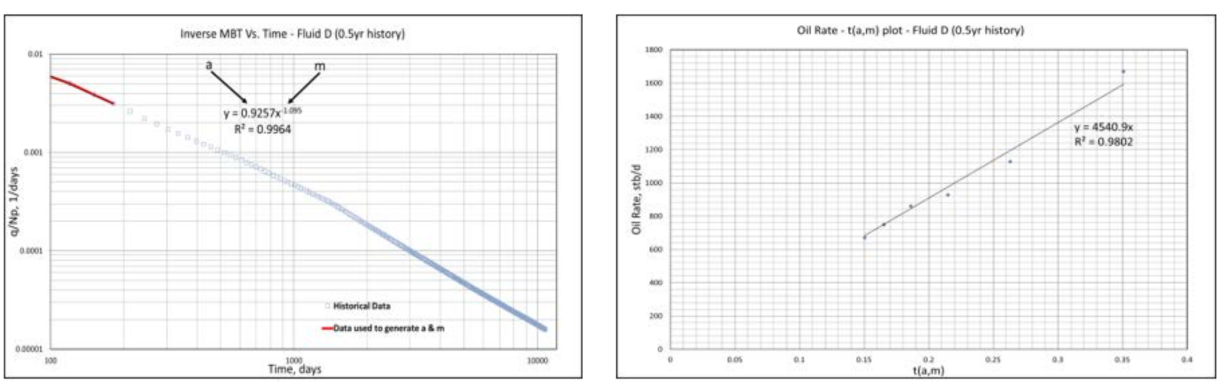

Figure 5-35 Inverse MBT vs. Time and Oil Rate vs. t(a,m) – Fluid D (0.5yr History)

Table 5-32 Modified Duong and Arps Parameters – Fluid D (0.5yr History)

Modified Duong Parameters – Fluid D (0.5yr history)		
a	0.926	
m	-1.095	
q_1, stb/d	4,541	
q_∞, stb/d	0	
Arps Parameters – Fluid D (0.5yr history)		
	Arps	Arps(1)
t_{sw}, days	1,400	212
D_{sw}, 1/days	0.012	0.045
q_{sw}, stb/d	207.8	627.5
b	0.95	0.9

5.2.1.9.2. 1 year of Production History – Fluid D

The first year of historical production data were used to generate the n and τ parameters for the YM-SEPD model. The same range of historical data were also used to generate the a and m parameters for the Modified Duong model. The results obtained are the following:

1. Plots and Parameters for YM-SEPD and YM-SEPD Hybrid Models: Figure 5-36 and Table 5-33 show the Yu plot and the parameters for the YM-SEPD and Arps' models.

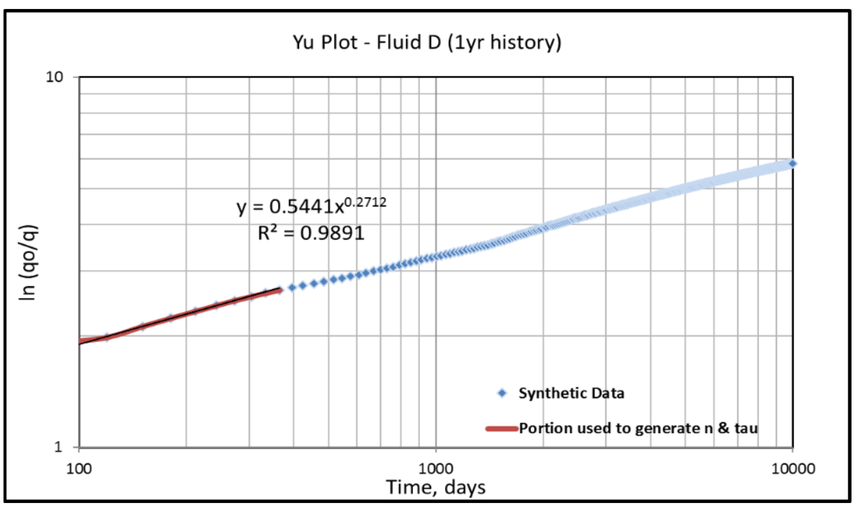

Figure 5-36 Yu Plot – Fluid D (1yr History)

Table 5-33 YM-SEPD and Arps Parameters – Fluid D (1yr History)

YM-SEPD Parameters – Fluid D (1yr history)		
n	0.271	
Intercept	0.544	
τ, days	9.43	
q_0, stb/d	6,244	
Arps Parameters – Fluid D (1yr history)		
	Arps	**Arps(1)**
t_{sw}, days	1,400	212
D_{sw}, 1/days	0.001	0.003
q_{sw}, stb/d	128.9	610.1
b	1.3	0.95

2. Plots and Parameters for Modified Duong and Modified Duong Hybrid Models: Figure 5-37 and Table 5-34 show the inverse MBT vs. time plot, oil rate vs. t(a,m) plot and parameters for the Modified Duong and Arps' models.

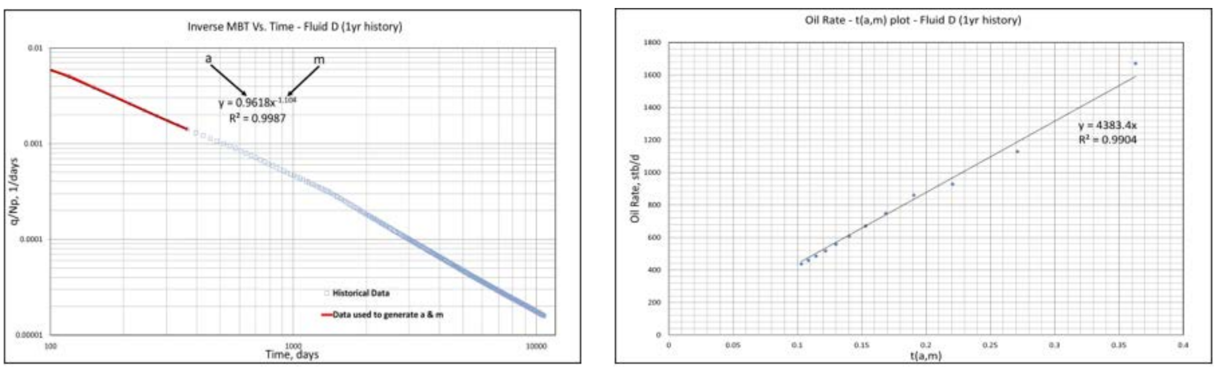

Figure 5-37 Inverse MBT vs. Time and Oil Rate vs. t(a,m) – Fluid D (1yr History)

Table 5-34 Modified Duong and Arps Parameters – Fluid D (1yr History)

Modified Duong Parameters – Fluid D (1yr history)		
a	0.962	
m	-1.104	
q_1, stb/d	4,383	
q_∞, stb/d	0	
Arps Parameters – Fluid D (1yr history)		
	Arps	**Arps(1)**
t_{sw}, days	1,400	212
D_{sw}, 1/days	0.012	0.05
q_{sw}, stb/d	196.8	615.2
b	0.85	0.9

5.2.1.9.3. 2 years of Production History – Fluid D

The first to second year of historical data were used to generate the n and τ parameters for the YM-SEPD model. The same range of historical data were also used to generate the a and m parameters for the Modified Duong model. The results obtained are the following:

1. Plots and Parameters for YM-SEPD and YM-SEPD Hybrid Models: Figure 5-38 and Table 5-35 show the Yu plot and the parameters for the YM-SEPD and Arps' models.

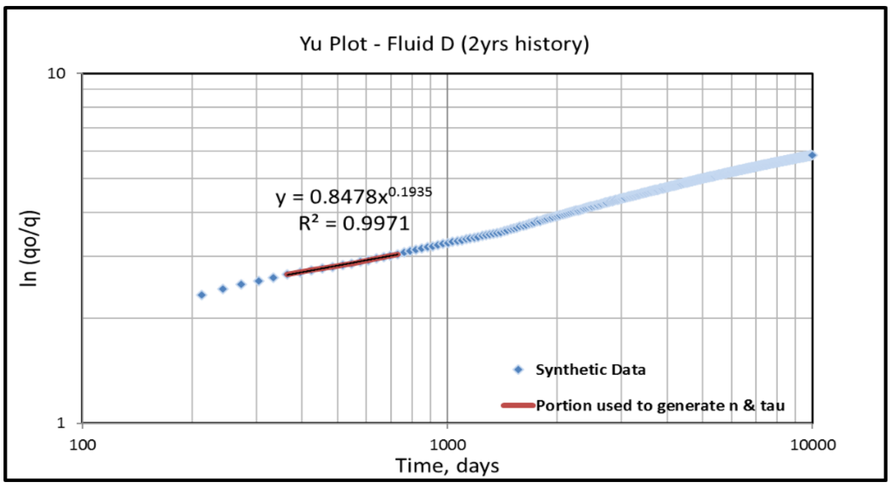

Figure 5-38 Yu Plot – Fluid D (2yrs History)

Table 5-35 YM-SEPD and Arps Parameters – Fluid D (2yrs History)

YM-SEPD Parameters – Fluid D (2yrs history)		
n	0.194	
Intercept	0.848	
τ, days	2.35	
q_o, stb/d	6,244	
Arps Parameters – Fluid D (2yrs history)		
	Arps	Arps(1)
t_{sw}, days	1,400	212
D_{sw}, 1/days	0.001	0.002
q_{sw}, stb/d	199.4	572.1
b	0.43	0.87

2. Plots and Parameters for Modified Duong and Modified Duong Hybrid Models: Figure 5-39 and Table 5-36 show the inverse MBT vs. time plot, oil rate vs. t(a,m) plot and parameters for the Modified Duong and Arps' models.

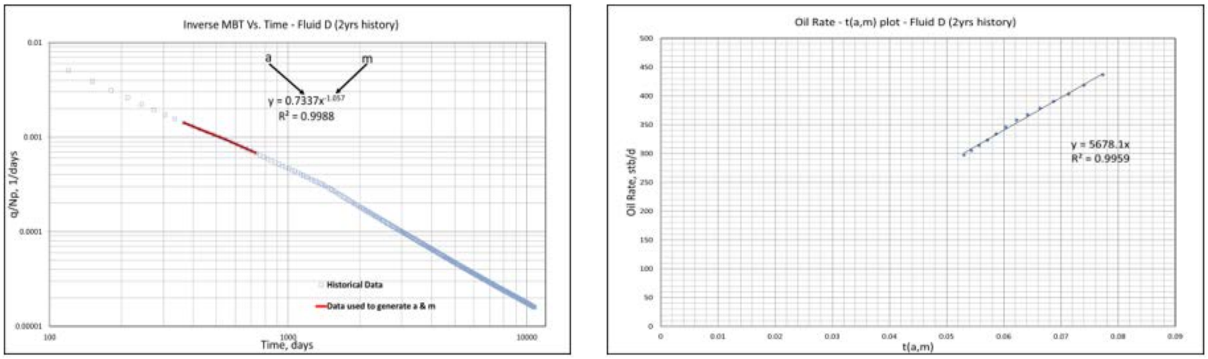

Figure 5-39 Inverse MBT vs. Time and Oil Rate vs. t(a,m) – Fluid D (2yrs History)

Table 5-36 Modified Duong and Arps Parameters – Fluid D (2yrs History)

Modified Duong Parameters – Fluid D (2yrs history)		
a	0.734	
m	-1.057	
q_1, stb/d	5,678	
q_∞, stb/d	0	
Arps Parameters – Fluid D (2yrs history)		
	Arps	Arps(1)
t_{sw}, days	1,400	212
D_{sw}, 1/days	0.01	0.045
q_{sw}, stb/d	208.9	583.6
b	0.85	0.9

5.2.1.9.4. 3 years of Production History – Fluid D

The second to third year of historical data were used to generate the n and τ parameters for the YM-SEPD model. The same range of historical data were also used to generate the a and m parameters for the Modified Duong model. The results obtained are the following:

1. Plots and Parameters for YM-SEPD and YM-SEPD Hybrid Models: Figure 5-40 and Table 5-37 show the Yu plot and the parameters for the YM-SEPD and Arps' models.

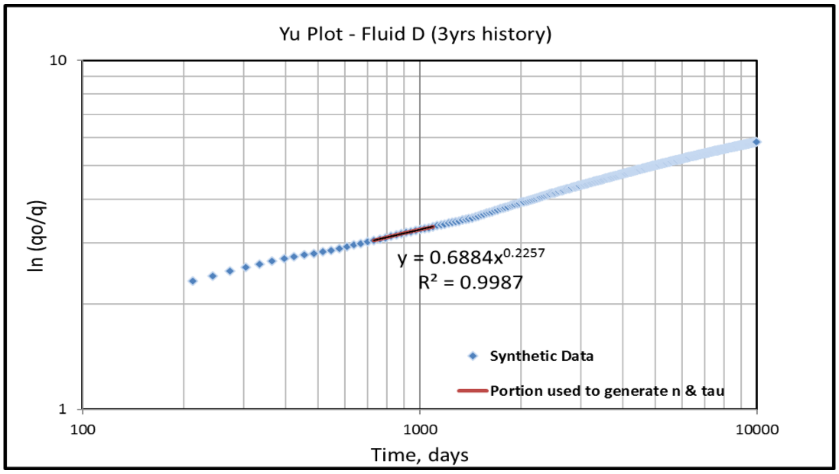

Figure 5-40 Yu Plot – Fluid D (3yrs History)

Table 5-37 YM-SEPD and Arps Parameters – Fluid D (3yrs History)

YM-SEPD Parameters – Fluid D (3yrs history)		
n	0.226	
Intercept	0.688	
τ, days	5.23	
q_o, stb/d	6,244	
Arps Parameters – Fluid D (3yrs history)		
	Arps	**Arps(1)**
t_{sw}, days	1,400	212
D_{sw}, 1/days	0.001	0.003
q_{sw}, stb/d	182.8	622.2
b	0.55	0.9

2. Plots and Parameters for Modified Duong and Modified Duong Hybrid Models: Figure 5-41 and Table 5-38 show the inverse MBT vs. time plot, oil rate vs. t(a,m) plot and parameters for the Modified Duong and Arps' models.

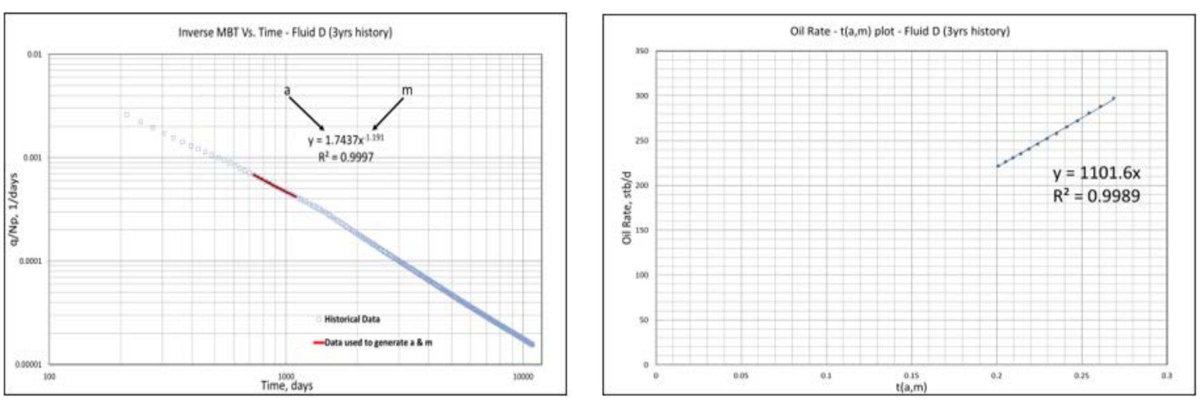

Figure 5-41 Inverse MBT vs. Time and Oil Rate vs. t(a,m) – Fluid D (3yrs History)

Table 5-38 Modified Duong and Arps Parameters – Fluid D (3yrs History)

Modified Duong Parameters – Fluid D (3yrs history)		
a	1.744	
m	-1.191	
q_1, stb/d	1,102	
q_∞, stb/d	0	
Arps Parameters – Fluid D (3yrs history)		
	Arps	**Arps(1)**
t_{sw}, days	1,400	212
D_{sw}, 1/days	0.014	0.061
q_{sw}, stb/d	184.5	647.0
b	0.75	0.98

Graphical production forecast results for all Fluid D cases are shown in Figure 5-42. It can be seen from the graphs that the YM-SEPD hybrid models provide reasonable results with production histories of 2 years or more and seriously underestimate production with availability of less than 2 years of historical data. The Modified Duong and its hybrid variants overestimated production and the Principal Components Methodology (PCM) provided consistently reasonable forecasts in all cases.

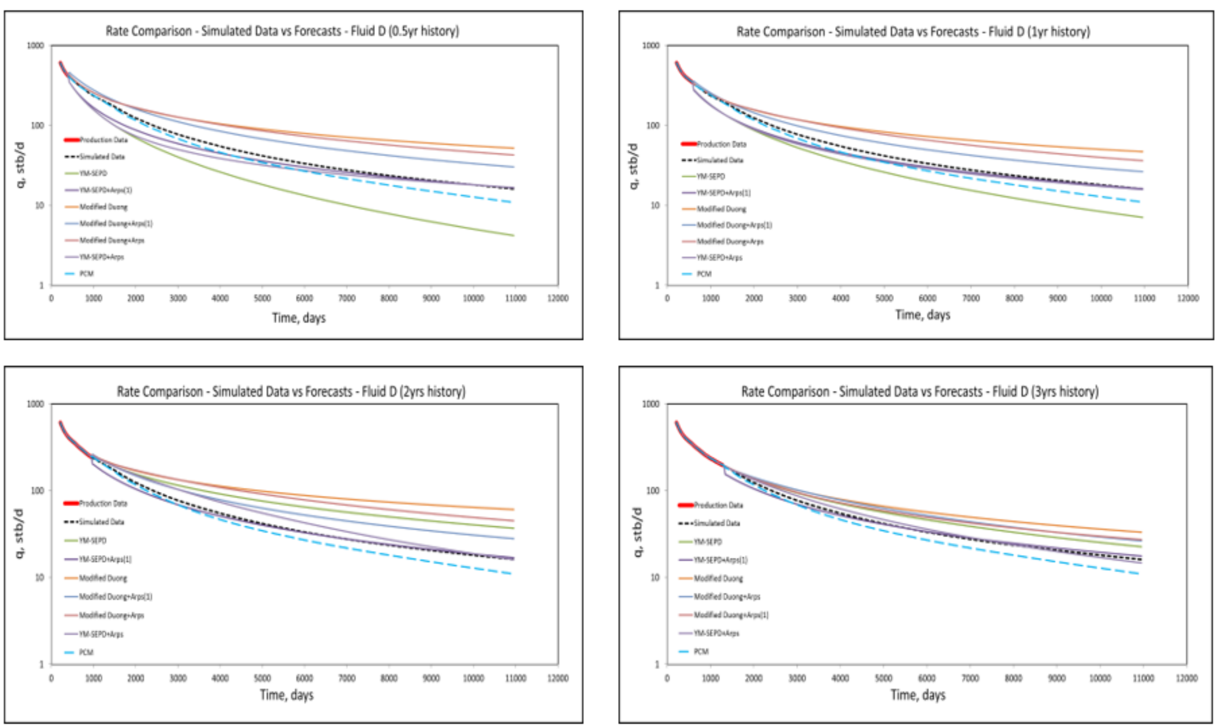

Figure 5-42 Rate Comparisons: Simulated Data vs. Forecasts – Fluid D (All Cases)

Table 5-39 shows the absolute errors, percentage errors and forecasts for all the models. Figures in red indicate the lowest percentage errors.

Table 5-39 Forecasts, Errors and Percentage Errors – Fluid D

Cumulative Oil Production Forecast Errors – Fluid D	Forecast, STB				Error (absolute value), STB				Percentage Error, %			
Matched Production Data	0.5 yr.	1 yr.	2 yrs.	3 yrs.	0.5 yr.	1 yr.	2 yrs.	3 yrs.	0.5 yr.	1 yr.	2 yrs.	3 yrs.
Simulated Data	23,613	21,368	17,932	15,336	0	0	0	0	-	-	-	-
YM-SEPD	13,216	14,463	27,472	18,967	-10,397	-6,905	+9,540	+3,631	-78.7	-47.7	+34.7	+19.1
YM-SEPD + Arps(1)	18,588	17,273	16,162	14,261	-5,025	-4,095	-1,770	-1,075	-27.0	-23.7	-11.0	-7.5
YM-SEPD + Arps	16,950	16,888	21,674	16,367	-6,663	-4,480	+3,742	+1,031	-39.3	-26.5	+17.3	+6.3
Modified Duong	37,821	32,969	34,387	21,917	+14,208	+11,601	+16,455	+6,581	+37.6	+35.2	+47.9	+30.0
Modified Duong + Arps(1)	32,451	26,880	24,121	19,932	+8,838	+5,512	+6,189	+4,596	+27.2	+20.5	+25.7	+23.1
Modified Duong + Arps	36,180	31,014	31,756	20,614	+12,567	+9,646	+13,824	+5,278	+34.7	+31.1	+43.5	+25.6
PCM	21,275	19,204	15,805	13,207	-2338	-2,164	-2,127	-2,129	-11.0	-11.3	-13.5	-16.1

5.2.2. Forecasting Oil Production Using the Principal Components Methodology (PCM)

PCM is a data-driven method of forecasting based on the statistical technique of principal components analysis (PCA). Principal components analysis (PCA) has numerous applications in various fields such as biology, finance, architecture, etc. The ability to use PCA to extract common trends and patterns from sets of data have made it applicable to oil production forecasting as well.

The same well model as in the previous subsection (Figure 5-2) was used here. A commercial compositional simulator was used to simulate production from wells with ten different reservoir fluids (volatile oils). 30 years of production was simulated from wells with different minimum bottomhole pressure (BHP) constraints of 500 psi and 1000 psi, reservoirs with different degrees of undersaturation – initial reservoir pressures of 4000 psi and 5000 psi, as well as reservoir fluids with different critical gas saturations – 5% and

10% respectively (shown in Table 5-40). The original basecases are wells (with the ten different fluid samples) having a minimum BHP of 1000 psi, initial reservoir pressure of 5000 psi and critical gas saturation of 5%. Altogether, production data were simulated from 40 different wells. Table 5-41 shows the ten different reservoir fluid compositions.

Table 5-40 Reservoir Data (2)

Permeability	0.001 md	
Porosity	0.06	
Reservoir Temperature	250°F	
Corey Relative Permeability Exponent	2.5	
Depth to top of formation	10,000 ft	
Reservoir Thickness	250 ft	
		BASECASE
Initial Reservoir Pressure	4,000 psi	5,000 psi
Critical gas saturation, S_{gc}	0.1	0.05
Minimum Bottomhole Pressure	500 psi	1,000 psi

Table 5-41 Fluid Compositions (2)

	Fluid 1	Fluid 2	Fluid 3	Fluid 4	Fluid 5	Fluid 6	Fluid 7	Fluid 8	Fluid 9	Fluid 10
Components	Composition (%)	Composition (%)	Composition (%)	Composition (%)	Composition (%)	Composition (%)	Composition (%)	Composition (%)	Composition (%)	Composition (%)
CH_4	58.77	58.07	61.82	53.47	49.43	49.96	48.78	51.93	44.42	41.52
C_2H_6	7.57	7.43	7.91	11.46	7.28	6.44	6.24	6.64	9.52	6.12
C_3H_8	4.09	4.16	4.42	8.79	8.02	3.48	3.49	3.71	7.30	6.74
$I\text{-}C_4H_{10}$	0.91	0.96	1.02	-	2.31	0.77	0.81	0.86	-	1.94
$N\text{-}C_4H_{10}$	2.09	1.63	1.74	4.56	3.61	1.78	1.37	1.46	3.79	3.03
$I\text{-}C_5H_{12}$	0.77	0.75	0.80	-	1.80	0.66	0.63	0.67	-	1.51
$N\text{-}C_5H_{12}$	1.15	0.80	0.86	2.09	1.79	0.98	0.67	0.72	1.74	1.50
C_6H_{14}	1.75	1.14	1.21	1.51	2.32	1.49	0.96	1.02	1.26	1.95
C_{7+}	21.76	22.59	17.59	16.92	22.41	33.50	34.98	30.78	30.98	34.82
CO_2	0.93	2.32	2.47	0.90	0.16	0.79	1.95	2.08	0.75	0.13
N_2	0.21	0.15	0.16	0.30	0.87	0.18	0.13	0.13	0.25	0.73
	Highly Volatile Oils					Moderately Volatile Oils				
GOR, scf/bbl	3,024	3,043	4,081	3,967	2,561	1,806	1,755	2,128	1,873	1,513
API	63.5	63.0	63.5	64.9	65.2	49.2	49.1	46.8	49.7	50.6
Oil FVF, bbl/stb	3.56	3.55	-	4.81	3.26	2.23	2.19	2.42	2.32	2.10

The basic workflow for PCM was followed, as outlined in subsection 5.2. We generated a representative collection of production data from 40 different wells with ten different reservoir fluid compositions by compositional simulation with a commercial compositional simulator. Singular value decomposition (SVD) was then used to obtain 40 sets of principal components (PCs). The first set of principal components are the primary principal components which reveal the structure or pattern that best captures most of the variance in the representative data from all 40 wells considered. The other sets of PCs portray certain characteristic features for each well. The first set of PCs capture the most data that maximize the variance from all representative wells, followed by the second set of PCs, the third set and so on (Makinde and Lee, 2016). Five sets of principal components out of the total 40 obtained were used for our analyses. Table 5-42 shows the percentage of data capture for each of the five sets of PCs. Graphical representations of each set of PCs are shown in Figures 5-43 to 5-45.

Table 5-42 Principal Components and % Data Capture

PRINCIPAL COMPONENTS (PCs)	% DATA CAPTURE
1st Set of PCs	86.4
2nd Set of PCs	5.5
3rd Set of PCs	2.7
4th Set of PCs	1.5
5th Set of PCs	0.9

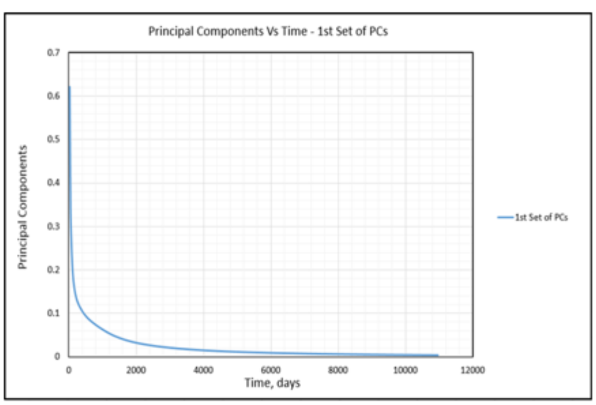

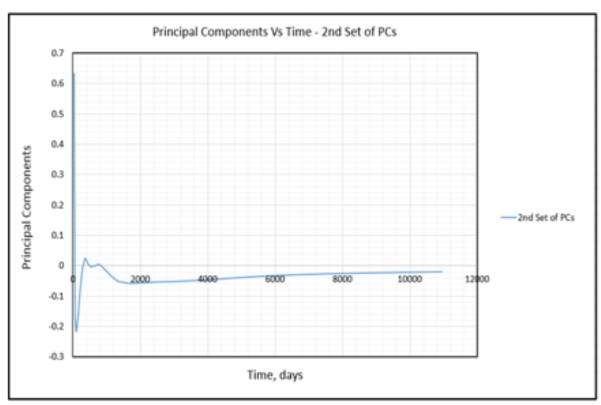

Figure 5-43 Principal Components vs. Time – 1st and 2nd Set of PCs

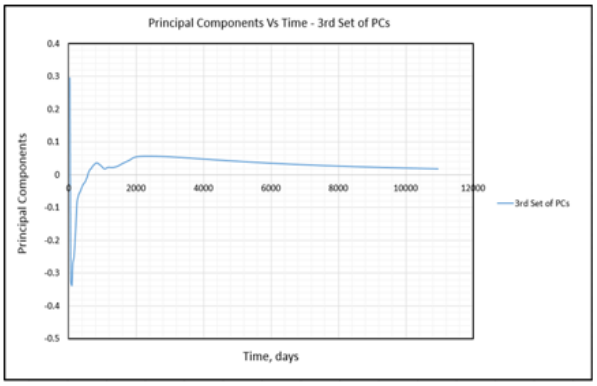

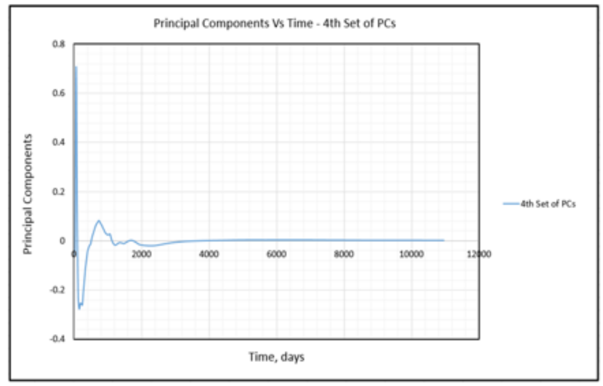

Figure 5-44 Principal Components vs. Time – 3rd and 4th Set of PCs

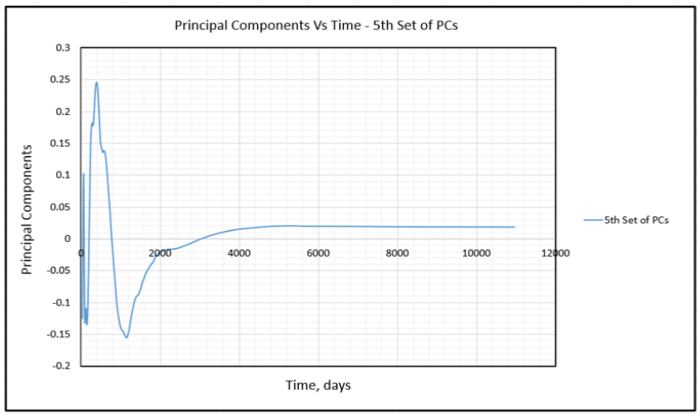

Figure 5-45 Principal Components vs. Time – 5th Set of PCs

5.2.2.1. Results

We used PCM to forecast 30 years of production for each of the ten fluid samples with availability of 0.5 to 3 yrs of simulated production history. The results were then compared to our basecase simulation study results. Analyses were done with PCM, using only the 1st primary set of principal components to using all five sets of PCs for estimating future production. Results for all the fluid samples will be shown in the following subsections.

5.2.2.1.1. Fluid 1 Cases

Graphical representations of production forecasts for all Fluid 1 cases are shown in Figure 5-46. From the graphical displays for Fluid 1, we observe that forecasting using the first 2 sets of principal components gave more accurate forecasts in all cases. This is expected as the first two sets of PCs capture approximately 92% of data that maximize the variance in the representative well data under consideration.

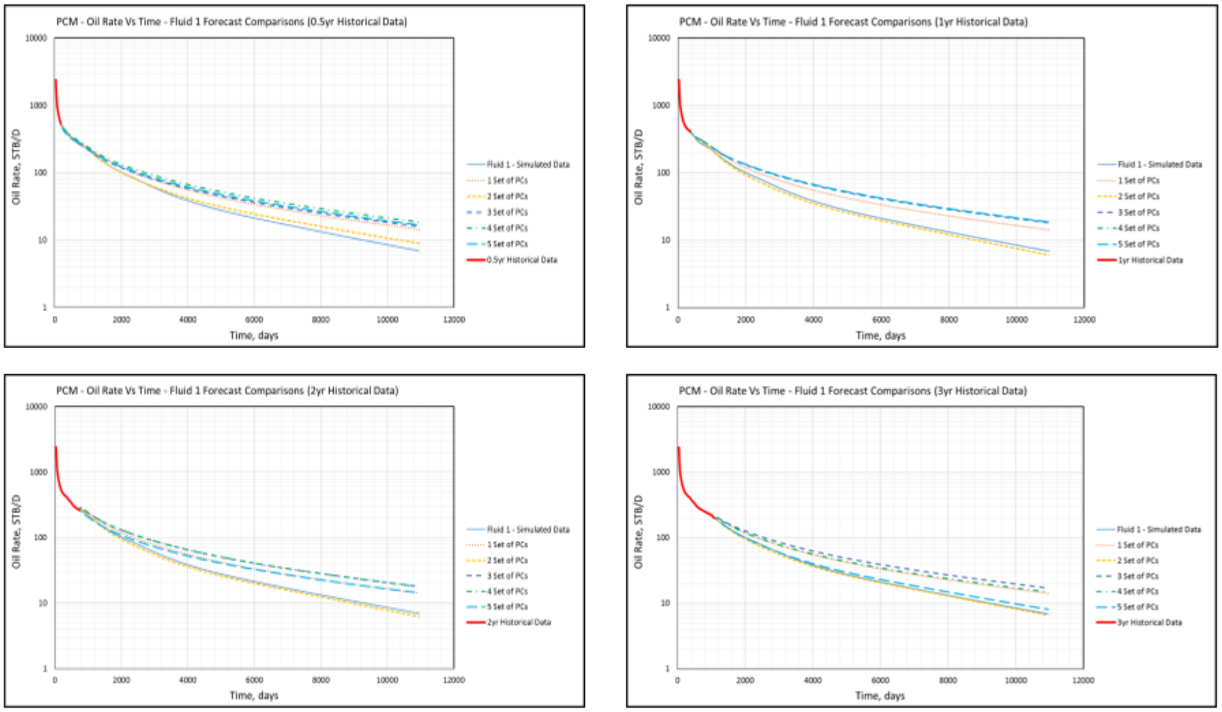

Figure 5-46 Forecast Comparisons: Fluid 1 (All Cases)

Table 5-43 shows the numerical forecast results for each Fluid 1 case. All figures are approximated and those in red indicate the lowest percentage error for each case.

Table 5-43 Forecasts, Errors and Percentage Errors – Fluid 1

FLUID 1 RESULTS																				
Principal Components (PCs)	1 Set of PCs				2 Sets of PCs				3 Sets of PCs				4 Sets of PCs				5 Sets of PCs			
Historical Data	0.5yr	1yr	2yrs	3yrs	0.5yr	1yr	2yrs	3yrs	0.5yr	1yr	2yrs	3yrs	0.5yr	1yr	2yrs	3yrs	0.5yr	1yr	2yrs	3yrs
Simulated Data, MSTB	21.4	18.7	15.0	12.2	21.4	18.7	15.0	12.2	21.4	18.7	15.0	12.2	21.4	18.7	15.0	12.2	21.4	18.7	15.0	12.2
PCM Forecast, MSTB	26.2	23.4	19.3	16.3	22.3	18.0	14.2	11.6	26.0	25.8	21.6	17.9	29.1	26.4	21.7	16.5	27.1	26.4	17.9	12.5
Error (absolute value), MSTB	4.8	4.7	4.3	4.1	0.9	-0.7	-0.8	-0.6	4.6	7.1	6.6	5.7	7.7	7.7	6.7	4.3	5.7	7.7	2.9	0.3
Percentage Error, %	18.2	19.9	22.3	25.0	3.7	-4.0	-5.7	-5.4	17.5	27.5	30.5	32.1	26.4	29.1	31.0	26.3	20.9	29.1	16.2	2.2

5.2.2.1.2. Fluid 2 Cases

Graphical representations of production forecasts for all Fluid 2 cases are displayed in Figure 5-47. From the graphs for Fluid 2, we observe that forecasting using the first 2 sets of principal components gave more precise forecasts in all cases.

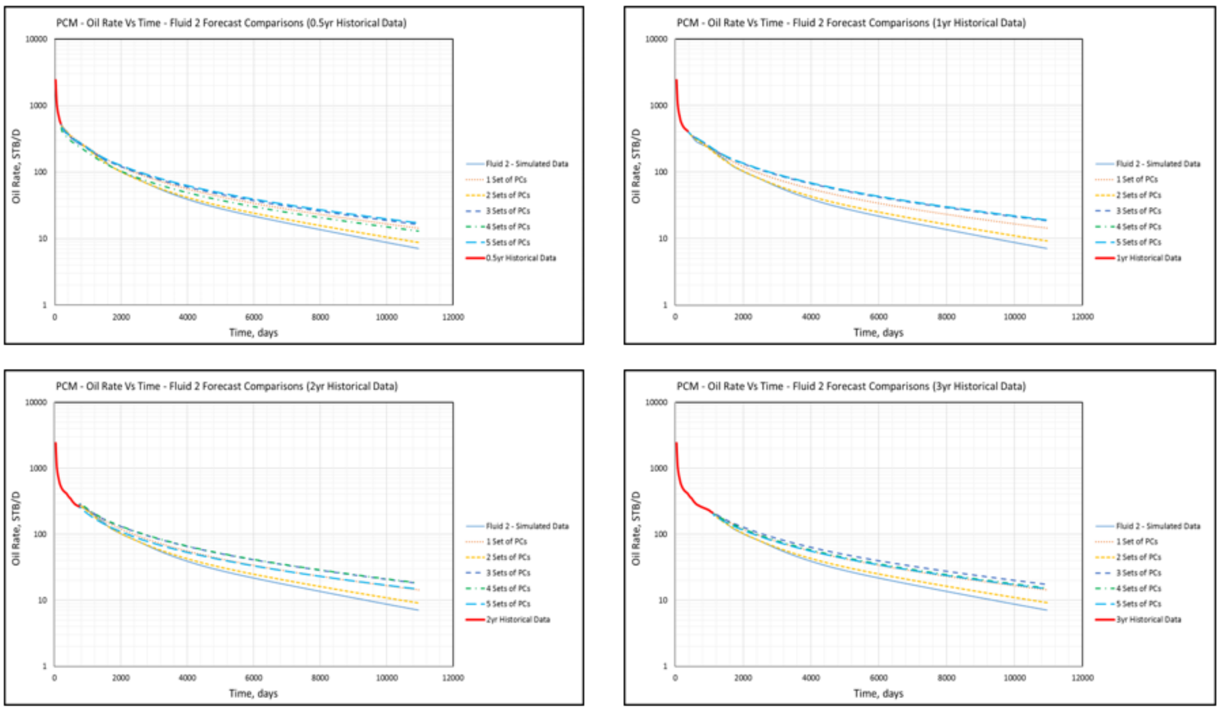

Figure 5-47 Forecast Comparisons: Fluid 2 (All Cases)

Table 5-44 shows the numerical forecast results for each Fluid 2 case. All figures are approximated and those in red indicate the lowest percentage error for each case.

Table 5-44 Forecasts, Errors and Percentage Errors – Fluid 2

FLUID 2 RESULTS																				
Principal Components (PCs)	1 Set of PCs				2 Sets of PCs				3 Sets of PCs				4 Sets of PCs				5 Sets of PCs			
Historical Data	0.5yr	1yr	2yrs	3yrs	0.5yr	1yr	2yrs	3yrs	0.5yr	1yr	2yrs	3yrs	0.5yr	1yr	2yrs	3yrs	0.5yr	1yr	2yrs	3yrs
Simulated Data, MSTB	21.8	19.1	15.3	12.4	21.8	19.1	15.3	12.4	21.8	19.1	15.3	12.4	21.8	19.1	15.3	12.4	21.8	19.1	15.3	12.4
PCM Forecast, MSTB	26.3	23.5	19.4	16.4	22.2	20.0	16.0	13.2	26.3	26.2	21.8	18.3	22.5	26.8	22.0	16.8	27.4	26.8	18.1	16.1
Error (absolute value), MSTB	4.5	4.4	4.1	4.0	0.4	0.9	0.7	0.8	4.5	7.1	6.5	5.9	0.7	7.7	6.7	4.4	5.6	7.7	2.8	3.7
Percentage Error, %	17.3	18.9	21.1	24.1	1.6	4.5	4.1	5.6	17.1	27.1	29.9	31.9	3.0	28.7	30.5	26.2	20.4	28.7	15.7	22.9

5.2.2.1.3. Fluid 3 Cases

Graphical displays of production forecasts for all Fluid 3 cases are shown in Figure 5-48. As with the previous cases already discussed, we observe from the graphs that forecasting using the first 2 sets of principal components gave more accurate forecasts in all cases.

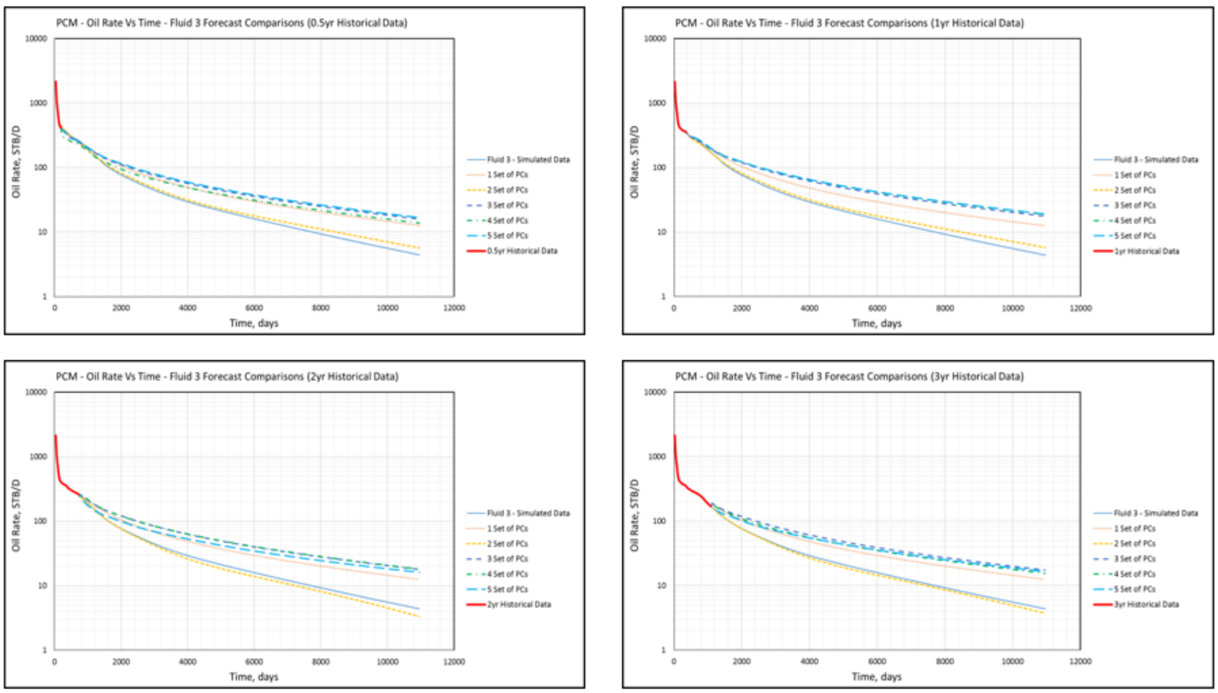

Figure 5-48 Forecast Comparisons: Fluid 3 (All Cases)

Table 5-45 shows the numerical forecast results for each Fluid 3 case. All figures are estimated and those in red indicate the lowest percentage error for each case.

Table 5-45 Forecasts, Errors and Percentage Errors – Fluid 3

FLUID 3 RESULTS																				
Principal Components (PCs)	1 Set of PCs				2 Sets of PCs				3 Sets of PCs				4 Sets of PCs				5 Sets of PCs			
Historical Data	0.5yr	1yr	2yrs	3yrs	0.5yr	1yr	2yrs	3yrs	0.5yr	1yr	2yrs	3yrs	0.5yr	1yr	2yrs	3yrs	0.5yr	1yr	2yrs	3yrs
Simulated Data, MSTB	17.5	15.3	11.8	9.3	17.5	15.3	11.8	9.3	17.5	15.3	11.8	9.3	17.5	15.3	11.8	9.3	17.5	15.3	11.8	9.3
PCM Forecast, MSTB	23.0	20.4	16.9	14.3	18.0	15.9	11.1	8.9	23.9	23.9	20.4	17.3	20.8	24.8	20.6	16.0	24.9	24.9	17.2	15.5
Error (absolute value), MSTB	5.5	5.1	5.1	5.0	0.5	0.6	-0.7	-0.4	6.4	8.6	8.6	8.0	3.3	9.5	8.8	6.7	7.4	9.6	5.4	6.2
Percentage Error, %	23.7	24.9	30.3	35.2	2.8	3.7	-6.3	-3.9	26.7	35.8	42.1	46.3	15.8	38.3	42.6	42.1	29.6	38.4	31.5	40.2

5.2.2.1.4. Fluid 4 Cases

Graphical illustrations of production forecasts for all Fluid 4 cases are shown in Figure 5-49.

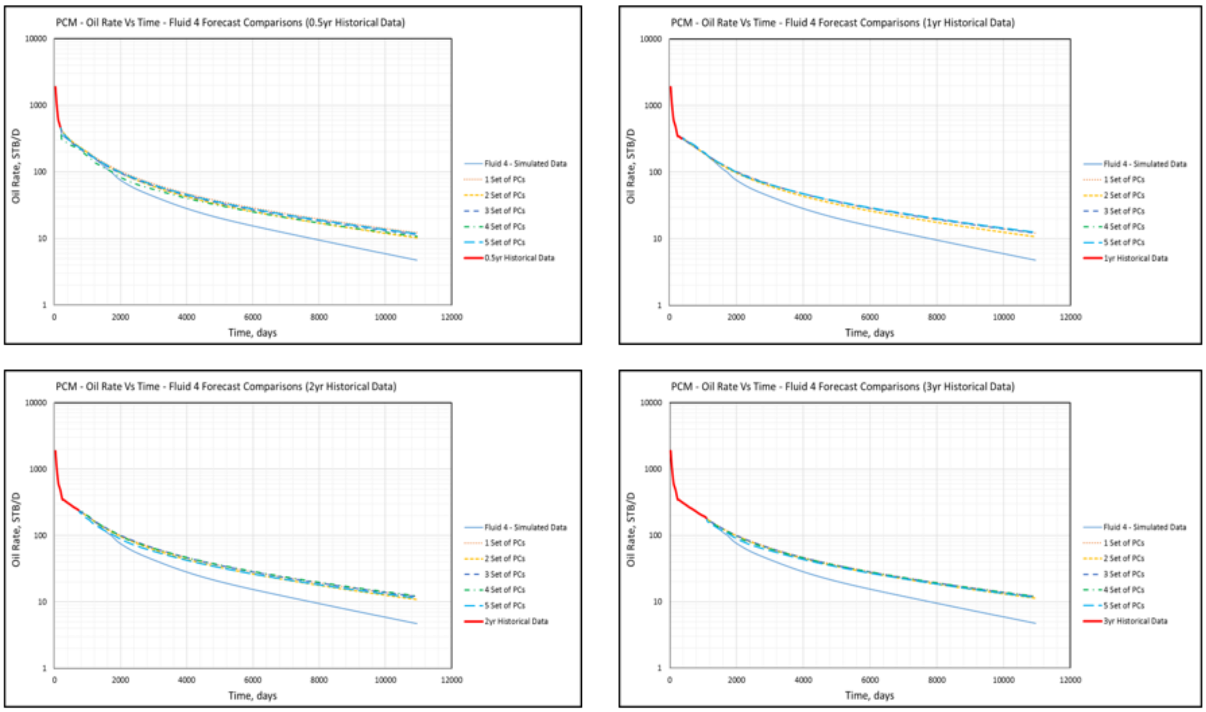

Figure 5-49 Forecast Comparisons: Fluid 4 (All Cases)

Table 5-46 displays the forecast results for each Fluid 4 case. All figures are estimated and those in red indicate the lowest percentage error for each case. Here, the overall lowest percentage error was approximately 8%, which was obtained by using the first 4 sets of PCs with only 6 months of production history available.

Table 5-46 Forecasts, Errors and Percentage Errors – Fluid 4

FLUID 4 RESULTS																				
Principal Components (PCs)	1 Set of PCs				2 Sets of PCs				3 Sets of PCs				4 Sets of PCs				5 Sets of PCs			
Historical Data	0.5yr	1yr	2yrs	3yrs	0.5yr	1yr	2yrs	3yrs	0.5yr	1yr	2yrs	3yrs	0.5yr	1yr	2yrs	3yrs	0.5yr	1yr	2yrs	3yrs
Simulated Data, MSTB	17.2	15.1	11.8	9.3	17.2	15.1	11.8	9.3	17.2	15.1	11.8	9.3	17.2	15.1	11.8	9.3	17.2	15.1	11.8	9.3
PCM Forecast, MSTB	22.2	19.7	16.3	13.8	20.9	18.8	15.5	13.3	20.9	19.7	16.3	13.7	18.7	19.8	16.3	13.4	21.4	19.8	14.8	12.7
Error (absolute value), MSTB	5.0	4.6	4.5	4.5	3.7	3.7	3.7	4.0	3.7	4.6	4.5	4.4	1.5	4.7	4.5	4.1	4.2	4.7	3.0	3.4
Percentage Error, %	22.7	23.1	27.2	32.2	17.8	19.5	23.8	30.0	17.5	23.1	27.2	31.6	8.0	23.7	27.5	30.6	19.8	23.7	19.8	26.6

5.2.2.1.5. Fluid 5 Cases

Graphical displays of production forecasts for all Fluid 5 cases are shown in Figure 5-50. Here, all forecasts are reasonable and consistent.

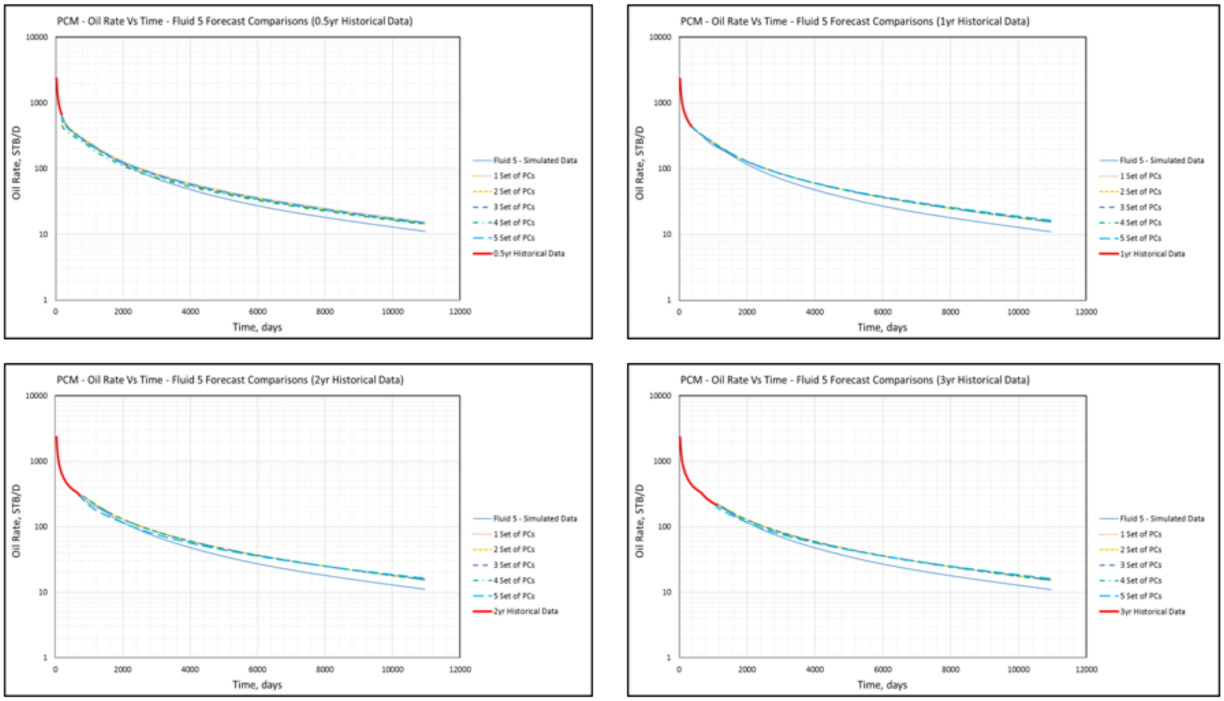

Figure 5-50 Forecast Comparisons: Fluid 5 (All Cases)

Table 5-47 shows the numerical forecast results for each Fluid 5 case. All figures are approximated and those in red indicate the lowest percentage error for each case. As can be seen on the table, percentage error can be quite low, even with just 6 months of production history.

Table 5-47 Forecasts, Errors and Percentage Errors – Fluid 5

FLUID 5 RESULTS																				
Principal Components (PCs)	1 Set of PCs				2 Sets of PCs				3 Sets of PCs				4 Sets of PCs				5 Sets of PCs			
Historical Data	0.5yr	1yr	2yrs	3yrs	0.5yr	1yr	2yrs	3yrs	0.5yr	1yr	2yrs	3yrs	0.5yr	1yr	2yrs	3yrs	0.5yr	1yr	2yrs	3yrs
Simulated Data, MSTB	25.2	22.1	17.8	14.8	25.2	22.1	17.8	14.8	25.2	22.1	17.8	14.8	25.2	22.1	17.8	14.8	25.2	22.1	17.8	14.8
PCM Forecast, MSTB	28.2	25.4	21.0	17.7	27.5	25.4	21.0	17.7	26.4	25.4	21.0	17.6	24.4	25.4	21.0	17.3	27.1	25.5	19.2	16.6
Error (absolute value), MSTB	3.0	3.3	3.2	2.9	2.3	3.3	3.2	2.9	1.2	3.3	3.2	2.8	-0.8	3.3	3.2	2.5	1.9	3.4	1.4	1.8
Percentage Error, %	10.6	13.0	15.5	16.4	8.4	13.0	15.5	16.4	4.6	13.0	15.5	15.7	-3.3	13.0	15.5	14.6	7.2	13.5	7.3	10.8

5.2.2.1.6. Fluid 6 Cases

Graphical displays of production forecasts for all Fluid 6 cases are shown in Figure 5-51. Here, all forecasts are highly accurate.

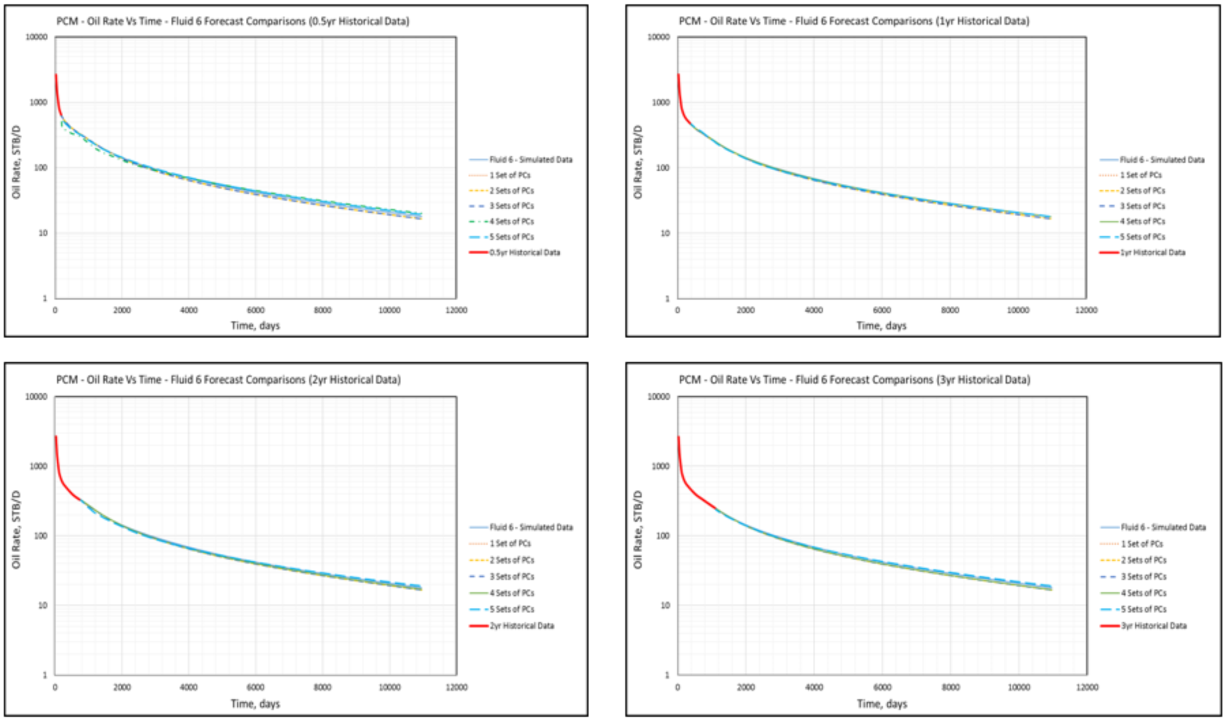

Figure 5-51 Forecast Comparisons: Fluid 6 (All Cases)

Table 5-48 shows the forecast results for each Fluid 6 case. All figures are approximated and those in red indicate the lowest percentage error for each case. Percentage errors here are consistently low in all cases.

Table 5-48 Forecasts, Errors and Percentage Errors – Fluid 6

FLUID 6 RESULTS																				
Principal Components (PCs)	1 Set of PCs				2 Sets of PCs				3 Sets of PCs				4 Sets of PCs				5 Sets of PCs			
Historical Data	0.5yr	1yr	2yrs	3yrs	0.5yr	1yr	2yrs	3yrs	0.5yr	1yr	2yrs	3yrs	0.5yr	1yr	2yrs	3yrs	0.5yr	1yr	2yrs	3yrs
Simulated Data, MSTB	31.3	28.1	23.4	20.0	31.3	28.1	23.4	20.0	31.3	28.1	23.4	20.0	31.3	28.1	23.4	20.0	31.3	28.1	23.4	20.0
PCM Forecast, MSTB	30.5	27.3	22.6	19.2	30.4	27.3	22.6	19.2	30.5	27.4	22.7	19.2	29.1	28.1	22.9	19.1	31.4	27.8	22.6	20.0
Error (absolute value), MSTB	-0.8	-0.8	-0.8	-0.8	-0.9	-0.8	-0.8	-0.8	-0.8	-0.7	-0.7	-0.8	-2.2	0.0	-0.5	-0.9	0.1	0.3	-0.8	0.0
Percentage Error, %	-2.6	-2.8	-3.6	-4.5	-2.9	-2.8	-3.6	-4.5	-2.6	-2.6	-3.4	-4.5	-7.6	-0.1	-2.3	-4.6	0.4	-1.1	-3.5	-0.3

5.2.2.1.7. Fluid 7 Cases

Graphical illustrations of production forecasts for all Fluid 7 cases are shown in Figure 5-52.

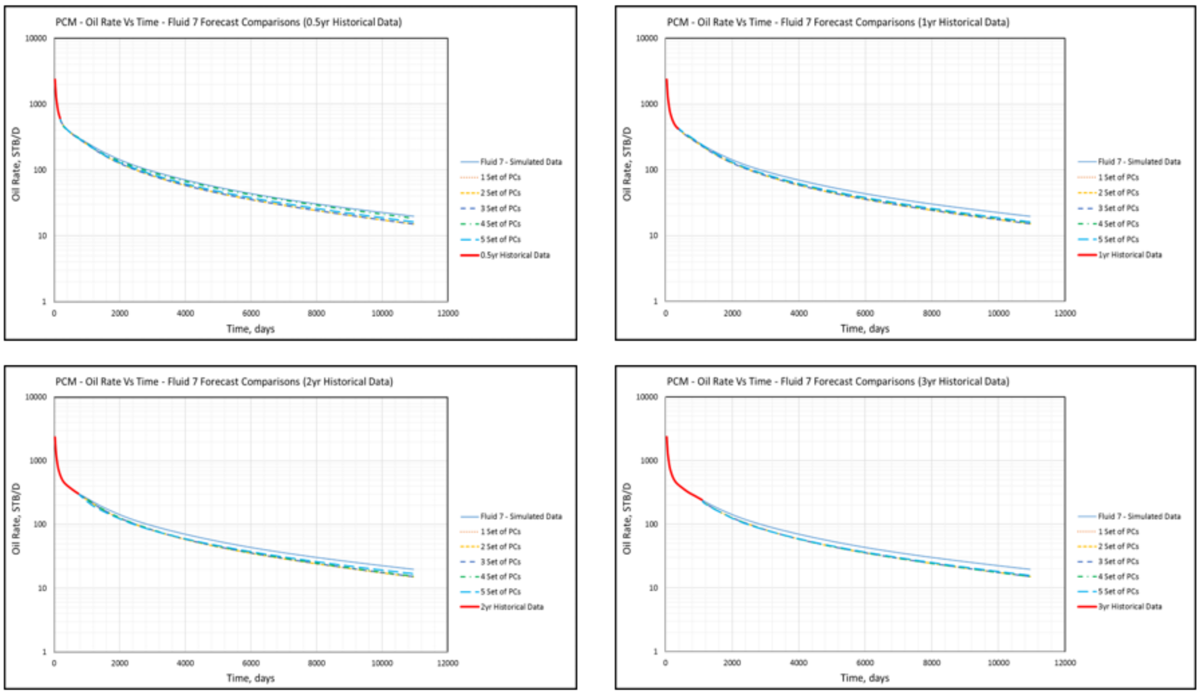

Figure 5-52 Forecast Comparisons: Fluid 7 (All Cases)

Table 5-49 shows the forecast results for each Fluid 7 case. All figures are estimated and those in red indicate the lowest percentage error for each case. The overall lowest percentage error was approximately 3%, which was obtained by using the first 4 sets of PCs with only 6 months of production history available.

Table 5-49 Forecasts, Errors and Percentage Errors – Fluid 7

FLUID 7 RESULTS																				
Principal Components (PCs)	1 Set of PCs				2 Sets of PCs				3 Sets of PCs				4 Sets of PCs				5 Sets of PCs			
Historical Data	0.5yr	1yr	2yrs	3yrs	0.5yr	1yr	2yrs	3yrs	0.5yr	1yr	2yrs	3yrs	0.5yr	1yr	2yrs	3yrs	0.5yr	1yr	2yrs	3yrs
Simulated Data, MSTB	30.7	27.8	23.5	20.3	30.7	27.8	23.5	20.3	30.7	27.8	23.5	20.3	30.7	27.8	23.5	20.3	30.7	27.8	23.5	20.3
PCM Forecast, MSTB	27.6	24.7	20.5	17.4	27.6	24.7	20.5	17.4	27.6	24.7	20.5	17.4	29.8	25.5	20.7	17.4	28.4	25.9	20.5	17.4
Error (absolute value), MSTB	-3.1	-3.1	-3.0	-2.9	-3.1	-3.1	-3.0	-2.9	-3.1	-3.1	-3.0	-2.9	-0.9	-2.3	-2.8	-2.9	-2.3	-1.9	-3.0	-2.9
Percentage Error, %	-11.1	-12.5	-14.8	-16.6	-11.1	-12.5	-14.8	-16.6	-11.1	-12.5	-14.8	-16.6	-2.8	-9.0	-13.4	-16.6	-8.0	-7.1	-14.8	-16.6

5.2.2.1.8. Fluid 8 Cases

Graphical illustrations of production forecasts for all Fluid 8 cases are shown in Figure 5-53.

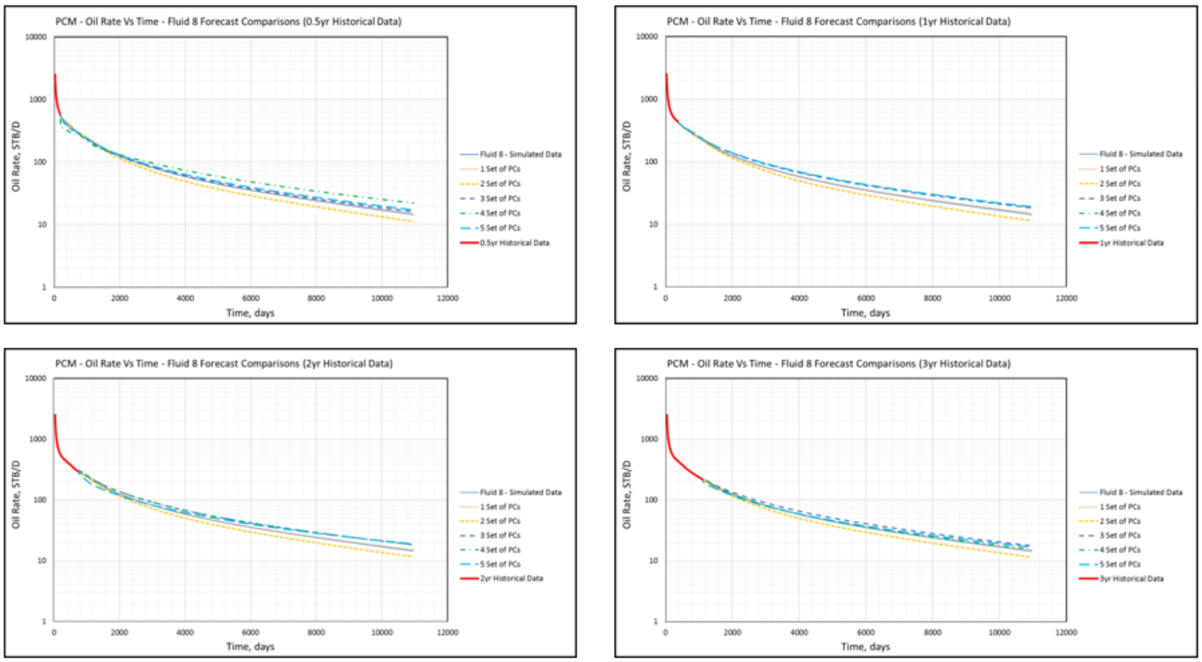

Figure 5-53 Forecast Comparisons: Fluid 8 (All Cases)

Table 5-50 shows the forecast results for each Fluid 8 case. All figures are approximated and those in red indicate the lowest percentage error for each case. The overall lowest percentage error was approximately 1%.

Table 5-50 Forecasts, Errors and Percentage Errors – Fluid 8

FLUID 8 RESULTS																				
Principal Components (PCs)	1 Set of PCs				2 Sets of PCs				3 Sets of PCs				4 Sets of PCs				5 Sets of PCs			
Historical Data	0.5yr	1yr	2yrs	3yrs	0.5yr	1yr	2yrs	3yrs	0.5yr	1yr	2yrs	3yrs	0.5yr	1yr	2yrs	3yrs	0.5yr	1yr	2yrs	3yrs
Simulated Data, MSTB	27.3	24.4	20.1	17.1	27.3	24.4	20.1	17.1	27.3	24.4	20.1	17.1	27.3	24.4	20.1	17.1	27.3	24.4	20.1	17.1
PCM Forecast, MSTB	27.7	24.8	20.6	17.4	25.0	22.4	18.3	15.1	27.0	26.9	22.6	18.9	28.8	27.4	22.7	17.4	28.2	27.4	20.3	16.9
Error (absolute value), MSTB	0.4	0.4	0.5	0.3	-2.3	-2.0	-1.8	-2.0	-0.3	2.5	2.5	1.8	1.5	3.0	2.6	0.3	0.9	3.0	0.2	-0.2
Percentage Error, %	1.4	1.7	2.3	1.9	-9.1	-8.9	-10.0	-12.8	-1.0	9.4	11.1	9.6	5.3	10.9	11.6	2.0	3.2	11.0	1.0	-0.8

5.2.2.1.9. Fluid 9 Cases

Graphical displays of production forecasts for all Fluid 9 cases are shown in Figure 5-54. Forecasts are consistently good in all cases regardless of the production history available.

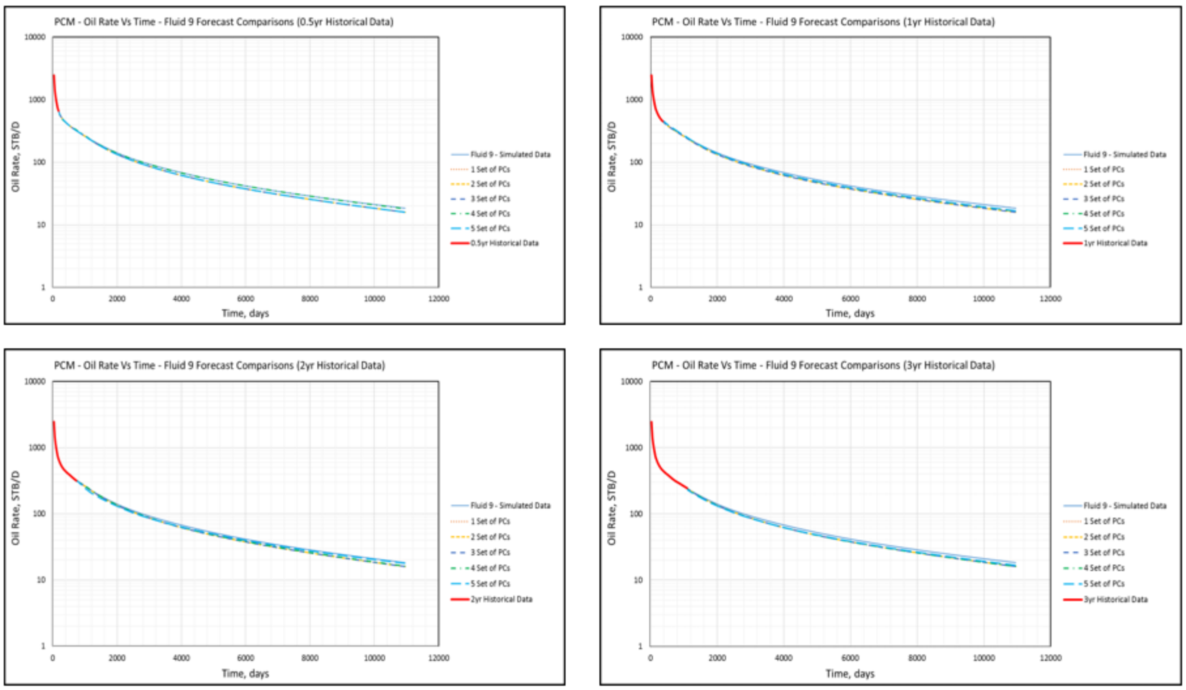

Figure 5-54 Forecast Comparisons: Fluid 9 (All Cases)

Table 5-51 shows the forecast results for each Fluid 9 case. All figures are estimated and those in red indicate the lowest percentage error for each case.

Table 5-51 Forecasts, Errors and Percentage Errors – Fluid 9

FLUID 9 RESULTS																				
Principal Components (PCs)	1 Set of PCs				2 Sets of PCs				3 Sets of PCs				4 Sets of PCs				5 Sets of PCs			
Historical Data	0.5yr	1yr	2yrs	3yrs	0.5yr	1yr	2yrs	3yrs	0.5yr	1yr	2yrs	3yrs	0.5yr	1yr	2yrs	3yrs	0.5yr	1yr	2yrs	3yrs
Simulated Data, MSTB	30.6	27.5	23.0	19.7	30.6	27.5	23.0	19.7	30.6	27.5	23.0	19.7	30.6	27.5	23.0	19.7	30.6	27.5	23.0	19.7
PCM Forecast, MSTB	29.1	26.1	21.7	18.3	29.1	26.1	21.7	18.3	29.1	26.2	21.7	18.3	30.4	27.0	21.9	18.3	29.1	27.2	21.7	18.4
Error (absolute value), MSTB	-1.5	-1.4	-1.3	-1.4	-1.5	-1.4	-1.3	-1.4	-1.5	-1.3	-1.3	-1.4	-0.2	-0.5	-1.1	-1.4	-1.5	-0.3	-1.3	-1.3
Percentage Error, %	-5.1	-5.3	-6.3	-7.5	-5.1	-5.4	-6.3	-7.5	-5.1	-5.1	-6.2	-7.5	-0.7	-2.1	-5.1	-7.6	-5.1	-1.3	-6.3	-7.1

5.2.2.1.10. Fluid 10 Cases

Graphs showing production forecasts for all Fluid 10 cases are in Figure 5-55. All forecasts are reasonable, regardless of the available historical production data.

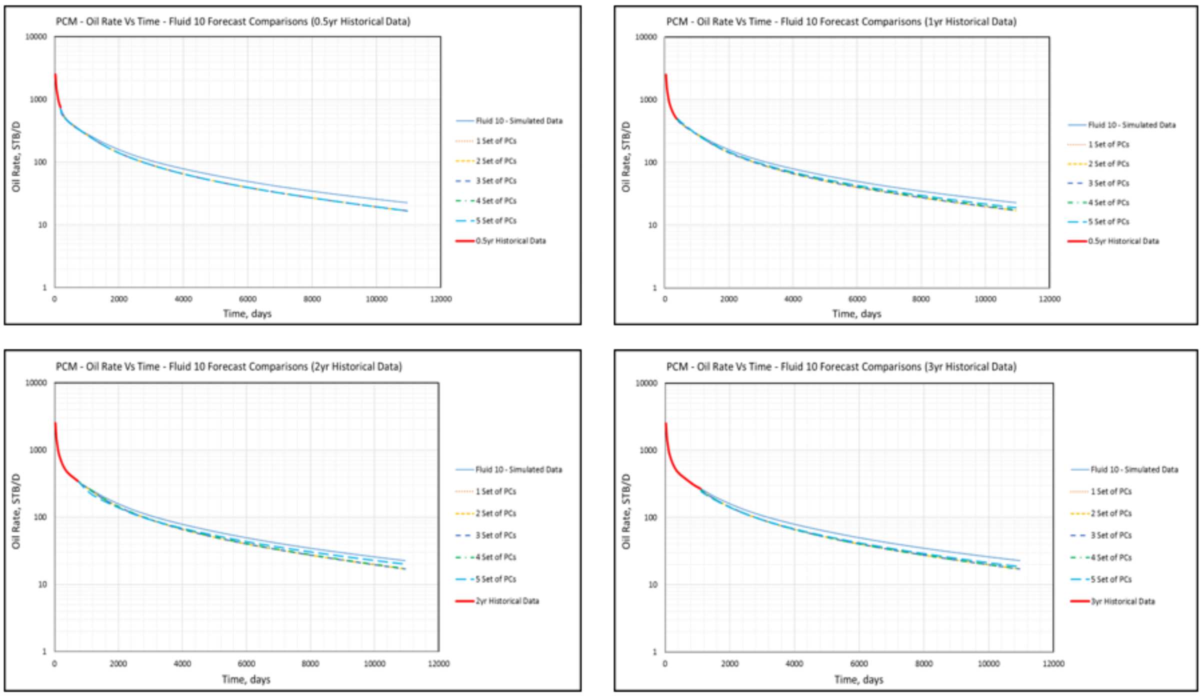

Figure 5-55 Forecast Comparisons: Fluid 10 (All Cases)

Table 5-52 shows the forecast results for each Fluid 10 case. All figures are approximated and those in red indicate the lowest percentage error for each case.

Table 5-52 Forecasts, Errors and Percentage Errors – Fluid 10

FLUID 10 RESULTS																				
Principal Components (PCs)	1 Set of PCs				2 Sets of PCs				3 Sets of PCs				4 Sets of PCs				5 Sets of PCs			
Historical Data	0.5yr	1yr	2yrs	3yrs	0.5yr	1yr	2yrs	3yrs	0.5yr	1yr	2yrs	3yrs	0.5yr	1yr	2yrs	3yrs	0.5yr	1yr	2yrs	3yrs
Simulated Data, MSTB	34.8	31.3	26.5	22.8	34.8	31.3	26.5	22.8	34.8	31.3	26.5	22.8	34.8	31.3	26.5	22.8	34.8	31.3	26.5	22.8
PCM Forecast, MSTB	30.8	27.8	23.1	19.6	30.8	27.8	23.1	19.6	30.8	27.9	23.1	19.6	30.7	28.6	23.4	19.6	30.8	29.0	23.1	19.7
Error (absolute value), MSTB	-4.0	-3.5	-3.4	-3.2	-4.0	-3.5	-3.4	-3.2	-4.8	-3.4	-3.4	-3.2	-4.1	-2.7	-3.1	-3.2	-4.0	-2.3	-3.4	-3.1
Percentage Error, %	-13.1	-12.6	-14.5	-16.6	-13.1	-12.6	-14.5	-16.6	-13.1	-12.4	-14.5	-16.6	-13.1	-9.4	-13.2	-16.6	-13.1	-8.1	-14.5	-15.9

Commonly, in some cases, only the first set of PCs (primary PCs) are sufficient for forecasting production with highly reasonable level of accuracy. Using more than 2 sets of PCs for PCM does not necessarily mean that production forecasts will be more precise. The other sets of PCs that capture lesser data, may portray particular features peculiar to only certain wells within the representative pool of wells. Thus, forecasts may be less accurate if these PCs are included in the analyses of wells for which they do not depict any of its features. Note that PCs obtained for these analyses are from reservoirs with different characteristics and fluids, as well as wells with different operating constraints.

We next studied the effects that the source of principal components can have on production forecasts. What if we obtain principal components from wells with similar operating conditions in reservoirs with similar characteristics and similar (or nearly similar) reservoir fluid types? Will there be any significant difference in production forecasts compared to those estimated with PCs from wells with varying fluids? To answer these questions, we calculated PCs from wells with highly volatile oils and separately from wells with moderately volatile oils. Figure 5-56 shows a graph of these principal components (PCs) compared to PCs gotten from wells with varying conditions (tagged “All Cases”).

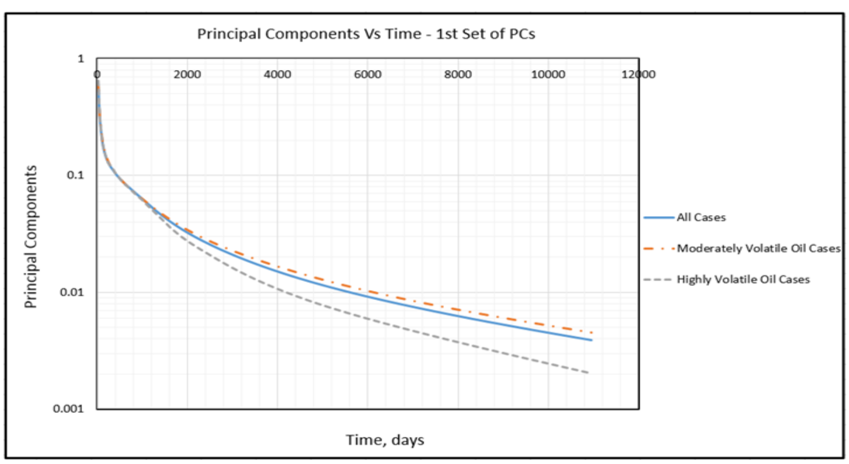

Figure 5-56 Principal Components vs. Time – 1st Set of PCs

5.2.2.2. Results (2)

Results for all the fluids are shown in the following subsections. Production forecasts (1) are estimates obtained with the use of PCs calculated from several wells with varying conditions, whereas production forecasts (2) are estimates obtained using PCs calculated from several wells with similar (or nearly similar) conditions.

5.2.2.2.1. Fluid 1 Cases

The cases for Fluid 1 are shown in the graphs in Figure 5-57 below:

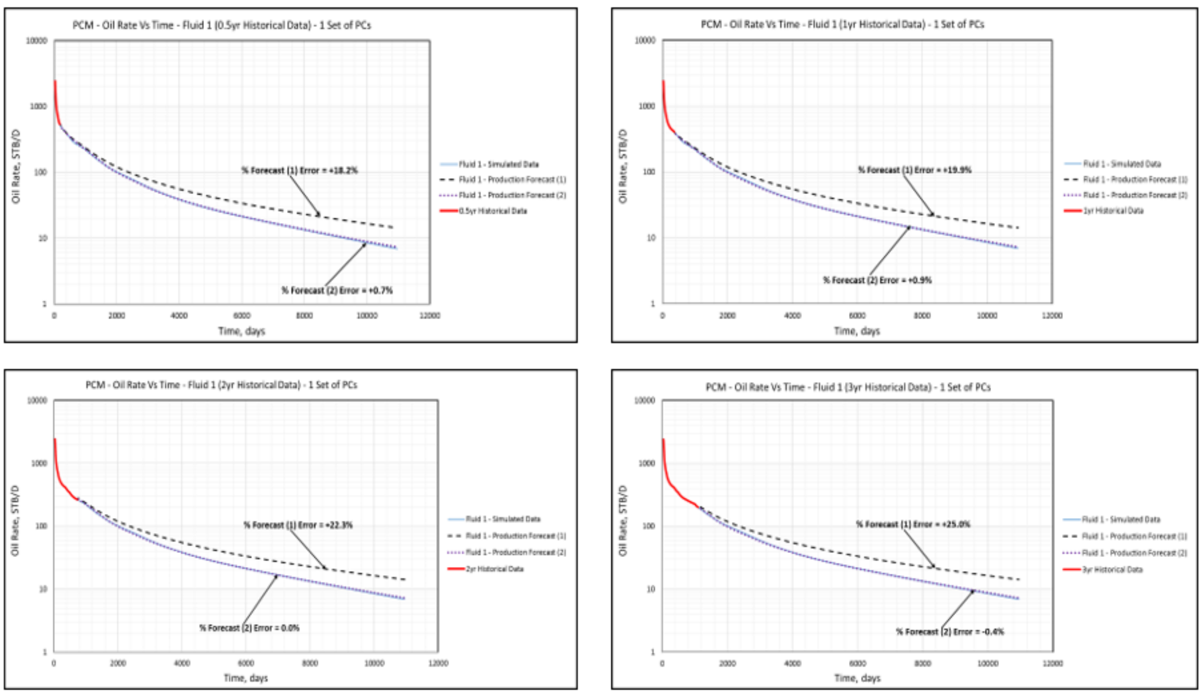

Figure 5-57 Production Forecasts (1) and (2) for Fluid 1 – 1st Set of PCs

From the graphs in Figure 5-57, we can observe that there are significant improvements in production estimates when PCs obtained from wells with similar fluids are used to forecast. Production forecasts are highly accurate in all these cases and the first set of PCs are enough to provide good estimates. Table 5-53 displays the numerical figures, errors and percentage errors for Fluid 1 forecasts (1) and (2). The red figures indicate the lower of the two percentage errors for each case.

Table 5-53 Errors and Percentage Errors for Forecasts (1) and (2) – Fluid 1

FLUID 1 RESULTS				
Principal Components (PCs)	1 Set of PCs (Primary PCs)			
Historical Data	0.5yr	1yr	2yrs	3yrs
Simulated Data, STB	21,420	18,737	14,965	12,183
PCM Forecast (1), STB	26,197	23,397	19,265	16,253
Error (1) (absolute value), STB	+4,777	+4,660	+4,300	+4,070
Percentage Error (1), %	+18.2	+19.9	+22.3	+25.0
PCM Forecast (2), STB	21,572	18,900	14,965	12,131
Error (2) (absolute value), STB	+152	+163	0	-52
Percentage Error (2), %	+0.7	+0.9	0.0	-0.4

5.2.2.2.2. Fluid 2 Cases

The cases for Fluid 2 are displayed in the graphs in Figure 5-58 below:

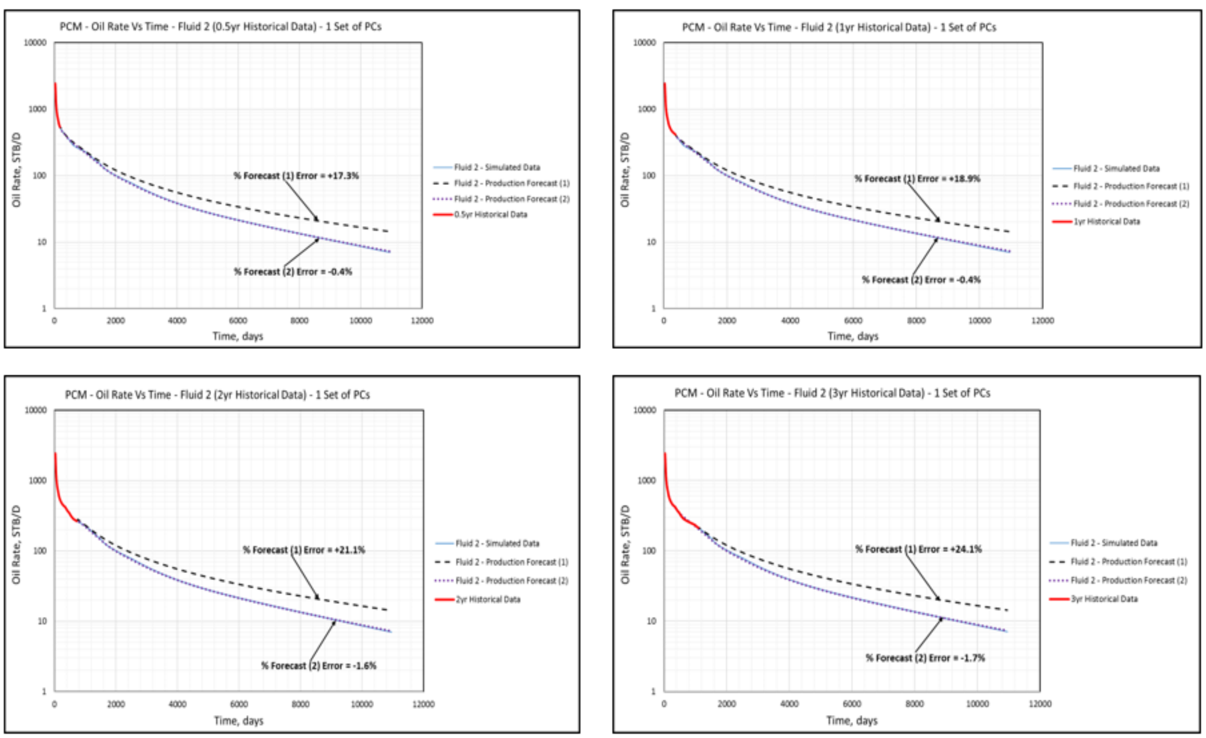

Figure 5-58 Production Forecasts (1) and (2) for Fluid 2 – 1st Set of PCs

Here, as in the previous case, we can see that there are significant improvements in production estimates when PCs obtained from wells with similar fluids are used to forecast. Production forecasts are very precise in all these cases and the first set of PCs are sufficient to provide good estimates. Table 5-54 shows the numerical figures, errors and percentage errors for Fluid 2 forecasts (1) and (2). The red figures indicate the lower of the two percentage errors for each case.

Table 5-54 Errors and Percentage Errors for Forecasts (1) and (2) – Fluid 2

FLUID 2 RESULTS				
Principal Components (PCs)	1 Set of PCs (Primary PCs)			
Historical Data	0.5yr	1yr	2yrs	3yrs
Simulated Data, STB	21,788	19,080	15,292	12,428
PCM Forecast (1), STB	26,341	23,536	19,377	16,368
Error (1) (absolute value), STB	+4,553	+4,456	+4,085	+3,940
Percentage Error (1), %	+17.3	+18.9	+21.1	+24.1
PCM Forecast (2), STB	21,692	19,013	15,053	12,217
Error (2) (absolute value), STB	-96	-67	-239	-211
Percentage Error (2), %	-0.4	-0.4	-1.6	-1.7

5.2.2.2.3. Fluid 3 Cases

The cases for Fluid 3 are shown in the graphs in Figure 5-59 below:

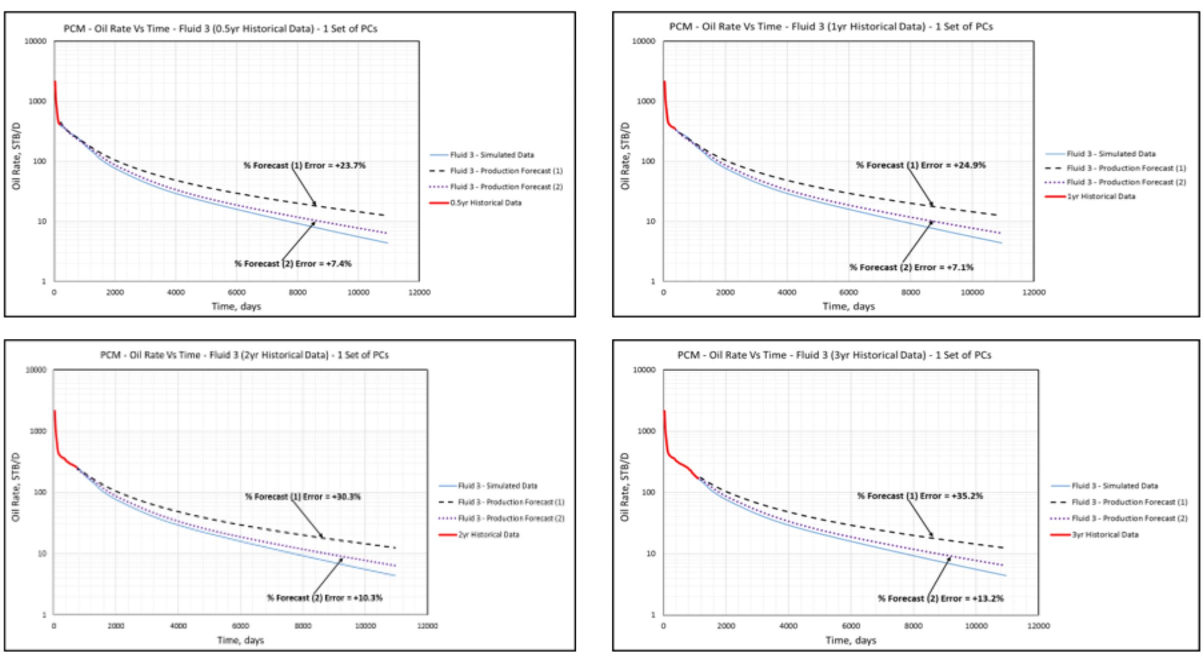

Figure 5-59 Production Forecasts (1) and (2) for Fluid 3 – 1st Set of PCs

From the graphs in Figure 5-59, we can notice that there are improvements in production estimates when PCs obtained from wells with similar fluids are used to forecast. Table 5-55 shows the forecasts, errors and percentage errors for Fluid 3 forecasts (1) and (2). The red figures indicate the lower of the two percentage errors for each case.

Table 5-55 Errors and Percentage Errors for Forecasts (1) and (2) – Fluid 3

FLUID 3 RESULTS				
Principal Components (PCs)	1 Set of PCs (Primary PCs)			
Historical Data	0.5yr	1yr	2yrs	3yrs
Simulated Data, STB	17,541	15,308	11,791	9,267
PCM Forecast (1), STB	22,981	20,392	16,912	14,299
Error (1) (absolute value), STB	+5,440	+5,084	+5,121	+5,032
Percentage Error (1), %	+23.7	+24.9	+30.3	+35.2
PCM Forecast (2), STB	18,933	16,482	13,141	10,674
Error (2) (absolute value), STB	+1,392	+1,174	+1,350	+1,407
Percentage Error (2), %	+7.4	+7.1	+10.3	+13.2

5.2.2.2.4. Fluid 4 Cases

The cases for Fluid 4 are shown in the graphs in Figure 5-60 below:

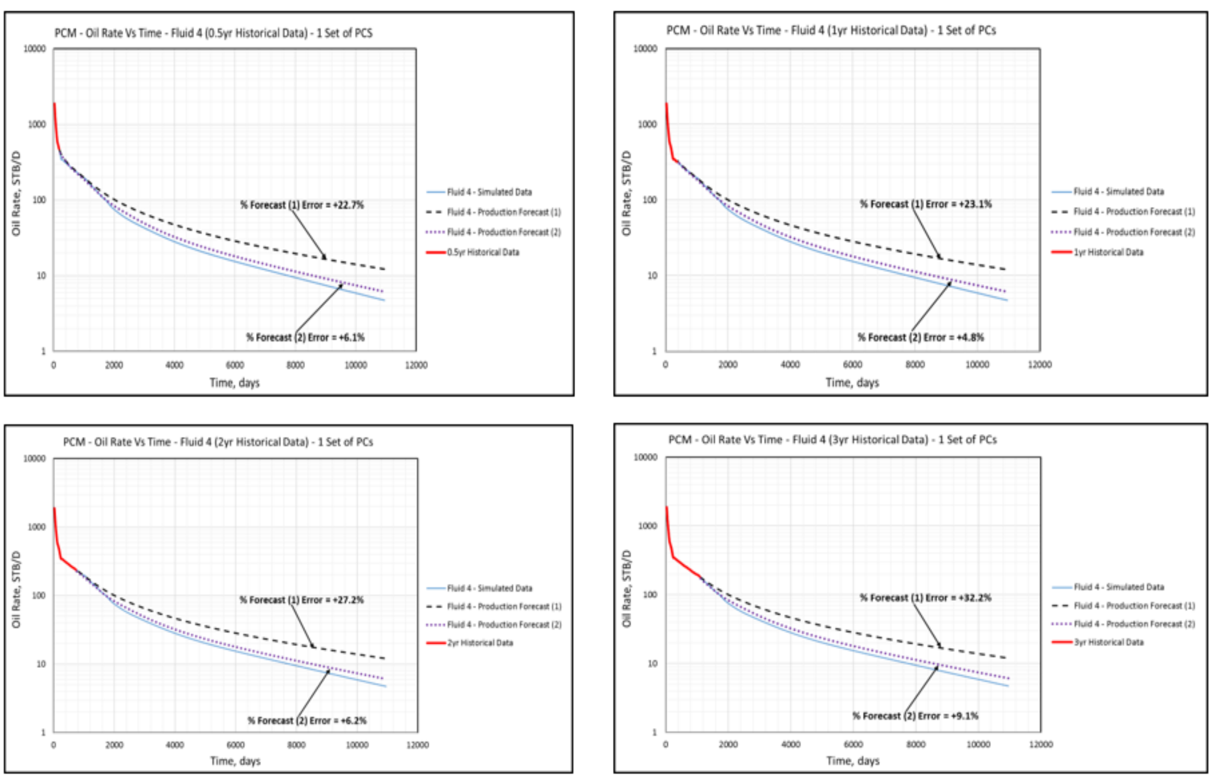

Figure 5-60 Production Forecasts (1) and (2) for Fluid 4 – 1st Set of PCs

As with other cases, we can observe in Figure 5-60 that there are improvements in production estimates when PCs obtained from wells with similar fluids are used to forecast. Table 5-56 displays the forecasts, errors and percentage errors for Fluid 4 forecasts (1) and (2). The red figures indicate the lower of the two percentage errors for each case.

Table 5-56 Errors and Percentage Errors for Forecasts (1) and (2) – Fluid 4

FLUID 4 RESULTS				
Principal Components (PCs)	1 Set of PCs (Primary PCs)			
Historical Data	0.5yr	1yr	2yrs	3yrs
Simulated Data, STB	17,209	15,128	11,837	9,334
PCM Forecast (1), STB	22,275	19,683	16,267	13,775
Error (1) (absolute value), STB	+5,066	+4,555	+4,430	+4,441
Percentage Error (1), %	+22.7	+23.2	+27.2	+32.2
PCM Forecast (2), STB	18,317	15,884	12,623	10,270
Error (2) (absolute value), STB	+1,108	+756	+786	+936
Percentage Error (2), %	+6.1	+4.8	+6.2	+9.1

5.2.2.2.5. Fluid 5 Cases

The cases for Fluid 5 are displayed in the graphs in Figure 5-61 below:

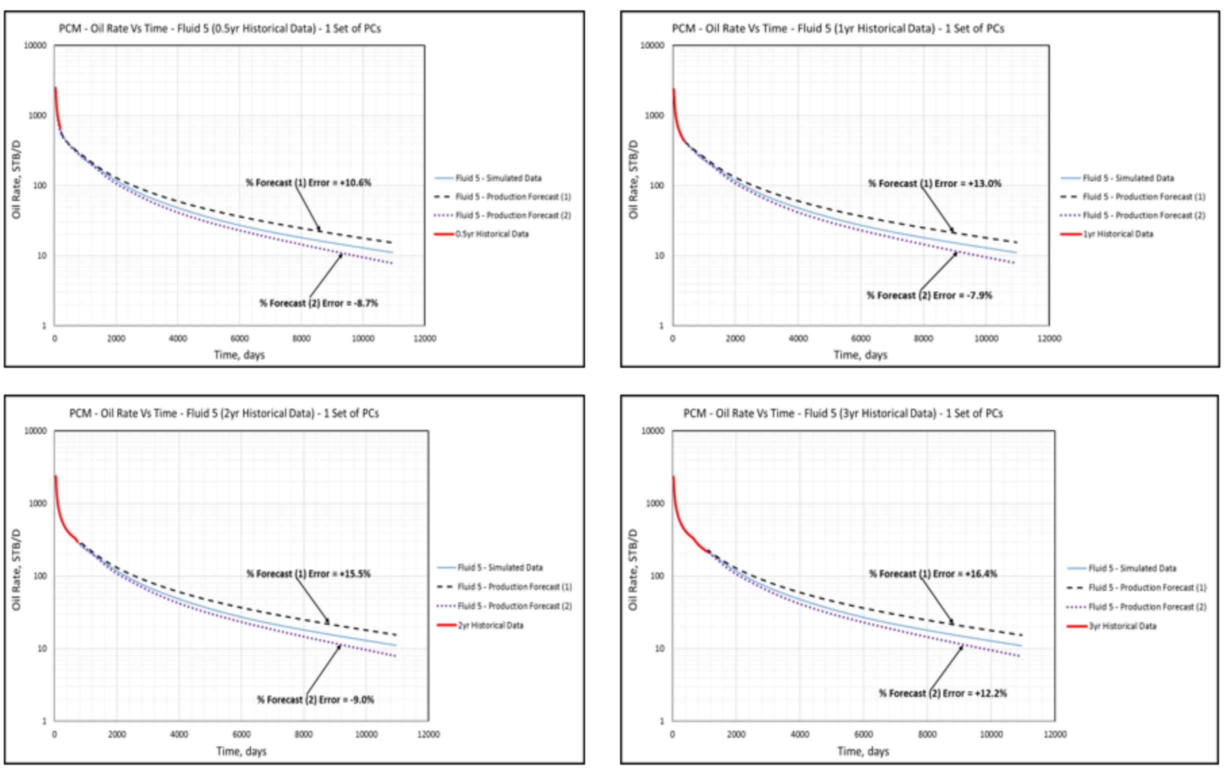

Figure 5-61 Production Forecasts (1) and (2) for Fluid 5 – 1st Set of PCs

When PCs obtained from wells with similar fluids are used to forecast, production estimates are better, as can be seen in Figure 5-61. Table 5-57 shows the forecasts, errors and percentage errors for Fluid 5 forecasts (1) and (2). The red figures indicate the lower of the two percentage errors for each case.

Table 5-57 Errors and Percentage Errors for Forecasts (1) and (2) – Fluid 5

FLUID 5 RESULTS				
Principal Components (PCs)	1 Set of PCs (Primary PCs)			
Historical Data	0.5yr	1yr	2yrs	3yrs
Simulated Data, STB	25,161	22,070	17,759	14,797
PCM Forecast (1), STB	28,152	25,373	21,013	17,704
Error (1) (absolute value), STB	+2,991	+3,303	+3,254	+2,907
Percentage Error (1), %	+10.6	+13.0	+15.5	+16.4
PCM Forecast (2), STB	23,143	20,461	16,296	13,193
Error (2) (absolute value), STB	-2,018	-1,609	-1,463	-1,604
Percentage Error (2), %	-8.7	-7.9	-9.0	-12.2

5.2.2.2.6. Fluid 6 Cases

The cases for Fluid 6 are displayed in the graphs in Figure 5-62 below:

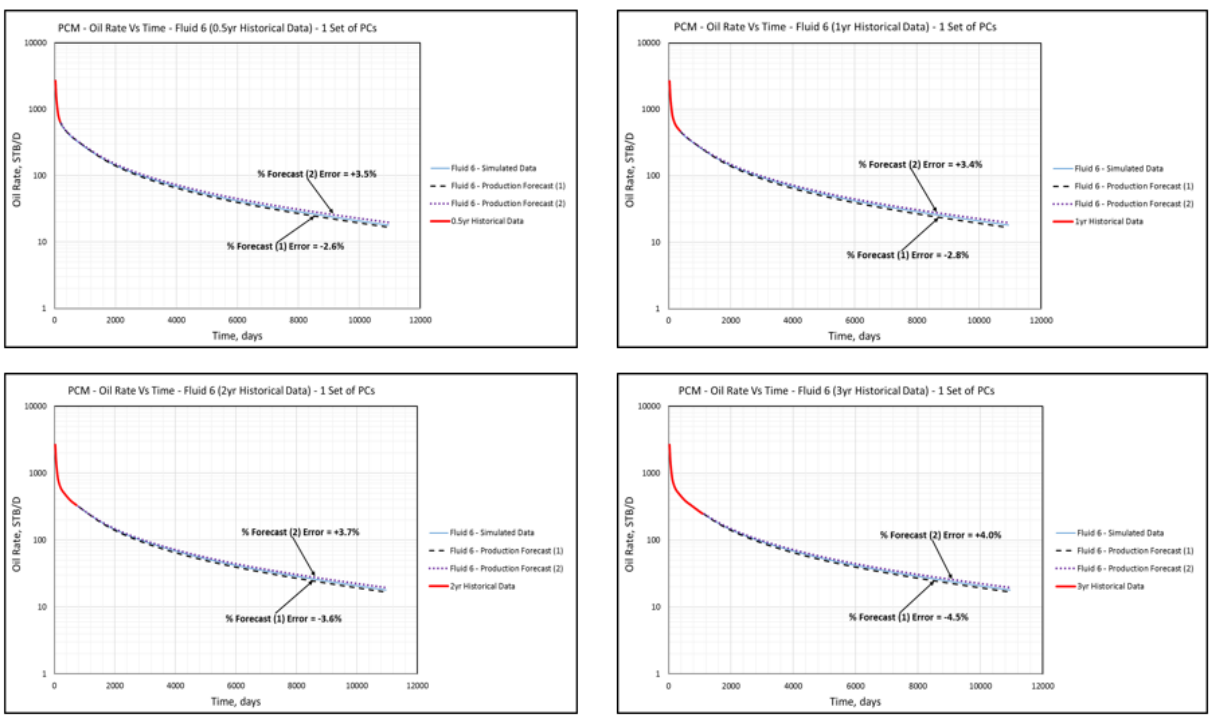

Figure 5-62 Production Forecasts (1) and (2) for Fluid 6 – 1st Set of PCs

From the graphs in Figure 5-62, we can observe that forecasts are quite accurate when PCs are calculated from wells with varying conditions. When PCs obtained from wells with similar fluids are used to forecast, results are approximately similar or slightly less accurate in some cases. Table 5-58 shows the forecasts, errors and percentage errors for Fluid 6 forecasts (1) and (2). The red figures indicate the lower of the two percentage errors for each case.

Table 5-58 Errors and Percentage Errors for Forecasts (1) and (2) – Fluid 6

FLUID 6 RESULTS				
Principal Components (PCs)	1 Set of PCs (Primary PCs)			
Historical Data	0.5yr	1yr	2yrs	3yrs
Simulated Data, STB	31,289	28,090	23,444	20,014
PCM Forecast (1), STB	30,507	27,329	22,634	19,150
Error (1) (absolute value), STB	-782	-761	-810	-864
Percentage Error (1), %	-2.6	-2.8	-3.6	-4.5
PCM Forecast (2), STB	32,406	29,075	24,334	20,848
Error (2) (absolute value), STB	+1,117	+985	+890	+834
Percentage Error (2), %	+3.5	+3.4	+3.7	+4.0

5.2.2.2.7. Fluid 7 Cases

The cases for Fluid 7 are shown in the graphs in Figure 5-63 below:

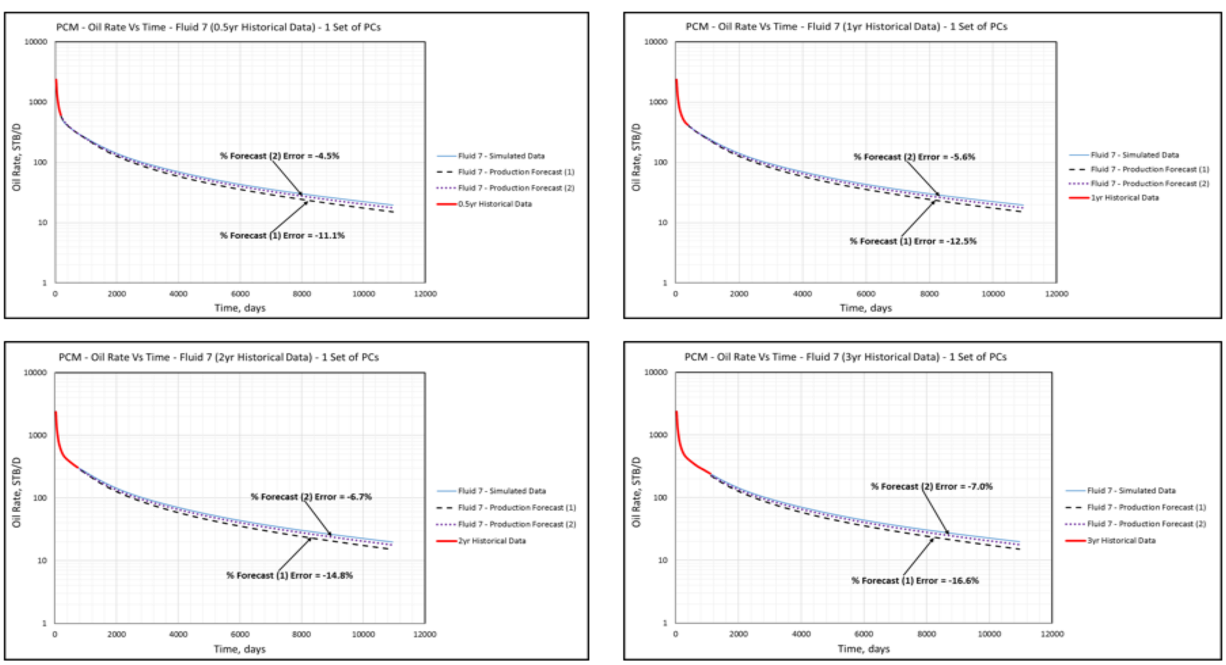

Figure 5-63 Production Forecasts (1) and (2) for Fluid 7 – 1st Set of PCs

We can notice in Figure 5-63 that there are improvements in production estimates when PCs obtained from wells with similar fluids are used to forecast. Table 5-59 displays the forecasts, errors and percentage errors for Fluid 7 forecasts (1) and (2). The red figures indicate the lower of the two percentage errors for each case.

Table 5-59 Errors and Percentage Errors for Forecasts (1) and (2) – Fluid 7

FLUID 7 RESULTS				
Principal Components (PCs)	1 Set of PCs (Primary PCs)			
Historical Data	0.5yr	1yr	2yrs	3yrs
Simulated Data, STB	30,650	27,774	23,512	20,260
PCM Forecast (1), STB	27,585	24,697	20,488	17,382
Error (1) (absolute value), STB	-3,065	-3,077	-3,024	-2,878
Percentage Error (1), %	-11.1	-12.5	-14.8	-16.6
PCM Forecast (2), STB	29,321	26,291	22,039	18,933
Error (2) (absolute value), STB	-1,329	1,483	-1,473	-1,327
Percentage Error (2), %	-4.5	-5.6	-6.7	-7.0

5.2.2.2.8. Fluid 8 Cases

The cases for Fluid 8 are displayed in the graphs in Figure 5-64 below:

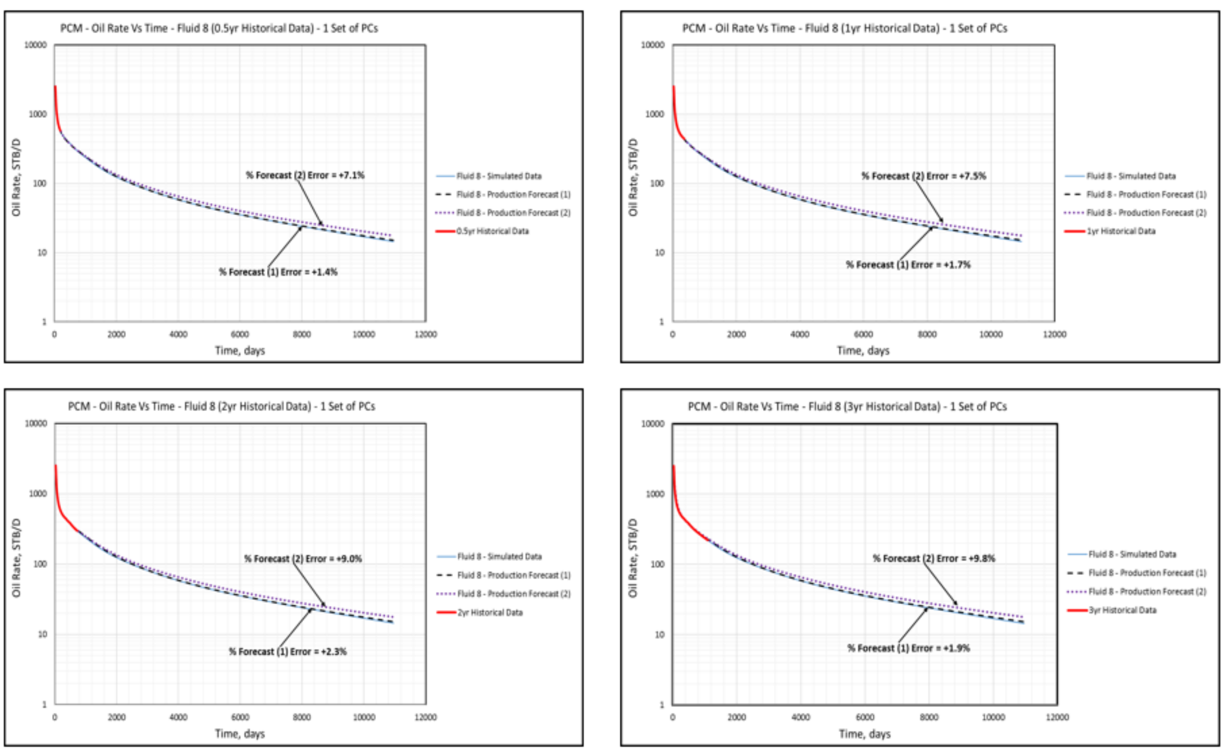

Figure 5-64 Production Forecasts (1) and (2) for Fluid 8 – 1st Set of PCs

This is one of the rare cases where PCs obtained from wells with similar fluids or operating under similar conditions did not improve forecasts. Results obtained from wells with varying conditions are highly accurate and those obtained from wells with similar (or near-similar) conditions are reasonable as well. This can be observed in Figure 5-64. Table 5-60 shows the forecasts, errors and percentage errors for Fluid 8 forecasts (1) and (2). The red figures indicate the lower of the two percentage errors for each case.

Table 5-60 Errors and Percentage Errors for Forecasts (1) and (2) – Fluid 8

FLUID 8 RESULTS				
Principal Components (PCs)	1 Set of PCs (Primary PCs)			
Historical Data	0.5yr	1yr	2yrs	3yrs
Simulated Data, STB	27,289	24,377	20,102	17,059
PCM Forecast (1), STB	27,676	24,801	20,577	17,384
Error (1) (absolute value), STB	+387	+424	+475	+325
Percentage Error (1), %	+1.4	+1.7	+2.3	+1.9
PCM Forecast (2), STB	29,360	26,356	22,100	18,908
Error (2) (absolute value), STB	+2,071	+1,979	+1,998	+1,849
Percentage Error (2), %	+7.1	+7.5	+9.0	+9.8

5.2.2.2.9. Fluid 9 Cases

The cases for Fluid 9 are shown in the graphs in Figure 5-65 below:

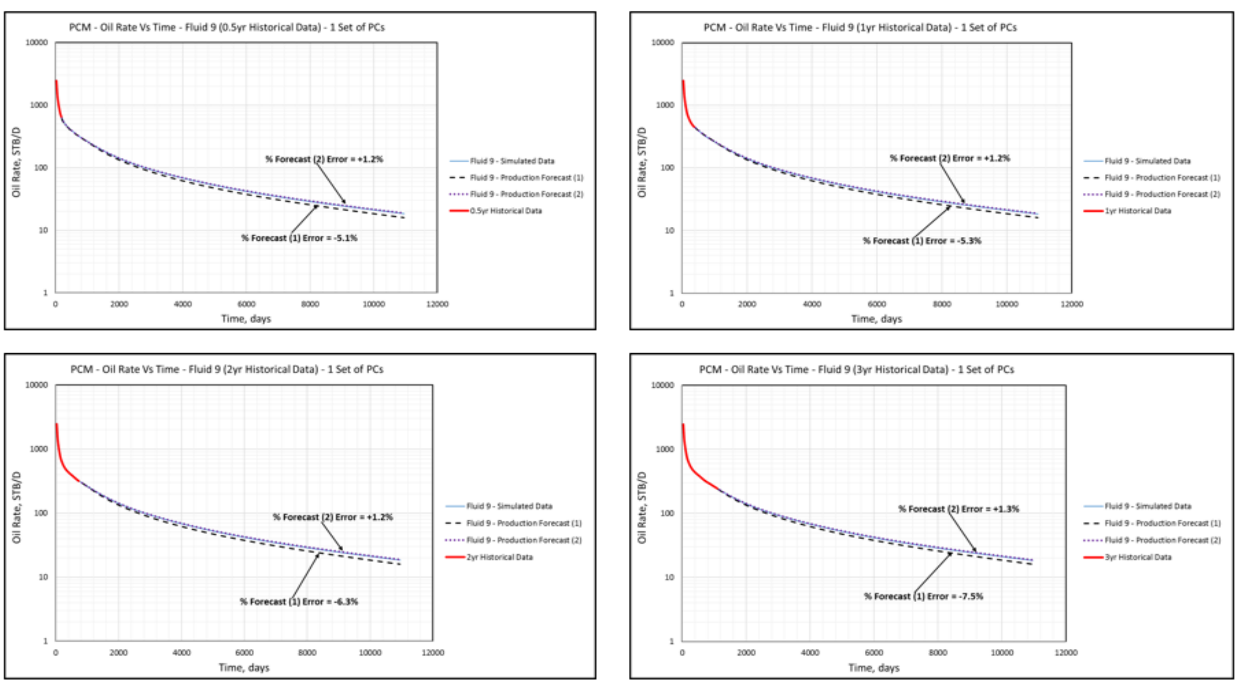

Figure 5-65 Production Forecasts (1) and (2) for Fluid 9 – 1st Set of PCs

When PCs obtained from wells with similar fluids are used to forecast, production estimates are better, as can be seen in Figure 5-65. Table 5-61 displays the forecasts, errors and percentage errors for Fluid 9 forecasts (1) and (2). The red figures indicate the lower of the two percentage errors for each case.

Table 5-61 Errors and Percentage Errors for Forecasts (1) and (2) – Fluid 9

FLUID 9 RESULTS				
Principal Components (PCs)	1 Set of PCs (Primary PCs)			
Historical Data	0.5yr	1yr	2yrs	3yrs
Simulated Data, STB	30,611	27,515	23,036	19,724
PCM Forecast (1), STB	29,121	26,137	21,667	18,341
Error (1) (absolute value), STB	-1,490	-1,378	-1,369	-1,383
Percentage Error (1), %	-5.1	-5.3	-6.3	-7.5
PCM Forecast (2), STB	30,969	27,838	23,317	19,985
Error (2) (absolute value), STB	+358	+323	+281	+261
Percentage Error (2), %	+1.2	+1.2	+1.2	+1.3

5.2.2.2.10. Fluid 10 Cases

The cases for Fluid 10 are shown in the graphs in Figure 5-66 below:

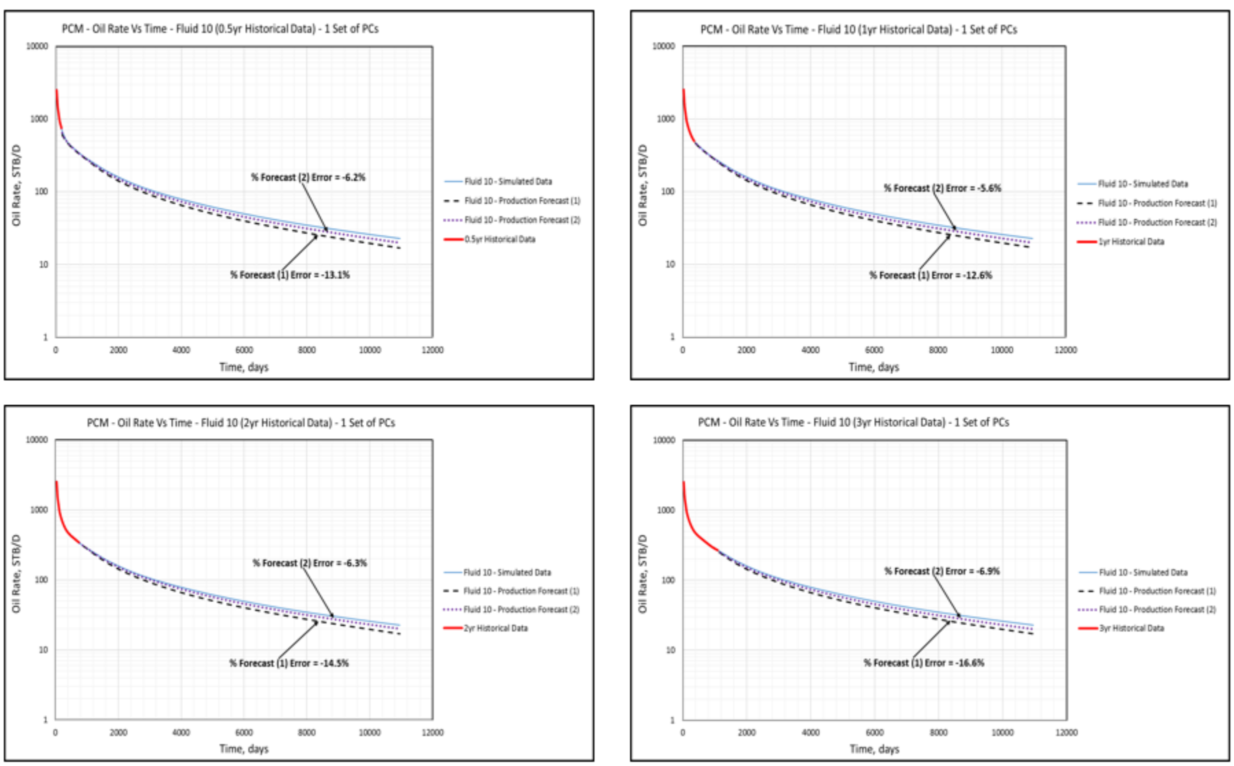

Figure 5-66 Production Forecasts (1) and (2) for Fluid 10 – 1st Set of PCs

We can observe in Figure 5-66 that there are improvements in production estimates when PCs obtained from wells with similar fluids are used to forecast. Table 5-62 displays the forecasts, errors and percentage errors for Fluid 10 forecasts (1) and (2). The red figures indicate the lower of the two percentage errors for each case.

Table 5-62 Errors and Percentage Errors for Forecasts (1) and (2) – Fluid 10

FLUID 10 RESULTS				
Principal Components (PCs)	1 Set of PCs (Primary PCs)			
Historical Data	0.5yr	1yr	2yrs	3yrs
Simulated Data, STB	34,777	31,314	26,449	22,843
PCM Forecast (1), STB	30,752	27,810	23,109	19,586
Error (1) (absolute value), STB	-4,025	-3,504	-3,340	-3,257
Percentage Error (1), %	-13.1	-12.6	-14.5	-16.6
PCM Forecast (2), STB	32,739	29,652	24,893	21,361
Error (2) (absolute value), STB	-2,038	-1,662	-1,556	-1,482
Percentage Error (2), %	-6.2	-5.6	-6.2	-6.9

5.2.2.3. Field Data Analyses

When actual field data is available, the application of PCM involves two main steps prior to following the already outlined basic workflow. Firstly, the historical field data are history-matched. The parameters obtained from the history-matching exercise can then be used to simulate production data for as long as we would like to forecast (in our case, 30 years). After this, the basic PCM workflow can be followed. In this study, we did this exercise for 10 different representative wells in the same liquid rich shale play. Therefore, 10 sets of principal components (PCs) were calculated using singular value decomposition (SVD). We then used the first set of PCs to forecast future production of the wells and other wells in the same region. An example for a well with about 1461 days of production data is shown here. Figure 5-67 shows the history-matched data and simulated forecast. Figure 5-68 shows comparison with the PCM forecast. In this case, the PCM forecast error was approximately 10%.

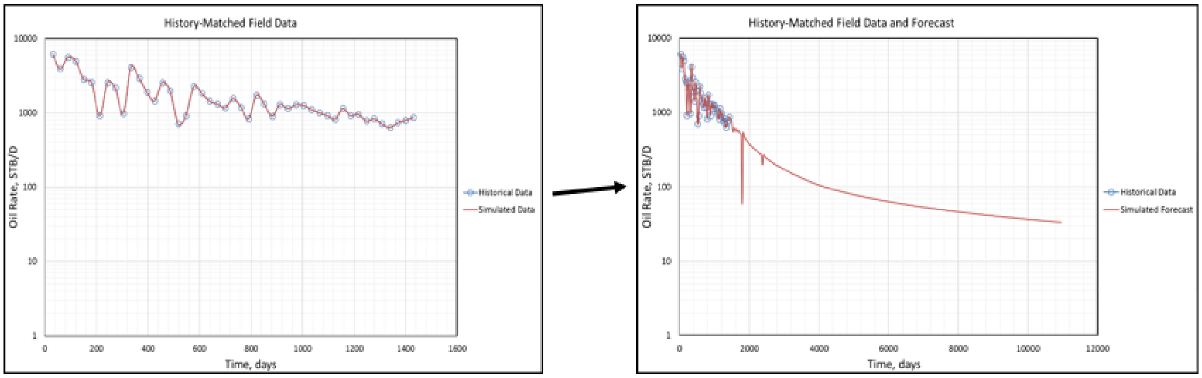

Figure 5-67 History-Matched Field Data and Forecast

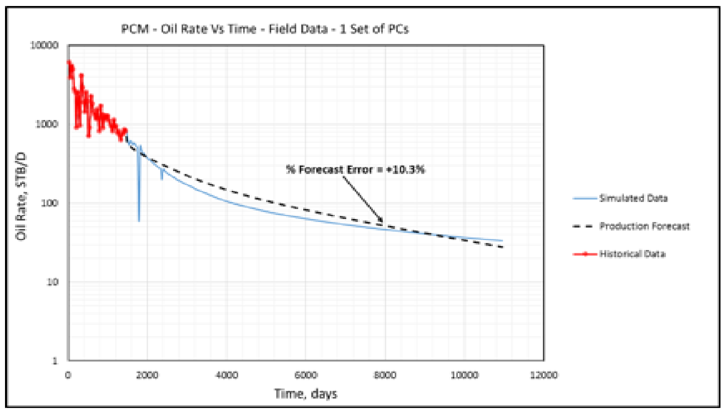

Figure 5-68 Forecast Comparisons: Field Data

Another example for a well with about 3,561 days of historical production data is presented here. Figure 5-69 displays the history-matched production data and simulated forecast. Figure 5-70 shows comparison with the PCM forecast. Here, the PCM forecast is highly accurate, with a forecast error of only 0.02%.

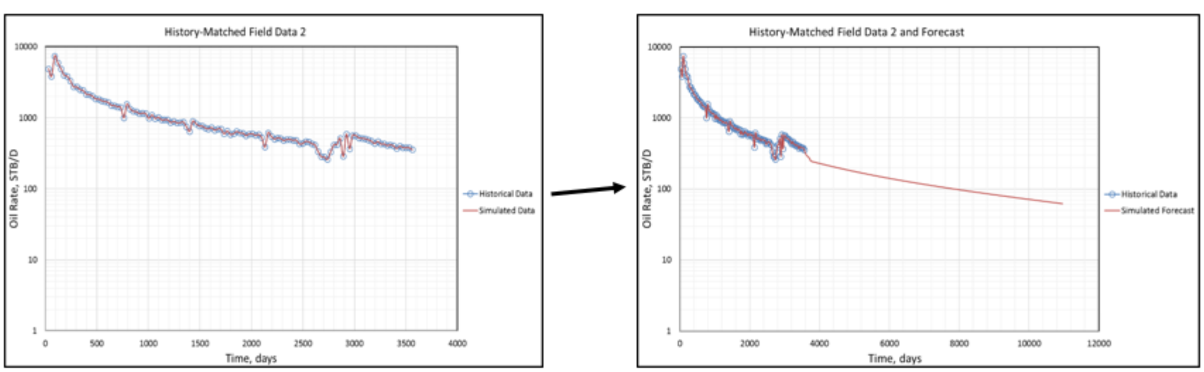

Figure 5-69 History-Matched Field Data 2 and Forecast

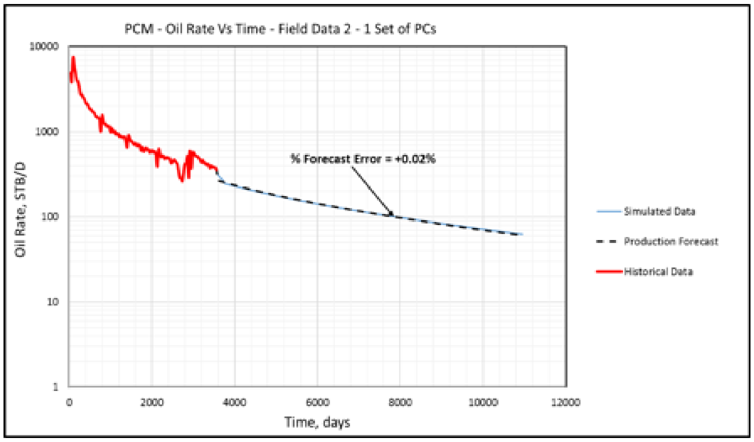

Figure 5-70 Forecast Comparisons: Field Data 2

5.2.3. Forecasting Gas-Oil Ratios (GOR) and Solution Gas Production Using the Principal Components Methodology (PCM)

Stakeholders often focus on oil forecasts for shale oil reservoirs, ignoring the equally important solution gas produced from these plays. Limited production data, complex flow mechanisms in liquid-rich shale reservoirs, patterns of producing gas-oil ratios and other factors, make the task of forecasting solution gas production difficult. Beliveau (2004) discussed several historical methods of estimating solution gas production depending on the reservoir production mechanism. He concluded that proper history-matching and reservoir simulation is the only way to generate good solution gas forecasts. Yu (2014) presented a simple methodology for forecasting solution gas production based on predicted oil production. He proposed a specialized plot based on a linear relationship between the logarithm of a well's cumulative gas-oil ratio (GOR_{cum}) and cumulative oil production (N_p). Makinde and Lee (2016) modified this approach by considering a power law relationship between these two variables. Principal components analysis (PCA) however, has enabled us to reveal the internal structure of data from the representative wells considered, in a way that best describes the variance in the data. This allowed us to get principal components (data from the PCA calculations) that helped us forecast gas-oil ratios from shale volatile oil reservoirs using the Principal Components Methodology (PCM).

The same multi-fractured horizontal well (MFHW) model as in Figure 5-2 was considered here. Production from wells with ten different fluid samples (volatile oils) were simulated using a commercial compositional simulator. As a basecase, 30 years of production were simulated from wells with a minimum bottomhole pressure (BHP) constraint of 1000 psi, initial reservoir pressure of 5000 psi and critical gas saturation of 5%. Later, we further simulated cases with wells having a minimum BHP of 500 psi, initial reservoir pressure of 4000 psi and critical gas saturation of 10%. In all, production was simulated from 40 different wells. The Peng-Robinson equation of state was used for the PVT, then pressure drop and fluid flow were modeled using logarithmically-spaced local grid refinement (LS-LGR). Tables 5-40 and 5-41 show the reservoir data as well as the ten different reservoir fluid compositions.

The basic procedure for PCM was followed as outlined in subsection 5.2. Producing gas-oil ratio (GOR) data from various wells were represented in a matrix form. Then, singular value decomposition (SVD) was used to break the matrix into simpler, more meaningful parts and as a result, obtain the principal components (PCs). The principal components are a set of normalized eigenvectors calculated with SVD. They are independent linear combinations of a set of normalized values that capture as much of the variability in the original data sets (producing GOR in this study) as possible. These principal components were then used to forecast future GOR data. From the estimated producing GOR, we were able to determine the solution gas production (in our cases, after

30 years). This cumulative gas production was calculated by using the trapezoidal rule to approximate the area under the forecasted producing GOR vs. cumulative oil production (Np) curve with Equation 14, shown here as

$$Cum.Gas = \sum_{i=1}^{n} \frac{GOR_{i+1} - GOR_i}{2(Np_{i+1} - Np_i)} \ . \tag{14}$$

The more data points that are available, the more accurate trapezoidal rule approximations are.

When working with field data, history-matching of the available data is the first step. Parameters obtained from simulator history-matches can then be used to simulate GOR data for as long as we desire. After these steps, the basic workflow for PCM can be followed as already outlined.

In this study, singular value decomposition (SVD) was used to generate 40 sets of principal components (PCs) with producing gas-oil ratio (GOR) data from 40 different wells with ten different reservoir fluid compositions. The first set of principal components are the primary principal components which capture the most variability in the representative data from all 40 wells considered. The other sets of PCs reveal certain specific characteristics for each well. The first set of PCs capture the most data that best describes the variance from all representative wells, followed by the second set of PCs. Each successive set of PCs capture less and less variance in the representative data under consideration (Makinde and Lee, 2016). Five sets of principal components out of the total of 40 obtained were used for our analyses. Table 5-63 shows the percentage of data capture for each of the 5 sets of PCs. Graphical descriptions (semi-log plots) of each set of PCs are shown in Figures 5-71 and 5-72.

Table 5-63 Principal Components and % Data Capture

PRINCIPAL COMPONENTS (PCs)	% DATA CAPTURE
1st Set of PCs	92.3
2nd Set of PCs	3.7
3rd Set of PCs	1.6
4th Set of PCs	0.5
5th Set of PCs	0.4

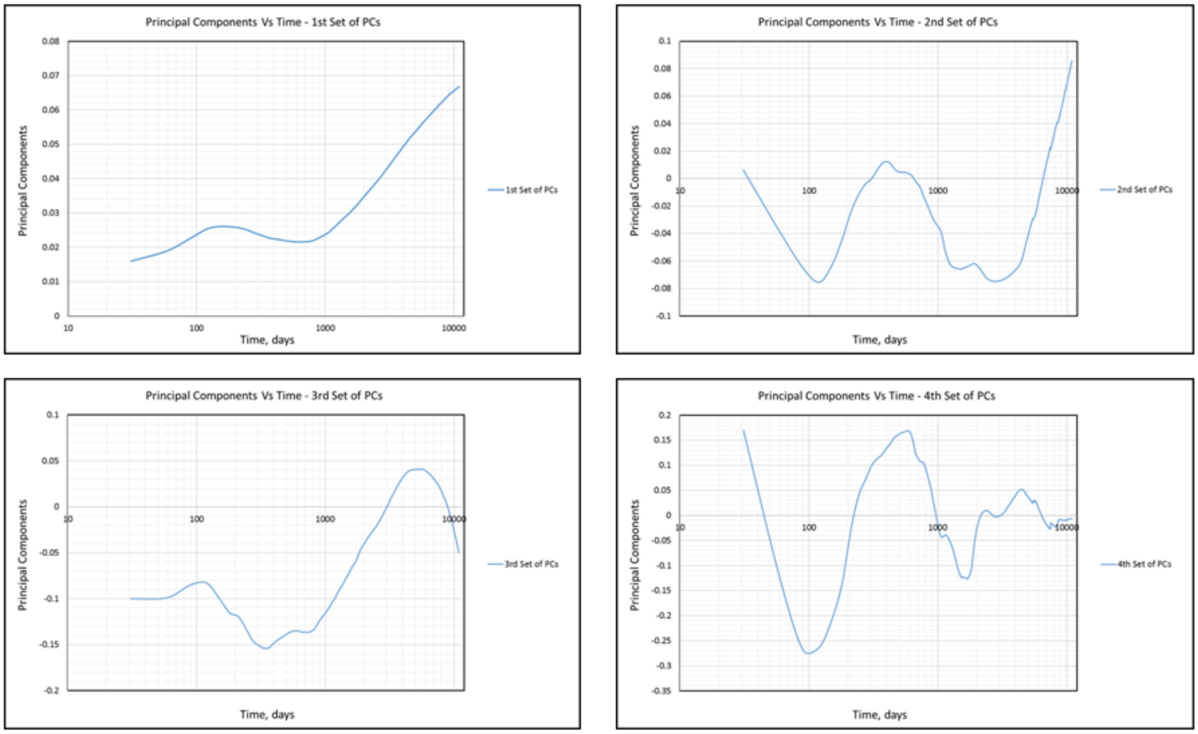

Figure 5-71 Principal Components vs. Time – 1st to 4th Set of PCs

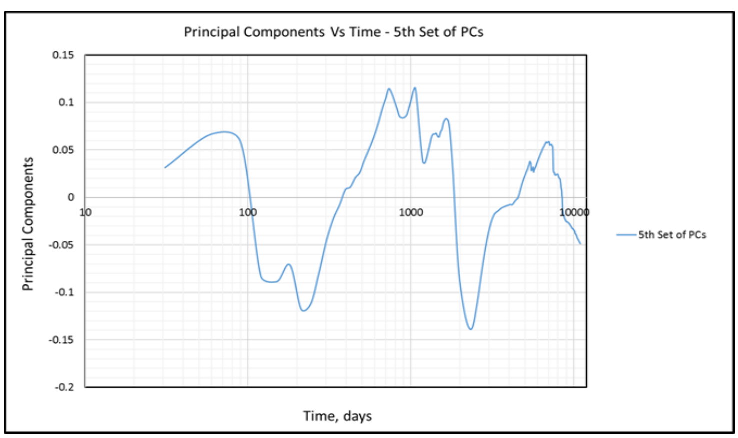

Figure 5-72 Principal Components vs. Time – 5th Set of PCs

5.2.3.1. Results

We used PCM to forecast 30 years of producing gas-oil ratio (GOR) data for the ten fluid samples with availability of 0.5 to 3 yrs of simulated GOR history. The results were then compared to our basecase simulation study results. Analyses were done with PCM, using from one to all five sets of PCs for estimating future GOR. Results for all the fluids under consideration are shown in the following subsections.

5.2.3.1.1. Fluid 1 Cases

Graphical displays of GOR forecasts and the plots of the estimated GOR forecasts versus cumulative oil production for Fluid 1 are shown in Figures 5-73 to 5-82.

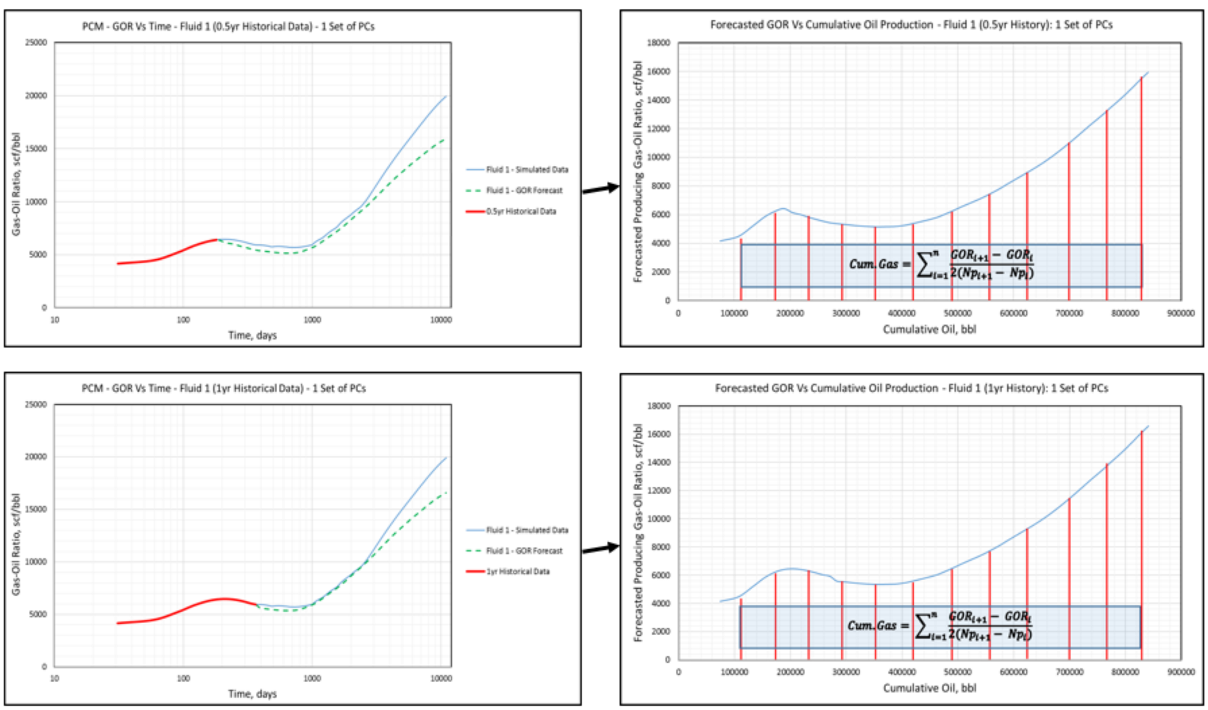

Figure 5-73 GOR Forecasts & Forecasted GOR vs. Cum. Oil – Fluid 1 (0.5yr. and 1 yr. Histories): 1 Set of PCs

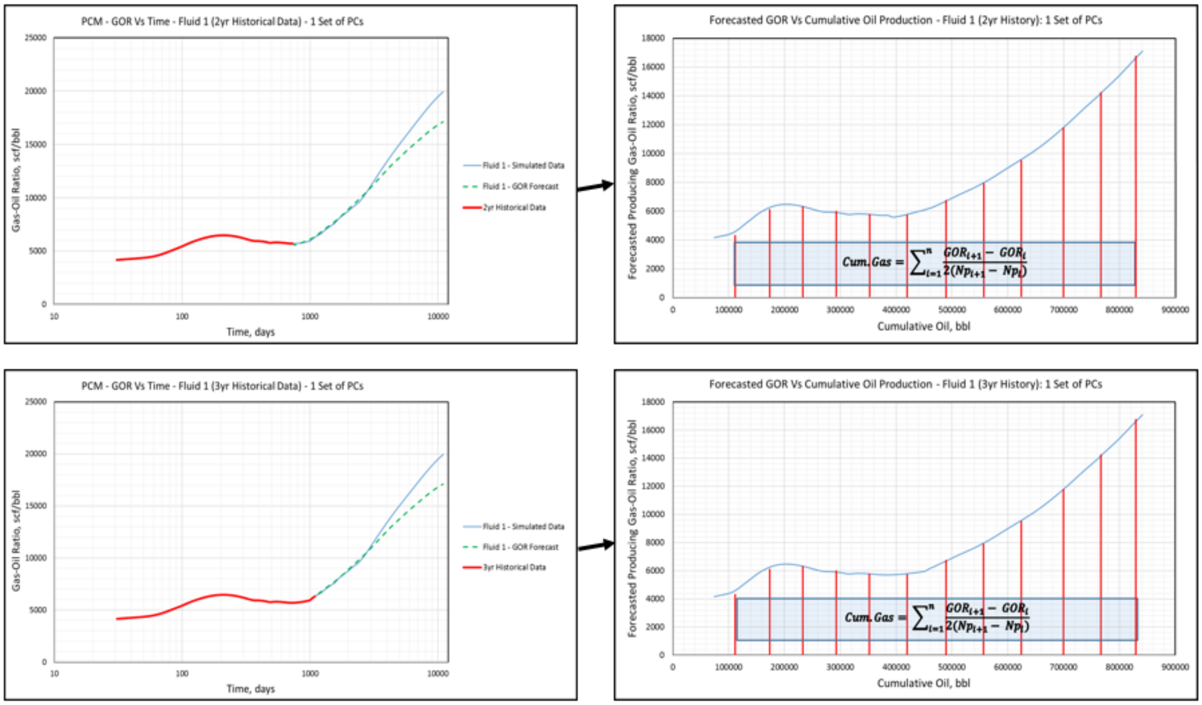

Figure 5-74 GOR Forecasts & Forecasted GOR vs. Cum. Oil – Fluid 1 (2yr. and 3yr. Histories): 1 Set of PCs

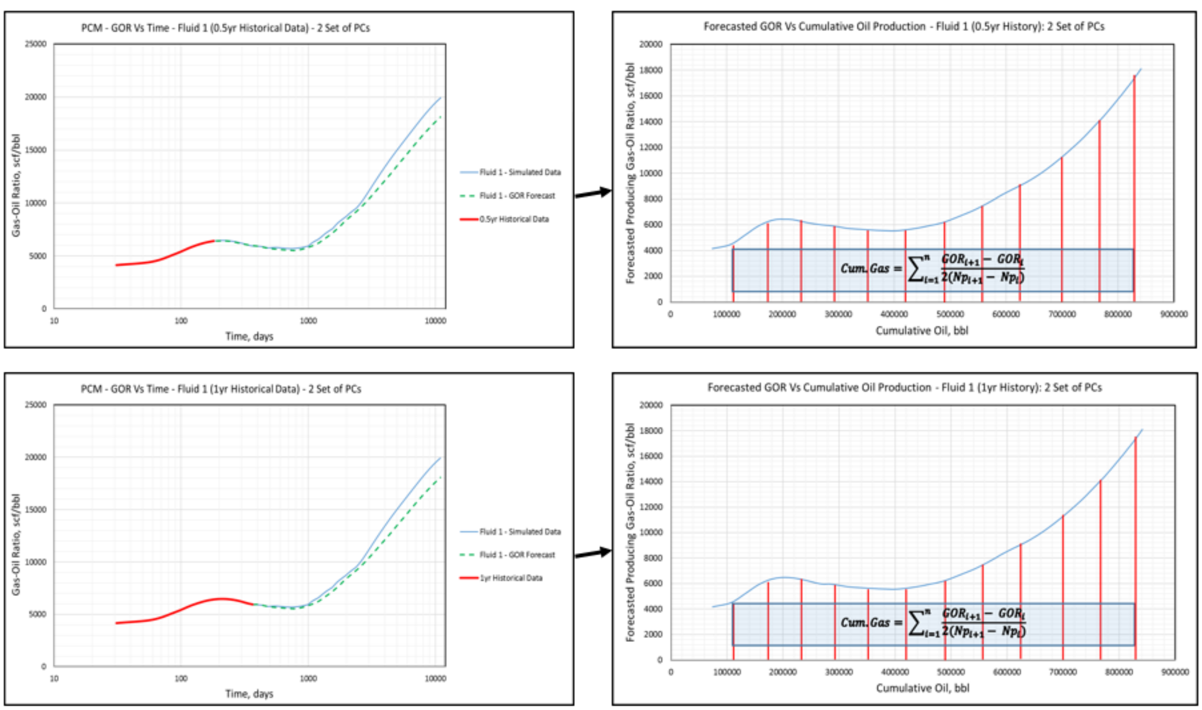

Figure 5-75 GOR Forecasts & Forecasted GOR vs. Cum. Oil – Fluid 1 (0.5yr. and 1yr. Histories): 2 Sets of PCs

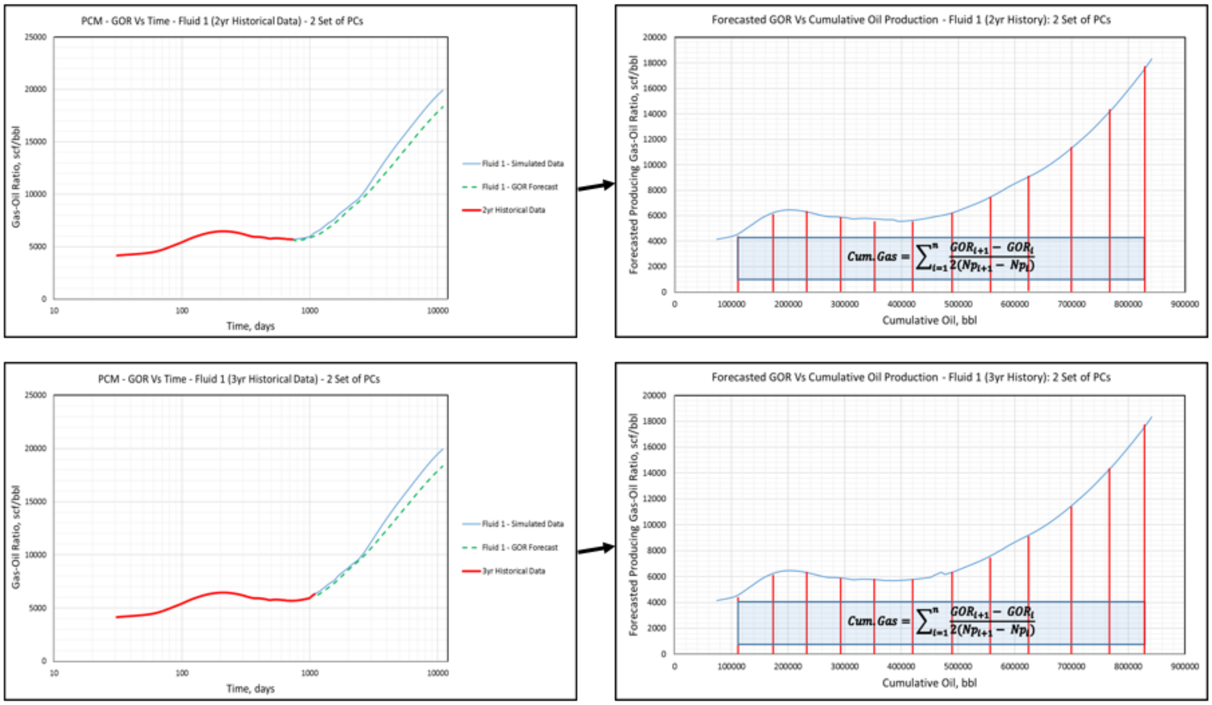

Figure 5-76 GOR Forecasts & Forecasted GOR vs. Cum. Oil – Fluid 1 (2yr. and 3yr. Histories): 2 Sets of PCs

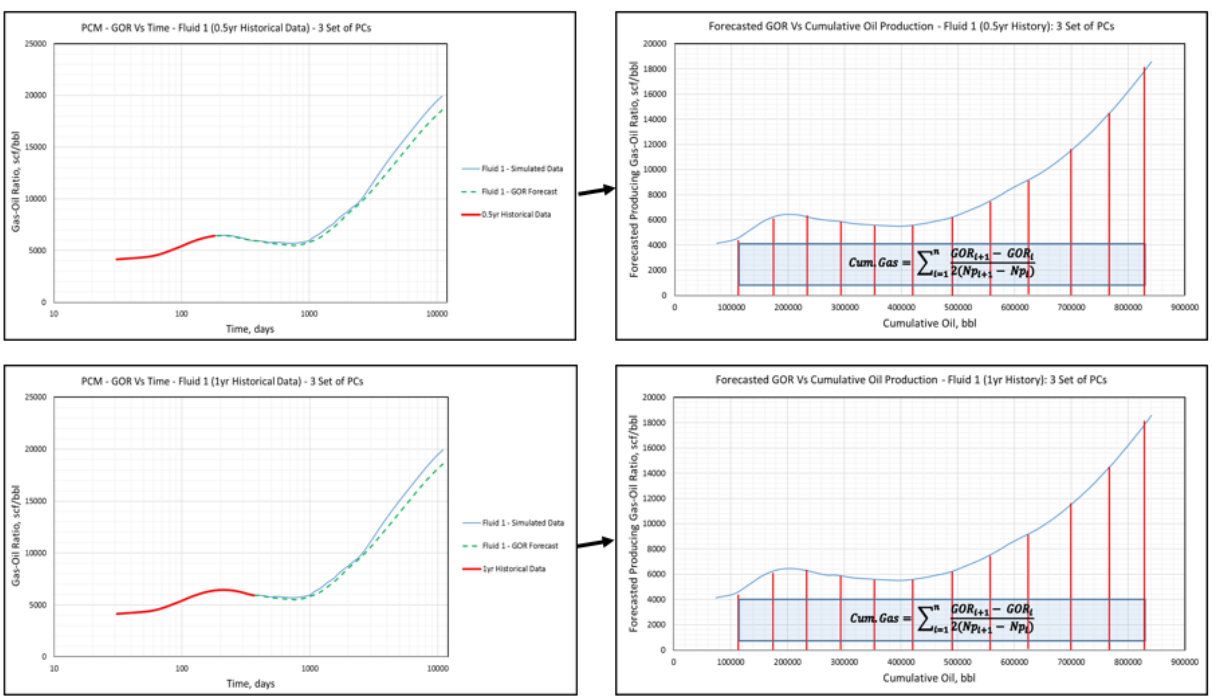

Figure 5-77 GOR Forecasts & Forecasted GOR vs. Cum. Oil – Fluid 1 (0.5yr. and 1yr. Histories): 3 Sets of PCs

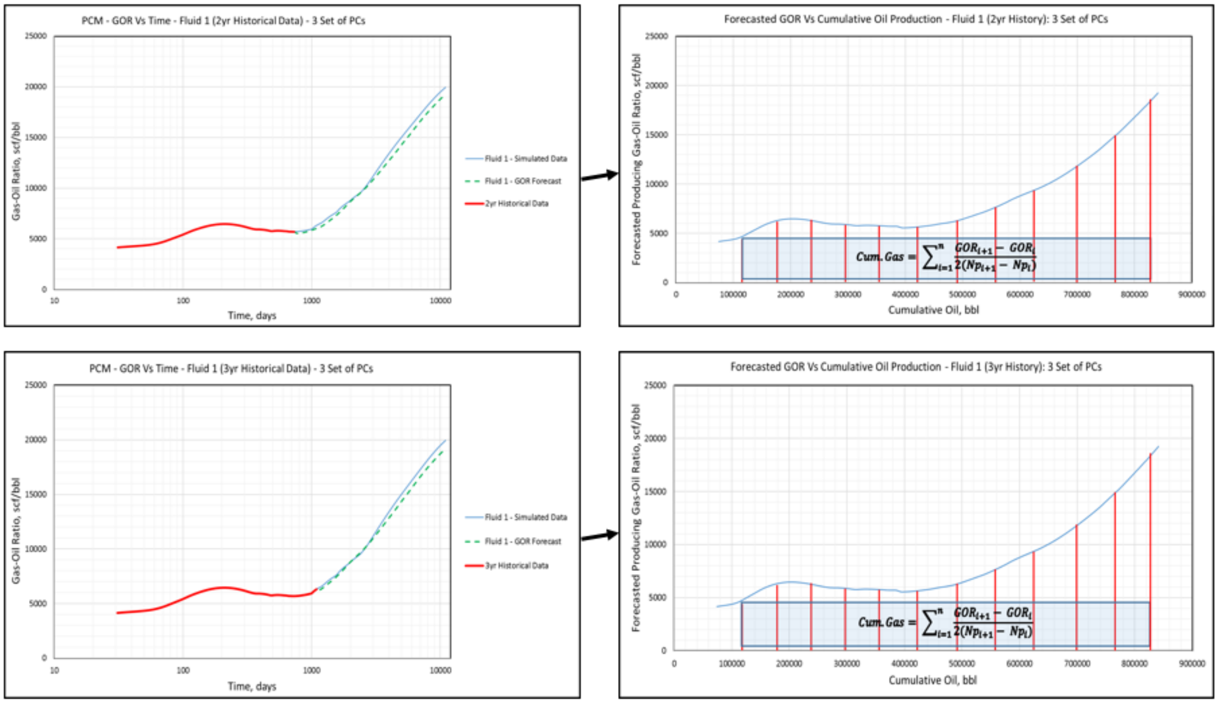

Figure 5-78 GOR Forecasts & Forecasted GOR vs. Cum. Oil – Fluid 1 (2yr. and 3yr. Histories): 3 Sets of PCs

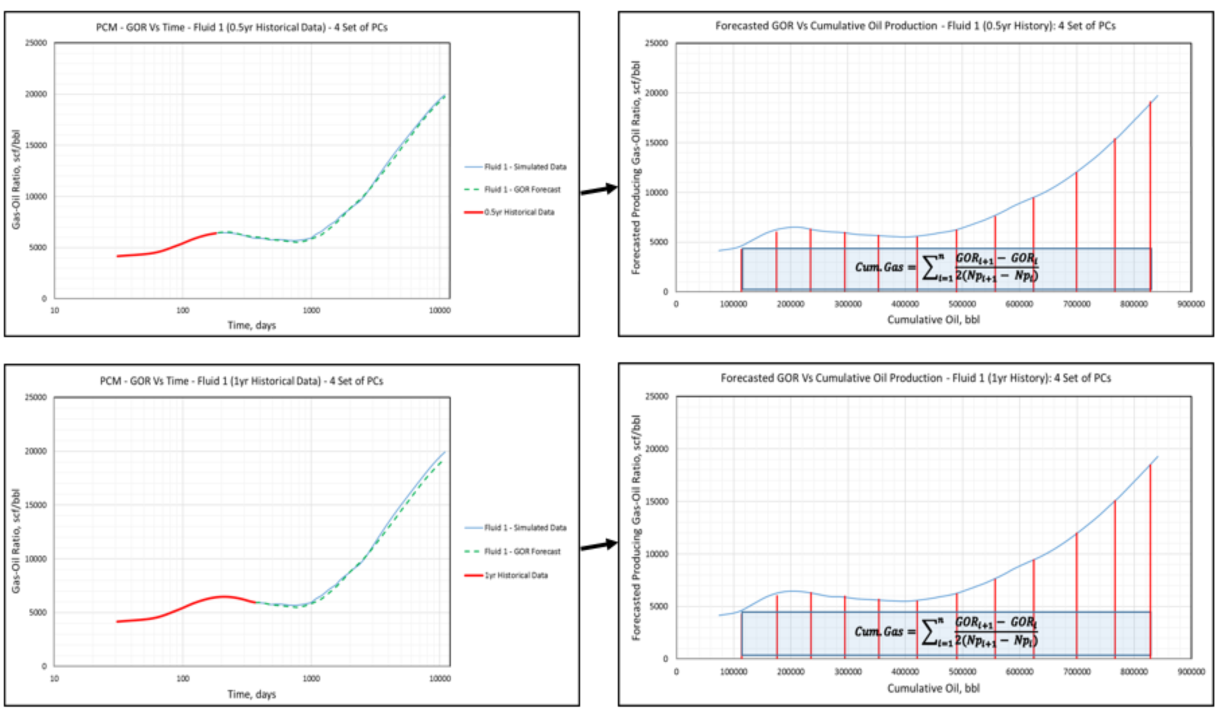

Figure 5-79 GOR Forecasts & Forecasted GOR vs. Cum. Oil – Fluid 1 (0.5yr. and 1yr. Histories): 4 Sets of PCs

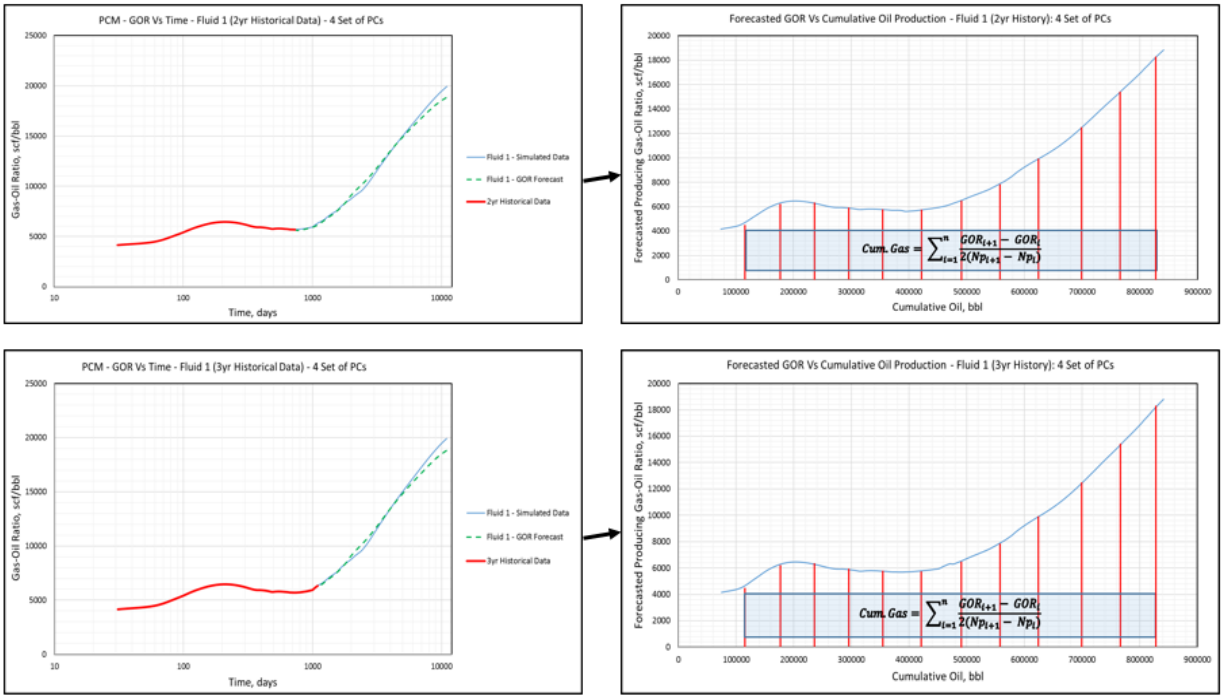

Figure 5-80 GOR Forecasts & Forecasted GOR vs. Cum. Oil – Fluid 1 (2yr. and 3yr. Histories): 4 Sets of PCs

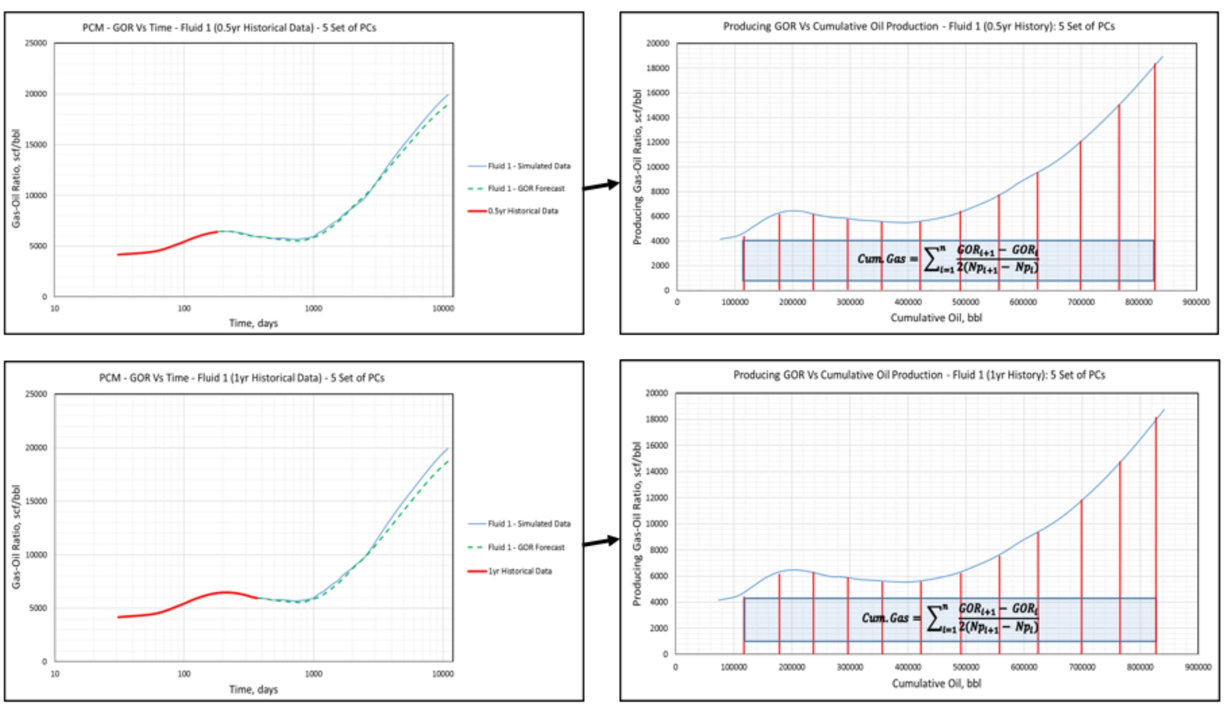

Figure 5-81 GOR Forecasts & Forecasted GOR vs. Cum. Oil – Fluid 1 (0.5yr. and 1yr. Histories): 5 Sets of PCs

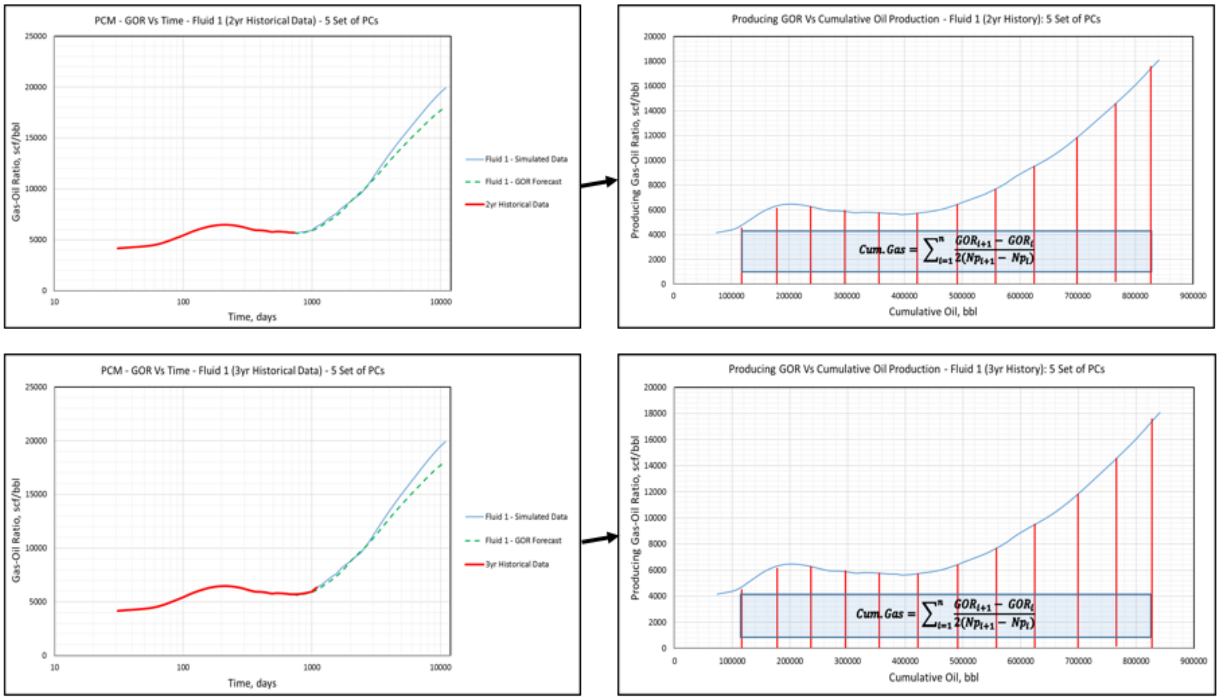

Figure 5-82 GOR Forecasts & Forecasted GOR vs. Cum. Oil – Fluid 1 (2yr. and 3yr. Histories): 5 Sets of PCs

Table 5-64 shows the results for all Fluid 1 cases. In all these cases, forecasts were reasonable and errors in the calculated solution gas produced (after 30 yrs) in most cases were relatively low. Percentage error was as low as 5.2% when 4 sets of PCs were used to forecast. The figures in red indicate the lowest percentage errors for each case.

Table 5-64 Solution Gas Production Forecasts, Errors and Percentage Errors – Fluid 1

FLUID 1 RESULTS																				
Principal Components (PCs)	1 Set of PCs				2 Sets of PCs				3 Sets of PCs				4 Sets of PCs				5 Sets of PCs			
Historical Data	0.5yr	1yr	2yrs	3yrs	0.5yr	1yr	2yrs	3yrs	0.5yr	1yr	2yrs	3yrs	0.5yr	1yr	2yrs	3yrs	0.5yr	1yr	2yrs	3yrs
Simulated Cum. Gas, bscf	6.9	6.9	6.9	6.9	6.9	6.9	6.9	6.9	6.9	6.9	6.9	6.9	6.9	6.9	6.9	6.9	6.9	6.9	6.9	6.9
PCM Forecast, bscf	5.9	6.2	6.3	6.3	6.2	6.2	6.2	6.3	6.3	6.3	6.4	6.4	6.4	6.4	6.5	6.5	6.4	6.3	6.3	6.5
Error (absolute value), bscf	-1.0	-0.7	-0.6	-0.6	-0.7	-0.7	-0.7	-0.6	-0.6	-0.6	-0.5	-0.5	-0.5	-0.5	-0.4	-0.4	-0.5	-0.6	-0.6	-0.4
Percentage Error, %	-14.1	-10.7	-8.2	-8.2	-10.2	-10.2	-9.7	-8.9	-9.0	-9.1	-7.5	-6.9	-6.4	-7.2	-5.2	-5.3	-7.1	-8.0	-8.0	-6.3

5.2.3.1.2. Fluid 2 Cases

Graphical displays of GOR forecasts and the plots of the estimated GOR forecasts versus cumulative oil production for Fluid 2 are shown in Figures 5-83 to 5-92.

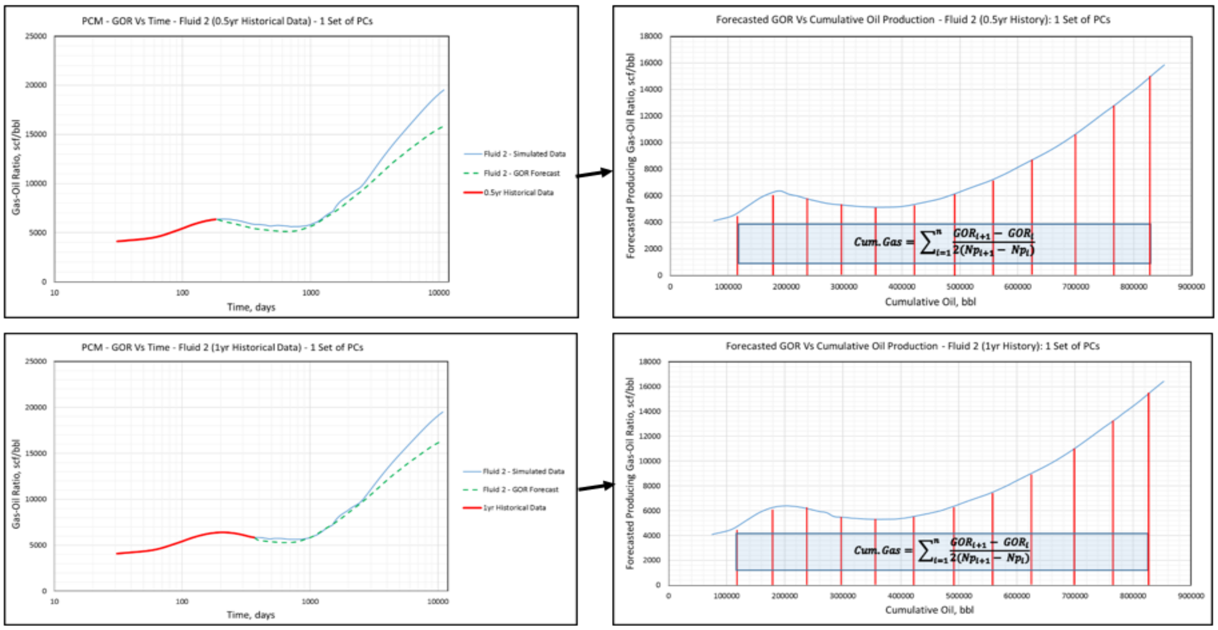

Figure 5-83 GOR Forecasts & Forecasted GOR vs. Cum. Oil – Fluid 2 (0.5yr. and 1yr. Histories): 1 Set of PCs

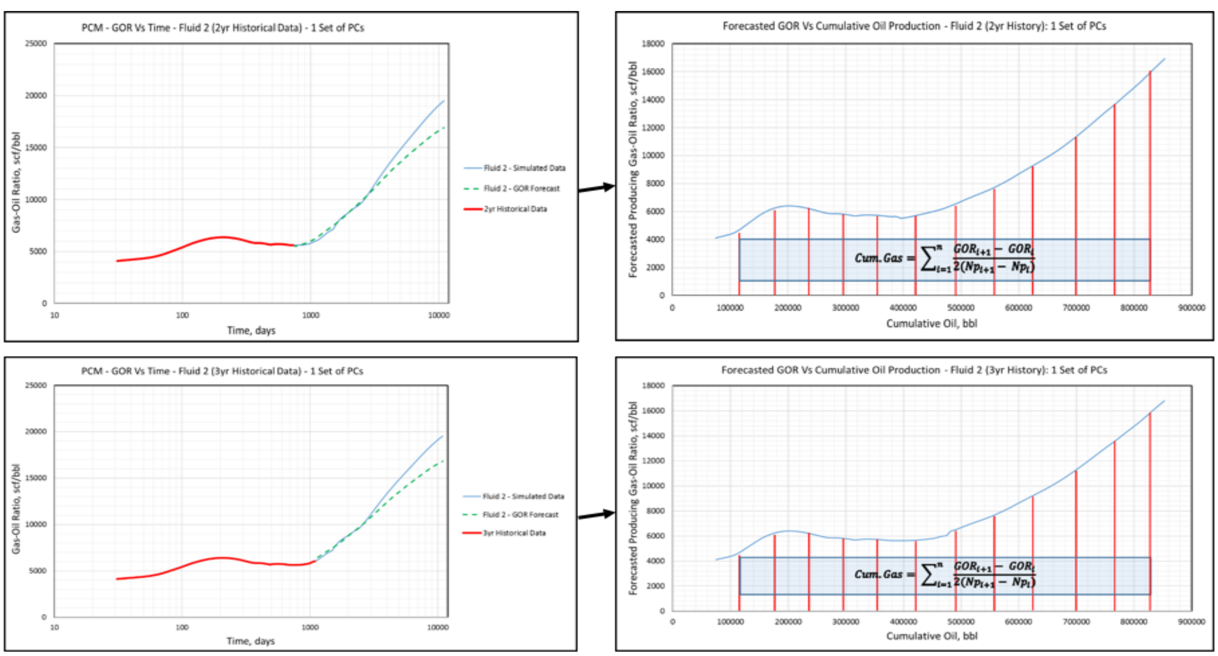

Figure 5-84 GOR Forecasts & Forecasted GOR vs. Cum. Oil – Fluid 2 (2yr. and 3yr. Histories): 1 Set of PCs

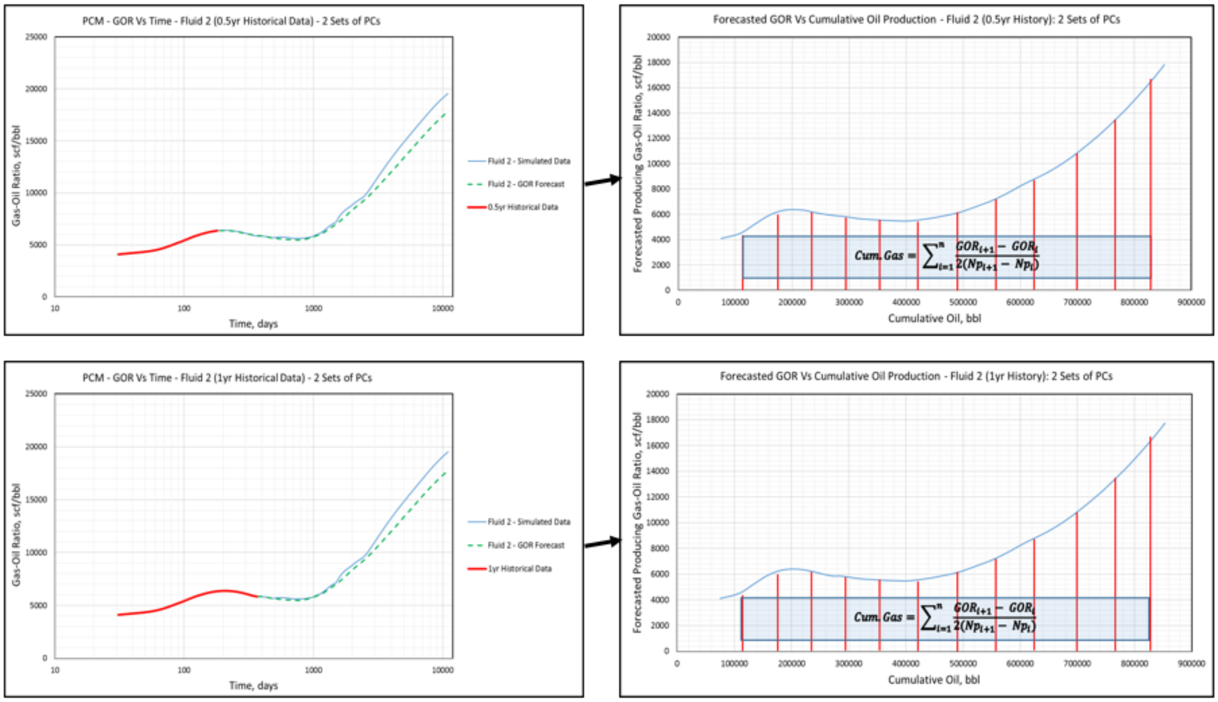

Figure 5-85 GOR Forecasts & Forecasted GOR vs. Cum. Oil – Fluid 2 (0.5yr. and 1yr. Histories): 2 Sets of PCs

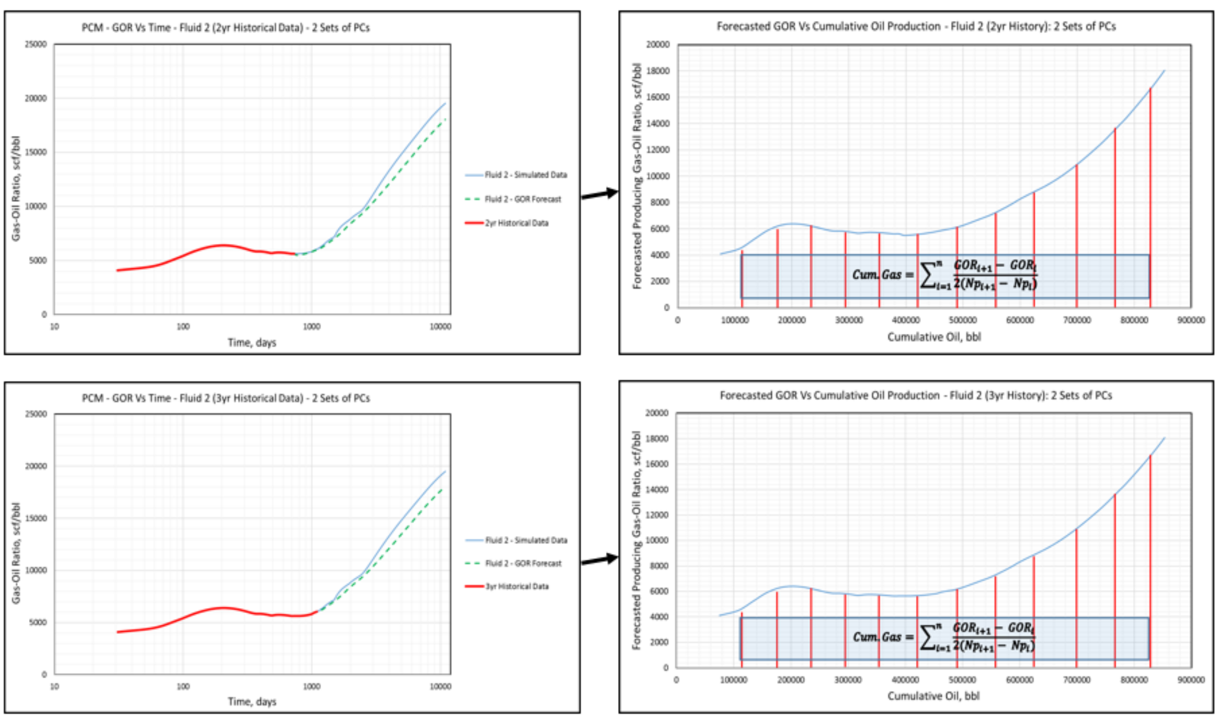

Figure 5-86 GOR Forecasts & Forecasted GOR vs. Cum. Oil – Fluid 2 (2yr. and 3yr. Histories): 2 Sets of PCs

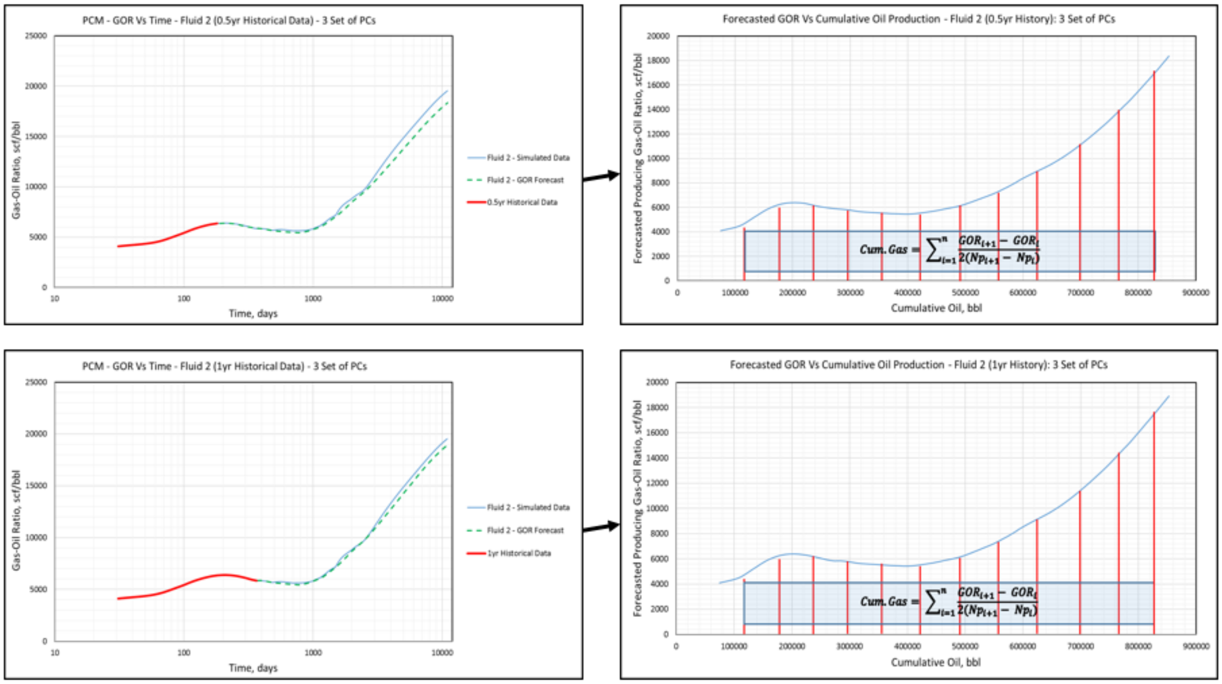

Figure 5-87 GOR Forecasts & Forecasted GOR vs. Cum. Oil – Fluid 2 (0.5yr. and 1yr. Histories): 3 Sets of PCs

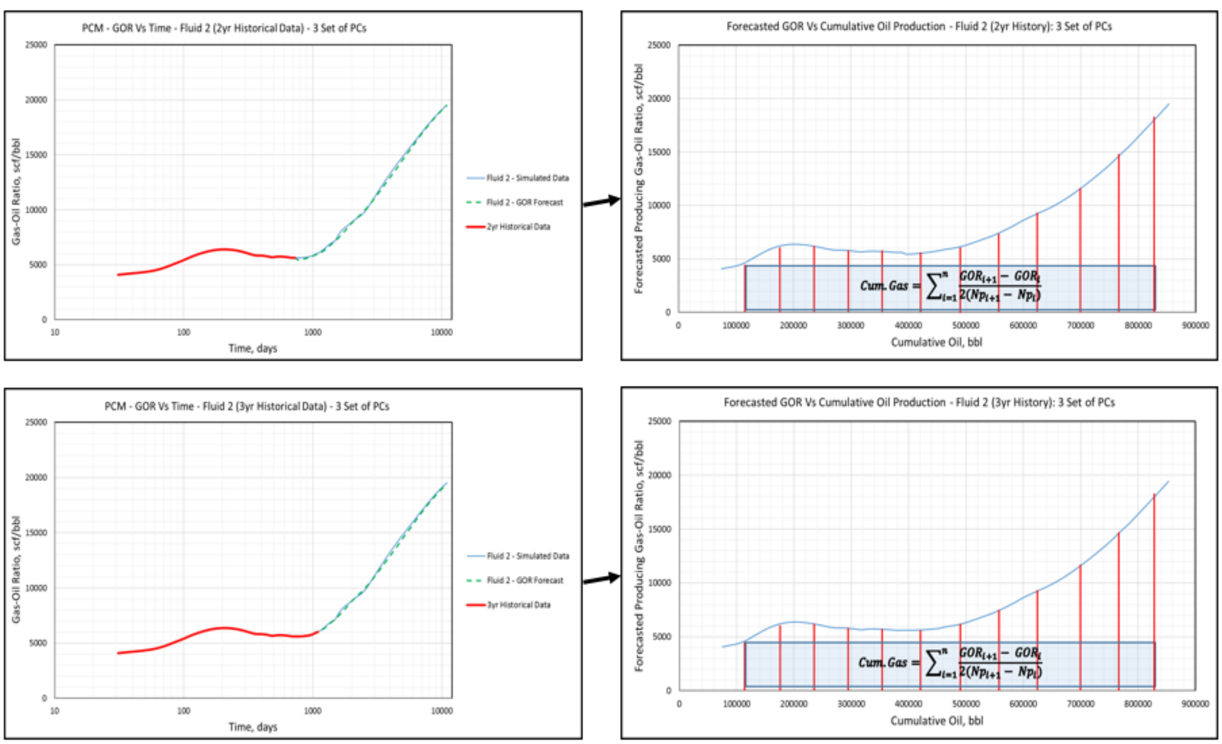

Figure 5-88 GOR Forecasts & Forecasted GOR vs. Cum. Oil – Fluid 2 (2yr. and 3yr. Histories): 3 Sets of PCs

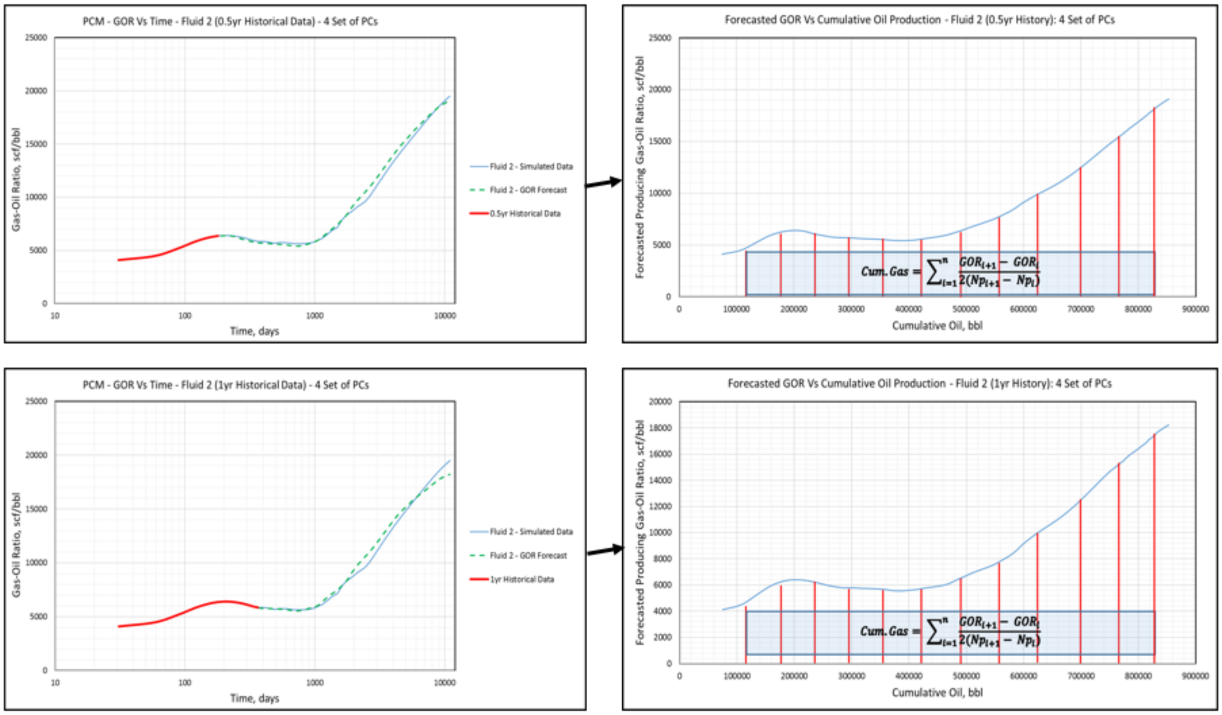

Figure 5-89 GOR Forecasts & Forecasted GOR vs. Cum. Oil – Fluid 2 (0.5yr. and 1yr. Histories): 4 Sets of PCs

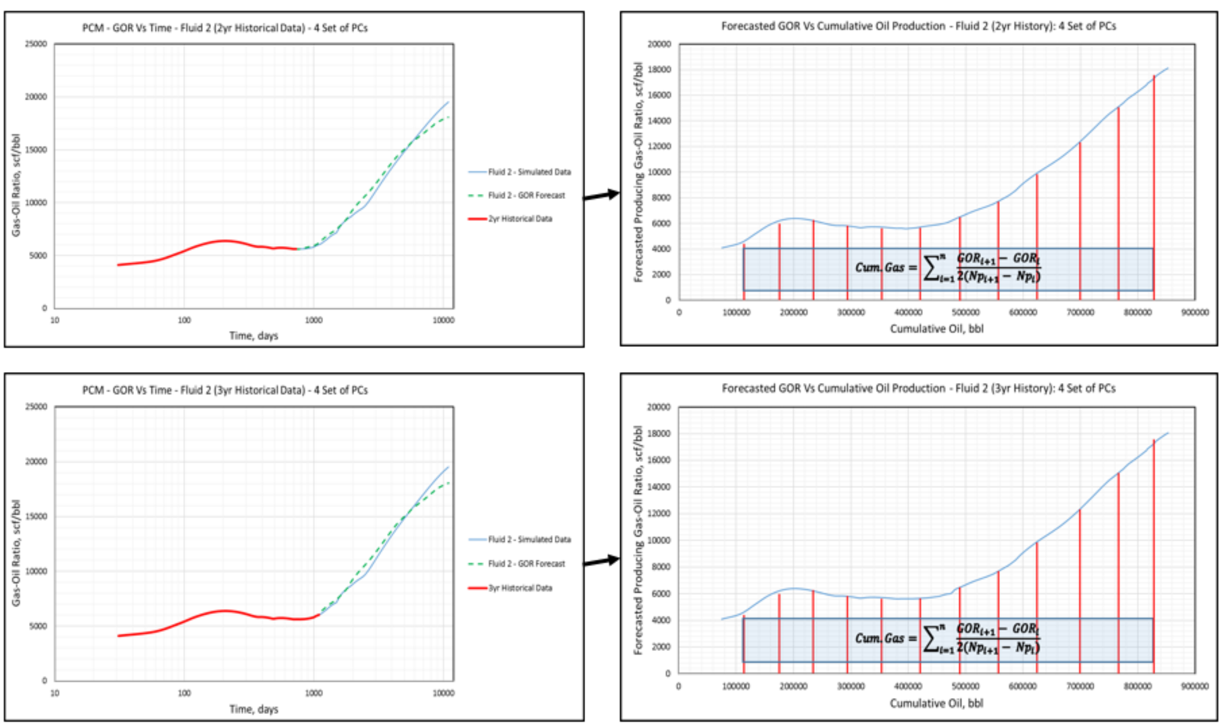

Figure 5-90 GOR Forecasts & Forecasted GOR vs. Cum. Oil – Fluid 2 (2yr. and 3yr. Histories): 4 Sets of PCs

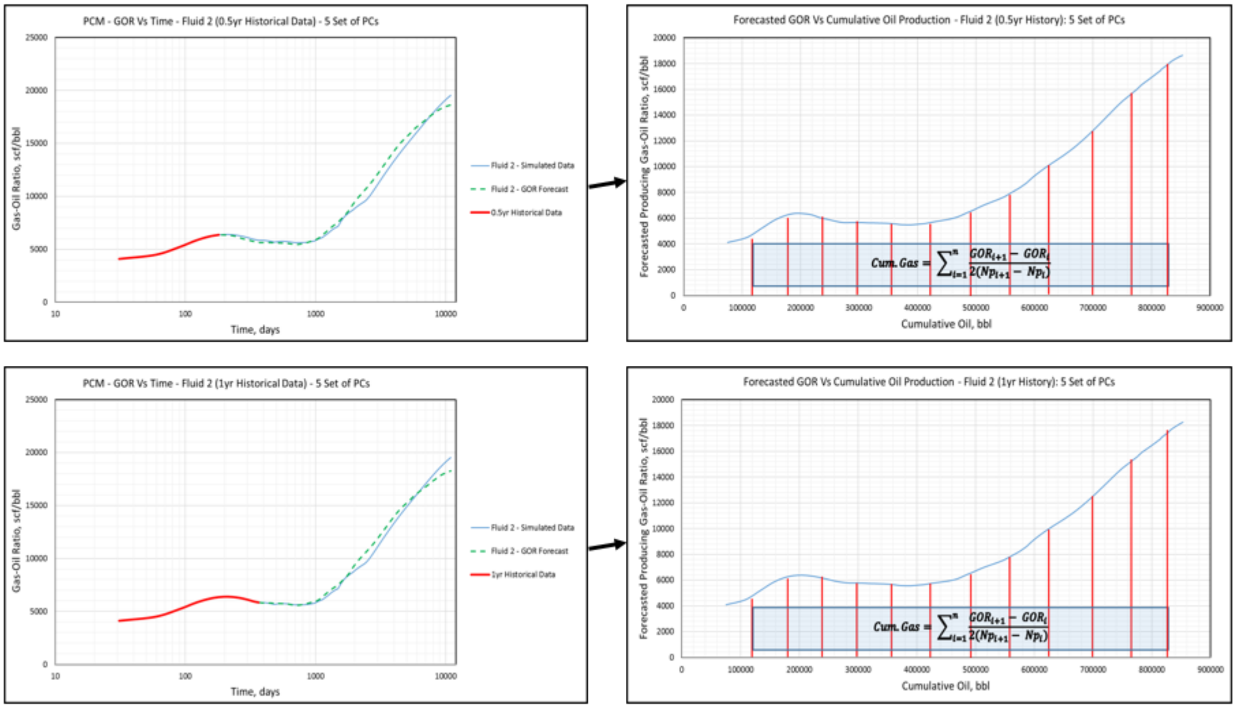

Figure 5-91 GOR Forecasts & Forecasted GOR vs. Cum. Oil – Fluid 2 (0.5yr. and 1yr. Histories): 5 Sets of PCs

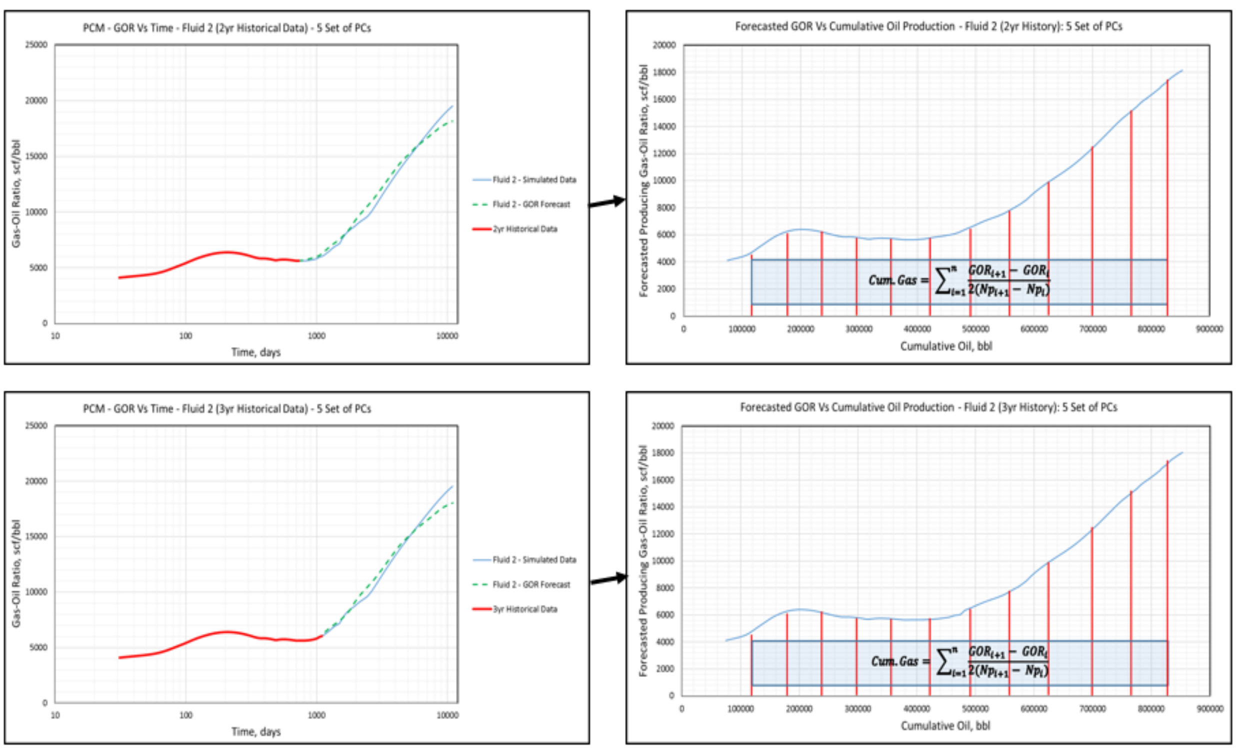

Figure 5-92 GOR Forecasts & Forecasted GOR vs. Cum. Oil – Fluid 2 (2yr. and 3yr. Histories): 5 Sets of PCs

Table 5-65 shows the results for all Fluid 2 cases. In all these cases, forecasts were reasonable and errors in the calculated solution gas produced (after 30 yrs) in most cases were relatively low. Percentage error was as low as 2.5% when all 5 sets of PCs were used to forecast. The figures in red indicate the lowest percentage errors for each case.

Table 5-65 Solution Gas Production Forecasts, Errors and Percentage Errors – Fluid 2

FLUID 2 RESULTS																				
Principal Components (PCs)	1 Set of PCs				2 Sets of PCs				3 Sets of PCs				4 Sets of PCs				5 Sets of PCs			
Historical Data	0.5yr	1yr	2yrs	3yrs	0.5yr	1yr	2yrs	3yrs	0.5yr	1yr	2yrs	3yrs	0.5yr	1yr	2yrs	3yrs	0.5yr	1yr	2yrs	3yrs
Simulated Cum. Gas, bscf	6.9	6.9	6.9	6.9	6.9	6.9	6.9	6.9	6.9	6.9	6.9	6.9	6.9	6.9	6.9	6.9	6.9	6.9	6.9	6.9
PCM Forecast, bscf	6.0	6.2	6.4	6.3	6.2	6.2	6.3	6.3	6.3	6.4	6.5	6.5	6.7	6.7	6.6	6.6	6.7	6.7	6.7	6.6
Error (absolute value), bscf	-0.9	-0.7	-0.5	-0.6	-0.7	-0.7	-0.6	-0.6	-0.6	-0.5	-0.4	-0.4	-0.2	-0.2	-0.3	-0.3	-0.2	-0.2	-0.2	-0.3
Percentage Error, %	-13.5	-10.4	-8.0	-8.4	-9.9	-10.0	-9.4	-9.1	-8.6	-7.2	-5.8	-5.8	-3.5	-3.5	-3.8	-4.0	-2.5	-3.2	-3.5	-4.1

5.2.3.1.3. Fluid 3 Cases

Graphical displays of GOR forecasts and the plots of the estimated GOR forecasts versus cumulative oil production for Fluid 3 are shown in Figures 5-93 to 5-102.

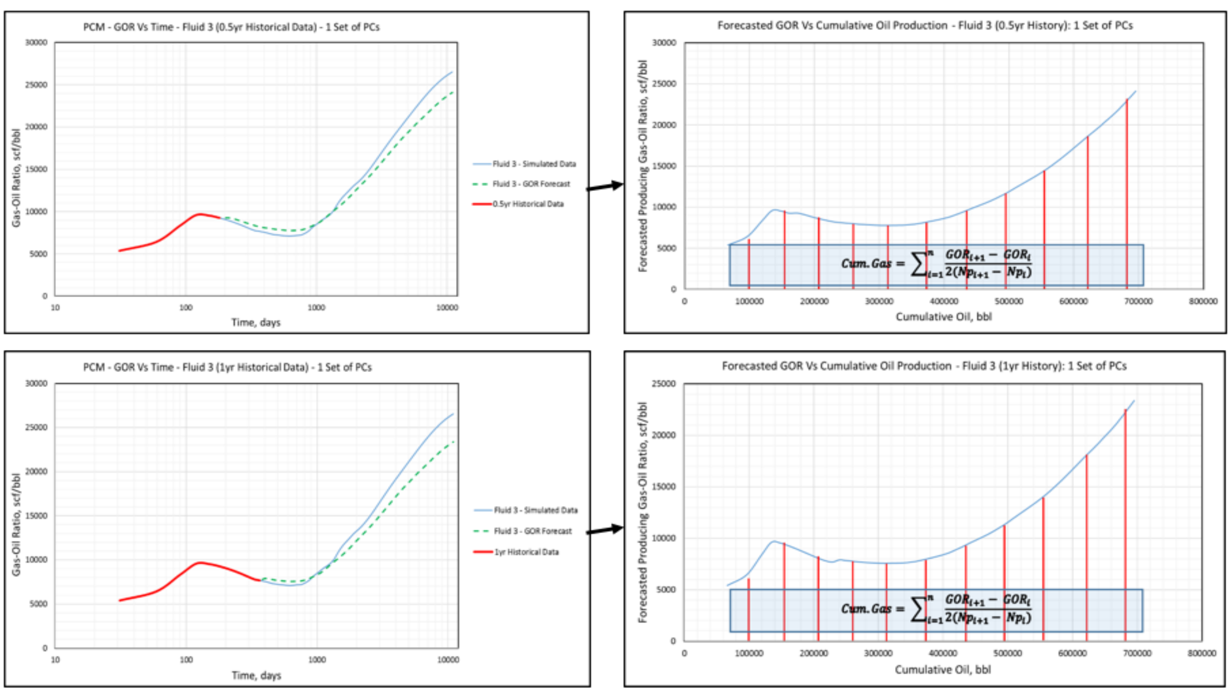

Figure 5-93 GOR Forecasts & Forecasted GOR vs. Cum. Oil – Fluid 3 (0.5yr. and 1yr. Histories): 1 Set of PCs

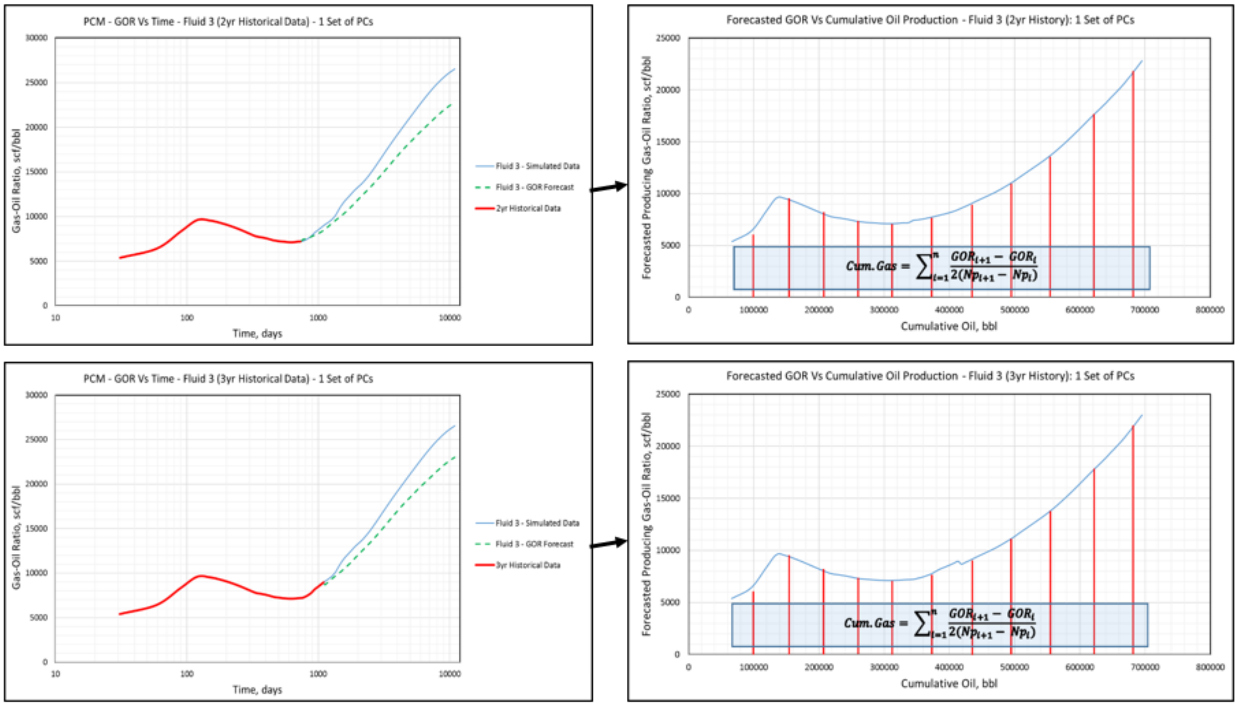

Figure 5-94 GOR Forecasts & Forecasted GOR vs. Cum. Oil – Fluid 3 (2yr. and 3yr. Histories): 1 Set of PCs

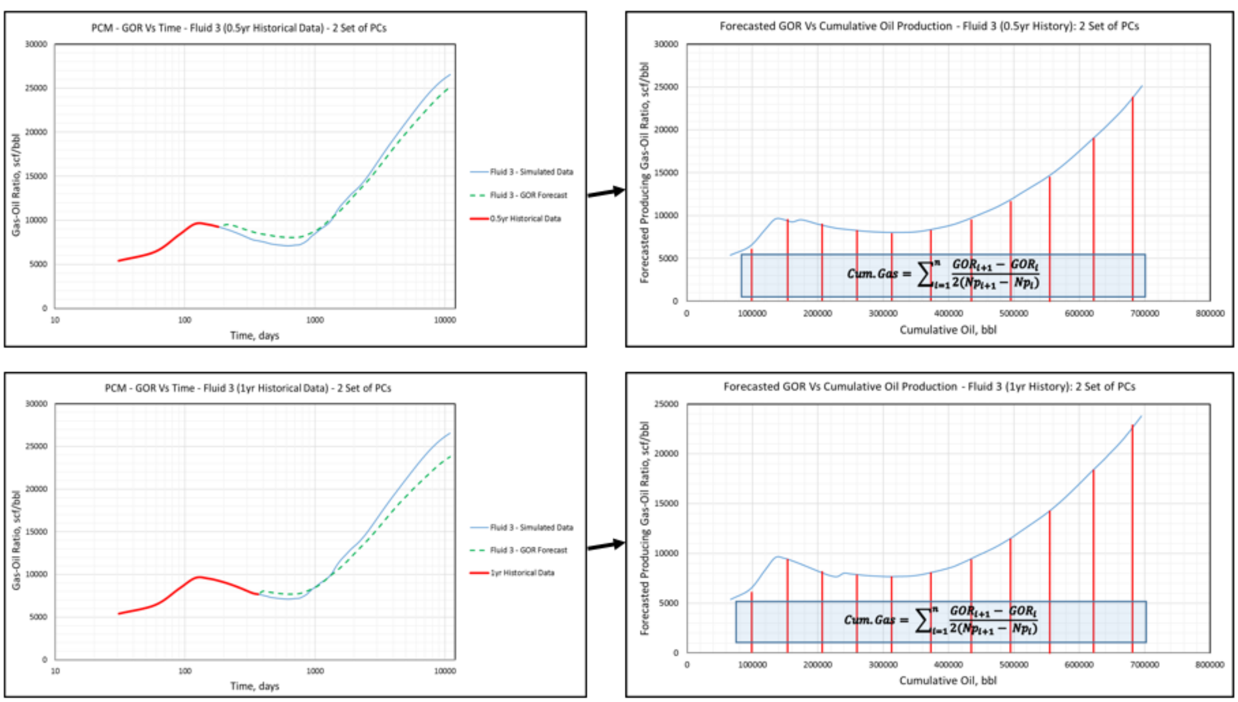

Figure 5-95 GOR Forecasts & Forecasted GOR vs. Cum. Oil – Fluid 3 (0.5yr. and 1yr. Histories): 2 Sets of PCs

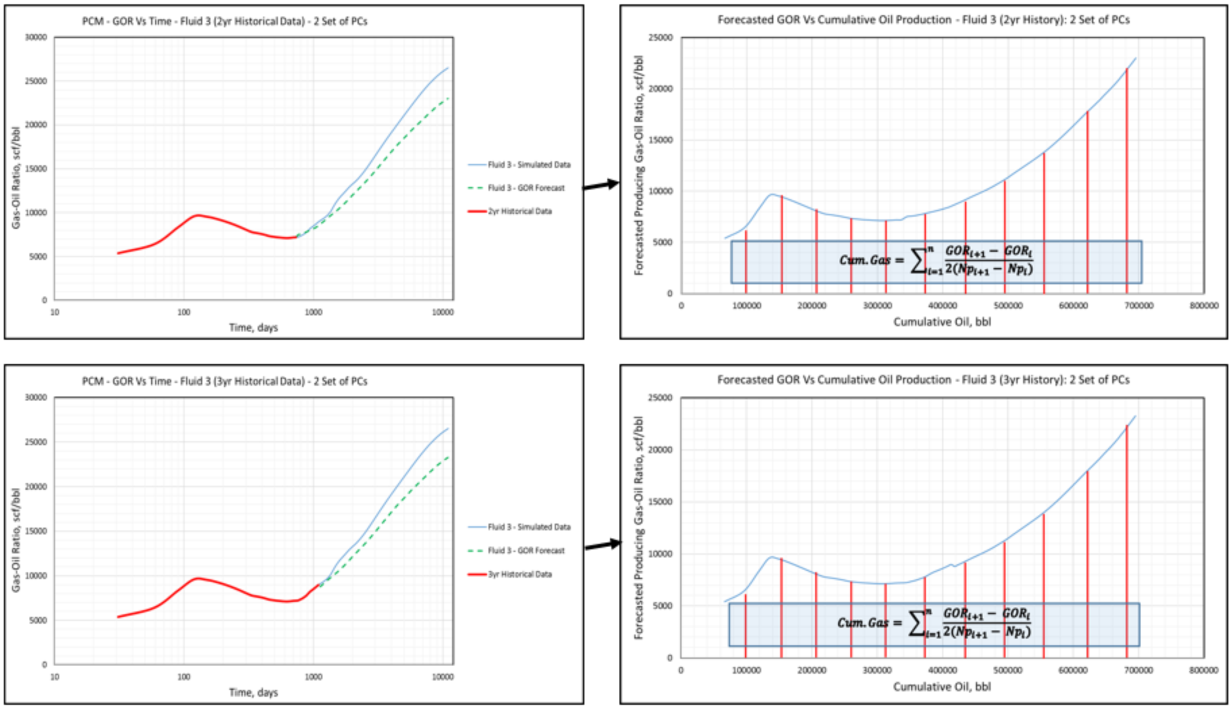

Figure 5-96 GOR Forecasts & Forecasted GOR vs. Cum. Oil – Fluid 3 (2yr. and 3yr. Histories): 2 Sets of PCs

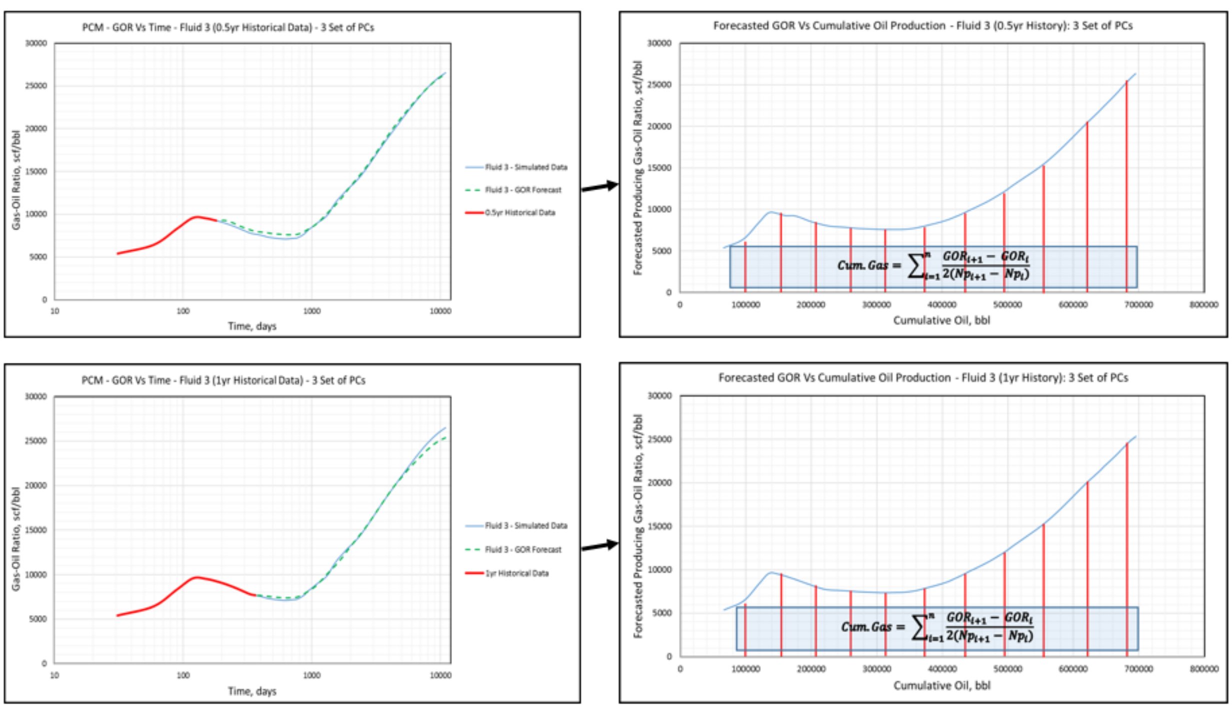

Figure 5-97 GOR Forecasts & Forecasted GOR vs. Cum. Oil – Fluid 3 (0.5yr. and 1yr. Histories): 3 Sets of PCs

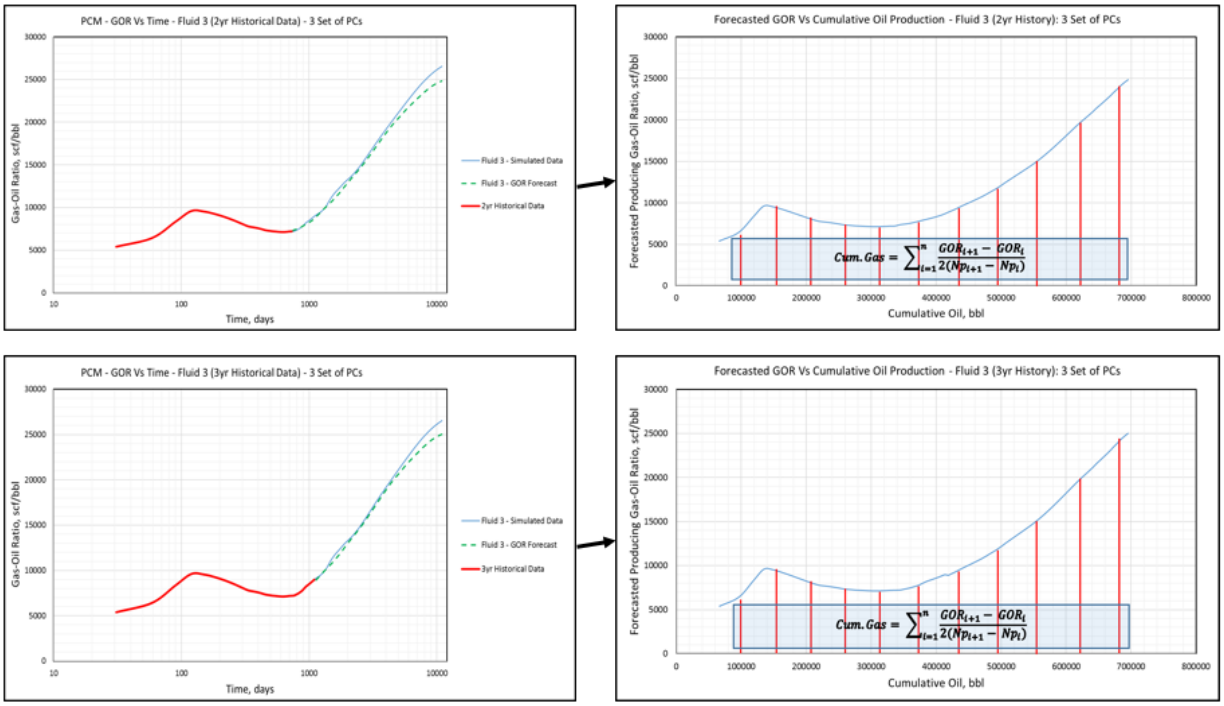

Figure 5-98 GOR Forecasts & Forecasted GOR vs. Cum. Oil – Fluid 3 (2yr. and 3yr. Histories): 3 Sets of PCs

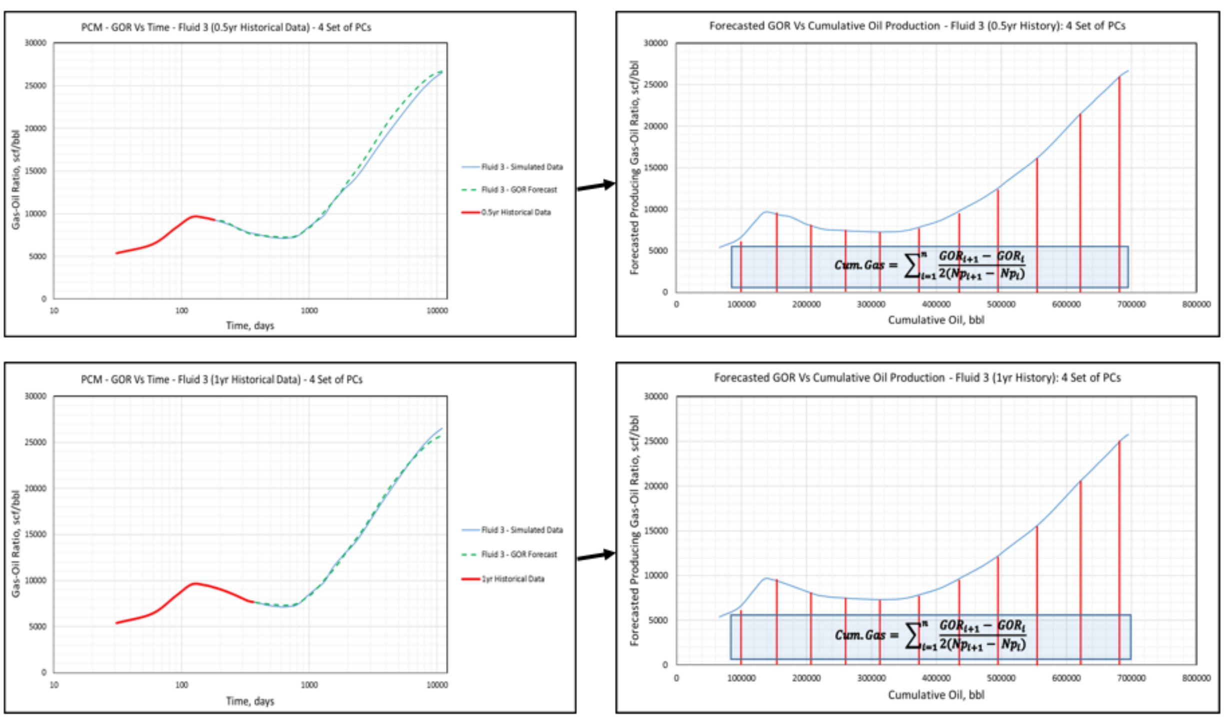

Figure 5-99 GOR Forecasts & Forecasted GOR vs. Cum. Oil – Fluid 3 (0.5yr. and 1yr. Histories): 4 Sets of PCs

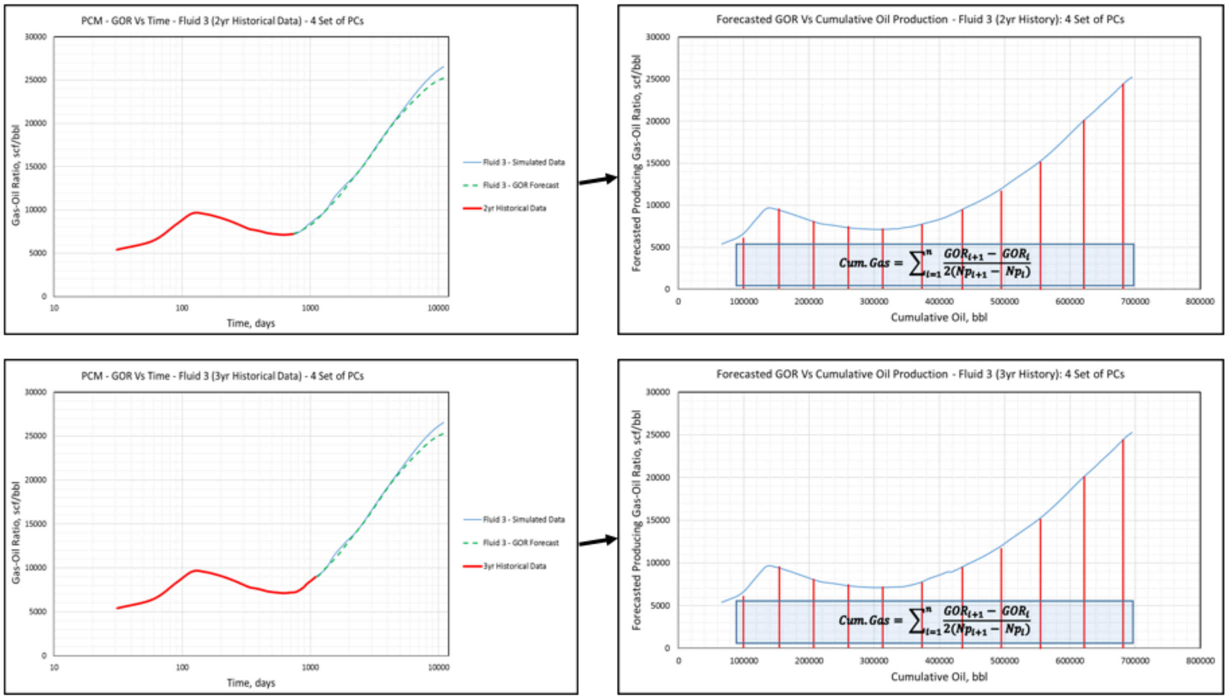

Figure 5-100 GOR Forecasts & Forecasted GOR vs. Cum. Oil – Fluid 3 (2yr. and 3yr. Histories): 4 Sets of PCs

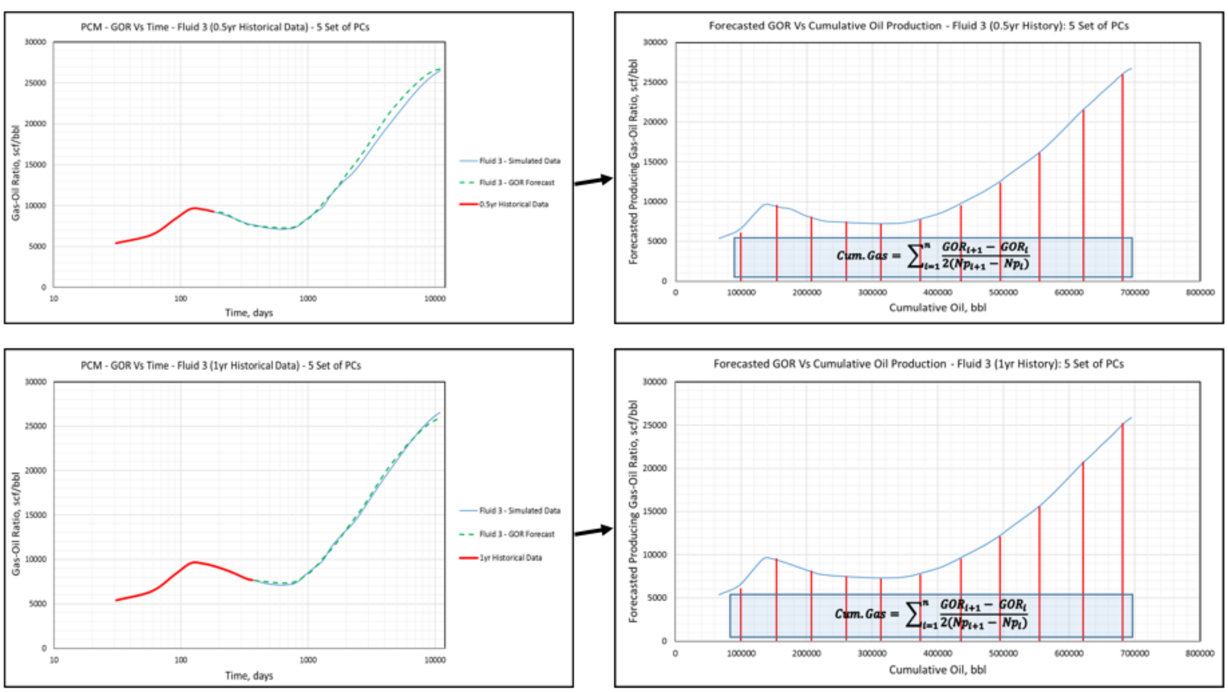

Figure 5-101 GOR Forecasts & Forecasted GOR vs. Cum. Oil – Fluid 3 (0.5yr. and 1yr. Histories): 5 Sets of PCs

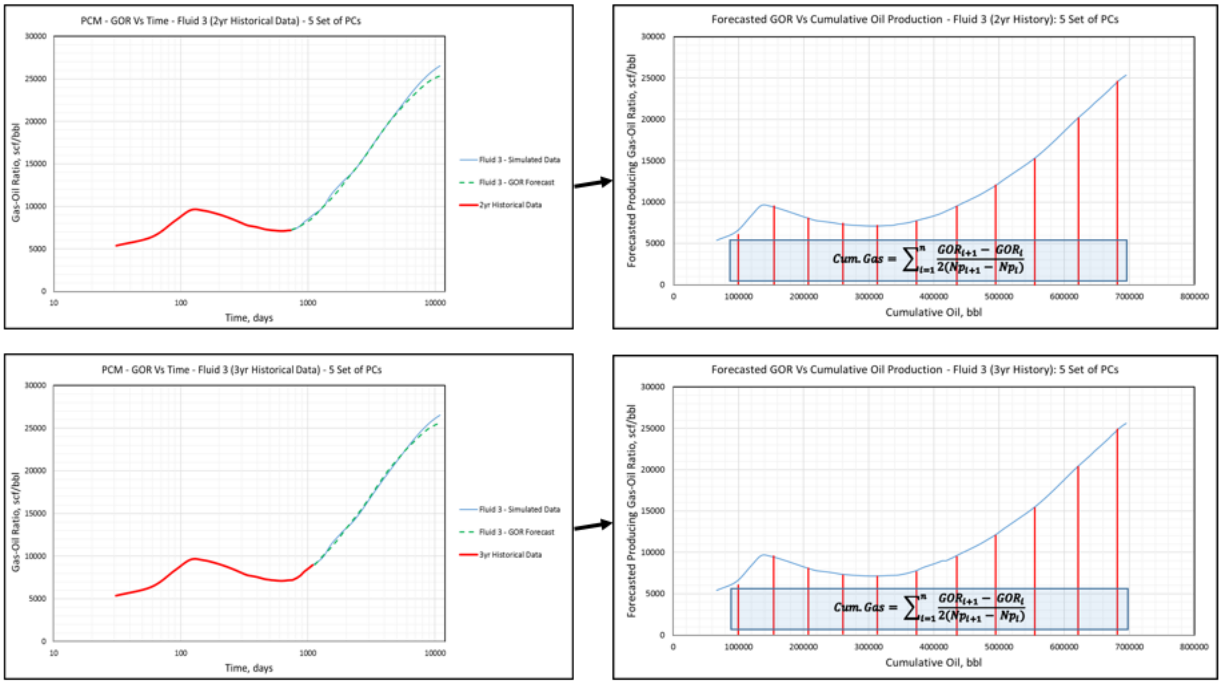

Figure 5-102 GOR Forecasts & Forecasted GOR vs. Cum. Oil – Fluid 3 (2yr. and 3yr. Histories): 5 Sets of PCs

Table 5-66 shows the results for all Fluid 3 cases. In all these cases, forecasts were reasonable and errors in the calculated solution gas produced (after 30 yrs) in most cases were relatively low. Percentage error was as low as 2.5% when all 5 sets of PCs were used to forecast. The figures in red indicate the lowest percentage errors for each case.

Table 5-66 Solution Gas Production Forecasts, Errors and Percentage Errors – Fluid 3

FLUID 3 RESULTS																				
Principal Components (PCs)	1 Set of PCs				2 Sets of PCs				3 Sets of PCs				4 Sets of PCs				5 Sets of PCs			
Historical Data	0.5yr	1yr	2yrs	3yrs	0.5yr	1yr	2yrs	3yrs	0.5yr	1yr	2yrs	3yrs	0.5yr	1yr	2yrs	3yrs	0.5yr	1yr	2yrs	3yrs
Simulated Cum. Gas, bscf	7.7	7.7	7.7	7.7	7.7	7.7	7.7	7.7	7.7	7.7	7.7	7.7	7.7	7.7	7.7	7.7	7.7	7.7	7.7	7.7
PCM Forecast, bscf	7.1	6.9	6.7	6.8	7.3	7.0	6.8	6.8	7.4	7.2	7.1	7.2	7.5	7.3	7.2	7.2	7.5	7.3	7.2	7.3
Error (absolute value), bscf	-0.6	-0.8	-1.0	-0.9	-0.4	-0.7	-0.9	-0.9	-0.3	-0.5	-0.6	-0.5	-0.2	-0.4	-0.5	-0.5	-0.2	-0.4	-0.5	-0.4
Percentage Error, %	-7.4	-10.0	-12.1	-11.5	-5.3	-8.8	-11.6	-10.9	-3.8	-5.5	-7.2	-6.6	-2.6	-4.7	-6.3	-6.0	-2.5	-4.3	-5.9	-5.2

5.2.3.1.4. Fluid 4 Cases

Graphical displays of GOR forecasts and the plots of the estimated GOR forecasts versus cumulative oil production for Fluid 4 are shown in Figures 5-103 to 5-112.

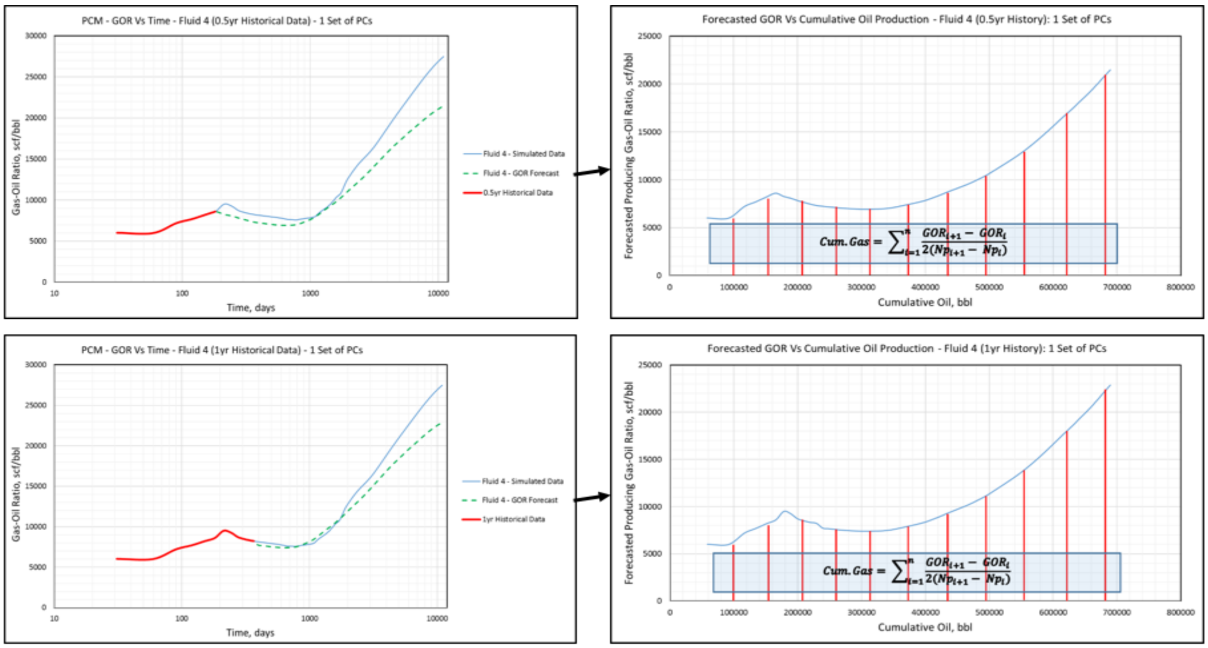

Figure 5-103 GOR Forecasts & Forecasted GOR vs. Cum. Oil -- Fluid 4 (0.5yr. and 1yr. Histories): 1 Set of PCs

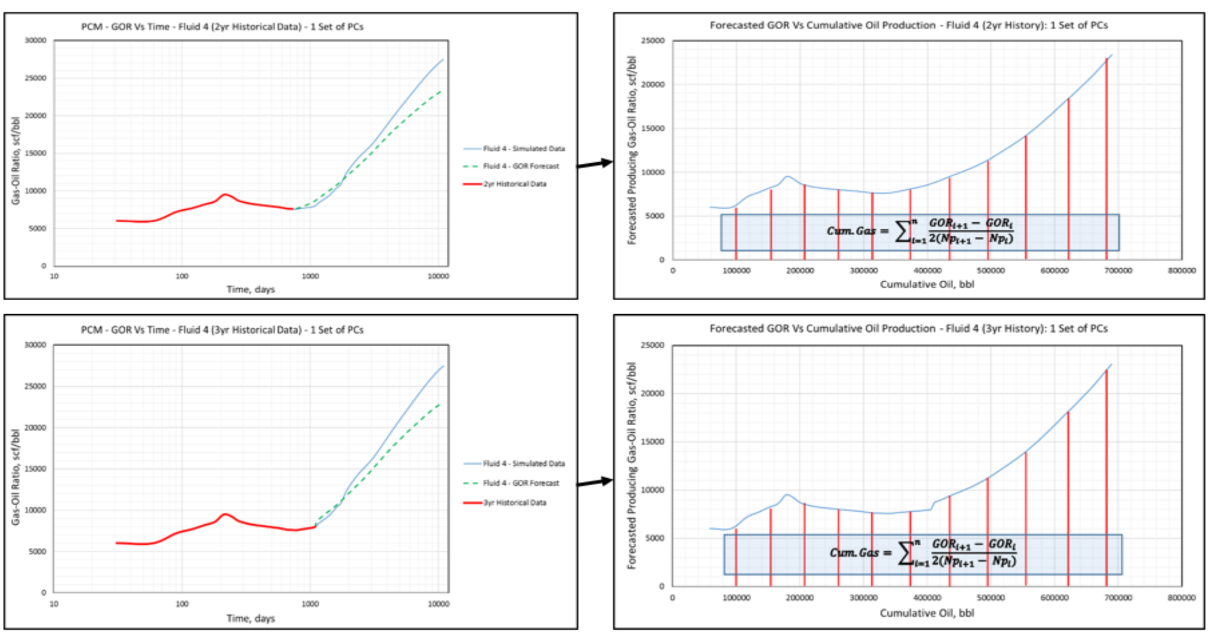

Figure 5-104 GOR Forecasts & Forecasted GOR vs. Cum. Oil – Fluid 4 (2yr. and 3yr. Histories): 1 Set of PCs

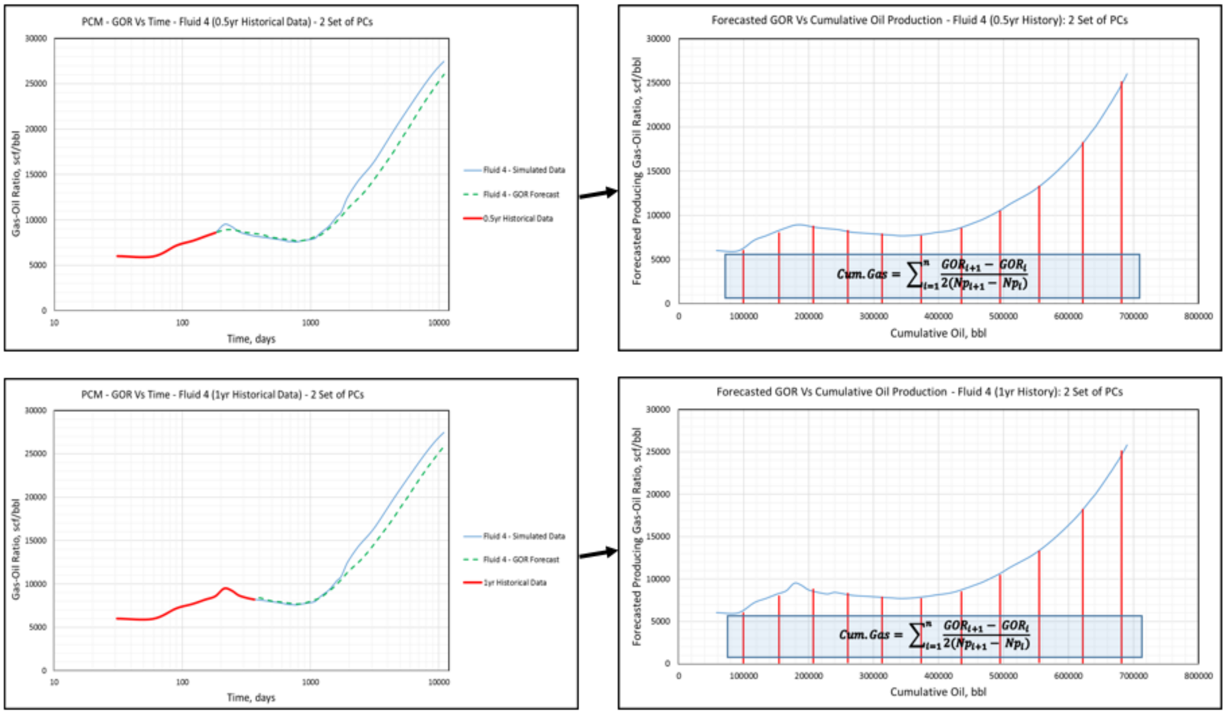

Figure 5-105 GOR Forecasts & Forecasted GOR vs. Cum. Oil – Fluid 4 (0.5yr. and 1yr. Histories): 2 Sets of PCs

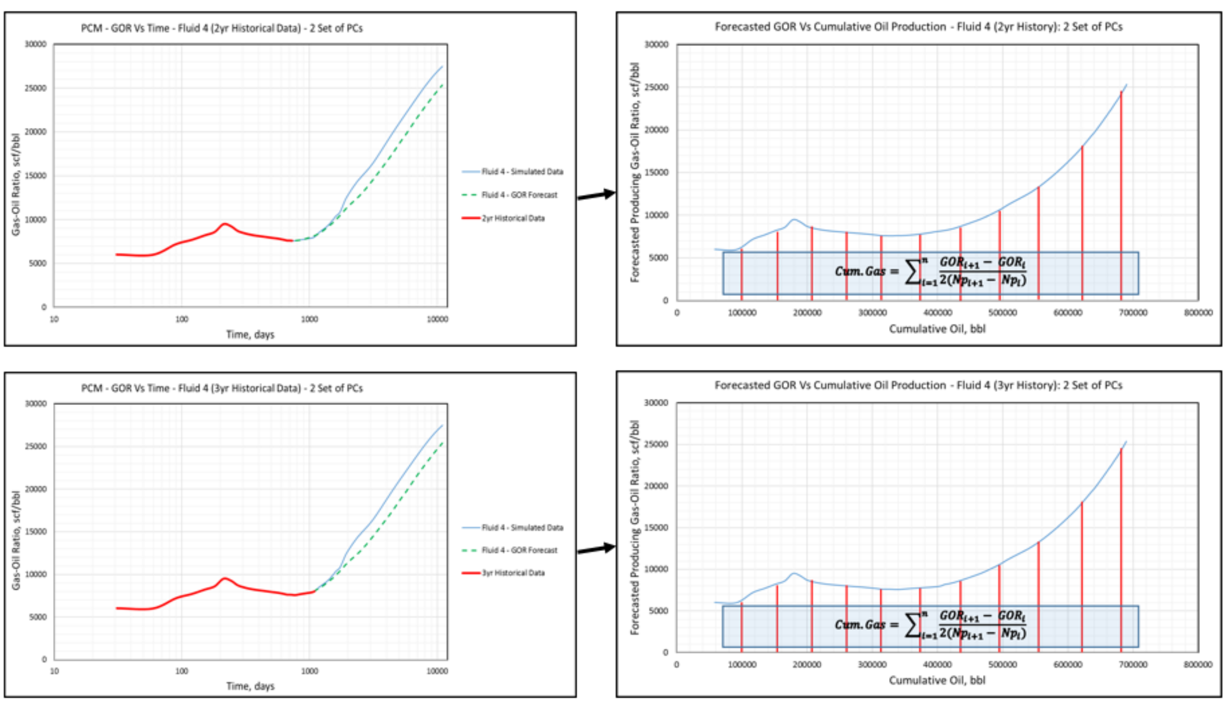

Figure 5-106 GOR Forecasts & Forecasted GOR vs. Cum. Oil – Fluid 4 (2yr. and 3yr. Histories): 2 Sets of PCs

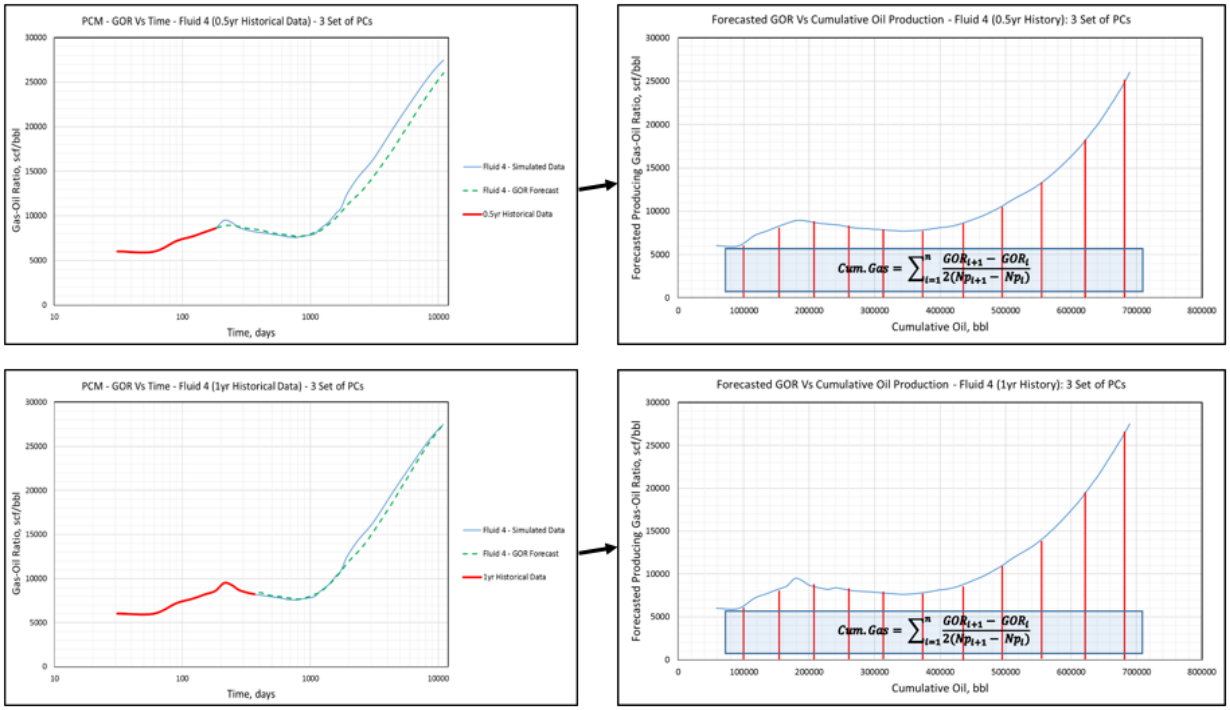

Figure 5-107 GOR Forecasts & Forecasted GOR vs. Cum. Oil – Fluid 4 (0.5yr. and 1yr. Histories): 3 Sets of PCs

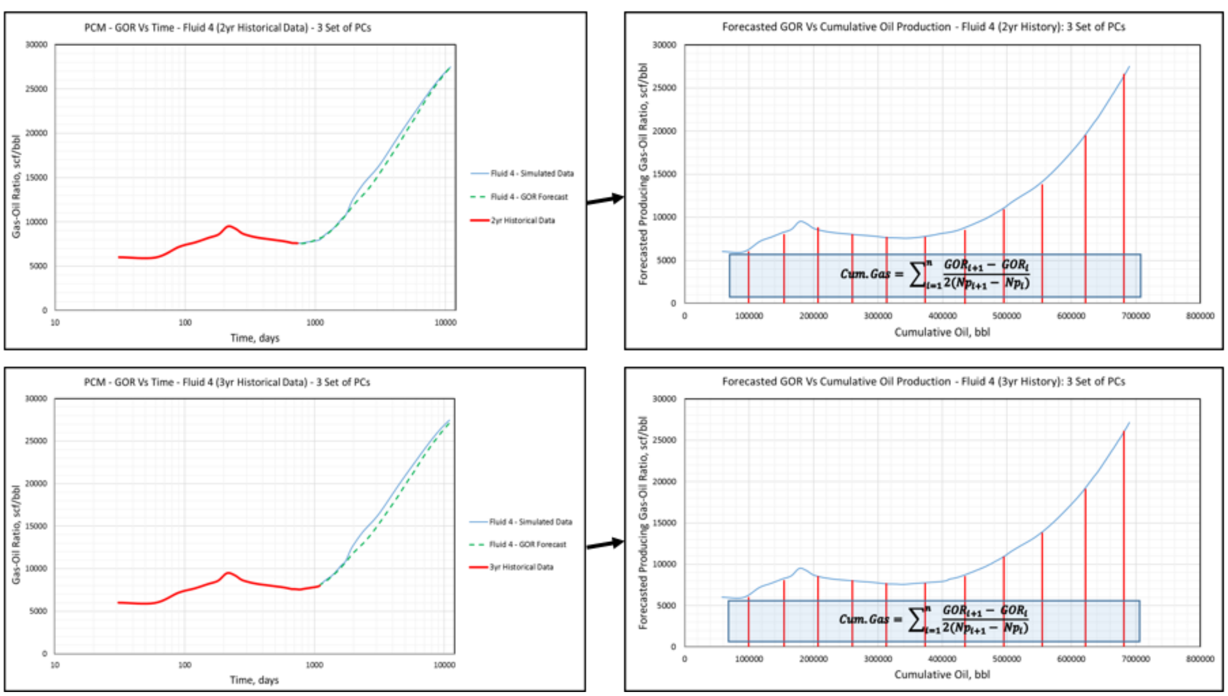

Figure 5-108 GOR Forecasts & Forecasted GOR vs. Cum. Oil – Fluid 4 (2yr. and 3yr. Histories): 3 Sets of PCs

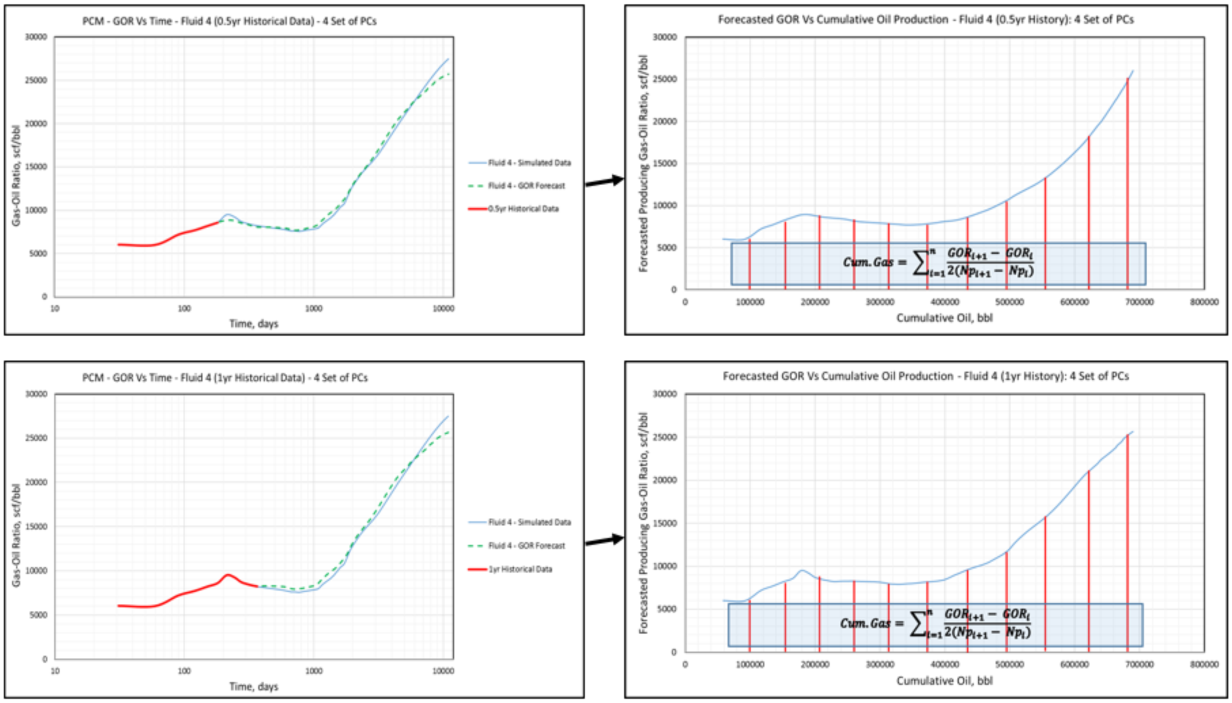

Figure 5-109 GOR Forecasts & Forecasted GOR vs. Cum. Oil – Fluid 4 (0.5yr. and 1yr. Histories): 4 Sets of PCs

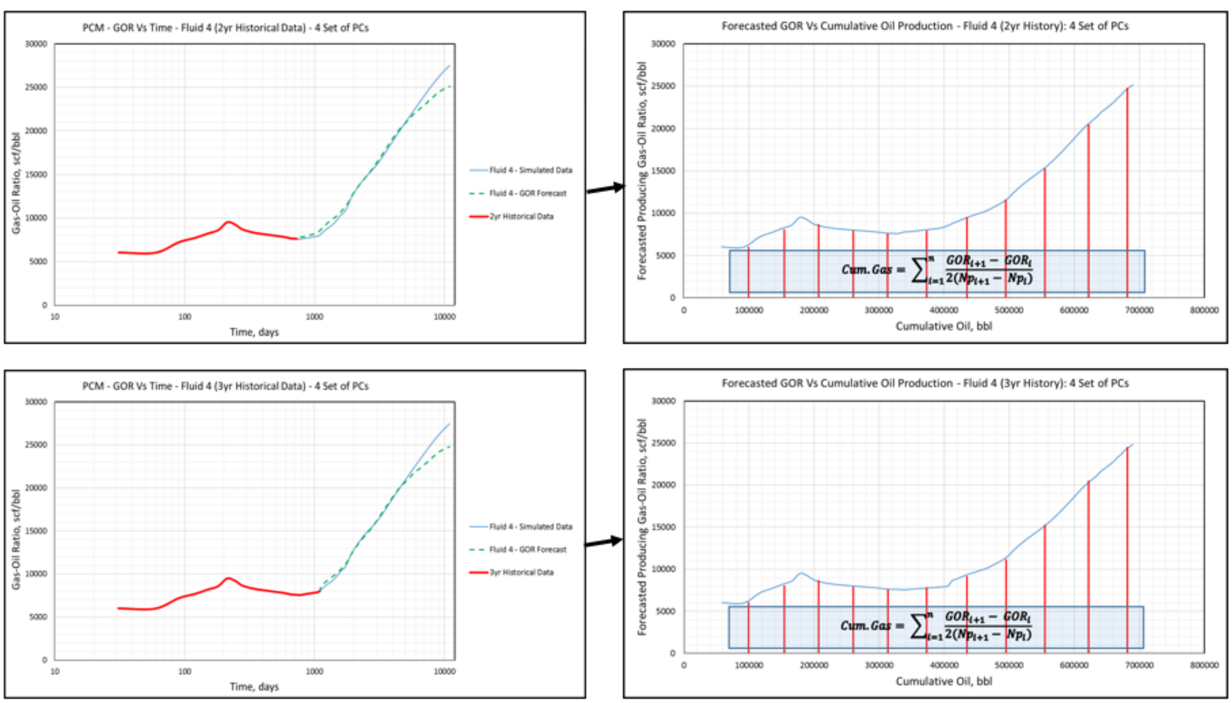

Figure 5-110 GOR Forecasts & Forecasted GOR vs. Cum. Oil – Fluid 4 (2yr. and 3yr. Histories): 4 Sets of PCs

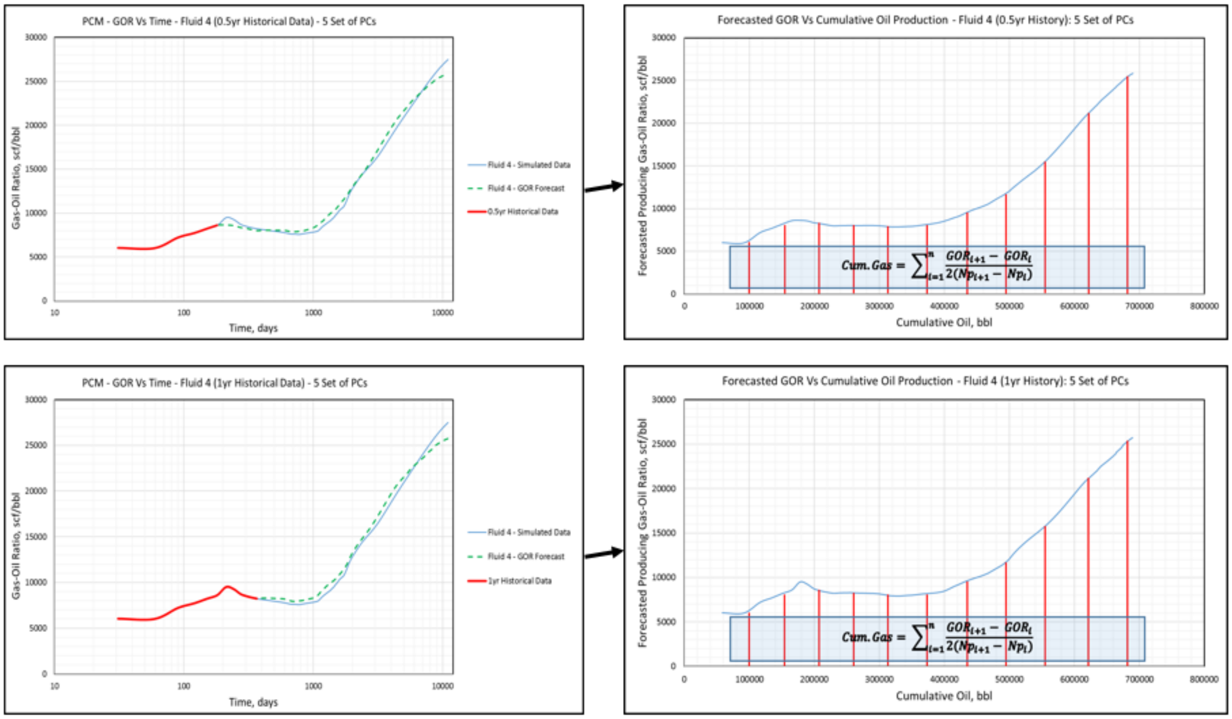

Figure 5-111 GOR Forecasts & Forecasted GOR vs. Cum. Oil – Fluid 4 (0.5yr. and 1yr. Histories): 5 Sets of PCs

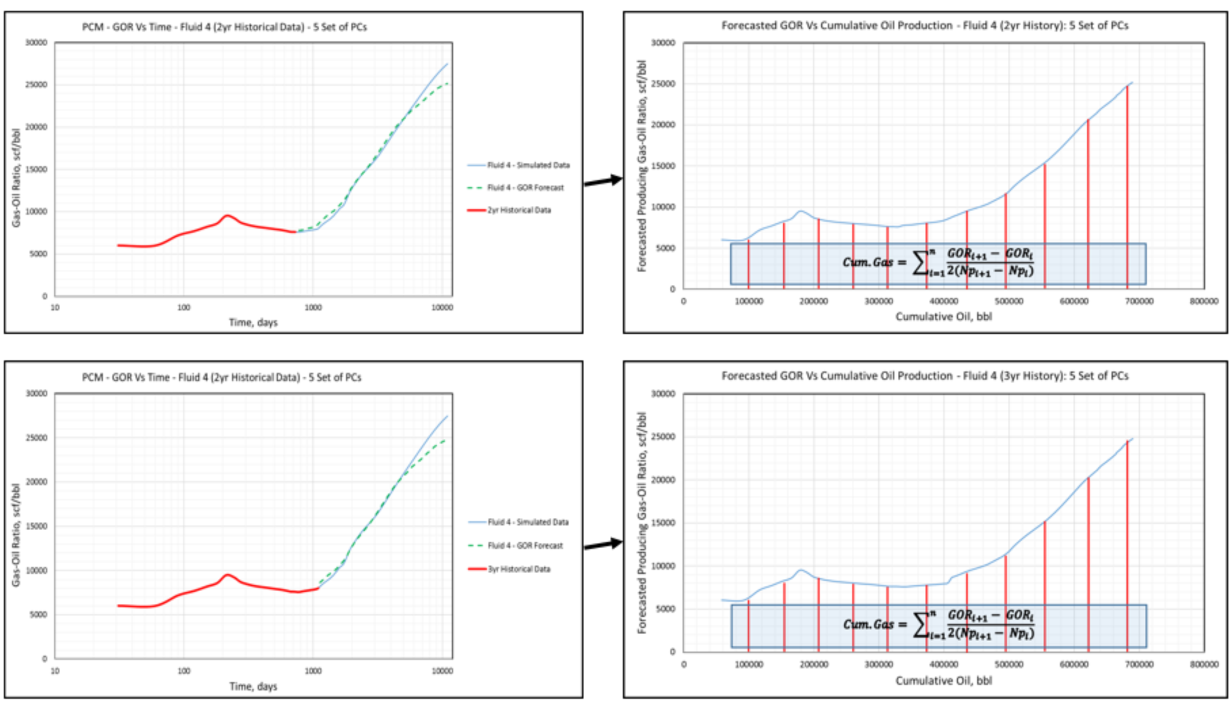

Figure 5-112 GOR Forecasts & Forecasted GOR vs. Cum. Oil – Fluid 4 (2yr. and 3yr. Histories): 5 Sets of PCs

Table 5-67 shows the results for all Fluid 4 cases. In all these cases, forecasts were reasonable and errors in the calculated solution gas produced (after 30 yrs) in most cases were relatively low. Percentage error was as low as 2.8% when all 5 sets of PCs were used to forecast. The figures in red indicate the lowest percentage errors for each case.

Table 5-67 Solution Gas Production Forecasts, Errors and Percentage Errors – Fluid 4

FLUID 4 RESULTS																				
Principal Components (PCs)	1 Set of PCs				2 Sets of PCs				3 Sets of PCs				4 Sets of PCs				5 Sets of PCs			
Historical Data	0.5yr	1yr	2yrs	3yrs	0.5yr	1yr	2yrs	3yrs	0.5yr	1yr	2yrs	3yrs	0.5yr	1yr	2yrs	3yrs	0.5yr	1yr	2yrs	3yrs
Simulated Cum. Gas, bscf	7.5	7.5	7.5	7.5	7.5	7.5	7.5	7.5	7.5	7.5	7.5	7.5	7.5	7.5	7.5	7.5	7.5	7.5	7.5	7.5
PCM Forecast, bscf	6.3	6.7	6.9	6.8	6.8	6.8	6.7	6.7	6.8	7.0	7.0	6.9	7.2	7.3	7.2	7.1	7.3	7.3	7.2	7.1
Error (absolute value), bscf	-1.2	-0.8	-0.6	-0.7	-0.7	-0.7	-0.8	-0.8	-0.7	-0.5	-0.5	-0.6	-0.3	-0.2	-0.5	-0.6	-0.2	-0.2	-0.3	-0.4
Percentage Error, %	-15.7	-10.4	-8.6	-9.7	-9.9	-9.8	-10.4	-10.7	-9.9	-7.1	-7.0	-7.9	-4.1	-2.9	-4.6	-5.7	-3.4	-2.8	-4.5	-5.7

5.2.3.1.5. Fluid 5 Cases

Graphical displays of GOR forecasts and the plots of the estimated GOR forecasts versus cumulative oil production for Fluid 5 are shown in Figures 5-113 to 5-122.

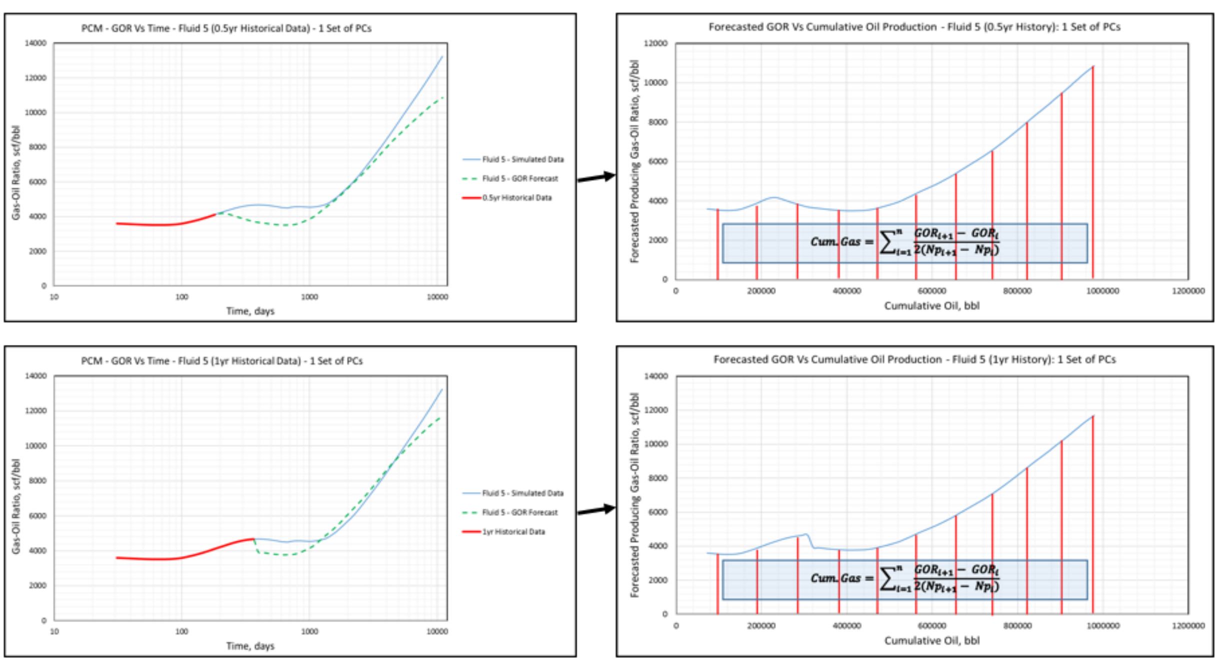

Figure 5-113 GOR Forecasts & Forecasted GOR vs. Cum. Oil – Fluid 5 (0.5yr. and 1yr. Histories): 1 Set of PCs

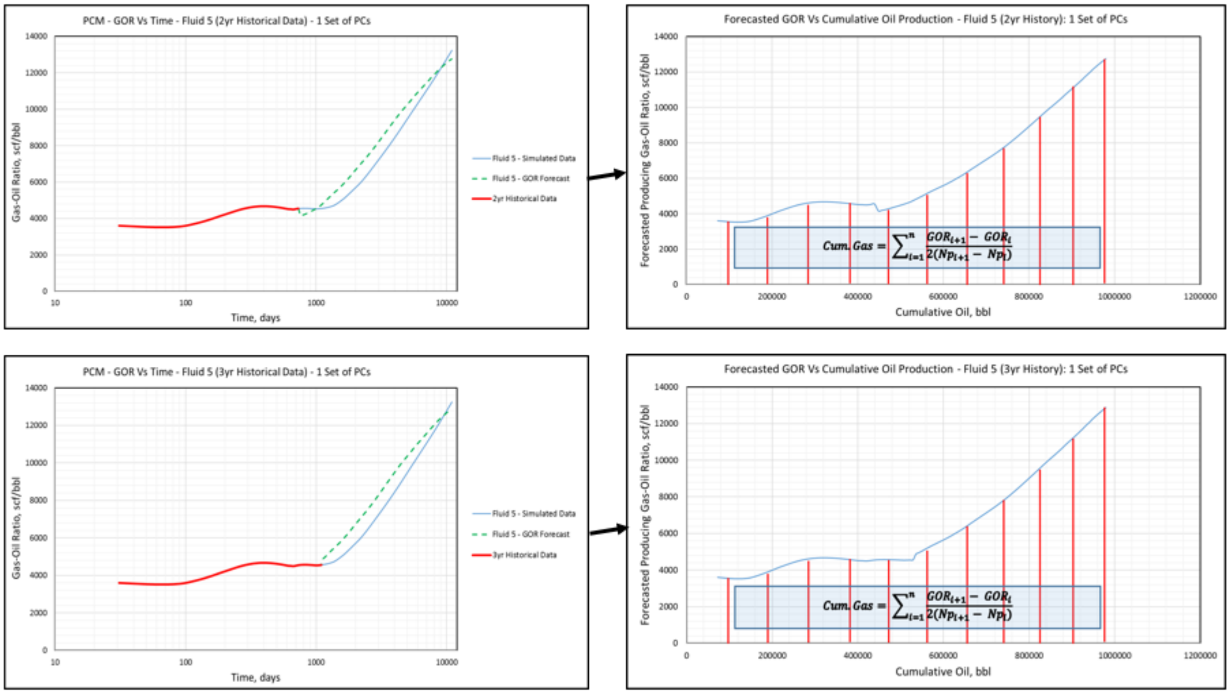

Figure 5-114 GOR Forecasts & Forecasted GOR vs. Cum. Oil – Fluid 5 (2yr. and 3yr. Histories): 1 Set of PCs

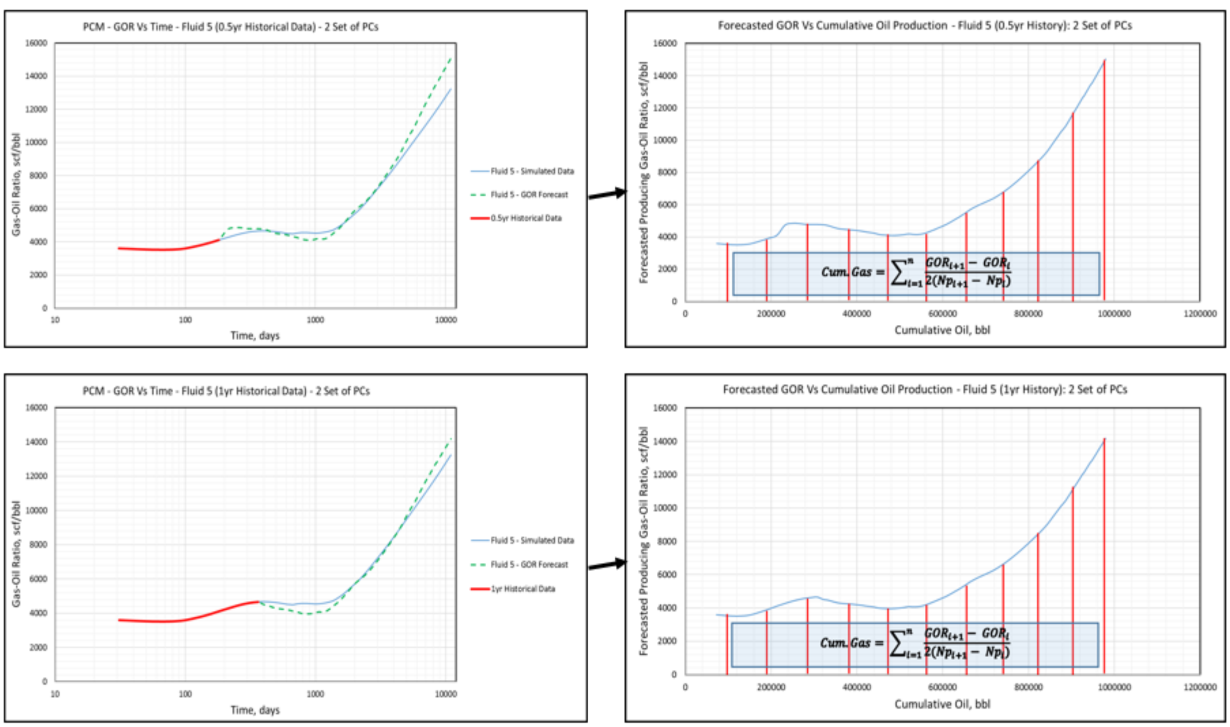

Figure 5-115 GOR Forecasts & Forecasted GOR vs. Cum. Oil – Fluid 5 (0.5yr. and 1yr. Histories): 2 Sets of PCs

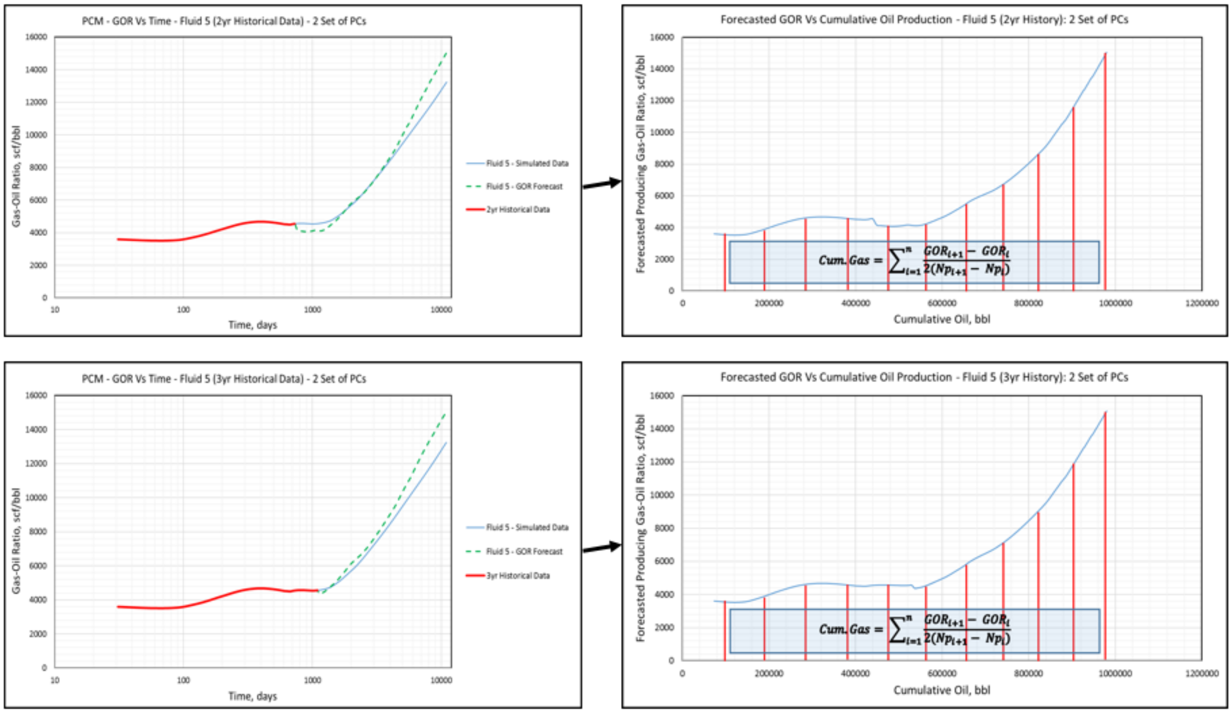

Figure 5-116 GOR Forecasts & Forecasted GOR vs. Cum. Oil – Fluid 5 (2yr. and 3yr. Histories): 2 Sets of PCs

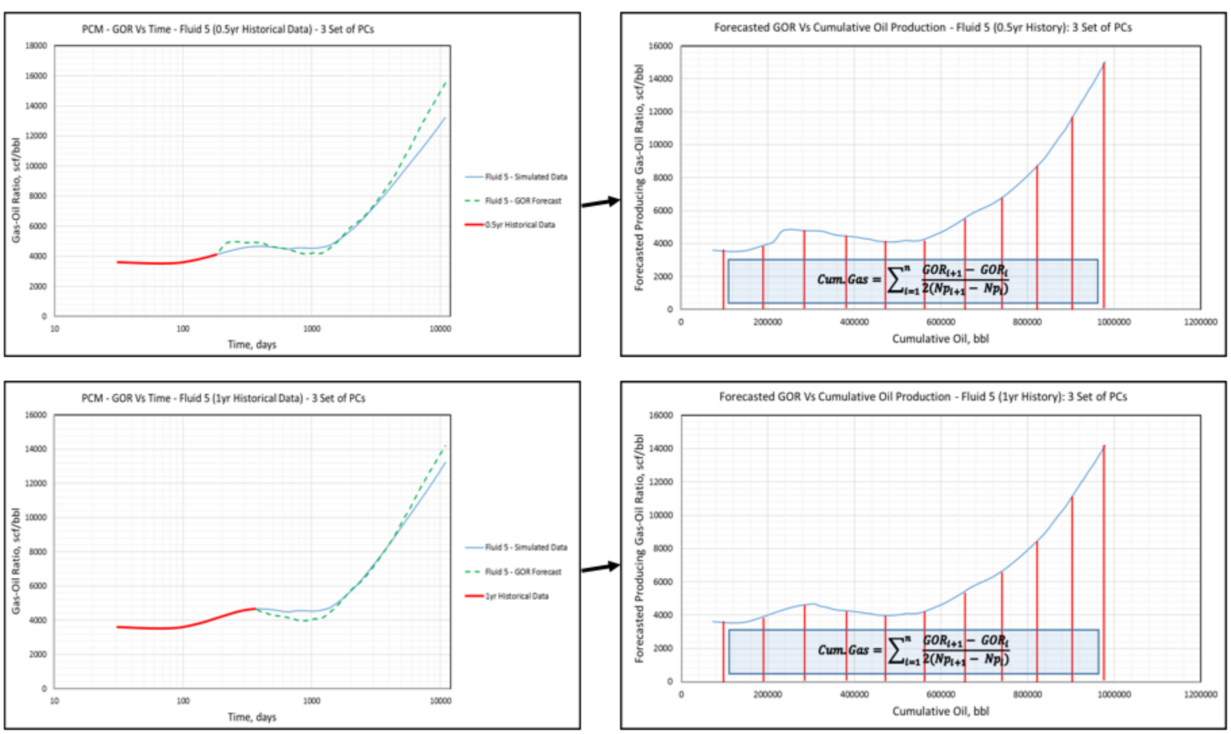

Figure 5-117 GOR Forecasts & Forecasted GOR vs. Cum. Oil – Fluid 5 (0.5yr. and 1yr. Histories): 3 Sets of PCs

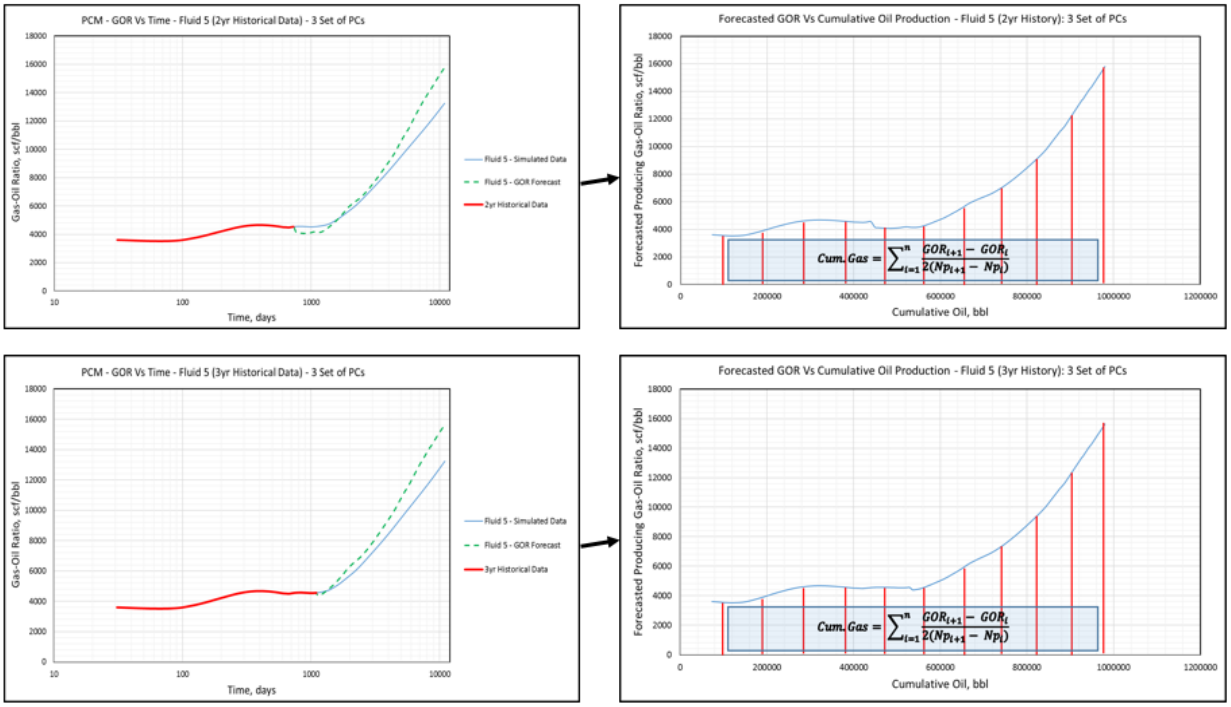

Figure 5-118 GOR Forecasts & Forecasted GOR vs. Cum. Oil – Fluid 5 (2yr. and 3yr. Histories): 3 Sets of PCs

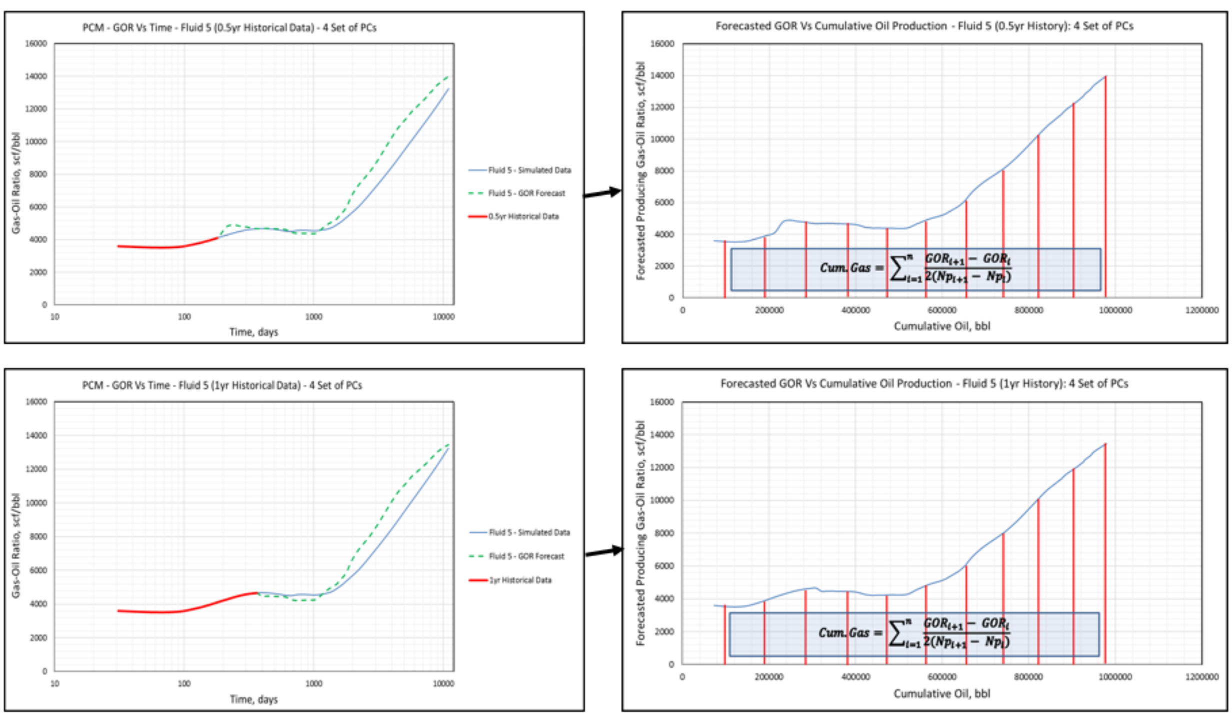

Figure 5-119 GOR Forecasts & Forecasted GOR vs. Cum. Oil – Fluid 5 (0.5yr. and 1yr. Histories): 4 Sets of PCs

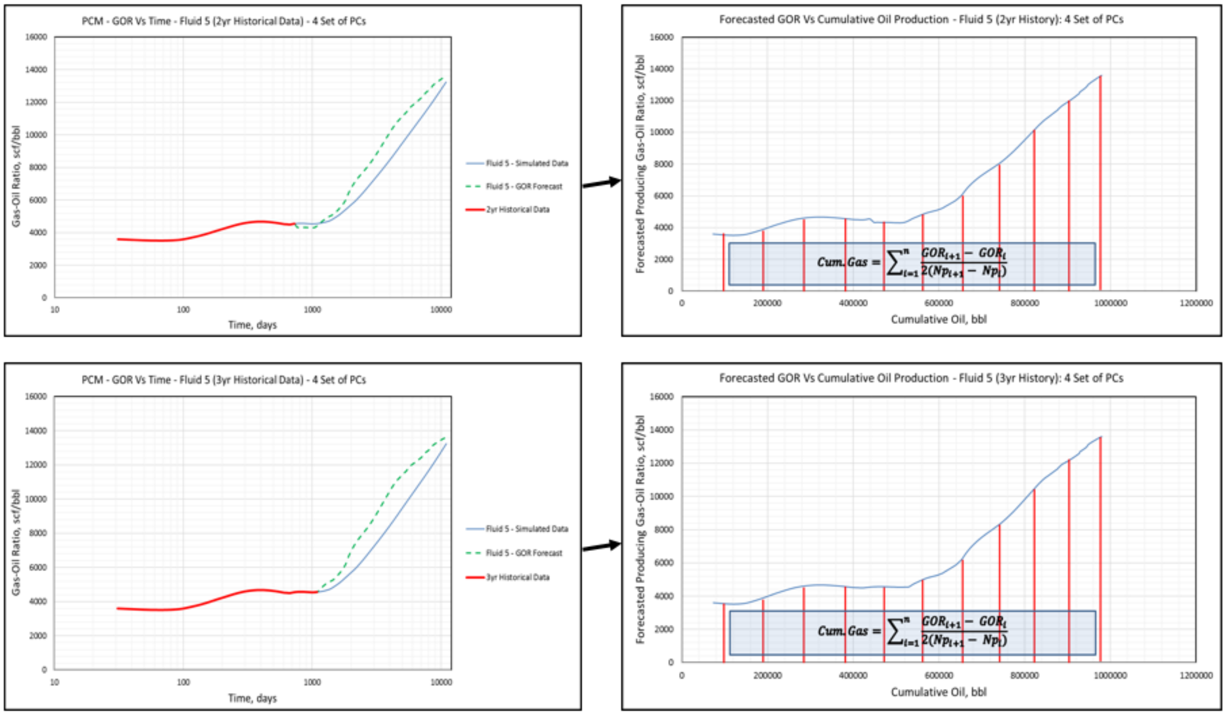

Figure 5-120 GOR Forecasts & Forecasted GOR vs. Cum. Oil – Fluid 5 (2yr. and 3yr. Histories): 4 Sets of PCs

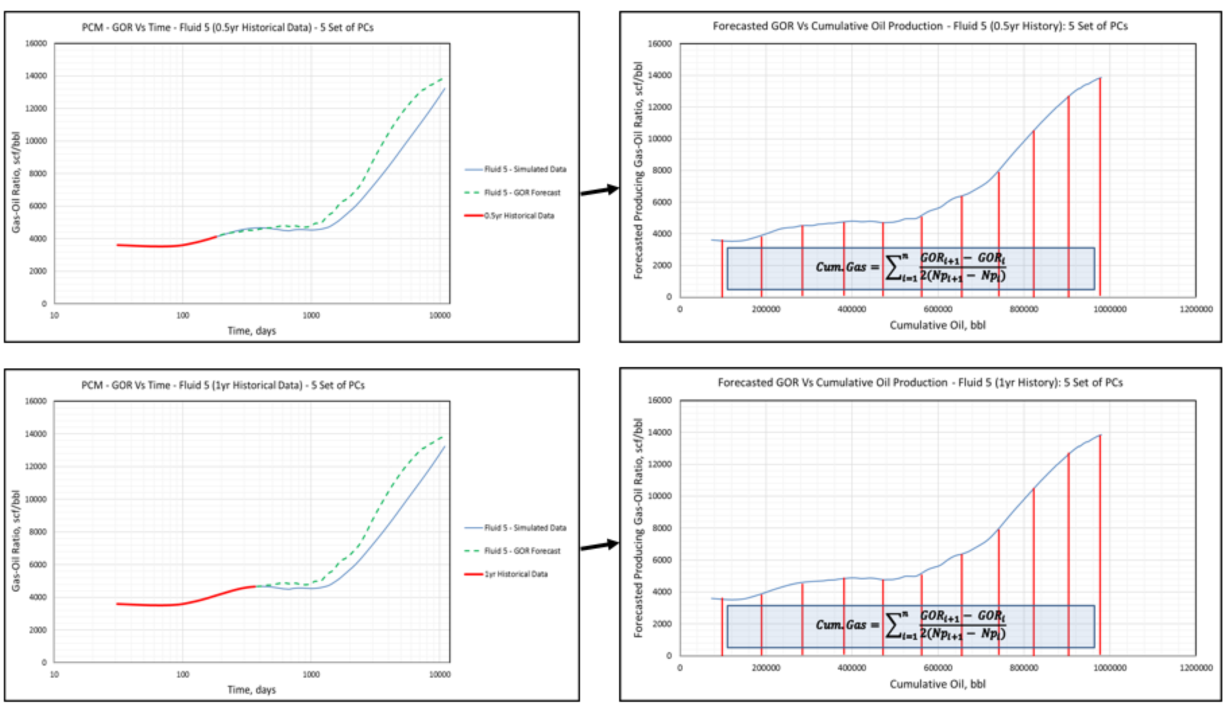

Figure 5-121 GOR Forecasts & Forecasted GOR vs. Cum. Oil – Fluid 5 (0.5yr. and 1yr. Histories): 5 Sets of PCs

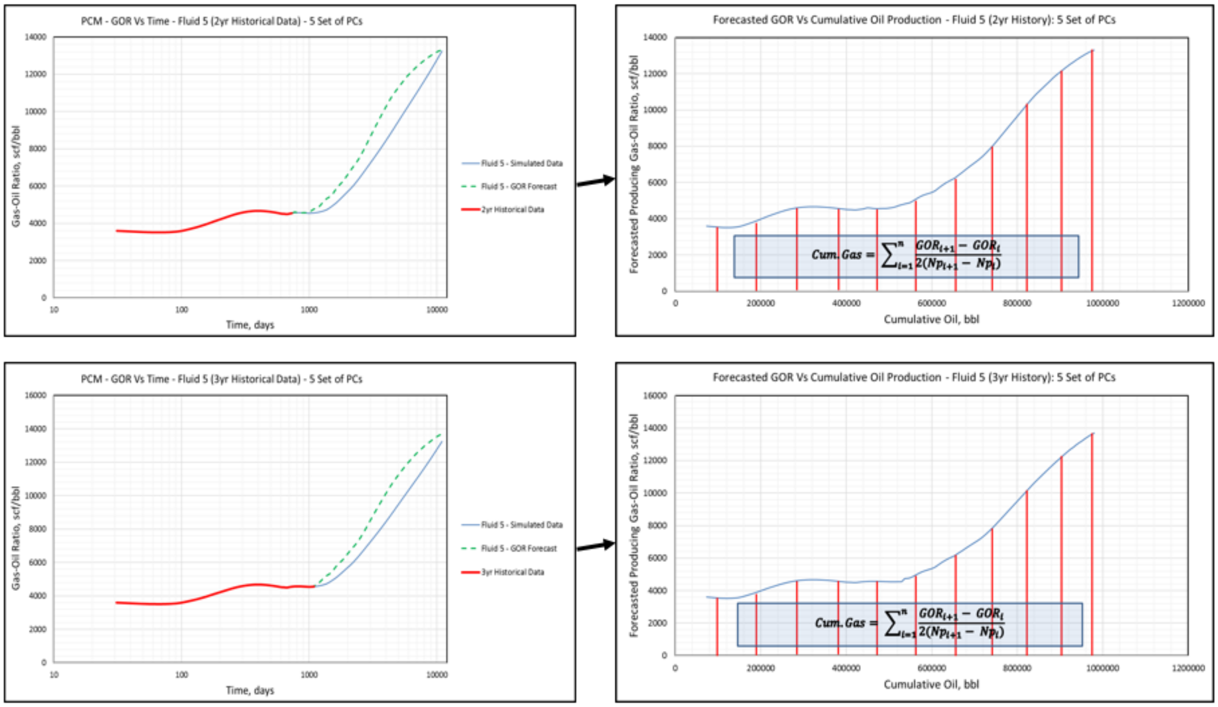

Figure 5-122 GOR Forecasts & Forecasted GOR vs. Cum. Oil – Fluid 5 (2yr. and 3yr. Histories): 5 Sets of PCs

Table 5-68 shows the results for all Fluid 5 cases. In all these cases, forecasts were reasonable and errors in the calculated solution gas produced (after 30 yrs) in most cases were relatively low. Percentage error was as low as 0.2% when just the first set of PCs were used to forecast. The figures in red indicate the lowest percentage errors for each case.

Table 5-68 Solution Gas Production Forecasts, Errors and Percentage Errors – Fluid 5

FLUID 5 RESULTS																				
Principal Components (PCs)	1 Set of PCs				2 Sets of PCs				3 Sets of PCs				4 Sets of PCs				5 Sets of PCs			
Historical Data	0.5yr	1yr	2yrs	3yrs	0.5yr	1yr	2yrs	3yrs	0.5yr	1yr	2yrs	3yrs	0.5yr	1yr	2yrs	3yrs	0.5yr	1yr	2yrs	3yrs
Simulated Cum. Gas, bscf	5.7	5.7	5.7	5.7	5.7	5.7	5.7	5.7	5.7	5.7	5.7	5.7	5.7	5.7	5.7	5.7	5.7	5.7	5.7	5.7
PCM Forecast, bscf	4.9	5.2	5.7	5.7	5.5	5.3	5.5	5.6	5.6	5.3	5.6	5.8	5.9	5.8	5.8	5.9	6.0	6.0	5.9	5.9
Error (absolute value), bscf	-0.8	-0.5	0.0	0.0	-0.2	-0.4	-0.2	-0.1	-0.1	-0.4	-0.1	0.1	0.2	0.1	0.1	0.2	0.3	0.3	0.2	0.2
Percentage Error, %	-13.9	-7.6	0.2	1.0	-2.8	-6.1	-3.5	-0.3	-1.3	-6.1	-0.7	1.8	4.3	1.8	2.7	4.7	5.9	6.3	3.9	3.3

5.2.3.1.6. Fluid 6 Cases

Graphical displays of GOR forecasts and the plots of the estimated GOR forecasts versus cumulative oil production for Fluid 6 are shown in Figures 5-123 to 5-132.

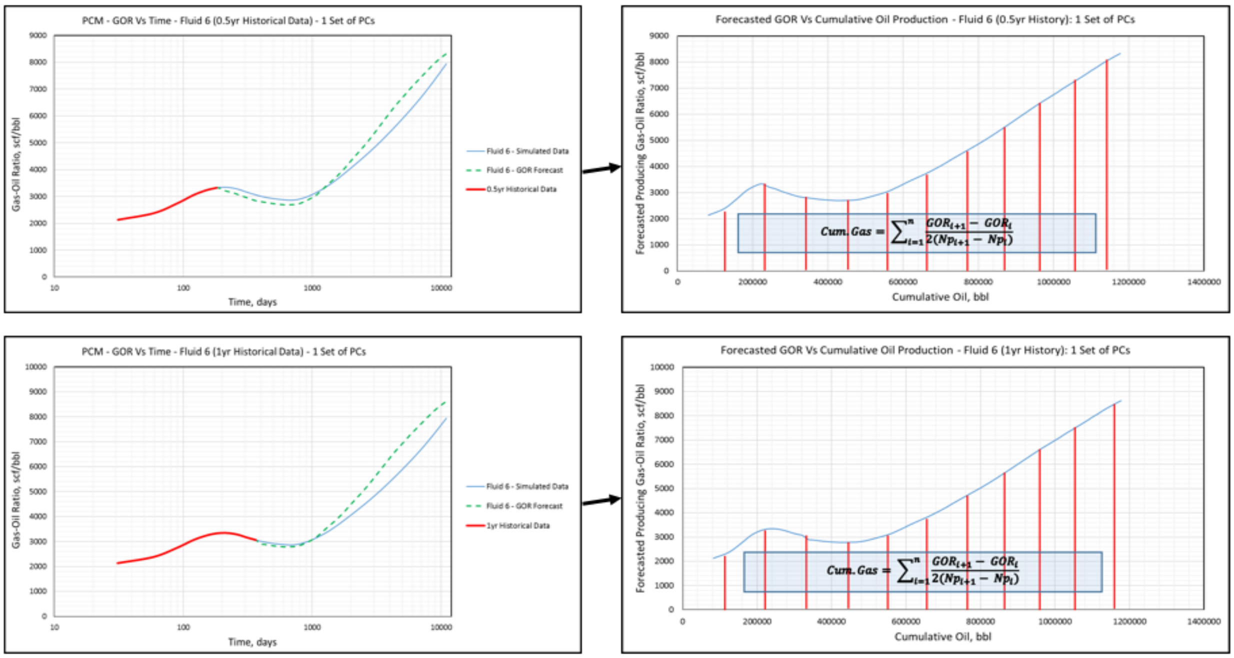

Figure 5-123 GOR Forecasts & Forecasted GOR vs. Cum. Oil – Fluid 6 (0.5yr. and 1yr. Histories): 1 Set of PCs

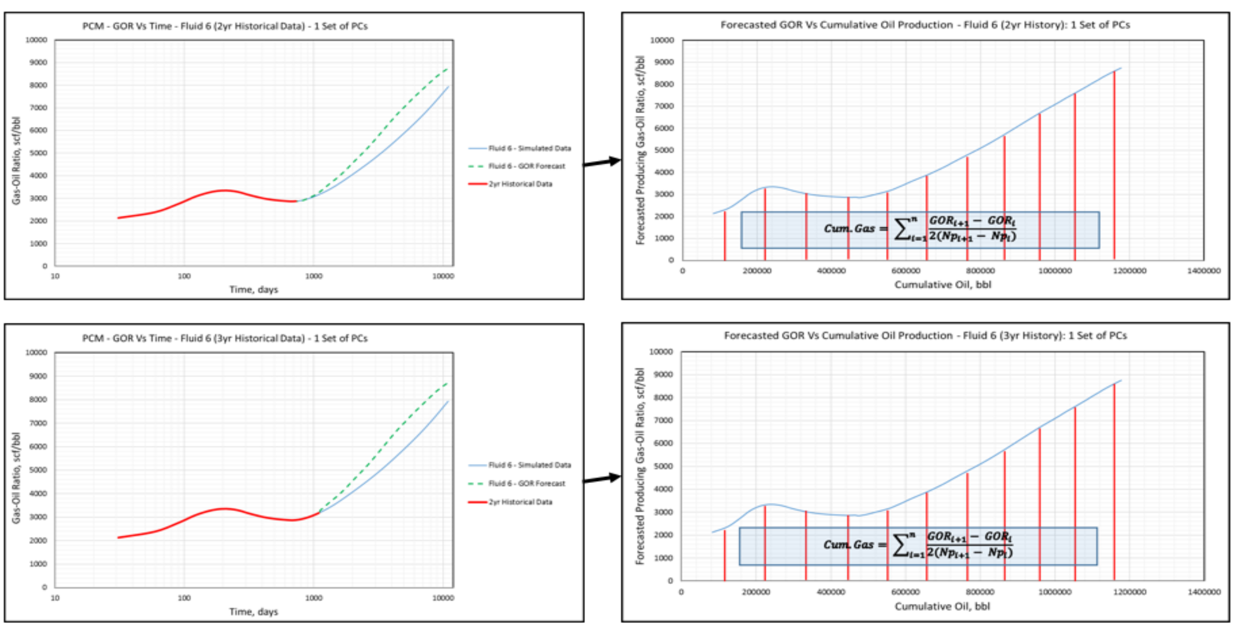

Figure 5-124 GOR Forecasts & Forecasted GOR vs. Cum. Oil – Fluid 6 (2yr. and 3yr. Histories): 1 Set of PCs

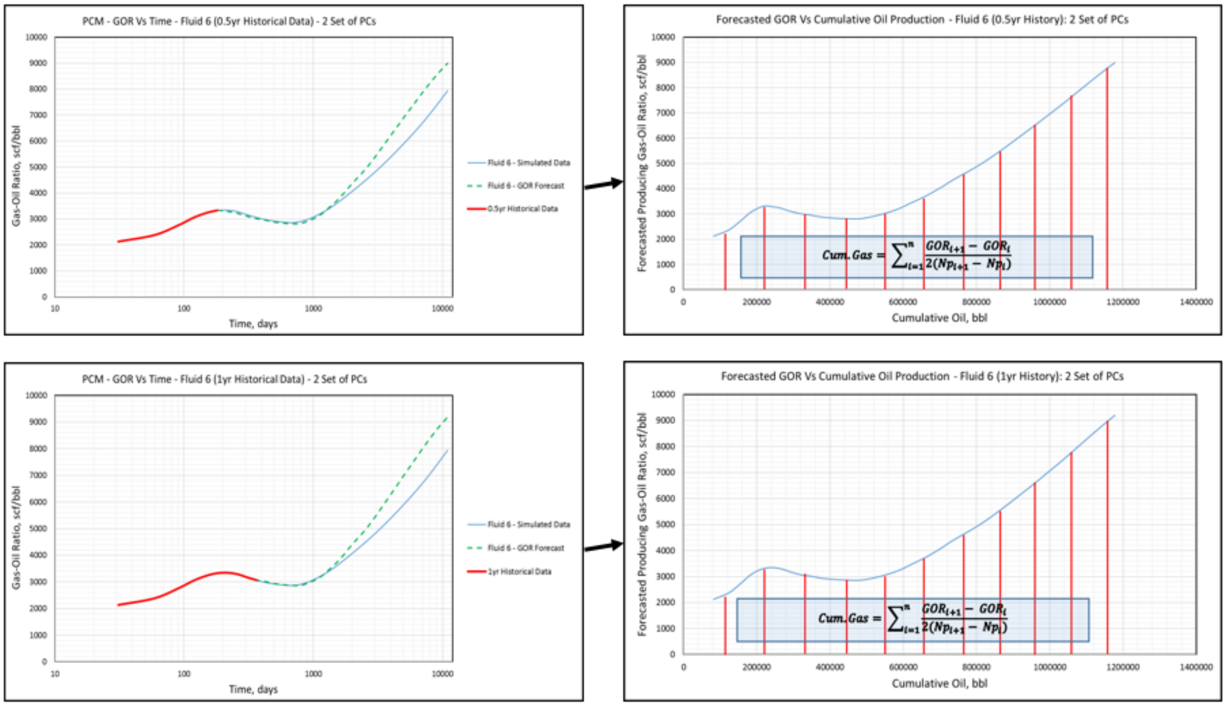

Figure 5-125 GOR Forecasts & Forecasted GOR vs. Cum. Oil – Fluid 6 (0.5yr. and 1yr. Histories): 2 Sets of PCs

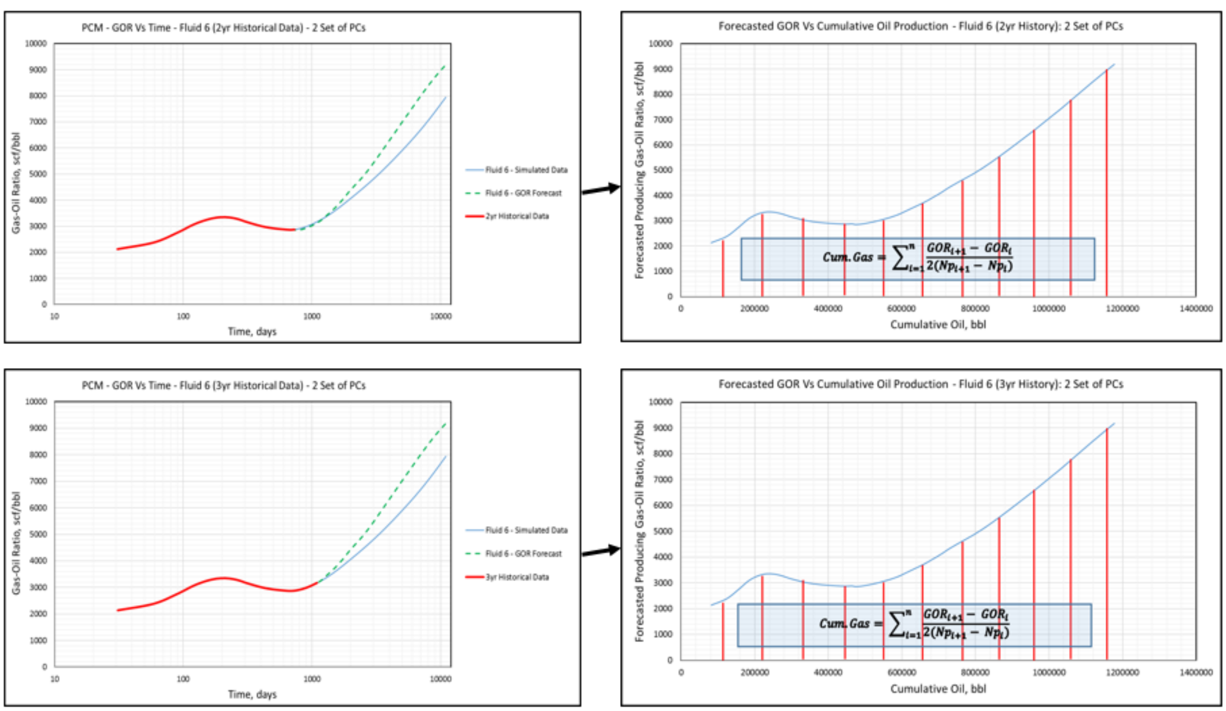

Figure 5-126 GOR Forecasts & Forecasted GOR vs. Cum. Oil – Fluid 6 (2yr. and 3yr. Histories): 2 Sets of PCs

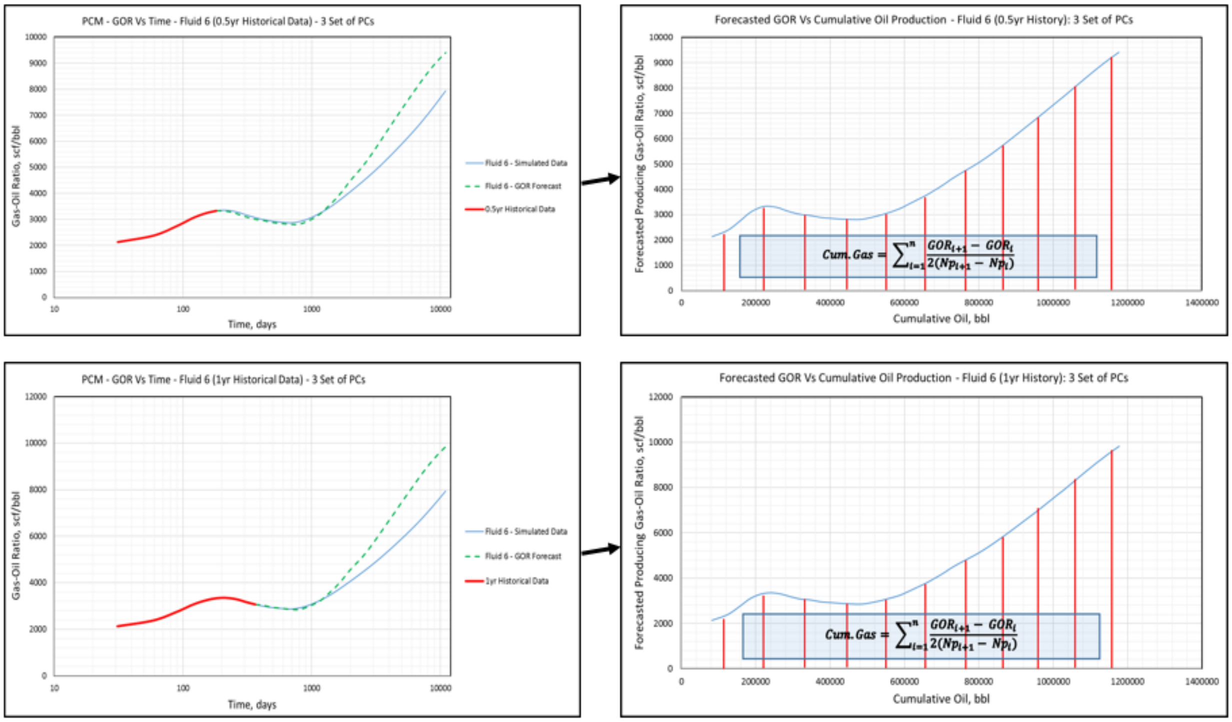

Figure 5-127 GOR Forecasts & Forecasted GOR vs. Cum. Oil – Fluid 6 (0.5yr. and 1yr. Histories): 3 Set of PCs

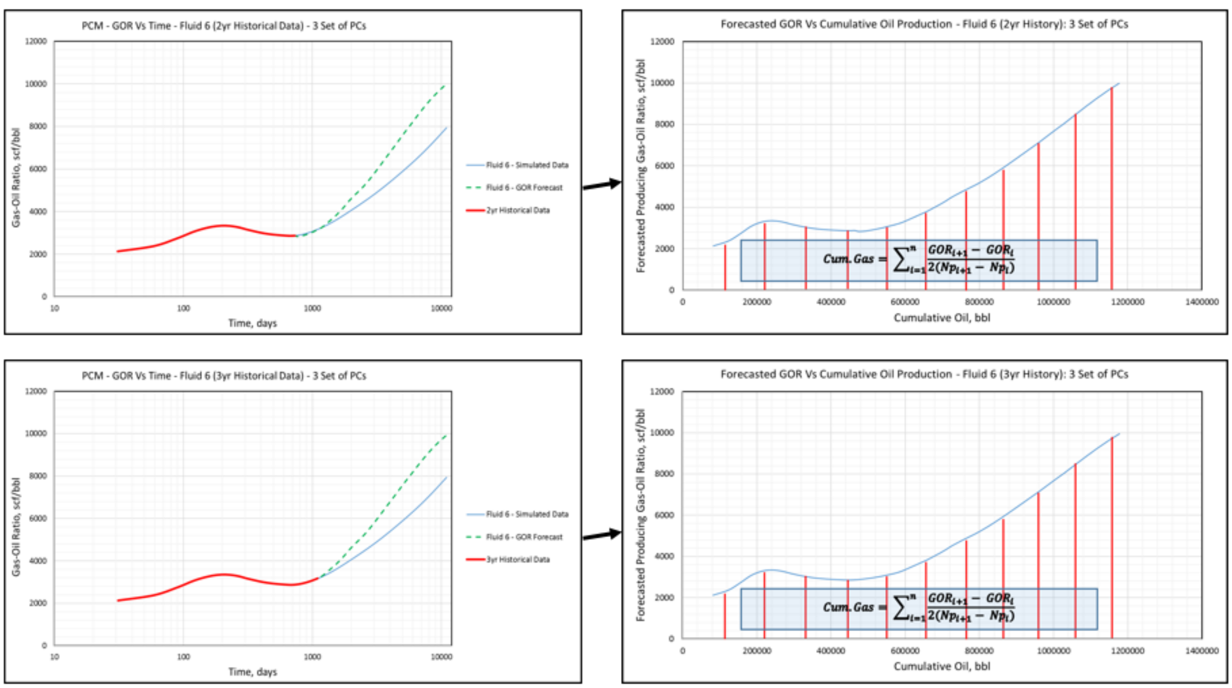

Figure 5-128 GOR Forecasts & Forecasted GOR vs. Cum. Oil – Fluid 6 (2yr. and 3yr. Histories): 3 Set of PCs

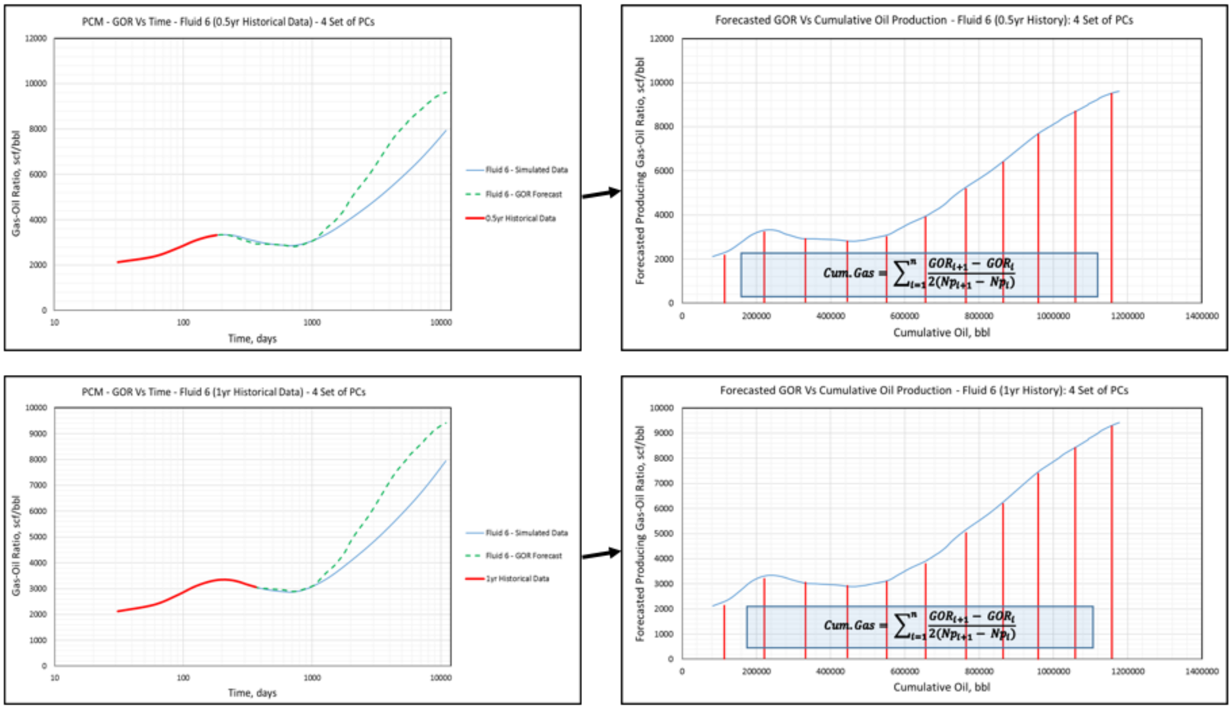

Figure 5-129 GOR Forecasts & Forecasted GOR vs. Cum. Oil – Fluid 6 (0.5yr. and 1yr. Histories): 4 Set of PCs

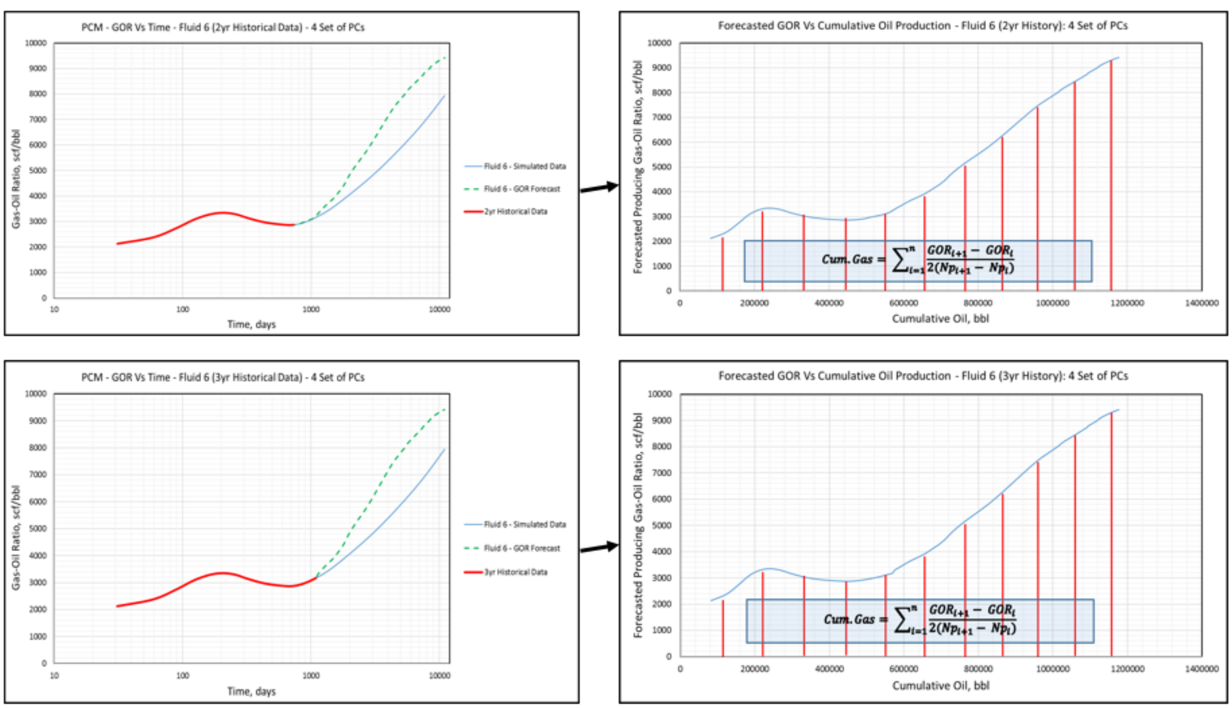

Figure 5-130 GOR Forecasts & Forecasted GOR vs. Cum. Oil – Fluid 6 (2yr. and 3yr. Histories): 4 Set of PCs

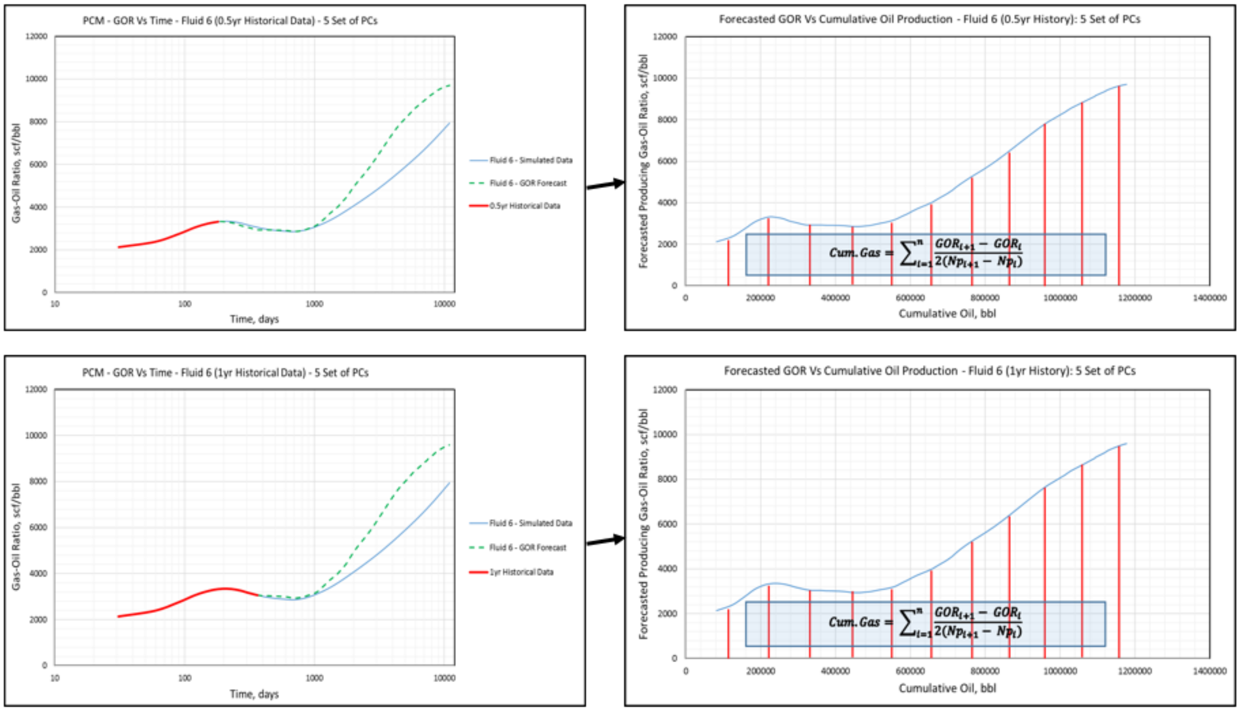

Figure 5-131 GOR Forecasts & Forecasted GOR vs. Cum. Oil – Fluid 6 (0.5yr. and 1yr. Histories): 5 Set of PCs

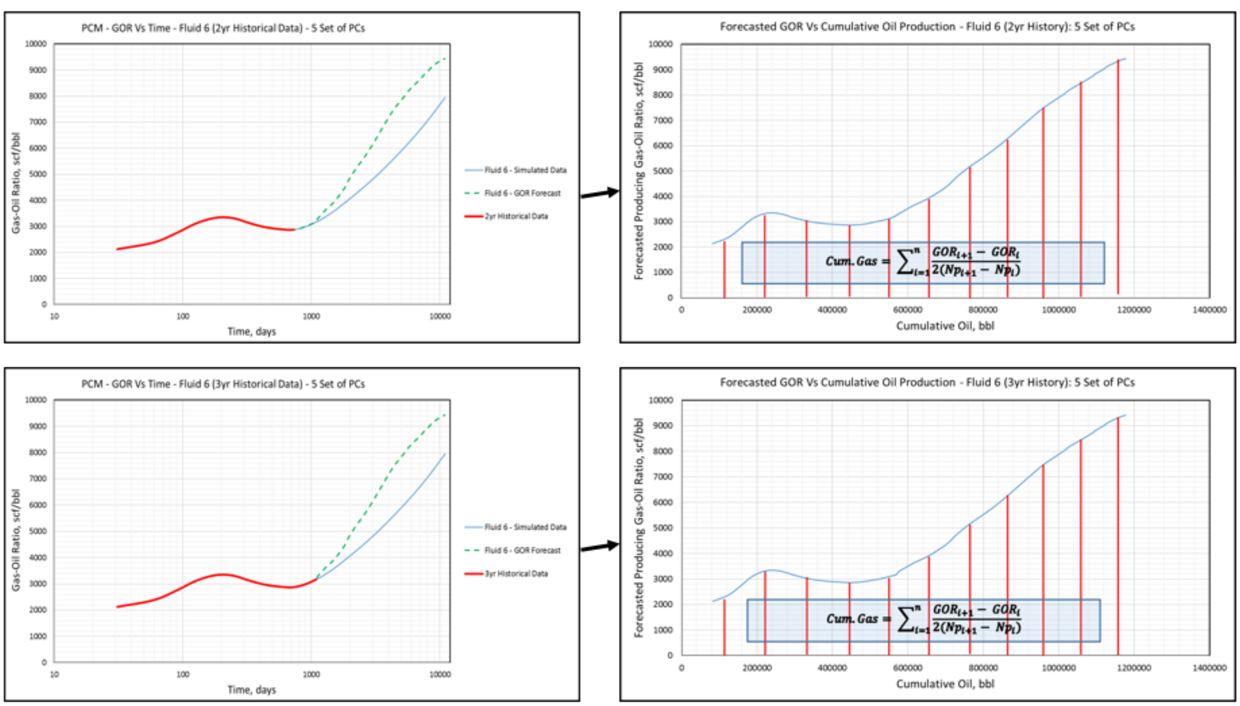

Figure 5-132 GOR Forecasts & Forecasted GOR vs. Cum. Oil – Fluid 6 (2yr. and 3yr. Histories): 5 Sets of PCs

Table 5-69 shows the results for all Fluid 6 cases. In all these cases, forecasts were reasonable and errors in the calculated solution gas produced (after 30 yrs) in most cases were relatively low. Percentage error was as low as 0.6% when the first set of PCs were used to forecast. The figures in red indicate the lowest percentage errors for each case.

Table 5-69 Solution Gas Production Forecasts, Errors and Percentage Errors – Fluid 6

FLUID 6 RESULTS																				
Principal Components (PCs)	1 Set of PCs				2 Sets of PCs				3 Sets of PCs				4 Sets of PCs				5 Sets of PCs			
Historical Data	0.5yr	1yr	2yrs	3yrs	0.5yr	1yr	2yrs	3yrs	0.5yr	1yr	2yrs	3yrs	0.5yr	1yr	2yrs	3yrs	0.5yr	1yr	2yrs	3yrs
Simulated Cum. Gas, bscf	4.8	4.8	4.8	4.8	4.8	4.8	4.8	4.8	4.8	4.8	4.8	4.8	4.8	4.8	4.8	4.8	4.8	4.8	4.8	4.8
PCM Forecast, bscf	4.8	5.0	5.0	5.0	4.9	5.0	5.0	5.0	5.1	5.2	5.2	5.2	5.4	5.3	5.3	5.3	5.4	5.4	5.3	5.3
Error (absolute value), bscf	0.0	0.2	0.2	0.2	0.1	0.2	0.2	0.2	0.3	0.4	0.4	0.4	0.6	0.5	0.5	0.5	0.6	0.6	0.5	0.5
Percentage Error, %	0.6	4.0	5.5	5.3	3.4	4.7	4.5	5.0	6.5	8.7	9.7	10.0	13.4	11.9	11.8	11.8	14.4	13.6	12.0	11.8

5.2.3.1.7. Fluid 7 Cases

Graphical displays of GOR forecasts and the plots of the estimated GOR forecasts versus cumulative oil production for Fluid 7 are shown in Figures 5-133 to 5-142.

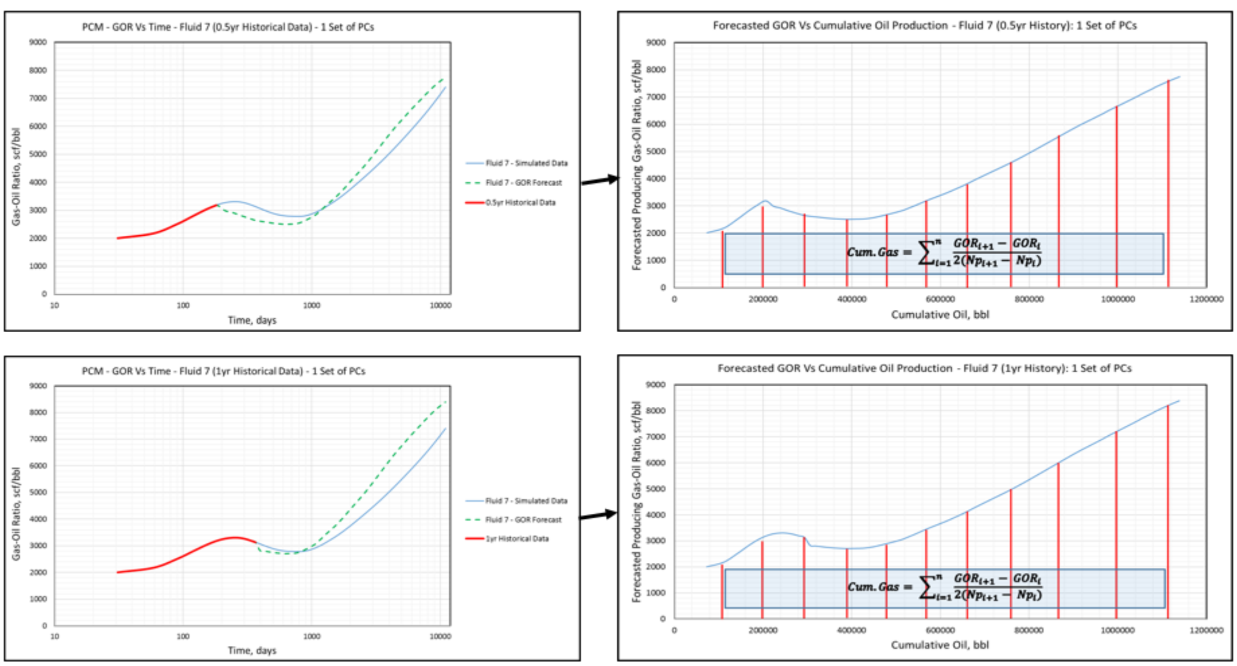

Figure 5-133 GOR Forecasts & Forecasted GOR vs. Cum. Oil – Fluid 7 (0.5yr. and 1yr. Histories): 1 Set of PCs

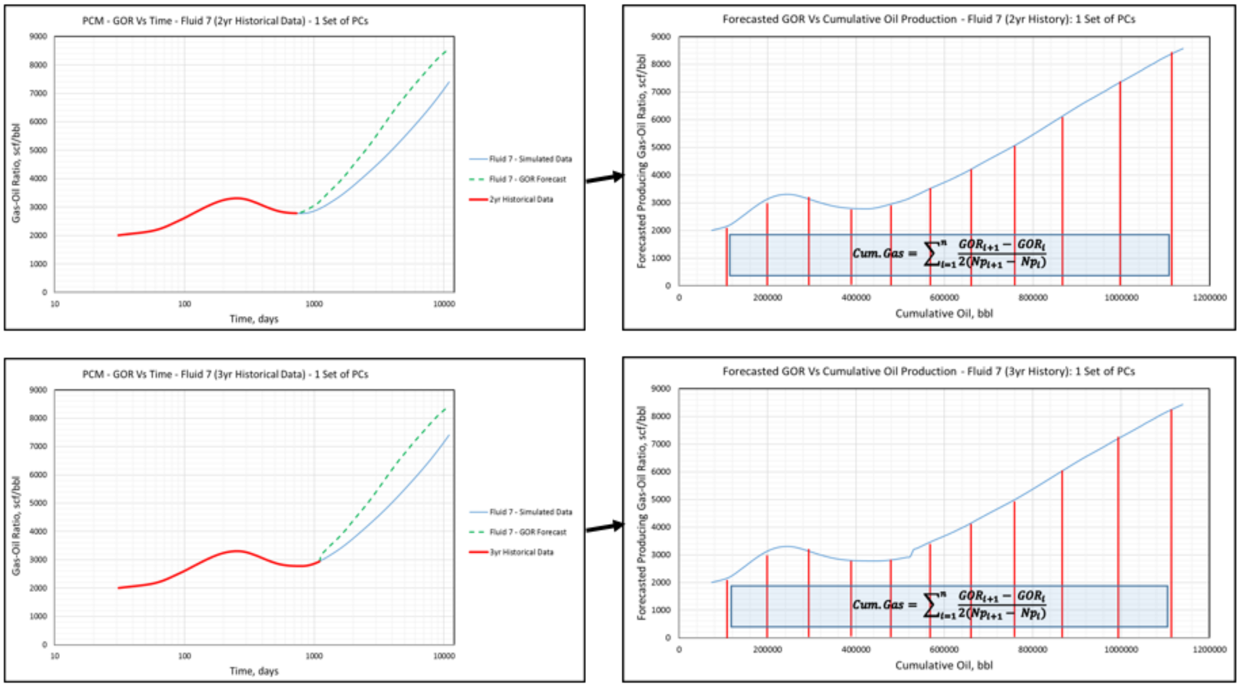

Figure 5-134 GOR Forecasts & Forecasted GOR vs. Cum. Oil – Fluid 7 (2yr. and 3yr. Histories): 1 Set of PCs

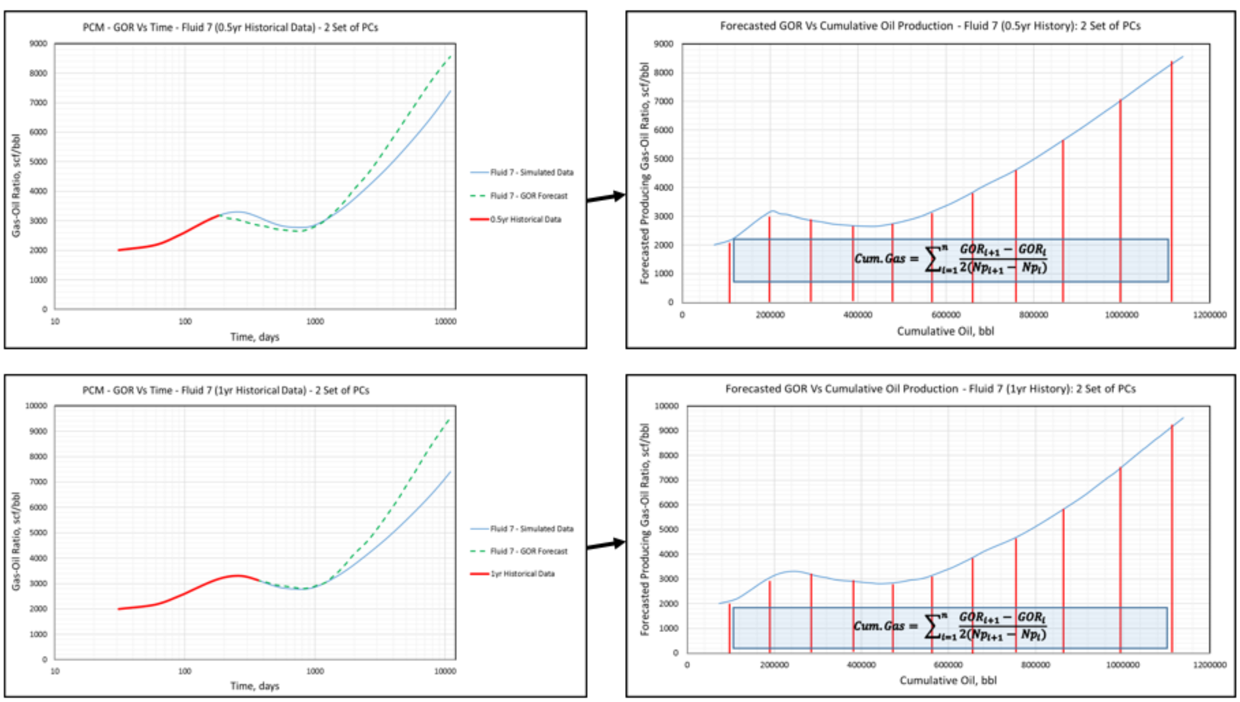

Figure 5-135 GOR Forecasts & Forecasted GOR vs. Cum. Oil – Fluid 7 (0.5yr. and 1yr. Histories): 2 Set of PCs

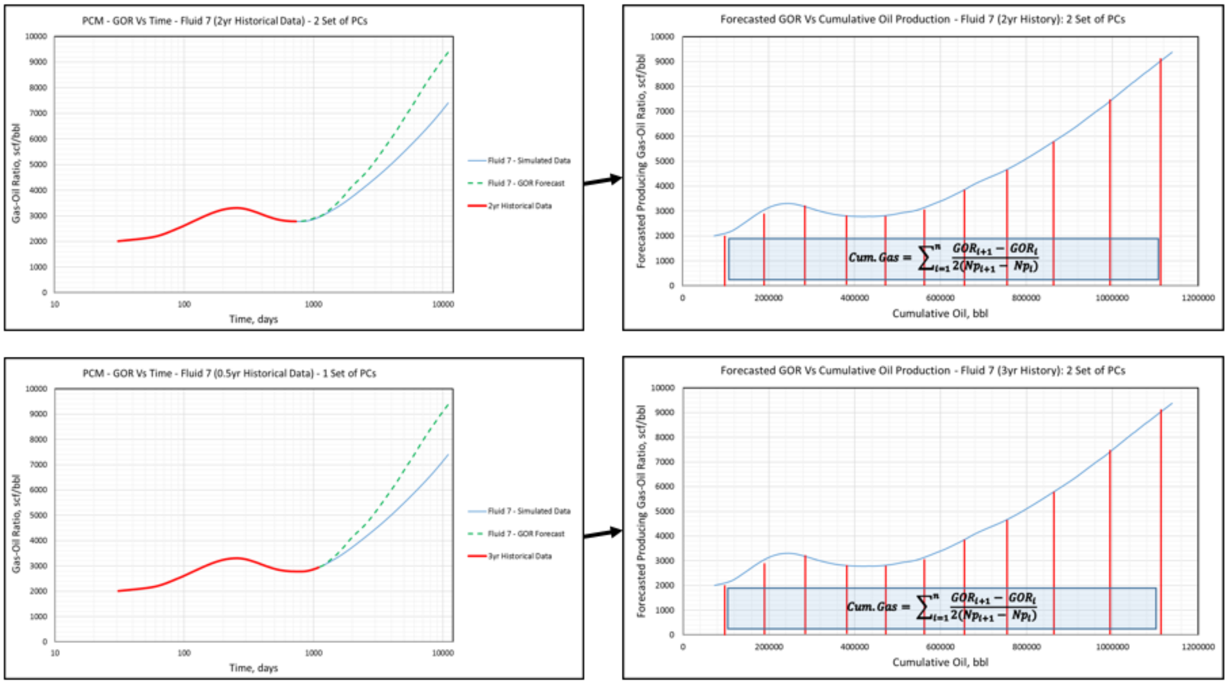

Figure 5-136 GOR Forecasts & Forecasted GOR vs. Cum. Oil – Fluid 7 (2yrs. and 3yrs. Histories): 2 Sets of PCs

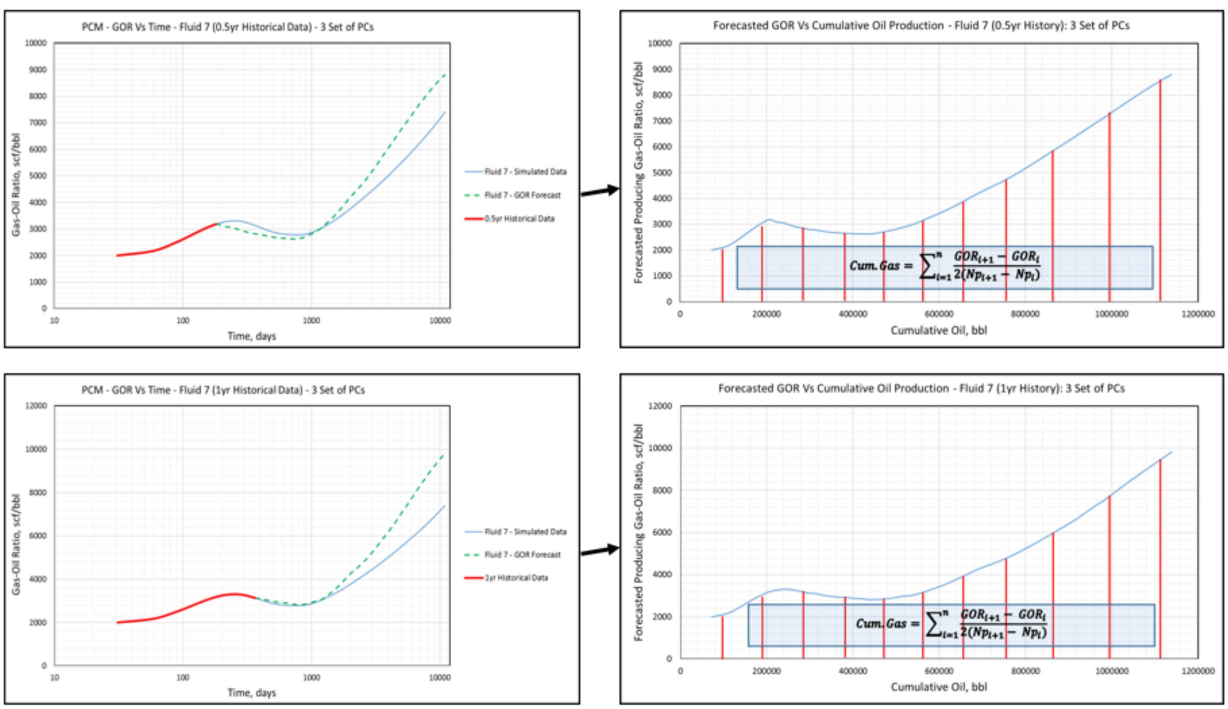

Figure 5-137 GOR Forecasts & Forecasted GOR vs. Cum. Oil – Fluid 7 (0.5yr. and 1yr. Histories): 3 Sets of PCs

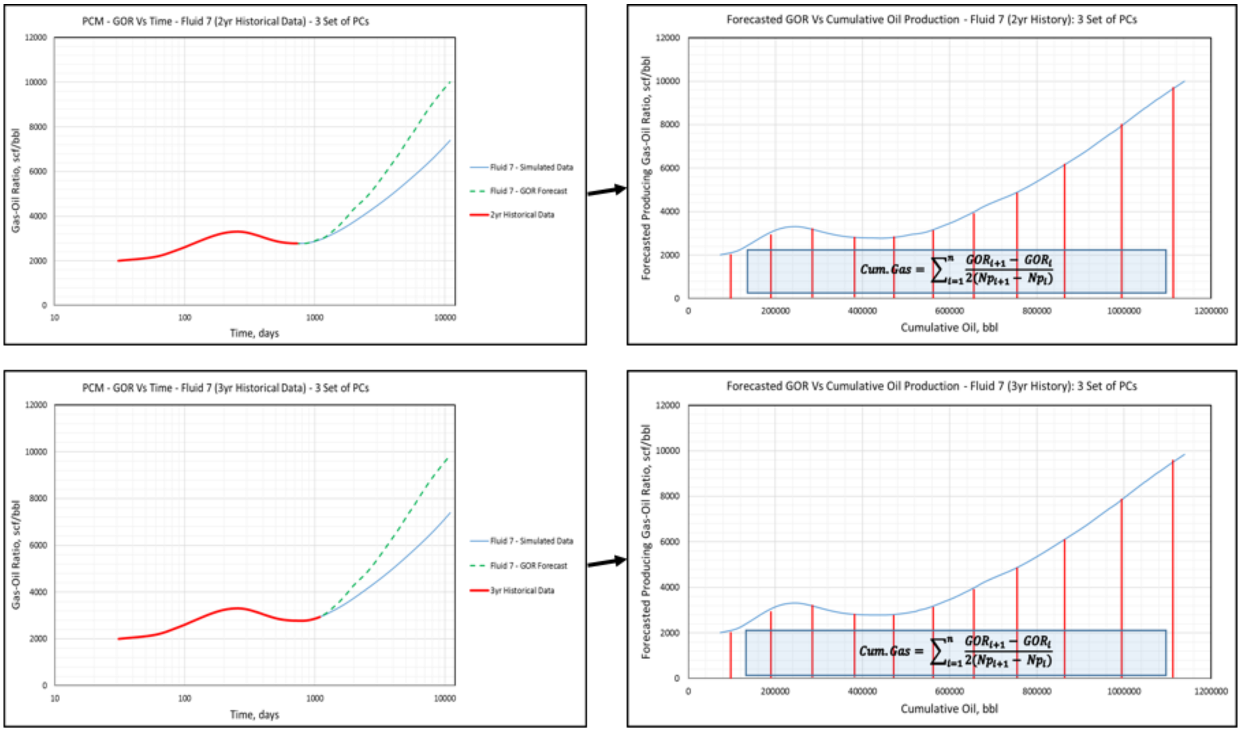

Figure 5-138 GOR Forecasts & Forecasted GOR vs. Cum. Oil – Fluid 7 (2yrs. and 3yrs. Histories): 3 Sets of PCs

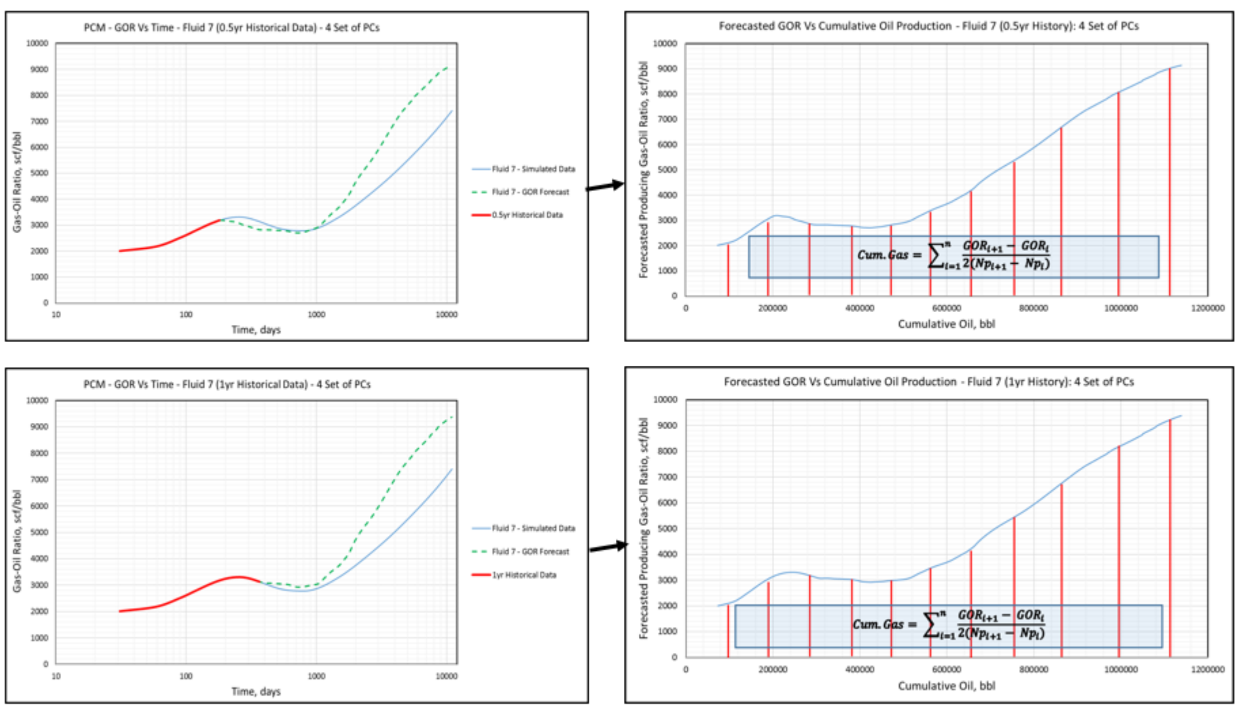

Figure 5-139 GOR Forecasts & Forecasted GOR vs. Cum. Oil – Fluid 7 (0.5yr. and 1yr. Histories): 4 Sets of PCs

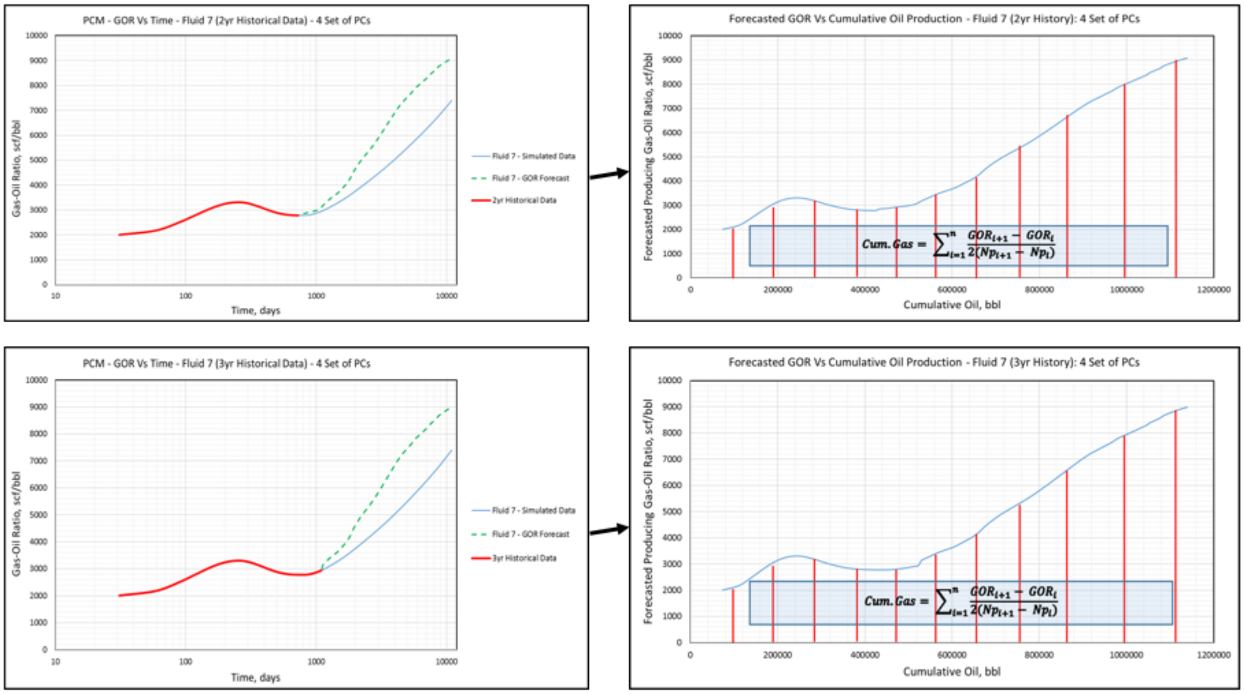

Figure 5-140 GOR Forecasts & Forecasted GOR vs. Cum. Oil – Fluid 7 (2yrs. and 3yrs. Histories): 4 Sets of PCs

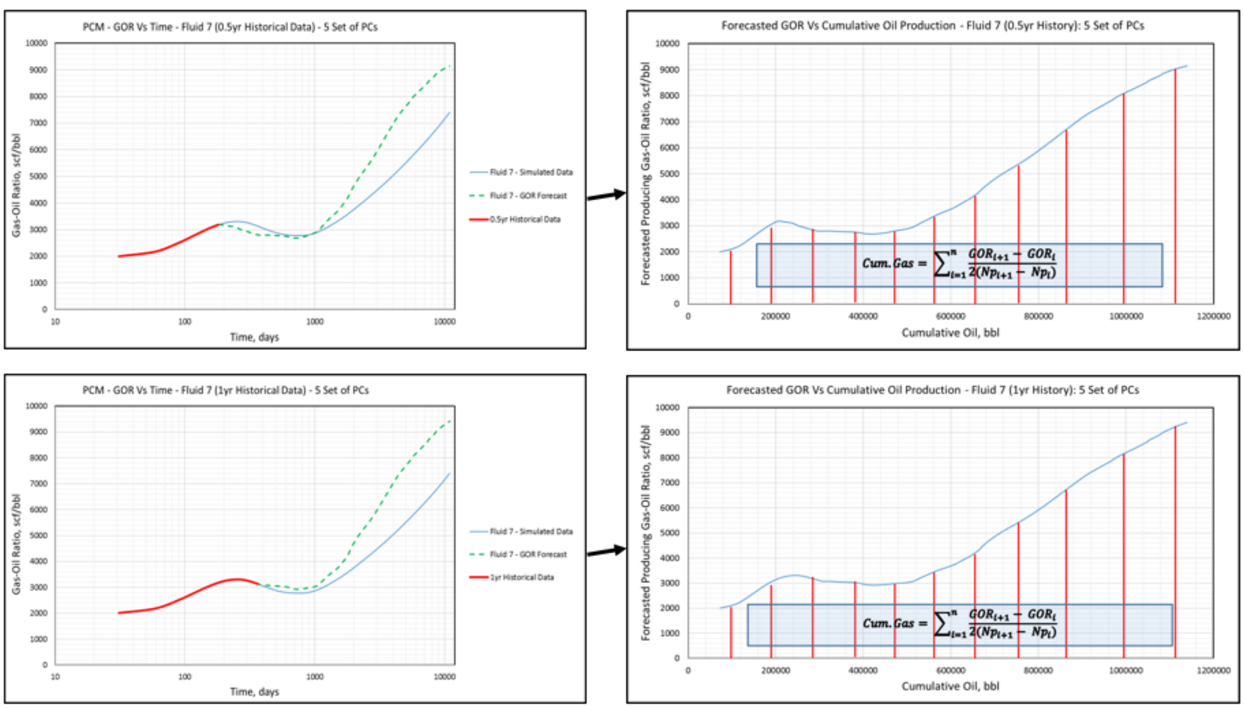

Figure 5-141 GOR Forecasts & Forecasted GOR vs. Cum. Oil – Fluid 7 (0.5yr. and 1yr. Histories): 5 Sets of PCs

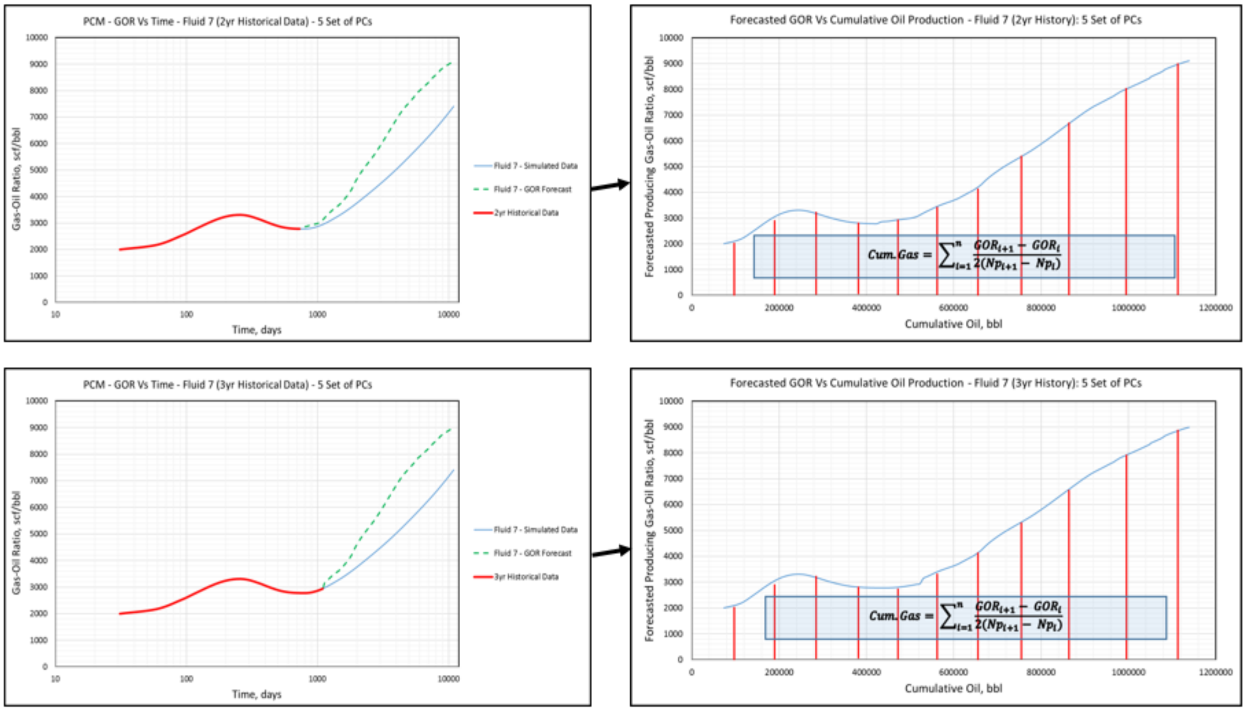

Figure 5-142 GOR Forecasts & Forecasted GOR vs. Cum. Oil – Fluid 7 (2yrs. and 3yrs. Histories): 5 Sets of PCs

Table 5-70 shows the results for all Fluid 7 cases. In all these cases, forecasts were reasonable and errors in the calculated solution gas produced (after 30 yrs) in most cases were relatively low. Percentage error was as low as 0.2% when the first set of PCs were used to forecast and only 6 months of historical data available. The figures in red indicate the lowest percentage errors for each case.

Table 5-70 Solution Gas Production Forecasts, Errors and Percentage Errors – Fluid 7

FLUID 7 RESULTS																				
Principal Components (PCs)	1 Set of PCs				2 Sets of PCs				3 Sets of PCs				4 Sets of PCs				5 Sets of PCs			
Historical Data	0.5yr	1yr	2yrs	3yrs	0.5yr	1yr	2yrs	3yrs	0.5yr	1yr	2yrs	3yrs	0.5yr	1yr	2yrs	3yrs	0.5yr	1yr	2yrs	3yrs
Simulated Cum. Gas, bscf	4.4	4.4	4.4	4.4	4.4	4.4	4.4	4.4	4.4	4.4	4.4	4.4	4.4	4.4	4.4	4.4	4.4	4.4	4.4	4.4
PCM Forecast, bscf	4.4	4.8	4.9	4.8	4.6	4.8	4.8	4.8	4.7	4.9	5.0	5.0	5.1	5.2	5.1	5.1	5.1	5.2	5.1	5.1
Error (absolute value), bscf	0.0	0.4	0.5	0.4	0.2	0.4	0.4	0.4	0.3	0.5	0.6	0.6	0.7	0.8	0.7	0.7	0.7	0.8	0.7	0.7
Percentage Error, %	0.2	8.1	10.3	8.8	3.9	9.3	8.5	8.3	6.3	11.4	13.1	12.2	14.9	17.7	15.5	14.4	14.9	17.6	15.8	14.4

5.2.3.1.8. Fluid 8 Cases

Graphical displays of GOR forecasts and the plots of the estimated GOR forecasts versus cumulative oil production for Fluid 8 are shown in Figures 5-143 to 5-152.

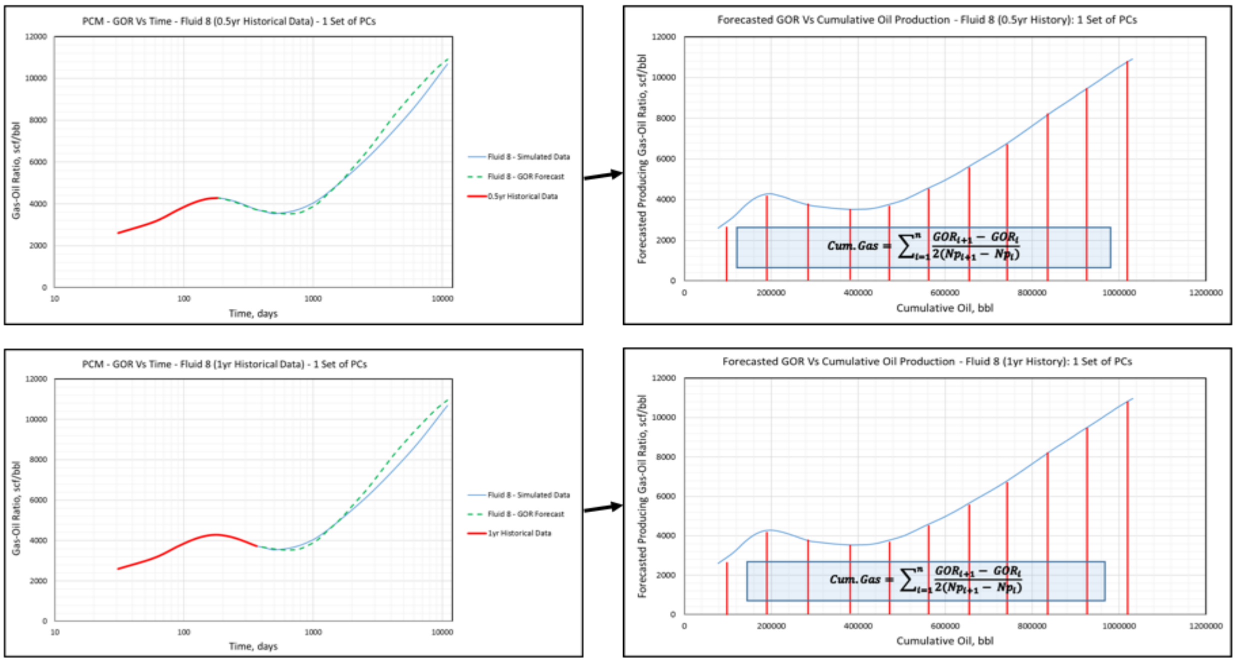

Figure 5-143 GOR Forecasts & Forecasted GOR vs. Cum. Oil – Fluid 8 (0.5yr. and 1yr. Histories): 1 Set of PCs

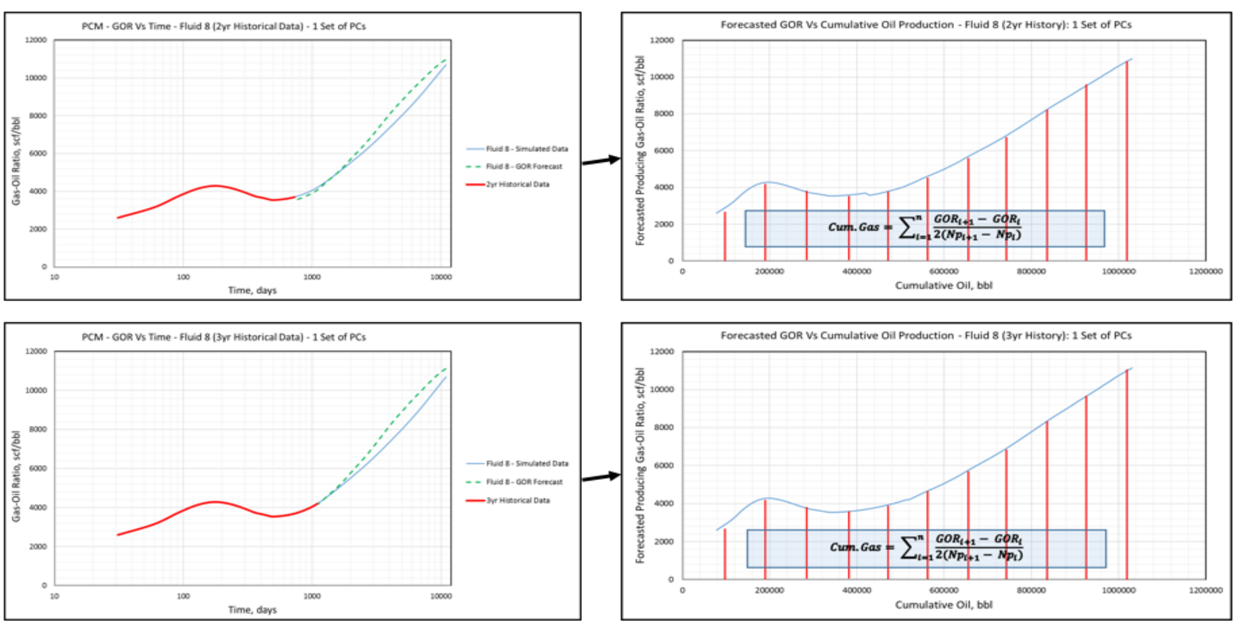

Figure 5-144 GOR Forecasts & Forecasted GOR vs. Cum. Oil – Fluid 8 (2yrs. and 3yrs. Histories): 1 Set of PCs

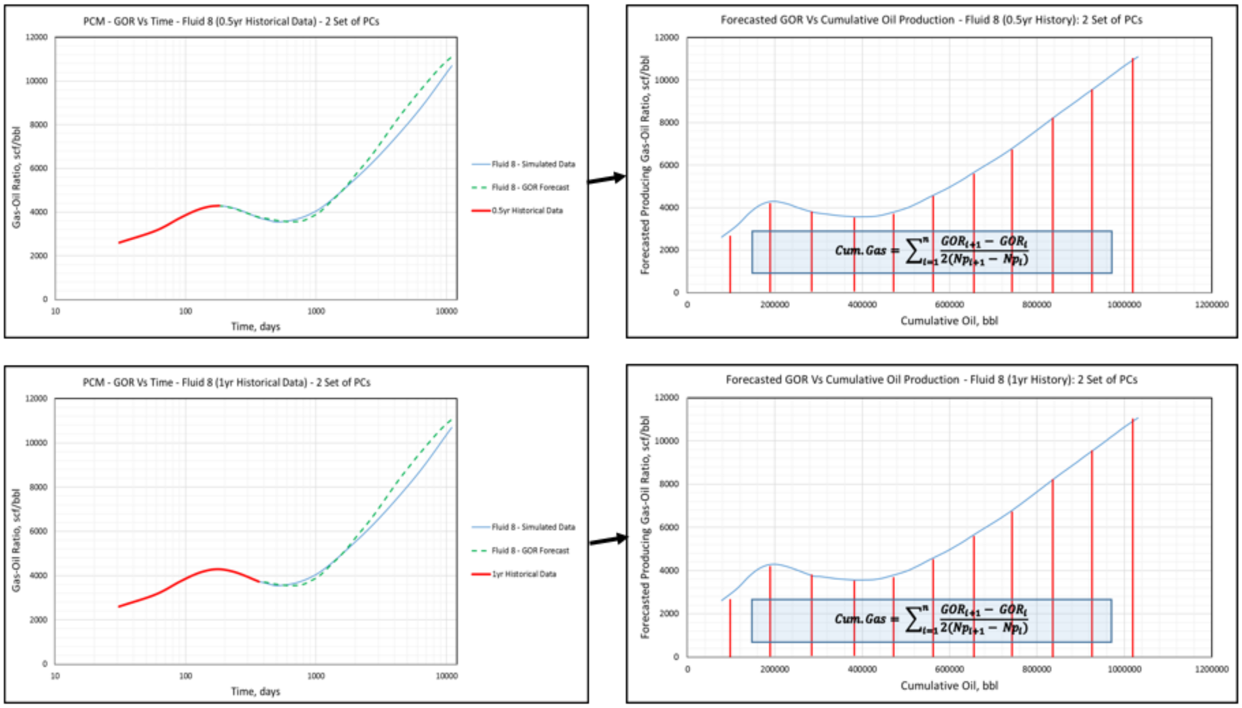

Figure 5-145 GOR Forecasts & Forecasted GOR vs. Cum. Oil – Fluid 8 (0.5yr. and 1yr. Histories): 2 Sets of PCs

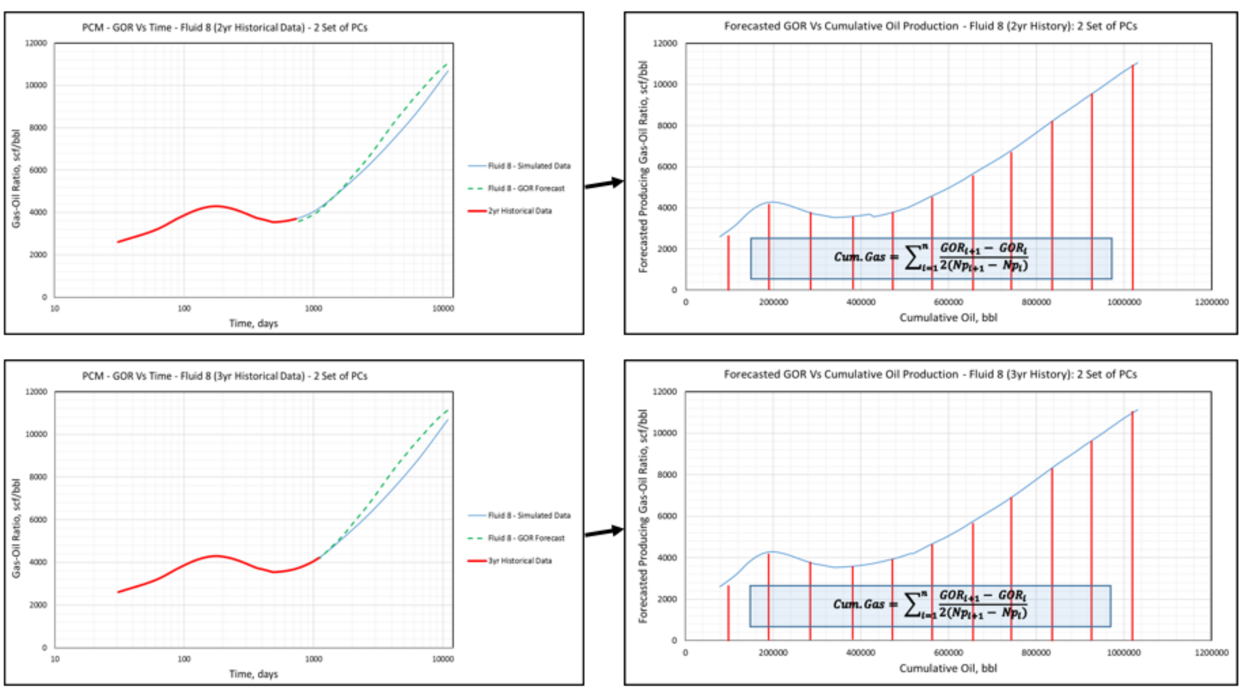

Figure 5-146 GOR Forecasts & Forecasted GOR vs. Cum. Oil – Fluid 8 (2yrs. and 3yrs. Histories): 2 Sets of PCs

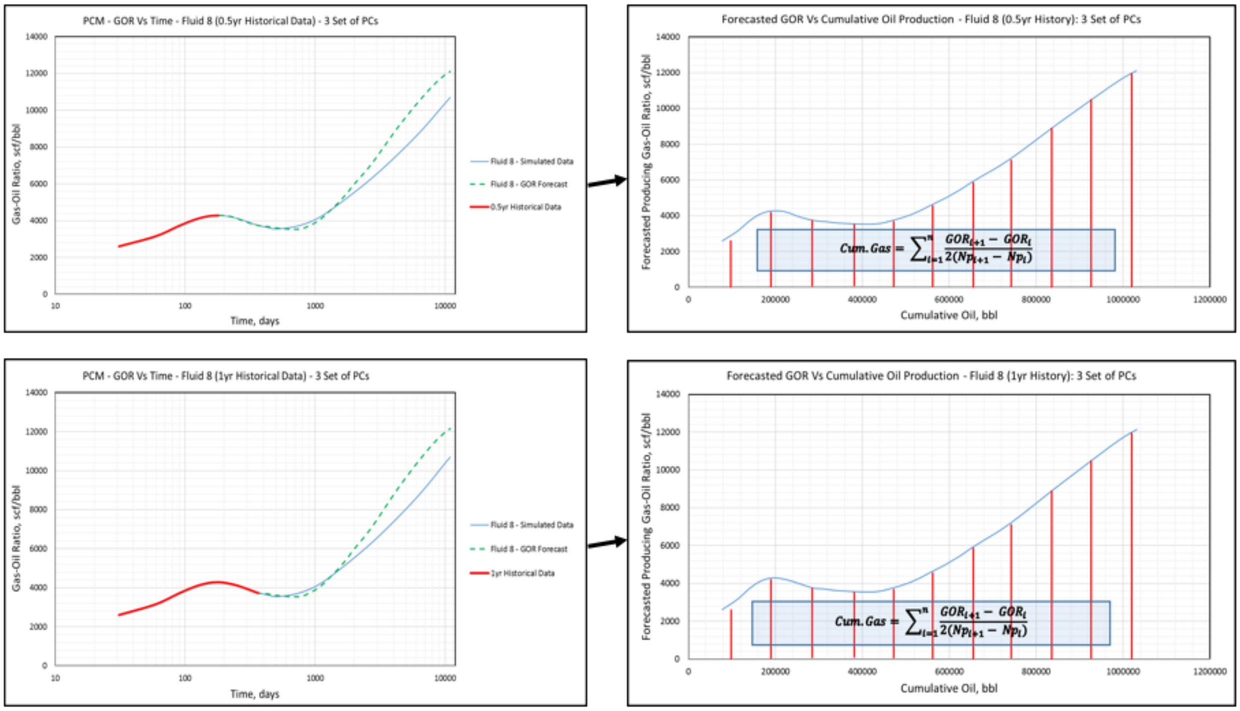

Figure 5-147 GOR Forecasts & Forecasted GOR vs. Cum. Oil – Fluid 8 (0.5yr. and 1yr. Histories): 3 Sets of PCs

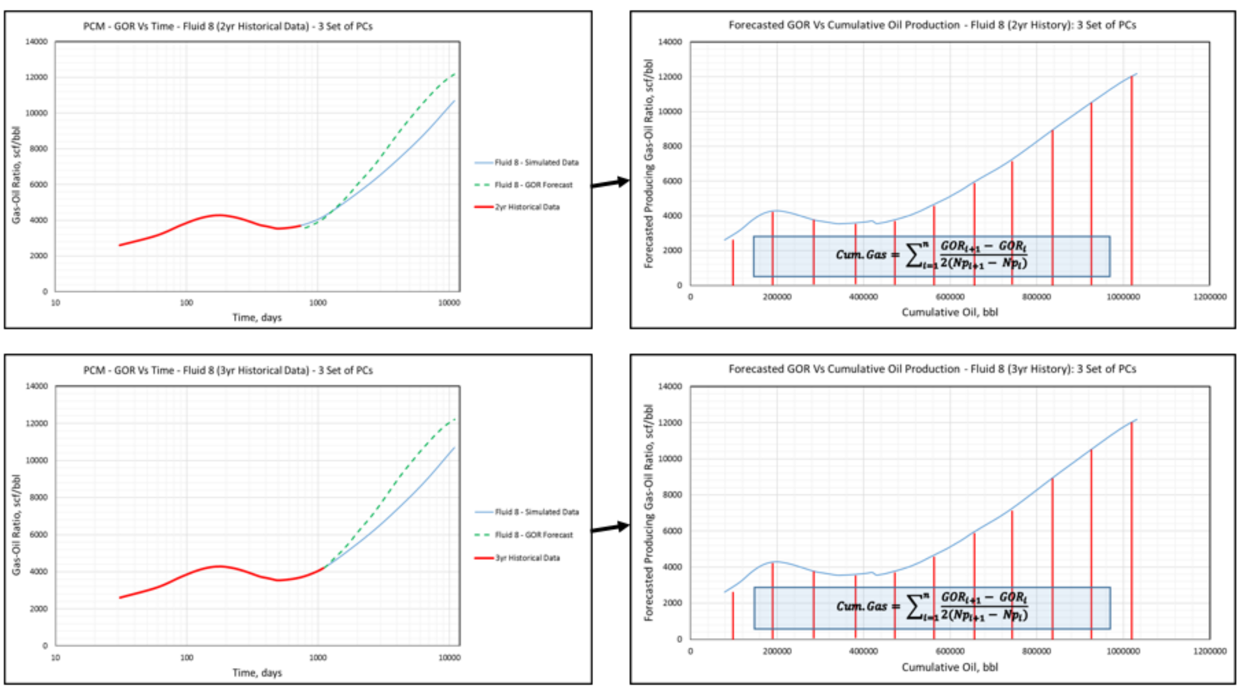

Figure 5-148 GOR Forecasts & Forecasted GOR vs. Cum. Oil – Fluid 8 (2yrs. and 3yrs. Histories): 3 Sets of PCs

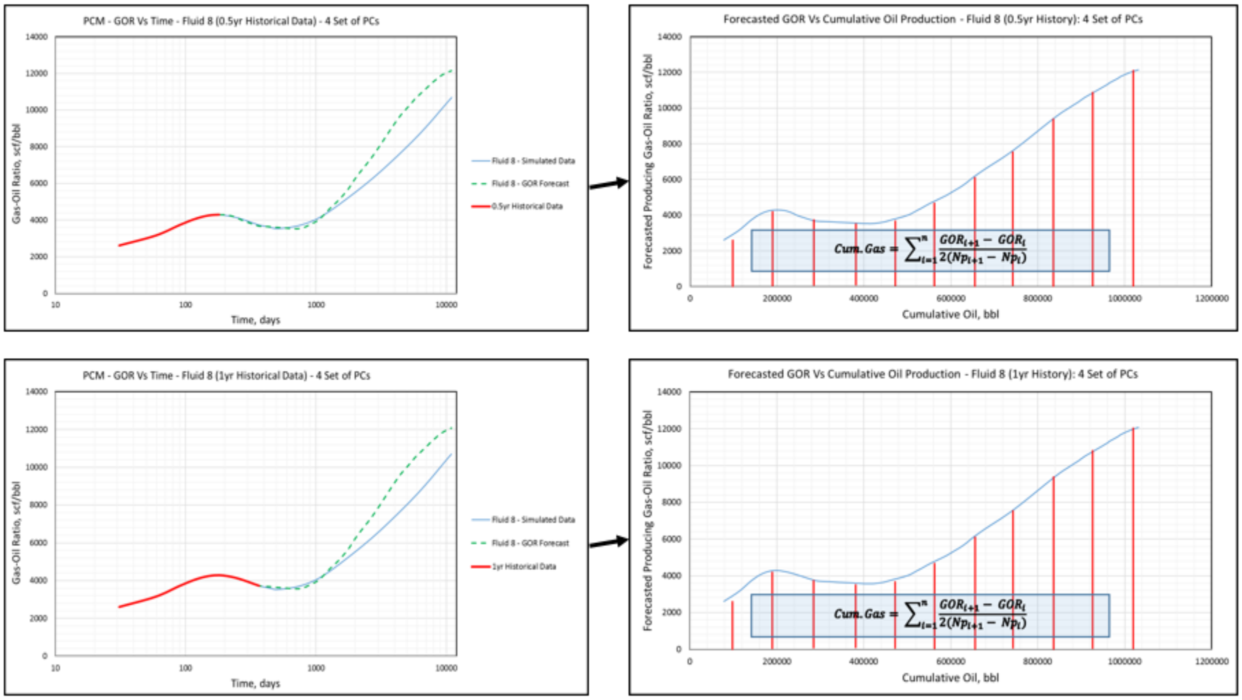

Figure 5-149 GOR Forecasts & Forecasted GOR vs. Cum. Oil – Fluid 8 (0.5yr. and 1yr. Histories): 4 Sets of PCs

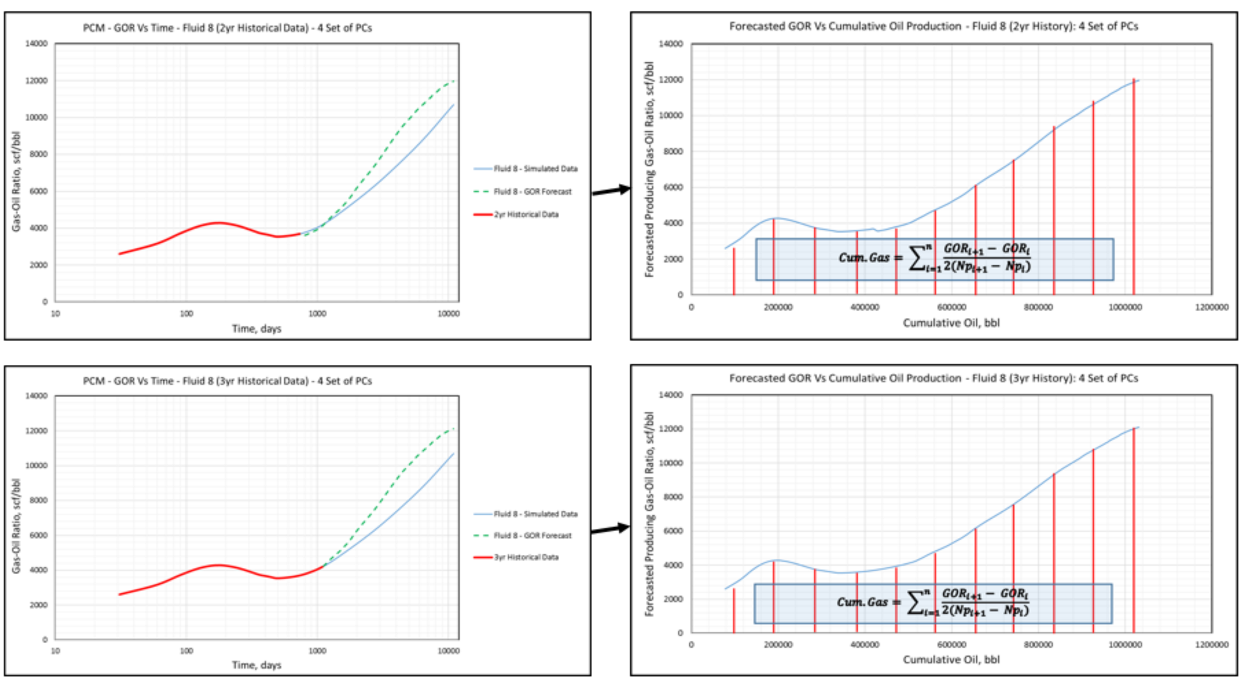

Figure 5-150 GOR Forecasts & Forecasted GOR vs. Cum. Oil – Fluid 8 (2yrs. and 3yrs. Histories): 4 Sets of PCs

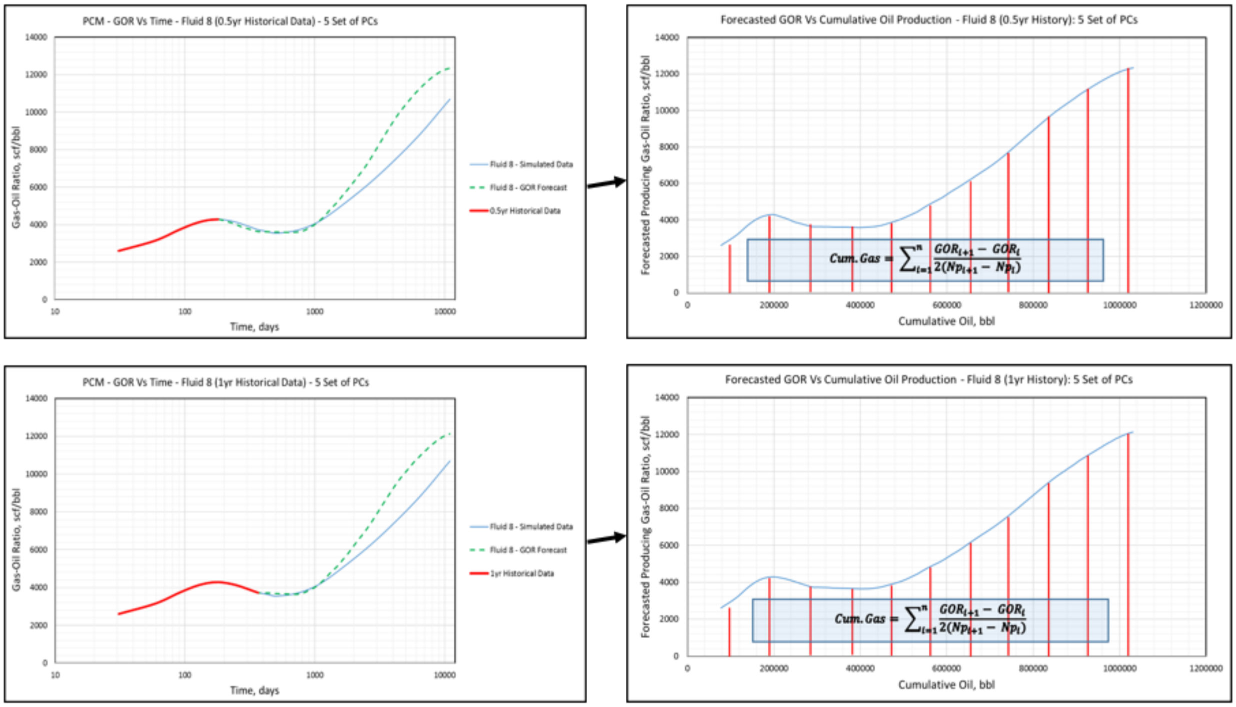

Figure 5-151 GOR Forecasts & Forecasted GOR vs. Cum. Oil – Fluid 8 (0.5yr. and 1yr. Histories): 5 Sets of PCs

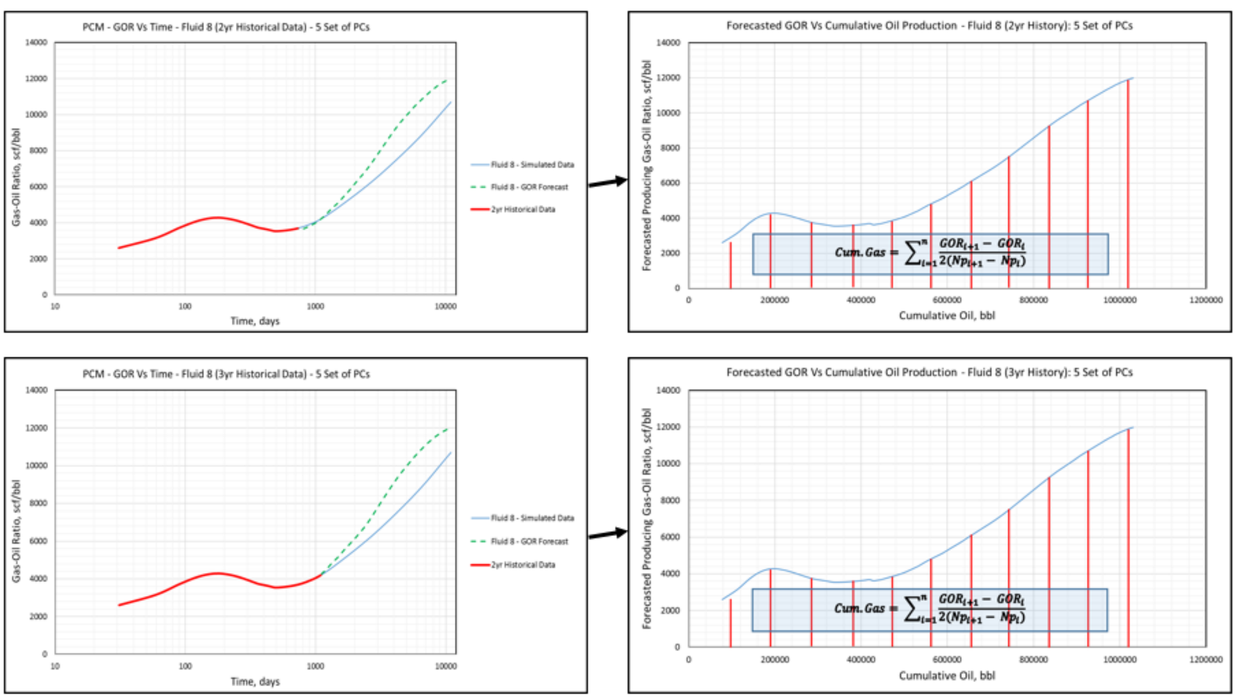

Figure 5-152 GOR Forecasts & Forecasted GOR vs. Cum. Oil – Fluid 8 (2yrs. and 3yrs. Histories): 5 Sets of PCs

Table 5-71 shows the results for all Fluid 8 cases. In all these cases, forecasts were reasonable and errors in the calculated solution gas produced (after 30 yrs) in most cases were relatively low. Percentage error was as low as 0.4% when the first set of PCs were used to forecast. The figures in red indicate the lowest percentage errors for each case.

Table 5-71 Solution Gas Production Forecasts, Errors and Percentage Errors – Fluid 8

FLUID 8 RESULTS																				
Principal Components (PCs)	1 Set of PCs				2 Sets of PCs				3 Sets of PCs				4 Sets of PCs				5 Sets of PCs			
Historical Data	0.5yr	1yr	2yrs	3yrs	0.5yr	1yr	2yrs	3yrs	0.5yr	1yr	2yrs	3yrs	0.5yr	1yr	2yrs	3yrs	0.5yr	1yr	2yrs	3yrs
Simulated Cum. Gas, bscf	5.5	5.5	5.5	5.5	5.5	5.5	5.5	5.5	5.5	5.5	5.5	5.5	5.5	5.5	5.5	5.5	5.5	5.5	5.5	5.5
PCM Forecast, bscf	5.4	5.4	5.4	5.5	5.4	5.4	5.4	5.5	5.7	5.7	5.7	5.8	5.9	5.9	5.8	5.9	6.0	5.9	5.8	5.9
Error (absolute value), bscf	-0.1	-0.1	-0.1	0.0	-0.1	-0.1	-0.1	0.0	0.2	0.2	0.2	0.3	0.4	0.4	0.3	0.4	0.5	0.4	0.3	0.4
Percentage Error, %	-1.1	-0.7	-0.4	0.7	-0.5	-0.6	-0.5	0.7	4.6	4.7	4.9	6.3	7.5	7.2	6.3	7.5	9.1	8.0	6.7	7.1

5.2.3.1.9. Fluid 9 Cases

Graphical displays of GOR forecasts and the plots of the estimated GOR forecasts versus cumulative oil production for Fluid 9 are shown in Figures 5-153 to 5-162.

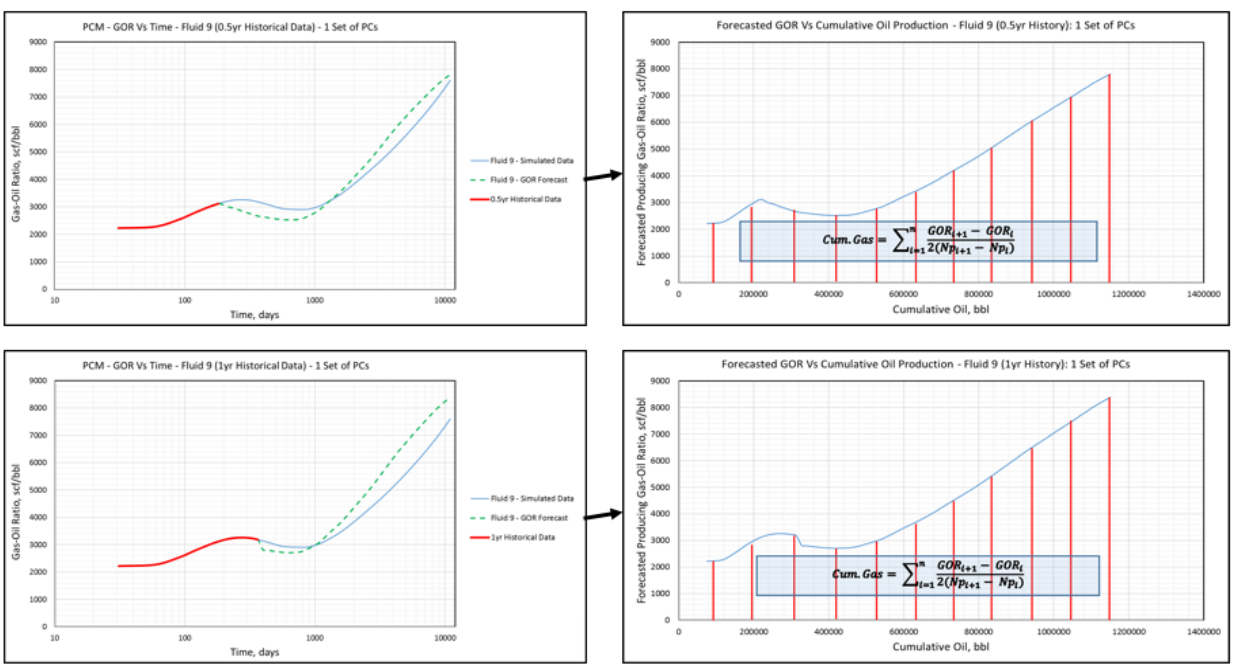

Figure 5-153 GOR Forecasts & Forecasted GOR vs. Cum. Oil – Fluid 9 (0.5yr. and 1yr. Histories): 1 Set of PCs

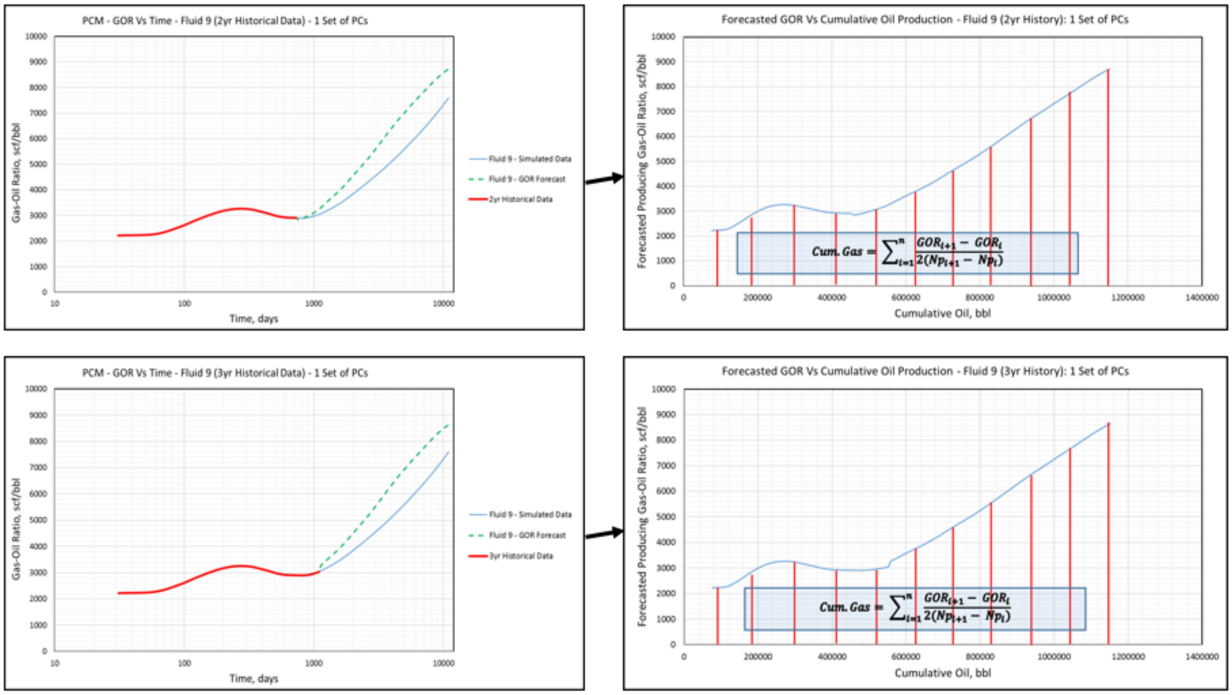

Figure 5-154 GOR Forecasts & Forecasted GOR vs. Cum. Oil – Fluid 9 (2yrs. and 3yrs. Histories): 1 Set of PCs

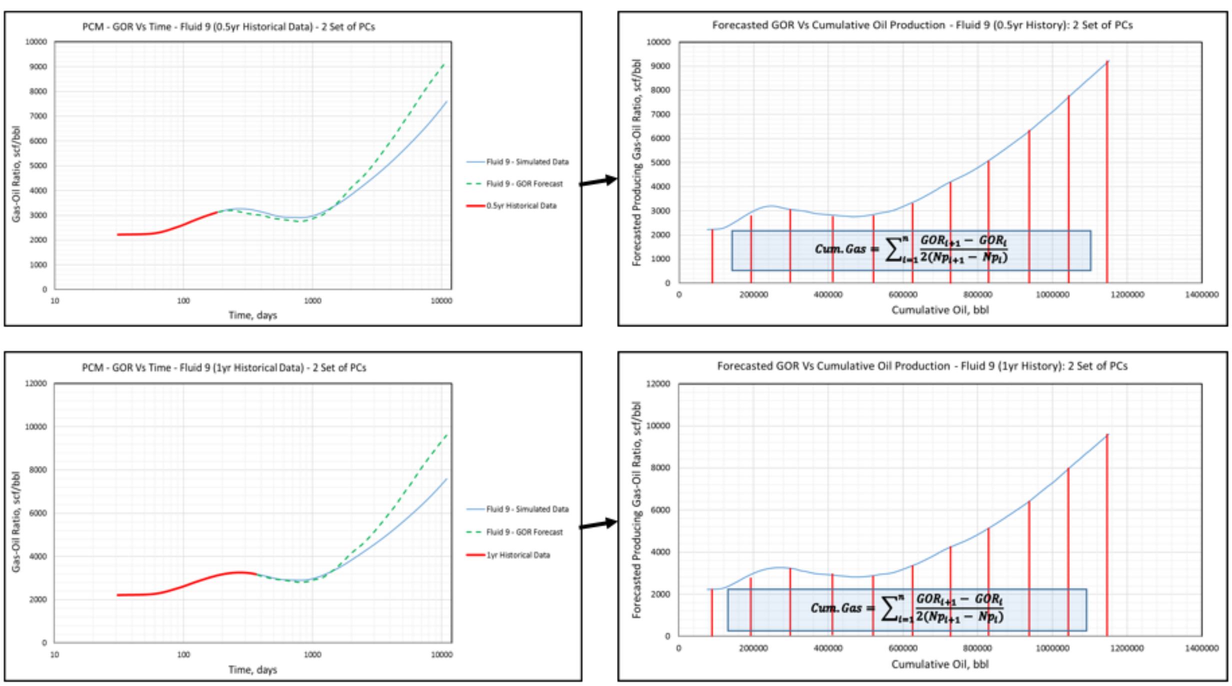

Figure 5-155 GOR Forecasts & Forecasted GOR vs. Cum. Oil – Fluid 9 (0.5yr. and 1yr. Histories): 2 Sets of PCs

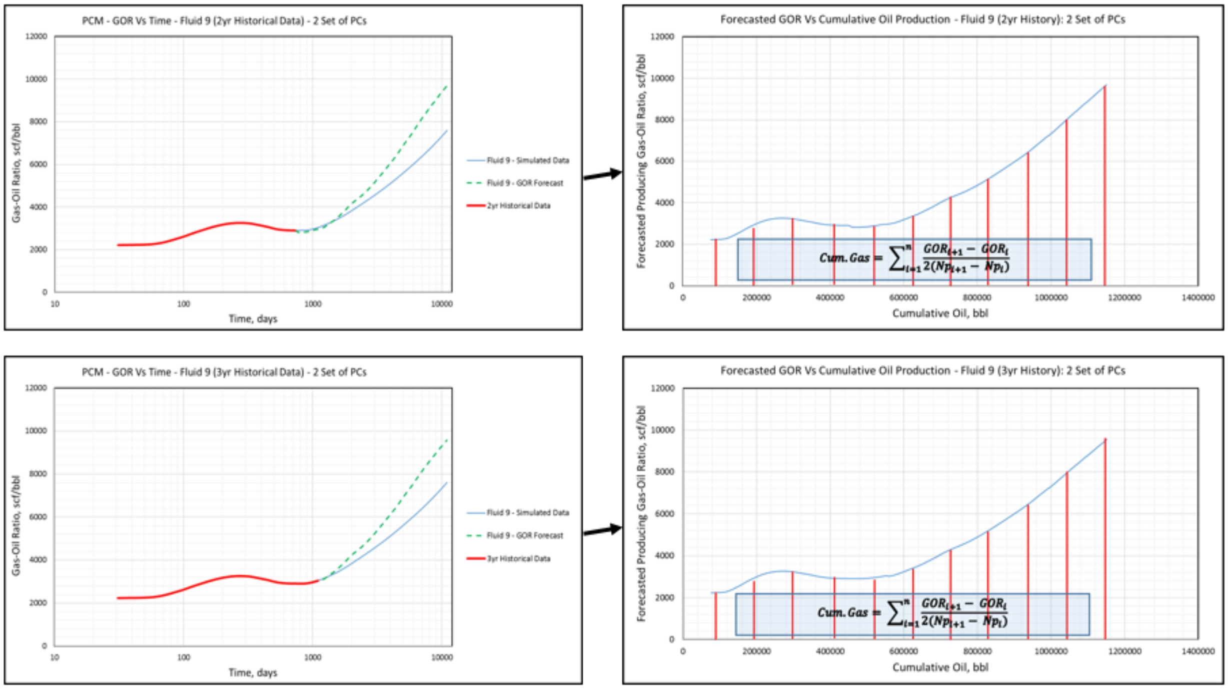

Figure 5-156 GOR Forecasts & Forecasted GOR vs. Cum. Oil – Fluid 9 (2yrs. and 3yrs. Histories): 2 Sets of PCs

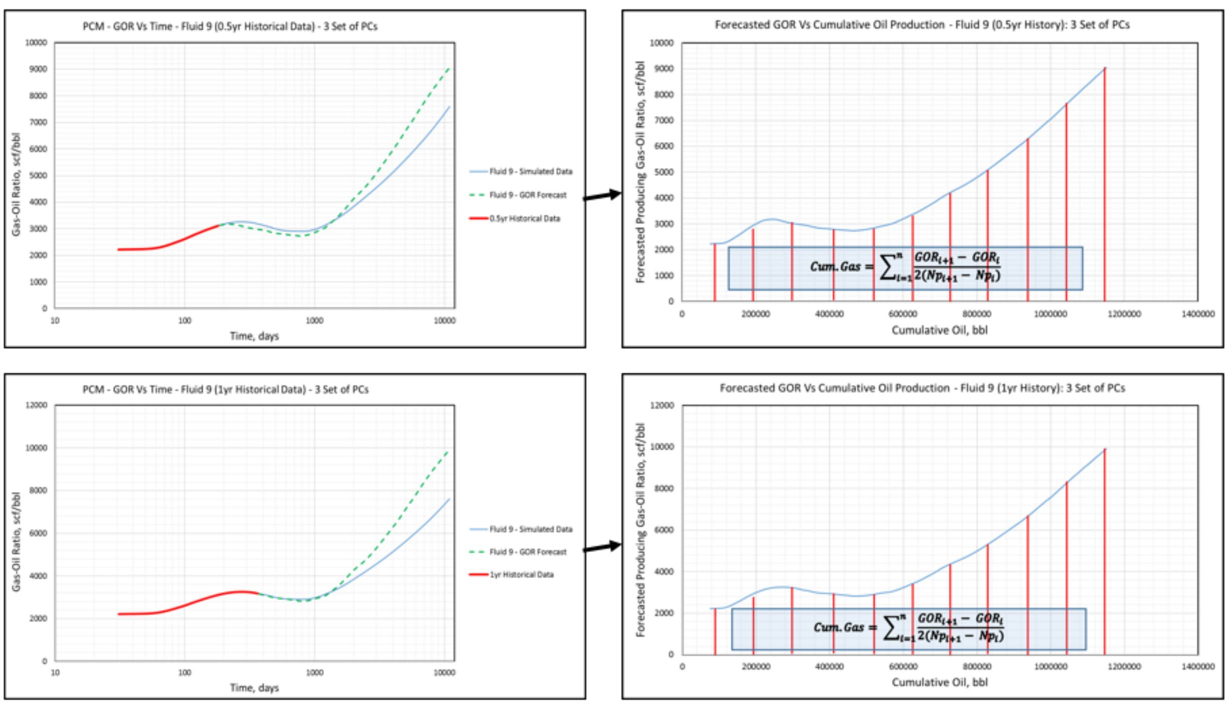

Figure 5-157 GOR Forecasts & Forecasted GOR vs. Cum. Oil – Fluid 9 (0.5yr. and 1yr. Histories): 3 Sets of PCs

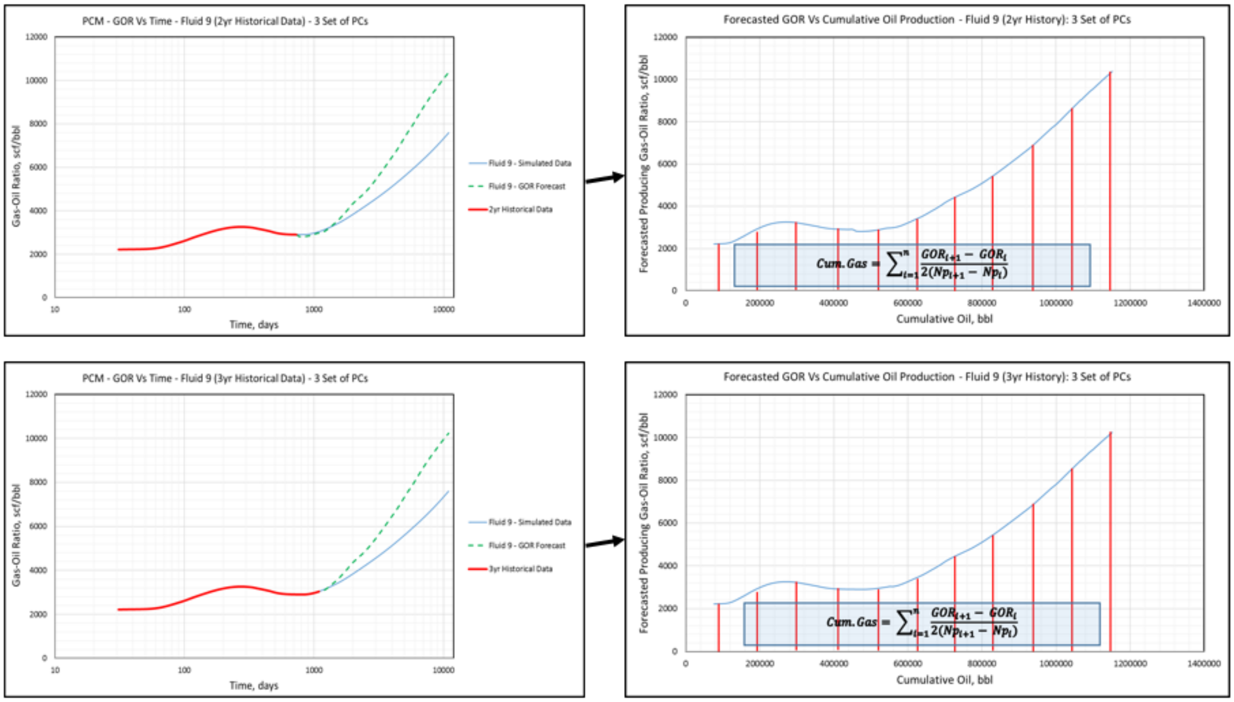

Figure 5-158 GOR Forecasts & Forecasted GOR vs. Cum. Oil – Fluid 9 (2yrs. and 3yrs. Histories): 3 Sets of PCs

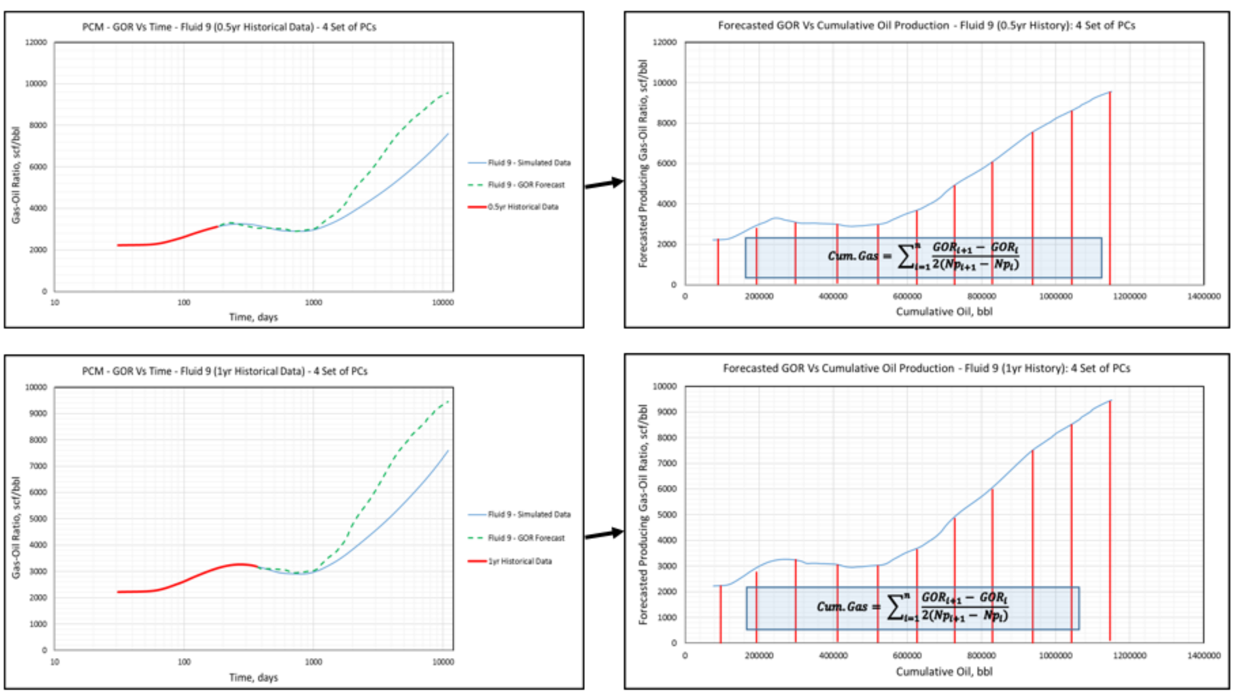

Figure 5-159 GOR Forecasts & Forecasted GOR vs. Cum. Oil – Fluid 9 (0.5yr. and 1yr. Histories): 4 Sets of PCs

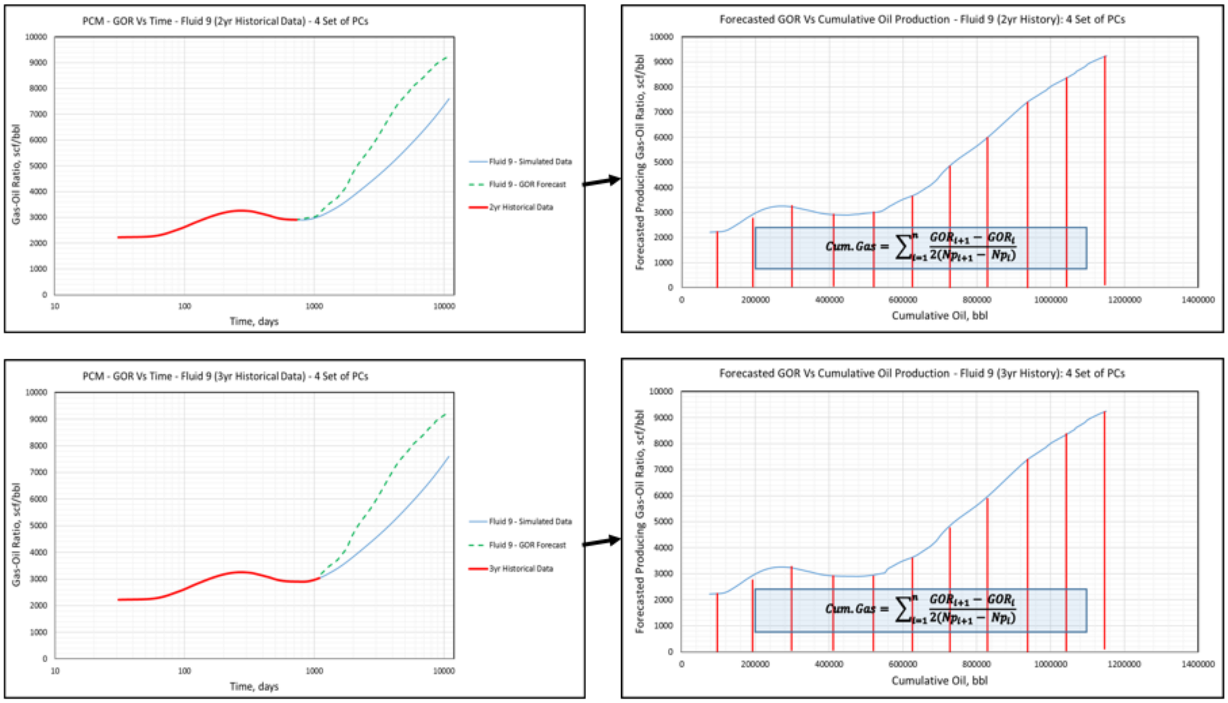

Figure 5-160 GOR Forecasts & Forecasted GOR vs. Cum. Oil – Fluid 9 (2yrs. and 3yrs. Histories): 4 Sets of PCs

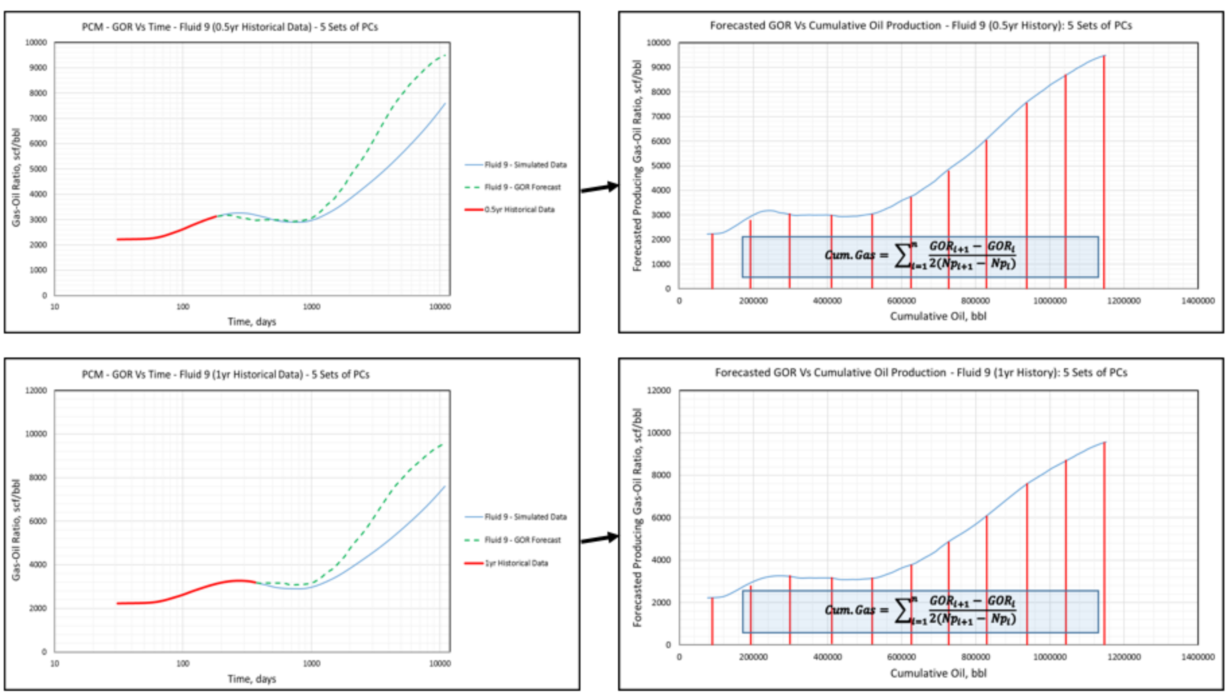

Figure 5-161 GOR Forecasts & Forecasted GOR vs. Cum. Oil – Fluid 9 (0.5yr. and 1yr. Histories): 5 Sets of PCs

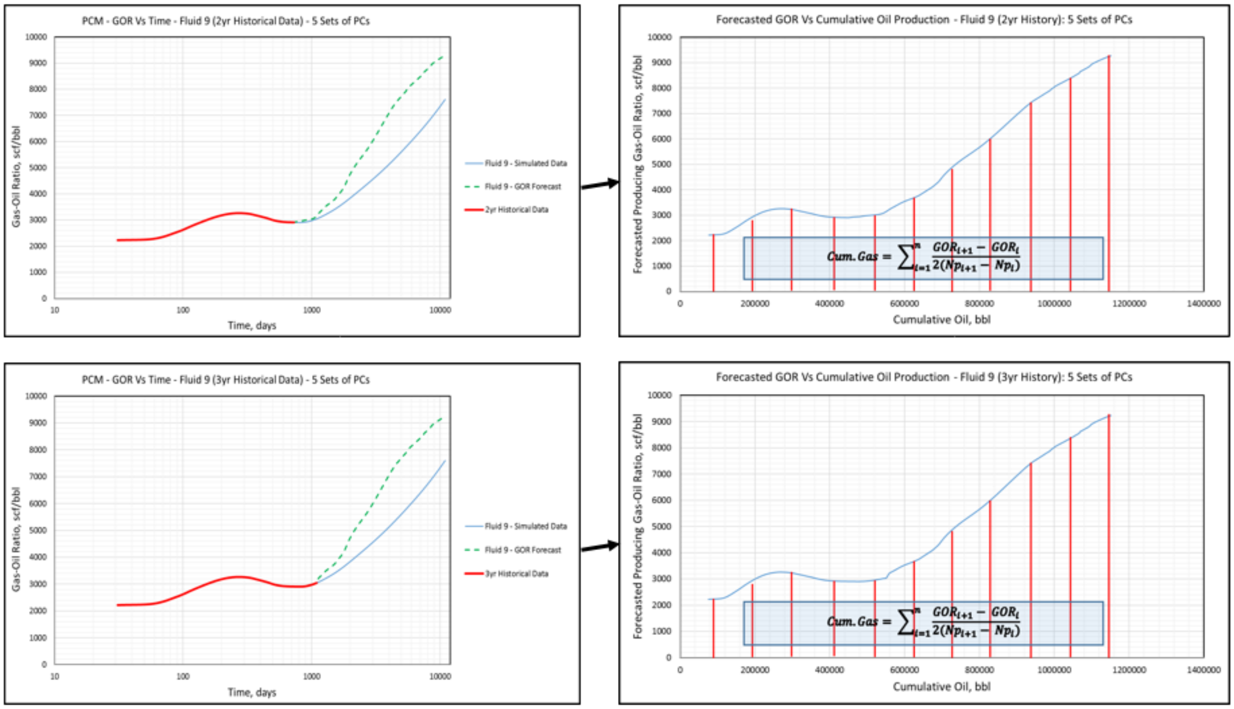

Figure 5-162 GOR Forecasts & Forecasted GOR vs. Cum. Oil – Fluid 9 (2yrs. and 3yrs. Histories): 5 Sets of PCs

Table 5-72 shows the results for all Fluid 9 cases. In all these cases, forecasts were reasonable and errors in the calculated solution gas produced (after 30 yrs) in most cases were relatively low. Percentage error was as low as 1.8% when the first set of PCs were used to forecast. The figures in red indicate the lowest percentage errors for each case.

Table 5-72 Solution Gas Production Forecasts, Errors and Percentage Errors – Fluid 9

FLUID 9 RESULTS																				
Principal Components (PCs)	1 Set of PCs				2 Sets of PCs				3 Sets of PCs				4 Sets of PCs				5 Sets of PCs			
Historical Data	0.5yr	1yr	2yrs	3yrs	0.5yr	1yr	2yrs	3yrs	0.5yr	1yr	2yrs	3yrs	0.5yr	1yr	2yrs	3yrs	0.5yr	1yr	2yrs	3yrs
Simulated Cum. Gas, bscf	4.5	4.5	4.5	4.5	4.5	4.5	4.5	4.5	4.5	4.5	4.5	4.5	4.5	4.5	4.5	4.5	4.5	4.5	4.5	4.5
PCM Forecast, bscf	4.4	4.7	4.9	4.9	4.7	4.8	4.8	4.8	4.7	4.9	5.0	5.0	5.2	5.2	5.1	5.1	5.2	5.3	5.2	5.1
Error (absolute value), bscf	-0.1	0.2	0.4	0.4	0.2	0.3	0.3	0.3	0.2	0.4	0.5	0.5	0.7	0.7	0.6	0.6	0.7	0.8	0.7	0.6
Percentage Error, %	-1.8	5.2	9.2	8.3	4.4	6.4	6.8	7.2	3.7	9.1	11.5	11.4	15.7	15.5	14.2	13.7	15.7	17.0	14.5	14.0

5.2.3.1.10. Fluid 10 Cases

Graphical displays of GOR forecasts and the plots of the estimated GOR forecasts versus cumulative oil production for Fluid 10 are shown in Figures 5-163 to 5-172.

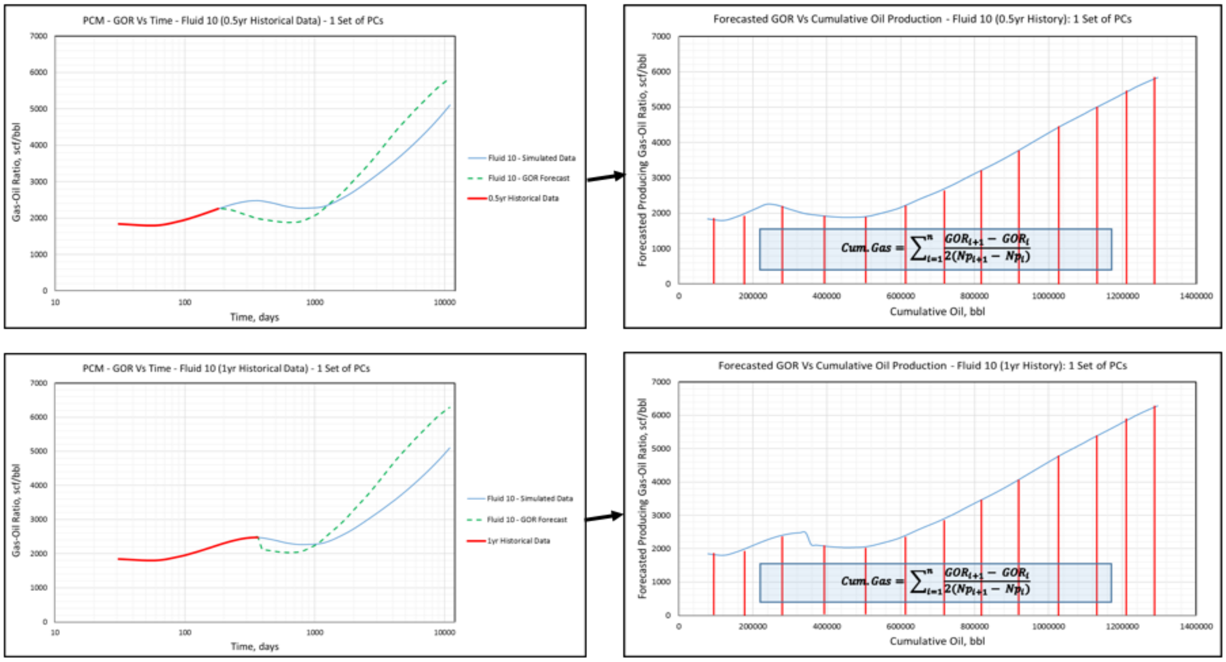

Figure 5-163 GOR Forecasts & Forecasted GOR vs. Cum. Oil – Fluid 10 (0.5yr. and 1yr. Histories): 1 Set of PCs

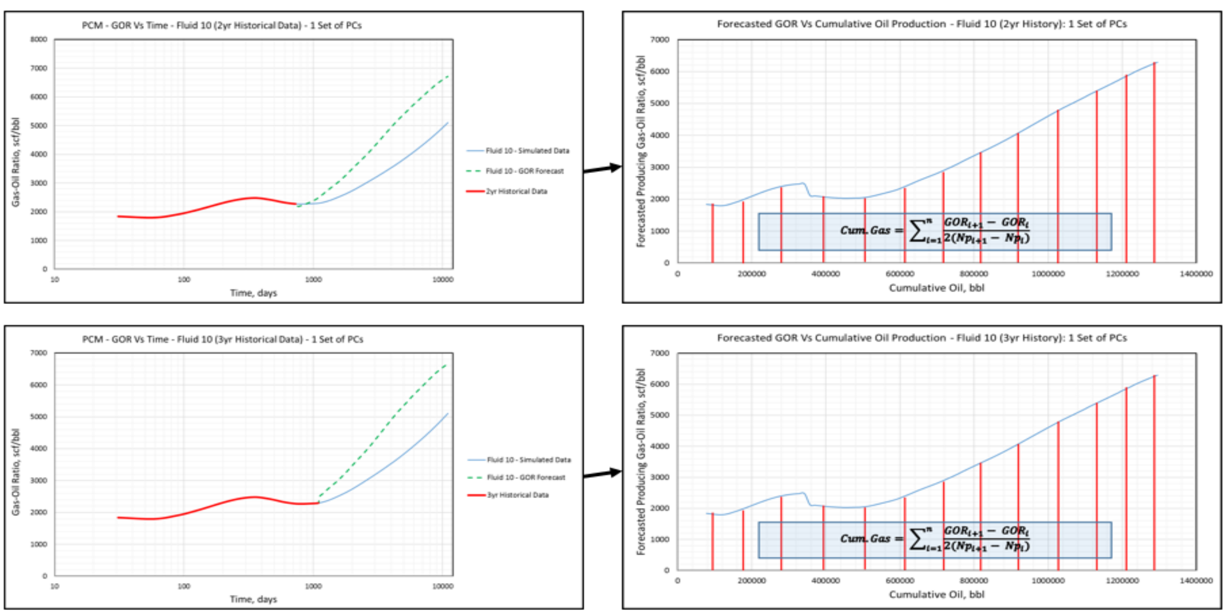

Figure 5-164 GOR Forecasts & Forecasted GOR vs. Cum. Oil – Fluid 10 (2yrs. and 3yrs. Histories): 1 Set of PCs

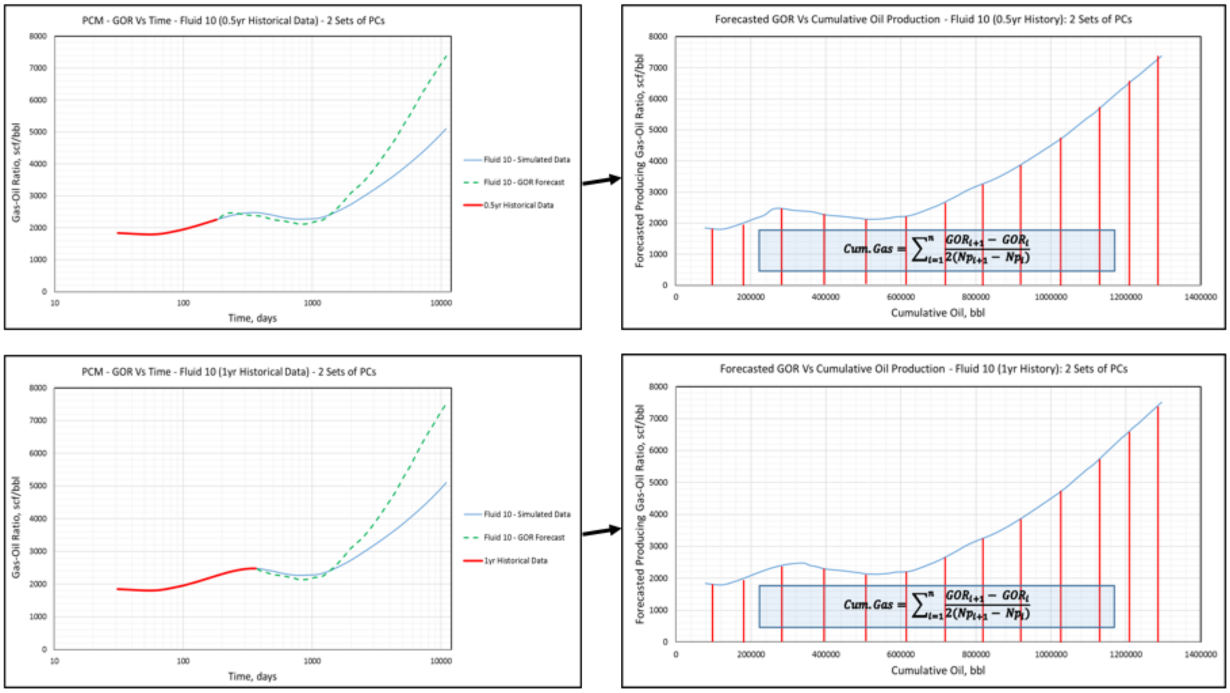

Figure 5-165 GOR Forecasts & Forecasted GOR vs. Cum. Oil – Fluid 10 (0.5yr. and 1yr. Histories): 2 Sets of PCs

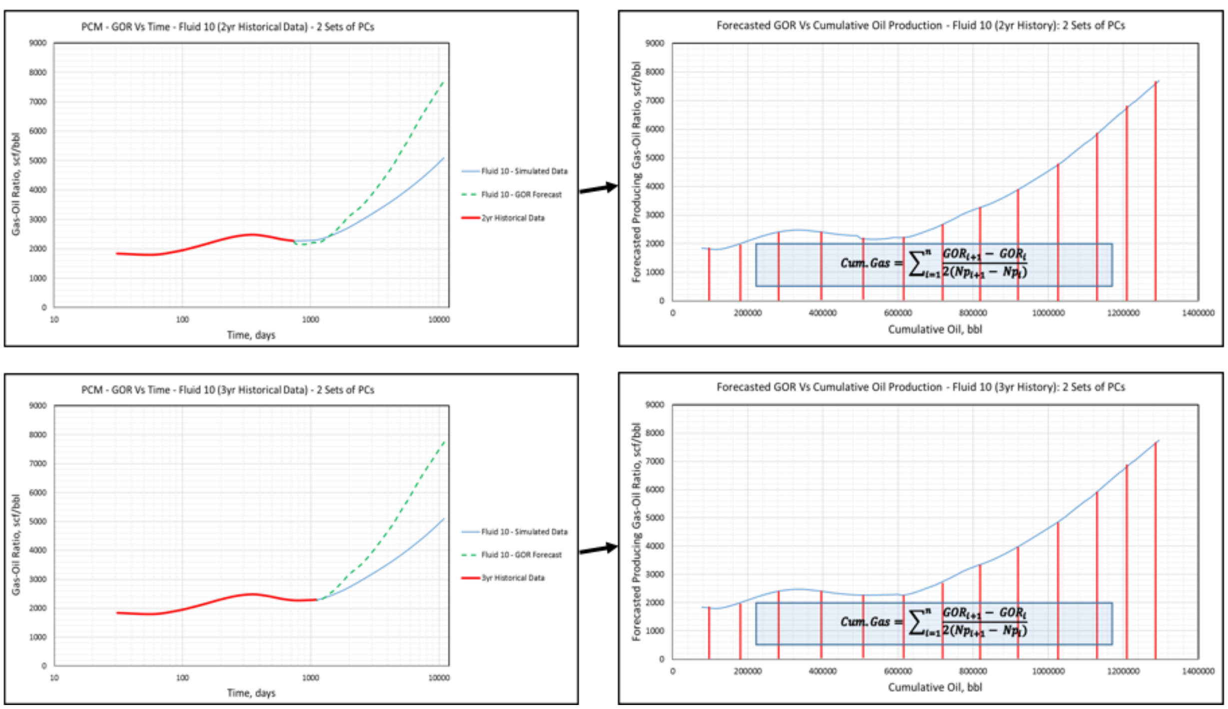

Figure 5-166 GOR Forecasts & Forecasted GOR vs. Cum. Oil – Fluid 10 (2yrs. and 3yrs. Histories): 2 Sets of PCs

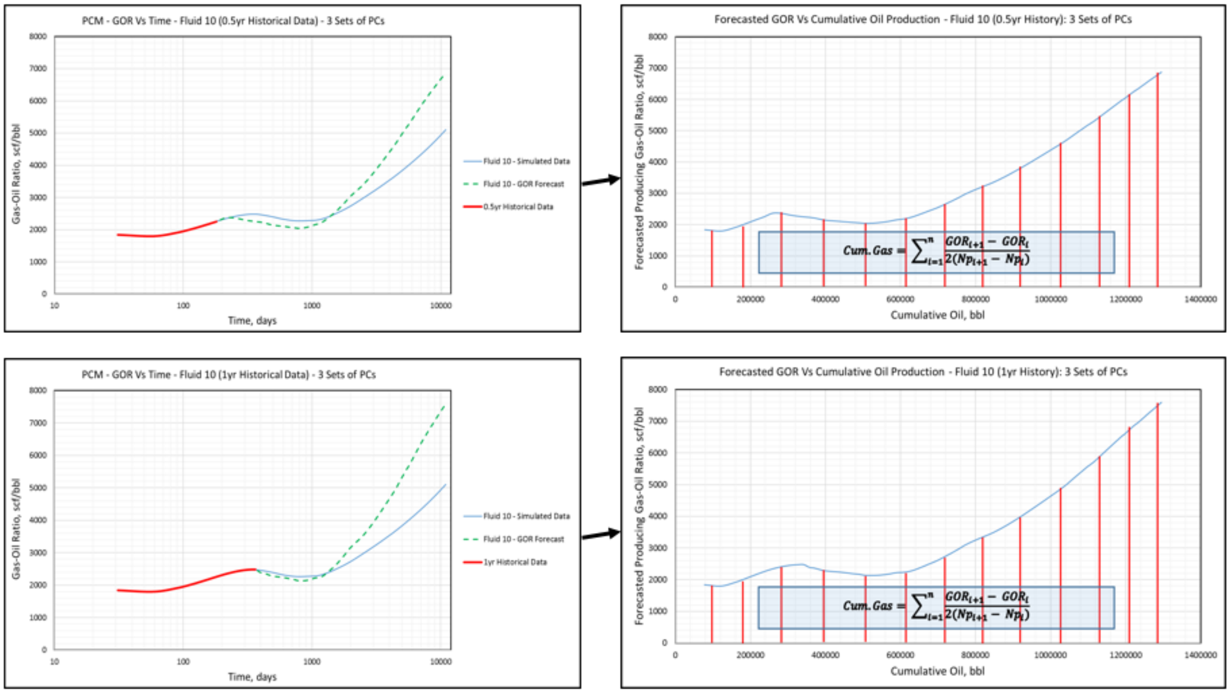

Figure 5-167 GOR Forecasts & Forecasted GOR vs. Cum. Oil – Fluid 10 (0.5yr. and 1yr. Histories): 3 Sets of PCs

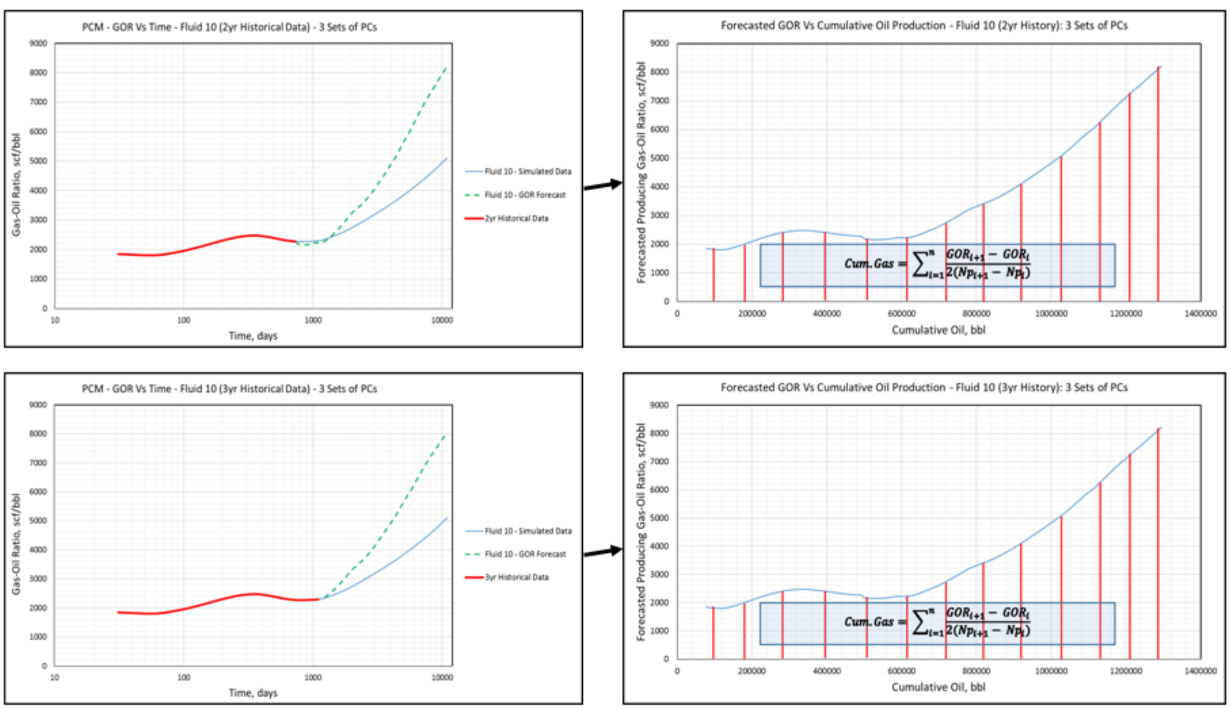

Figure 5-168 GOR Forecasts & Forecasted GOR vs. Cum. Oil – Fluid 10 (2yrs. and 3yrs. Histories): 3 Sets of PCs

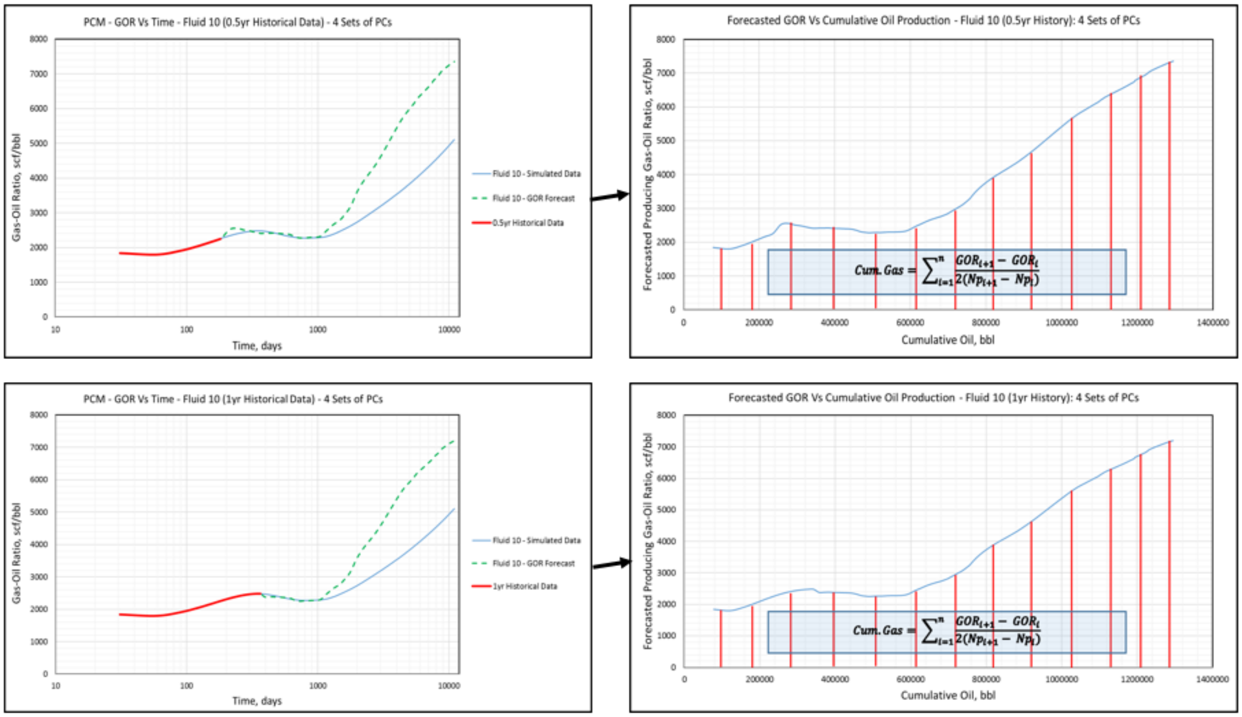

Figure 5-169 GOR Forecasts & Forecasted GOR vs. Cum. Oil – Fluid 10 (0.5yr. and 1yr. Histories): 4 Sets of PCs

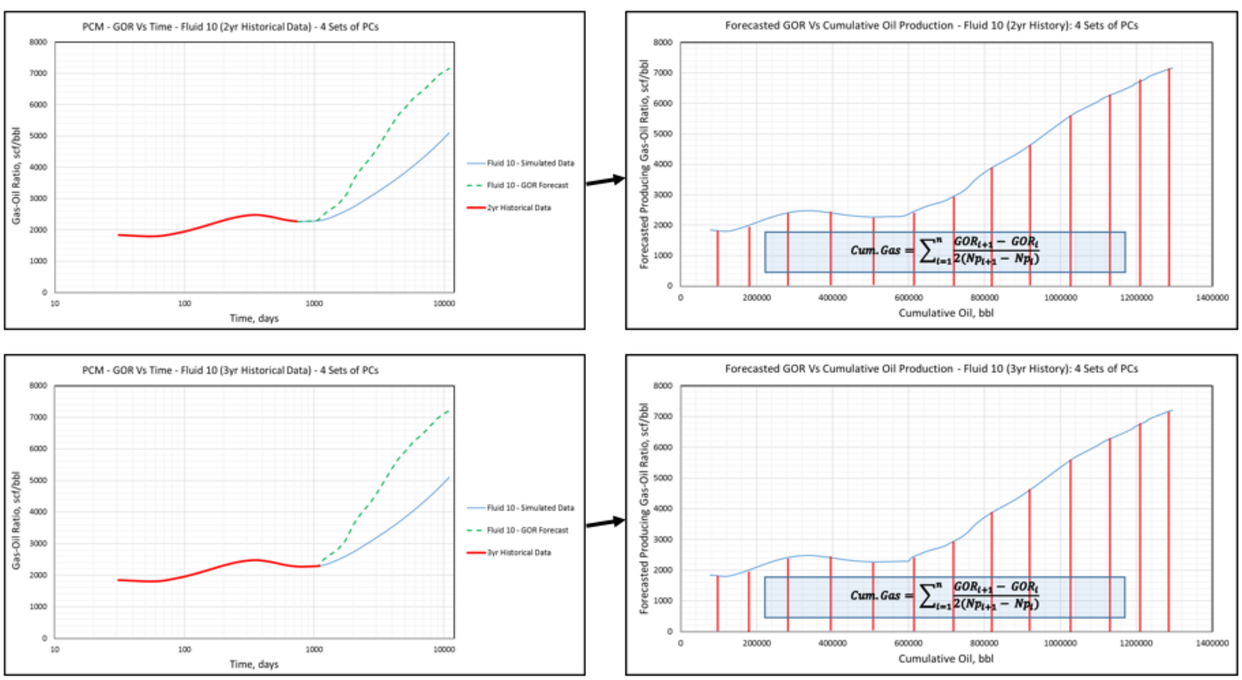

Figure 5-170 GOR Forecasts & Forecasted GOR vs. Cum. Oil – Fluid 10 (2yrs. and 3yrs. Histories): 4 Sets of PCs

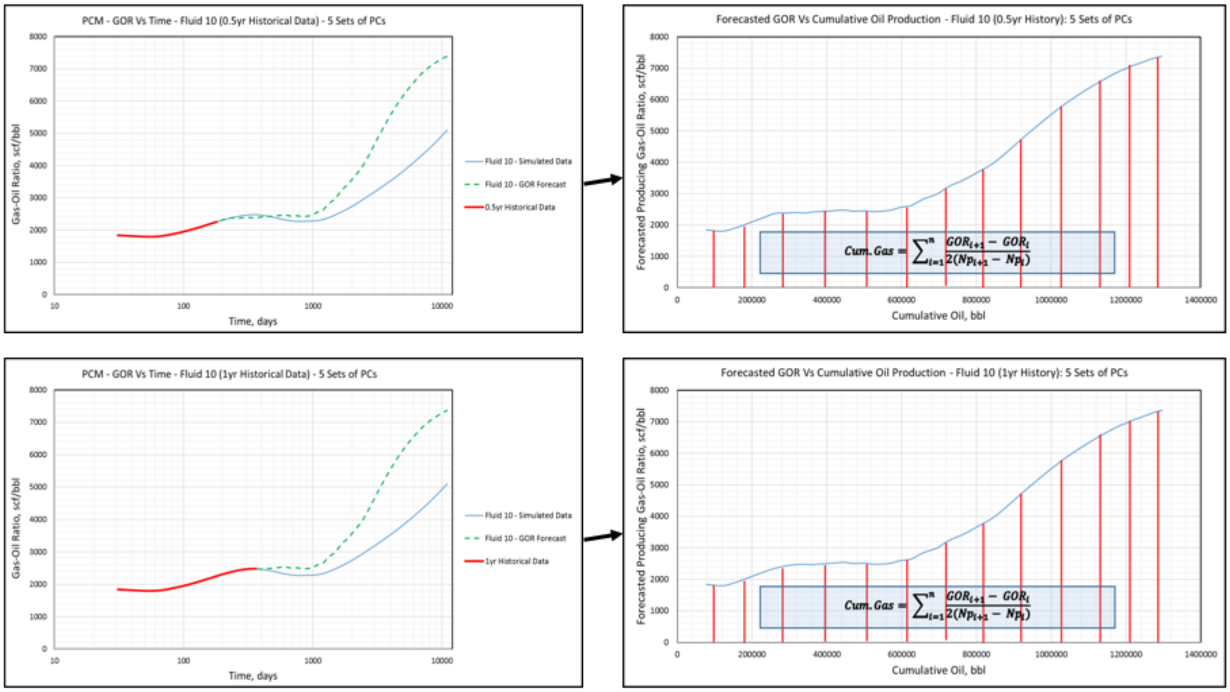

Figure 5-171 GOR Forecasts & Forecasted GOR vs. Cum. Oil – Fluid 10 (0.5yr. and 1yr. Histories): 5 Sets of PCs

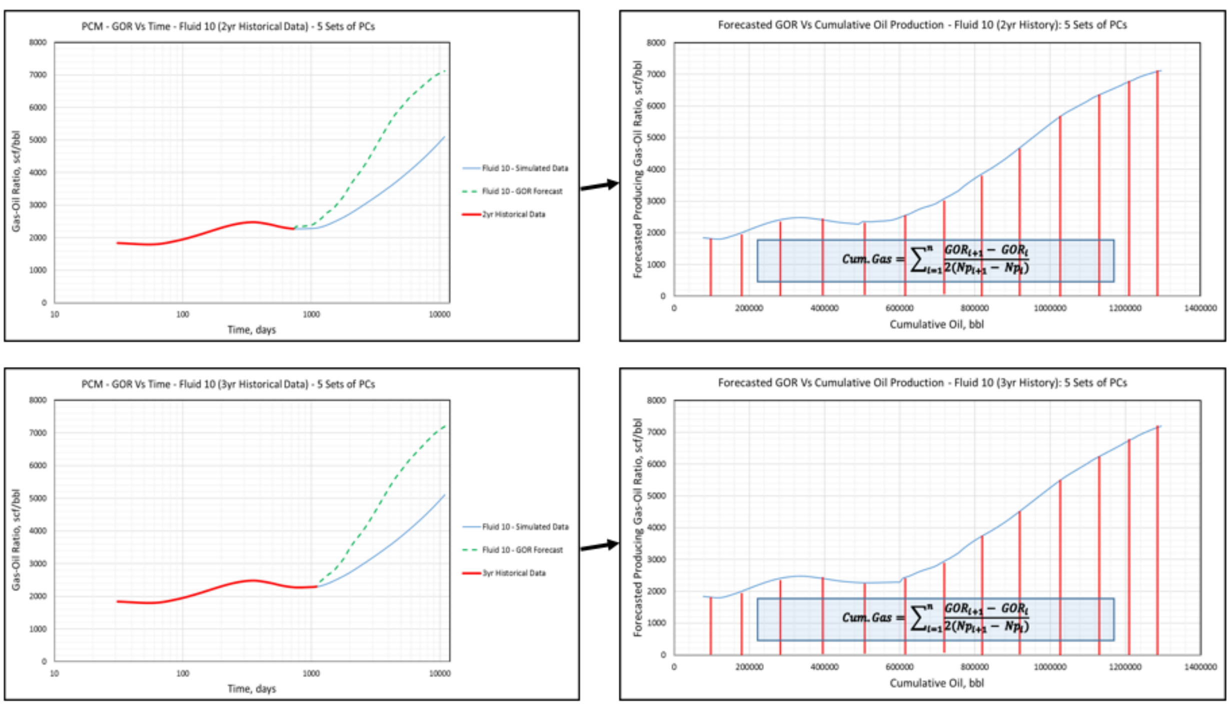

Figure 5-172 GOR Forecasts & Forecasted GOR vs. Cum. Oil – Fluid 10 (2yrs. and 3yrs. Histories): 5 Sets of PCs

Table 5-73 shows the results for all Fluid 10 cases. In all these cases, forecasts were reasonable and errors in the calculated solution gas produced (after 30 yrs) in most cases were relatively low. Percentage error was as low as 2.6% when the first set of PCs were used to forecast. The figures in red indicate the lowest percentage errors for each case.

Table 5-73 Solution Gas Production Forecasts, Errors and Percentage Errors – Fluid 10

FLUID 10 RESULTS																				
Principal Components (PCs)	1 Set of PCs				2 Sets of PCs				3 Sets of PCs				4 Sets of PCs				5 Sets of PCs			
Historical Data	0.5yr	1yr	2yrs	3yrs	0.5yr	1yr	2yrs	3yrs	0.5yr	1yr	2yrs	3yrs	0.5yr	1yr	2yrs	3yrs	0.5yr	1yr	2yrs	3yrs
Simulated Cum. Gas, bscf	3.7	3.7	3.7	3.7	3.7	3.7	3.7	3.7	3.7	3.7	3.7	3.7	3.7	3.7	3.7	3.7	3.7	3.7	3.7	3.7
PCM Forecast, bscf	3.8	4.1	4.4	4.3	4.2	4.2	4.2	4.3	4.0	4.3	4.4	4.4	4.6	4.5	4.5	4.5	4.7	4.7	4.6	4.5
Error (absolute value), bscf	0.1	0.4	0.7	0.6	0.5	0.5	0.5	0.6	0.3	0.6	0.7	0.7	0.9	0.8	0.8	0.8	1.0	1.0	0.9	0.8
Percentage Error, %	2.6	10.3	17.3	16.5	12.2	12.7	14.0	15.8	8.5	14.6	18.9	19.8	23.8	22.3	22.2	22.1	25.9	26.4	23.5	21.2

Next, we calculated PCs from wells with similar operating conditions in reservoirs with similar characteristics and similar (or approximately similar) reservoir fluid types. We calculated PCs from wells with moderately volatile oils and separately from wells with highly volatile oils. Figure 5-173 shows a graph of these principal components compared to PCs obtained from wells with varying conditions (tagged "All Cases").

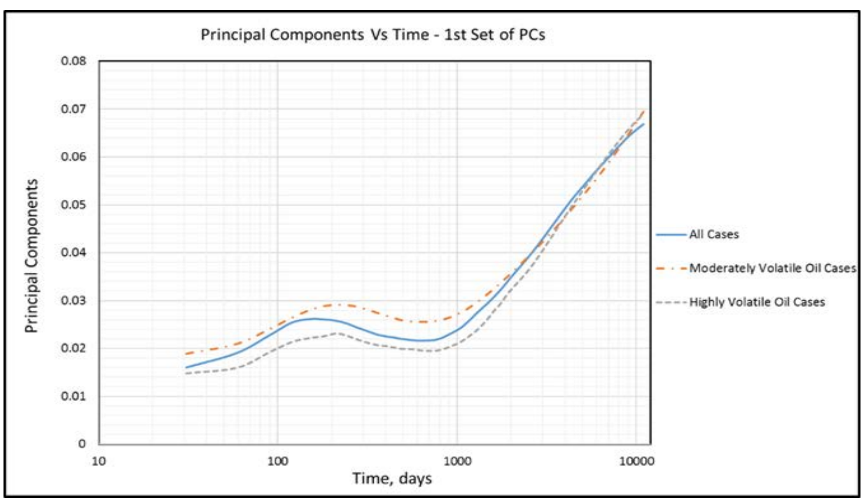

Figure 5-173 Principal Components vs. Time – 1st Set of PCs

5.2.3.2. Results (2)

Results for all the fluids are shown in the following subsections. GOR forecasts (1) are estimates obtained with the use of PCs calculated from several wells with varying conditions, whereas GOR forecasts (2) are estimates obtained using PCs calculated from several wells with similar (or nearly similar) conditions.

5.2.3.2.1. Fluid 1 Cases

The following sets of graphs show the results of cases for Fluid 1.

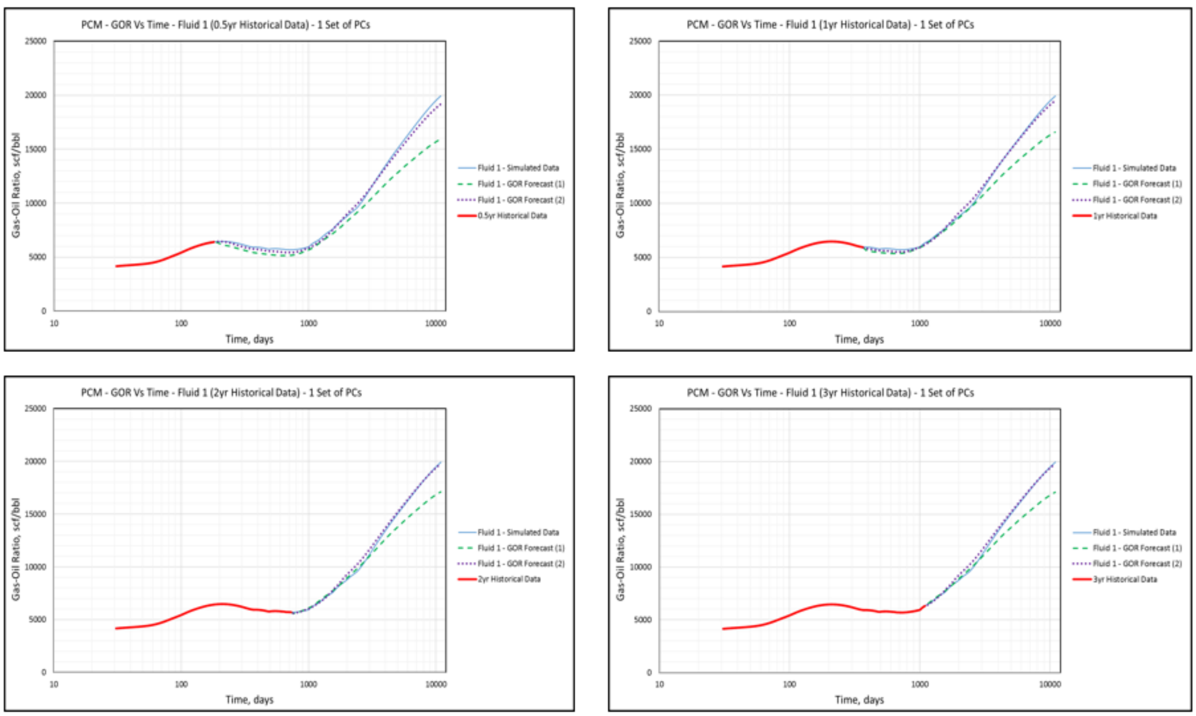

Figure 5-174 GOR Forecasts (1) and (2) for Fluid 1 – 1st Set of PCs

Forecasts are reasonably accurate in all these cases and the first set of PCs are enough to provide good estimates. The results can be seen in Figure 5-174. Calculated solution gas production after 30 yrs for forecasts (2) had a percentage error as low as approximately 3.9%. Table 5-74 displays the PCM forecasts, errors and percentage errors for Fluid 1 cases. The red figures indicate the lower of the two percentage errors for each case.

Table 5-74 Errors and % Errors: Solution Gas Production Forecasts (1) and (2) – Fluid 1

FLUID 1 RESULTS				
Principal Components (PCs)	1 Set of PCs (Primary PCs)			
Historical Data	0.5yr	1yr	2yrs	3yrs
Simulated Cum. Gas, bscf	6.88	6.88	6.88	6.88
PCM Forecast (1), bscf	5.91	6.15	6.32	6.32
Error (1) (absolute value), bscf	-0.97	-0.73	-0.56	-0.56
Percentage Error (1), %	-14.14	-10.69	-8.18	-8.24
PCM Forecast (2), bscf	6.43	6.52	6.61	6.62
Error (2) (absolute value), bscf	-0.45	-0.36	-0.27	-0.26
Percentage Error (2), %	-6.58	-5.31	-3.98	-3.86

5.2.3.2.2. Fluid 2 Cases

The following sets of graphs show the results of cases for Fluid 2.

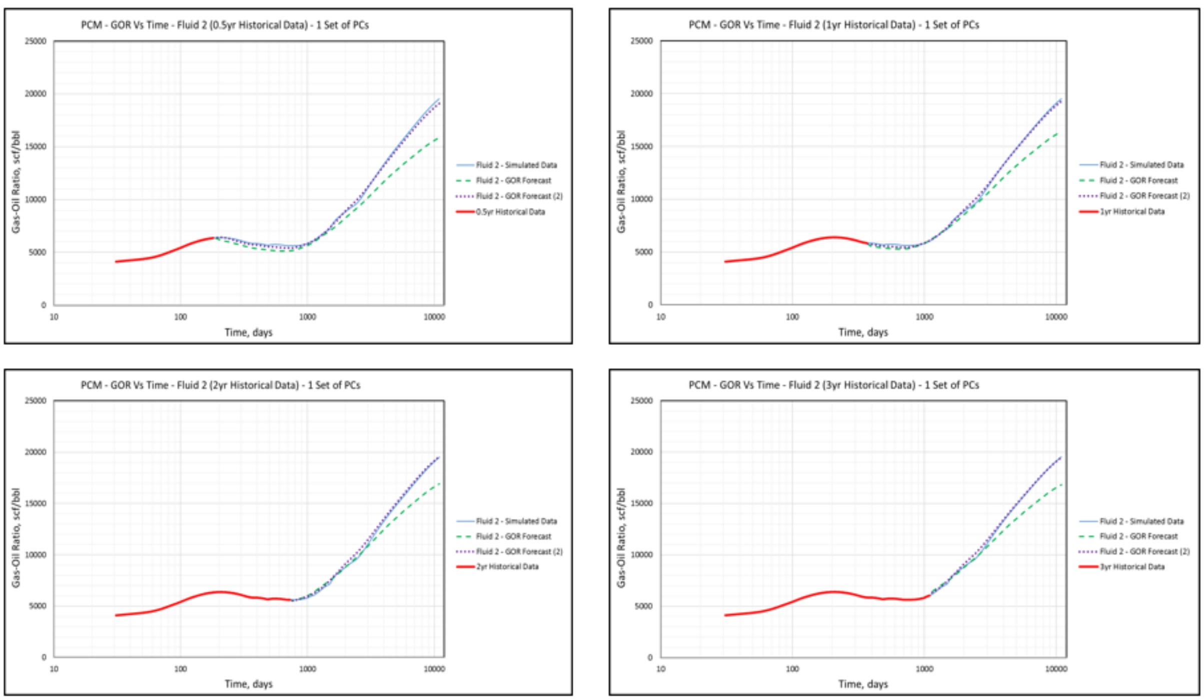

Figure 5-175 GOR Forecasts (1) and (2) for Fluid 2 – 1st Set of PCs

Forecasts are reasonably accurate in all these cases and the first set of PCs are enough to provide good estimates. The results can be seen in Figure 5-175. Calculated solution gas production after 30 yrs for forecasts (2) had a percentage error as low as approximately 3.8%. Table 5-75 displays the PCM forecasts, errors and percentage errors for Fluid 2 cases. The red figures indicate the lower of the two percentage errors for each case.

Table 5-75 Errors and % Errors: Solution Gas Production Forecasts (1) and (2) – Fluid 2

FLUID 2 RESULTS				
Principal Components (PCs)	1 Set of PCs (Primary PCs)			
Historical Data	0.5yr	1yr	2yrs	3yrs
Simulated Cum. Gas, bscf	6.90	6.90	6.90	6.90
PCM Forecast (1), bscf	5.97	6.18	6.35	6.32
Error (1) (absolute value), bscf	-0.93	-0.72	-0.55	-0.58
Percentage Error (1), %	-13.45	-10.40	-7.95	-8.40
PCM Forecast (2), bscf	6.49	6.55	6.64	6.62
Error (2) (absolute value), bscf	-0.41	-0.35	-0.26	-0.28
Percentage Error (2), %	-5.84	-5.02	-3.76	-4.03

5.2.3.2.3. Fluid 3 Cases

The following sets of graphs show the results of cases for Fluid 3.

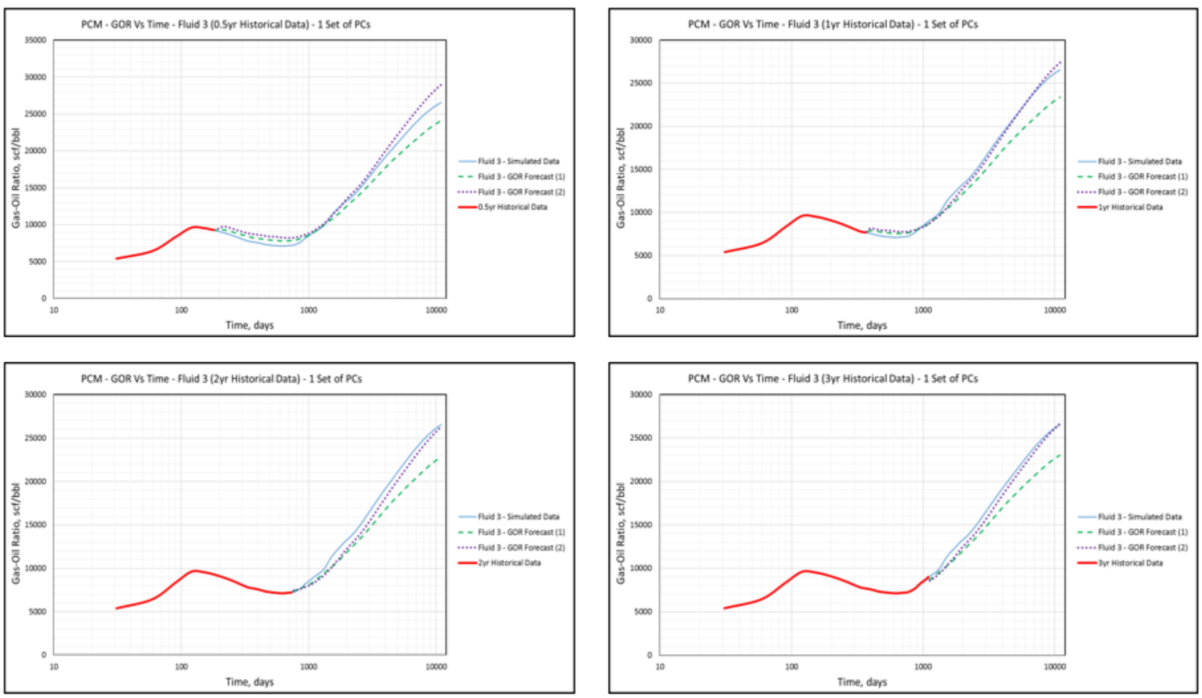

Figure 5-176 GOR Forecasts (1) and (2) for Fluid 3 – 1st Set of PCs

Forecasts are reasonably accurate in all these cases and the first set of PCs are enough to provide good estimates. The results can be seen in Figure 5-176. Calculated solution gas production after 30 yrs for forecasts (2) had a percentage error as low as approximately 0.3%. Table 5-76 displays the PCM forecasts, errors and percentage errors for Fluid 3 cases. The red figures indicate the lower of the two percentage errors for each case.

Table 5-76 Errors and % Errors: Solution Gas Production Forecasts (1) and (2) – Fluid 3

FLUID 3 RESULTS				
Principal Components (PCs)	1 Set of PCs (Primary PCs)			
Historical Data	0.5yr	1yr	2yrs	3yrs
Simulated Cum. Gas, bscf	7.67	7.67	7.67	7.67
PCM Forecast (1), bscf	7.10	6.90	6.74	6.78
Error (1) (absolute value), bscf	-0.57	-0.77	-0.93	-0.89
Percentage Error (1), %	-7.39	-10.01	-12.10	-11.54
PCM Forecast (2), bscf	7.69	7.27	7.01	7.07
Error (2) (absolute value), bscf	0.02	-0.40	-0.66	-0.60
Percentage Error (2), %	+0.28	-5.13	-8.59	-7.78

5.2.3.2.4. Fluid 4 Cases

The following sets of graphs show the results of cases for Fluid 4.

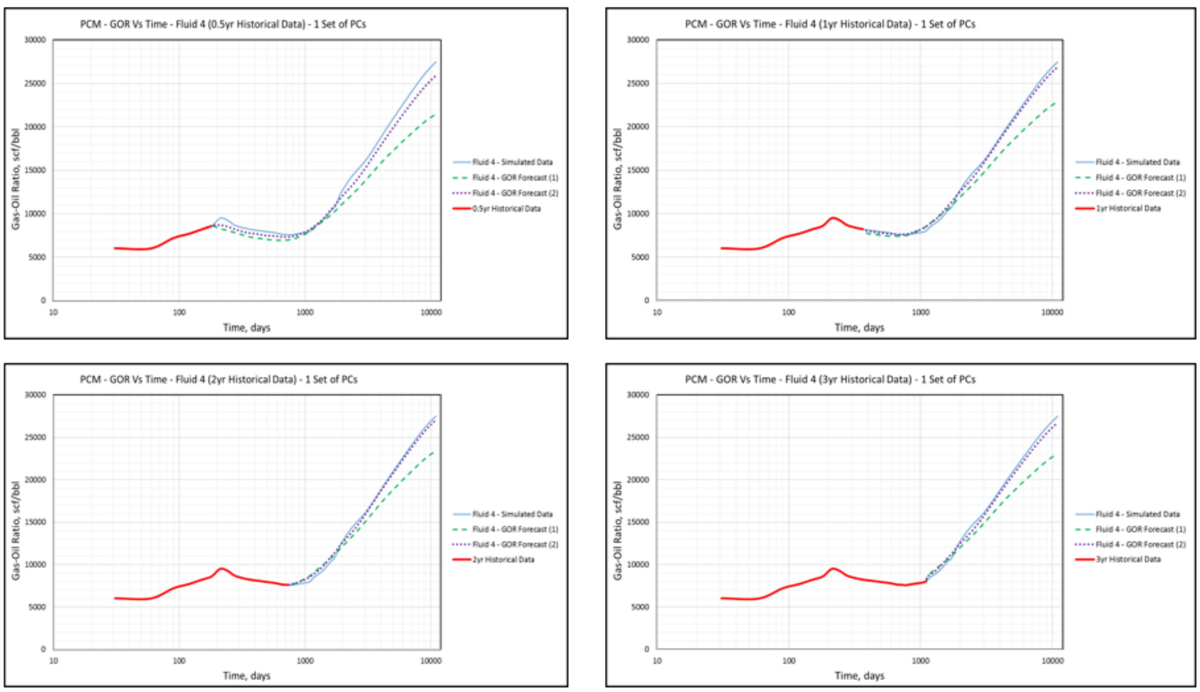

Figure 5-177 GOR Forecasts (1) and (2) for Fluid 4 – 1st Set of PCs

Forecasts are reasonably accurate in all these cases and the first set of PCs are enough to provide good estimates. The results can be seen in Figure 5-177. Calculated solution gas production after 30 yrs for forecasts (2) had a percentage error as low as approximately 4.8%. Table 5-77 displays the PCM forecasts, errors and percentage errors for Fluid 4 cases. The red figures indicate the lower of the two percentage errors for each case.

Table 5-77 Errors and % Errors: Solution Gas Production Forecasts (1) and (2) – Fluid 4

FLUID 4 RESULTS				
Principal Components (PCs)	1 Set of PCs (Primary PCs)			
Historical Data	0.5yr	1yr	2yrs	3yrs
Simulated Cum. Gas, bscf	7.52	7.52	7.52	7.52
PCM Forecast (1), bscf	6.34	6.74	6.87	6.79
Error (1) (absolute value), bscf	-1.18	-0.78	-0.65	-0.73
Percentage Error (1), %	-15.70	-10.39	-8.58	-9.71
PCM Forecast (2), bscf	6.86	7.11	7.16	7.08
Error (2) (absolute value), bscf	-0.66	-0.41	-0.36	-0.44
Percentage Error (2), %	-8.68	-5.34	-4.80	-5.80

5.2.3.2.5. Fluid 5 Cases

The following sets of graphs show the results of cases for Fluid 5.

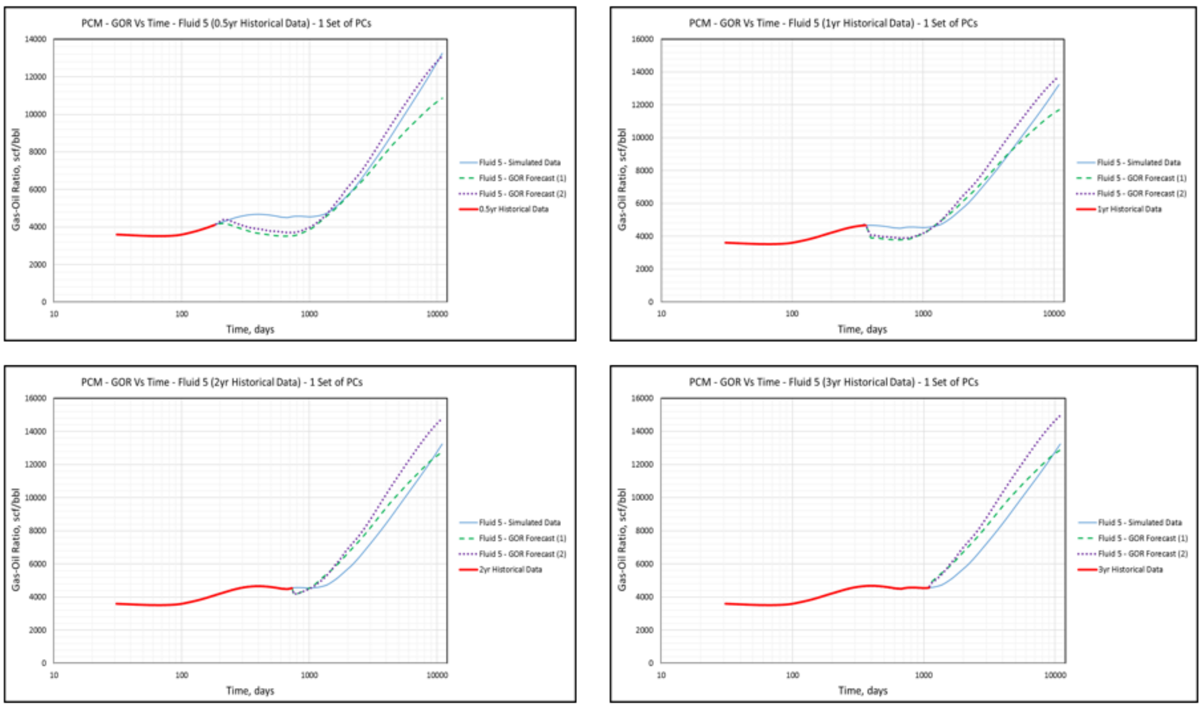

Figure 5-178 GOR Forecasts (1) and (2) for Fluid 5 – 1st Set of PCs

Forecasts are reasonably accurate in all these cases and the first set of PCs are enough to provide good estimates. The results can be seen in Figure 5-178. Calculated solution gas production after 30 yrs for forecasts (2) had a percentage error as low as approximately 1.6%. Table 5-78 displays the PCM forecasts, errors and percentage errors for Fluid 5 cases. The red figures indicate the lower of the two percentage errors for each case.

Table 5-78 Errors and % Errors: Solution Gas Production Forecasts (1) and (2) – Fluid 5

FLUID 5 RESULTS				
Principal Components (PCs)	1 Set of PCs (Primary PCs)			
Historical Data	0.5yr	1yr	2yrs	3yrs
Simulated Cum. Gas, bscf	5.66	5.66	5.66	5.66
PCM Forecast (1), bscf	4.88	5.23	5.67	5.72
Error (1) (absolute value), bscf	-0.78	-0.43	+0.01	+0.06
Percentage Error (1), %	-13.88	-7.62	+0.17	+1.04
PCM Forecast (2), bscf	5.33	5.57	5.96	6.02
Error (2) (absolute value), bscf	-0.33	-0.09	+0.30	+0.36
Percentage Error (2), %	-5.85	-1.58	+5.27	+6.35

5.2.3.2.6. Fluid 6 Cases

The following sets of graphs show the results of cases for Fluid 6.

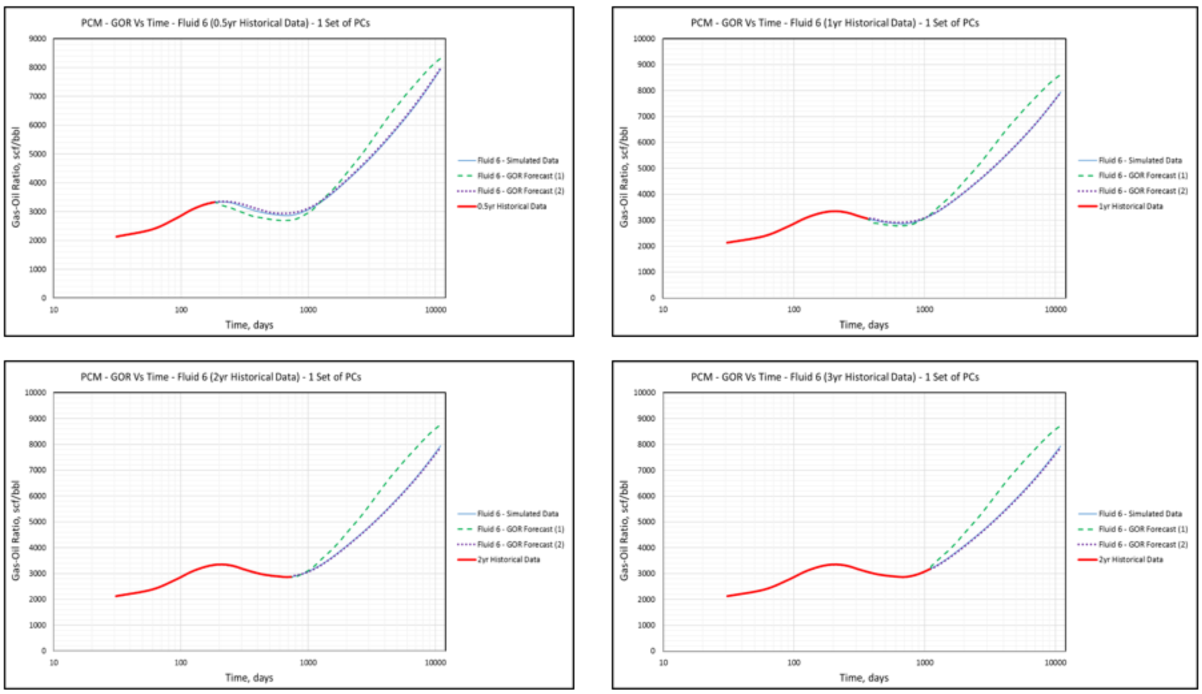

Figure 5-179 GOR Forecasts (1) and (2) for Fluid 6 – 1st Set of PCs

Forecasts are reasonably accurate in all these cases and the first set of PCs are enough to provide good estimates. The results can be seen in Figure 5-179. Calculated solution gas production after 30 yrs for forecasts (2) had a percentage error as low as approximately 3.3%. Table 5-79 displays the PCM forecasts, errors and percentage errors for Fluid 6 cases. The red figures indicate the lower of the two percentage errors for each case.

Table 5-79 Errors and % Errors: Solution Gas Production Forecasts (1) and (2) – Fluid 6

FLUID 6 RESULTS				
Principal Components (PCs)	1 Set of PCs (Primary PCs)			
Historical Data	0.5yr	1yr	2yrs	3yrs
Simulated Cum. Gas, bscf	4.76	4.76	4.76	4.76
PCM Forecast (1), bscf	4.79	4.95	5.02	5.01
Error (1) (absolute value), bscf	+0.03	+0.19	+0.26	+0.25
Percentage Error (1), %	+0.62	+3.97	+5.49	+5.32
PCM Forecast (2), bscf	4.60	4.56	4.54	4.54
Error (2) (absolute value), bscf	-0.16	-0.20	-0.22	-0.22
Percentage Error (2), %	-3.25	-4.06	-4.59	-4.64

5.2.3.2.7. Fluid 7 Cases

The following sets of graphs show the results of cases for Fluid 7.

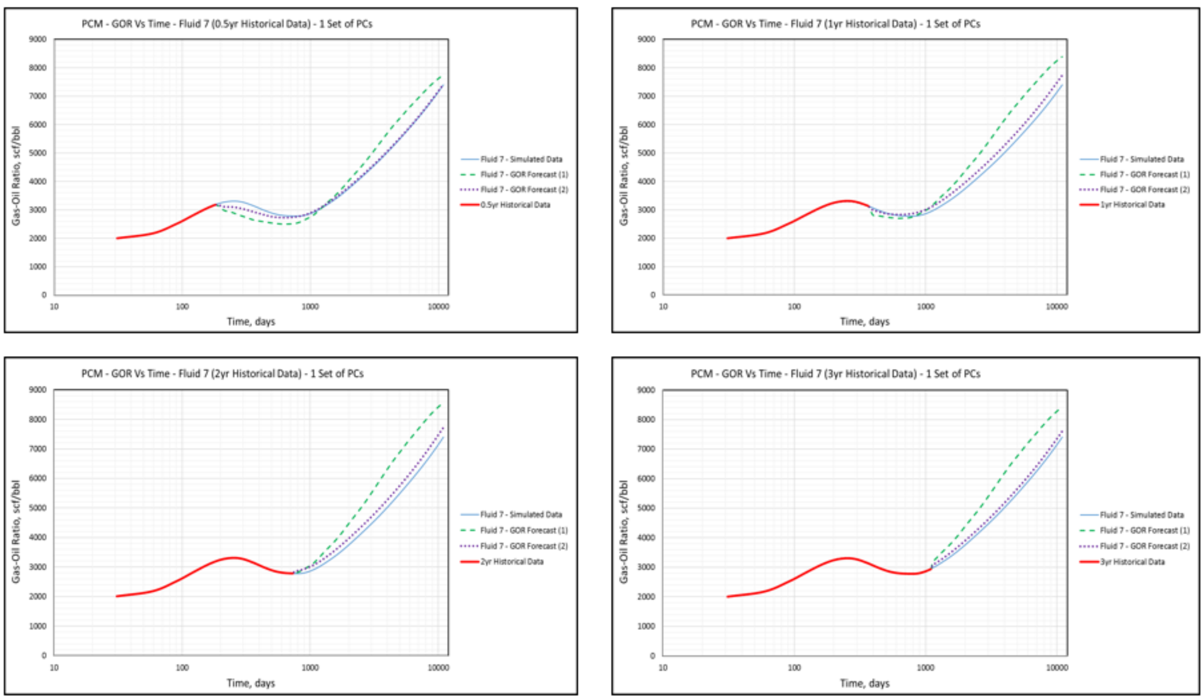

Figure 5-180 GOR Forecasts (1) and (2) for Fluid 7 – 1st Set of PCs

Forecasts are reasonably accurate in all these cases and the first set of PCs are enough to provide good estimates. The results can be seen in Figure 5-180. Calculated solution gas production after 30 yrs for forecasts (2) had a percentage error as low as approximately 0.4%. Table 5-80 displays the PCM forecasts, errors and percentage errors for Fluid 7 cases. The red figures indicate the lower of the two percentage errors for each case.

Table 5-80 Errors and % Errors: Solution Gas Production Forecasts (1) and (2) – Fluid 7

FLUID 7 RESULTS				
Principal Components (PCs)	1 Set of PCs (Primary PCs)			
Historical Data	0.5yr	1yr	2yrs	3yrs
Simulated Cum. Gas, bscf	4.42	4.42	4.42	4.42
PCM Forecast (1), bscf	4.42	4.78	4.87	4.80
Error (1) (absolute value), bscf	0.00	+0.36	+0.45	+0.38
Percentage Error (1), %	+0.17	+8.10	+10.29	+8.77
PCM Forecast (2), bscf	4.24	4.40	4.39	4.34
Error (2) (absolute value), bscf	-0.18	-0.02	-0.03	-0.08
Percentage Error (2), %	-3.96	-0.41	-0.51	-1.78

5.2.3.2.8. Fluid 8 Cases

The following sets of graphs show the results of cases for Fluid 8.

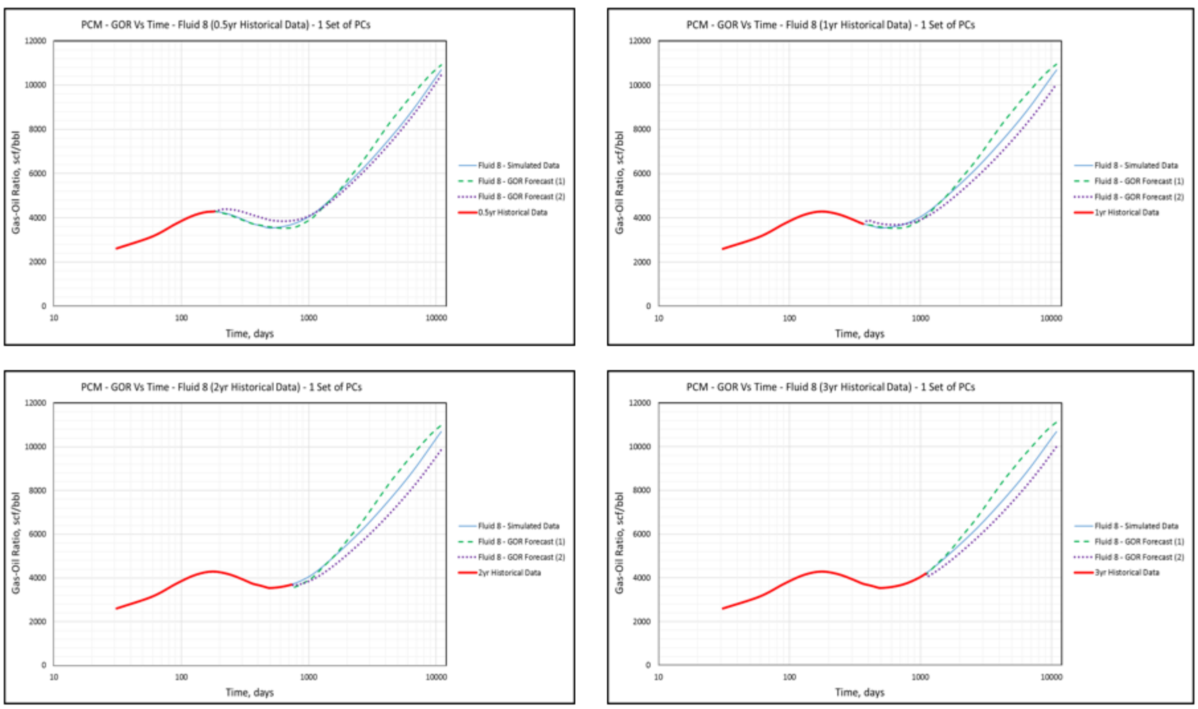

Figure 5-181 GOR Forecasts (1) and (2) for Fluid 8 – 1st Set of PCs

Forecasts are reasonably accurate in all these cases and the first set of PCs are enough to provide good estimates. The results can be seen in Figure 5-181. Calculated solution gas production after 30 yrs for forecasts (2) had a percentage error as low as approximately 4.8%. Table 5-81 displays the PCM forecasts, errors and percentage errors for Fluid 8 cases. The red figures indicate the lower of the two percentage errors for each case.

Table 5-81 Errors and % Errors: Solution Gas Production Forecasts (1) and (2) – Fluid 8

FLUID 8 RESULTS				
Principal Components (PCs)	1 Set of PCs (Primary PCs)			
Historical Data	0.5yr	1yr	2yrs	3yrs
Simulated Cum. Gas, bscf	5.46	5.46	5.46	5.46
PCM Forecast (1), bscf	5.40	5.43	5.44	5.50
Error (1) (absolute value), bscf	-0.06	-0.03	-0.02	+0.04
Percentage Error (1), %	-1.11	-0.67	-0.38	+0.74
PCM Forecast (2), bscf	5.20	5.01	4.93	4.99
Error (2) (absolute value), bscf	-0.26	-0.45	-0.53	-0.47
Percentage Error (2), %	-4.79	-8.28	-9.79	-8.67

5.2.3.2.9. Fluid 9 Cases

The following sets of graphs show the results of cases for Fluid 9.

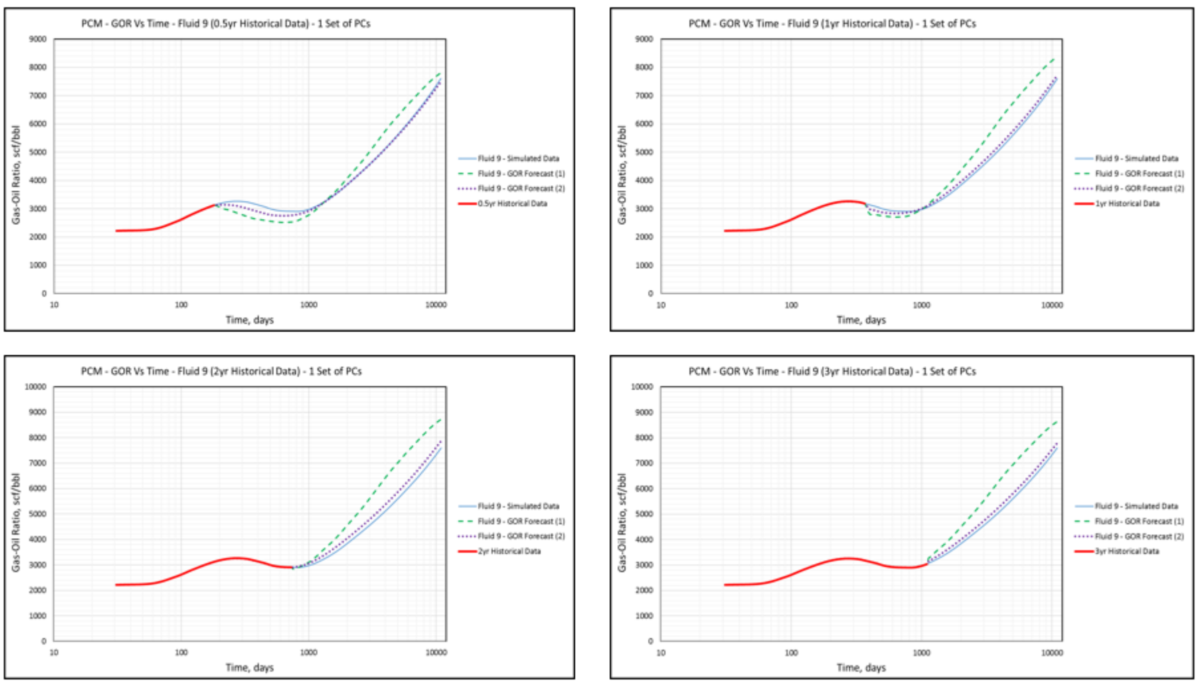

Figure 5-182 GOR Forecasts (1) and (2) for Fluid 9 – 1st Set of PCs

Forecasts are reasonably accurate in all these cases and the first set of PCs are enough to provide good estimates. The results can be seen in Figure 5-182. Calculated solution gas production after 30 yrs for forecasts (2) had a percentage error as low as approximately 1.2%. Table 5-82 displays the PCM forecasts, errors and percentage errors for Fluid 9 cases. The red figures indicate the lower of the two percentage errors for each case.

Table 5-82 Errors and % Errors: Solution Gas Production Forecasts (1) and (2) – Fluid 9

FLUID 9 RESULTS				
Principal Components (PCs)	1 Set of PCs (Primary PCs)			
Historical Data	0.5yr	1yr	2yrs	3yrs
Simulated Cum. Gas, bscf	4.50	4.50	4.50	4.50
PCM Forecast (1), bscf	4.42	4.74	4.92	4.88
Error (1) (absolute value), bscf	-0.08	+0.24	+0.42	+0.38
Percentage Error (1), %	-1.80	+5.22	+9.16	+8.33
PCM Forecast (2), bscf	4.25	4.38	4.45	4.42
Error (2) (absolute value), bscf	-0.25	-0.12	-0.05	-0.08
Percentage Error (2), %	-5.52	-2.77	-1.21	-1.88

5.2.3.2.10. Fluid 10 Cases

The following sets of graphs show the results of cases for Fluid 10.

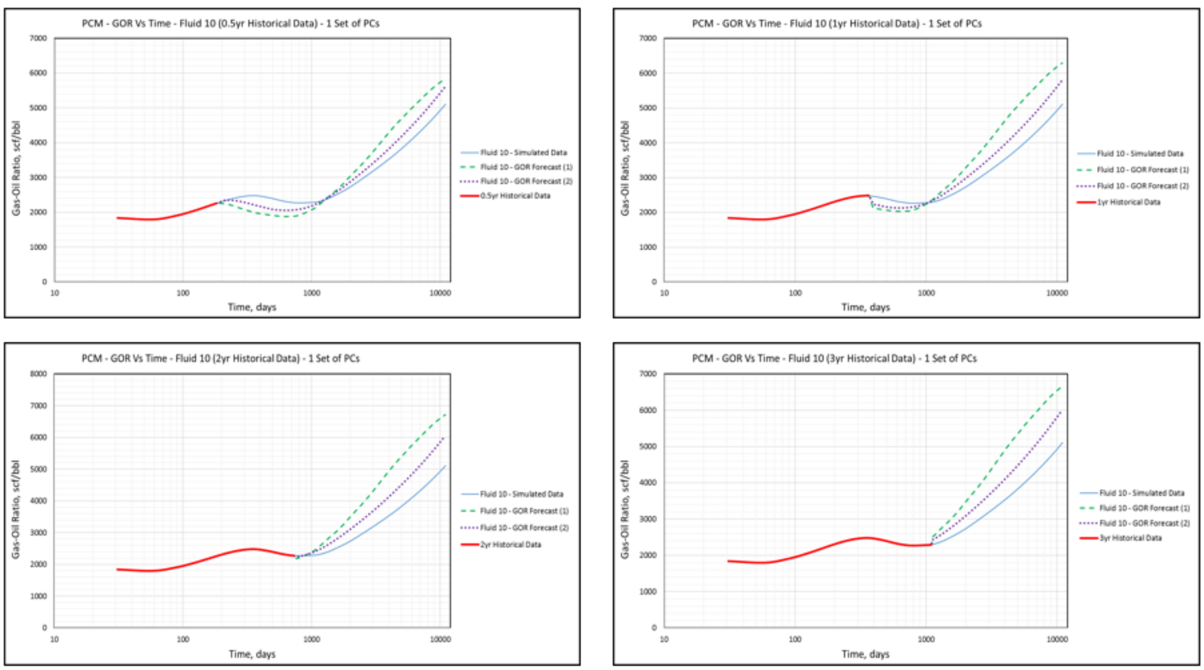

Figure 5-183 GOR Forecasts (1) and (2) for Fluid 10 – 1st Set of PCs

Forecasts are reasonably accurate in all these cases and the first set of PCs are enough to provide good estimates. The results can be seen in Figure 5-183. Calculated solution gas production after 30 yrs for forecasts (2) had a percentage error as low as approximately 1.4%. Table 5-83 displays the PCM forecasts, errors and percentage errors for Fluid 10 cases. The red figures indicate the lower of the two percentage errors for each case.

Table 5-83 Errors and % Errors: Solution Gas Production Forecasts (1) and (2) – Fluid 10

FLUID 10 RESULTS				
Principal Components (PCs)	1 Set of PCs (Primary PCs)			
Historical Data	0.5yr	1yr	2yrs	3yrs
Simulated Cum. Gas, bscf	3.70	3.70	3.70	3.70
PCM Forecast (1), bscf	3.80	4.09	4.35	4.32
Error (1) (absolute value), bscf	+0.10	+0.39	+0.65	+0.62
Percentage Error (1), %	+2.63	+10.30	+17.31	+16.54
PCM Forecast (2), bscf	3.65	3.77	3.93	3.90
Error (2) (absolute value), bscf	-0.05	+0.07	+0.23	+0.20
Percentage Error (2), %	-1.38	+1.78	+6.01	+5.37

When PCs obtained from wells with comparable conditions are used to forecast, there are improvements in producing GOR estimates. Forecasts are reasonably accurate in all cases and the first set of PCs are enough to provide good estimates. In practice, data from a minimum of 4-5 representative wells up to as many wells as possible should be sufficient for establishing PCs to be used in the Principal Components Methodology (PCM). PCM can reasonably forecast future production irrespective of the length of production history available. For field data analyses, history-matching and simulation (for as long as forecast is needed) are necessary steps prior to following the PCM procedure.

5.3. Inferences

1. Hybrid decline curve analysis (DCA) models are better for forecasting production from shale volatile oil reservoirs than traditional DCA models. They provide a much better match to compositionally simulated data in most circumstances than traditional DCA models;
2. When historical data of 2-3 years or more are available, the YM-SEPD hybrid models forecast production reasonably well in most cases. However, with short production history (usually less than 2 years), YM-SEPD and its hybrid models underestimate production;

3. The Modified Duong and its hybrid variants overestimate production in most cases. With sufficient historical data of 2 years or more, the overestimation by the hybrid Modified Duong models are not severe;
4. In most instances, the Modified Duong and its hybrid alternatives perform observably better than the YM-SEPD models for wells with short production history (typically less than 2 years);
5. Principal Components Methodology (PCM) is a simple, easy-to-use method based on pattern recognition and feature extraction;
6. PCM consistently forecasts with reasonable certainty irrespective of the length of production or GOR history available;
7. If principal components (PCs) are obtained from a representative group of wells from the same shale play, exhibiting similar (or nearly similar) characteristics, PCM can forecast with a reasonably high level of accuracy.
8. PCM has the following advantages over empirical and analytical forecasting methods:

- It eliminates the need to determine vital decline curve analysis (DCA) model parameters like the hyperbolic decline exponents (b values);
- Diagnostic plots are not necessary prior to forecasting with PCM;
- It avoids the complication of switching from one DCA model to another, as is the case with hybrid (combination) DCA models;
- It does not involve complex and rigorous calculations.

Chapter 6 – Overall Conclusions

The following are key conclusions and contributions from this study:

1. Reservoir simulation is a vital tool for estimating reserves, forecasting production, decision-making and optimizing production practices;
2. The type of reservoir simulator used for analyses is critical especially when considering multiphase flow scenarios;
3. The use of empirical correlations for calculation of bubble point pressure and PVT properties in black-oil simulators may lead to erroneous forecasts;
4. Compositional simulators are better for forecasting production from shale volatile oil reservoirs, as it includes more of the physics that are important for modeling production;
5. Despite the relative ease-of-use, black-oil simulators may be well worth considering if appropriate and better empirical correlations are used;
6. Methane composition in reservoir fluids impact oil recovery estimates in shale volatile oil reservoirs;
7. Reservoir fluid sampling or recombination errors can have substantial impact on oil recovery estimates;
8. Ultra-low permeability and multi-phase flow effects lead to lengthy transition flow regimes between the end of linear flow (ELF) and the start of boundary dominated flow (STBDF) in shale volatile oil reservoirs;
9. A noticeable change of slope was observed on the inverse MBT (material balance time) vs. Time and Yu plots. This point of change corresponds to the start of

boundary effects (STBE) and the STBDF on the rate-MBT and rate-time diagnostic plots;

10. Traditional decline curve analysis (DCA) models are not completely appropriate for forecasting production from shale volatile oil reservoirs;
11. Hybrid (combination) decline curve analysis (DCA) models were developed. They led to better production forecasts in most cases than the simple, traditional DCA models;
12. The time of switch from one model (in our cases – YM-SEPD, Duong and Modified Duong) to another (in our cases – Arps) in hybrid DCA models determines how sensitive production data are to changes in “b” values (Arp’s decline exponents);
13. A power law relationship between the logarithm of known cumulative gas-oil ratio and the logarithm of available cumulative oil production was used to estimate future cumulative gas-oil ratios and ultimately forecast solution gas production;
14. Modified Duong model was developed to reduce the potential overestimates of the Duong model. Modified Duong and its hybrid alternatives significantly reduce the overestimates and led to better forecasts than those obtained with the original Duong model;
15. Solution gas drive mechanism is the primary production mechanism in shale volatile oil reservoirs;
16. Six critical points in the GOR history of shale volatile oil reservoirs were identified;
17. The degree of volatility of volatile oils and gas saturation play an important role in the production performance of shale volatile oil reservoirs;

18. The Principal Components Methodology (PCM) was developed. It is a simple, easy-to-use method of forecasting production that eliminates many complexities associated with existing forecasting methods.

References

Alkouh, A.B., Patel, K., Schechter, D. and Wattenbarger, R. 2012. "Practical Use of Simulators for Characterization of Shale Reservoirs." SPE paper 162645 presented at the SPE Canadian Unconventional Resources Conference, Calgary, Alberta, Canada.

Arps, J.J. 1945. "Analysis of Decline Curves." *AIME* **160**: 228 – 247.

Beliveau, D. 2004. "Solution Gas Production Profiling." Paper 2004-201 presented at the Petroleum Society's 5th Canadian International Petroleum Conference (55th Annual Technical Meeting), Calgary, Alberta, Canada, June 8–10, 2004.

Bhattacharya, S. and Nikolaou, M. 2013. "Analysis of Production History for Unconventional Gas Reservoirs with Statistical Methods", SPE 147658, *SPE Journal*, October 2013.

Cander, H. 2012. "What Are Unconventional Resources? A Simple Definition Using Viscosity and Permeability." Presented at the AAPG Annual Convention and Exhibition, Long Beach, California, 22 – 25 April 2012.

Clarkson, C.R. and Qanbari, F. 2015. "A Semianalytical Forecasting Method for Unconventional Gas and Light Oil Wells: A Hybrid Approach for Addressing the Limitations of Existing Empirical and Analytical Methods." *SPE Reservoir Evaluation & Engineering* ***18*** *(1). SPE 170767-PA.*

Duong, A.N. 2011. "Rate-Decline Analysis for Fracture-Dominated Shale Reservoirs." *SPE Reservoir Evaluation & Engineering* ***14*** *(3). SPE 137748-PA.*

GEM Advanced Compositional Reservoir Simulator, Version 2013 User Guide. 2013. Calgary, Alberta: CMG.

Ilk, D., Rushing, J.A., Perego, A.D. and Blasingame, T.A. 2008. “Exponential vs. Hyperbolic Decline in Tight Gas Sands: Understanding the Origin and Implications for Reserve Estimates Using Arps’ Decline Curves.” SPE paper 116731 presented at the SPE Annual Technical Conference and Exhibition held in Denver, CO, 21 – 24 September 2008.

Jones, R. S. Jr. “Producing Gas-Oil Ratio Behavior of Multi-Fractured Horizontal Wells in Tight Oil Reservoirs.” URTeC 2460396 presented at the Unconventional Resources Technology Conference held in San Antonio, Texas, USA, 1 – 3 August 2016.

Khanal, A., Khoshghadam, M., Makinde, I. and Lee, W.J. 2015. “Modeling Production Decline in Liquid Rich Shale (LRS) Gas Condensate Reservoirs.” SPE paper 175913 presented at the SPE/CSUR Unconventional Resources Conference held in Calgary, AB, Canada, 20 – 22 October 2015.

Khoshghadam, M., Khanal, A., Makinde, I., Lee, W. J., & Rabinejadganji, N. “Numerical Study of Production Mechanisms in Unconventional Liquid-Rich Shale Volatile Oil Reservoirs.” SPE paper 175994 presented at the SPE/CSUR Unconventional Resources Conference held in Calgary, AB, Canada, 20 – 22 October 2015.

Makinde, I. 2014. *Production Forecasting in Shale Volatile Oil Reservoirs.* MS Thesis, University of Houston, Houston, Texas (May 2014).

Makinde, I. and Lee, W.J. 2016. “Production Forecasting in Shale Volatile Oil Reservoirs”. SPE paper 179965 prepared for presentation at the SPE/IAEE Hydrocarbon Economics and Evaluation Symposium held in Houston, Texas, USA, 17–18 May 2016.

Makinde, I. and Lee, W.J. 2016. "Forecasting Production of Shale Volatile Oil Reservoirs Using Simple Models." SPE paper 179964 prepared for presentation at the SPE/IAEE Hydrocarbon Economics and Evaluation Symposium held in Houston, Texas, USA, 17–18 May 2016.

Makinde, I. and Lee, W.J. 2016. "Production Forecasting in Shale Volatile Oil Reservoirs Using Reservoir Simulation, Empirical and Analytical Methods." URTeC: 2429922 presented at the Unconventional Resources Technology Conference held in San Antonio, Texas, USA, 1–3 August 2016.

Makinde, I. and Lee, W.J. 2016. "A New Approach to Forecasting Production from Liquid Rich Shale Reservoirs." SPE paper 183021 presented at the Abu Dhabi International Petroleum Exhibition and Conference held in Abu Dhabi, UAE, 7 – 10 November, 2016.

Makinde, I. and Lee, W.J. 2016. "Statistical Approach to Forecasting Gas-Oil Ratios and Solution Gas Production from Shale Volatile Oil Reservoirs." SPE paper 182933 presented at the Abu Dhabi International Petroleum Exhibition and Conference held in Abu Dhabi, UAE, 7 – 10 November, 2016.

Matthews, C. 2016. America Now Leads the World In This Surprising Category. *Fortune*, 5 July, 2016, http://fortune.com/2016/07/05/oil-reserves-us/ (accessed October 24, 2016).

McCain, W.D. Jr. 1994. "Heavy Components Control Reservoir Fluid Behavior." *Journal of Petroleum Technology, Technology Today Series.* SPE 28214.

McCain, W.D. Jr., Soto, R.B., Valko, P.P. and Blasingame, T.A. 1998. "Correlation of Bubblepoint Pressures for Reservoir Oils – A Comparative Study." SPE paper 51086 presented at the 1998 SPE Eastern Regional Conference and Exhibition held in Pittsburgh, PA, 9 – 11 November 1998.

Ozkan, E., Brown, M., Raghavan, R. and Kazemi, H. 2011. “Comparison of Fractured-Horizontal-Well Performance in Tight Sand and Shale Reservoirs.” *SPE Reservoir Evaluation & Engineering **14** (2). SPE 121290-PA.*

Permadi, P. “Effect of Drainage Area and Producing Rate on Horizontal-Well Oil Recovery in Bottom Water Drive Reservoirs.” SPE 39557 presented at the SPE India Oil and Gas Conference and Exhibition held in New Delhi, India, 17 – 19 February 1998.

Rubis, Ecrin Version 4.30, Rubis Guided Session #7. 1988 – 2013. KAPPA.

Smith, L.I. 2002. “A Tutorial on Principal Components Analysis”, February 26, 2002.

Stalgorova, E. and Mattar, L. 2013. “Analytical Model for Unconventional Multifractured Composite Systems.” *SPE Reservoir Evaluation & Engineering **16** (3). SPE 162516-PA.*

Valko, P.P. and Lee, W.J. 2010. “A Better Way to Forecast Production from Unconventional Gas Wells.” SPE paper 134231 presented at the SPE Annual Technical Conference and Exhibition held in Florence, Italy, 19 – 22 September 2010.

Winprop – Phase behavior and Fluid Property Program, Version 2013 User Guide. 2013. Calgary, Alberta: CMG.

Yu, S. and Miocevic, D.J. 2013. “An Improved Method to Obtain Reliable Production and EUR Prediction for Wells with Short Production History in Tight/Shale Reservoirs.” SPE paper 168684 presented at the Unconventional Resource Technology Conference held in Denver, CO, 12 – 14 August 2013.

Yu, S. 2014. “A New Methodology to Forecast Solution Gas Production in Tight Oil Reservoirs.” SPE paper 171580 presented at the SPE/CSUR Unconventional Resources Conference held in Calgary, AB, Canada, 30 September – 2 October 2014.